Transformer and Inductor Design Handbook

Fourth Edition

© 2011 by Taylor and Francis Group, LLC

Transformer and Inductor Design Handbook

Fourth Edition

Colonel Wm. T. McLyman

CRC Press
Taylor & Francis Group
Boca Raton London New York

CRC Press is an imprint of the
Taylor & Francis Group, an **informa** business

© 2011 by Taylor and Francis Group, LLC

CRC Press
Taylor & Francis Group
6000 Broken Sound Parkway NW, Suite 300
Boca Raton, FL 33487-2742

© 2011 by Taylor and Francis Group, LLC
CRC Press is an imprint of Taylor & Francis Group, an Informa business

No claim to original U.S. Government works

Printed in the United States of America on acid-free paper
10 9 8 7 6 5 4 3 2 1

International Standard Book Number-13: 978-1-4398-3688-0 (Ebook-PDF)

This book contains information obtained from authentic and highly regarded sources. Reasonable efforts have been made to publish reliable data and information, but the author and publisher cannot assume responsibility for the validity of all materials or the consequences of their use. The authors and publishers have attempted to trace the copyright holders of all material reproduced in this publication and apologize to copyright holders if permission to publish in this form has not been obtained. If any copyright material has not been acknowledged please write and let us know so we may rectify in any future reprint.

Except as permitted under U.S. Copyright Law, no part of this book may be reprinted, reproduced, transmitted, or utilized in any form by any electronic, mechanical, or other means, now known or hereafter invented, including photocopying, microfilming, and recording, or in any information storage or retrieval system, without written permission from the publishers.

For permission to photocopy or use material electronically from this work, please access www.copyright.com (http://www.copyright.com/) or contact the Copyright Clearance Center, Inc. (CCC), 222 Rosewood Drive, Danvers, MA 01923, 978-750-8400. CCC is a not-for-profit organization that provides licenses and registration for a variety of users. For organizations that have been granted a photocopy license by the CCC, a separate system of payment has been arranged.

Trademark Notice: Product or corporate names may be trademarks or registered trademarks, and are used only for identification and explanation without intent to infringe.

Visit the Taylor & Francis Web site at
http://www.taylorandfrancis.com

and the CRC Press Web site at
http://www.crcpress.com

© 2011 by Taylor and Francis Group, LLC

To My Wife, Bonnie

© 2011 by Taylor and Francis Group, LLC

Contents

Foreword *ix*

Preface *xi*

Acknowledgements *xiii*

About the Author *xv*

Symbols *xvii*

Chapter 1

Fundamentals of Magnetics 1-1

Chapter 2

Magnetic Materials and Their Characteristics 2-1

Chapter 3

Magnetic Cores 3-1

Chapter 4

Window Utilization, Magnet Wire, and Insulation 4-1

Chapter 5

Transformer Design Trade-Offs 5-1

Chapter 6

Transformer-Inductor Efficiency, Regulation, and Temperature Rise 6-1

Chapter 7

Power Transformer Design 7-1

Chapter 8

DC Inductor Design, Using Gapped Cores 8-1

Chapter 9

DC Inductor Design, Using Powder Cores 9-1

Chapter 10

AC Inductor Design 10-1

Chapter 11

Constant Voltage Transformer (CVT) 11-1

Chapter 12

Three-Phase Transformer Design 12-1

© 2011 by Taylor and Francis Group, LLC

Chapter 13

Flyback Converters, Transformer Design 13-1

Chapter 14

Forward Converter, Transformer Design, and Output Inductor Design 14-1

Chapter 15

Input Filter Design 15-1

Chapter 16

Current Transformer Design 16-1

Chapter 17

Winding Capacitance and Leakage Inductance 17-1

Chapter 18

Quiet Converter Design 18-1

Chapter 19

Rotary Transformer Design 19-1

Chapter 20

Planar Transformers and Inductors 20-1

Chapter 21

Derivations for the Design Equations 21-1

Chapter 22

Autotransformer Design 22-1

Chapter 23

Common-Mode Inductor Design 23-1

Chapter 24

Series Saturable Reactor Design 24-1

Chapter 25

Self-Saturating, Magnetic Amplifiers 25-1

Chapter 26

Designing Inductors for a Given Resistance 26-1

Index I-1

© 2011 by Taylor and Francis Group, LLC

Foreword

Colonel McLyman is a well-known author, lecturer and magnetic circuit designer. His previous books on transformer and inductor design, magnetic core characteristics and design methods for converter circuits have been widely used by magnetics circuit designers.

In his 4th edition, Colonel McLyman has combined and updated the information found in his previous books. He has also added five new subjects such as autotransformer design, common-mode inductor design, series saturable reactor design, self-saturating magnetic amplifier and designing inductors for a given resistance. The author covers magnetic design theory with all of the relevant formulas. He has complete information on all of the magnetic materials and core characteristics along with the real world, step-by-step design examples.

This book is a must for engineers doing magnetic design. Whether you are working on high "rel" state of the art design or high volume, or low cost production, this book will help you. Thanks Colonel for a well-done, useful book.

Robert G. Noah
Application Engineering Manager (Retired)
Magnetics, Division of Spang and Company
Pittsburgh, Pennsylvania

© 2011 by Taylor and Francis Group, LLC

Preface

I have had many requests to update my book *Transformer and Inductor Design Handbook*, because of the way power electronics has changed in the past few years. I have been requested to add and expand on the present Chapters. There are now twenty-six Chapters. The new Chapters are autotransformer design, common-mode inductor design, series saturable reactor design, self-saturating magnetic amplifier and designing inductors for a given resistance, all with step-by-step design examples.

This book offers a practical approach with design examples for design engineers and system engineers in the electronics industry, as well as the aerospace industry. While there are other books available on electronic transformers, none of them seem to have been written with the user's viewpoint in mind. The material in this book is organized so that the design engineer, student engineer or technician, starting at the beginning of the book and continuing through the end, will gain a comprehensive knowledge of the state of the art in transformer and inductor design. The more experienced engineers and system engineers will find this book a useful tool when designing or evaluating transformers and inductors.

Transformers are to be found in virtually all electronic circuits. This book can easily be used to design lightweight, high-frequency aerospace transformers or low-frequency commercial transformers. It is, therefore, a design manual.

The conversion process in power electronics requires the use of transformers, components that frequently are the heaviest and bulkiest item in the conversion circuit. Transformer components also have a significant effect on the overall performance and efficiency of the system. Accordingly, the design of such transformers has an important influence on overall system weight, power conversion efficiency, and cost. Because of the interdependence and interaction of these parameters, judicious trade-offs are necessary to achieve design optimization.

Manufacturers have for years assigned numeric codes to their cores to indicate their power-handling ability. This method assigns to each core a number called the area product, A_p, that is the product of its window area, W_a, and core cross-section area, A_c. These numbers are used by core suppliers to summarize dimensional and electrical properties in their catalogs. The product of the window area, W_a, and the core area, A_c, gives the area product, A_p, a dimension to the fourth power. I have developed a new equation for the power-handling ability of the core, the core geometry, K_g. The core geometry, K_g, has a dimension to the fifth power. This new equation gives engineers faster and tighter control of their design. The core geometry coefficient, K_g, is a relatively new concept, and magnetic core manufacturers are now beginning to put it in their catalogs.

Because of their significance, the area product, A_p, and the core geometry, K_g, are treated extensively in this handbook. A great deal of other information is also presented for the convenience of the designer. Much of the material is in tabular form to assist the designer in making the trade-offs best suited for the particular application in a minimum amount of time.

© 2011 by Taylor and Francis Group, LLC

Designers have used various approaches in arriving at suitable transformer and inductor designs. For example, in many cases a rule of thumb used for dealing with current density is that a good working level is 1000 circular mils per ampere. This is satisfactory in many instances; however, the wire size used to meet this requirement may produce a heavier and bulkier inductor than desired or required. The information presented here will make it possible to avoid the use of this and other rules of thumb, and to develop a more economical and better design.

The author or the publisher assumes no responsibility for any infringement of patent or other rights of third parties that may result from the use of circuits, systems, or processes described or referred to in this handbook.

I wish to thank the manufacturers represented in this book for their assistance in supplying technical data.

Colonel Wm. T. McLyman

© 2011 by Taylor and Francis Group, LLC

Acknowledgements

In gathering the material for this book, I have been fortunate in having the assistance and cooperation of several companies and many colleagues. As the author, I wish to express my gratitude to all of them. The list is too long to mention them all. However, there are some individuals and companies whose contributions have been significant. Colleagues that have retired from Magnetics include Robert Noah and Harry Savisky who helped so greatly with the editing of the final draft. Other contributions were given by my colleagues at Magnetics, Lowell Bosley and his staff with the sending of up-to-date catalogs and sample cores. I would like to thank colleagues at Micrometals Corp., Jim Cox and Dale Nicol, and George Orenchak of TSC International. I would like to give a special thanks to Richard (Oz) Ozenbaugh of Linear Magnetics Corp. for his assistance in the detailed derivations of many of the equations and his efforts in checking all the design examples. I would also like to give special thanks to Steve Freeman of Rodon Products, Inc. and Charles Barnett of Leightner Electronics, Inc. for building and testing all of the magnetic components used in the design examples.

There are individuals I would like to thank: Dr. Vatche Vorperian of Jet Propulsion Laboratory (JPL) for his help in generating and clarifying equations for the Quiet Converter; Jerry Fridenberg of Fridenberg Research, Inc. for modeling circuits on his SPICE program; Dr. Gene Wester of (JPL) for his inputs and Kit Sum for his assistance in the energy storage equations. I also want to thank the late Robert Yahiro for his help and encouragement over the years.

© 2011 by Taylor and Francis Group, LLC

About The Author

Colonel Wm. T. McLyman has retired as a senior member of the Avionics Equipment Section of the Jet Propulsion Laboratory (JPL) affiliated with the California Institute of Technology in Pasadena, California. He has fifty-four years of experience in the field of Magnetics and holds fourteen United States Patents on magnetics-related concepts. Through his thirty years at JPL, he has written over seventy JPL technical memorandums, new technology reports, and tech-briefs on the subject of magnetics and circuit designs for power conversion. He has worked on projects for NASA including the Pathfinder Mission to Mars, Cassini, Galileo, Magellan, Viking, Voyager, MVM, Hubble Space Telescope, and many others.

He has been on the lecture circuit for over twenty-nine years speaking in the United States, Canada, Mexico, and Europe on the design and fabrication of magnetic components. He is known as a recognized authority in magnetic design. He is the president of his company called Kg Magnetics, Inc., which specializes in power magnetics design.

He has also written a book entitled *Design and Fabrication of High Reliability Magnetic Devices.* This book is based on fabricating and testing Hi-Rel magnetic devices. He also markets through Kg Magnetics, Inc. a magnetics design and analysis software computer program called "Titan" for transformers and inductors, see Figure 1. This program operates on Windows 95, 98, 2000, and NT.

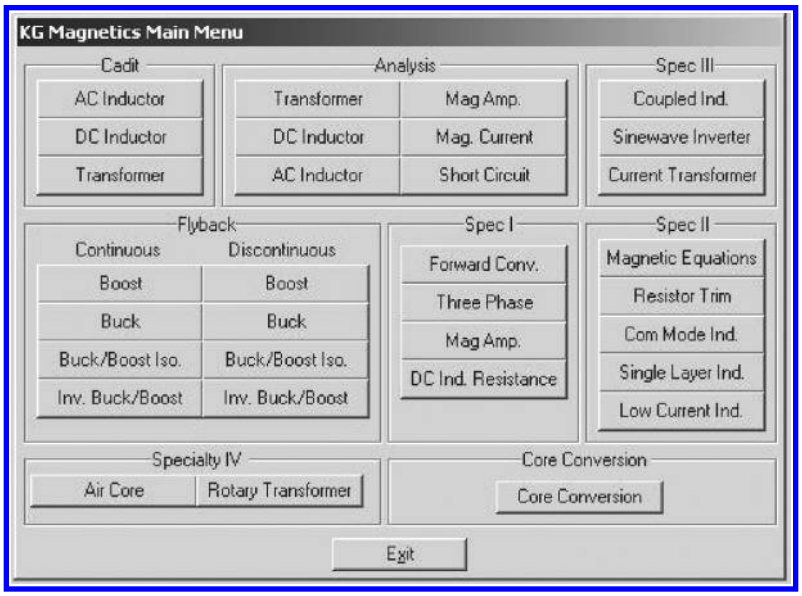

Figure 1. Computer Design Program Main Menu.

Kg Magnetics, Inc.
Colonel Wm. T. McLyman, (President)
www.kgmagnetics.com
colonel@kgmagnetics.com
Idyllwild, CA 92549

© 2011 by Taylor and Francis Group, LLC

Symbols

α	regulation, %
A_c	effective cross section of the core, cm^2
A_p	area product, cm^4
A_t	surface area of the transformer, cm^2
A_w	wire area, cm^2
$A_{w(B)}$	bare wire area, cm^2
$A_{w(I)}$	insulated wire area, cm^2
A_{wp}	primary wire area, cm^2
A_{ws}	secondary wire area, cm^2
A-T	amp turn
AWG	American wire gage
B	flux, teslas
B_{ac}	alternating current flux density, teslas
ΔB	change in flux, teslas
B_{dc}	direct current flux density, teslas
B_m	flux density, teslas
B_{max}	maximum flux density, teslas
B_o	operating peak flux density, teslas
B_{pk}	peak flux density, teslas
B_r	residual flux density, teslas
B_s	saturation flux density, teslas
C	capacitance
C_n	new capacitance
C_p	lumped capacitance
C_s	stray capacitance
CM	circular mils
CM	common mode
D_{AWG}	wire diameter, cm
$D_{(min)}$	minimum duty ratio
$D_{(max)}$	maximum duty ratio
D_w	dwell time duty ratio
DM	differential mode
E	voltage
E_{Line}	line-to-line voltage
E_{Phase}	Line to neutral voltage
Energy	energy, watt-second
ESR	equivalent series resistance

© 2011 by Taylor and Francis Group, LLC

η	efficiency
f	frequency, Hz
F	fringing flux factor
F_m	magneto-motive force, mmf
F.L.	full load
G	winding length, cm
γ	density, in grams-per-cm^2
ε	skin depth, cm
H	magnetizing force, oersteds
H	magnetizing force, amp-turns
H_c	magnetizing force required to return flux to zero, oersteds
ΔH	delta magnetizing force, oersteds
H_o	operating peak magnetizing force
H_s	magnetizing force at saturation, oersteds
I	current, amps
I_c	charge current, amps
I_c	control current, amps
ΔI	delta current, amps
I_{dc}	dc current, amps
I_g	gate current, amps
I_{in}	input current, amps
I_{Line}	input line current, amps
I_m	magnetizing current, amps
I_o	load current, amps
$I_{o(max)}$	maximum load current, amps
$I_{o(min)}$	minimum load current, amps
I_p	primary current, amps
I_{Phase}	input phase current, amps
I_s	secondary current, amps
$I_{s(Phase)}$	secondary phase current, amps
$I_{s(Line)}$	secondary line current, amps
J	current density, amps per cm^2
K_c	copper loss constant
K_c	quasi-voltage waveform factor
K_e	electrical coefficient
K_{cw}	control winding coefficient
K_f	waveform coefficient

© 2011 by Taylor and Francis Group, LLC

K_g	core geometry coefficient, cm^5
K_j	constant related to current density
K_s	constant related to surface area
K_u	window utilization factor
K_{up}	primary window utilization factor
K_{us}	secondary window utilization factor
K_{vol}	constant related to volume
K_w	constant related to weight
L	inductance, henry
l	is a linear dimension
λ	density, grams per cm^3
L_c	open circuit inductance, henrys
L_c	control winding inductance, henrys
$L_{(crt)}$	critical inductance
l_g	gap, cm
l_m	magnetic path length, cm
L_p	primary inductance, henrys
l_t	total path length, cm
MA	magnetic amplifier
mks	meters-kilogram-seconds
MLT	mean length turn, cm
mmf	magnetomotive force, F_m
MPL	magnetic path length, cm
mW/g	milliwatts-per-gram
μ	permeability
μ_e	effective permeability
μ_i	initial permeability
μ_Δ	incremental permeability
μ_m	core material permeability
μ_o	permeability of air
μ_r	relative permeability
n	turns ratio
N	turns
N_c	control turns
N_g	gate turns
N_L	inductor turns
N_n	new turns

© 2011 by Taylor and Francis Group, LLC

N_p	primary turns
N_s	secondary turns
N.L.	no load
P	watts
P_c	control power loss, watts
P_{cu}	copper loss, watts
P_{fe}	core loss, watts
P_g	gap loss, watts
P_{gain}	power gain, factor
ϕ	magnetic flux
P_{in}	input power, watts
P_L	inductor copper loss, watts
P_o	output power, watts
P_p	primary copper loss, watts
P_s	secondary copper loss, watts
P_Σ	total loss (core and copper), watts
P_t	total apparent power, watts
P_{tin}	autotransformer input power, volt-amps
P_{to}	autotransformer output power, volt-amps
P_{VA}	primary, volt-amps
R	resistance, ohms
R_{ac}	ac resistance, ohms
R_c	control resistance, ohms
R_{cu}	copper resistance, ohms
R_{dc}	dc resistance, ohms
R_e	equivalent core loss (shunt) resistance, ohms
R_g	reluctance of the gap
$R_{in(equiv)}$	reflected load resistance, ohms
R_L	load resistance, ohms
R_m	reluctance
R_{mt}	total reluctance
R_o	load resistance, ohms
$R_{o(R)}$	reflected load resistance, ohms
R_p	primary resistance, ohms
R_R	ac/dc resistance ratio
R_s	secondary resistance, ohms
R_t	total resistance, ohms

© 2011 by Taylor and Francis Group, LLC

ρ	resistivity, ohm-cm
S_1	conductor area/wire area
S_2	wound area/usable window
S_3	usable window area/window area
S_4	usable window area/usable window area + insulation area
S_{np}	number of primary strands
S_{ns}	number of secondary strands
S_{VA}	secondary volt-amps
SR	saturable reactor
T	total period, seconds
t_{off}	off time, seconds
t_{on}	on time, seconds
t_r	time constant, seconds
T_r	temperature rise, degrees C
t_w	dwell time, seconds
U	multiplication factor
V_{ac}	applied voltage, volts
V_c	control voltage, volts
$V_{c(pk)}$	peak voltage, volts
V_d	diode voltage drop, volts
V_{in}	input voltage, volts
$V_{in(max)}$	maximum input voltage, volts
$V_{in(min)}$	minimum input voltage, volts
V_n	new voltage, volts
V_o	output voltage, volts
V_p	primary voltage, volts
$V_{p(rms)}$	primary rms voltage, volts
$V_{r(pk)}$	peak ripple voltage
$V_{s(LL)}$	secondary line-to-line voltage, volts
$V_{s(LN)}$	secondary line to neutral voltage, volts
V_s	secondary voltage, volts
ΔV_{CC}	capacitor voltage, volts
ΔV_{CR}	capacitor ESR voltage, volts
ΔV_p	delta primary voltage, volts
ΔV_s	delta secondary voltage, volts
VA	volt-amps
W	watts

© 2011 by Taylor and Francis Group, LLC

W/kg	watts-per-kilogram
WK	watts-per-kilogram
W_a	window area, cm^2
W_{ac}	control window area, cm^2
$W_{a(eff)}$	effective window area, cm^2
W_{ag}	gate window area, cm^2
W_{ap}	primary window area, cm^2
W_{as}	secondary window area, cm^2
W_t	weight, grams
W_{tcu}	copper weight, grams
W_{tfe}	iron weight, grams
w-s	watt-seconds
X_L	inductive reactance, ohms

© 2011 by Taylor and Francis Group, LLC

Chapter 1

Fundamentals of Magnetics

© 2011 by Taylor and Francis Group, LLC

Table of Contents

1. Introduction 1-3
2. Magnetic Properties in Free Space 1-3
3. Intensifying the Magnetic Field 1-4
4. Simple Transformer 1-7
5. Magnetic Core 1-8
6. Fundamental Characteristics of a Magnetic Core 1-9
7. Hysteresis Loop (B-H Loop) 1-11
8. Permeability 1-12
9. Magnetomotive Force (mmf) and Magnetizing Force (H) 1-15
10. Reluctance 1-16
11. Air Gap 1-18
12. Controlling the dc Flux with an Air Gap 1-20
13. Types of Air Gaps 1-21
14. Fringing Flux 1-22
15. Material Permeability, (μ_m) 1-23
16. Air Gaps 1-23
17. Fringing Flux, F 1-24
18. Gapped, dc Inductor Design 1-25
19. Fringing Flux and Coil Proximity 1-26
20. Fringing Flux, Crowding 1-27
21. Fringing Flux and Powder Cores 1-28

© 2011 by Taylor and Francis Group, LLC

Introduction

Considerable difficulty is encountered in mastering the field of magnetics because of the use of so many different systems of units – the centimeter-gram-second (cgs) system, the meter-kilogram-second (mks) system, and the mixed English units system. Magnetics can be treated in a simple way by using the cgs system. There always seems to be one exception to every rule and that is permeability.

Magnetic Properties in Free Space

A long wire with a dc current, I, flowing through it, produces a circulatory magnetizing force, H, and a magnetic field, B, around the conductor, as shown in Figure 1-1, where the relationship is:

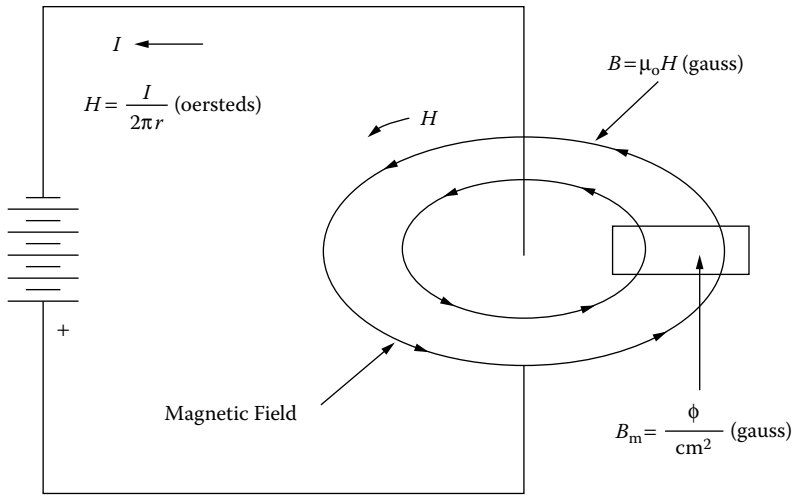

Figure 1-1. A Magnetic Field Generated by a Current Carrying Conductor.

The direction of the line of flux around a straight conductor may be determined by using the "right hand rule" as follows: When the conductor is grasped with the right hand, so that the thumb points in the direction of the current flow, the fingers point in the direction of the magnetic lines of force. This is based on so-called conventional current flow, not the electron flow.

When a current is passed through the wire in one direction, as shown in Figure 1-2(A), the needle in the compass will point in one direction. When the current in the wire is reversed, as in Figure 1-2(B), the needle will also reverse direction. This shows that the magnetic field has polarity and that, when the current I, is reversed, the magnetizing force, H, will follow the current reversals.

© 2011 by Taylor and Francis Group, LLC

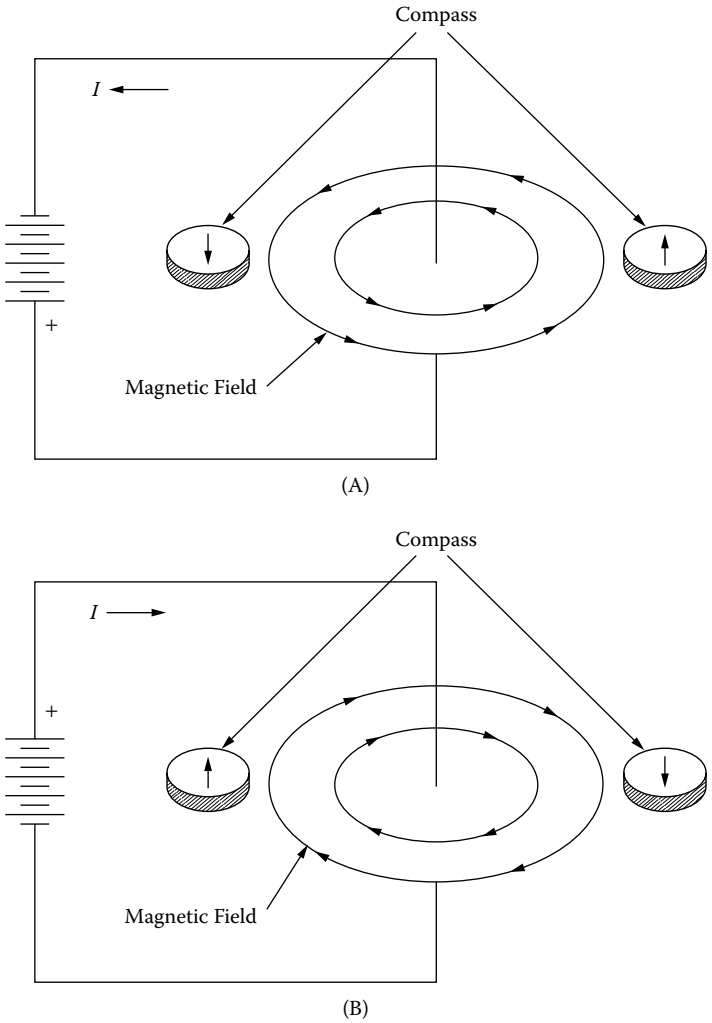

Figure 1-2. The Compass Illustrates How the Magnetic Field Changes Polarity.

Intensifying the Magnetic Field

When a current passes through a wire, a magnetic field is set up around the wire. If the conductors, as shown in Figure 1-3, carrying current in the same direction are separated by a relatively large distance, the magnetic fields generated will not influence each other. If the same two conductors are placed close to each other, as shown in Figure 1-4, the magnetic fields add, and the field intensity doubles.

$$\gamma = \frac{B^2}{8\pi\mu}, \quad \text{[energy density]} \qquad [1\text{-}1]$$

If the wire is wound on a dowel, its magnetic field is greatly intensified. The coil, in fact, exhibits a magnetic field exactly like that of a bar magnet, as shown in Figure 1-5. Like the bar magnet, the coil has a north pole and a neutral center region. Moreover, the polarity can be reversed by reversing the current, I, through the coil. Again, this demonstrates the dependence of the magnetic field on the current direction.

© 2011 by Taylor and Francis Group, LLC

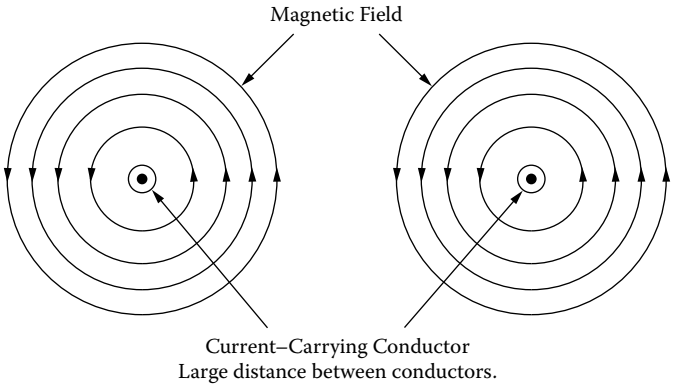

Figure 1-3. Magnetic Fields Produced Around Spaced Conductors.

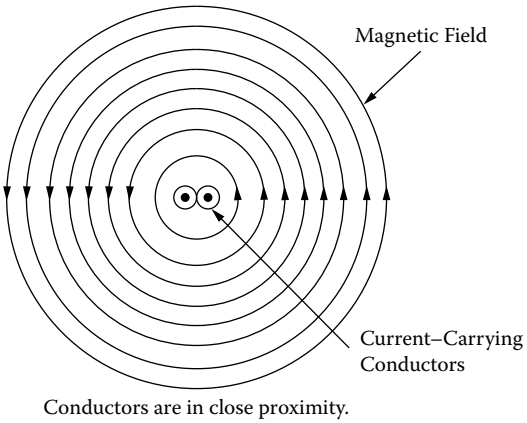

Figure 1-4. Magnetic Fields Produced Around Adjacent Conductors.

The magnetic circuit is the space in which the flux travels around the coil. The magnitude of the flux is determined by the product of the current, I, and the number of turns, N, in the coil. The force, NI, required to create the flux is magnetomotive force (mmf). The relationship between flux density, B, and magnetizing force, H, for an air-core coil is shown in Figure 1-6. The ratio of B to H is called the permeability, μ, and for this air-core coil the ratio is unity in the cgs system, where it is expressed in units of gauss per oersteds, (gauss/oersteds).

$$\mu_o = 1$$
$$B = \mu_o H \qquad [1\text{-}2]$$

If the battery, in Figure 1-5, were replaced with an ac source, as shown in Figure 1-7, the relationship between B and H would have the characteristics shown in Figure 1-8. The linearity of the relationship between B and H represents the main advantage of air-core coils. Since the relationship is linear, increasing H increases B, and therefore the flux in the coil, and, in this way, very large fields can be produced with large currents. There is obviously a practical limit to this, which depends on the maximum allowable current in the conductor and the resulting rise.

© 2011 by Taylor and Francis Group, LLC

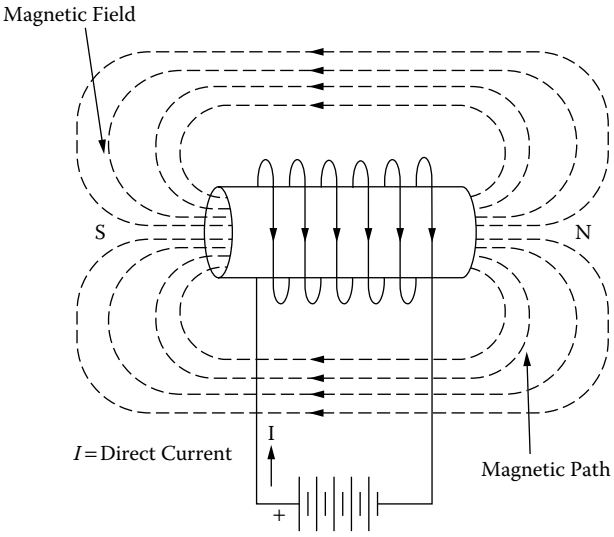

Figure 1-5. Air-Core Coil with dc Excitation.

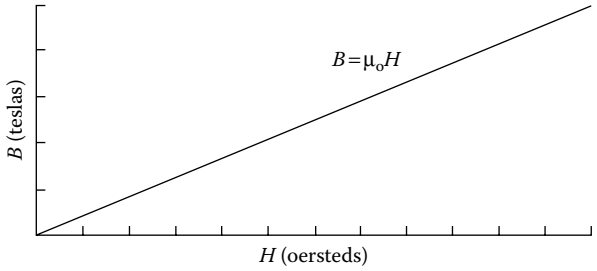

Figure 1-6. Relationship between B and H with dc Excitation.

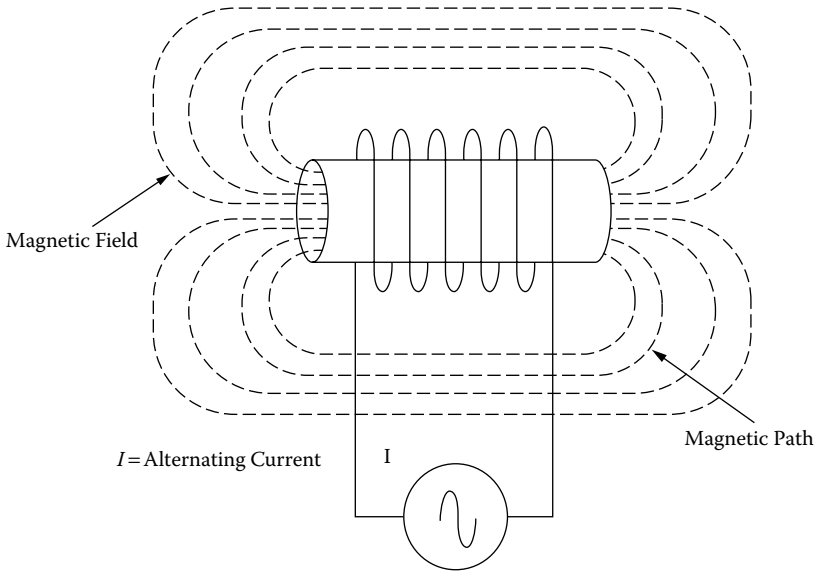

Figure 1-7. Air-Core Coil Driven from an ac Source.

© 2011 by Taylor and Francis Group, LLC

Fields of the order of 0.1 tesla are feasible for a 40°C temperature rise above room ambient temperature. With super cooled coils, fields of 10 tesla have been obtained.

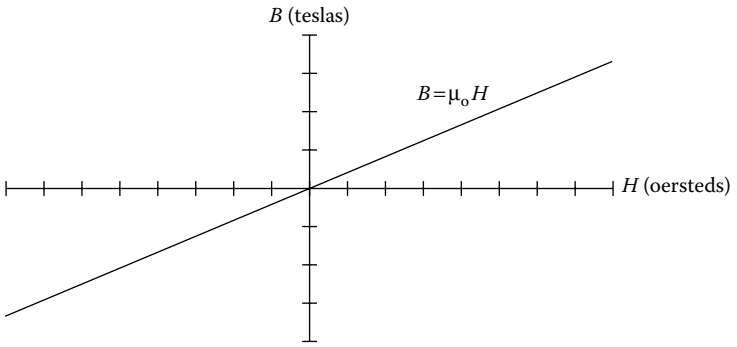

Figure 1-8. Relationship between B and H with ac Excitation.

Simple Transformer

A transformer in its simplest form is shown in Figure 1-9. This transformer has two air coils that share a common flux. The flux diverges from the ends of the primary coil in all directions. It is not concentrated or confined. The primary is connected to the source and carries the current that establishes a magnetic field. The other coil is open-circuited. Notice that the flux lines are not common to both coils. The difference between the two is the leakage flux; that is, leakage flux is the portion of the flux that does not link both coils.

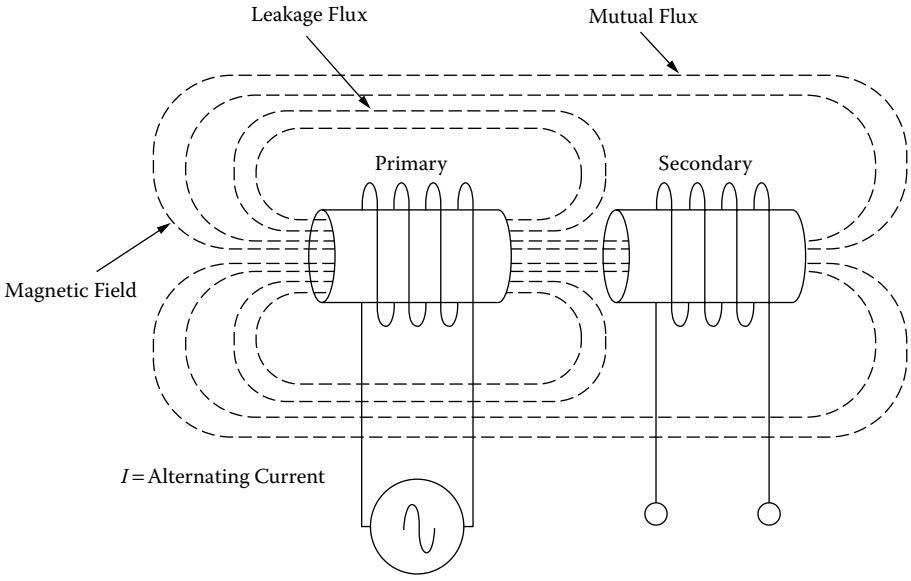

Figure 1-9. The Simplest Type of Transformer.

© 2011 by Taylor and Francis Group, LLC

Magnetic Core

Most materials are poor conductors of magnetic flux; they have low permeability. A vacuum has a permeability of 1.0, and nonmagnetic materials, such as air, paper, and copper have permeabilities of the same order. There are a few materials, such as iron, nickel, cobalt, and their alloys that have high permeability, sometimes ranging into the hundreds of thousands. To achieve an improvement over the air-coil, as shown in Figure 1-10, a magnetic core can be introduced, as shown in Figure 1-11. In addition to its high permeability, the advantages of the magnetic core over the air-core are that the Magnetic Path Length (MPL) is well-defined, and the flux is essentially confined to the core, except in the immediate vicinity of the winding. There is a limit as to how much magnetic flux can be generated in a magnetic material before the magnetic core goes into saturation, and the coil reverts back to an air-core, as shown in Figure 1-12.

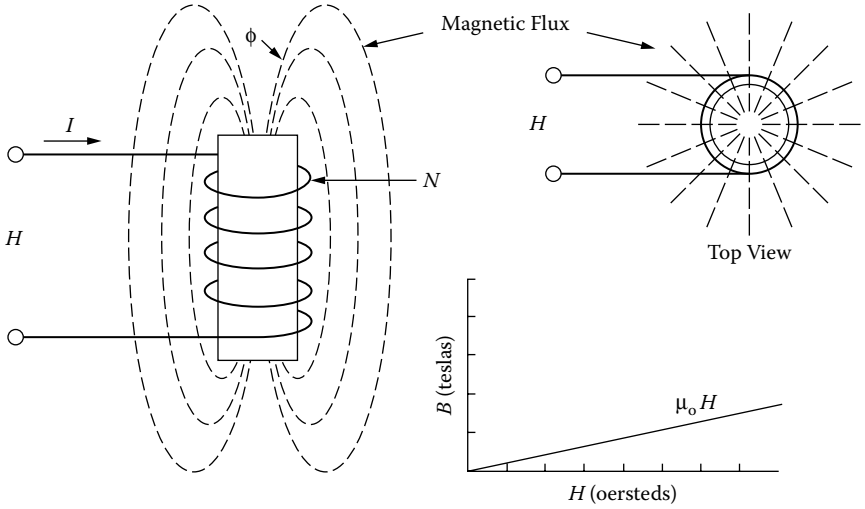

Figure 1-10. Air-Core Coil Emitting Magnetic Flux when Excited.

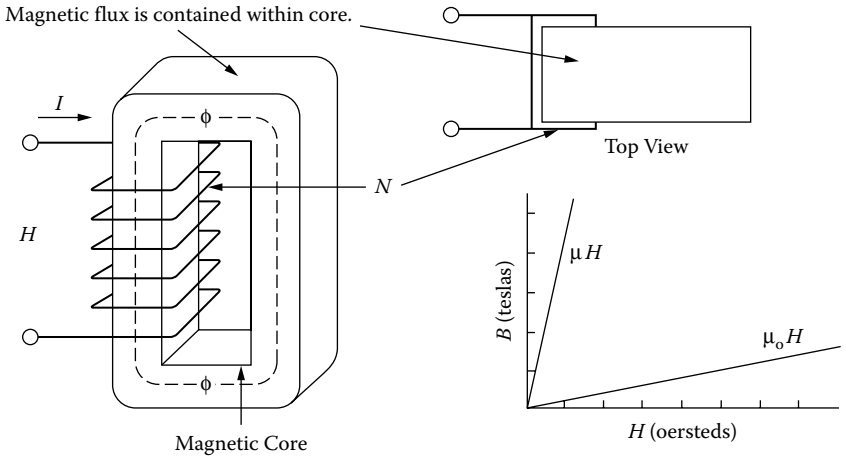

Figure 1-11. Introduction of a Magnetic Core.

© 2011 by Taylor and Francis Group, LLC

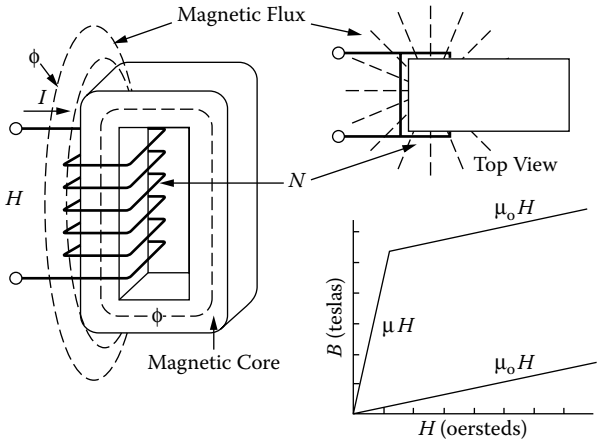

Figure 1-12. Excited Magnetic Core Driven into Saturation.

Fundamental Characteristics of a Magnetic Core

The effect of exciting a completely demagnetized, ferromagnetic material, with an external magnetizing force, H, and increasing it slowly, from zero, is shown in Figure 1-13, where the resulting flux density is plotted as a function of the magnetizing force, H. Note that, at first, the flux density increases very slowly up to point A, then, increases very rapidly up to point B, and then, almost stops increasing. Point B is called the knee of the curve. At point C, the magnetic core material has saturated. From this point on, the slope of the curve is shown in Equation [1-3].

$$\frac{B}{H} = 1, \quad \text{[gauss/oersteds]} \tag{1-3}$$

The coil is now behaving as if it had an air-core. When the magnetic core is in hard saturation, the coil has the same permeability as air, or unity. Following the magnetization curve in Figure 1-14, Figures 1-15 through Figures 1-16 show how the flux in the core is generated from the inside of the core to the outside until the core saturates.

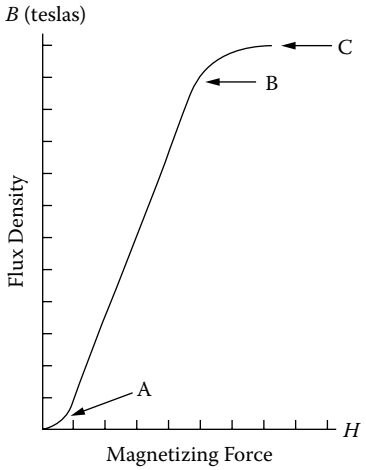

Figure 1-13. Typical Magnetization Curve.

© 2011 by Taylor and Francis Group, LLC

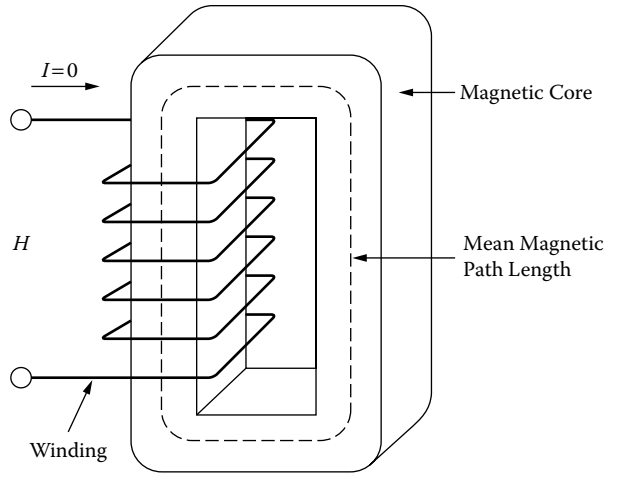

Figure 1-14. Magnetic Core with Zero Excitation.

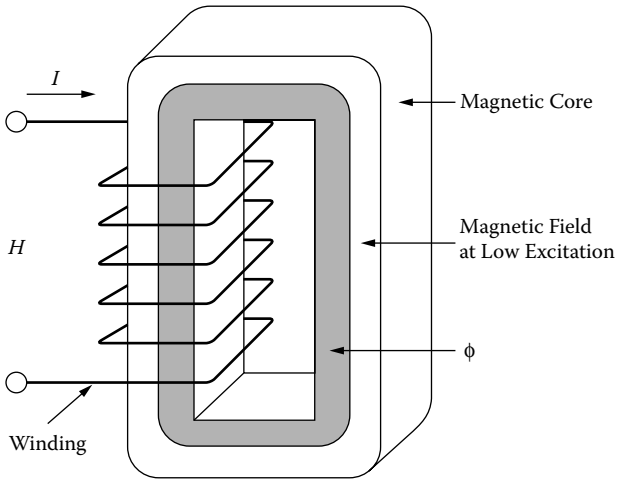

Figure 1-15. Magnetic Core with Low Excitation.

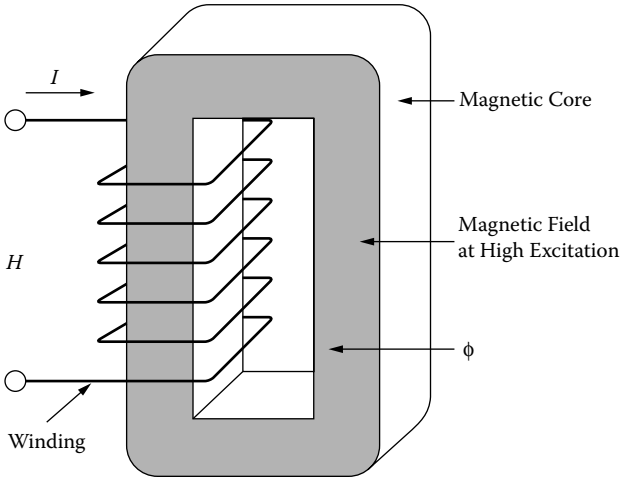

Figure 1-16. Magnetic Core with High Excitation.

© 2011 by Taylor and Francis Group, LLC

Hysteresis Loop (B-H Loop)

An engineer can take a good look at the hysteresis loop and get a first order evaluation of the magnetic material. When the magnetic material is taken through a complete cycle of magnetization and demagnetization, the results are as shown in Figure 1-17. It starts with a neutral magnetic material, traversing the B-H loop at the origin X. As H is increased, the flux density B increases along the dashed line to the saturation point, B_s. When H is now decreased and B is plotted, B-H loop transverses a path to B_r, where H is zero and the core is still magnetized. The flux at this point is called remanent flux, and has a flux density, B_r.

The magnetizing force, H, is now reversed in polarity to give a negative value. The magnetizing force required to reduce the flux B_r to zero is called the coercive force, H_c. When the core is forced into saturation, the retentivity, B_{rs}, is the remaining flux after saturation, and coercivity, H_{cs}, is the magnetizing force required to reset to zero. Along the initial magnetization curve at point X, the dashed line in Figure 1-17, B increases from the origin nonlinearly with H, until the material saturates. In practice, the magnetization of a core in an excited transformer never follows this curve, because the core is never in the totally demagnetized state, when the magnetizing force is first applied.

The hysteresis loop represents energy lost in the core. The best way to display the hysteresis loop is to use a dc current, because the intensity of the magnetizing force must be so slowly changed so that no eddy currents are generated in the material. Only under this condition is the area inside the closed B-H loop indicative of the hysteresis. The enclosed area is a measure of energy lost in the core material during that cycle. In ac applications, this process is repeated continuously and the total hysteresis loss is dependent upon the frequency.

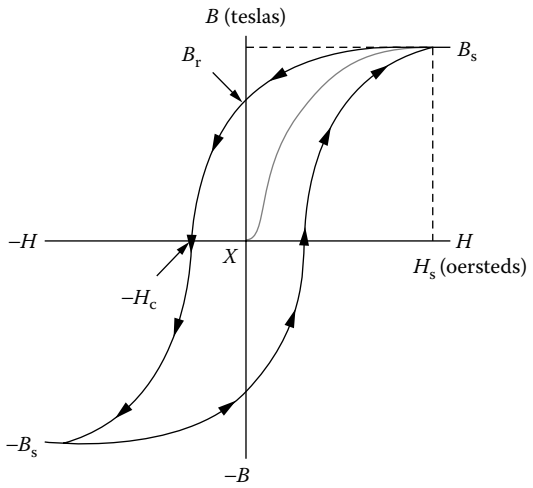

Figure 1-17. Typical Hysteresis Loop.

© 2011 by Taylor and Francis Group, LLC

Permeability

In magnetics, permeability is the ability of a material to conduct flux. The magnitude of the permeability at a given induction is the measure of the ease with which a core material can be magnetized to that induction. It is defined as the ratio of the flux density, B, to the magnetizing force, H. Manufacturers specify permeability in units of gauss per oersteds, as shown in Equation [1-4].

$$\text{Permeability} = \frac{B}{H}, \quad \left[\frac{\text{gauss}}{\text{oersteds}}\right] \tag{1-4}$$

The absolute permeability, μ_o in cgs units is unity 1 (gauss per oersteds) in a vacuum, as shown in Equation [1-5].

$$\begin{aligned} &\text{cgs}: \quad \mu_o = 1, \quad \left[\frac{\text{gauss}}{\text{oersteds}}\right] = \left[\frac{\text{teslas}}{\text{oersteds}} \left(10^4\right)\right] \\ &\text{mks}: \quad \mu_o = 0.4\pi\left(10^{-8}\right), \quad \left[\frac{\text{henrys}}{\text{meter}}\right] \end{aligned} \tag{1-5}$$

When B is plotted against H, as in Figure 1-18, the resulting curve is called the magnetization curve. These curves are idealized. The magnetic material is totally demagnetized and is then subjected to gradually increasing magnetizing force, while the flux density is plotted. The slope of this curve at any given point gives the permeability at that point. Permeability can be plotted against a typical B-H curve, as shown in Figure 1-19. Permeability is not constant; therefore, its value can be stated only at a given value of B or H.

There are many different kinds of permeability, and each is designated by a different subscript on the symbol μ.

μ_o 1. Absolute permeability, defined as the permeability in a vacuum.

μ_i 2. Initial permeability is the slope of the initial magnetization curve at the origin. It is measured at very small induction, as shown in Figure 1-20.

μ_Δ 3. Incremental permeability is the slope of the magnetization curve for finite values of peak-to-peak flux density with superimposed dc magnetization, as shown in Figure 1-21.

μ_e 4. Effective permeability. If a magnetic circuit is not homogeneous (i.e., contains an air gap), the effective permeability is the permeability of hypothetical homogeneous (ungapped) structure of the same shape, dimensions, and reluctance that would give the inductance equivalent to the gapped structure.

μ_r 5. Relative permeability is the permeability of a material relative to that of free space.

μ_n 6. Normal permeability is the ratio of B/H at any point of the curve, as shown in Figure 1-22.

μ_{max} 7. Maximum permeability is the slope of a straight line drawn from the origin tangent to the curve at its knee, as shown in Figure 1-23.

μ_p 8. Pulse permeability is the ratio of peak B to peak H for unipolar excitation.

μ_m 9. Material permeability is the slope of the magnetization curve measure at less than 50 gauss, as shown in Figure 1-24.

© 2011 by Taylor and Francis Group, LLC

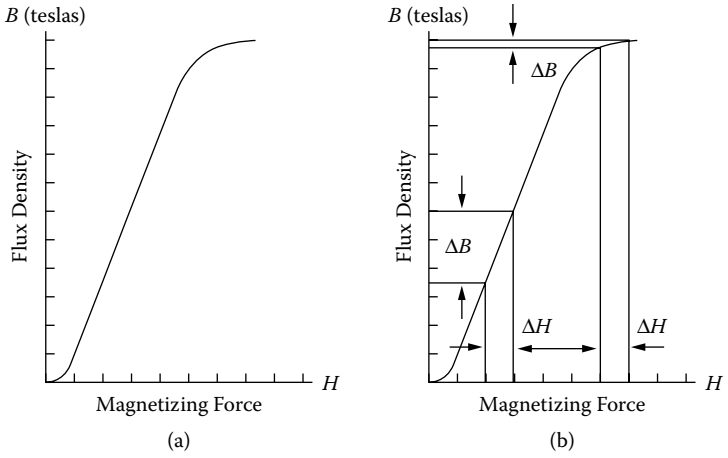

Figure 1-18. Magnetizing Curve.

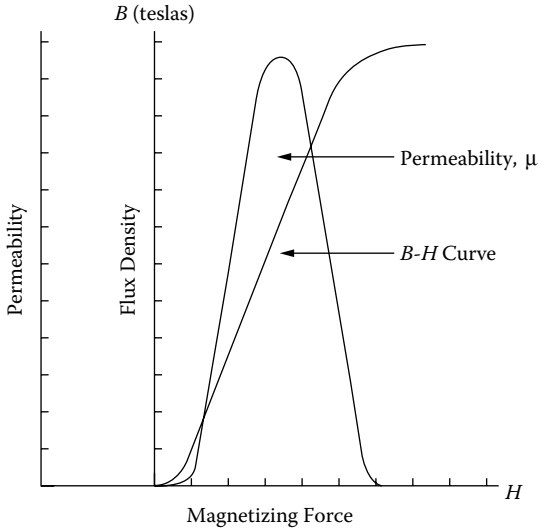

Figure 1-19. Variation of Permeability μ along the Magnetizing Curve.

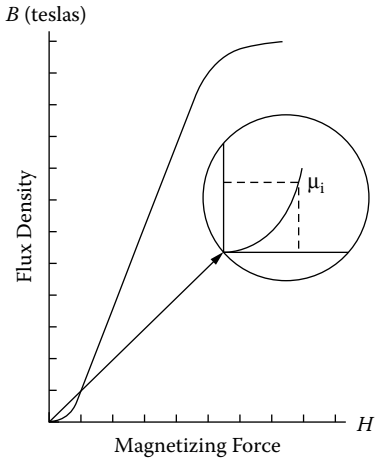

Figure 1-20. Initial Permeability.

© 2011 by Taylor and Francis Group, LLC

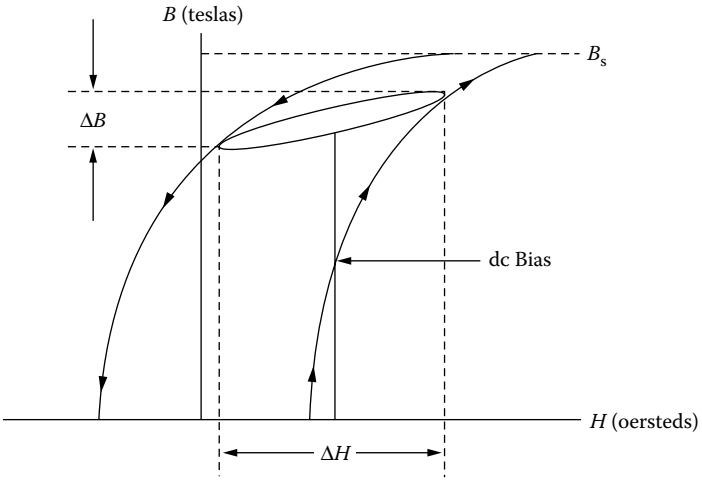

Figure 1-21. Incremental Permeability.

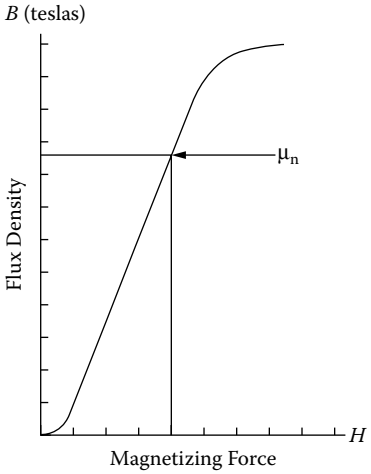

Figure 1-22. Normal Permeability.

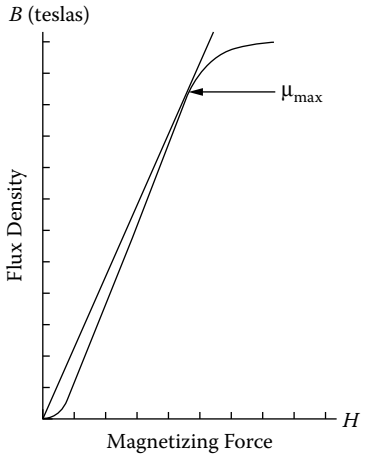

Figure 1-23. Maximum Permeability.

© 2011 by Taylor and Francis Group, LLC

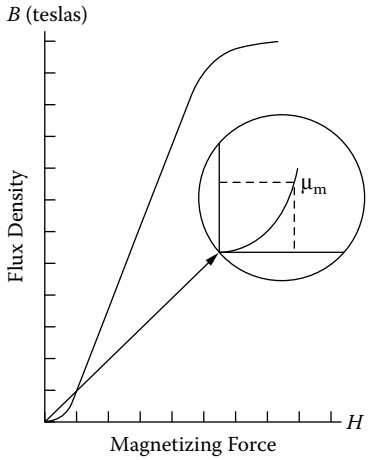

Figure 1-24. Material Permeability.

Magnetomotive Force (mmf) and Magnetizing Force (H)

There are two force functions commonly encountered in magnetics: magnetomotive force, mmf, and magnetizing force, H. Magnetomotive force should not be confused with magnetizing force; the two are related as cause and effect. Magnetomotive force is given by the Equation [1-6].

$$\text{mmf} = 0.4\pi\, NI, \quad [\text{gilberts}] \tag{1-6}$$

N is the number of turns and I is the current in amperes. Whereas mmf is the force, H is a force field, or force per unit length, as shown in Equation [1-7].

$$H = \frac{\text{mmf}}{\text{MPL}}, \quad \left[\frac{\text{gilberts}}{\text{cm}} = \text{oersteds}\right] \tag{1-7}$$

Substituting,

$$H = \frac{0.4\pi\, NI}{\text{MPL}}, \quad [\text{oersteds}] \tag{1-8}$$

MPL = Magnetic Path Length in cm.

If the flux is divided by the core area, A_c, we get flux density, B, in lines per unit area, as shown in Equation [1-9].

$$B = \frac{\phi}{A_c}, \quad [\text{gauss}] \tag{1-9}$$

The flux density, B, in a magnetic medium, due to the existence of a magnetizing force H, depends on the permeability of the medium and the intensity of the magnetic field, as shown in Equation [1-10].

$$B = \mu\, H, \quad [\text{gauss}] \tag{1-10}$$

© 2011 by Taylor and Francis Group, LLC

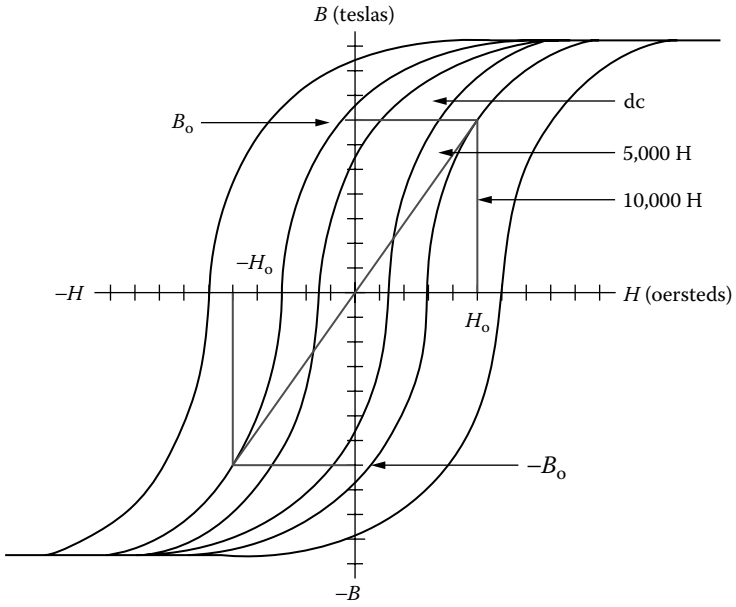

Figure 1-25. Typical B-H Loops Operating at Various Frequencies.

The peak magnetizing current, I_m, for a wound core can be calculated from the following Equation [1-11].

$$I_m = \frac{H_o(MPL)}{0.4\pi N}, \quad \text{[amps]} \qquad \text{[1-11]}$$

H_o is the field intensity at the peak operating point. To determine the magnetizing force, H_o, use the manufacturer's core loss curves at the appropriate frequency and operating flux density, B_o, as shown in Figure 1-25.

Reluctance

The flux produced in a given material by magnetomotive force (mmf) depends on the material's resistance to flux, which is called reluctance, R_m. The reluctance of a core depends on the composition of the material and its physical dimension and is similar in concept to electrical resistance. The relationship between mmf, flux, and magnetic reluctance is analogous to the relationship between emf, current, and resistance, as shown in Figure 1-26.

$$\begin{aligned} emf\ (E) &= IR = \text{ Current x Resistance} \\ mmf\ (F_m) &= \Phi R_m = \text{ Flux x Reluctance} \end{aligned} \qquad \text{[1-12]}$$

A poor conductor of flux has a high magnetic resistance, R_m. The greater the reluctance, the higher the magnetomotive force that is required to obtain a given magnetic field.

© 2011 by Taylor and Francis Group, LLC

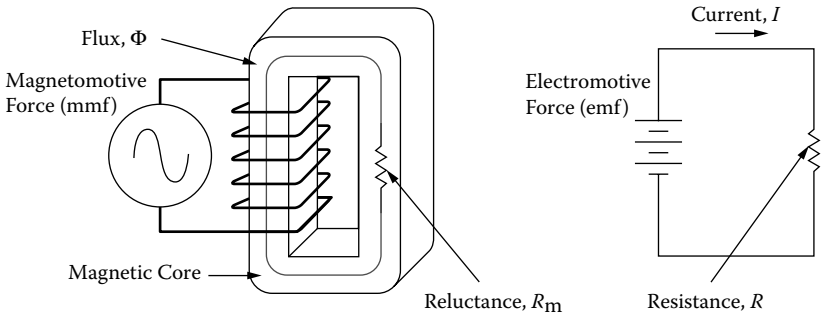

Figure 1-26. Comparing Magnetic Reluctance and Electrical Resistance.

The electrical resistance of a conductor is related to its length l, cross-sectional area A_w, and specific resistance ρ, which is the resistance per unit length. To find the resistance of a copper wire of any size or length, we merely multiply the resistivity by the length, and divide by the cross-sectional area, as shown in Equation [1-13].

$$R = \frac{\rho l}{A_w}, \quad \text{[ohms]} \tag{1-13}$$

In the case of magnetics, 1/μ is analogous to ρ and is called reluctivity. The reluctance, R_m, of a magnetic circuit, is shown in Equation [1-14].

$$R_m = \frac{\text{MPL}}{\mu_r \mu_o A_c} \tag{1-14}$$

Where MPL, is the magnetic path length, cm.

A_c is the cross-section of the core, cm^2.

μ_r is the permeability of the magnetic material.

μ_o is the permeability of air.

A typical magnetic core is shown in Figure 1-27, illustrating the Magnetic Path Length (MPL) and the cross-sectional area, A_c, of a C core.

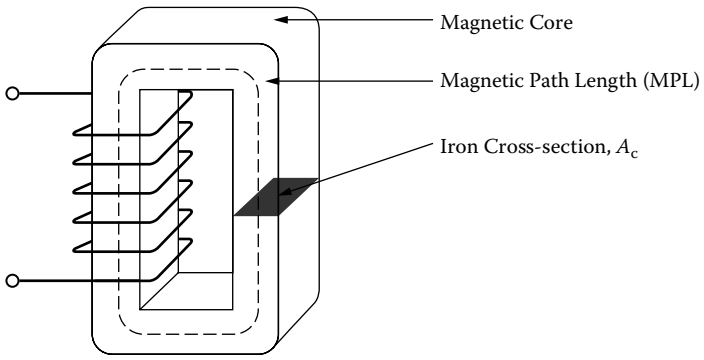

Figure 1-27. Magnetic Core Showing the Magnetic Path Length (MPL) and Iron Cross-section, A_c.

© 2011 by Taylor and Francis Group, LLC

Air Gap

A high permeability material is one that has a low reluctance for a given magnetic path length (MPL) and iron cross-section, A_c. If an air gap is included in a magnetic circuit, as shown in Figure 1-28, which is otherwise composed of low reluctivity material like iron, almost all of the reluctance in the circuit will be at the gap. The reason for this is because the reluctivity of air is much greater than that of a magnetic material. For all practical purposes, controlling the size of the air gap controls the reluctance.

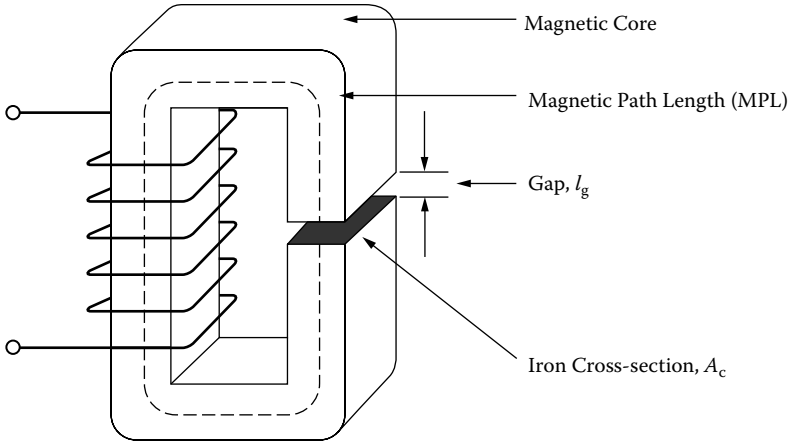

Figure 1-28. A Typical Magnetic Core with an Air Gap.

An example can best show this procedure. The total reluctance of the core is the sum of the iron reluctance and the air gap reluctance, in the same way that two series resistors are added in an electrical circuit. The equation for calculating the air gap reluctance, R_g, is basically the same as the equation for calculating the reluctance of the magnetic material, R_m. The difference is that the permeability of air is 1 and the gap length, l_g, is used in place of the Magnetic Path Length (MPL). The equation is shown in Equation [1-15].

$$R_g = \left(\frac{1}{\mu_o}\right)\left(\frac{l_g}{A_c}\right) \qquad [1\text{-}15]$$

But, since $\mu_o = 1$, the Equation simplifies to:

$$R_g = \frac{l_g}{A_c} \qquad [1\text{-}16]$$

Where:

l_g = the gap length, cm.

A_c = the cross-section of the core, cm^2.

μ_o = the permeability of air.

The total reluctance, R_{mt}, for the core shown in Figure 1-28 is therefore:

© 2011 by Taylor and Francis Group, LLC

$$R_{mt} = R_m + R_g$$
$$R_{mt} = \frac{MPL}{\mu_r \mu_o A_c} + \frac{l_g}{\mu_o A_c} \quad [1\text{-}17]$$

Where μ_r is the relative permeability, which is used exclusively with magnetic materials.

$$\mu_r = \frac{\mu}{\mu_o} = \frac{B}{\mu_o H}, \quad \left[\frac{\text{gauss}}{\text{oersteds}}\right] \quad [1\text{-}18]$$

The magnetic material permeability, μ_m, is given by:

$$\mu_m = \mu_r \mu_o \quad [1\text{-}19]$$

The reluctance of the gap is higher than that of the iron even when the gap is small. The reason is because the magnetic material has a relatively high permeability, as shown in Table 1-1. So the total reluctance of the circuit depends more on the gap than on the iron.

Table 1-1. Material Permeability

Material Permeability, μ_m	
Material Name	Permeability
Iron Alloys	0.8K to 25K
Ferrites	0.8K to 20K
Amorphous	0.8K to 80K

After the total reluctance, R_t, has been calculated, the effective permeability, μ_e, can be calculated.

$$R_{mt} = \frac{l_t}{\mu_e A_c},$$
$$l_t = l_g + \text{MPL} \quad [1\text{-}20]$$

Where l_t is the total path length and μ_e is the effective permeability.

$$R_{mt} = \frac{l_t}{\mu_e A_c} = \frac{l_g}{\mu_o A_c} + \frac{\text{MPL}}{\mu_o \mu_r A_c} \quad [1\text{-}21]$$

Simplifying yields:

$$\frac{l_t}{\mu_e} = \frac{l_g}{\mu_o} + \frac{\text{MPL}}{\mu_o \mu_r} \quad [1\text{-}22]$$

Then:

$$\mu_e = \frac{l_t}{\frac{l_g}{\mu_o} + \frac{\text{MPL}}{\mu_o \mu_r}}$$
$$\mu_e = \frac{l_g + \text{MPL}}{\frac{l_g}{\mu_o} + \frac{\text{MPL}}{\mu_o \mu_r}} \quad [1\text{-}23]$$

© 2011 by Taylor and Francis Group, LLC

If $l_g \ll$ MPL, multiply both sides of the equation by $(\mu_r\mu_o \text{ MPL})/(\mu_r\mu_o \text{ MPL})$.

$$\mu_e = \frac{\mu_o \mu_r}{1 + \mu_r\left(\frac{l_g}{\text{MPL}}\right)} \quad [1\text{-}24]$$

The classic equation is:

$$\mu_e = \frac{\mu_m}{1 + \mu_m\left(\frac{l_g}{\text{MPL}}\right)} \quad [1\text{-}25]$$

Introducing an air gap, l_g, to the core cannot correct for the dc flux, but can sustain the dc flux. As the gap is increased, so is the reluctance. For a given magnetomotive force, the flux density is controlled by the gap.

Controlling the dc Flux with an Air Gap

There are two similar equations used to calculate the dc flux. The first equation is used with powder cores. Powder cores are manufactured from very fine particles of magnetic materials. This powder is coated with an inert insulation to minimize eddy currents losses and to introduce a distributed air gap into the core structure.

$$\mu_r = \mu_e$$
$$B_{dc} = (\mu_r)\left(\frac{0.4\pi NI}{\text{MPL}}\right), \quad \text{[gauss]} \quad [1\text{-}26]$$
$$\mu_r = \frac{\mu_m}{1 + \mu_m\left(\frac{l_g}{\text{MPL}}\right)}$$

The second equation is used, when the design calls for a gap to be placed in series with the Magnetic Path Length (MPL), such as a ferrite cut core, a C core, or butt-stacked laminations.

$$\mu_r = \mu_e$$
$$B_{dc} = (\mu_r)\left(\frac{0.4\pi NI}{\text{MPL}}\right), \quad \text{[gauss]} \quad [1\text{-}27]$$

Substitute $(\text{MPL}\mu_m)$ /$(\text{MPL}\mu_m)$ for 1:

$$\mu_r = \frac{\mu_m}{1 + \mu_m\left(\frac{l_g}{\text{MPL}}\right)} = \frac{\mu_m}{\frac{\text{MPL}\mu_m}{\text{MPL}\mu_m} + \mu_m\left(\frac{l_g}{\text{MPL}}\right)} \quad [1\text{-}28]$$

© 2011 by Taylor and Francis Group, LLC

Then, simplify:

$$\mu_r = \frac{\text{MPL}}{\frac{\text{MPL}}{\mu_m} + l_g} \quad [1\text{-}29]$$

$$B_{dc} = \left(\frac{\text{MPL}}{\frac{\text{MPL}}{\mu_m} + l_g} \right) \left(\frac{0.4\pi NI}{\text{MPL}} \right), \quad \text{[gauss]} \quad [1\text{-}30]$$

Then, simplify:

$$B_{dc} = \frac{0.4\pi NI}{l_g + \frac{\text{MPL}}{\mu_m}}, \quad \text{[gauss]} \quad [1\text{-}31]$$

Types of Air Gaps

Basically, there are two types of gaps used in the design of magnetic components: bulk and distributed. Bulk gaps are maintained with materials, such as paper, Mylar, or even glass. The gapping materials are designed to be inserted in series with the magnetic path to increase the reluctance, R, as shown in Figure 1-29.

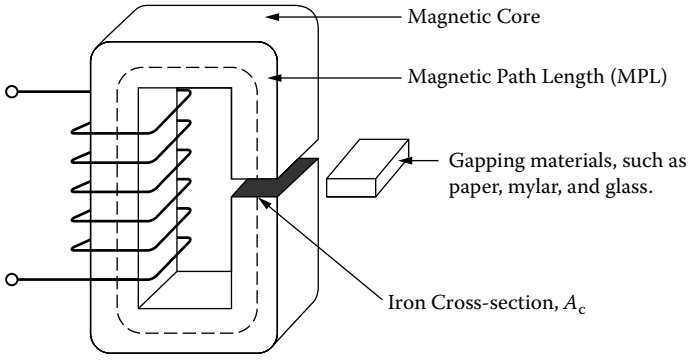

Figure 1-29. Placement of the Gapping Materials.

Placement of the gapping material is critical in keeping the core structurally balanced. If the gap is not proportioned in each leg, then the core will become unbalanced and create even more than the required gap. There are designs where it is important to place the gap in an area to minimize the noise that is caused by the fringing flux at the gap. The gap placement for different core configurations is shown in Figure 1-30. The standard gap placement is shown in Figure 1-30A, C, and D. The EE or EC cores shown in Figure 1-30B, are best-suited, when the gap has to be isolated within the magnetic assembly to minimize fringing flux noise. When the gap is used as shown in Figure 1-30A, C, and D, then, only half the thickness of the calculated gap dimension is used in each leg of the core.

© 2011 by Taylor and Francis Group, LLC

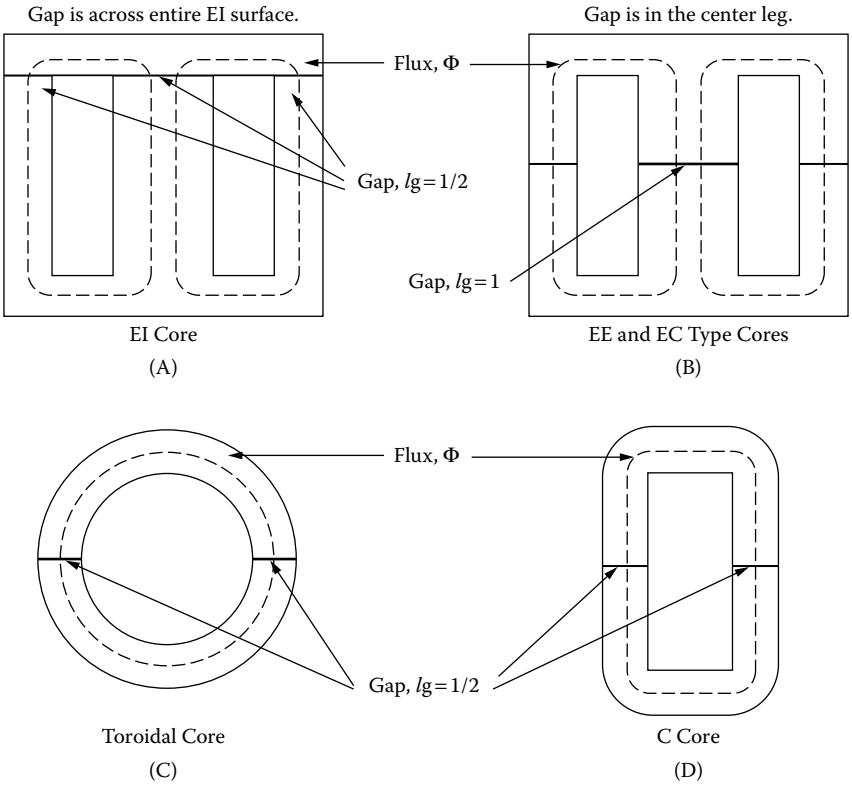

Figure 1-30. Gap Placement using Different Core Configurations.

Fringing Flux

Introduction

Fringing flux has been around since time began for the power conversion engineer. Designing power conversion magnetics that produce a minimum of fringing flux has always been a problem. Engineers have learned to design around fringing flux, and minimize its effects. It seems that when engineers do have a problem, it is usually at the time when the design is finished and ready to go. It is then that the engineer will observe something that was not recognized before. This happens during the final test when the unit becomes unstable, the inductor current is nonlinear, or the engineer just located a hot spot during testing. Fringing flux can cause a multitude of problems. Fringing flux can reduce the overall efficiency of the converter, by generating eddy currents that cause localized heating in the windings and/or the brackets. When designing inductors, fringing flux must to be taken into consideration. If the fringing flux is not handled correctly, there will be premature core saturation. More and more magnetic components are now designed to operate in the sub-megahertz region. High frequency has really brought out the fringing flux and its parasitic eddy currents. Operating at high frequency has made the engineer very much aware of what fringing flux can do to hamper a design.

© 2011 by Taylor and Francis Group, LLC

Material Permeability, (μ_m)

The B-H loops that are normally seen in the manufacturers' catalogs are usually taken from a toroidal sample of the magnetic material. The toroidal core, without a gap, is the ideal shape to view the B-H loop of a given material. The material permeability, u_m, will be seen at its highest in the toroidal shape, as shown in Figure 1-31.

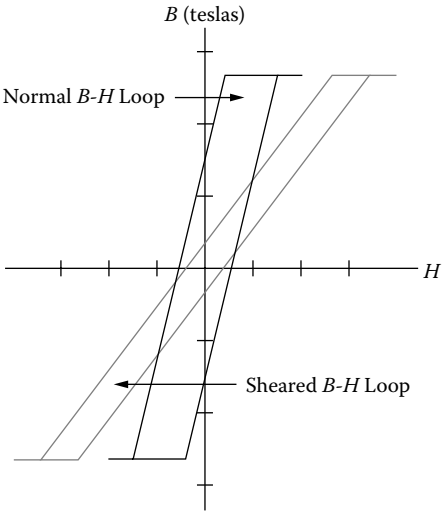

Figure 1-31. The Shearing of an Idealized B-H Loop due to an Air Gap.

A small amount of air gap, less than 25 microns, has a powerful effect by shearing over the B-H loop. This shearing over of the B-H loop reduces the permeability. High permeability ferrites that are cut, like E cores, have only about 80 percent of the permeability, than that of a toroid of the same material. This is because of the induced gap, even though the mating surfaces are highly polished. In general, magnetic materials with high-permeability, are sensitive to temperature, pressure, exciting voltage, and frequency. The inductance change is directly proportional to the permeability change. This change in inductance will have an effect on the exciting current. It is very easy to see, that inductors that are designed into an LC, tuned circuit, must have a stable permeability, u_e.

$$L = \frac{0.4\pi N^2 A_c \Delta\mu\left(10^{-8}\right)}{\text{MPL}}, \quad \text{[henrys]} \qquad \text{[1-32]}$$

Air Gaps

Air gaps are introduced into magnetic cores for a variety of reasons. In a transformer design a small air gap, l_g, inserted into the magnetic path, will lower and stabilize the effective permeability, μ_e.

© 2011 by Taylor and Francis Group, LLC

$$\mu_e = \frac{\mu_m}{1 + \mu_m \left(\frac{l_g}{\text{MPL}} \right)} \qquad [1\text{-}33]$$

This will result in a tighter control of the permeability change with temperature, and exciting voltage. Inductor designs will normally require a large air gap, l_g, to handle the dc flux.

$$l_g = \frac{0.4\pi N I_{dc} \left(10^{-4}\right)}{B_{dc}}, \quad [\text{cm}] \qquad [1\text{-}34]$$

Whenever an air gap is inserted into the magnetic path, as shown in Figure 1-32, there is an induced, fringing flux at the gap.

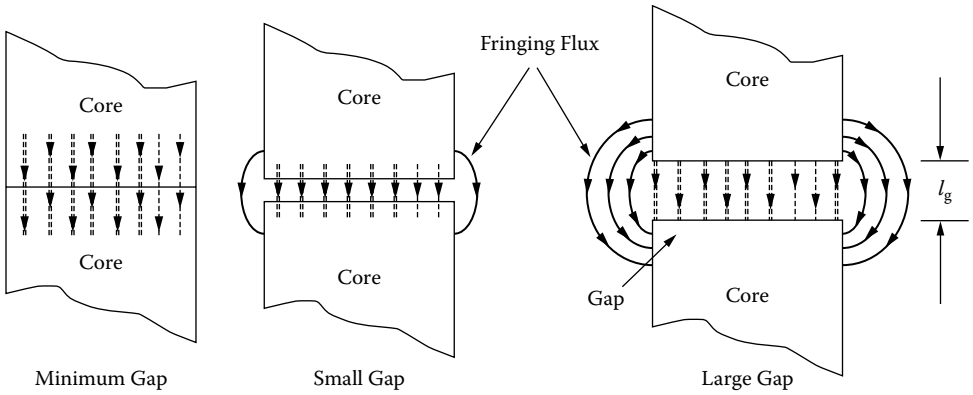

Figure 1-32. Fringing Flux at the Gap.

The fringing flux effect is a function of gap dimension, the shape of the pole faces, and the shape, size, and location of the winding. Its net effect is to shorten the air gap. Fringing flux decreases the total reluctance of the magnetic path and, therefore, increases the inductance by a factor, F, to a value greater than the one calculated.

Fringing Flux, F

Fringing flux is completely around the gap and re-enters the core in a direction of high loss, as shown in Figure 1-33. Accurate prediction of gap loss, P_g, created by fringing flux is very difficult to calculate.

This area around the gap is very sensitive to metal objects, such as clamps, brackets and banding materials. The sensitivity is dependent on the intensity of the magnetomotive force, gap dimensions and the operating frequency. If a metal bracket or banding material is used to secure the core, and it passes over the gap, two things can happen: (1) If the material ferromagnetic is placed over the gap, or is in close proximity so it conducts the magnetic field, this is called “shorting the gap.” Shorting the gap is the same as reducing the gap

© 2011 by Taylor and Francis Group, LLC

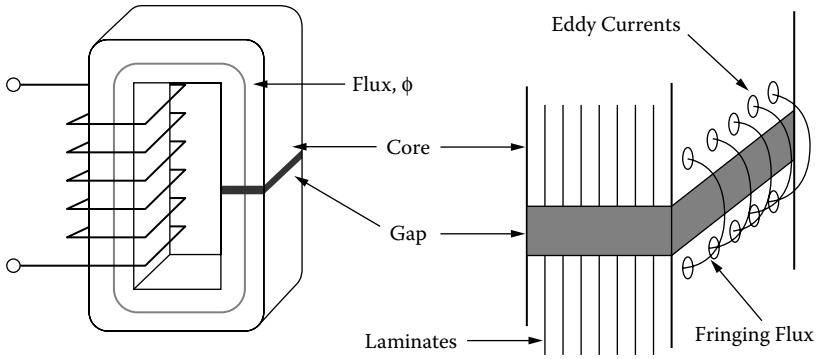

Figure 1-33. Fringing Flux, with High Loss Eddy Currents.

dimension, thereby producing a higher inductance, than designed, and could drive the core into saturation. (2) If the material is metallic, (such as copper, or phosphor bronze), but not ferromagnetic, it will not short the gap or change the inductance. In both cases, if the fringing flux is strong enough, it will induce eddy currents that will cause localized heating. This is the same principle used in induction heating.

Gapped, dc Inductor Design

The fringing flux factor, F, has an impact on the basic inductor design equations. When the engineer starts a design, he or she must determine the maximum values for B_{dc} and for B_{ac}, which will not produce magnetic saturation. The magnetic material that has been selected will dictate the saturation flux density. The basic equation for maximum flux density is:

$$B_{\max} = \frac{0.4\pi N\left(I_{dc} + \dfrac{\Delta I}{2}\right)\left(10^{-4}\right)}{l_g + \dfrac{\text{MPL}}{\mu_{\text{m}}}}, \quad \text{[teslas]} \qquad \text{[1-35]}$$

The inductance of an iron-core inductor, carrying dc and having an air gap, may be expressed as:

$$L = \frac{0.4\pi N^2 A_c\left(10^{-8}\right)}{l_g + \dfrac{\text{MPL}}{\mu_m}}, \quad \text{[henrys]} \qquad \text{[1-36]}$$

The inductance is dependent on the effective length of the magnetic path, which is the sum of the air gap length, l_g, and the ratio of the core magnetic path length to the material permeability, (MPL/u_m). The final determination of the air gap size requires consideration of the fringing flux effect which is a function of the gap dimension, the shape of the pole faces, and the shape, size, and location of the winding. The winding length, or the G dimension of the core, has a big influence on the fringing flux. See, Figure 1-34 and Equation 1-37.

© 2011 by Taylor and Francis Group, LLC

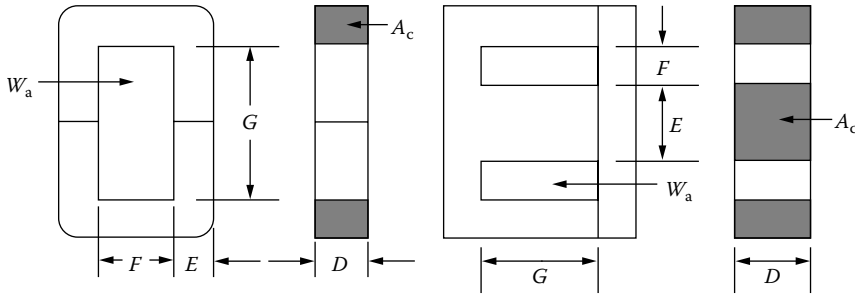

Figure 1-34. Dimensional, Call Out for C and E Cores.

The fringing flux decreases the total reluctance of the Magnetic Path Length and, therefore, increases the inductance by a factor of F to a value greater than that calculated. The fringing flux factor is:

$$F = \left(1 + \frac{l_g}{\sqrt{A_c}} \ln \frac{2G}{l_g}\right) \qquad [1\text{-}37]$$

After the inductance has been calculated using Equation 1-36, the fringing flux factor has to be incorporated into Equation 1-36. Equation 1-36 can now be rewritten to include the fringing flux factor, as shown in Equation 1-38

$$L = F\left(\frac{0.4\pi N^2 A_c \left(10^{-8}\right)}{l_g + \dfrac{\text{MPL}}{\mu_m}}\right), \quad \text{[henrys]} \qquad [1\text{-}38]$$

The fringing flux factor, F, can now be included into Equation 1-35. This will check for premature, core saturation.

$$B_{\max} = F\left(\frac{0.4\pi N\left(I_{dc} + \dfrac{\Delta I}{2}\right)\left(10^{-4}\right)}{l_g + \dfrac{\text{MPL}}{\mu_m}}\right), \quad \text{[teslas]} \qquad [1\text{-}39]$$

Now that the fringing flux factor, F, is known and inserted into Equation 1-38. Equation 1-38 can be rewritten to solve for the required turns so that premature core saturation will not happen, as shown in Equation 1-40.

$$N = \sqrt{\frac{L\left(l_g + \dfrac{\text{MPL}}{\mu_m}\right)}{0.4\pi A_c F\left(10^{-8}\right)}}, \quad \text{[turns]} \qquad [1\text{-}40]$$

Fringing Flux and Coil Proximity

As the air gap increases, the fringing flux will increase. Fringing flux will fringe out away from the gap by the distance of the gap. If a coil was wound tightly around the core and encompasses the gap, the flux generated

© 2011 by Taylor and Francis Group, LLC

around the magnet wire will force the fringing flux back into the core. The end result will not produce any fringing flux at all, as shown in Figure 1-35. As the coil distance moves away from the core, the fringing flux will increase until the coil distance from the core is equal to the gap dimension.

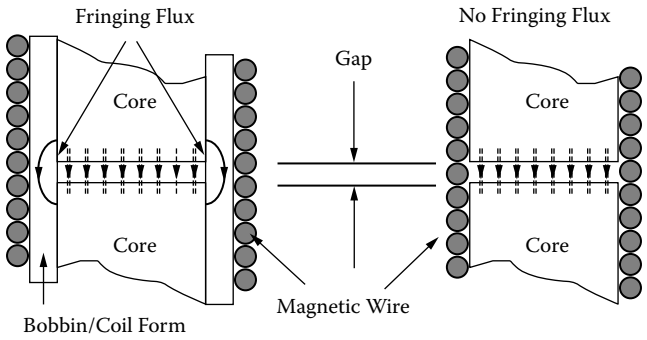

Figure 1-35. Comparing a Tightly-Wound Coil, and a Coil Wound on a Coil Form.

Fringing Flux, Crowding

Flux will always take the path of highest permeability. This can best be seen in transformers with interleaved laminations. The flux will traverse along the lamination until it meets its mating, I or E. At this point, the flux will jump to the adjacent lamination and bypass the mating point, as shown in Figure 1-36.

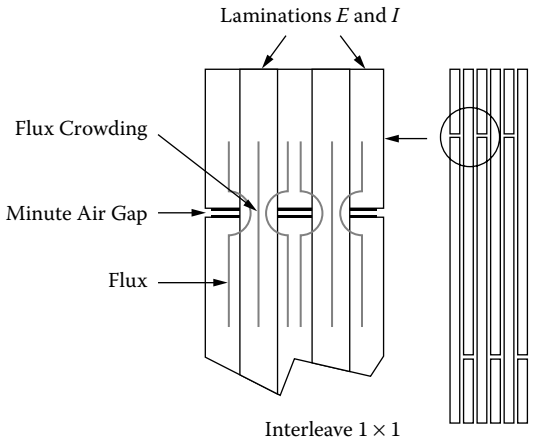

Figure 1-36. Flux Crowding in Adjacent Laminations.

This phenomena can best be seen by observing the exciting current at low, medium and high flux levels, as shown in Figure 1-37. At low levels of excitation, the exciting current is almost square, due to the flux taking the high permeability path, by jumping to the adjacent lamination, as shown in Figure 1-36. As the excitation is increased, the adjoining lamination will start to saturate, and the exciting current will increase and become nonlinear. When the adjacent lamination approaches saturation, the permeability drops. It is then that the flux will go in a straight line and cross the minute air gap, as shown in Figure 1-36.

© 2011 by Taylor and Francis Group, LLC

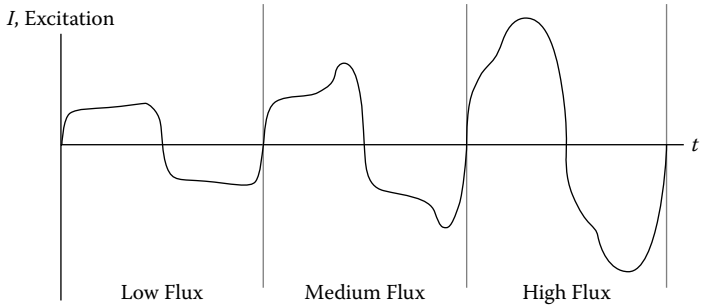

Figure 1-37. Exciting Current, at Different Levels of Flux Density, B.

Fringing Flux and Powder Cores

Designing high frequency converters, using low permeability powder cores, will usually require very few turns. Low perm power cores (less than 60), exhibit fringing flux. Powder cores with a distributed gap will have fringing flux that shorts the gap and gives the impression of a core with a higher permeability. Because of the fringing flux and a few turns, it is very important to wind uniformly and in a consistent manner. This winding is done to control the fringing flux and get inductance repeatability from one core to another, as shown in Figures 1-38 and 1-39.

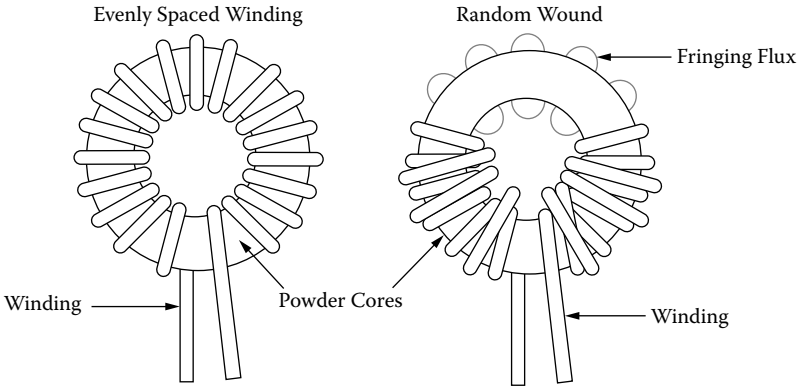

Figure 1-38. Comparing Toroidal, Winding Methods.

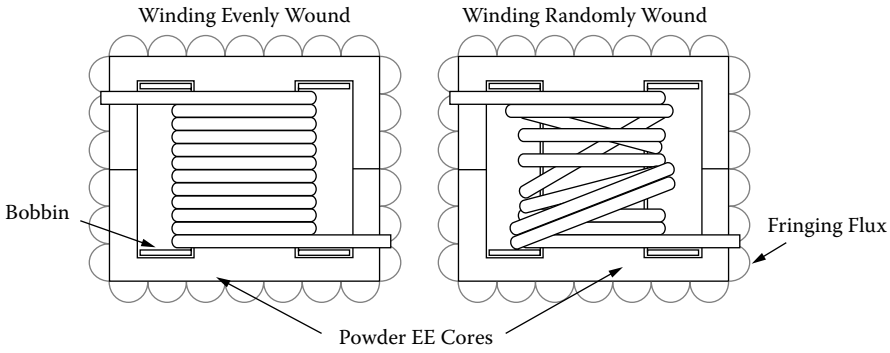

Figure 1-39. Comparing EE Cores, Winding Methods.

© 2011 by Taylor and Francis Group, LLC

Chapter 2

Magnetic Materials and Their Characteristics

© 2011 by Taylor and Francis Group, LLC

Table of Contents

1. Introduction....2-3
2. Saturation....2-3
3. Remanence Flux, B_r, and Coercivity H_c....2-4
4. Permeability, μ....2-4
5. Hysteresis Loss, Resistivity, ρ, (core loss)....2-4
6. Introduction to Silicon Steel....2-5
7. Introduction to Thin Tape Nickel Alloys....2-5
8. Introduction to Metallic Glass....2-9
9. Introduction to Soft Ferrites....2-12
10. Manganese-Zinc Ferrites....2-13
11. Nickel-Zinc Ferrites....2-13
12. Ferrite Cross Reference....2-16
13. Introduction to Molypermalloy Powder Cores....2-17
14. Introduction to Iron Powder Cores....2-17
15. Core Loss....2-24
16. Core Loss Equations....2-25
17. Selection of Magnetic Materials....2-29
18. Typical Operation....2-29
19. Material Characteristics....2-30
20. Magnetic Material Saturation Defined....2-33
21. Test Conditions....2-36
22. Magnetic Material Saturation Theory....2-41
23. Air Gap Effect....2-42
24. Effect of Gapping....2-42
25. Composite Core Configuration....2-50
26. Summary....2-53

© 2011 by Taylor and Francis Group, LLC

Introduction

The magnetic material is the paramount player in the design of magnetic components. The magnetics design engineer has three standard words when making the normal design trade-off study: cost, size, and performance. He will be happy to stuff any two into the bag. The magnetics engineer is now designing magnetic components that operate from below the audio range to the megahertz range. He is normally asked to design for maximum performance, with the minimum of his parasitic friends' capacitance and leakage inductance. Today, the magnetic materials the engineer has to work with are silicon steel, nickel iron (permalloy), cobalt iron (permendur), amorphous metallic alloys, and ferrites. These also have spin-off material variants, such as moly-permalloy powder, sendust powder, and iron powder cores. From this group of magnetic materials, the engineer will make trade-offs with the magnetic properties for his design. These properties are: saturation, B_s, permeability, μ, resistivity, ρ (core loss), remanence, B_r, and coercivity, H_c.

Saturation

A typical hysteresis loop of a soft magnetic material is shown in Figure 2-1. When a high magnetizing force is encountered, a point is reached where further increase in, H, does not cause useful increase in, B. This point is known as the saturation point of that material. The saturation flux density, B_s, and the required magnetizing force, H_s, to saturate the core are shown with dashed lines.

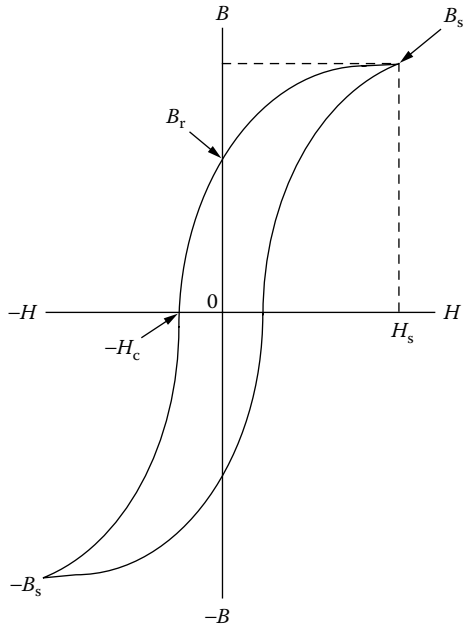

Figure 2-1. Typical B-H or Hysteresis Loop of a Soft Magnetic Material.

© 2011 by Taylor and Francis Group, LLC

Remanence Flux, B_r, and Coercivity H_c

In Figure 2-1 the hysteresis loop clearly shows the remanence flux density, B_r. The remanence flux is the polarized flux remaining in the core after the excitation has been removed. The magnetizing force, $-H_c$, is called coercivity. It is the amount of magnetizing force required to bring the remanence flux density back to zero.

Permeability, μ

The permeability of a magnetic material is a measure of the ease in magnetizing the material. Permeability, μ, is the ratio of the flux density, B, to the magnetizing force, H, as shown in Equation [2-1].

$$\mu = \frac{B}{H}, \quad \text{[permeability]} \qquad [2\text{-}1]$$

The relationship between B and H is not linear, as shown in the hysteresis loop in Figure 2-1. Then, it is evident that the ratio, B/H, (permeability), also varies. The variation of permeability with flux density, B, is shown in Figure 2-2. Also, it shows the flux density at which the permeability is at a maximum.

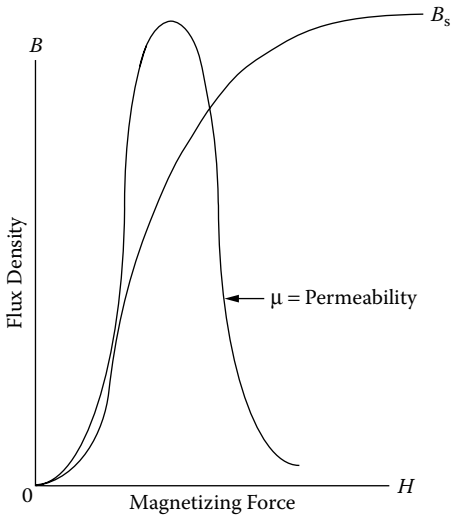

Figure 2-2. Variation in Permeability μ with B and H.

Hysteresis Loss, Resistivity, ρ, (core loss)

The enclosed area within the hysteresis, shown in Figure 2-1, is a measure of the energy lost in the core material during that cycle. This loss is made up in two components: (1) the hysteresis loss and (2) eddy current loss. The hysteresis loss is the energy loss when the magnetic material is going through a cycling state. The

© 2011 by Taylor and Francis Group, LLC

eddy current loss is caused when the lines of flux pass through the core, inducing electrical currents in it. These currents are called eddy currents and produce heat in the core. If the electrical resistance of the core is high, the current will be low; therefore, a feature of low-loss material is high electrical resistance. In the norm, when designing magnetic components, the core loss is a major design factor. Core loss can be controlled by selecting the right material and thickness. Selecting the correct material, and operating within its limits, will prevent overheating that could result in damage to the wire insulation and/or the potting compound.

Introduction to Silicon Steel

Silicon steel was one of the first alloys to be used in transformers and inductors. It has been greatly improved over the years and is probably, pound for pound, the most widely used magnetic material. One of the drawbacks in using steel in the early years was, as the material became older, the losses would increase. With the addition of silicon to the steel, the advantages were twofold: it increased the electrical resistivity, therefore reducing the eddy current losses, and it also improved the material's stability with age.

Silicon steel offers high saturation flux density, a relatively good permeability at high flux density, and a moderate loss at audio frequency. One of the important improvements made to the silicon steel was in the process called cold-rolled, grain-oriented, AISI type M6. This M6 grain-oriented steel has exceptionally low losses and high permeability. It is used in applications requiring high performance and the losses will be at a minimum.

Introduction to Thin Tape Nickel Alloys

High permeability metal alloys are based primarily on the nickel-iron system. Although Hopkinson investigated nickel-iron alloys as early as 1889, it was not until the studies by Elmen, starting in about 1913, on properties in weak magnetic fields and effects of heat-treatments, that the importance of the Ni-Fe alloys was realized. Elmen called his Ni-Fe alloys, "Permalloys," and his first patent was filed in 1916. His preferred composition was the 78Ni-Fe alloy. Shortly after Elmen, Yensen started an independent investigation that resulted in the 50Ni-50Fe alloy, "Hipernik," which has lower permeability and resistivity but higher saturation than the 78-Permalloy, (1.5 teslas compared to 0.75 teslas), making it more useful in power equipment.

Improvements in the Ni-Fe alloys were achieved by high temperature anneals in hydrogen atmosphere, as first reported by Yensen. The next improvement was done by using grain-oriented material and annealing it, in a magnetic field, which was also in a hydrogen atmosphere. Kelsall and Bozorth did this work. Using these two methods, a new material, called Supermalloy, was achieved. It has a higher permeability, a lower coercive force, and about the same flux density as 78-Permalloy. Perhaps the most important of these factors is the

© 2011 by Taylor and Francis Group, LLC

magnetic anneal, which, not only increases permeability, but also provides a "square" magnetization curve, important in high frequency power conversion equipment.

In order to obtain high resistance, and therefore lower core losses for high frequency applications, two approaches have been followed: (1) modification of the shape of metallic alloys and (2) development of magnetic oxides. The result was the development of thin tapes and powdered alloys in the 1920's, and thin films in the 1950's. The development of thin film has been spurred by the requirements of aerospace, power conversion electronics from the mid 1960's to the present.

The Ni-Fe alloys are available in thicknesses of 2 mil, 1 mil, 0.5 mil, 0.25 and 0.125 mil. The material comes with a round or square B-H loop. This gives the engineer a wide range of sizes and configurations from which to select for a design. The iron alloy properties for some of the most popular materials are shown in Table 2-1. Also, given in Table 2-1, is the Figure number for the B-H loop of each of the magnetic materials.

Table 2-1. Magnetic Properties for Selected Iron Alloys Materials

Iron Alloy Material Properties								
Material Name	Composition	Initial Permeability μ_i	Flux Density Teslas B_s	Curie Temp. °C	dc, Coercive Force, Hc Oersteds	Density grams/cm^3 δ	Weight Factor x	Typical B-H Loop Figures
Silicon	3% Si 97% Fe	1.5 K	1.5-1.8	750	0.4-0.6	7.63	1.000	(2-3)
Supermendur*	49% Co 49% Fe 2% V	0.8 K	1.9-2.2	940	0.15-0.35	8.15	1.068	(2-4)
Orthonol	50% Ni 50% Fe	2 K	1.42-1.58	500	0.1-0.2	8.24	1.080	(2-5)
Permalloy	79% Ni 17% Fe 4% Mo	12 K-100 K	0.66-0.82	460	0.02-0.04	8.73	1.144	(2-6)
Supermalloy	78% Ni 17% Fe 5% Mo	10 K-50 K	0.65-0.82	460	0.003-0.008	8.76	1.148	(2-7)
* Field Anneal. x Silicon has unity weight factor.								

© 2011 by Taylor and Francis Group, LLC

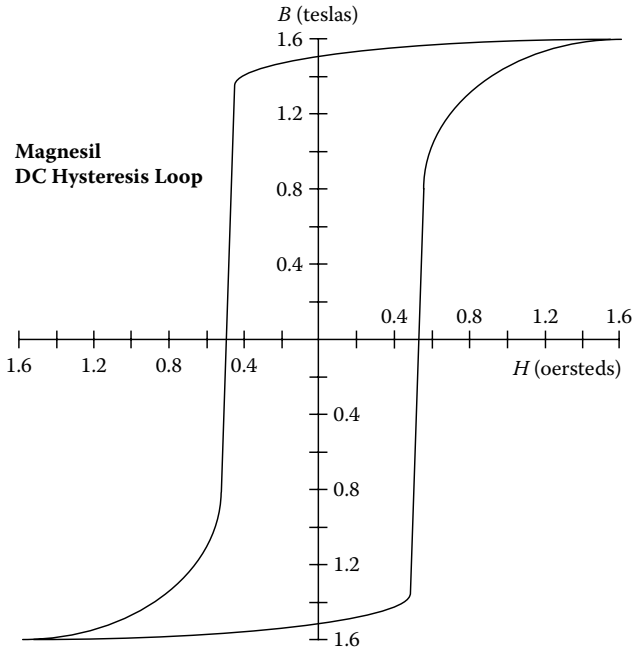

Figure 2-3. Silicon B-H Loop: 97% Fe 3% Si.

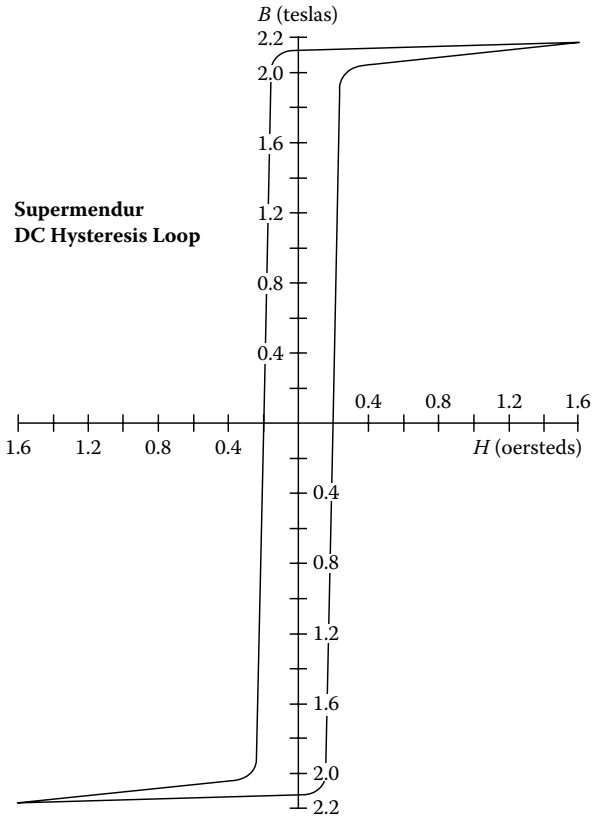

Figure 2-4. Supermendur B-H Loop: 49% Fe 49% Co 2% V.

© 2011 by Taylor and Francis Group, LLC

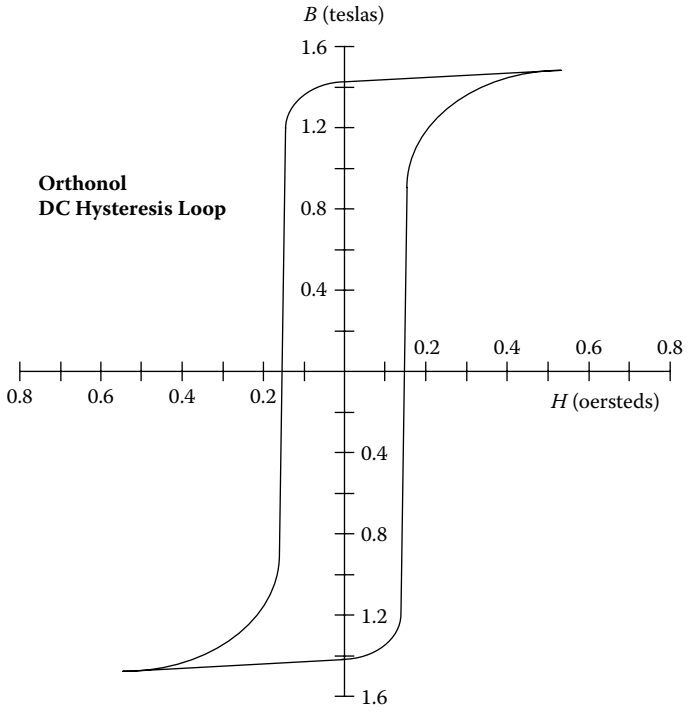

Figure 2-5. Orthonol B-H Loop: 50% Fe 50% Ni.

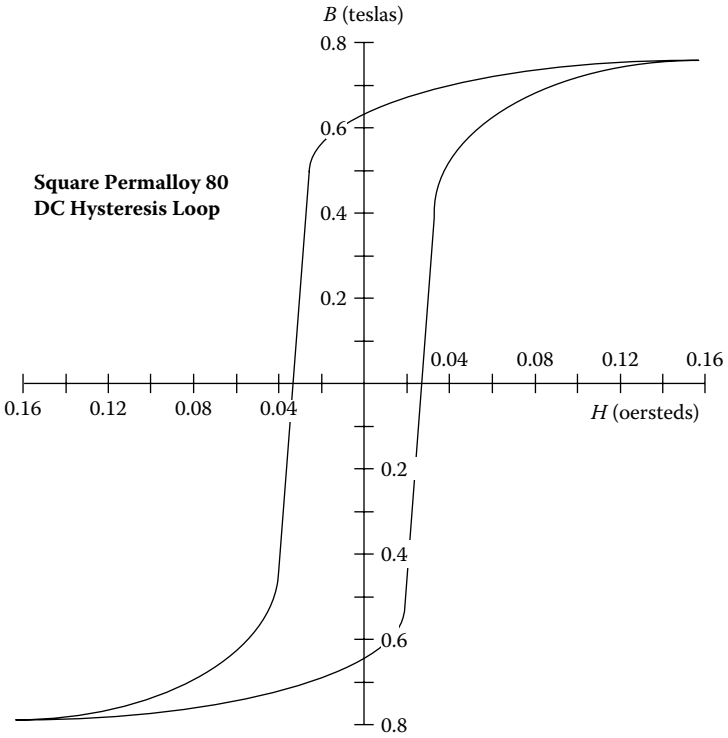

Figure 2-6. Square Permalloy 80 B-H Loop: 79% Ni 17% Fe 4% Mo.

© 2011 by Taylor and Francis Group, LLC

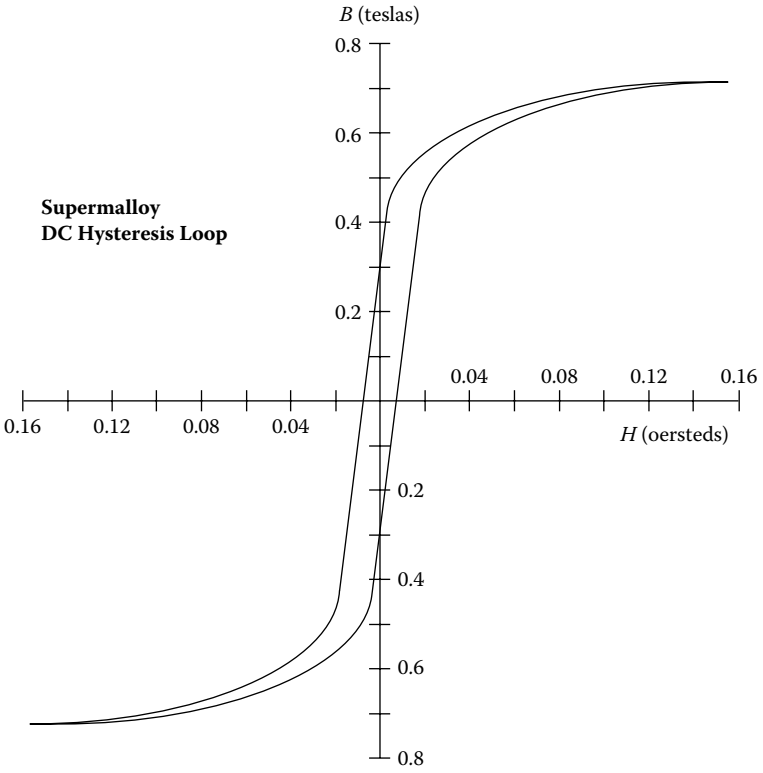

Figure 2-7. Supermalloy B-H Loop: 78% Ni 17% Fe 5% Mo.

Introduction to Metallic Glass

The first synthesis of a metallic glass drawing wide attention among material scientists, occurred in 1960. Klement, Willens and Duwez reported that a liquid, AuSi alloy, when rapidly quenched to liquid nitrogen temperature, would form an amorphous solid. It was twelve years later that Chen and Polk produced ferrous-based metallic glasses in useful shapes with significant ductility. Metallic glasses have since survived the transition from laboratory curiosities to useful products, and currently are the focus of intensive technological and fundamental studies.

Metallic glasses are generally produced, by liquid quenching, in which a molten metal alloy is rapidly cooled, at rates on the order of 10^5 degrees/sec., through the temperature at which crystallization normally occurs. The basic difference between crystalline (standard magnetic material) and glassy metals is in their atomic structures. Crystalline metals are composed of regular, three-dimensional arrays of atoms, which exhibit long-range order. Metallic glasses do not have long-range structural order. Despite their structural differences, crystalline and glassy metals of the same compositions exhibit nearly the same densities.

The electrical resistivities of metallic glasses are much larger, (up to three times higher), than those of crystalline metals of similar compositions. The magnitude of the electrical resistivities and their temperature coefficients in the glassy and liquid states are almost identical.

© 2011 by Taylor and Francis Group, LLC

Metallic glasses are quite soft magnetically. The term, "soft," refers to a large response of the magnetization to a small-applied field. A large magnetic response is desirable in such applications as transformers and inductors. The obvious advantages of these new materials are in high frequency applications with their high induction, high permeability, and low core loss.

There are four amorphous materials that have been used in high frequency applications: 2605SC, 2714A, 2714AF and Vitroperm 500F. Material 2605SC offers a unique combination of high resistivity, high saturation induction, and low core loss, making it suitable for designing high frequency dc inductors. Material 2714A is a cobalt material that offers a unique combination of high resistivity, high squareness ratio B_r/B_s, and very low core loss, making it suitable for designing high frequency aerospace transformers and mag-amps. The Vitroperm 500F is an iron based material with a saturation of 1.2 teslas and is well-suited for high frequency transformers and gapped inductors. The high frequency core loss for the nanocrystalline 500F is lower than some ferrite, even operating at a high flux density. The amorphous properties for some of the most popular materials are shown in Table 2-2. Also, given in Table 2-2, is the Figure number for the B-H loop of each of the magnetic materials.

Table 2-2. Magnetic Properties for Selected Amorphous Materials

Amorphous Material Properties								
Material Name	Major Composition	Initial Permeability μ_i	Flux Density Telsas B_s	Curie Temperature °C	dc, Coercive Force, Hc Oersteds	Density grams/cm^3 δ	Weight Factor x	Typical B-H Loop Figures
2605SC	81% Fe 13.5% B 3.5% Si	1.5K	1.5-1.6	370	0.4-0.6	7.32	0.957	(2-8)
2714A	66% Co 15% Si 4% Fe	0.8K	0.5-0.65	205	0.15-0.35	7.59	0.995	(2-9)
2714AF	66% Co 15% Si 4% Fe	2K	0.5-0.65	205	0.1-0.2	7.59	0.995	(2-10)
Nanocrystal Vitroperm 500F*	73.5% Fe 1% Cu 15.5% Si	30K-80K	1.0-1.2	460	0.02-0.04	7.73	1.013	(2.11)

* Vitroperm is the trademark of Vacuumschmelze.
x Silicon has a unity weight factor. See Table 2.1.

© 2011 by Taylor and Francis Group, LLC

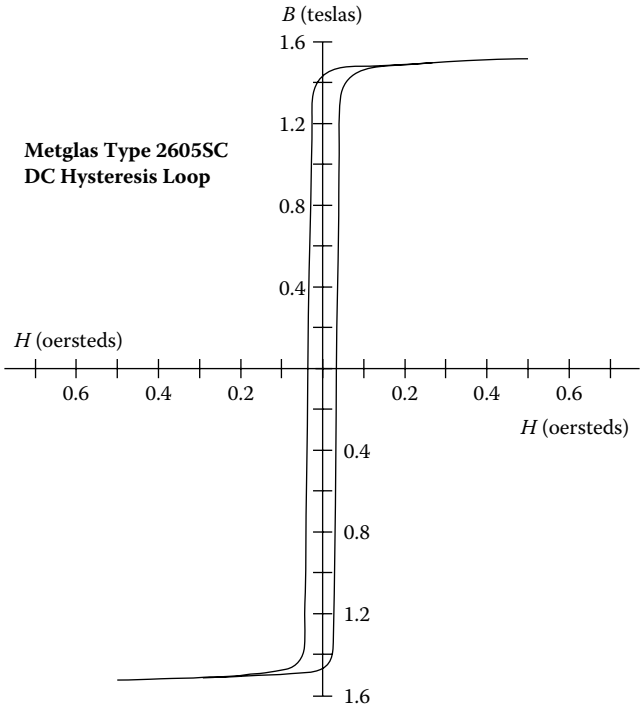

Figure 2-8. Amorphous 2605SC B-H Loop: 81% Fe 13.5% B 3.5% Si.

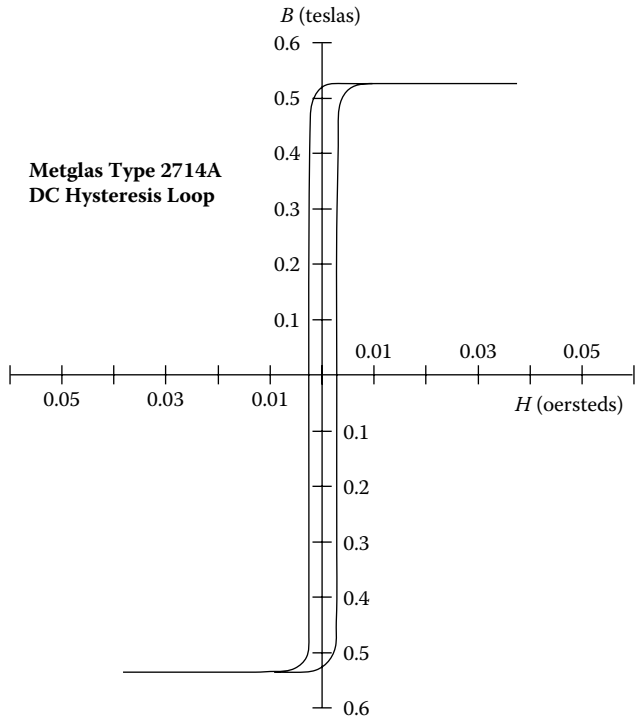

Figure 2-9. Amorphous 2714A B-H Loop: 66% Co 15% Si 4% Fe.

© 2011 by Taylor and Francis Group, LLC

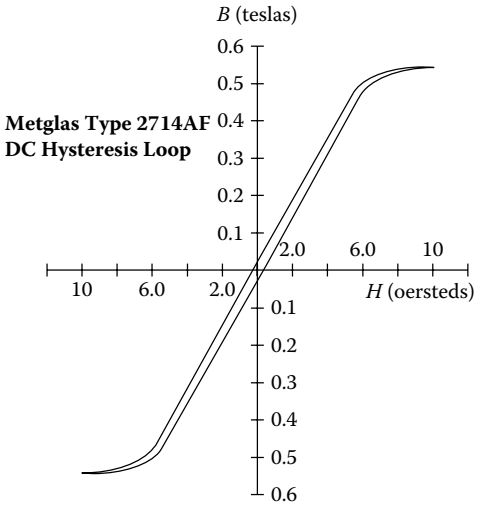

Figure 2-10. Amorphous 2714AF B-H Loop: 66% Co 15% Si 4% Fe.

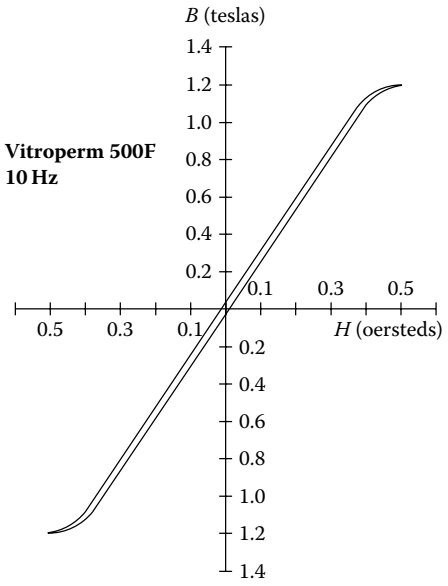

Figure 2-11. Vitroperm 500F B-H Loop: 73.5% Fe 15.5% Si 1% Cu.

Introduction to Soft Ferrites

In the early days of electrical industry, the need for the indispensable magnetic material was served by iron and its magnetic alloys. However, with the advent of higher frequencies, the standard techniques of reducing eddy current losses, (using laminations or iron powder cores), was no longer efficient or cost effective.

This realization stimulated a renewed interest in "magnetic insulators," as first reported by S. Hilpert in Germany, in 1909. It was readily understood that, if the high electrical resistivity of oxides could be combined with desired magnetic characteristics, a magnetic material that was particularly well-suited for high frequency operation would result.

© 2011 by Taylor and Francis Group, LLC

Research to develop such a material was being performed by scientists in various laboratories all over the world, such as V. Kato, T. Takei, and N. Kawai in the 1930's in Japan, and by J. Snoek of the Philips' Research Laboratories in the period 1935-1945 in The Netherlands. By 1945, Snoek had laid down the basic fundamentals of the physics and technology of practical ferrite materials. In 1948, the Neel Theory of ferromagnetism provided the theoretical understanding of this type of magnetic material.

Ferrites are ceramic, homogeneous materials composed of oxides; iron oxide is their main constituent. Soft ferrites can be divided into two major categories; manganese-zinc and nickel-zinc. In each of these categories, changing the chemical composition, or manufacturing technology, can manufacture many different Mn-Zn and Ni-Zn material grades. The two families of Mn-Zn and Ni-Zn ferrite materials complement each other, and allow the use of soft ferrites from audio frequencies to several hundred megahertz. Manufacturers do not like to handle manganese-zinc in the same area, or building with nickel-zinc, because one contaminates the other, which leads to poor performance yields. The basic difference between manganese-zinc and nickel-zinc is shown in Table 2-3. The biggest difference is manganese-zinc has a higher permeability and nickel-zinc has a higher resistivity. Shown in Table 2-4 are some of the most popular and new ferrite materials. Also, given in Table 2-4, is the Figure number for the B-H loop of each of the materials.

Table 2-3. Comparing Manganese-Zinc and Nickel-Zinc Basic Properties

Basic Ferrite Material Properties					
Materials	Initial Permeability μ_i	Flux Density B_{max} Teslas	Curie Temperature, °C	dc, Coercive Force, H_c Oersteds	Resistivity Ω - cm
Manganese Zinc	750-15 K	0.3-0.5	100-300	0.04-0.25	10-100
Nickel Zinc	15-1500	0.3-0.5	150-450	0.3-0.5	10^6

Manganese-Zinc Ferrites

This type of soft ferrite is the most common, and is used in many more applications than the nickel-zinc ferrites. Within the Mn-Zn category, a large variety of materials are possible. Manganese-zinc ferrites are primarily used at frequencies less than 2 MHz.

Nickel-Zinc Ferrites

This class of soft ferrite is characterized by its high material resistivity, several orders of magnitude higher than Mn-Zn ferrites. Because of its high resistivity, Ni-Zn ferrite is the material of choice for operating from 1-2 MHz to several hundred megahertz.

The material permeability, μ_m, has little influence on the effective permeability, μ_e, when the gap dimension is relatively large, as shown in Table 2-5.

© 2011 by Taylor and Francis Group, LLC

Table 2-4. Magnetic Properties for Selected Ferrite Materials

Ferrites Material Properties							
*Magnetics Material Name	Initial Permeability μ_i	Flux Density Teslas B_s@15 Oe	Residual Flux Teslas B_r	Curie Temperature °C	dc, Coercive Force, Hc Oersteds	Density grams/cm^3 δ	Typical B-H Loop Figures
L	900	0.42 T	0.15 T	>300	0.94	4.8	(2-12)
R	2300	0.50 T	0.12 T	>230	0.18	4.8	(2-13)
P	2500	0.50 T	0.12 T	>230	0.18	4.8	(2-13)
T	2300	0.47 T	0.16 T	>215	0.25	4.8	NA
F	5000	0.49 T	0.10 T	>250	0.2	4.8	(2-14)
W	10,000	0.43 T	0.07 T	>125	0.15	4.8	(2-15)
* Magnetics, a Division of Spang & Company.							

Table 2-5. Permeability, and Its Effect on Gapped Inductors

Comparing Material Permeabilities					
*Material	μ_m	Gap, inch	Gap, cm	**MPL, cm	μ_e
L	900	0.04	0.101	10.4	92
R	2300	0.04	0.101	10.4	98
P	2500	0.04	0.101	10.4	99
F	3000	0.04	0.101	10.4	100
* The materials are from Magnetics, a Division of Spang & Company. ** Core, ETD44.					

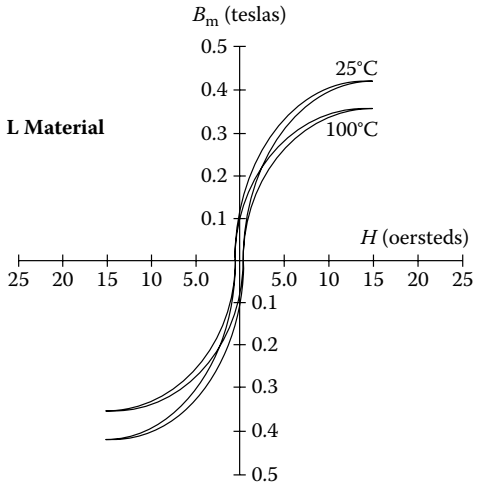

Figure 2-12. Ferrite B-H Loop, L Material at 25 and 100°C.

© 2011 by Taylor and Francis Group, LLC

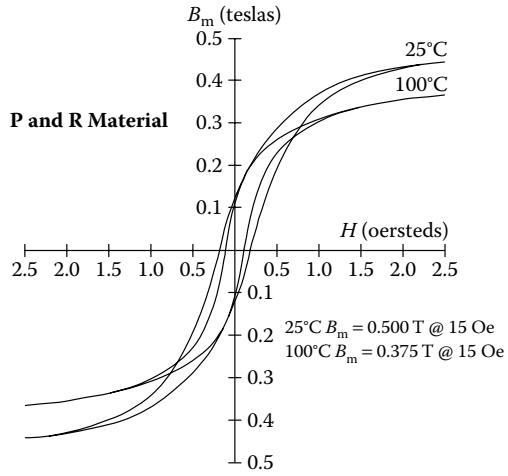

Figure 2-13. Ferrite B-H Loop, P & R Material at 25 and 100°C.

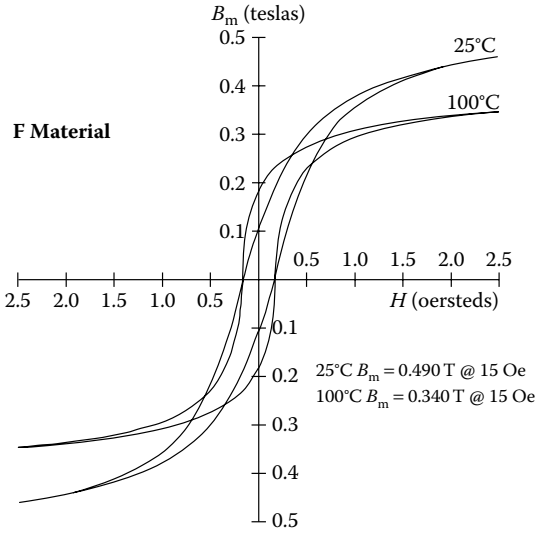

Figure 2-14. Ferrite B-H Loop, F Material at 25 and 100°C.

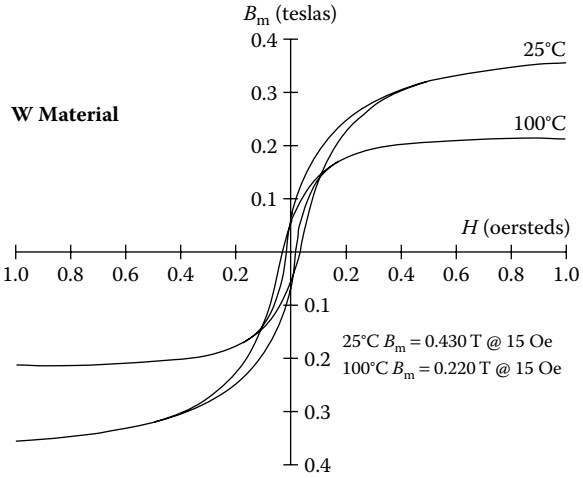

Figure 2-15. Ferrite B-H Loop, W & H Material at 25 and 100°C.

© 2011 by Taylor and Francis Group, LLC

Ferrite Cross Reference

A similar ferrite cross-reference has been made in Table 2-6. This table has been put together using some of the leading ferrite manufacturers. The ferrite materials in Table 2-6 have been organized for materials best suited for power transformers, power inductors and common-mode filters.

Table 2-6. Similar Ferrite Materials Best Suited for Power and Filters

Similar Ferrite Materials Used for Power and Filters							
Application	Power	Power	Power	Power	Filter	Filter	Filter
Manufacturers	Material Designation						
Magnetics	1* L	2* R	3* P	F	J	W	
Permeability, μ_i	900	2300	2500	3000	5000	10000	
Ferroxcube	3F45	3F3	3C94	3C91	3E27	3E5	3E7
Permeability, μ_i	900	2000	2300	3000	6000	10000	15000
Fair-Rite		77	78		75	76	
Permeability, μ_i		2000	2300		5000	10000	
EPCOS		N97	N72	T41	T65	T38	T46
Permeability, μ_i		2300	2500	2800	5200	10000	15000
TDK Corp.		PC40	PC44	H5A	HP5	H5C2	H5C3
Permeability, μ_i		2300	2400	3300	5000	10000	15000
MMG		F44	F45	F5A	F-10	FTA	FTF
Permeability, μ_i		1800	2000	2300	6000	10000	15000
Ceramic Mag			MN80C	MN8CX	MN60	MN100	
Permeability, μ_i			2050	3100	6500	9000	
TSC Ferrite Int.		TSF-7099	TSF-7070	TSF-8040	TSF-5000	TSF-010K	
Permeability, μ_i		2000	2200	3100	5000	10000	

1. High Frequency power material 500 kHz & up.
2. Lowest loss at 80°C-100°C, 25kHz to 250 kHz.
3. Lowest loss at 60°C-80°C.

© 2011 by Taylor and Francis Group, LLC

Introduction to Molypermalloy Powder Cores

The nickel-iron (Ni-Fe) high permeability magnetic alloys (permalloy) were discovered in 1923 and 1927. Permalloy alloys were successfully used in powder cores, greatly contributing to the carrier wave communications of the time.

In the early 1940's, the Bell Telephone Laboratory and the Western Electric Company developed a new material, trademarked Molybdenum Permalloy Powder (MPP), into cores. This new material was developed for loading coils, filtering coils, and transformers at audio and carrier frequencies in the telephone facility. The use of such cores has been extended to many industrial and military circuits. The stability of permeability and core losses with time, temperature, and flux level, are particularly important to engineers designing tuned circuits and timing circuits. This new material has given reliable and superior performance over all past powder core materials.

Molybdenum permalloy powder, [2 Molybdenum (Mo)-82 Nickel (Ni)-16 Iron (Fe)], is made by grinding hot-rolled and embrittled cast ingots; then, the alloy is insulated and screened to a fineness of 120 mesh for use in audio frequency applications, and 400 mesh for use at high frequencies.

In the power conversion field, the MPP core has made its greatest impact in switching power supplies. The use of MPP cores and power MOSFET transistors has permitted increased frequency, resulting in greater compactness and weight reduction in computer systems. The power supply is the heart of the system. When the power supply is designed correctly, using a moderate temperature rise, the system will last until it becomes obsolete. In these power systems there are switching inductors, smoothing choke coils, common mode filters, input filters, output filters, power transformers, current transformers and pulse transformers. They cannot all be optimally designed using MPP cores. But, in some cases, MPP cores are the only ones that will perform in the available space with the proper temperature rise.

Introduction to Iron Powder Cores

The development of compressed iron powder cores as a magnetic material for inductance coils, stemmed from efforts of Bell Telephone Laboratory engineers to find a substitute for fine iron-wire cores. The use of iron powder cores was suggested by Heaviside in 1887, and again, by Dolezalek in 1900.

The first iron powder cores of commercially valuable properties were described by Buckner Speed, in U.S. Patent No. 1274952, issued in 1918. Buckner Speed and G.W. Elman published a paper in the A.I.E.E.

© 2011 by Taylor and Francis Group, LLC

Transactions, "Magnetic Properties of Compressed Powdered Iron," in 1921. This paper describes a magnetic material, which is well suited to the construction of cores in small inductance coils and transformers, such as those used in a telephone system. These iron powder cores were made from 80 Mesh Electrolytic Iron Powder. The material was annealed, then, insulated by oxidizing the surface of the individual particles. In this way, a very thin and tough insulation of grains of iron was obtained; this did not break down when the cores were compressed. A shellac solution was applied to the insulated powder as a further insulator and binder. This was how Western Electric Company manufactured toroidal iron powder cores until about 1929. Today's iron powder cores are manufactured in much the same way, using highly pure iron powder and a more exotic insulator and binder. The prepared powder is compressed under extremely high pressures to produce a solid-looking core. This process creates a magnetic structure with a distributed air-gap. The inherent high saturation flux density of iron, combined with the distributed air-gap, produces a core material with initial permeability of less than 100, and with high-energy storage capabilities.

The dc current does not generate core loss, but an ac or ripple current does generate core loss. Iron powder material has higher core loss than some other, more expensive, core materials. Most dc-biased inductors have a relatively small percentage of ripple current and, thus, core loss will be minimal. However, core loss will sometimes become a limiting factor in applications with a relatively high percentage of ripple current at very high frequency. Iron powder is not recommended for inductors with discontinuous current or transformers with large ac flux swings.

In today's market low cost, iron powder cores are typically used in low and high frequency power switching conversion applications for differential-mode, input and output power inductors. Because iron powder cores have such low permeability, a relatively large number of turns are required for the proper inductance, thus keeping the ac flux at a minimum. The penalty for using iron powder cores is usually found in the size and efficiency of the magnetic component.

There are four standard powder materials available for power magnetic devices: Molypermalloy (MPP) Powder Cores with a family of curves, as shown in Figure 2-20; High flux (HF) Powder Cores with a family of curves, as shown in Figure 2-21; Sendust Powder Cores, *(Kool Mμ), with a family of curves, as shown in Figure 2-22; and Iron Powder Cores, with a family of curves, as shown in Figure 2-23. The powder cores come in a variety of permeabilities. This gives the engineer a wide range in which to optimize the design. The powder core properties for the most popular materials are shown in Table 2-7. Also, given in Table 2-7, is the Figure number for the B-H loop of each of the powder core materials. In Table 2-8 is a listing of the most popular permeabilities for each of the powder core materials.

* Trademark of Magnetics Division, Spang and Company.

© 2011 by Taylor and Francis Group, LLC

Table 2-7. Powder Core Material Properties

Powder Core Material Properties							
Material Name	Composition	Initial Permeability μ_i	Flux Density Teslas B_s	Curie Temperature °C	dc, Coercive Force, Hc Oersteds	Density grams/cm^3 δ	Typical B-H Loop Figures
MPP	80% Ni 20% Fe	14-550	0.7	460	0.3	8	(2-16)
High flux	50% Ni 50% Fe	14-160	1.5	500	1	7.6	(2-17)
Sendust (Kool Mμ)	85% Fe 9% Si 6% Al	26-125	1	500	0.5	5.5	(2-18)
Iron Powder	100% Fe	4.0-125	0.5-1.4	770	5.0-9.0	3.3-7.2	(2-19)

Table 2-8. Standard Powder Core Permeabilities

Standard Powder Core Permeabilities				
Powder Material	MPP	High Flux	Sendust (Kool Mμ)	Iron Powder
Initial Permeability μ_i				
10				X
14	X	X		X
26	X	X	X	
35				X
40			X	
55				X
60	X	X	X	X
75			X	X
90			X	
100				X
125	X	X	X	X
147	X	X		
160	X	X		
173	X			
200	X			
300	X			
550	X			

© 2011 by Taylor and Francis Group, LLC

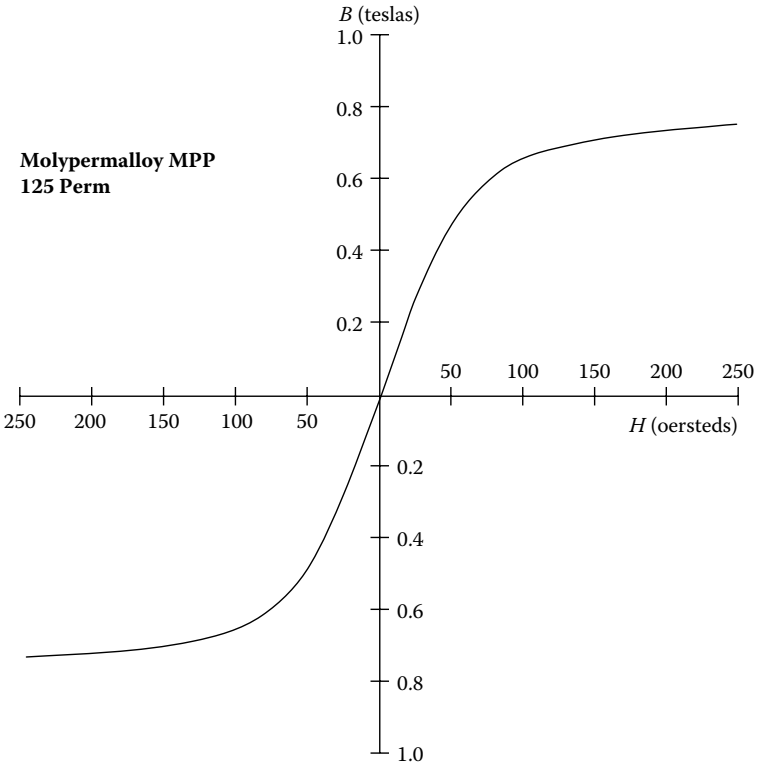

Figure 2-16. Molypermalloy Powder Core, 125 Perm.

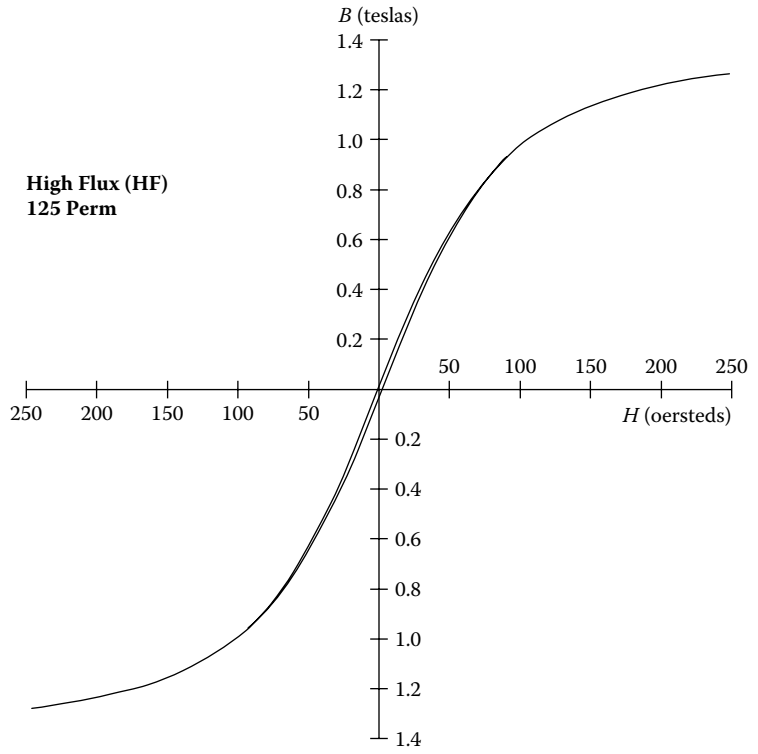

Figure 2-17. High Flux Powder Core, 125 Perm.

© 2011 by Taylor and Francis Group, LLC

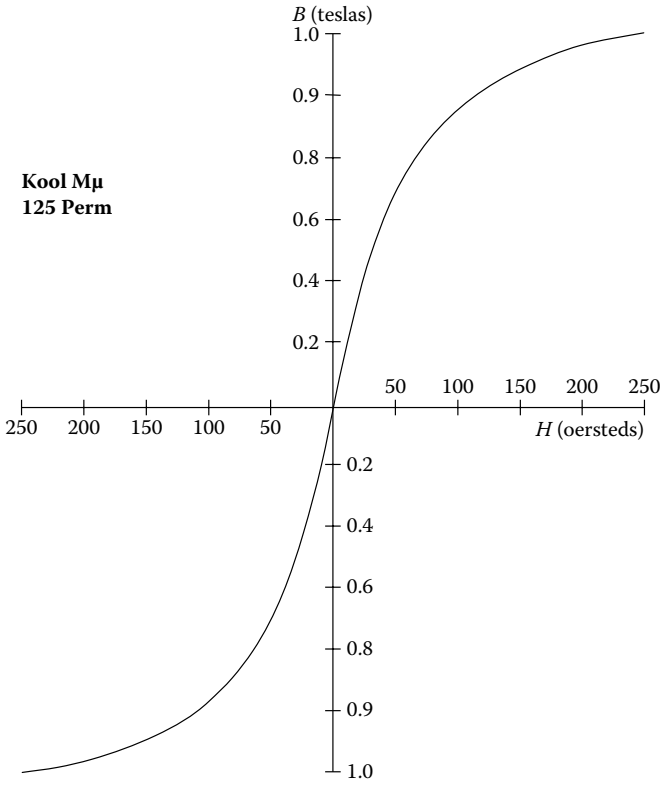

Figure 2-18. Sendust (Kool Mμ) Powder Core, 125 Perm.

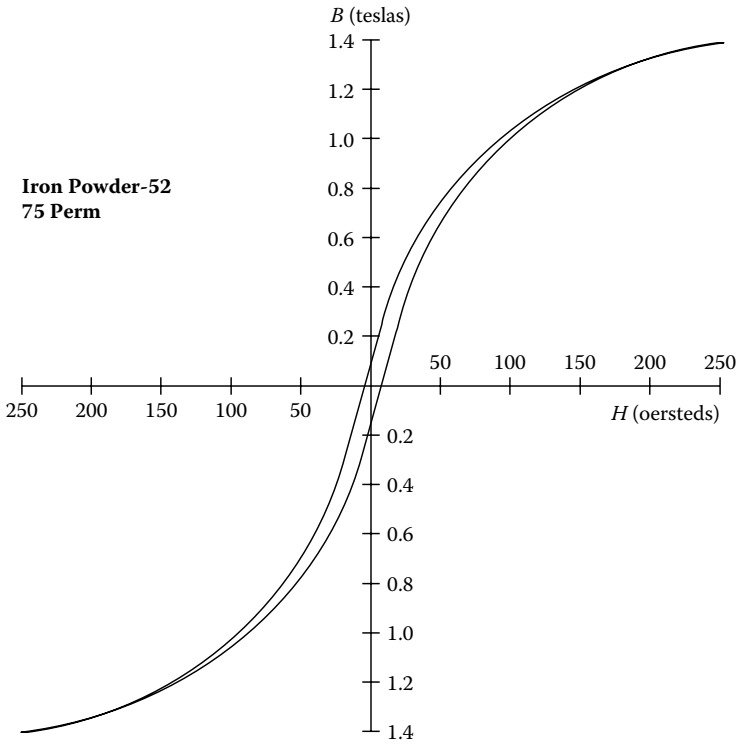

Figure 2-19. Iron Powder (-52) Core, 75 Perm.

© 2011 by Taylor and Francis Group, LLC

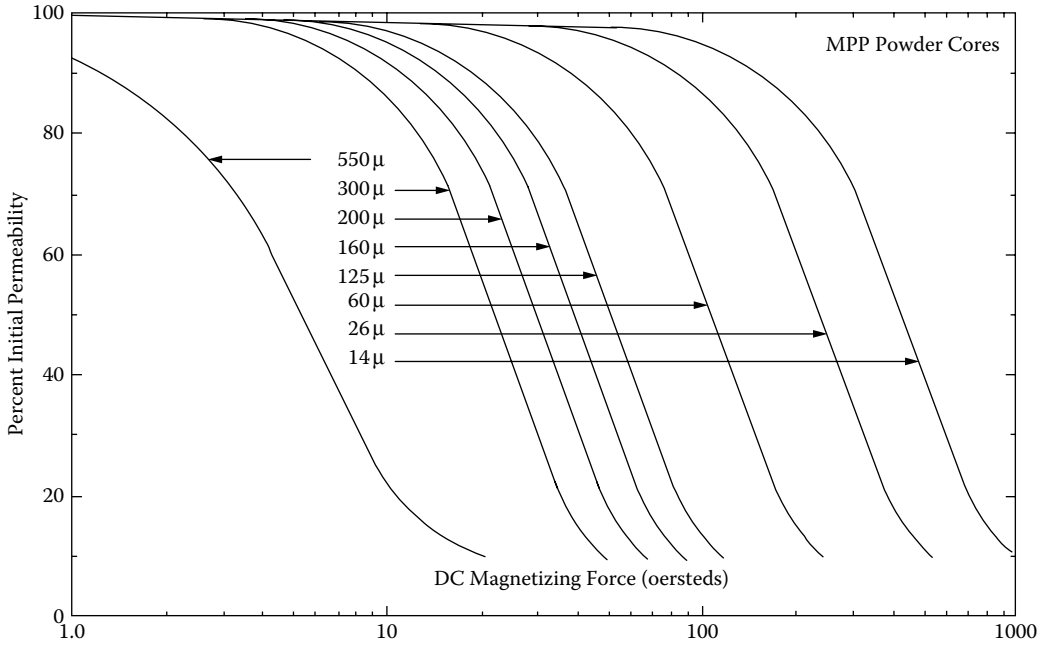

Figure 2-20. Permeability Versus dc Bias for Molypermalloy Powder Cores.

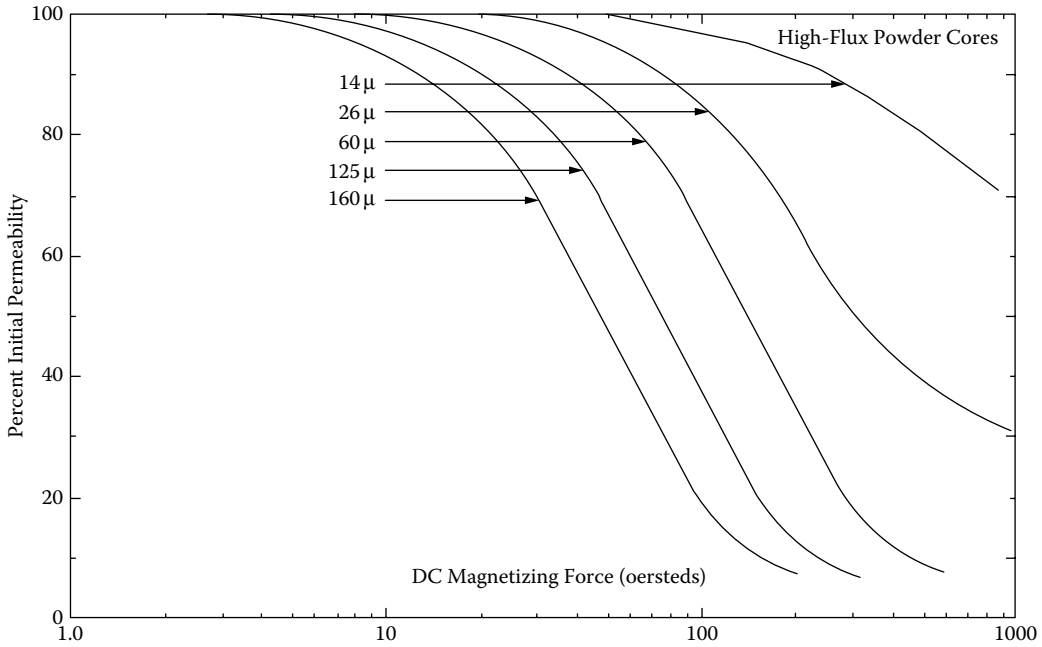

Figure 2-21. Permeability Versus dc Bias for High Flux Powder Cores.

© 2011 by Taylor and Francis Group, LLC

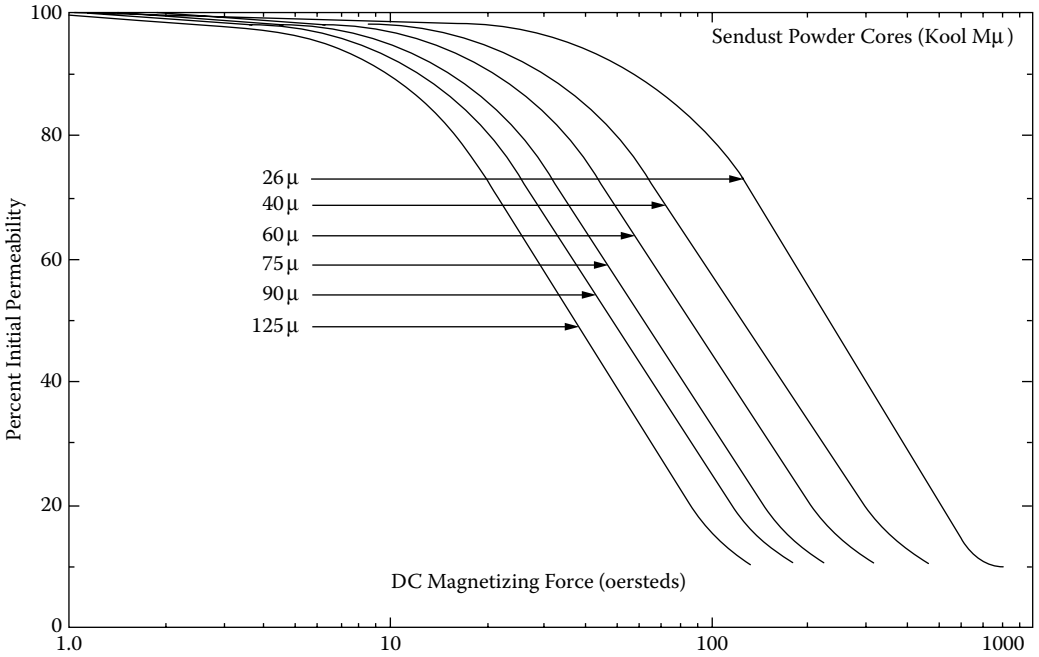

Figure 2-22. Permeability Versus dc Bias for Sendust Powder Cores.

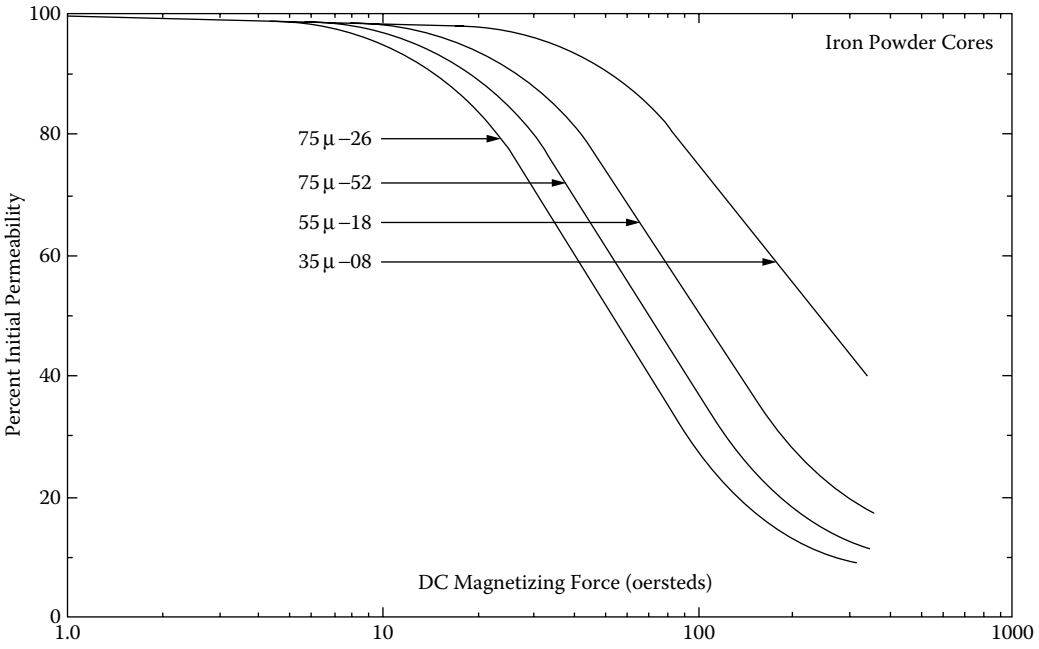

Figure 2-23. Permeability Versus dc Bias for Iron Powder Cores.

© 2011 by Taylor and Francis Group, LLC

Core Loss

The designer of power magnetic components, such as transformers and inductors, requires specific knowledge about the electrical and magnetic properties of the magnetic materials used in these components. There are two magnetic properties that are of interest, the dc and the ac. The dc B-H hysteresis loop is a very useful guide for comparing the different types of magnetic materials. It is the ac magnetic properties that are of interest to the design engineer. One of the most important ac properties is the core loss. The ac core loss is a function of the magnetic material, magnetic material thickness, magnetic flux density, B_{ac}, frequency, f, and operating temperature. Thus, the choice of the magnetic material is based upon achieving the best characteristic using the standard trade-off, such as cost, size, and performance.

All manufacturers do not use the same units when describing their core loss. The user should be aware of the different core loss units when comparing different magnetic materials. A typical core loss graph is shown in Figure 2-24. The vertical scale is core loss, and the horizontal scale is flux density. The core loss data is plotted at different frequencies, as shown in Figure 2-24.

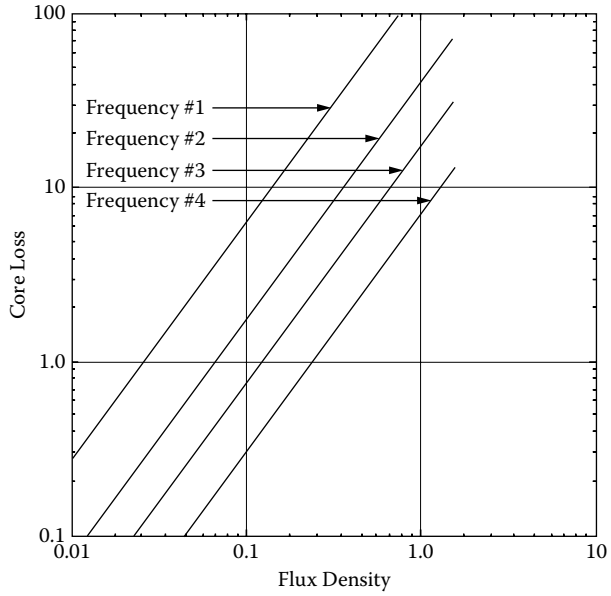

Figure 2-24. Typical Graph for Plotting Core Loss at Different Frequencies.

Vertical Scale

Here is a list of core loss units used by manufacturers:

1. watts per pound
2. watts per kilogram
3. milliwatts per gram
4. milliwatts per cubic centimeter (cm^3)

© 2011 by Taylor and Francis Group, LLC

Horizontal Scale

Here is a list of flux density units used by manufacturers:

1. gauss
2. kilogauss
3. teslas
4. millitesla

The data can be plotted or presented in either hertz or kilohertz.

Core Loss Equations

Manufacturers are now presenting the core loss in the form as shown in Equation [2-2].

$$\text{watts / kilogram} = k\, f^{(m)}\, B^{(n)} \qquad [2\text{-}2]$$

Here, again, the units will change from one manufacturer to another. In the following tables the manufacturer's core loss data has been organized with the same units for all core losses. The data was modified to put the data in metric units, gauss to teslas, and watts per pound to watts per kilogram. The coefficients for Magnetics Inc. molypermalloy powder cores, (MPP), using Equation [2-2] are shown in Table 2-9. The coefficients for Magnetics Inc. High Flux powder cores, (HF), using Equation [2-2] are shown in Table 2-10. The coefficients for Magnetics Inc. Sendust powder cores, (Kool-Mμ), using Equation [2-2] are shown in Table 2-11. The coefficients for iron alloy materials using Equation [2-2] are shown in Table 2-12.

Table 2-9. Core Loss Coefficients for MPP Powder Cores

Core Loss Equation Factors				
Magnetics MPP Powder Cores				
Material	Permeability μ	Coefficient k	Coefficient (m)	Coefficient (n)
MPP	14	0.005980	1.320	2.210
MPP	26	0.001190	1.410	2.180
MPP	60	0.000788	1.410	2.240
MPP	125	0.001780	1.400	2.310
MPP	147-160-173	0.000489	1.500	2.250
MPP	200-300	0.000250	1.640	2.270
MPP	550	0.001320	1.590	2.360

© 2011 by Taylor and Francis Group, LLC

Table 2-10. Core Loss Coefficients for High Flux Powder Cores

Core Loss Equation Factors				
Magnetics HF Powder Cores				
Material	Permeability μ	Coefficient k	Coefficient (m)	Coefficient (n)
High Flux	14	0.04280	1.26	2.52
High Flux	26	0.04180	1.25	2.55
High Flux	60	0.04140	1.23	2.56
High Flux	125	0.01300	1.32	2.59
High Flux	147	0.00940	1.41	2.56
High Flux	160	0.00940	1.41	2.56

Table 2-11. Core Loss Coefficients for Sendust Powder Cores

Core Loss Equation Factors				
Magnetics Kool-Mμ Powder Cores				
Material	Permeability μ	Coefficient k	Coefficient (m)	Coefficient (n)
Sendust	26	0.000693	1.460	2.000
Sendust	40	0.000693		
Sendust	60	0.000634		
Sendust	75	0.000620		
Sendust	90	0.000614		
Sendust	125	0.000596		

The coefficients for amorphous materials, using Equation [2-2] are shown in Table 2-13. The coefficients for Magnetics ferrite materials, using Equation [2-2] are shown in Table 2-14. The coefficients for Micrometals iron powder materials, using Equation [2-3] are shown in Table 2-15.

$$\text{watts/kilogram} = \left(\frac{f B_{ac}^3}{(a) + (b) B_{ac}^{0.7} + (c) B_{ac}^{1.35}} \right) + (d) f^2 B_{ac}^2 \qquad [2\text{-}3]$$

© 2011 by Taylor and Francis Group, LLC

Table 2-12. Core Loss Coefficients for Iron Alloy Cores

Core Loss Equation Factors					
Iron Alloy					
Material	Thickness mil's	Frequency Range	Coefficient k	Coefficient (m)	Coefficient (n)
50/50 Ni-Fe	1.00		0.0028100	1.210	1.380
	2.00		0.0005590	1.410	1.270
	4.00		0.0006180	1.480	1.440
Supermendur	2.00		0.0236000	1.050	1.300
	4.00	400 Hz	0.0056400	1.270	1.360
Permalloy 80	1.00		0.0000774	1.500	1.800
	2.00		0.0001650	1.410	1.770
	4.00		0.0002410	1.540	1.990
Supermalloy	1.00		0.0002460	1.350	1.910
	2.00		0.0001790	1.480	2.150
	4.00		0.0000936	1.660	2.060
Silicon	1.00		0.0593000	0.993	1.740
	2.00		0.0059700	1.260	1.730
	4.00		0.0035700	1.320	1.710
	12.00		0.0014900	1.550	1.870
	14.00		0.0005570	1.680	1.860
	24 M27 non-or	50-60 Hz	0.0386000	1.000	2.092

Table 2-13. Core Loss Coefficients for Amorphous Materials

Core Loss Equation Factors				
Amorphous				
Material	Thickness mils	Coefficient k	Coefficient (m)	Coefficient (n)
2605SC	0.80	$8.79(10^{-6})$	1.730	2.230
2714A	0.80	$10.1(10^{-6})$	1.550	1.670
Vitroperm 500	0.80	$0.864(10^{-6})$	1.834	2.112

© 2011 by Taylor and Francis Group, LLC

Table 2-14. Core Loss Coefficients for Magnetics Ferrites Materials

Core Loss Equation Factors				
Magnetic's Ferrite Core Materials				
Material	Frequency Range	Coefficient k	Coefficient (m)	Coefficient (n)
L	The loss coefficients for the L material was not available at this time.			
L				
L				
R	f < 100kHz	$5.597(10^{-4})$	1.43	2.85
R	100kHz <= f < 500kHz	$4.316(10^{-5})$	1.64	2.68
R	f => 500kHz	$1.678(10^{-6})$	1.84	2.28
P	f < 100kHz	$1.983(10^{-3})$	1.36	2.86
P	100kHz <= f < 500kHz	$4.855(10^{-5})$	1.63	2.62
P	f => 500kHz	$2.068(10^{-15})$	3.47	2.54
F	f =< 10kHz	$7.698(10^{-2})$	1.06	2.85
F	10kHz < f < 100kHz	$4.724(10^{-5})$	1.72	2.66
F	100kHz <= f < 500kHz	$5.983(10^{-5})$	1.66	2.68
F	f => 500kHz	$1.173(10^{-6})$	1.88	2.29
J	f =< 20kHz	$1.091(10^{-3})$	1.39	2.50
J	f > 20kHz	$1.658(10^{-8})$	2.42	2.50
W	f =< 20kHz	$4.194(10^{-3})$	1.26	2.60
W	f > 20kHz	$3.638(10^{-8})$	2.32	2.62

Table 2-15. Core Loss Coefficients for Iron Powder Cores

Core Loss Equation Factors					
Micrometals Iron Powder Cores					
Material	Permeability μ	Coefficient (a)	Coefficient (b)	Coefficient (c)	Coefficient (d)
Mix-08	35	0.01235	0.8202	1.4694	$3.85(10^{-7})$
Mix-18	55	0.00528	0.7079	1.4921	$4.70(10^{-7})$
Mix-26	75	0.00700	0.4858	3.3408	$2.71(10^{-6})$
Mix-52	75	0.00700	0.4858	3.6925	$9.86(10^{-7})$

© 2011 by Taylor and Francis Group, LLC

Selection of Magnetic Materials

Transformers used in static inverters, converters, and transformer-rectifier, (T-R), supplies, intended for aerospace and electronics industry power applications, are usually square loop tape, toroidal design. The design of reliable, efficient, and lightweight devices for this use has been seriously hampered by the lack of engineering data, describing the behavior of both the commonly used and more exotic core materials, with higher-frequency square wave excitation.

A program was carried out at the Jet Propulsion Laboratory, JPL, to develop this data from measurements of the dynamic B-H loop characteristics of the tape core materials presently available from various industry sources. Cores were produced in both toroidal and C forms, and were tested in both ungapped (uncut) and gapped (cut) configurations. The following section describes the results of that investigation.

Typical Operation

A transformer used for inverters, converters, and transformer-rectifier suppliers operates from a power bus, which could be dc or ac. In some power applications, a commonly used circuit is a driven transistor switch arrangement, such as that shown in Figure 2.25.

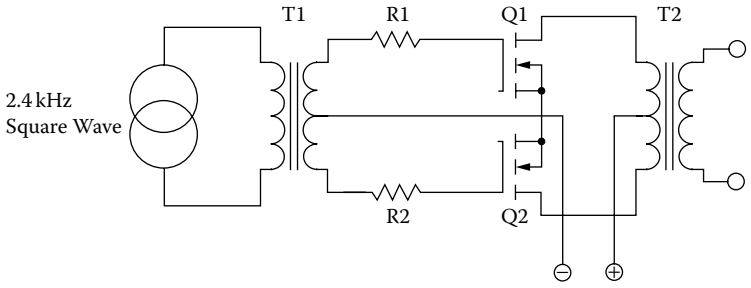

Figure 2-25. Typical Driven Power MOSFET Inverter.

One important consideration affecting the design of suitable transformers is that care must be taken to ensure that operation involves a balanced drive to the transformer primary. In the absence of a balanced drive, a net dc current will flow in the transformer primary, which causes the core to saturate easily during alternate half-cycles. A saturated core cannot support the applied voltage, limited mainly by its on resistance. The resulting high current, in conjunction with the transformer leakage inductance, results in a high-voltage spike during the switching sequence, which could be destructive to the power MOSFET. To provide a balanced drive, it is necessary to exactly match the MOSFETs for, $R_{DS(on)}$. But, this is not always sufficiently effective. Also, exact matching of the MOSFETs is a major problem in a practical sense.

© 2011 by Taylor and Francis Group, LLC

Material Characteristics

Many available core materials approximate the ideal square loop characteristic, illustrated by the B-H curve, as shown in Figure 2-26. Representative, dc B-H loops for commonly available core materials, are shown in Figure 2-27. Other characteristics are tabulated in Table 2-16.

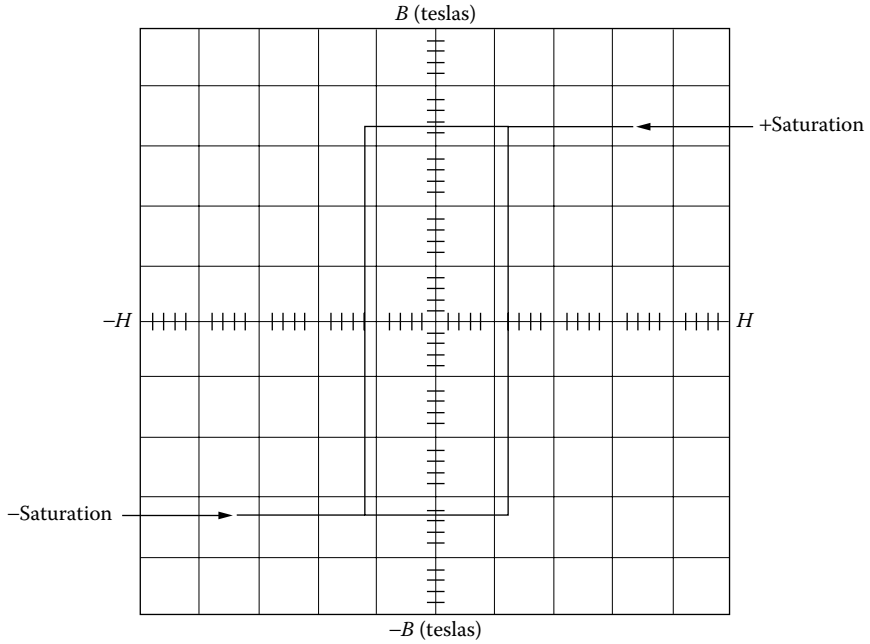

Figure 2-26. Ideal Square B-H Loop.

Many articles have been written about inverter and converter transformer design. Usually, authors' recommendations represent a compromise among material characteristics, such as those tabulated in Table 2-16, and displayed in Figure 2-27. These data are typical of commercially available core materials that are suitable for the particular application.

As can be seen, the material that provides the highest flux density (supermendur) would result in the smallest component size, and this would influence the choice if size were the most important consideration. The ferrite material, (See the ferrite curve in Figure 2-27), has the lowest flux density. This results in the largest transformer. Magnetic materials selected for transformers or inductors cannot be chosen by flux alone. There are other parameters, such as frequency and core configuration that must be taken into consideration.

© 2011 by Taylor and Francis Group, LLC

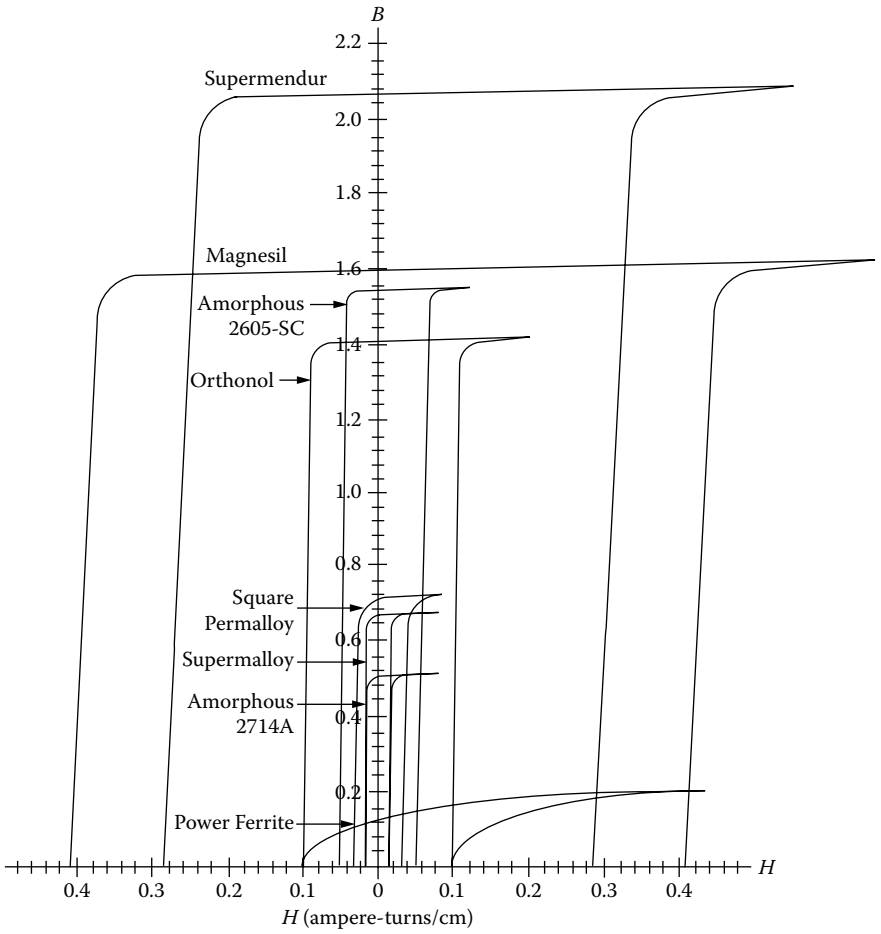

Figure 2-27. Typical dc B-H Loops of Magnetic Materials.

Usually, inverter transformer design is aimed at the smallest size, the highest efficiency and adequate performance under the widest range of environmental conditions. Unfortunately, the core material that can produce the smallest size has the lowest efficiency, and the highest efficiency materials result in the largest size. Thus, the transformer designer must make trade-offs between allowable transformer size and the minimum efficiency that can be tolerated. Then, the choice of core material will be based upon achieving the best characteristic on the most critical or important design parameter, and upon acceptable compromises on the other parameters.

After analysis of a number of designs, most engineers choose size rather than efficiency as the most important criterion, and select an intermediate loss factor on core material for their transformers. Consequently, as the frequency is increased, ferrites have become the most popular material.

© 2011 by Taylor and Francis Group, LLC

Table 2-16. Magnetic Core Material Characteristics

Magnetic Core Material Characteristics						
Material Name	Composition	Initial Permeability μ_i	Flux Density Teslas B_s	Curie Temperature °C	dc, Coercive Force, Hc Oersteds	Density grams/cm^3 δ
Magnesil	3% Si 97% Fe	1.5K	1.5-1.8	750	0.4-0.6	7.3
Supermendur*	49% Co 49% Fe 2% V	0.8K	1.9-2.2	940	0.15-0.35	8.15
Orthonol	50% Ni 50% Fe	2K	1.42-1.58	500	0.1-0.2	8.24
Sq. Permalloy	79% Ni 17% Fe 4% Mo	12K-100K	0.66-0.82	460	0.02-0.04	8.73
Supermalloy	78% Ni 17% Fe 5% Mo	10K-50K	0.65-0.82	460	0.003-0.008	8.76
Amorphous 2605-SC	81% Fe 13.5% B 3.5% Fe	3K	1.5-1.6	370	0.03-0.08	7.32
Amorphous 2714A	66% Co 15% Si 4% Fe	20K	0.5-0.58	205	0.008-0.02	7.59
Amorphous nano-crystal	73.5% Fe 1% Cu 15.5% Si	30K-80K	1.0-1.2	460	0.02-0.04	7.73
Ferrite	MnZn	0.75-15K	0.3-0.5	100-300	0.04-0.25	4.8
* Field Anneal.						

© 2011 by Taylor and Francis Group, LLC

Magnetic Material Saturation Defined

To standardize the definition of saturation, several unique points on the B-H loop are defined, as shown in Figure 2-28.

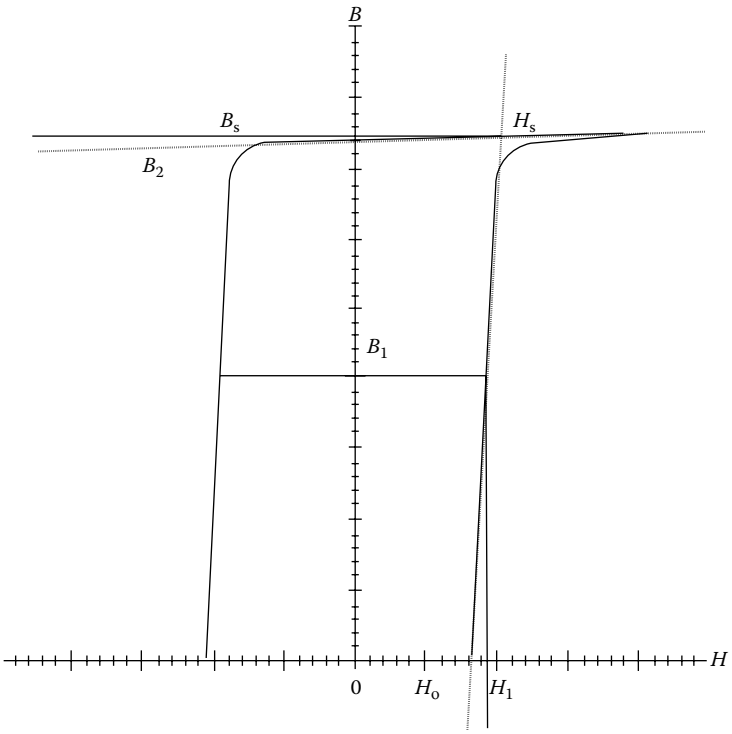

Figure 2-28. Defining the B-H Loop.

The straight line through (H_o, 0) and (H_s, B_s) may be written as:

$$B = \left(\frac{\Delta B}{\Delta H}\right)(H - H_o) \qquad [2\text{-}4]$$

The line through (0, B_2) and (H_s, B_s) has essentially zero slope and may be written as:

$$B = B_2 \approx B_s \qquad [2\text{-}5]$$

Equations [2-4] and [2-5] together define saturation conditions as follows:

$$B_s = \left(\frac{\Delta B}{\Delta H}\right)(H_s - H_o) \qquad [2\text{-}6]$$

Solving Equation [2-6] for H_s yields:

$$H_s = H_o + \frac{B_s}{\mu_o} \qquad [2\text{-}7]$$

© 2011 by Taylor and Francis Group, LLC

Where by definition:

$$\mu_o = \frac{\Delta B}{\Delta H} \quad [2\text{-}8]$$

By definition, saturation occurs when the peak exciting current (B) is twice the average exciting current (A), as shown in Figure 2-29. Analytically, this means that:

$$H_{pk} = 2H_s \quad [2\text{-}9]$$

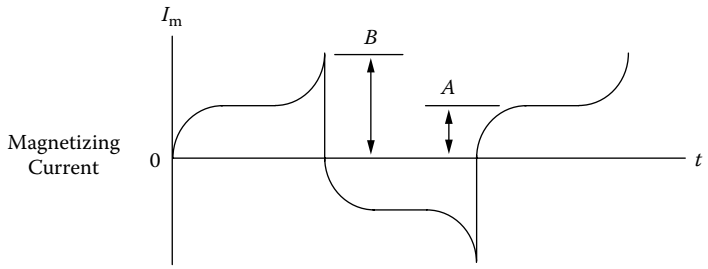

Figure 2-29. Defining the Excitation Current.

Solving Equation [2-1] for H_1, we obtain:

$$H_1 = H_o + \frac{B_1}{\mu_o} \quad [2\text{-}10]$$

To obtain the pre-saturation dc margin (ΔH), Equation [2-4] is subtracted from Equation [2-6]:

$$\Delta H = H_s - H_1 = \left(\frac{B_s - B_1}{\mu_o} \right) \quad [2\text{-}11]$$

The actual unbalanced dc current must be limited to:

$$I_{dc} \leq \left(\frac{\Delta H(\text{MPL})}{N} \right), \quad \text{[amperes]} \quad [2\text{-}12]$$

Where, N is the number of turns

MPL is the mean magnetic path length.

Combining Equations [2-7] and [2-8] gives:

$$I_{dc} \leq \left(\frac{(B_s - B_1)(\text{MPL})}{\mu_o N} \right), \quad \text{[amperes]} \quad [2\text{-}13]$$

© 2011 by Taylor and Francis Group, LLC

As mentioned earlier, in an effort to prevent core saturation, the drive to the switching power MosFet must be symmetrical and the power MosFet on resistance $R_{DS(on)}$ must be matched. The effect of core saturation, using an uncut or ungapped core, is shown in Figure 2-30, which illustrates the effect on the B-H loop transversed with a dc bias. Figure 2-31 shows typical B-H loops of 50-50 nickel-iron material excited from an ac source, with progressively reduced excitation; the vertical scale is 0.4 T/cm. It can be noted that the minor loop remains at one extreme position within the B-H major loop after reduction of excitation. The unfortunate effect of this random minor loop positioning is that, when conduction begins again in the transformer winding after shutdown, the flux swing could begin from the extreme ends rather than from the normal zero axis. The effect of this is to drive the core into saturation, with the production of spikes that can destroy transistors.

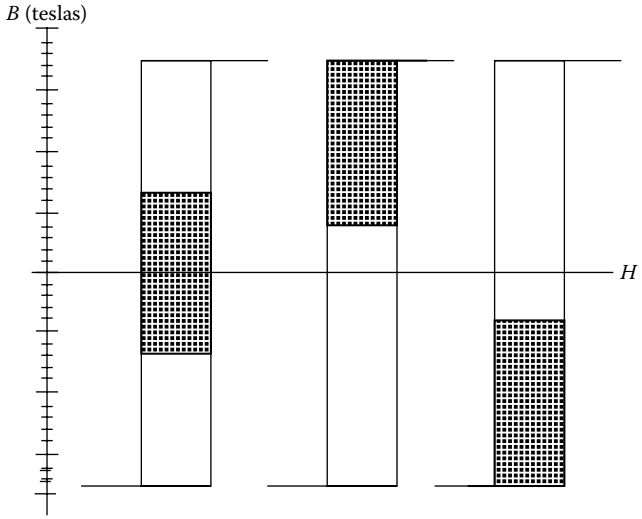

Figure 2-30. B-H Loop with dc Bias.

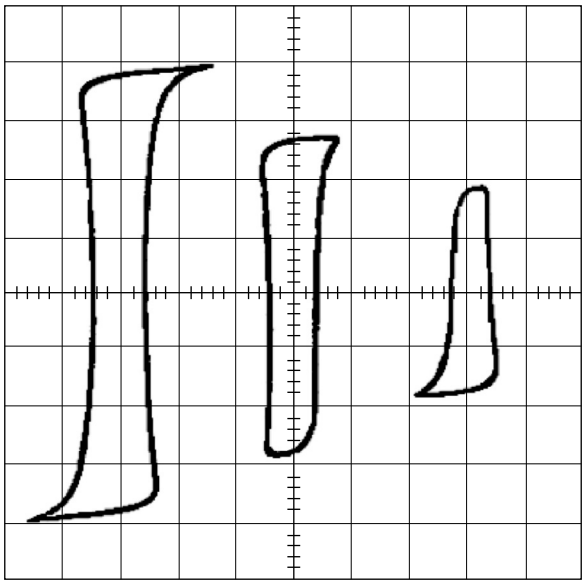

Figure 2-31. Typical Square Loop Material with dc Bias.

© 2011 by Taylor and Francis Group, LLC

Test Conditions

The test fixture, schematically illustrated in Figure 2-32, was built to affect comparison of dynamic B-H loop characteristics of various core materials. Cores were fabricated from various core materials in the basic core configuration, designated No. 52029 for toroidal cores, manufactured by Magnetics Inc. The materials used were those most likely to be of interest to designers of inverter or converter transformers. Test conditions are listed in Table 2-17.

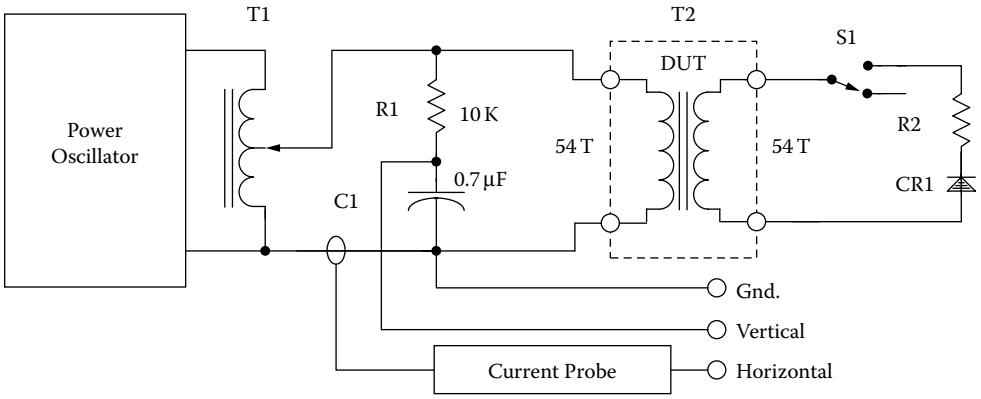

Figure 2-32. B-H Loop with dc Bias.

Winding Data were derived from the following:

$$N = \frac{V\left(10^4\right)}{4.0 B_m f A_c}, \quad \text{[turns]} \qquad \text{[2-14]}$$

Table 2-17. Materials and Test Conditions

Test Conditions					
Core Number*	Trade Name	B_s Teslas	Turns N	Frequency kHz	MPL cm
52029-2A	Orthonol	1.45	54	2.4	9.47
52029-2D	Sq. Permalloy	0.75	54	2.4	9.47
52029-2F	Supermalloy	0.75	54	2.4	9.47
52029-2H	48 Alloy	1.15	54	2.4	9.47
52029-2K	Magnesil	1.6	54	2.4	9.47
* Magnetics toroidal cores.					

The test transformer, represented in Figure 2-32, consists of 54-turn primary and secondary windings, with square wave excitation on the primary. Normally, switch S1 is open. With switch S1 closed, the secondary current is rectified by the diode to produce a dc bias in the secondary winding.

© 2011 by Taylor and Francis Group, LLC

Cores were fabricated from each of the materials by winding a ribbon of the same thickness on a mandrel of a given diameter. Ribbon termination was affected by welding in the conventional manner. The cores were vacuum impregnated, baked, and finished as usual.

Figures 2-33 through 2-36 show the dynamic B-H loops obtained for various core materials. In each of these Figures, switch S1 was in the open position, so there was no dc bias applied to the core and windings.

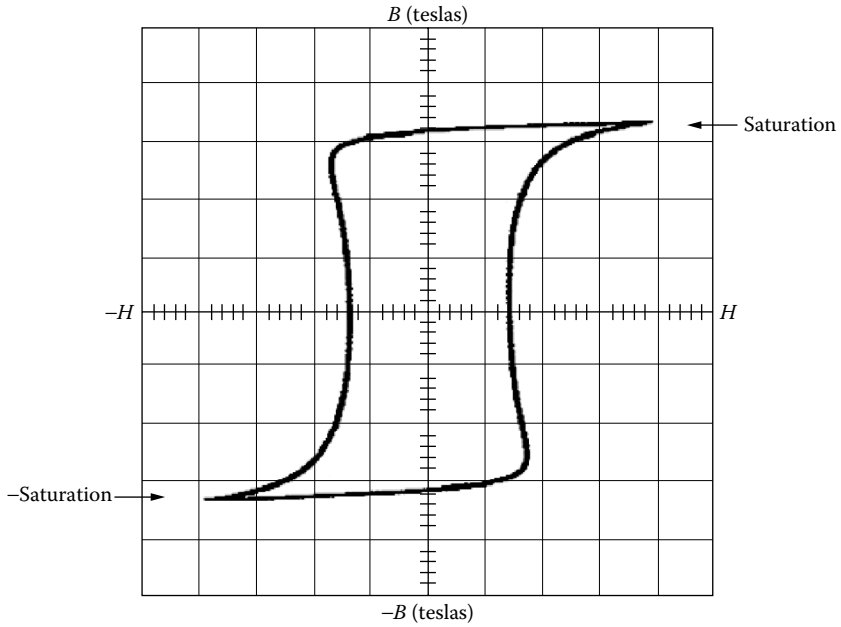

Figure 2-33. Magnesil (K) B-H Loop, B = 0.5 T/cm, H = 100 ma/cm.

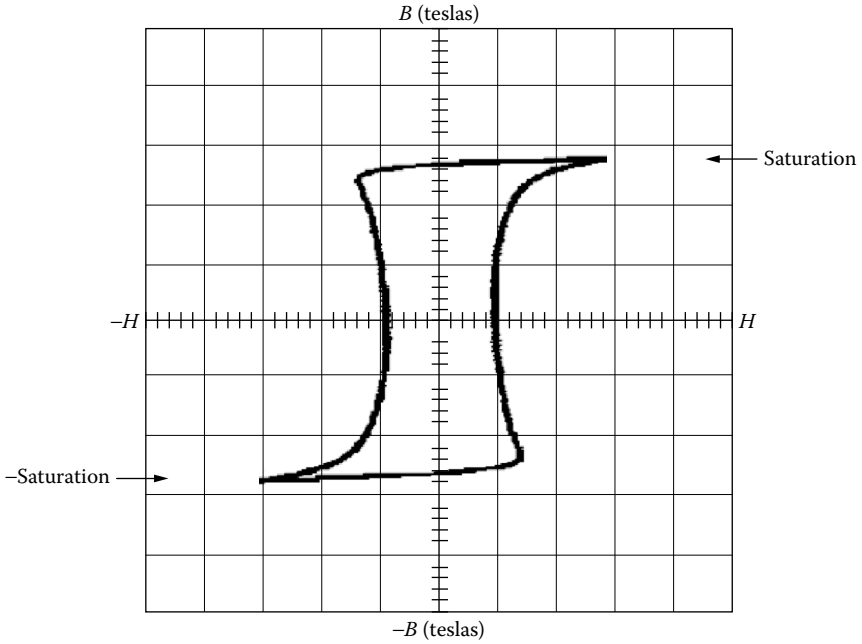

Figure 2-34. Orthonol (2A) B-H Loop, B = 0.5 T/cm, H = 50 ma/cm.

© 2011 by Taylor and Francis Group, LLC

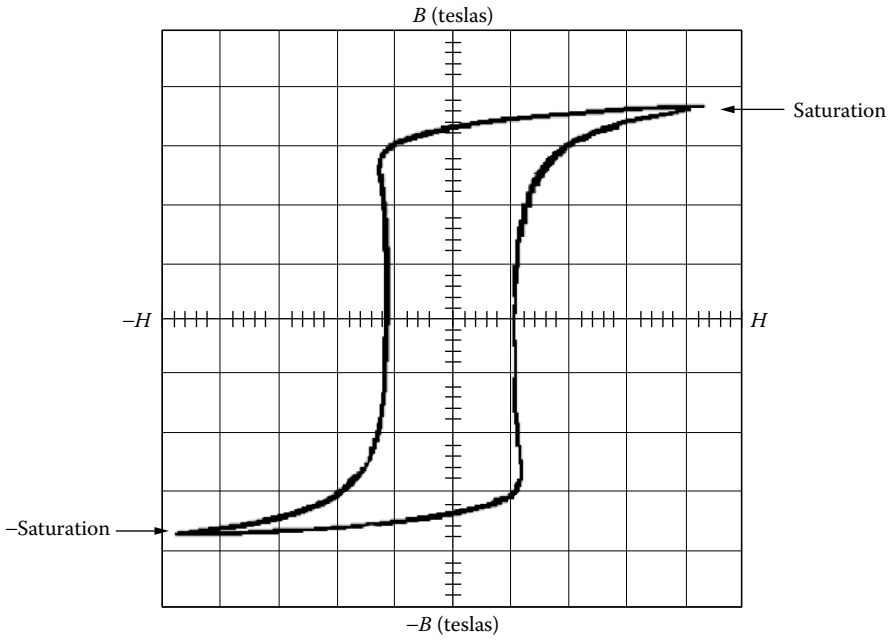

Figure 2-35. Square Permalloy (2D) B-H Loop, B = 0.2 T/cm, H = 20 ma/cm.

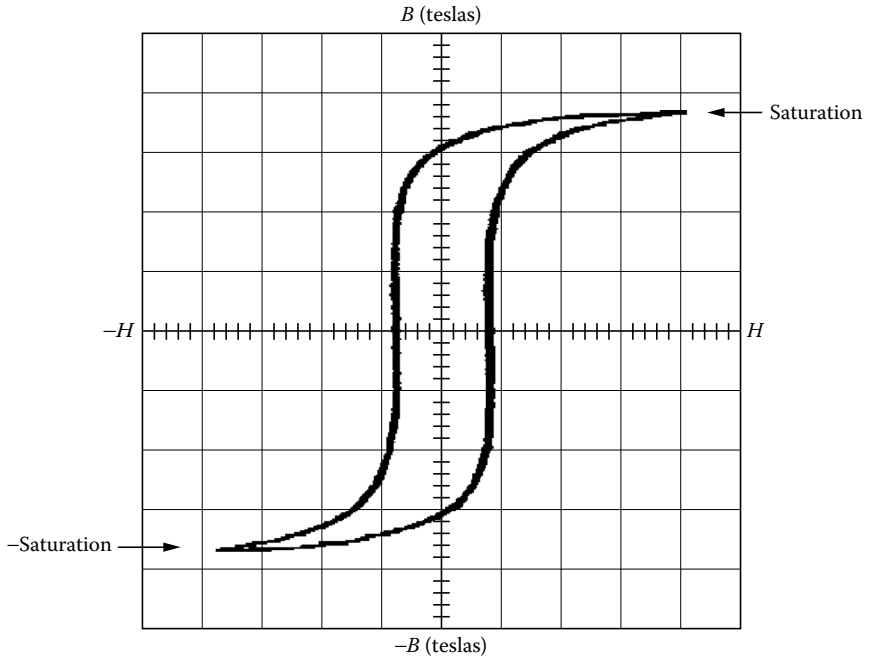

Figure 2-36. Supermalloy (2F) B-H Loop, B = 0.2 T/cm, H = 10 ma/cm.

Figures 2-37 to 2-40 show the dynamic B-H loop patterns obtained for various core materials when the test conditions are included in a sequence, in which S1 was in open condition (A), then in closed condition (B), and then, opened again, in condition (C). It is apparent from this data that, with a small amount of dc bias, the minor dynamic B-H loop can traverse the major B-H loop from saturation to saturation. Note that after the dc

© 2011 by Taylor and Francis Group, LLC

bias has been removed, the minor B-H loops remained shifted to one side or the other. Because of the ac coupling of the integrator to the oscilloscope, the photographs in these figures do not present a complete picture of what really happens during the flux swing.

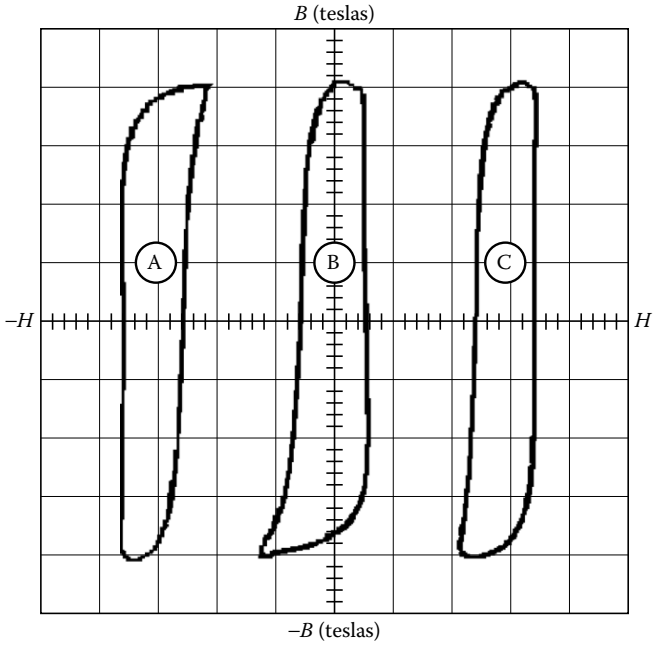

Figure 2-37. Magnesil (2K) B-H Loop, B = 0.3 T/cm, H = 200 ma/cm.

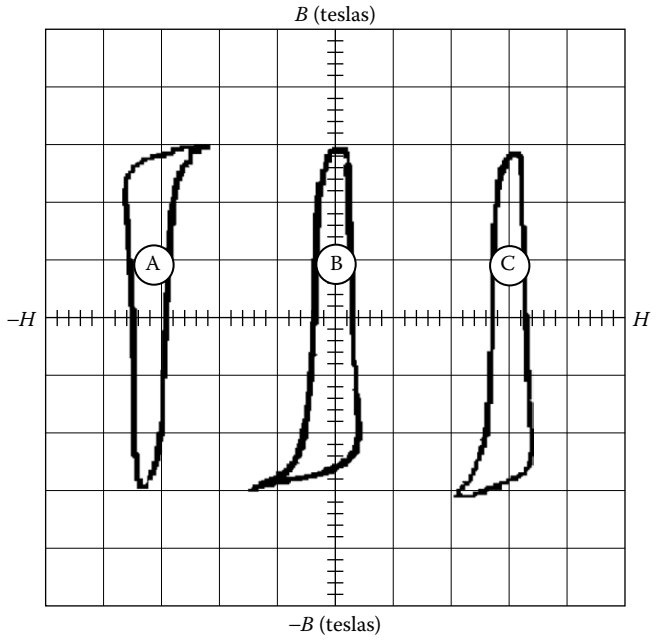

Figure 2-38. Orthonol (2A) B-H Loop, B = 0.2 T/cm, H = 100 ma/cm.

© 2011 by Taylor and Francis Group, LLC

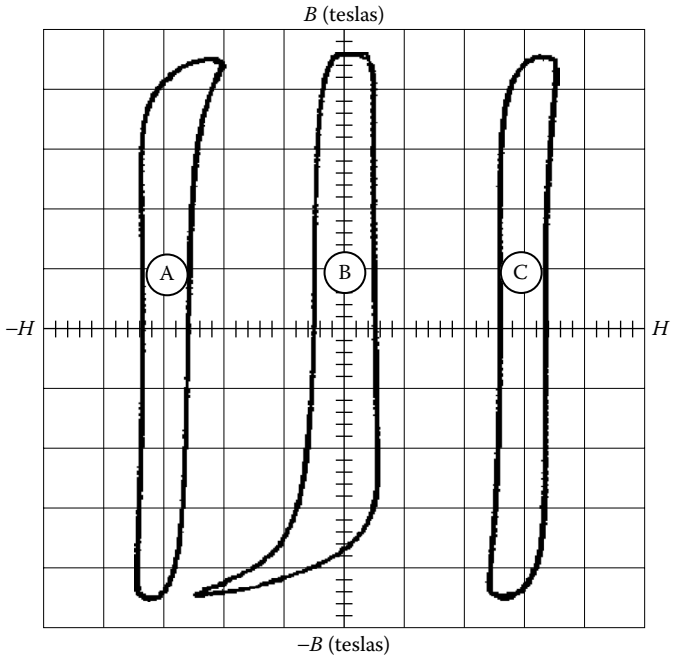

Figure 2-39. Sq. Permalloy (2D) B-H Loop, B = 0.1 T/cm, H = 20 ma/cm.

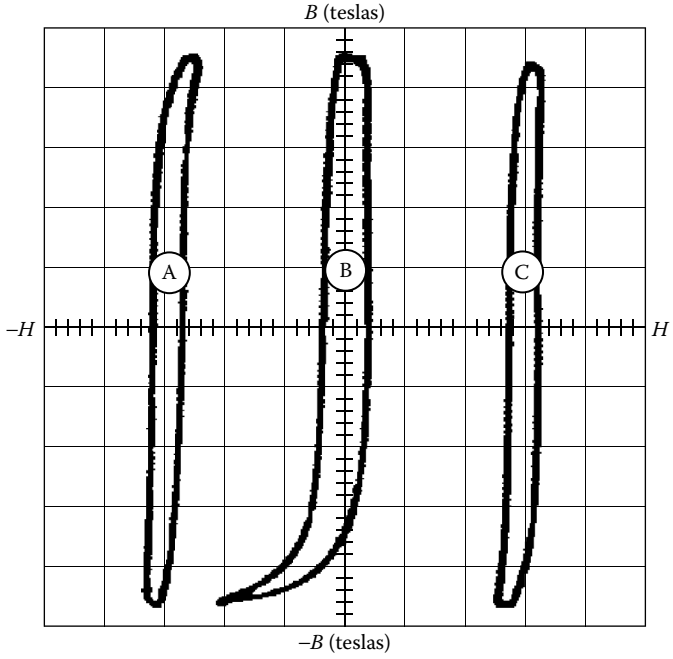

Figure 2-40. Supermalloy (2F) B-H Loop, B = 0.1 T/cm, H = 10 ma/cm.

© 2011 by Taylor and Francis Group, LLC

Magnetic Material Saturation Theory

The domain theory of the nature of magnetism is based on the assumption that all magnetic materials consist of individual molecular magnets. These minute magnets are capable of movement within the material. When a magnetic material is in its unmagnetized state, the individual magnetic particles are arranged at random, and effectively neutralize each other. An example of this is shown in Figure 2-41, where the tiny magnetic particles are arranged in a disorganized manner. (The north poles are represented by the darkened ends of the magnetic particles.) When a material is magnetized, the individual particles are aligned or oriented in a definite direction, as shown in Figure 2-42.

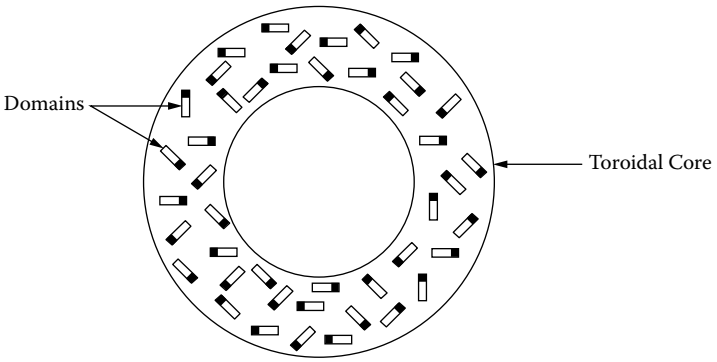

Figure 2-41. Magnetic Domains, Arranged in a Random Manner.

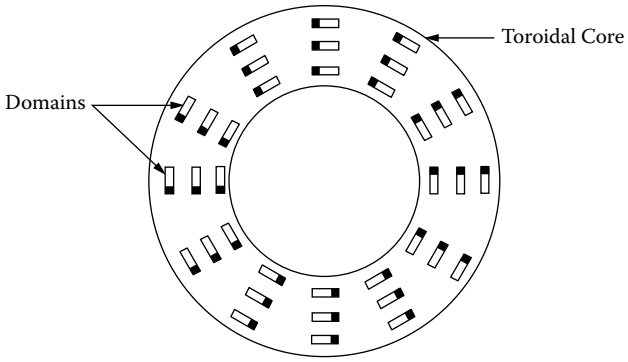

Figure 2-42. Magnetic Domains, Aligned in a Definite Direction.

The degree of magnetization of a material depends on the degree of alignment of the particles. The external magnetizing force can continue to affect the material up to the point of saturation, the point at which essentially all of the domains are lined up in the same direction.

In a typical toroidal core, the effective air gap is less than 10^{-6} cm. Such a gap is negligible in comparison to the ratio of mean length to permeability. If the toroid was subjected to a strong magnetic field (enough to saturate), essentially all of the domains would line up in the same direction. If suddenly the field were

© 2011 by Taylor and Francis Group, LLC

removed at B_m, the domains would remain lined up, and be magnetized along that axis. The amount of flux density that remains is called the residual flux, B_r. The result of this effect was shown earlier in Figures 2-37 through 2-40.

Air Gap Effect

An air gap introduced into the core has a powerful demagnetizing effect, resulting in a "shearing over" of the hysteresis loop, and a considerable decrease in permeability of high-permeability materials. Direct current excitation follows the same pattern. However, the core bias is considerably less affected than the magnetization characteristics by the introduction of a small air gap. The magnitude of the air gap effect also depends on the length of the mean magnetic path and on the characteristics of the uncut core. For the same air gap, the decrease in permeability will be less with a greater magnetic flux path, but more pronounced in a high-permeability core with a low coercive force.

Effect of Gapping

Figure 2-43 shows a comparison of a typical toroidal core B-H loop, without and with a gap. The gap increases the effective length of the magnetic path. When voltage E is impressed across primary winding, N_p, of a transformer, the resulting current, I_m, will be small because of the highly inductive circuit, as shown in Figure 2-44. For a particular core size, maximum inductance occurs when the air gap is minimum.

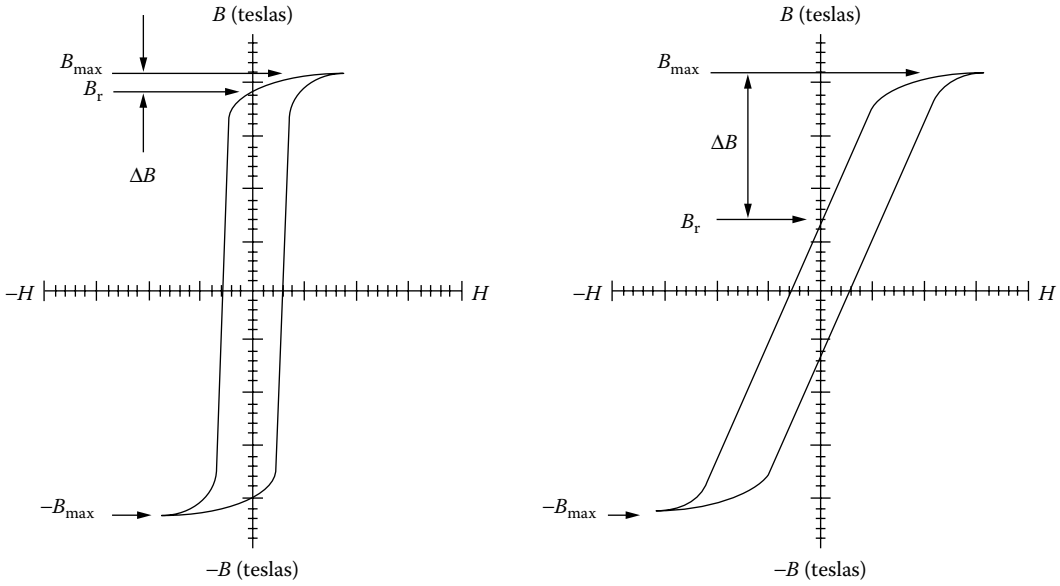

Figure 2-43. Comparing Magnetic Materials With and Without a Gap.

© 2011 by Taylor and Francis Group, LLC

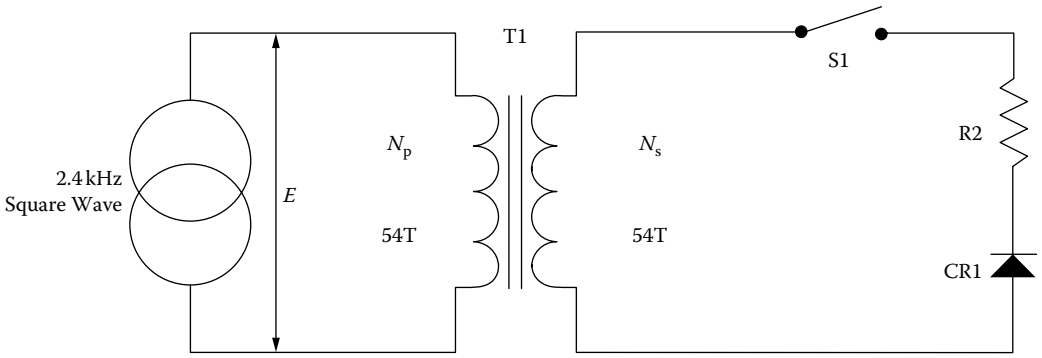

Figure 2-44. Implementing dc Unbalance.

When S1 is closed, an unbalanced dc current flows in the secondary, N_s turns, and the core is subjected to a dc magnetizing force, resulting in a flux density that may be expressed as:

$$B_{dc} = \frac{0.4\pi N_s I_{dc}\left(10^{-4}\right)}{l_g + \frac{\text{MPL}}{\mu_r}}, \quad \text{[teslas]} \qquad \text{[2-15]}$$

In converter and inverter design, this dc flux is augmented by the ac flux swing, which is:

$$B_{ac} = \frac{E\left(10^4\right)}{K_f f A_c N}, \quad \text{[teslas]} \qquad \text{[2-16]}$$

If the sum of B_{dc} and B_{ac} shifts operations above the maximum operating flux density of the core material, the incremental permeability, (μ_{ac}), is reduced. This condition lowers the impedance and increases the flow of magnetizing current, I_m. This condition can be remedied by introducing into the core assembly an air gap which causes a decrease in dc magnetization in the core. However, the size of the air gap that can be incorporated has a practical limitation. Since the air gap lowers impedance, it results in increased magnetizing current, I_m, which is inductive. The resultant voltage spikes produced by such currents apply a high stress to the switching transistors, and may cause failure. This stress can be minimized by tight control of lapping and etching of the gap to keep the gap to a minimum.

From Figure 2-43, it can be seen that the B-H curves depict maximum flux density, B_m, and residual flux, B_r, for ungapped and gapped cores, and that the useful flux swing is designated, ΔB, which is the difference between, B_m and B_r. It is noted, in Figure 2-43(a), that, B_r, approaches, B_m, but, in Figure 2-43(b), there is a much greater, ΔB, between them. In either case, when excitation voltage is removed at the peak of the excursion of the B-H loop, flux falls to the, B_r, point. It is apparent that introducing an air gap reduces, B_r, to a lower level, and increases the useful flux density. Thus, insertion of an air gap in the core eliminates, or markedly reduces, the voltage spikes produced by the leakage inductance, due to the transformer saturation.

© 2011 by Taylor and Francis Group, LLC

Two types of core configurations were investigated in the ungapped and gapped states. Figure 2-45 shows the type of toroidal core that was cut, and Figure 2-46 shows the type of C core that was cut. Toroidal cores are virtually gapless, when conventionally fabricated. To increase the gap, the cores were physically cut in half, and the cut edges were lapped, acid-etched to remove cut debris, and banded to form the cores. A minimum air gap, on the order of less than 25 μm, was established.

As is noted from Figures 2-47 through 2-50, which show the B-H loops of the uncut and cut cores, the results obtained indicated that the effect of gapping was the same for both the C cores and the toroidal cores subjected to testing. It is noted, however, that gapping of the toroidal cores produced a lowered square characteristic for the B-H loop, as shown in Table 2-18. This data was obtained from Figures 2-47 through 2-50. ΔH values extracted from the same figures, as shown in Figure 2-51, are tabulated in Table 2-19.

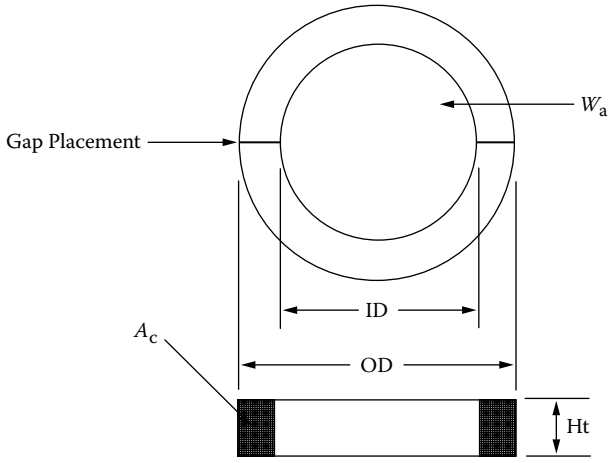

Figure 2-45. Typical Cut Toroidal Core.

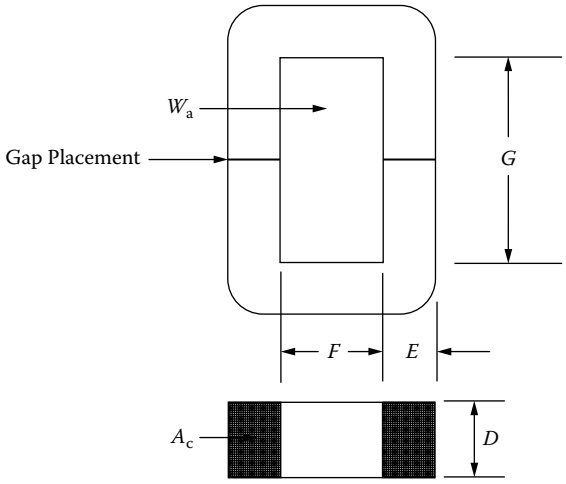

Figure 2-46. Typical Middle Cut C Core.

© 2011 by Taylor and Francis Group, LLC

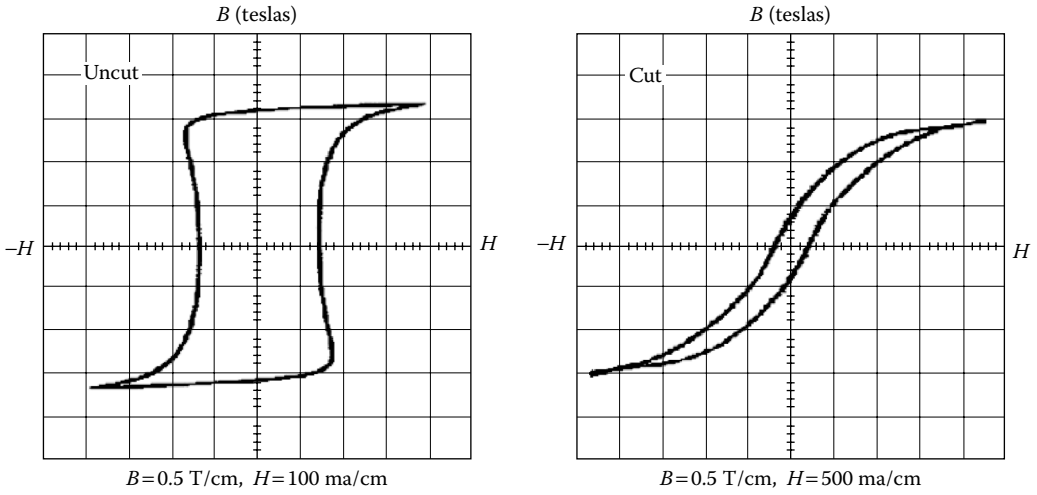

Figure 2-47. Magnesil (K) B-H Loop, Uncut and Cut with Minimum Gap.

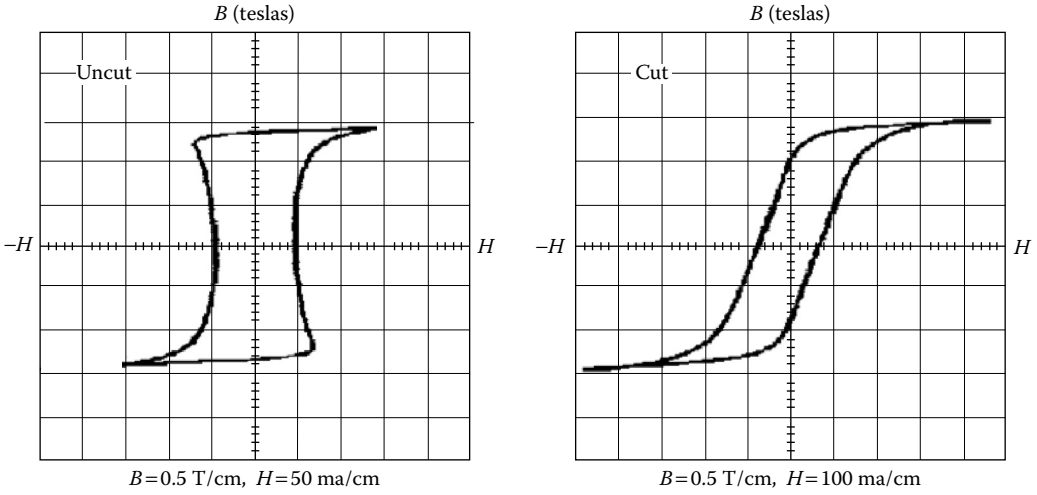

Figure 2-48. Orthonal (A) B-H Loop, Uncut and Cut with Minimum Gap.

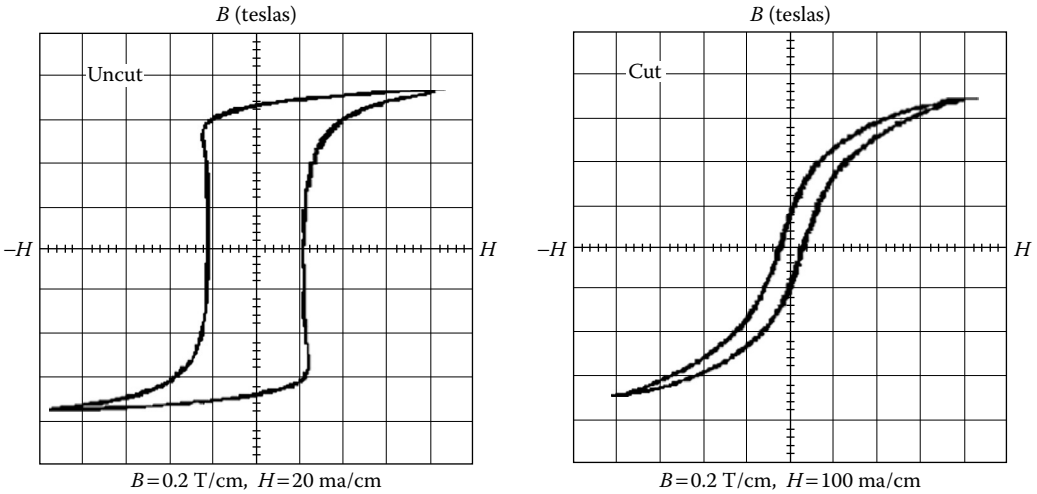

Figure 2-49. Square Permalloy (D) B-H Loop, Uncut and Cut with Minimum Gap.

© 2011 by Taylor and Francis Group, LLC

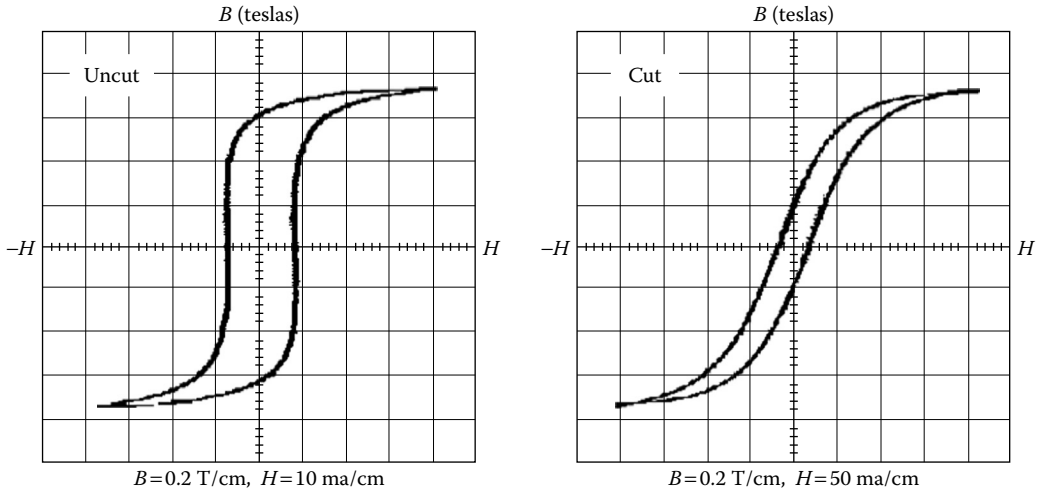

Figure 2-50. Supermalloy (F) B-H Loop, Uncut and Cut with Minimum Gap.

Table 2-18.

Comparing B_r/B_m on Uncut and Cut Cores					
Core Number*	Trade Name	Teslas B_s	Turns N	Uncut B_r/B_m	Cut B_r/B_m
52029-2A	Orthonol	1.45	54	0.96	0.62
52029-2D	Sq. Permalloy	0.75	54	0.86	0.21
52029-2F	Superpermalloy	0.75	54	0.81	0.24
52029-2K	Magnesil	1.60	54	0.93	0.22
* Magnetics toroidal cores.					

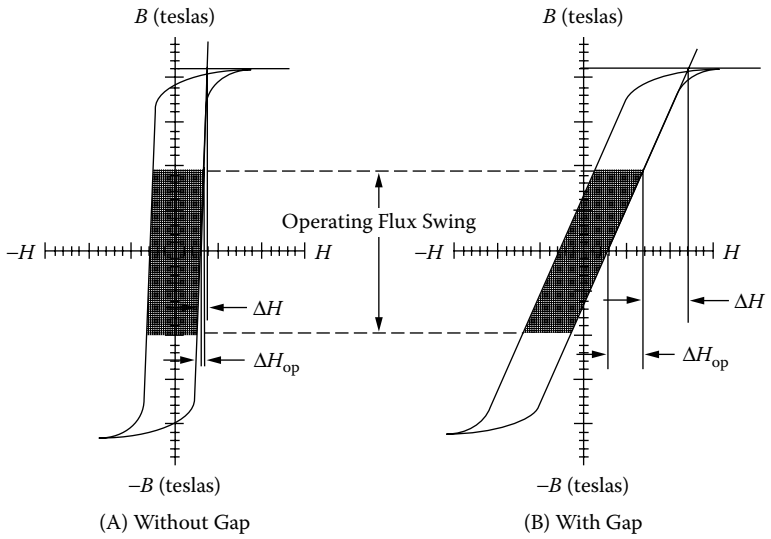

Figure 2-51. Defining ΔH_{op} and ΔH.

© 2011 by Taylor and Francis Group, LLC

Table 2-19. Comparing ΔH and ΔH_{op} on Uncut and Cut Cores

Comparing ΔH and ΔH_{op} on Uncut and Cut Cores							
				Ampere-turns/cm			
Material *Trade Name	Teslas B_m	Teslas B_{ac}	Teslas B_{dc}	Uncut		Cut	
				ΔH_{op}	ΔH	ΔH_{op}	ΔH
Orthonol	1.44	1.15	0.288	0.0125	0	0.895	0.178
Sq permalloy	0.73	0.58	0.146	0.0100	0.005	0.983	0.178
Supermalloy	0.63	0.58	0.136	0.0175	0.005	0.491	0.224
Magnesil	1.54	1.23	0.310	0.0750	0.025	7.150	1.780
* Magnetics cores.							

A direct comparison of cut and uncut cores was made electrically by means of two different test circuits. The magnetic material used in this branch of the test was Orthonol. The frequency was 2.4 kHz, and the flux density was 0.6 T. The first test circuit, shown in Figure 2-52, was a driven inverter operating into a 30-W load, with the power MOSFETs, operating into and out of saturation. Drive was applied continuously. S1 controls the supply voltage to Q1 and Q2.

With switch, S1, closed, transistor, Q1, was turned on and allowed to saturate. This applied voltage, E-$V_{DS(on)}$, across the transformer winding. Switch, S1, was then opened. Then, the flux in transformer, T2, dropped to the residual flux density, B_r. Switch, S1, was closed again. This was done several times in succession to catch the flux in an additive direction. Figures 2-53 and 2-54 show the inrush current measured at the center tap of, T2.

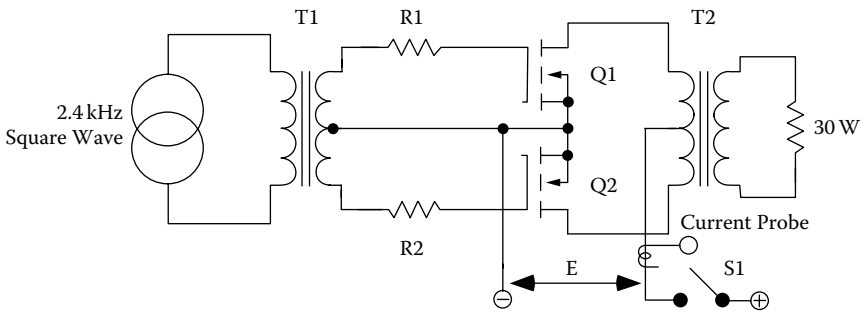

Figure 2-52. Inverter Inrush Current Test Fixture.

© 2011 by Taylor and Francis Group, LLC

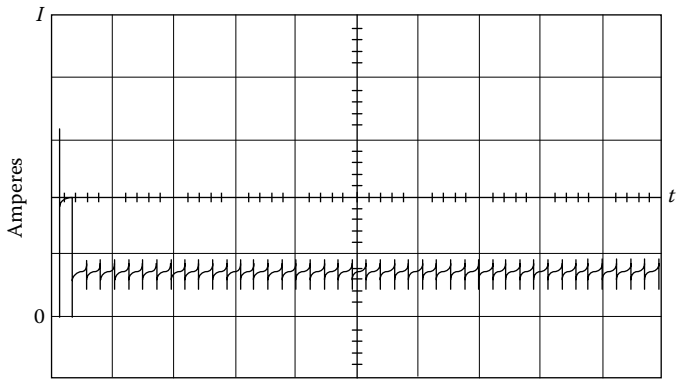

Figure 2-53. Typical Inrush Current of a Uncut Core in a Driven Inverter.

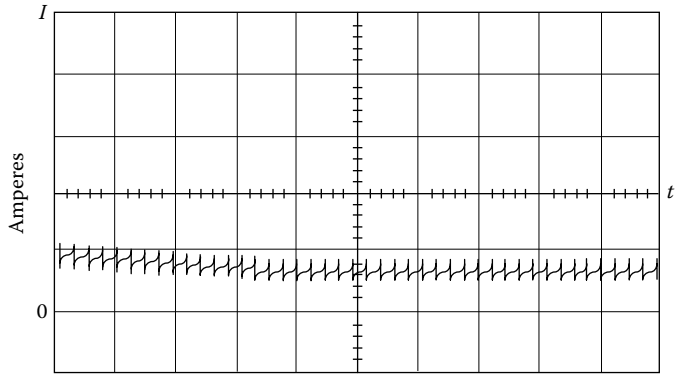

Figure 2-54. Resulting Inrush Current using a Cut Core.

It will be noted, in Figure 2-53, that the uncut core saturated, and the inrush current was limited only by circuit resistance and power, MOSFETs $R_{DS(on)}$. Figure 2-54 shows that saturation did not occur in the case of the cut core. Thus, the high inrush current and transistor stress were virtually eliminated.

The second test circuit arrangement is shown in Figure 2-55. The purpose of this test was to excite a transformer and measure the inrush current, using a current probe. A square wave power oscillator was used to excite transformer, T2. Switch, S1, was opened and closed several times to catch the flux in an additive direction. Figures 2-56 and 2-57 show inrush current for an uncut and cut core, respectively.

A small amount of air gap, less than 25 µm, has a powerful effect on the demagnetizing force, but little effect on the core loss. This small air gap decreases the residual magnetism by "shearing over" the hysteresis loop, which eliminates the problem of the core tending to remain saturated.

A typical example of the merits of the cut core occurred in the checkout of a Mariner spacecraft. During the checkout of a prototype science package, a large (8 A, 200 us) turn-on transient was observed. The normal running current was 0.06 A, fused with a parallel-redundant 1/8-A fuse, as required by the Mariner Mars design philosophy. With the 8-A inrush current, the 1/8-A fuses were easily blown. This did not happen, on

© 2011 by Taylor and Francis Group, LLC

every turn-on, but only when the core would "latch up" in the wrong direction for turn-on. Upon inspection, the transformer turned out to be a 50-50 nickel-iron toroid. The design was changed from a toroidal core to a cut core, with a 25 μm, air gap. The new design was completely successful in eliminating the 8-A turn-on transient.

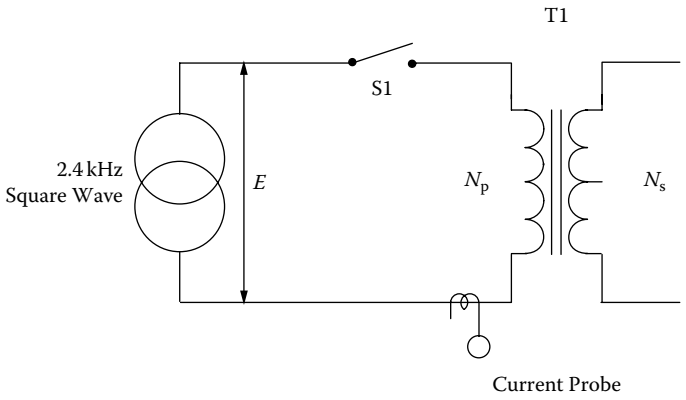

Figure 2-55. Transformer Rectifier Inrush Current Measurement.

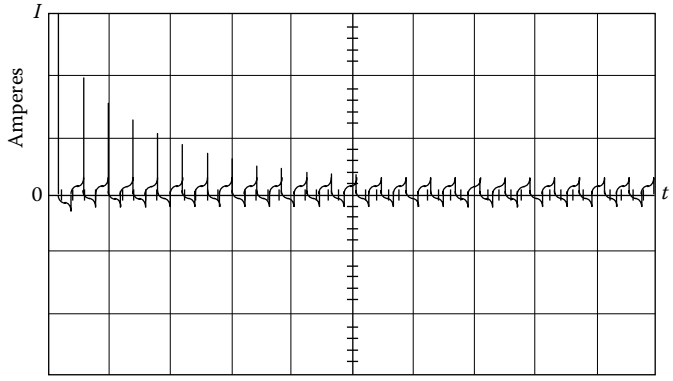

Figure 2-56. Inrush Current of a Transformer using a Uncut Core.

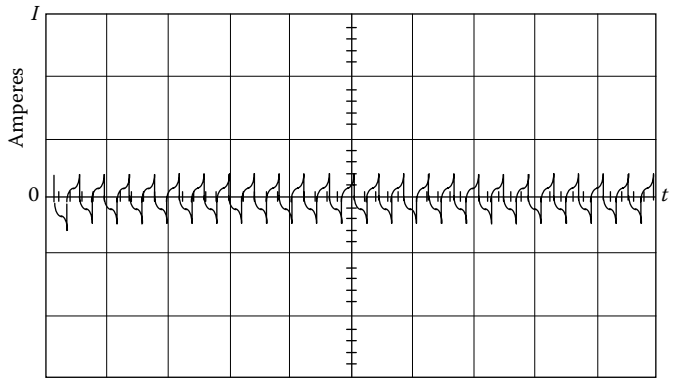

Figure 2-57. Inrush Current of a Transformer using a Cut Core.

© 2011 by Taylor and Francis Group, LLC

Composite Core Configuration

A composite core configuration has been developed for transformers that combine the protective feature of a gapped core with the much lower magnetizing current requirement of an uncut core. The uncut core functions, under normal operating conditions, and the cut core takes over during abnormal conditions to prevent high switching transients and their potentially destructive effect on the transistors.

This configuration is a composite of cut and uncut cores assembled together concentrically, with the uncut core nested within the cut core. The uncut core has high permeability, and thus requires a very small magnetizing current. On the other hand, the cut core has a low permeability and thus requires a much higher magnetization current. The uncut core is designed to operate at a flux density that is sufficient for normal operation of the converter. The uncut core may saturate under the abnormal conditions previously described. The cut core then takes over and supports the applied voltage so that excessive current does not flow. In a sense, it acts like a ballast resistor in some circuits to limit current flow to a safe level.

Figures 2-58 and 2-59 show the magnetization curves for an uncut core and a composite core of the same material at the same flux density. The much lower, B_r characteristic of the composite compared to the uncut core is readily apparent.

The desired features of the composite core can be obtained more economically by using different materials for the cut and uncut portions of the core. It was found that when the design required high nickel (4/79), the cut portion could be low nickel, (50/50), and because low nickel has twice as high a flux density as high nickel, the core was made of 66% high nickel, and 33% low nickel.

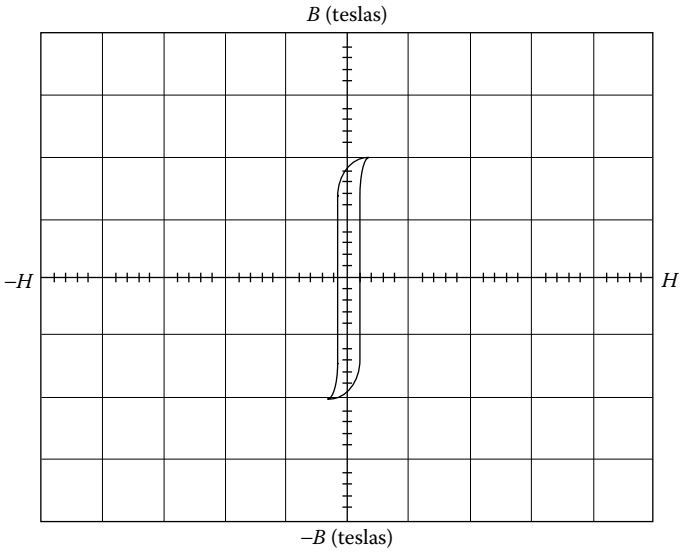

Figure 2-58. Uncut Core Excited at 0.2 T/cm.

© 2011 by Taylor and Francis Group, LLC

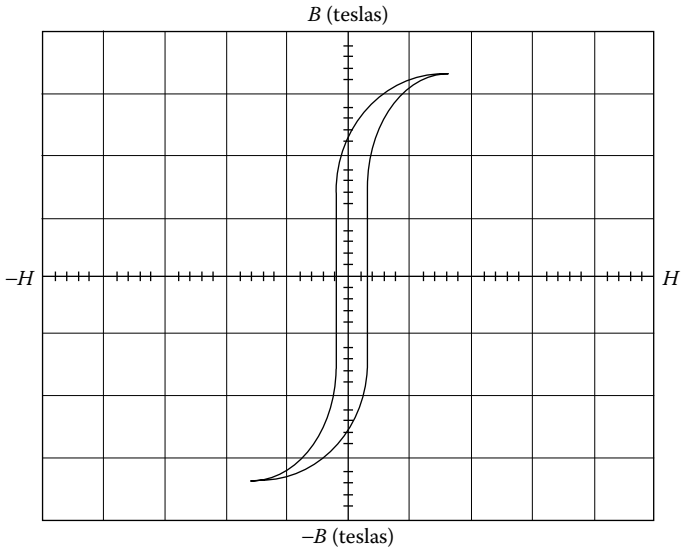

Figure 2-59. Both Cut and Uncut Cores Excited at 0.2 T/cm.

Figure 2-60 shows cut and uncut cores that have been impregnated to bond the ribbon layers together. The uncut core was first trimmed to fit within the inner diameter of the cut core by peeling off a wrap or two of the ribbon steel. The two cores are assembled into a composite core (Figure 2-61, on the right).

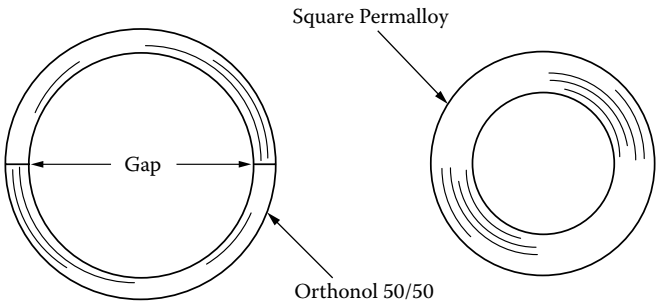

Figure 2-60. Composite Cores Ready for Final Assembly.

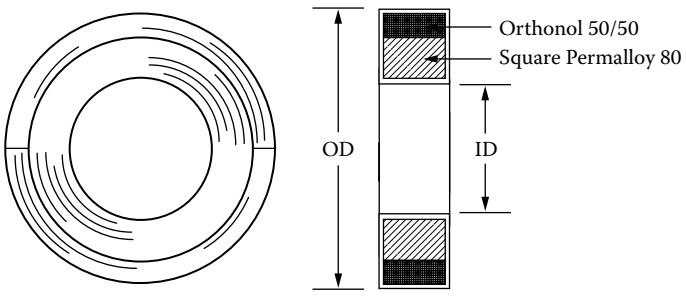

Figure 2-61. Composite Cores Assembled in Final Form.

© 2011 by Taylor and Francis Group, LLC

To ensure uniform characteristics for gapped cores, a gap dimension of 50 μm is recommended, because variations produced by thermal cycling will not affect this gap greatly. In the composite core, the gap is obtained by inserting a sheet of paper Mylar or Kapton film material between the core ends during banding. The same protective feature can be accomplished in transformers with laminated cores. When laminations are stacked by interleaving them one-by-one, the result will be a minimum air gap, as shown in Figure 2-62 by the squareness of the B-H loop. Shearing over of the B-H loop, or decreasing the residual flux, as shown in Figure 2-63, is accomplished by butt joining half the laminations in the core-cross section, which introduces a small, additional air gap.

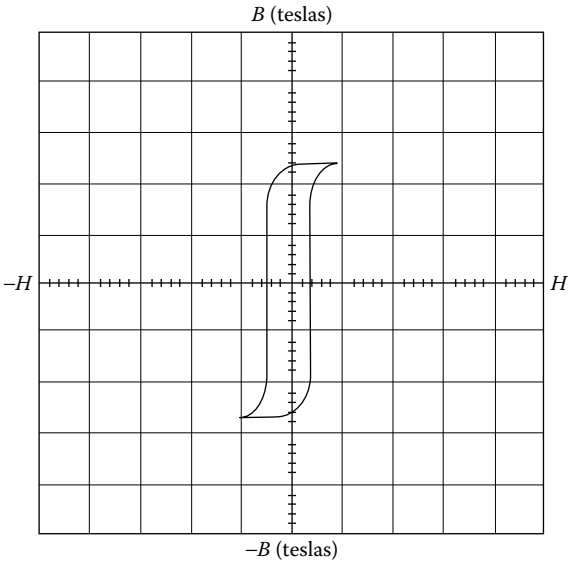

Figure 2-62. B-H Loop with Laminations Stacked 1×1 Interleaved.

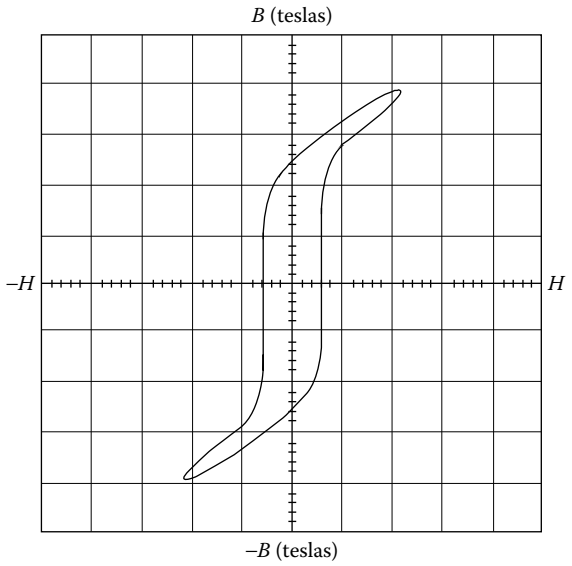

Figure 2-63. B-H Loop with Laminations Stack Half 1×1 and Half Butt Stack.

© 2011 by Taylor and Francis Group, LLC

Table 2-20 is a compiling of composite cores manufactured by Magnetics Inc., alongside their standard dimensional equivalent cores. Also, included in Table 2-20, is the cores' area product, A_p, and the core geometry K_g, which is discussed in Chapter 7.

Table 2-20. Composite Core Listing Along with the Area Product and Core Geometry

Magnetics Inc. Composite Cores			
Composite Number	Standard Core Number	A_p (cm^4)	K_g (cm^5)
01605-2D	52000	0.0728	0.00105
01754-2D	52002	0.1440	0.00171
01755-2D	52076	0.2850	0.00661
01609-D2	52061	0.3890	0.00744
01756-2D	52106	0.4390	0.00948
01606-2D	52094	0.6030	0.02210
01761-2D	52318	0.7790	0.02600
01757-2D	52029	1.0900	0.02560
01760-2D	52188	1.1520	0.05120
02153-2D	52181	1.2200	0.04070
01758-2D	52032	1.4550	0.04310
01607-2D	52026	2.1800	0.08740
01966-2D	52030	2.3370	0.06350
01759-2D	52038	2.9100	0.14000
01608-2D	52035	4.6760	0.20600
01623-2D	52425	5.2550	0.26200
01624-2D	52169	7.1300	0.41800
A_c = 66% Square Permalloy 4/79. A_c = 33% Orthonol 50/50. l_g = 2 mil Kapton.			

Summary

Low-loss tape-wound toroidal core materials, that have a very square hysteresis characteristic, (B-H loop), have been used extensively in the design of spacecraft transformers. Due to the squareness of the B-H loops of these materials, transformers designed with them tend to saturate quite easily. As a result, large voltage and current spikes, which cause undue stress on the electronic circuitry, can occur. Saturation occurs when there is any unbalance in the ac drive to the transformer, or when any dc excitation exists. Also, due to the square characteristic, a high residual flux state, (high, B_r), may remain when excitation is removed. Reapplication of excitation in the same direction may cause deep saturation, and an extremely large current spike. Limited by source impedance and transformer winding resistance can result. This can produce catastrophic failure.

© 2011 by Taylor and Francis Group, LLC

With the introduction of a small, (less than 25 μm), air gap into the core, the problems described above can be avoided while retaining the low-loss properties of the materials. The air gap has the effect of "shearing over" the B-H loop of the material so that the residual flux state is low. The margin between operating flux density and saturation flux density is high. The air gap thus has a powerful demagnetizing effect upon the square loop materials. Properly designed transformers, using cut toroid or C core square-loop materials, will not saturate upon turn-on, and can tolerate a certain amount of unbalanced drive or dc excitation.

It must be emphasized, however, that because of the nature of the material and the small size of the gap, extreme care and control must be taken in performing the gapping operation. Otherwise, the desired shearing effect will not be achieved, and the low-loss properties will be lost. The cores must be very carefully cut, lapped, and etched to provide smooth, residue-free surfaces. Reassembly must be performed with equal care.

A conversion, Table 2-21, has been added by popular request.

Table 2-21. Conversion Table

Conversion Table			
Item	Multiply	By	To Obtain
1	oersteds	79.5	amp-turn/m
2	oersteds	0.795	amp-turn/cm
3	amp-turn/m	0.0126	oersteds
4	amp-turn/cm	1.26	oersteds
5	gausses	0.0001	teslas
6	gausses	0.1	millitesla
7	teslas	10000	gausses
8	millitesla	10	gausses
9	inch	2.54	cm
10	cm	0.3937	inch
11	$inch^2$	6.452	cm^2
12	cm^2	0.155	$inch^2$
13	circular mils	5.07×10^{-6}	cm^2
14	cm^2	0.197×10^{6}	circular mils
15	ounces	28.35	grams
16	grams	0.0353	ounces
17	pounds	453.6	grams
18	grams	0.002205	pounds

© 2011 by Taylor and Francis Group, LLC

Chapter 3

Magnetic Cores

© 2011 by Taylor and Francis Group, LLC

Table of Contents

1. Introduction....3-4
2. Core Type and Shell Type Construction....3-5
3. Types of Core Materials....3-5
4. Eddy Currents and Insulation....3-6
5. Laminations....3-7
6. Annealing and Stress-Relief....3-8
7. Stacking Laminations and Polarity....3-9
8. Flux Crowding....3-10
9. Exciting Current....3-11
10. Tape Wound C, EE, and Toroidal Cores....3-12
11. Tape Toroidal Cores....3-14
12. Toroidal, Powder Core....3-15
13. Stacking Factors....3-15
14. Introduction to the Magnetic Cores....3-16
15. Design and Dimensional Data for EI Laminations....3-17
16. Design and Dimensional Data for UI Laminations....3-18
17. Design and Dimensional Data for LL Laminations....3-19
18. Design and Dimensional Data for DU Laminations....3-20
19. Design and Dimensional Data for Three-Phase Laminations....3-21
20. Design and Dimensional Data for Tape Wound C Cores....3-22
21. Dimensional Outline for Tape Wound EE Cores....3-23
22. Design and Dimensional Data for Tape Wound Toroidal Cores....3-24
23. Design and Dimensional Data for EE Ferrite Cores....3-25
24. Design and Dimensional Data for EE and EI Planar, Ferrite Cores....3-26
25. Design and Dimensional Data for EC, Ferrite Cores....3-27
26. Design and Dimensional Data for ETD, Ferrite Cores....3-28
27. Design and Dimensional Data for ETD/(low profile), Ferrite Cores....3-29
28. Design and Dimensional Data for ER, Ferrite Cores....3-30
29. Design and Dimensional Data for EFD, Ferrite Cores....3-31
30. Design and Dimensional Data for EPC, Ferrite Cores....3-32
31. Design and Dimensional Data for PC, Ferrite Cores....3-33
32. Design and Dimensional Data for EP, Ferrite Cores....3-34
33. Design and Dimensional Data for PQ, Ferrite Cores....3-35

© 2011 by Taylor and Francis Group, LLC

34. Design and Dimensional Data for PQ/(low profile), Ferrite Cores 3-36
35. Design and Dimensional Data for RM, Ferrite Cores 3-37
36. Design and Dimensional Data for RM/(low profile), Ferrite Cores 3-38
37. Design and Dimensional Data for DS, Ferrite Cores 3-39
38. Design and Dimensional Data for UUR, Ferrite Cores 3-40
39. Design and Dimensional Data for UUS, Ferrite Cores 3-41
40. Design and Dimensional Data for Toroidal, Ferrite Cores 3-42
41. Design and Dimensional Data for Toroidal, MPP Powder Cores 3-43
42. Design and Dimensional Data for Toroidal, Iron Powder Cores 3-44
43. Design and Dimensional Data for Toroidal, Sendust Powder Cores 3-45
44. Design and Dimensional Data for Toroidal, High Flux Powder Cores 3-46
45. Design and Dimensional Data for EE, Iron Powder Cores 3-47
46. Design and Dimensional Data for EE, Sendust Powder Cores 3-48
47. Manufacturers' Material Product List 3-49
48. References 3-50

© 2011 by Taylor and Francis Group, LLC

Introduction

The key ingredient in a magnetic device is the magnetic field (flux) created when current is passed through a coiled wire. The ability to control (channel, predict, conduct), the magnetic field (flux) is critical to controlling the operation of the magnetic device.

The ability of a material to conduct magnetic flux is defined as permeability. A vacuum is defined as having a permeability of 1.0 and the permeability of all other materials is measured against this baseline. Most materials, such as air, paper, and wood are poor conductors of magnetic flux, in that they have low permeability. If wire is wound on a dowel, it exhibits an exact magnetic field, as shown in Figure 3-1. There are a few materials, such as iron, nickel, cobalt, and their alloys that have high permeabilities, sometimes ranging into the hundreds of thousands. These materials and their alloys are used as the base materials for all core materials.

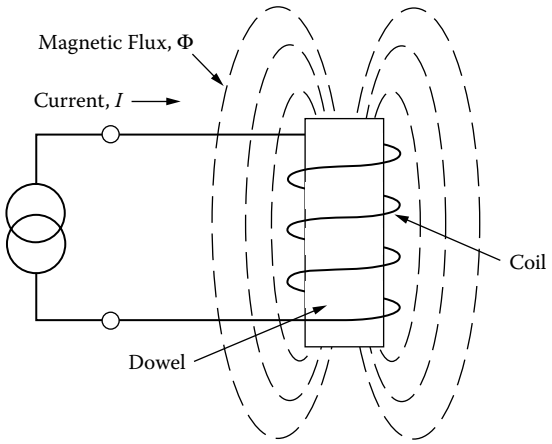

Figure 3-1. Air Core with an Intensified Magnetic Field.

The main purpose of the core is to contain the magnetic flux and create a well-defined, predictable path for the flux. This flux path, and the mean distance covered by the flux within the magnetic material, is defined as the Magnetic Path Length (MPL) (see Figure 3-2). The Magnetic Path Length and permeability are vital keys

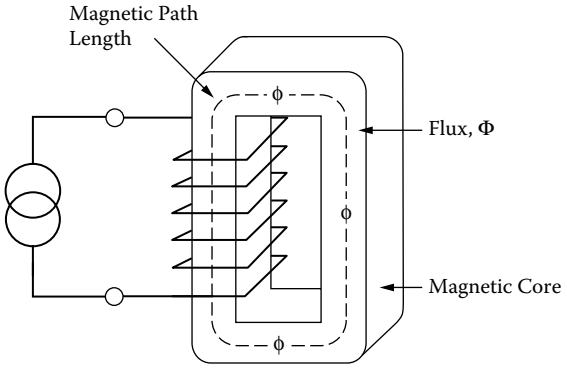

Figure 3-2. Magnetic Core Confines the Magnetic Field.

© 2011 by Taylor and Francis Group, LLC

in predicting the operation characteristic of a magnetic device. Selection of a core material and geometry are usually based on a compromise between conflicting requirements, such as size, weight, temperature rise, flux density, core loss, and operating frequency.

Core Type and Shell Type Construction

There are two types of construction for magnetic cores, core type and shell type. The shell type construction is shown in Figure 3-3, and the core type construction is shown in Figure 3-4. In the shell type, shown in Figure 3-3, the core surrounds the coil. Here, the magnetic fields are around the outside of the coil. The advantage of this configuration is that it requires only one coil. In the core type of construction, shown in Figure 3-4, the coils are outside of the core. A good example of this is a toroid, where the coil is wound on the outside of a core.

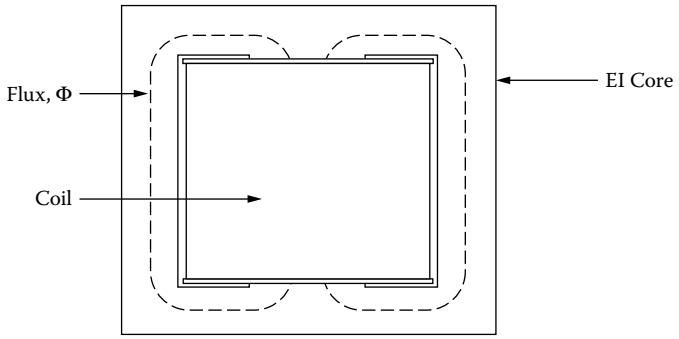

Figure 3-3. Shell Type Construction: the Core Surrounds the Coil.

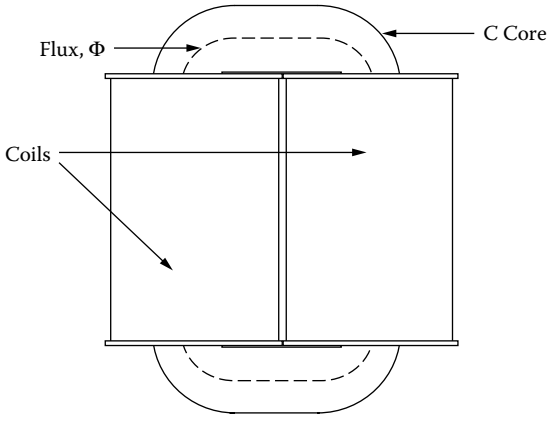

Figure 3-4. Core Type Construction the Coil Surrounds the Core.

Types of Core Materials

Magnetic cores are made of three basic materials. The first is bulk metal, the second is powdered materials, and the third is ferrite material.

© 2011 by Taylor and Francis Group, LLC

The bulk metals are processed from the furnace into ingots. Then, the material is put into a process of hot and cold rolling. The rolling process produces a sheet of material with a thickness ranging from 0.004 to 0.031 inches that can be punched into laminations. It can be further rolled into thicknesses ranging from 0.002 to 0.000125 inches, then slit and wound into tape cores, such as C cores, E cores and toroids.

The powder cores, such as powder molypermalloy and powdered iron materials, are die-pressed into toroids, EE cores and slugs. Powder core processing starts at the ingot, then goes through various steps of grinding until the powder is the right consistency for the required performance. Normally, powder cores are not machined after processing.

Ferrites are ceramic materials of iron oxide, alloyed with oxides or carbonate of manganese, zinc, nickel, magnesium, or cobalt. Alloys are selected and mixed, based on the required permeability of the core. Then, these mixtures are molded into the desired shape with pressure of approximately 150-200 tons per square inch and fired at temperatures above 2000 degrees F. After the parts are made, they are usually tumbled to remove burrs and sharp edges, which are characteristic of this process. Ferrites can be machined to almost any shape to meet the engineer's needs.

Eddy Currents and Insulation

Transformers, operating at moderate frequency, require the reduction of eddy current losses in the magnetic material. To reduce the eddy current losses to a reasonable value requires electrical steel to have adequate resistivity. Also, it needs to be rolled to a specific thickness, and it needs effective electrical insulation or coating of the magnetic material.

If an alternating voltage is applied to the primary winding, as shown in Figure 3-5, it will induce an alternating flux in the core. The alternating flux will, in turn, induce a voltage on the secondary winding. This alternating

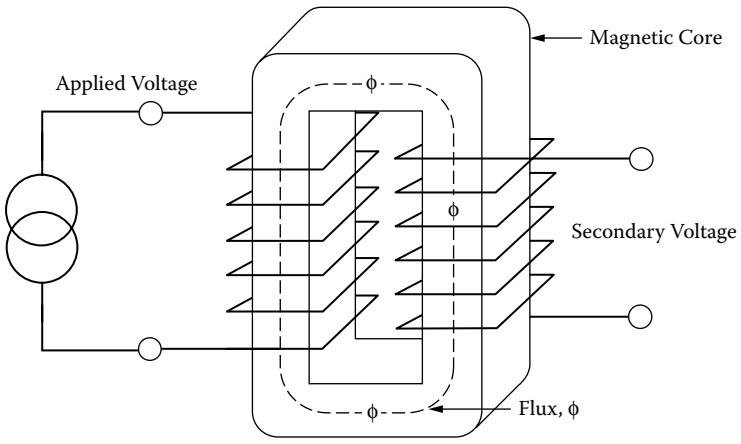

Figure 3-5. Applied Alternating Voltage Induces an Alternating Flux.

© 2011 by Taylor and Francis Group, LLC

flux also induces a small alternating voltage in the core material. These voltages produce currents called eddy currents, which are proportional to the voltage. The magnitude of these eddy currents is also limited by the resistivity of the material. The alternating flux is proportional to the applied voltage. Doubling the applied voltage will double the eddy currents. This will raise the core loss by a factor of four. Eddy currents not only flow in the lamination itself, but could flow within the core as a unit, if the lamination is not properly stamped, and if the lamination is not adequately insulated, as shown in Figure 3-6.

There are two eddy currents, as shown in Figure 3-6, i_a and i_b. The intralaminar eddy current, i_a, is governed by flux, per lamination and resistance of the lamination. It is, therefore, dependent on lamination width, thickness, and volume resistivity.

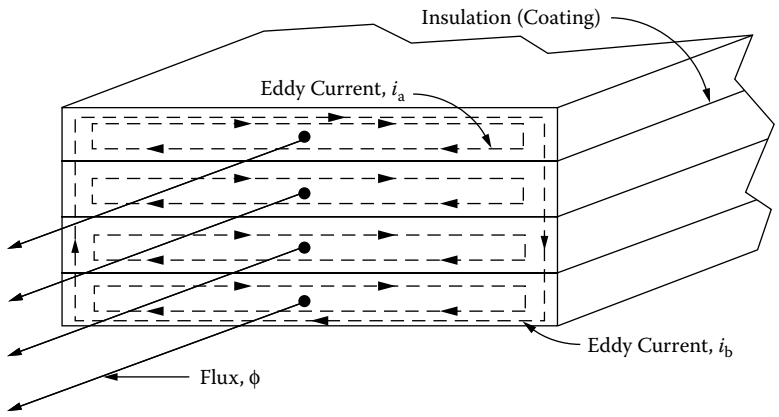

Figure 3-6. Insulation is Required between Laminations to Reduce Eddy Currents.

The interlaminar eddy current, i_b, is governed by total flux and resistance of the core stack. It is primarily dependent upon stack width and height, the number of laminations, and the surface insulation resistance, per lamination.

The magnetic materials used for tape cores and laminations are coated with an insulating material. The insulating coating is applied to reduce eddy currents. The American Iron and Steel Institute (AISI) has set up insulation standards for transformer steels used in different applications. High permeability, nickel-iron cores are very strain sensitive. Manufacturers of these cores normally have their own proprietary, insulating material.

Laminations

Laminations are available in scores of different shapes and sizes. The punch press technology for fabricating laminations has been well-developed. Most lamination sizes have been around forever. The most commonly used laminations are the EI, EE, FF, UI, LL, and the DU, as shown in Figure 3-7. The laminations differ from each other by the location of the cut in the Magnetic Path Length. This cut introduces an air gap, which results

© 2011 by Taylor and Francis Group, LLC

in the loss of permeability. To minimize the resulting air gap, the laminations are generally stacked in such a way that the air gaps in each layer are staggered.

There are bobbins and brackets for almost all standard stacking dimensions. Most of the EI lamination is the scrapless. The name, scrapless, is derived from shapes that are punched with minimum waste, as shown in Figure 3-8.

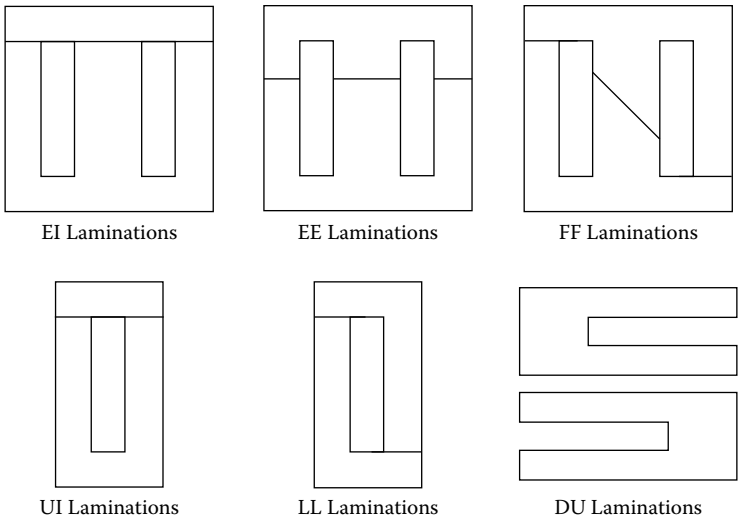

Figure 3-7. Commonly Used, Lamination Shapes.

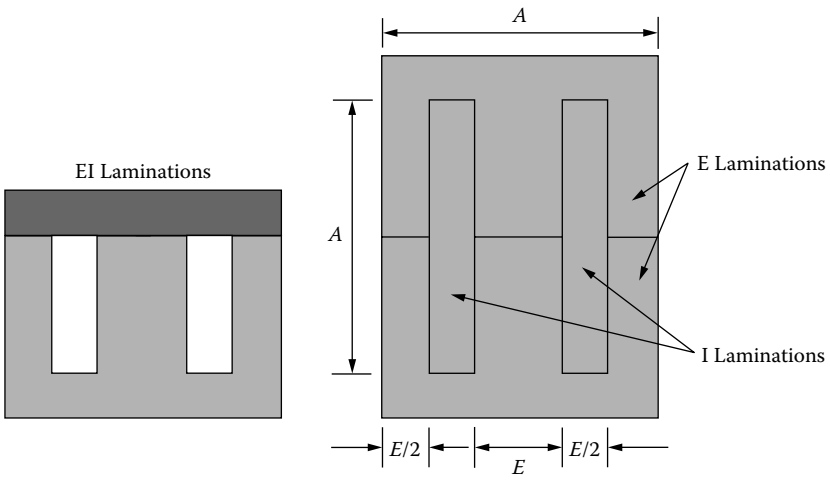

Figure 3-8. Typical, Scrapless EI Lamination.

Annealing and Stress-Relief

One of the most important parameters in transformer steels is permeability. Any stress or strain of the magnetic materials will have an impact on the permeability. The resulting stress could cause higher magnetizing current, or a lower inductance. When the transformer is being assembled (in the stacking process), and

© 2011 by Taylor and Francis Group, LLC

a lamination is bent, (does not return to its original shape), that lamination has been stressed and should be replaced.

Some of the important magnetic properties are lost due to stress and strain after stamping, shearing and slitting. These properties, that have been lost or seriously reduced, can be restored to the magnetic materials by annealing. Basically, stress relief is accomplished by heating (annealing) the magnetic material to prescribed temperature, (depending on the material), followed by cooling to room temperature. The entire annealing process is a delicate operation. The annealing must be done under controlled conditions of time, temperature and the ambient atmosphere that will avoid, even minute, adverse changes in the chemistry of the steel.

Stacking Laminations and Polarity

The edges of the magnetic material that have been stamped, sheared, or slit, will have a burr, as shown in Figure 3-9. The quality of the equipment will keep the burr to a minimum. This burr now gives the lamination a polarity. When a transformer is being stacked, the lamination build is normally sized by dimensions, or it just fills the bobbin.

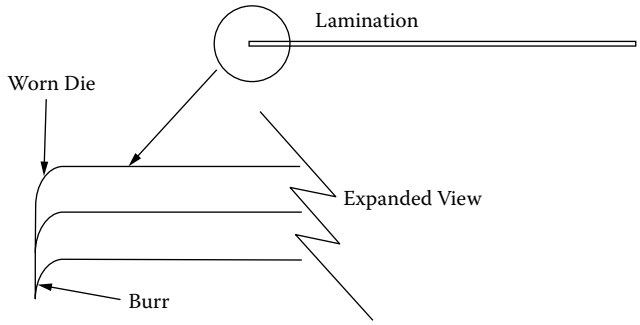

Figure 3-9. Expanded View, Showing Lamination Burr.

If the laminations are stacked correctly, all of the burred ends will be aligned. If the laminations are stacked randomly, such as the burr ends facing each other, then, the stacking factor would be affected. The stacking factor has a direct impact on the cross-section of the core. The end result would be less iron. This could lead to premature saturation, as an increase in the magnetizing current, or a loss of inductance.

There are several methods used in stacking transformer laminations. The most common technique used in stacking laminations is the alternate method. The alternate method is where one set of laminations, such as an E and an I, are assembled. Then, the laminations are reversed, as shown in Figure 3-10. This technique, used in stacking, provides the lowest air gap and the highest permeability. Another method for stacking laminations is to interleave two-by-two, also shown in Figure 3-10. The second method of stacking would be in groups of two

© 2011 by Taylor and Francis Group, LLC

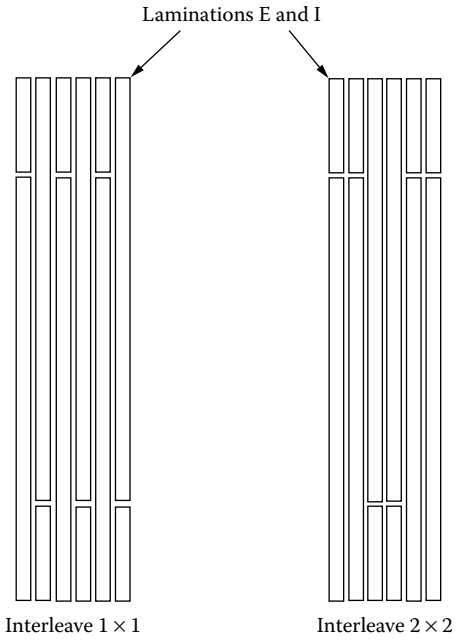

Figure 3-10. Methods for Stacking Laminations.

or more. This is done to cut the assembly time. The loss in performance in stacking, other than one-by-one, is the increase in magnetizing current and a loss of permeability.

Flux Crowding

When laminations are stacked, as shown in Figure 3-11, there is flux crowding. This flux crowding is caused by the difference in spacing between the E, I, and the adjacent lamination. The adjacent lamination has a minimum air gap, which translates into a higher permeability.

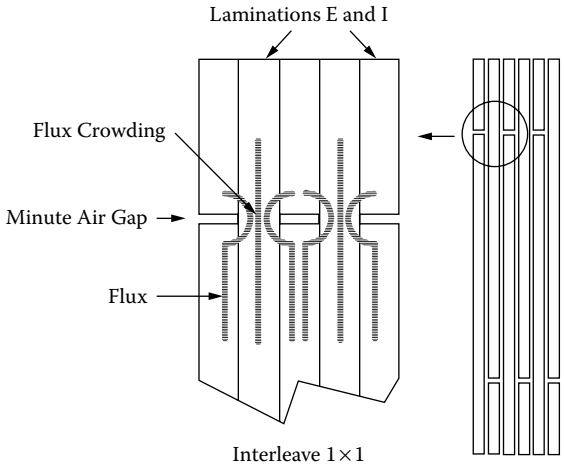

Figure 3-11. Flux Crowding, when Laminations are Interleaved.

© 2011 by Taylor and Francis Group, LLC

Exciting Current

The flux will skirt the low permeability air gap and migrate into the adjacent lamination, causing flux crowding in that lamination. Eventually, this crowding will cause saturation in that portion of the lamination, and the excitation current will rise. After that portion of the lamination has saturated, the flux will migrate back to the lower permeability segment of the lamination from where it left. This effect can be easily viewed by observing the B-H loops at low and high flux densities, and comparing them with a toroidal core of the same material, with a minimum air gap, as shown in Figure 3-12. The B-H loop, along with the magnetizing current, I_m, of a toroidal core, is shown in Figure 3-12A. The toroidal core, with its inherit minimum air gap, will have almost a square of current. Using the same material in lamination form will exhibit a B-H loop, and a magnetizing current, I_m, similar to Figure 3-12B operating at low flux densities. Increasing the excitation will cause premature saturation of the lamination, as seen by the non-linear, exciting current, as shown in Figure 3-12C.

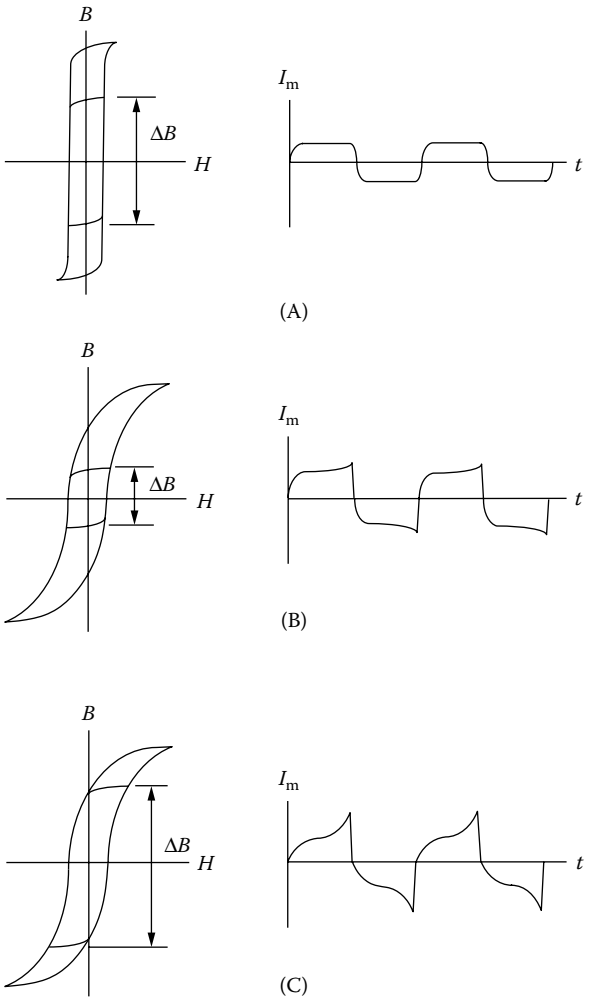

Figure 3-12. Comparing the Exciting Currents and Three B-H Loops.

© 2011 by Taylor and Francis Group, LLC

Most finished transformers or inductors will have some sort of bracket, such as an L bracket, end bells, a channel bracket or maybe a bolt through the mounting holes to the chassis. When transformers are being assembled, there is a certain amount of attention that has to be used to get proper performance. The insulation material used to coat the lamination is normally very durable, but it can be scratched off and degrade the performance. When brackets are used in the transformer assembly, as shown in Figure 3-13, care must be taken on how the bolts and brackets are put together. The transformer assembly bolts, shown in Figure 3-13, should be the recommended size for the mounting hole and use all of the required hardware. This hardware should include the correct bolt size and length, and correct surface washer, lock washer and nut. Also, included in this hardware, should be fiber shoulder washers and proper sleeving to cover the bolt threads. If insulating hardware is not used, there is a good chance of a partial, shorted turn. The continuity for this partial turn can be created through the bolts and bracket, or the bolts, bracket, and the chassis. This partial shorted turn will downgrade the performance of the transformer.

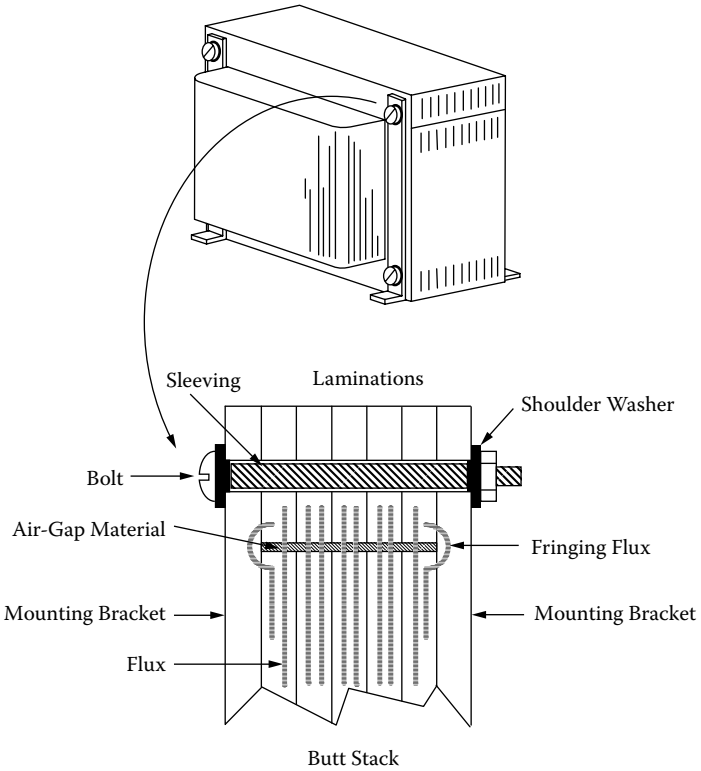

Figure 3-13. Lamination Mounting Hardware.

Tape Wound C, EE, and Toroidal Cores

Tape wound cores are constructed by winding around a mandrel, a magnetic material in the form of a preslit tape, as shown in Figure 3-14. This tape material comes in all of the iron alloys, plus the amorphous materials. The tape thickness varies from 0.0005 inch (0.0127 mm) to 0.012 inch (0.305 mm). The advantage of this type

© 2011 by Taylor and Francis Group, LLC

of construction is that the flux is parallel with the direction of rolling of the magnetic material. This provides the maximum utilization of flux with the minimum of magnetizing force. There are two disadvantages in this type of construction. When the core is cut in half, as shown in Figure 3-15, the mating surface has to be ground, lapped, and then, acid-etched. This is done to provide a smooth mating surface with the minimum of air gap and the maximum of permeability. The other disadvantage is when the cores are reassembled, the method used is normally done with a band and buckle, and this procedure requires a little skill to provide the right alignment and correct tension, as shown in Figure 3-16. The C cores are impregnated for strength, prior to being cut. The cut C core can be used in many configurations in the design of a magnetic component, as

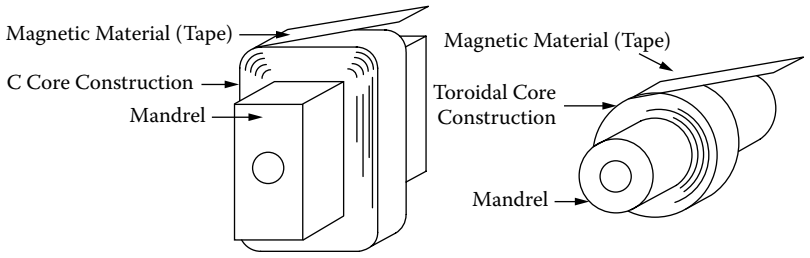

Figure 3-14. Tape Cores Being Wound on a Mandrel.

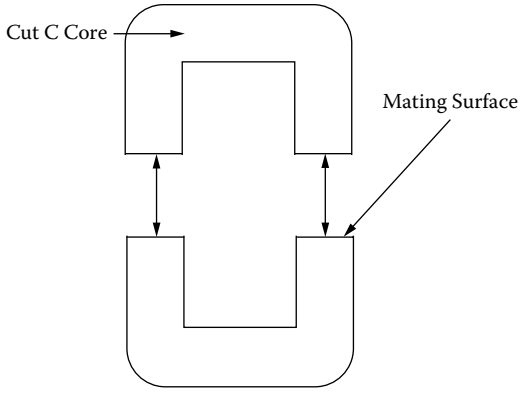

Figure 3-15. Two Halves of a Cut C Core.

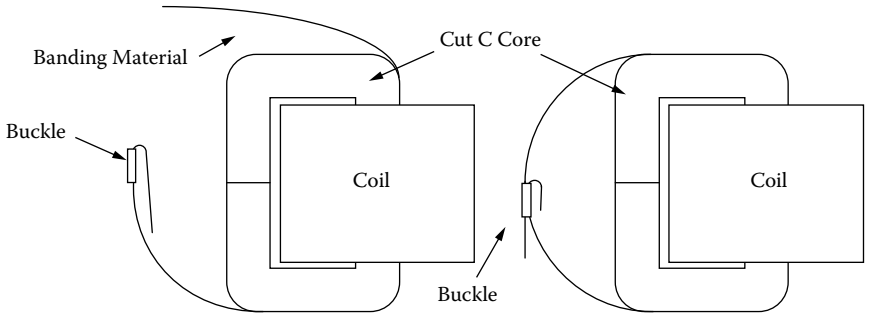

Figure 3-16. Banding the Cut C Core.

© 2011 by Taylor and Francis Group, LLC

shown in Figure 3-17. The EE cores are constructed in the same way as C cores, but they have an additional overwind, as shown in Figure 3-18. The assembled three-phase transformer is shown in Figure 3-19.

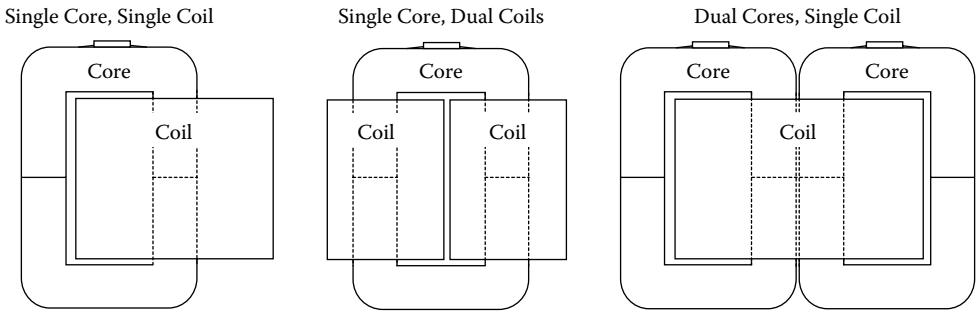

Figure 3-17. Three Different C Core Configurations.

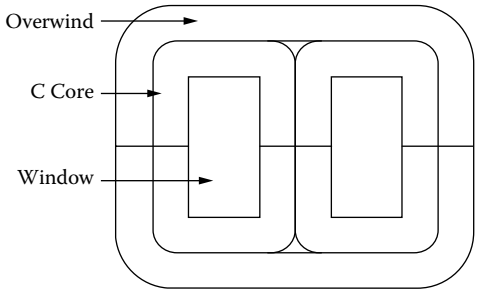

Figure 3-18. Three-Phase, Cut EE Core.

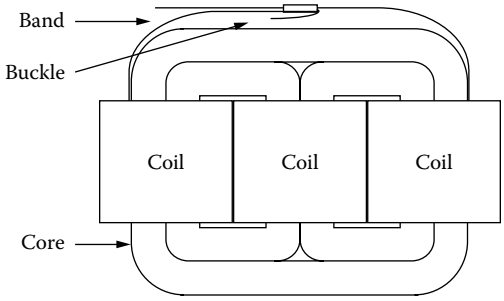

Figure 3-19. Typical, Assembled EE Cut Core.

Tape Toroidal Cores

Tape toroidal cores are constructed in the same way as tape C cores, by winding the magnetic material around a mandrel, in the form of a preslit tape. This tape material comes in all of the iron alloys, plus the amorphous materials. The tape thickness varies from 0.000125 inch (0.00318 mm) to 0.012 inch (0.305 mm). The tape toroid is normally offered in two configurations, cased and encapsulated, as shown in Figure 3-20. The cased toroid offers superior electrical properties and stress protection against winding. The encapsulated cores are used when not all of the fine magnetic properties are important to the design, as in power transformers.

© 2011 by Taylor and Francis Group, LLC

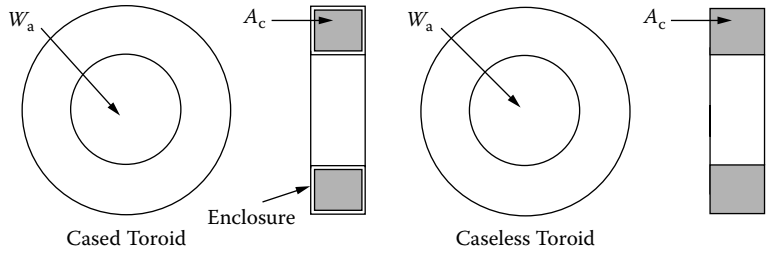

Figure 3-20. Outline of a Cased and a Caseless Toroidal Core.

Toroidal, Powder Core

Powder cores, as shown in Figure 3-21, are very unique. They give the engineer another tool to speed the initial design. Powder cores have a built-in air gap. They come in a variety of materials and are very stable with time and temperature. The cores are manufactured with good engineering aids. Manufacturers provide catalogs for their cores, listing not only the size, but also permeability and Millihenrys per 1000 turns. The data is presented to the engineer in such a way that it takes the minimum amount of time to have a design such that will function.

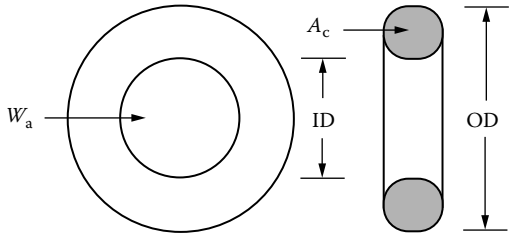

Figure 3-21. Outline of a Powder Toroidal Core.

Stacking Factors

The standard stacking factors for tape cores, wound cut cotes and laminations are shown in Table 3-1.

Table 3-1. Standard Stacking Factors

Standard Stacking Factors					
Thickness	Tape Cores	Wound Cut Cores	Laminations		$(S.F.)^2$
mils			Butt Stack	Interleave 1×1	
0.125	0.250				0.062
0.250	0.375				0.141
0.500	0.500				0.250
1.000	0.750	0.830			0.562
2.000	0.850	0.890			0.722
4.000	0.900	0.900	0.900	0.800	0.810
6.000		0.900	0.900	0.850	0.810
12.000	0.940	0.950			0.884
14.000	0.940	0.950	0.950	0.900	0.902
18.000			0.950	0.900	0.810
25.000			0.950	0.920	0.846

© 2011 by Taylor and Francis Group, LLC

Introduction to the Magnetic Core

The magnetic core data for this chapter has been taken from the catalogs of the leading manufacturers in the magnetics industry. The author has compiled dimensional data for over 200 magnetic cores. This compiled data has been placed into 32 tables. The 200 magnetic cores include:

1. Lamination, EI, UI, LL, DU and 3 phase EE cores.
2. Tape cores, C cores, Toroidal cores and 3 phase EE cores.
3. Ferrite cores, EE, UU, EC, ETD, Pot cores, PQ cores, RM cores, EFD cores, EPC cores.
4. Ferrite low profile core, EE, PQ cores, RM cores.
5. Molypermalloy powder cores, MPP cores.
6. High Flux powder cores, HF cores.
7. Sendust powder cores, Toroidal and EE cores.
8. Iron Powder cores, Toroidal and EE cores.

Following each dimensional table there is another table with design variables for each magnetic core. The list of variables are listed below:

1. The Weight of the copper, W_{tcu}.
2. The Weight of the core, W_{tfe}, is supplied by the manufacturer.
3. The Mean Length Turn, MLT, See Chapter 4.
4. The Magnetic Path Length, MPL, is supplied by the manufacturer.
5. The ratio of the Window Area, W_a, over the Iron Area, A_c. Magnetic cores that have small ratio are considered low frequency line transformers. For high frequency transformers the ratio should be three and above.
6. The Iron area, A_c, this is supplied by the manufacturer.
7. The Window area, W_a, is calculated from the dimensional table.
8. The Area Product, A_p, is a power handling equation. See Chapter 21.

$$A_p = W_a A_c, \quad [\text{cm}^4] \tag{3-1}$$

9. The Core Geometry, K_g, is a power handling equation. See Chapter 21.

$$K_g = \frac{W_a A_c^2 K_u}{\text{MLT}}, \quad [\text{cm}^5] \tag{3-2}$$

   The window utilization, K_u, has been calculated with 0.4 for all cores. When designing with ferrites or at high frequency, the window utilization, K_u, changes. See Chapter 4.
10. The Surface area, A_t, is calculated from the dimensional table. See Chapter 5.
11. The Millihenrys per 1000 turns, A_L, have been normalized for a permeability of 1000. For a close approximation, multiply this, A_L, value by the new permeability in kilo-perm. The permeability would change when using a 2500 perm by multiplying by 2.5.

© 2011 by Taylor and Francis Group, LLC

Design and Dimensional Data for EI Laminations

Laminations are still one of the most widely-used cores in power conversion. The dimensional outline for EI laminations and an assembled transformer is shown in Figure 3-22. Dimensional data for EI laminations is given in Table 3-2; design data is given in Table 3-3.

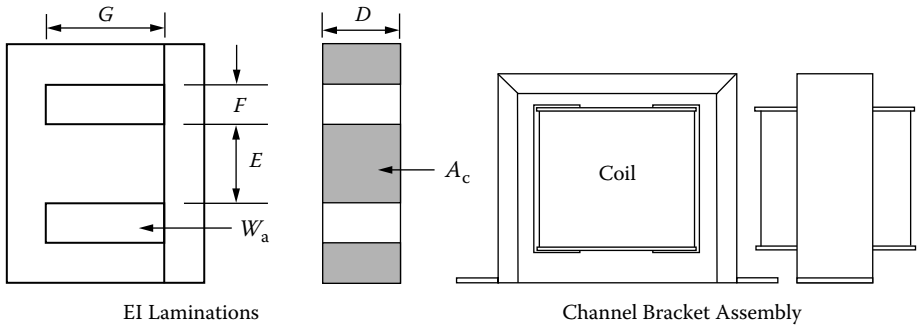

Figure 3-22. EI Lamination Outline.

Table 3-2. Dimensional Data for EI Laminations

EI, Laminations, (Tempel) 14 mil									
Part No.	D cm	E cm	F cm	G cm	Part No.	D cm	E cm	F cm	G cm
EI-375	0.953	0.953	0.794	1.905	EI-112	2.857	2.857	1.429	4.286
EI-021	1.270	1.270	0.794	2.064	EI-125	3.175	3.175	1.588	4.763
EI-625	1.588	1.588	0.794	2.381	EI-138	3.493	3.493	1.746	5.239
EI-750	1.905	1.905	0.953	2.857	EI-150	3.810	3.810	1.905	5.715
EI-875	2.223	2.223	1.111	3.333	EI-175	4.445	4.445	2.223	6.668
EI-100	2.540	2.540	1.270	3.810	EI-225	5.715	5.715	2.858	8.573

Table 3-3. Design Data for 14 mil EI Laminations

EI, Laminations, (Tempel) 14 mil										
Part No.	W_{tcu} grams	W_{tfe} grams	MLT cm	MPL cm	W_a/A_c	A_c cm^2	W_a cm^2	A_p cm^4	K_g cm^5	A_t cm^2
EI-375	36.1	47.2	6.7	7.3	1.754	0.862	1.512	1.303	0.067	46.2
EI-021	47.6	94.3	8.2	8.3	1.075	1.523	1.638	2.510	0.188	62.1
EI-625	63.5	170.0	9.5	9.5	0.418	2.394	1.890	4.525	0.459	83.2
EI-750	108.8	296.0	11.2	11.4	0.790	3.448	2.723	9.384	1.153	120.0
EI-875	171.0	457.0	13.0	13.3	0.789	4.693	3.705	17.384	2.513	163.0
EI-100	254.0	676.0	14.8	15.2	0.790	6.129	4.839	29.656	4.927	212.9
EI-112	360.0	976.0	16.5	17.2	0.789	7.757	6.124	47.504	8.920	269.4
EI-125	492.0	1343.0	18.3	19.1	0.789	9.577	7.560	72.404	15.162	333.0
EI-138	653.0	1786.0	20.1	21.0	0.789	11.588	9.148	106.006	24.492	403.0
EI-150	853.0	2334.0	22.0	22.9	0.789	13.790	10.887	150.136	37.579	479.0
EI-175	1348.0	3711.0	25.6	26.7	0.789	18.770	14.818	278.145	81.656	652.0
EI-225	2844.0	7976.0	32.7	34.3	0.789	31.028	24.496	760.064	288.936	1078.0

© 2011 by Taylor and Francis Group, LLC

Design and Dimensional Data for UI Laminations

The dimensional outline for UI laminations and an assembled transformer is shown in Figure 3-23. Dimensional data for UI laminations is given in Table 3-4; design data is given in Table 3-5.

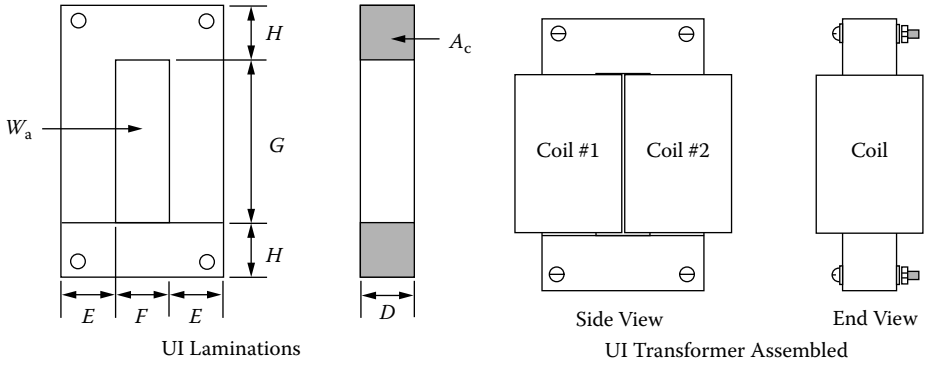

Figure 3-23. UI Lamination Outline.

Table 3-4. Dimensional Data for UI Laminations

UI, Standard Laminations 14 mil											
Part No.	D cm	E cm	F cm	G cm	H cm	Part No.	D cm	E cm	F cm	G cm	H cm
50UI	1.270	1.270	1.270	3.810	1.270	125UI	3.175	3.175	3.175	9.525	3.175
60UI	1.429	1.429	2.223	5.398	1.429	150UI	3.810	3.810	3.810	11.430	3.810
75UI	1.905	1.905	1.905	5.715	1.905	180UI	4.572	4.572	4.572	11.430	4.572
100UI	2.540	2.540	2.540	7.620	2.540	240UI	6.096	6.096	6.096	15.240	6.096

Table 3-5. Design Data for 14 mil UI Laminations

UI, Standard Laminations 14 mil										
Part No.	W_{tcu} grams	W_{tfe} grams	MLT cm	MPL cm	$\frac{W_a}{A_c}$	A_c cm^2	W_a cm^2	A_p cm^4	K_g cm^5	A_t cm^2
50UI	132	173	7.68	15.24	3.159	1.532	4.839	7.414	0.592	110
60UI	418	300	9.81	18.10	6.187	1.939	11.996	23.263	1.839	209
75UI	434	585	11.22	22.86	3.157	3.448	10.887	37.534	4.614	247
100UI	1016	1384	14.76	30.48	3.158	6.129	19.355	118.626	19.709	439
125UI	1967	2725	18.29	38.10	3.158	9.577	30.242	289.614	60.647	685
150UI	3413	4702	22.04	45.72	3.158	13.790	43.548	600.544	150.318	987
180UI	4884	7491	26.28	50.29	2.632	19.858	52.258	1037.740	313.636	1296
240UI	11487	17692	34.77	67.06	2.632	35.303	92.903	3279.770	1331.997	2304

© 2011 by Taylor and Francis Group, LLC

Design and Dimensional Data for LL Laminations

The dimensional outline for LL laminations and an assembled transformer is shown in Figure 3-24. Dimensional data for LL laminations is given in Table 3-6; design data is given in Table 3-7.

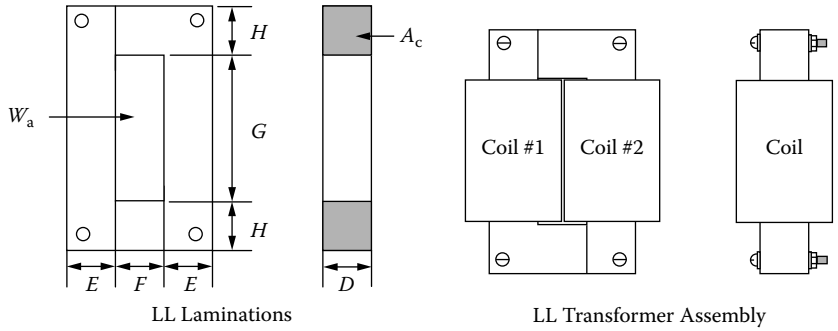

Figure 3-24. LL Lamination Outline.

Table 3-6. Dimensional Data for 14 mil LL Laminations

LL, Standard Laminations 14 mil											
Part No.	D cm	E cm	F cm	G cm	H cm	Part No.	D cm	E cm	F cm	G cm	H cm
141L	0.635	0.635	1.270	2.858	0.635	104L	1.270	1.270	1.984	5.555	1.270
108L	1.031	1.031	0.874	3.334	1.111	105L	1.270	1.270	1.905	6.826	1.270
250L	1.031	1.031	0.874	5.239	1.111	102L	1.429	1.429	1.588	5.398	1.429
101L	1.111	1.111	1.588	2.858	1.111	106L	1.429	1.429	2.223	5.398	1.429
7L	1.270	1.270	1.270	3.810	1.270	107L	1.588	1.588	2.064	6.350	1.588
4L	1.270	1.270	1.905	3.810	1.270						

Table 3-7. Design Data for 14 mil LL Laminations

LL, Standard Laminations 14 mil										
Part No.	W_{tcu} grams	W_{tfe} grams	MLT cm	MPL cm	$\frac{W_a}{A_c}$	A_c cm^2	W_a cm^2	A_p cm^4	K_g cm^5	A_t cm^2
141L	63.8	31.3	4.9	10.8	9.473	0.383	3.629	1.390	0.043	55.2
108L	61.2	97.9	5.9	12.7	2.884	1.010	2.913	2.943	0.201	70.3
250L	96.1	127.1	5.9	16.5	4.532	1.010	4.577	4.624	0.316	92.0
101L	118.5	115.9	7.3	13.3	3.867	1.173	4.536	5.322	0.340	97.3
7L	132.2	173.9	7.7	15.2	3.159	1.532	4.839	7.414	0.592	109.7
4L	224.0	185.2	8.7	16.5	4.737	1.532	7.258	11.121	0.785	141.9
104L	344.9	228.0	8.8	20.2	7.193	1.532	11.020	16.885	1.176	180.2
105L	401.3	256.5	8.7	22.5	8.488	1.532	13.004	19.925	1.407	199.4
102L	268.6	284.1	8.8	19.7	4.419	1.939	8.569	16.617	1.462	167.6
106L	418.6	302.1	9.8	21.0	6.187	1.939	11.996	23.263	1.839	208.8
107L	475.2	409.5	10.2	23.2	5.474	2.394	13.105	31.375	2.946	235.8

© 2011 by Taylor and Francis Group, LLC

Design and Dimensional Data for DU Laminations

The dimensional outline for DU laminations and an assembled transformer is shown in Figure 3-25. Dimensional data for DU laminations is given in Table 3-8; design data is given in Table 3-9.

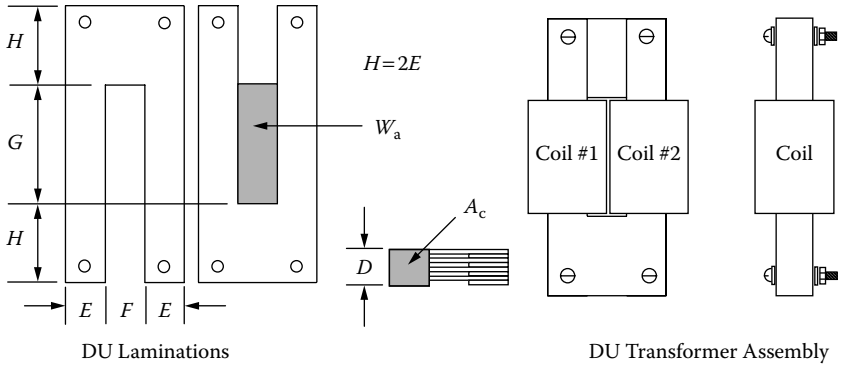

Figure 3-25. DU Lamination Outline.

Table 3-8. Dimensional Data for 14 mil DU Laminations

DU, Standard Laminations 14 mil											
Part No.	D cm	E cm	F cm	G cm	H cm	Part No.	D cm	E cm	F cm	G cm	H cm
DU-63	0.159	0.159	0.318	0.794	0.318	DU-39	0.953	0.953	0.953	2.858	1.905
DU-124	0.318	0.318	0.476	1.191	0.635	DU-37	0.953	0.953	1.905	3.810	1.905
DU-18	0.476	0.476	0.635	1.588	0.953	DU-50	1.270	1.270	2.540	5.080	2.540
DU-26	0.635	0.635	0.635	1.905	1.270	DU-75	1.905	1.905	3.810	7.620	3.810
DU-25	0.635	0.635	0.953	2.064	1.270	DU-1125	2.858	2.858	5.715	11.430	5.715
DU-1	0.635	0.635	0.953	3.810	1.270	DU-125	3.175	3.175	5.080	10.160	6.350

Table 3-9. Design Data for 14 mil DU Laminations

DU, Standard Laminations 14 mil										
Part No.	W_{tcu} grams	W_{tfe} grams	MLT cm	MPL cm	$\frac{W_a}{A_c}$	A_c cm^2	W_a cm^2	A_p cm^4	K_g cm^5	A_t cm^2
DU-63	1.4	0.6	1.5	3.2	10.500	0.024	0.252	0.006	0.00003	4.2
DU-124	4.9	4.3	2.4	5.2	5.906	0.096	0.567	0.054	0.0009	11.8
DU-18	11.9	13.5	3.3	7.3	4.688	0.215	1.008	0.217	0.0057	23.4
DU-26	17.0	28.9	3.9	8.9	3.159	0.383	1.210	0.463	0.0180	33.9
DU-25	31.1	30.4	4.4	9.9	5.133	0.383	1.966	0.753	0.0260	44.3
DU-1	57.3	42.4	4.4	13.3	9.634	0.383	3.630	1.390	0.0479	60.9
DU-39	55.3	104.5	5.7	13.3	3.158	0.862	2.722	2.346	0.1416	76.2
DU-37	186.0	124.5	7.2	17.2	8.420	0.862	7.258	6.256	0.2992	134.3
DU-50	443.9	287.8	9.7	22.8	8.422	1.532	12.903	19.771	1.2524	238.0
DU-75	1467.0	985.2	14.2	34.3	8.420	3.448	29.032	100.091	9.7136	537.1
DU-1125	4880.0	3246.0	21.0	51.4	8.421	7.757	65.322	506.709	74.8302	1208.0
DU-125	3906.0	3966.0	21.3	41.4	5.389	9.577	51.610	494.275	88.9599	1147.0

© 2011 by Taylor and Francis Group, LLC

Design and Dimensional Data for Three-Phase Laminations

The dimensional outline for 3Phase EI laminations and an assembled transformer is shown in Figure 3-26. Dimensional data for 3Phase EI laminations is given in Table 3-10; design data is given in Table 3-11.

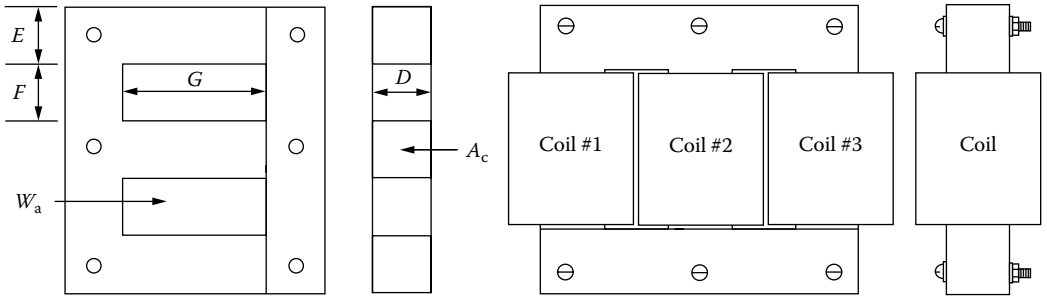

Figure 3-26. EI Three Phase Laminations Outline.

Table 3-10. Dimensional Data for 14 mil EI Three-Phase Laminations

3Phase, Standard Laminations, Thomas & Skinner 14 mil									
Part No.	D cm	E cm	F cm	G cm	Part No.	D cm	E cm	F cm	G cm
0.250EI	0.635	0.635	0.871	2.858	1.000EI	2.540	2.540	3.810	7.620
0.375EI	0.953	0.953	1.270	3.175	1.200EI	3.048	3.048	3.048	7.620
0.500EI	1.270	1.270	1.588	3.493	1.500EI	3.810	3.810	3.810	9.525
0.562EI	1.427	1.427	1.588	5.398	1.800EI	4.572	4.572	4.572	11.430
0.625EI	1.588	1.588	1.984	5.634	2.400EI	6.096	6.096	6.096	15.240
0.875EI	2.223	2.223	2.779	6.111	3.600EI	9.144	9.144	9.144	22.860

Table 3-11. Design Data for 14 mil EI Three Phase Laminations

3Phase, Standard Laminations, Thomas & Skinner 14 mil									
Part No.	W_{tcu} grams	W_{tfe} grams	MLT cm	$\frac{W_a}{2A_c}$	A_c cm^2	W_a cm^2	A_p cm^4	K_g cm^5	A_t cm^2
0.250EI	57	54	4.3	3.251	0.383	2.49	1.43	0.051	53
0.375EI	134	154	6.2	2.339	0.862	4.03	5.21	0.289	102
0.500EI	242	324	8.2	1.810	1.532	5.54	12.74	0.955	159
0.562EI	403	421	8.8	2.213	1.936	8.57	24.88	2.187	207
0.625EI	600	706	10.1	2.334	2.394	11.18	40.13	3.816	275
0.875EI	1255	1743	13.9	1.809	4.693	16.98	119.53	16.187	487
1.000EI	2594	2751	16.7	2.368	6.129	29.03	266.91	39.067	730
1.200EI	2178	3546	17.6	1.316	8.826	23.23	307.48	61.727	725
1.500EI	4266	6957	22.0	1.316	13.790	36.29	750.68	187.898	1132
1.800EI	7326	12017	26.3	1.316	19.858	52.26	1556.61	470.453	1630
2.400EI	17230	28634	34.8	1.316	35.303	92.90	4919.66	1997.995	2899
3.600EI	58144	96805	52.2	1.316	79.432	209.03	24905.75	15174.600	6522

© 2011 by Taylor and Francis Group, LLC

Design and Dimensional Data for Tape Wound C Cores

The dimensional outline for C cores is shown in Figure 3-27. Dimensional data for C cores is given in Table 3-12; design data is given in Table 3-13.

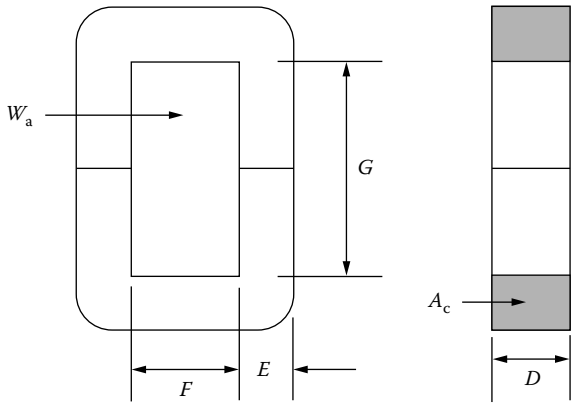

Figure 3-27. Tape C Core Dimensional Outline.

Table 3-12. Dimensional Data for Tape C Cores

C Cores, Magnetic Metals, 2 mil									
Part No.	D cm	E cm	F cm	G cm	Part No.	D cm	E cm	F cm	G cm
ML-002	0.635	0.476	0.635	1.588	ML-014	1.270	1.270	1.270	3.969
ML-004	0.635	0.635	0.635	2.223	ML-016	1.905	1.270	1.270	3.969
ML-006	1.270	0.635	0.635	2.223	ML-018	1.270	1.111	1.588	3.969
ML-008	0.953	0.953	0.953	3.016	ML-020	2.540	1.588	1.588	3.969
ML-010	1.588	0.953	0.953	3.016	ML-022	2.540	1.588	1.588	4.921
ML-012	1.270	1.111	1.270	2.858	ML-024	2.450	1.588	1.905	5.874

Table 3-13. Design Data for Tape C Cores

C Cores, Magnetic Metals, 2 mil										
Part No.	W_{tcu} grams	W_{tfe} grams	MLT cm	MPL cm	$\frac{W_a}{A_c}$	A_c cm^2	W_a cm^2	A_p cm^4	K_g cm^5	A_t cm^2
ML-002	13.0	13.0	3.6	6.4	3.747	0.269	1.008	0.271	0.0080	21.0
ML-004	19.8	22.6	3.9	8.3	3.933	0.359	1.412	0.507	0.0184	29.8
ML-006	27.2	45.2	5.4	8.3	1.967	0.718	1.412	1.013	0.0537	37.5
ML-008	58.4	72.5	5.7	11.8	3.556	0.808	2.874	2.323	0.1314	63.6
ML-010	73.5	120.8	7.2	11.8	2.134	1.347	2.874	3.871	0.2902	74.7
ML-012	95.1	121.7	7.4	12.7	2.891	1.256	3.630	4.558	0.3109	87.1
ML-014	137.7	170.4	7.7	15.6	3.513	1.435	5.041	7.236	0.5408	112.1
ML-016	160.5	255.6	9.0	15.6	2.341	2.153	5.041	10.854	1.0443	126.8
ML-018	176.2	149.1	7.9	15.6	5.019	1.256	6.303	7.915	0.5056	118.9
ML-020	254.5	478.4	11.4	17.5	1.756	3.590	6.303	22.626	2.8607	182.0
ML-022	315.6	530.5	11.4	19.4	2.177	3.590	7.815	28.053	3.5469	202.0
ML-024	471.7	600.1	11.9	21.9	3.117	3.590	11.190	40.170	4.8656	244.8

© 2011 by Taylor and Francis Group, LLC

Dimensional Outline for Tape Wound EE Cores

The dimensional outline for EE cores is shown in Figure 3-28. Dimensional data for EE cores is given in Table 3-14; design data is given in Table 3-15.

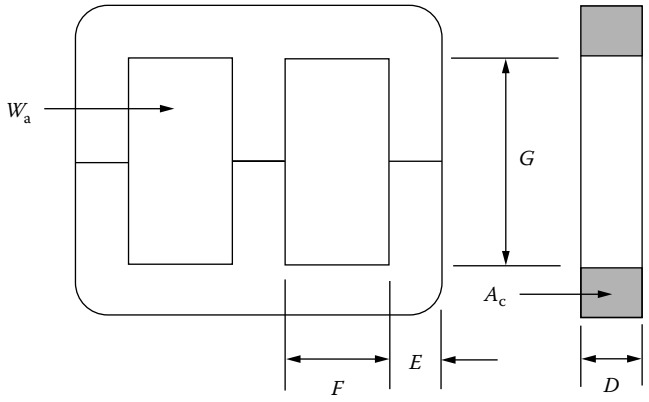

Figure 3-28. Tape EE Core Dimensional Outline.

Table 3-14. Dimensional Data for Tape EE Cores

3Phase E Cores, Magnetic Metals, 12 mil									
Part No.	D cm	E cm	F cm	G cm	Part No.	D cm	E cm	F cm	G cm
MTA-25	1.905	1.905	1.905	2.858	MTA-12	3.810	2.540	2.381	6.350
MTA-22	3.175	1.429	1.905	5.239	MTA-20	5.715	2.540	2.540	6.350
MTA-17	3.175	1.746	1.905	6.350	MTA-03	4.445	2.540	3.493	9.843
MTA-14	3.175	2.223	2.381	4.763	MTA-15	5.080	3.493	2.540	7.620

Table 3-15. Design Data for Tape EE Cores

3Phase E Cores, Magnetic Metals, 12 mil									
Part No.	W_{tcu} grams	W_{tfe} grams	MLT cm	$\frac{W_a}{2A_c}$	A_c cm^2	W_a cm^2	A_p cm^4	K_g cm^5	A_t cm^2
MTA-25	326	686	11.2	0.789	3.448	5.44	28.16	3.461	261
MTA-22	682	1073	12.8	1.158	4.310	9.98	64.53	8.686	324
MTA-17	867	1422	13.4	1.148	5.266	12.10	95.56	14.977	400
MTA-14	916	1803	15.1	0.846	6.705	11.34	114.06	20.203	468
MTA-12	1391	2899	17.3	0.822	9.194	15.12	208.50	44.438	613
MTA-20	1834	4420	21.3	0.585	13.790	16.13	333.64	86.347	737
MTA-03	3717	4597	20.3	1.602	10.730	34.38	553.15	117.079	993
MTA-15	2266	6544	22.0	0.574	16.860	19.35	489.40	150.340	956

© 2011 by Taylor and Francis Group, LLC

Design and Dimensional Data for Tape Wound Toroidal Cores

The dimensional outline for tape wound Toroidal cores is shown in Figure 3-29. Dimensional data for cased tape wound Toroidal cores is given in Table 3-16; design data is given in Table 3-17.

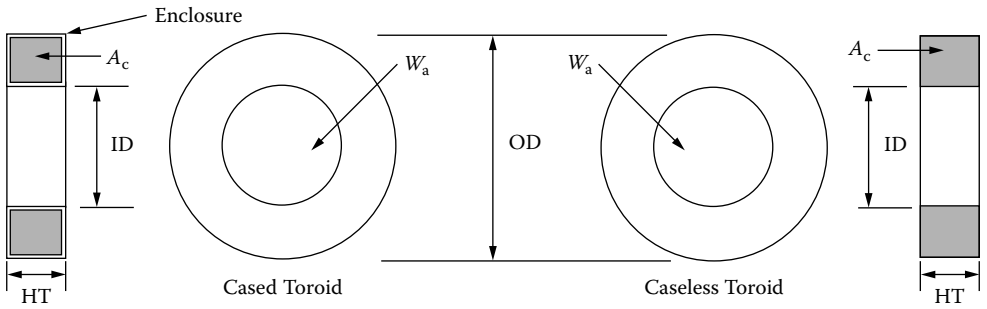

Figure 3-29. Tape Toroidal Core Dimensional Outline.

Table 3-16. Dimensional Data for Tape Toroidal Cores

Toroidal Tape Cores, Magnetics 2 mil Iron Alloy (cased and coated)											
Part No.	OD cm	ID cm	HT cm	Part No.	OD cm	ID cm	HT cm	Part No.	OD cm	ID cm	HT cm
52402	1.346	0.724	0.610	52057	2.134	1.359	0.610	52061	2.781	1.664	0.927
52107	1.651	1.041	0.610	52000	2.134	1.041	0.610	52004	3.429	2.286	0.927
52153	1.499	0.724	0.610	52155	1.659	0.884	0.927	52076	2.794	1.334	0.762
52056	1.816	1.041	0.610	52176	2.134	1.041	0.927	52007	2.794	1.334	0.927

Table 3-17. Design Data for Tape Toroidal Cores

Toroidal Tape Cores, Magnetics 2 mil Iron Alloy (cased)										
Part No.	W_{tcu} grams	W_{tfe} grams	MLT cm	MPL cm	$\frac{W_a}{A_c}$	A_c cm^2	W_a cm^2	A_p cm^4	K_g cm^5	A_t cm^2
52402	2.84	0.50	2.16	3.25	18.727	0.022	0.412	0.00906	0.0000369	9.80
52107	6.76	0.70	2.30	4.24	38.682	0.022	0.851	0.01872	0.0000716	15.50
52153	3.20	1.10	2.20	3.49	9.581	0.043	0.412	0.01772	0.0001385	11.20
52056	7.40	1.50	2.40	4.49	19.791	0.043	0.851	0.03659	0.0002622	16.80
52057	13.80	1.80	2.70	5.48	33.744	0.043	1.451	0.06239	0.0003975	23.70
52000	8.10	3.30	2.70	4.99	9.895	0.086	0.851	0.07319	0.0009324	20.60
52155	6.10	2.60	2.80	3.99	7.140	0.086	0.614	0.05280	0.0006487	16.00
52176	9.70	6.50	3.20	4.99	4.977	0.171	0.851	0.14552	0.0031105	23.30
52061	28.70	9.10	3.70	6.98	12.719	0.171	2.175	0.37193	0.0068756	40.30
52004	61.70	11.70	4.20	8.97	24.000	0.171	4.104	0.70178	0.0114291	62.20
52076	17.20	9.50	3.50	6.48	7.244	0.193	1.398	0.26981	0.0059513	34.60
52007	18.50	12.70	3.70	6.48	5.440	0.257	1.398	0.35929	0.0099823	36.40

© 2011 by Taylor and Francis Group, LLC

Design and Dimensional Data for EE Ferrite Cores

The dimensional outline for EE ferrite cores is shown in Figure 3-30. Dimensional data for EE ferrite cores is given in Table 3-18; design data is given in Table 3-19.

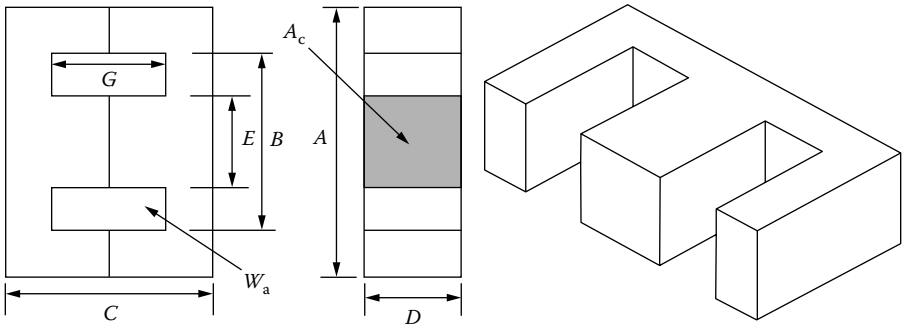

Figure 3-30. Dimension Outline for EE Ferrite Cores.

Table 3-18. Dimensional Data for EE Ferrite Cores

EE, Ferrite Cores (Magnetics)													
Part No.	A cm	B cm	C cm	D cm	E cm	G cm	Part No.	A cm	B cm	C cm	D cm	E cm	G cm
EE-187	1.910	1.433	1.620	0.475	0.475	1.140	EE-21	4.060	2.860	3.320	1.245	1.245	2.080
EE-2425	2.540	1.880	1.930	0.635	0.635	1.280	EE-625	4.690	3.920	3.920	1.560	1.560	2.420
EE-375	3.420	2.550	2.820	0.930	0.930	1.960	EE-75	5.610	3.810	4.720	1.880	1.880	2.920

Table 3-19. Design Data for EE Ferrite Cores

EE, Ferrite Cores (Magnetics)											
Part No.	W_{tcu} grams	W_{tfe} grams	MLT cm	MPL cm	$\frac{W_a}{A_c}$	A_c cm^2	W_a cm^2	A_p cm^4	K_g cm^5	A_t cm^2	*AL mh/1K
EE-187	6.8	4.4	3.8	4.01	2.239	0.226	0.506	0.114	0.0027	14.4	501
EE-2425	13.9	9.5	4.9	4.85	2.010	0.395	0.794	0.314	0.0101	23.5	768
EE-375	36.4	33.0	6.6	6.94	1.769	0.870	1.539	1.339	0.0706	45.3	1160
EE-21	47.3	57.0	8.1	7.75	1.103	1.490	1.643	2.448	0.1801	60.9	1696
EE-625	64.4	103.0	9.4	8.90	0.825	2.340	1.930	4.516	0.4497	81.8	2330
EE-75	111.1	179.0	11.2	10.70	0.831	3.370	2.799	9.433	1.1353	118.0	3519

* This AL value has been normalized for a permeability of 1K. For a close approximation of AL for other values of permeability, multiply this AL value by the new permeability in kilo-perm. If the new permeability is 2500, then use 2.5.

© 2011 by Taylor and Francis Group, LLC

Design and Dimensional Data for EE and EI Planar, Ferrite Cores

The dimensional outline for EE and EI planar ferrite cores is shown in Figure 3-31. Dimensional data for EE and EI planar ferrite cores is given in Table 3-20; design data is given in Table 3-21.

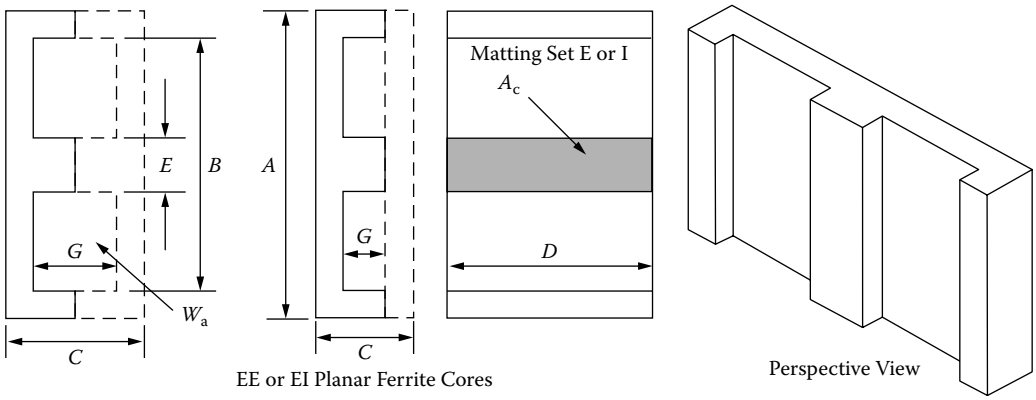

Figure 3-31. Dimension Outline for EE, EI Planar Ferrite Cores.

Table 3-20. Dimensional Data for EE, EI Planar Ferrite Cores

EE&EI/LP, Ferrite Cores (Magnetics)													
Part No.	A cm	B cm	C cm	D cm	E cm	G cm	Part No.	A cm	B cm	C cm	D cm	E cm	G cm
EI-41805	1.800	1.370	0.639	1.000	0.400	0.200	EI-43208	3.175	2.490	0.953	2.032	0.635	0.318
EE-41805	1.800	1.370	0.800	1.000	0.400	0.400	EE-43208	3.175	2.490	1.270	2.032	0.635	0.636
EI-42216	2.180	1.610	0.865	1.580	0.500	0.305	EI-44310	4.320	3.470	1.360	2.790	0.810	0.540
EE-42216	2.180	1.610	1.140	1.580	0.500	0.610	EE-44310	4.320	3.470	1.900	2.790	0.810	1.080

Table 3-21. Design Data for EE, EI Planar Ferrite Cores

EE&EI/LP, Ferrite Cores (Magnetics)											
Part No.	W_{tcu} grams	W_{tfe} grams	MLT cm	MPL cm	$\frac{W_a}{A_c}$	A_c cm^2	W_a cm^2	A_p cm^4	K_g cm^5	A_t cm^2	*AL mh/1K
EI-41805	1.5	4.1	4.7	2.03	0.2269	0.401	0.091	0.0365	0.00125	10.4	1410
EE-41805	3.1	4.9	4.7	2.42	0.4564	0.401	0.183	0.0734	0.00250	11.6	1460
EI-42216	3.8	10.4	6.5	2.58	0.2035	0.806	0.164	0.1322	0.00656	17.8	2699
EE-42216	7.8	13.0	6.5	3.21	0.4169	0.806	0.336	0.2708	0.01343	20.5	2203
EI-43208	8.9	22.0	8.9	3.54	0.2223	1.300	0.289	0.3757	0.02195	33.4	3183
EE-43208	17.8	26.0	8.9	4.17	0.4354	1.300	0.566	0.7358	0.04299	37.9	2913
EI-44310	29.7	58.0	11.9	5.06	0.3057	2.290	0.700	1.6030	0.12339	65.4	4622
EE-44310	59.4	70.8	11.9	6.15	0.6114	2.290	1.400	3.2060	0.24678	75.3	3944

* This AL value has been normalized for a permeability of 1K. For a close approximation of AL for other values of permeability, multiply this AL value by the new permeability in kilo-perm. If the new permeability is 2500, then use 2.5.

© 2011 by Taylor and Francis Group, LLC

Design and Dimensional Data for EC, Ferrite Cores

The dimensional outline for EC ferrite cores is shown in Figure 3-32. Dimensional data for EC ferrite cores is given in Table 3-22; design data is given in Table 3-23.

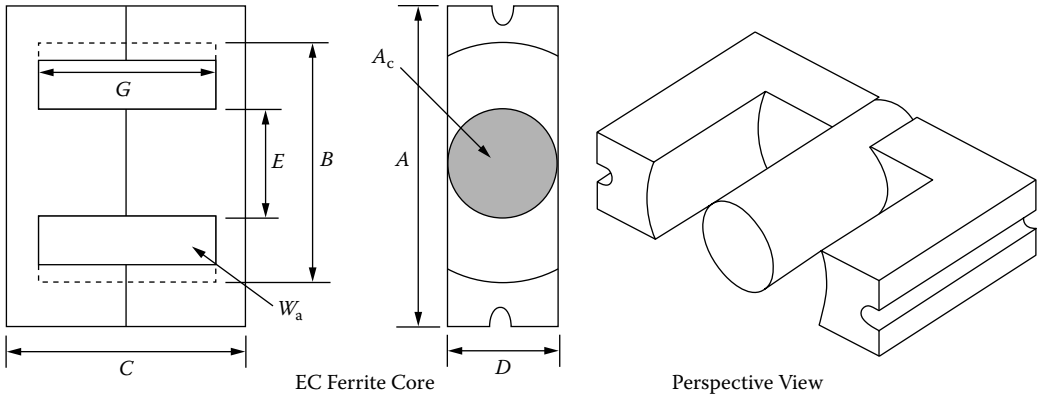

Figure 3-32. Dimension Outline for EC Ferrite Cores.

Table 3-22. Dimensional Data for EC Ferrite Cores

EC, Ferrite Cores (Magnetics)						
Part No.	A cm	B cm	C cm	D cm	E cm	G cm
EC-35	3.450	2.275	3.460	0.950	0.950	2.460
EC-41	4.060	2.700	3.900	1.160	1.160	2.780
EC-52	5.220	3.300	4.840	1.340	1.340	3.180
EC-70	7.000	4.450	6.900	1.640	1.640	4.450

Table 3-23. Design Data for EC Ferrite Cores

EC, Ferrite Cores (Magnetics)											
Part No.	W_{tcu} grams	W_{tfe} grams	MLT cm	MPL cm	$\frac{W_a}{A_c}$	A_c cm^2	W_a cm^2	A_p cm^4	K_g cm^5	A_t cm^2	*AL mh/1K
EC-35	35.1	36.0	6.3	7.59	1.864	0.843	1.571	1.324	0.071	50.2	962
EC-41	55.4	52.0	7.5	8.76	1.721	1.210	2.082	2.519	0.163	67.6	1510
EC-52	97.8	111.0	9.0	10.30	1.689	1.800	3.040	5.472	0.438	106.5	1681
EC-70	256.7	253.0	11.7	14.10	2.214	2.790	6.177	17.234	1.644	201.7	1917

* This AL value has been normalized for a permeability of 1K. For a close approximation of AL for other values of permeability, multiply this AL value by the new permeability in kilo-perm. If the new permeability is 2500, then use 2.5.

© 2011 by Taylor and Francis Group, LLC

Design and Dimensional Data for ETD, Ferrite Cores

The dimensional outline for ETD ferrite cores is shown in Figure 3-33. Dimensional data for ETD ferrite cores is given in Table 3-24; design data is given in Table 3-25.

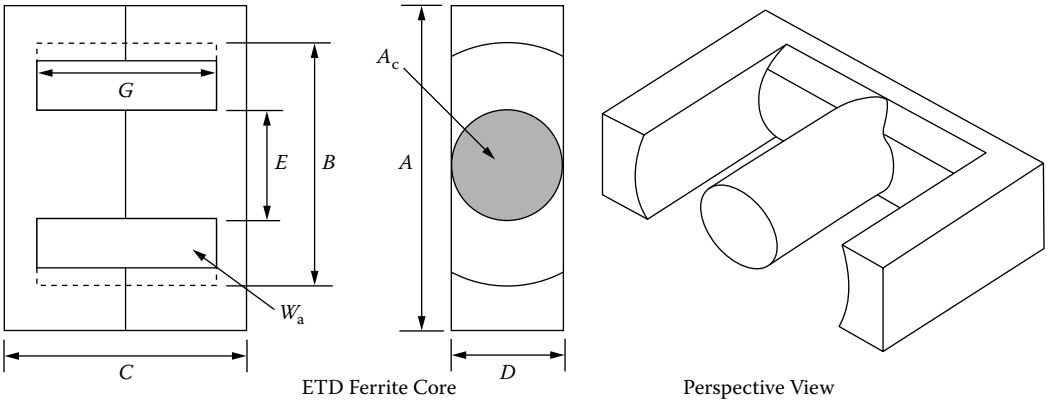

Figure 3-33. Dimension Outline for ETD Ferrite Cores.

Table 3-24. Dimensional Data for ETD Ferrite Cores

ETD, Ferrite Cores (Ferroxcube)													
Part No.	A cm	B cm	C cm	D cm	E cm	G cm	Part No.	A cm	B cm	C cm	D cm	E cm	G cm
ETD-29	3.060	2.270	3.160	0.980	0.980	2.200	ETD-49	4.980	3.610	4.940	1.670	1.670	3.540
ETD-34	3.500	2.560	3.460	1.110	1.110	2.360	ETD-54	5.450	4.120	5.520	1.890	1.890	4.040
ETD-39	4.000	2.930	3.960	1.280	1.280	2.840	ETD-59	5.980	4.470	6.200	2.165	2.165	4.500
ETD-44	4.500	3.250	4.460	1.520	1.520	3.220							

Table 3-25. Design Data for ETD Ferrite Cores

ETD, Ferrite Cores (Ferroxcube)											
Part No.	W_{tcu} grams	W_{tfe} grams	MLT cm	MPL cm	W_a/A_c	A_c cm^2	W_a cm^2	A_p cm^4	K_g cm^5	A_t cm^2	*AL mh/1K
ETD-29	32.1	28.0	6.4	7.20	1.865	0.761	1.419	1.0799	0.0514	42.5	1000
ETD-34	43.4	40.0	7.1	7.87	1.757	0.974	1.711	1.6665	0.0914	53.4	1182
ETD-39	69.3	60.0	8.3	9.22	1.871	1.252	2.343	2.9334	0.1770	69.9	1318
ETD-44	93.2	94.0	9.4	10.30	1.599	1.742	2.785	4.8515	0.3596	87.9	1682
ETD-49	126.2	124.0	10.3	11.40	1.627	2.110	3.434	7.2457	0.5937	107.9	1909
ETD-54	186.9	180.0	11.7	12.70	1.609	2.800	4.505	12.6140	1.2075	133.7	2273
ETD-59	237.7	260.0	12.9	13.90	1.410	3.677	5.186	19.0689	2.1742	163.1	2727

* This AL value has been normalized for a permeability of 1K. For a close approximation of AL for other values of permeability, multiply this AL value by the new permeability in kilo-perm. If the new permeability is 2500, then use 2.5.

© 2011 by Taylor and Francis Group, LLC

Design and Dimensional Data for ETD/(low profile), Ferrite Cores

The dimensional outline for ETD/lp low profile ferrite cores is shown in Figure 3-34. Dimensional data for ETD/lp low profile ferrite cores is given in Table 3-26; design data is given in Table 3-27.

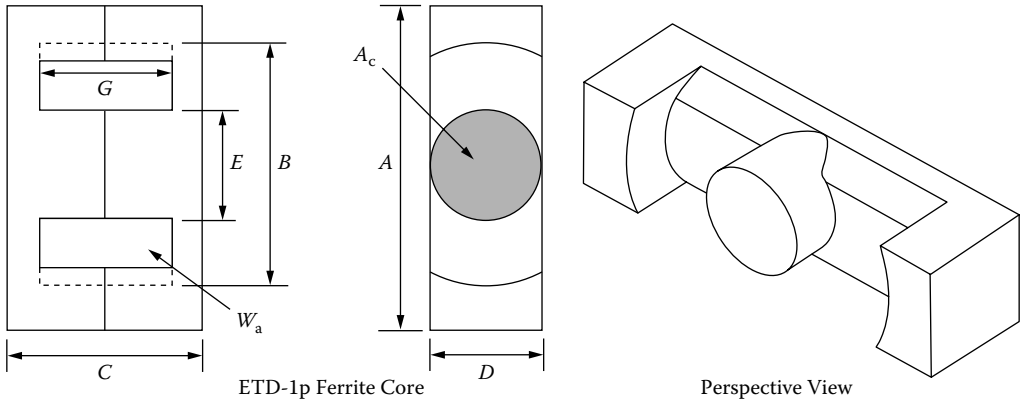

Figure 3-34. Dimension Outline for ETD/lp Ferrite Cores.

Table 3-26. Dimensional Data for ETD/lp Ferrite Cores

ETD/lp, Ferrite Cores (TSC Ferrite International)						
Part No.	A cm	B cm	C cm	D cm	E cm	G cm
ETD34(lp)	3.421	2.631	1.804	1.080	1.080	0.762
ETD39(lp)	3.909	3.010	1.798	1.250	1.250	0.762
ETD44(lp)	4.399	3.330	1.920	1.481	1.481	0.762
ETD49(lp)	4.869	3.701	2.082	1.631	1.631	0.762

Table 3-27. Design Data for ETD/lp Ferrite Cores

ETD/lp, Ferrite Cores (TSC Ferrite International)											
Part No.	W_{tcu} grams	W_{tfe} grams	MLT cm	MPL cm	W_a/A_c	A_c cm^2	W_a cm^2	A_p cm^4	K_g cm^5	A_t cm^2	*AL mh/1K
ETD34(lp)	15.1	32.7	7.2	4.65	0.609	0.970	0.591	0.5733	0.0309	33.1	2382
ETD39(lp)	20.0	46.3	8.4	5.03	0.559	1.200	0.671	0.8052	0.0460	39.6	2838
ETD44(lp)	24.6	72.1	9.5	5.40	0.420	1.730	0.727	1.2577	0.0916	48.4	3659
ETD49(lp)	29.1	95.0	10.4	5.85	0.374	2.110	0.789	1.6648	0.1351	58.2	4120

* This AL value has been normalized for a permeability of 1K. For a close approximation of AL for other values of permeability, multiply this AL value by the new permeability in kilo-perm. If the new permeability is 2500, then use 2.5.

© 2011 by Taylor and Francis Group, LLC

Design and Dimensional Data for ER, Ferrite Cores

Surface Mount Device, SMD

The dimensional outline for ER ferrite cores is shown in Figure 3-35. Dimensional data for ER ferrite cores is given in Table 3-28; design data is given in Table 3-29.

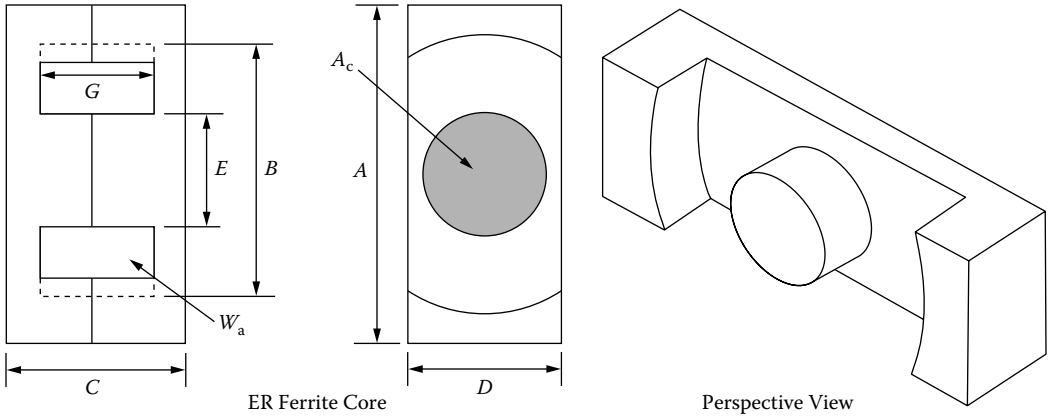

Figure 3-35. Dimension Outline for ER Ferrite Cores.

Table 3-28. Dimensional Data for ER Ferrite Cores

ER, Ferrite Cores (Ferroxcube)													
Part No.	A cm	B cm	C cm	D cm	E cm	G cm	Part No.	A cm	B cm	C cm	D cm	E cm	G cm
ER 9.5	0.950	0.750	0.490	0.500	0.350	0.320	ER 42	4.200	3.005	4.480	1.560	1.550	3.090
ER 11	1.100	0.870	0.490	0.600	0.425	0.300	ER 48	4.800	3.800	4.220	2.100	1.800	2.940
ER 35	3.500	2.615	4.140	1.140	1.130	2.950	ER 54	5.350	4.065	3.660	1.795	1.790	2.220

Table 3-29. Design Data for ER Ferrite Cores

ER, Ferrite Cores (Ferroxcube)											
Part No.	W_{tcu} grams	W_{tfe} grams	MLT cm	MPL cm	$\frac{W_a}{A_c}$	A_c cm^2	W_a cm^2	A_p cm^4	K_g cm^5	A_t cm^2	*AL mh/1K
ER 9.5	0.6	0.7	2.700	1.42	0.842	0.076	0.0640	0.00486	0.000055	3.0	435
ER 11	0.7	1.0	3.200	1.47	0.650	0.103	0.0670	0.00690	0.000089	3.7	609
ER 35	56.7	46.0	7.300	9.08	2.190	1.000	2.1900	2.19000	0.120000	62.4	1217
ER 42	72.9	96.0	9.100	9.88	1.189	1.890	2.2480	4.24872	0.352971	81.0	2000
ER 48	120.7	128.0	11.500	10.00	1.185	2.480	2.9400	7.29120	0.628945	100.1	2478
ER 54	101.9	122.0	11.400	9.18	1.052	2.400	2.5250	6.06000	0.510316	96.2	2652

* This AL value has been normalized for a permeability of 1K. For a close approximation of AL for other values of permeability, multiply this AL value by the new permeability in kilo-perm. If the new permeability is 2500, then use 2.5.

© 2011 by Taylor and Francis Group, LLC

Design and Dimensional Data for EFD, Ferrite Cores

Surface Mount Device, SMD

The EFD cores, (**E**conomic **F**lat **D**esign), offer a significant advance in power transformer circuit miniaturization. The dimensional outline for EFD ferrite cores is shown in Figure 3-36. Dimensional data for EFD ferrite cores is given in Table 3-30; design data is given in Table 3-31.

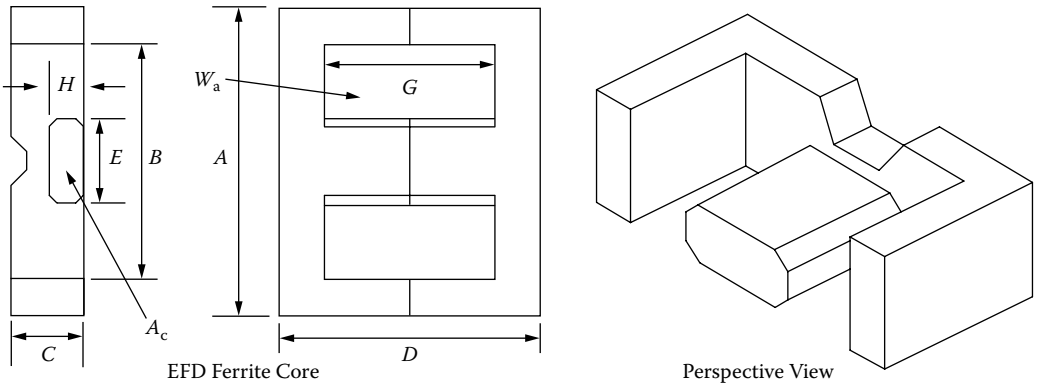

Figure 3-36. Dimension Outline for EFD Ferrite Cores.

Table 3-30. Dimensional Data for EFD Ferrite Cores

EFD, Ferrite Cores (Ferroxcube)							
Part No.	A cm	B cm	C cm	D cm	E cm	G cm	H cm
EFD-10	1.050	0.765	0.270	1.040	0.455	0.750	0.145
EFD-15	1.500	1.100	0.465	1.500	0.530	1.100	0.240
EFD-20	2.000	1.540	0.665	2.000	0.890	1.540	0.360
EFD-25	2.500	1.870	0.910	2.500	1.140	1.860	0.520
EFD-30	3.000	2.240	0.910	3.000	1.460	2.240	0.490

Table 3-31. Design Data for EFD Ferrite Cores

EFD, Ferrite Cores (Ferroxcube)											
Part No.	W_{tcu} grams	W_{tfe} grams	MLT cm	MPL cm	$\frac{W_a}{A_c}$	A_c cm^2	W_a cm^2	A_p cm^4	K_g cm^5	A_t cm^2	*AL mh/1K
EFD-10	0.8	0.90	1.8	2.37	1.611	0.072	0.116	0.00835	0.00013	3.3	254
EFD-15	3.0	2.80	2.7	3.40	2.093	0.150	0.314	0.04710	0.00105	7.3	413
EFD-20	6.8	7.00	3.8	4.70	1.616	0.310	0.501	0.15531	0.00507	13.3	565
EFD-25	11.5	16.00	4.8	5.70	1.171	0.580	0.679	0.39382	0.01903	21.6	957
EFD-30	17.0	24.00	5.5	6.80	1.267	0.690	0.874	0.60306	0.03026	28.9	913

* This AL value has been normalized for a permeability of 1K. For a close approximation of AL for other values of permeability, multiply this AL value by the new permeability in kilo-perm. If the new permeability is 2500, then use 2.5.

© 2011 by Taylor and Francis Group, LLC

Design and Dimensional Data for EPC, Ferrite Cores

Surface Mount Device, SMD

The dimensional outline for EPC ferrite cores is shown in Figure 3-37. Dimensional data for EPC ferrite cores is given in Table 3-32; design data is given in Table 3-33.

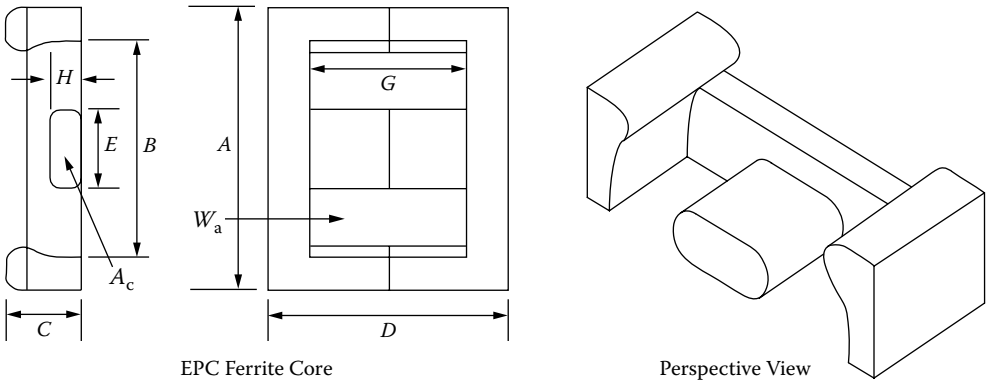

Figure 3-37. Dimension Outline for EPC Ferrite Cores.

Table 3-32. Dimensional Data for EPC Ferrite Cores

EPC, Ferrite Cores (TDK)							
Part No.	A cm	B cm	C cm	D cm	E cm	G cm	H cm
EPC-10	1.020	0.760	0.340	0.810	0.500	0.530	0.190
EPC-13	1.325	1.050	0.460	1.320	0.560	0.900	0.205
EPC-17	1.760	1.430	0.600	1.710	0.770	1.210	0.280
EPC-19	1.910	1.580	0.600	1.950	0.850	1.450	0.250
EPC-25	2.510	2.040	0.800	2.500	1.150	1.800	0.400
EPC-27	2.710	2.160	0.800	3.200	1.300	2.400	0.400
EPC-30	3.010	2.360	0.800	3.500	1.500	2.600	0.400

Table 3-33. Design Data for EPC Ferrite Cores

EPC, Ferrite Cores (TDK)											
Part No.	W_{tcu} grams	W_{tfe} grams	MLT cm	MPL cm	$\frac{W_a}{A_c}$	A_c cm^2	W_a cm^2	A_p cm^4	K_g cm^5	A_t cm^2	*AL mh/1K
EPC-10	0.5	1.1	1.9	1.78	0.735	0.094	0.069	0.00648	0.000128	2.9	416
EPC-13	2.0	2.1	2.5	3.06	1.768	0.125	0.221	0.02763	0.000553	5.9	363
EPC-17	4.9	4.5	3.4	4.02	1.750	0.228	0.399	0.09097	0.002440	10.2	479
EPC-19	6.9	5.3	3.7	4.61	2.330	0.227	0.529	0.12008	0.002947	12.1	392
EPC-25	14.8	13.0	5.0	5.92	1.804	0.464	0.837	0.38837	0.014416	20.6	650
EPC-27	18.8	18.0	5.1	7.31	1.890	0.546	1.032	0.56347	0.024130	26.8	642
EPC-30	21.9	23.0	5.5	8.16	1.833	0.610	1.118	0.68198	0.030255	31.5	654

* This AL value has been normalized for a permeability of 1K. For a close approximation of AL for other values of permeability, multiply this AL value by the new permeability in kilo-perm. If the new permeability is 2500, then use 2.5.

© 2011 by Taylor and Francis Group, LLC

Design and Dimensional Data for PC, Ferrite Cores

The dimensional outline for PC ferrite pot cores is shown in Figure 3-38. Dimensional data for PC ferrite pot cores is given in Table 3-34; design data is given in Table 3-35.

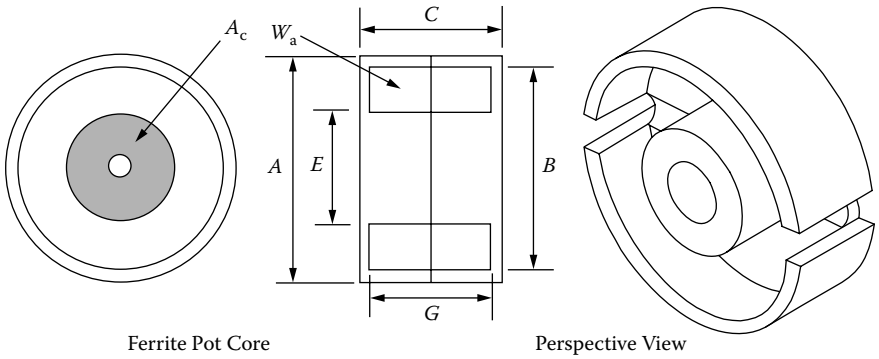

Figure 3-38. Dimension Outline for PC Ferrite Cores.

Table 3-34. Dimensional Data for PC Ferrite Cores

PC, Ferrite Cores (Magnetics)											
Part No.	A cm	B cm	C cm	E cm	G cm	Part No.	A cm	B cm	C cm	E cm	G cm
PC-40905	0.915	0.763	0.526	0.380	0.345	PC-42616	2.550	2.160	1.610	1.130	1.102
PC-41408	1.405	1.160	0.840	0.580	0.580	PC-43019	3.000	2.540	1.890	1.330	1.300
PC-41811	1.800	1.515	1.060	0.740	0.740	PC-43622	3.560	3.040	2.190	1.590	1.460
PC-42213	2.160	1.820	1.340	0.940	0.940	PC-44229	4.240	3.630	2.940	1.740	2.040

Table 3-35. Design Data for PC Ferrite Cores

PC, Ferrite Cores (Magnetics)											
Part No.	W_{tcu} grams	W_{tfe} grams	MLT cm	MPL cm	$\frac{W_a}{A_c}$	A_c cm^2	W_a cm^2	A_p cm^4	K_g cm^5	A_t cm^2	*AL mh/1K
PC-40905	0.5	1.0	1.9	1.25	0.654	0.101	0.066	0.00668	0.000142	2.8	440
PC-41408	1.6	3.2	2.9	1.97	0.670	0.251	0.168	0.04222	0.001462	6.8	893
PC-41811	3.5	7.3	3.7	2.59	0.662	0.433	0.287	0.12418	0.005813	11.1	1333
PC-42213	6.2	13.0	4.4	3.12	0.652	0.634	0.414	0.26222	0.015114	16.4	1757
PC-42616	10.1	20.0	5.3	3.76	0.604	0.939	0.568	0.53288	0.037764	23.1	2267
PC-43019	16.7	34.0	6.3	4.50	0.574	1.370	0.787	1.07751	0.093726	31.9	2904
PC-43622	26.7	57.0	7.5	5.29	0.524	2.020	1.059	2.13817	0.230352	44.5	3783
PC-44229	55.9	104.0	8.6	6.85	0.718	2.686	1.928	5.17807	0.646898	67.7	4000

* This AL value has been normalized for a permeability of 1K. For a close approximation of AL for other values of permeability, multiply this AL value by the new permeability in kilo-perm. If the new permeability is 2500, then use 2.5.

© 2011 by Taylor and Francis Group, LLC

Design and Dimensional Data for EP, Ferrite Cores

The EP ferrite cores are typically used in transformer applications. The shape of the assembly is almost cubical, allowing high package densities on the PCB. The dimensional outline for EP ferrite cores is shown in Figure 3-39. Dimensional data for EP ferrite cores is given in Table 3-36; design data is given in Table 3-37.

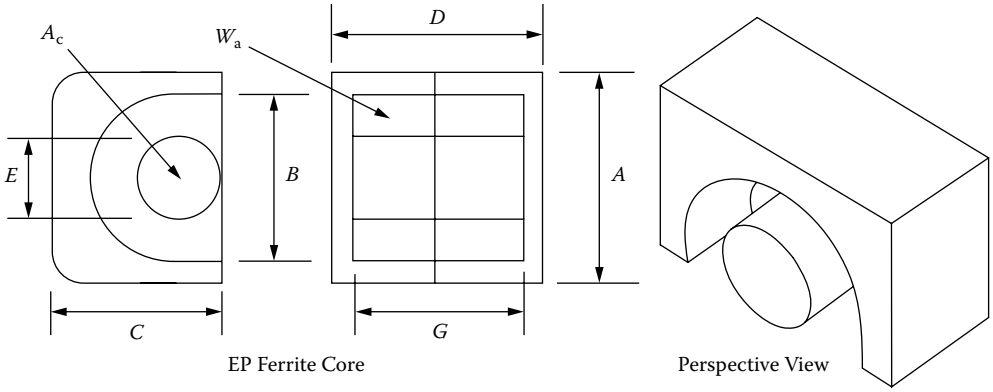

Figure 3-39. Dimension Outline for EP Ferrite Cores.

Table 3-36. Dimensional Data for EP Ferrite Cores

EP, Ferrite Cores (Magnetics)						
Part No.	A cm	B cm	C cm	D cm	E cm	G cm
EP-07	0.920	0.720	0.635	0.740	0.340	0.500
EP-10	1.150	0.920	0.760	1.030	0.345	0.720
EP-13	1.250	1.000	0.880	1.290	0.435	0.920
EP-17	1.800	1.200	1.100	1.680	0.570	1.140
EP-20	2.400	1.650	1.500	2.140	0.880	1.440

Table 3-37. Design Data for EP Ferrite Cores

EP, Ferrite Cores (Magnetics)											
Part No.	W_{tcu} grams	W_{tfe} grams	MLT cm	MPL cm	W_a/A_c	A_c cm^2	W_a cm^2	A_p cm^4	K_g cm^5	A_t cm^2	*AL mh/1K
EP-07	1.4	1.4	1.8	1.55	0.888	0.107	0.095	0.01017	0.00024	3.5	414
EP-10	1.6	2.8	2.1	1.93	1.832	0.113	0.207	0.02339	0.00050	5.7	400
EP-13	2.0	5.1	2.4	2.42	1.200	0.195	0.234	0.04563	0.00148	7.7	667
EP-17	11.6	11.6	2.9	2.95	0.955	0.337	0.322	0.10851	0.00504	13.7	1034
EP-20	7.4	27.6	4.2	4.11	0.632	0.787	0.497	0.39114	0.02932	23.8	1667

* This AL value has been normalized for a permeability of 1K. For a close approximation of AL for other values of permeability, multiply this AL value by the new permeability in kilo-perm. If the new permeability is 2500, then use 2.5.

© 2011 by Taylor and Francis Group, LLC

Design and Dimensional Data for PQ, Ferrite Cores

The PQ ferrite cores, (**P**ower **Q**uality), feature round center legs with rather small cross-sections. The dimensional outline for PQ ferrite cores is shown in Figure 3-40. Dimensional data for PQ ferrite cores is given in Table 3-38; design data is given in Table 3-39.

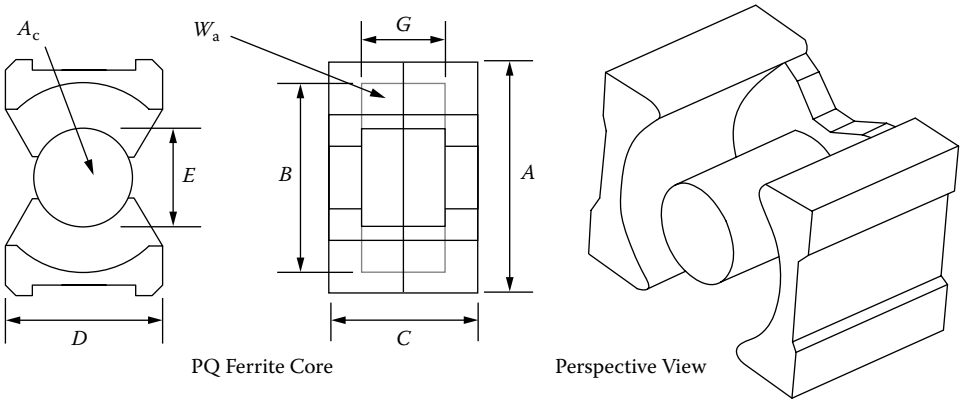

Figure 3-40. Dimension Outline for PQ Ferrite Cores.

Table 3-38. Dimensional Data for PQ Ferrite Cores

PQ, Ferrite Cores (TDK)													
Part No.	A cm	B cm	C cm	D cm	E cm	G cm	Part No.	A cm	B cm	C cm	D cm	E cm	G cm
PQ20/16	2.050	1.800	1.620	1.400	0.880	1.030	PQ32/30	3.200	2.750	3.035	2.200	1.345	2.130
PQ20/20	2.050	1.800	2.020	1.400	0.880	1.430	PQ35/35	3.510	3.200	3.475	2.600	1.435	2.500
PQ26/20	2.650	2.250	2.015	1.900	1.200	1.150	PQ40/40	4.050	3.700	3.975	2.800	1.490	2.950
PQ26/25	2.650	2.250	2.475	1.900	1.200	1.610	PQ50/50	5.000	4.400	4.995	3.200	2.000	3.610
PQ32/20	3.200	2.750	2.055	2.200	1.345	1.150							

Table 3-39. Design Data for PQ Ferrite Cores

PQ, Ferrite Cores (TDK)											
Part No.	W_{tcu} grams	W_{tfe} grams	MLT cm	MPL cm	W_a/A_c	A_c cm^2	W_a cm^2	A_p cm^4	K_g cm^5	A_t cm^2	*AL mh/1K
PQ20/16	7.4	13.0	4.4	3.74	0.765	0.620	0.474	0.294	0.0166	16.9	1617
PQ20/20	10.4	15.0	4.4	4.54	1.061	0.620	0.658	0.408	0.0230	19.7	1313
PQ26/20	31.0	31.0	5.6	4.63	0.508	1.190	0.604	0.719	0.0611	28.4	2571
PQ26/25	17.0	36.0	5.7	5.55	0.716	1.180	0.845	0.997	0.0826	32.6	2187
PQ32/20	18.9	42.0	6.6	5.55	0.475	1.700	0.808	1.374	0.1415	36.3	3046
PQ32/30	35.5	55.0	6.7	7.46	0.929	1.610	1.496	2.409	0.2315	46.9	2142
PQ35/35	59.0	73.0	7.5	8.79	1.126	1.960	2.206	4.324	0.4520	60.7	2025
PQ40/40	97.2	95.0	8.4	10.20	1.622	2.010	3.260	6.553	0.6272	77.1	1792
PQ50/50	158.5	195.0	10.3	11.30	1.321	3.280	4.332	14.209	1.8099	113.9	2800

* This AL value has been normalized for a permeability of 1K. For a close approximation of AL for other values of permeability, multiply this AL value by the new permeability in kilo-perm. If the new permeability is 2500, then use 2.5.

© 2011 by Taylor and Francis Group, LLC

Design and Dimensional Data for PQ/(low profile), Ferrite Cores

The PQ/lp cores are a cut-down version of the standard PQ cores. The PQ/lp cores have a substantially reduced total height. The dimensional outline for PQ ferrite cores is shown in Figure 3-41. Dimensional data for PQ ferrite cores is given in Table 3-40; design data is given in Table 3-41.

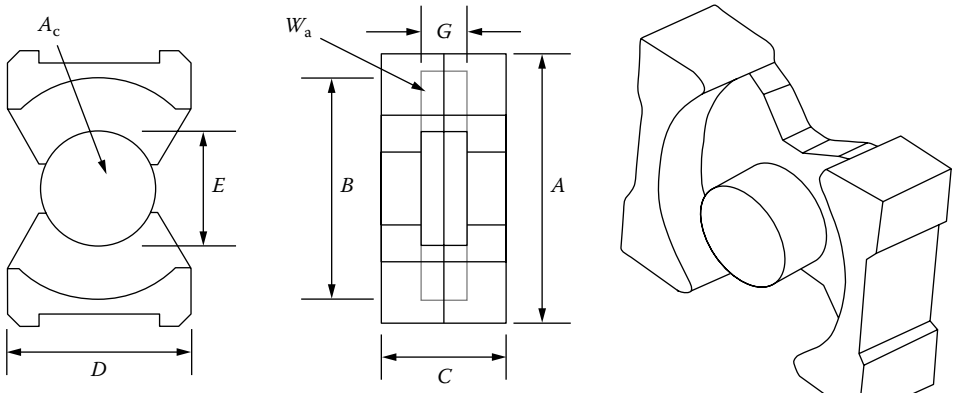

Figure 3-41. Dimension Outline for PQ/lp Ferrite Cores.

Table 3-40. Dimensional Data for PQ/lp Ferrite Cores

PQ/lp, Ferrite Cores (Ferrite International)						
Part No.	A cm	B cm	C cm	D cm	E cm	G cm
PQ20-14-14lp	2.125	1.801	1.352	1.400	0.884	0.762
PQ26-16-14lp	2.724	2.250	1.630	1.900	1.199	0.762
PQ32-17-22lp	3.302	2.751	1.670	2.200	1.348	0.762
PQ35-17-26lp	3.612	3.200	1.738	2.601	1.435	0.762
PQ40-18-28lp	4.148	3.701	1.784	2.799	1.491	0.762

Table 3-41. Design Data for PQ/lp Ferrite Cores

PQ/lp, Ferrite Cores (TSC Ferrite International)											
Part No.	W_{tcu} grams	W_{tfe} grams	MLT cm	MPL cm	$\frac{W_a}{A_c}$	A_c cm^2	W_a cm^2	A_p cm^4	K_g cm^5	A_t cm^2	*AL mh/1K
PQ20-14-14lp	5.4	12.5	4.4	3.2	0.563	0.620	0.349	0.216	0.0122	15.4	1948
PQ26-16-19lp	7.9	28.0	5.6	3.9	0.336	1.190	0.400	0.476	0.0405	25.4	3170
PQ32-17-22lp	12.5	39.4	6.6	4.8	0.315	1.700	0.535	0.910	0.0937	32.9	3659
PQ35-17-26lp	17.8	44.9	7.4	5.3	0.343	1.960	0.672	1.317	0.1395	40.4	3893
PQ40-18-28lp	24.9	63.5	8.3	5.8	0.419	2.010	0.842	1.692	0.1639	48.0	3850

* This AL value has been normalized for a permeability of 1K. For a close approximation of AL for other values of permeability, multiply this AL value by the new permeability in kilo-perm. If the new permeability is 2500, then use 2.5.

© 2011 by Taylor and Francis Group, LLC

Design and Dimensional Data for RM, Ferrite Cores

The RM cores, (**R**ectangular **M**odular), were developed for high Printed Circuit Board, (PCB), packing densities. The dimensional outline for RM ferrite cores is shown in Figure 3-42. Dimensional data for RM ferrite cores is given in Table 3-42; design data is given in Table 3-43.

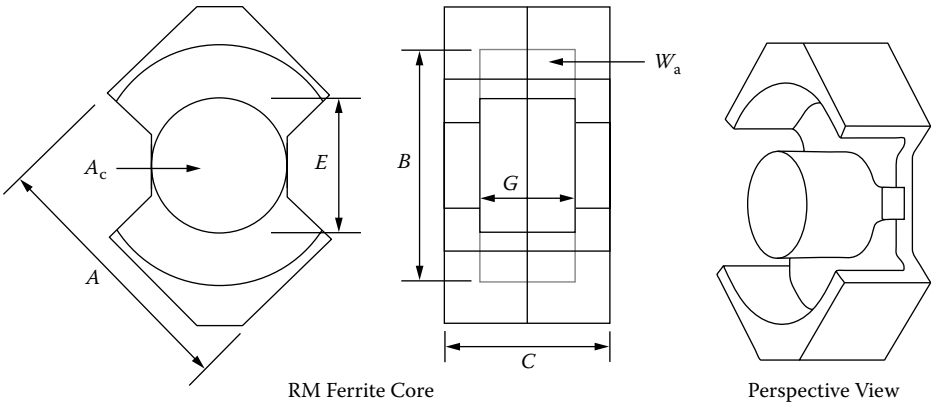

Figure 3-42. Dimension Outline for RM Ferrite Cores.

Table 3-42. Dimensional Data for RM Ferrite Cores

RM, Ferrite Cores (TDK)											
Part No.	A cm	B cm	C cm	E cm	G cm	Part No.	A cm	B cm	C cm	E cm	G cm
RM-4	0.963	0.815	1.04	0.38	0.72	RM-10	2.415	2.165	1.86	1.07	1.27
RM-5	1.205	1.04	1.04	0.48	0.65	RM-12	2.925	2.55	2.35	1.26	1.71
RM-6	1.44	1.265	1.24	0.63	0.82	RM-14	3.42	2.95	2.88	1.47	2.11
RM-8	1.935	1.73	1.64	0.84	1.1						

Table 3-43. Design Data for RM Ferrite Cores

RM, Ferrite Cores (TDK)											
Part No.	W_{tcu} grams	W_{tfe} grams	MLT cm	MPL cm	$\frac{W_a}{A_c}$	A_c cm^2	W_a cm^2	A_p cm^4	K_g cm^5	A_t cm^2	*AL mh/1K
RM-4	1.1	1.7	2.0	2.27	1.121	0.140	0.157	0.0220	0.0006	5.9	489
RM-5	1.6	3.0	2.5	2.24	0.768	0.237	0.182	0.0431	0.0016	7.9	869
RM-6	2.9	5.5	3.1	2.86	0.710	0.366	0.260	0.0952	0.0045	11.3	1130
RM-8	7.3	13.0	4.2	3.80	0.766	0.640	0.490	0.3136	0.0191	20.2	1233
RM-10	13.2	23.0	5.3	4.40	0.709	0.980	0.695	0.6811	0.0504	29.6	1833
RM-12	24.4	42.0	6.2	5.69	0.788	1.400	1.103	1.5442	0.1395	44.6	2434
RM-14	39.9	70.0	7.2	6.90	0.830	1.880	1.561	2.9347	0.3065	62.8	2869

* This AL value has been normalized for a permeability of 1K. For a close approximation of AL for other values of permeability, multiply this AL value by the new permeability in kilo-perm. If the new permeability is 2500, then use 2.5.

© 2011 by Taylor and Francis Group, LLC

Design and Dimensional Data for RM/(low profile), Ferrite Cores

Surface Mount Device, SMD

The RM/lp ferrite cores are a cut down version of the standard RM cores. The dimensional outline for RM/lp ferrite cores is shown in Figure 3-43. Dimensional data for RM/lp ferrite cores is given in Table 3-44; design data is given in Table 3-45.

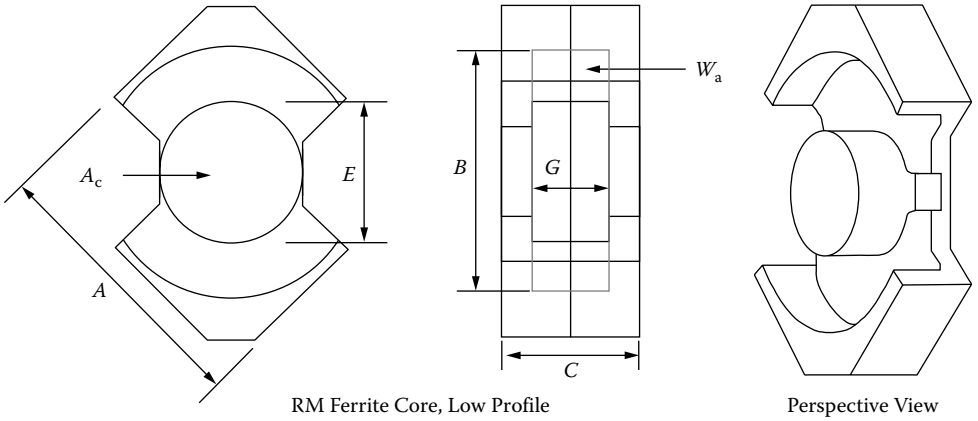

Figure 3-43. Dimension Outline for RM/lp Ferrite Cores.

Table 3-44. Dimensional Data for RM/lp Ferrite Cores

RM/lp, Ferrite Cores (Ferroxcube)											
Part No.	A cm	B cm	C cm	E cm	G cm	Part No.	A cm	B cm	C cm	E cm	G cm
RM4/ILP	0.980	0.795	0.780	0.390	0.430	RM8/ILP	1.970	1.700	1.160	0.855	0.590
RM5/ILP	1.230	1.020	0.780	0.490	0.360	RM10/ILP	2.470	2.120	1.300	1.090	0.670
RM6S/LP	1.470	1.240	0.900	0.640	0.450	RM12/ILP	2.980	2.500	1.680	1.280	0.900
RM7/ILP	1.720	1.475	0.980	0.725	0.470	RM14/ILP	3.470	2.900	2.050	1.500	1.110

Table 3-45. Design Data for RM/lp Ferrite Cores

RM/lp, Ferrite Cores (Ferroxcube)											
Part No.	W_{tcu} grams	W_{tfe} grams	MLT cm	MPL cm	$\frac{W_a}{A_c}$	A_c cm^2	W_a cm^2	A_p cm^4	K_g cm^5	A_t cm^2	*AL mh/1K
RM4/ILP	0.6	1.5	2.0	1.73	0.770	0.113	0.087	0.00983	0.00022	5.0	609
RM5/ILP	0.9	2.2	2.5	1.75	0.525	0.181	0.095	0.01720	0.00050	6.9	1022
RM6S/LP	1.5	4.2	3.1	2.18	0.433	0.312	0.135	0.04212	0.00170	9.6	1380
RM7/ILP	2.3	6.0	3.6	2.35	0.444	0.396	0.176	0.06970	0.00307	12.7	1587
RM8/ILP	3.7	10.0	4.2	2.87	0.449	0.554	0.249	0.13795	0.00728	16.9	1783
RM10/ILP	6.4	17.0	5.2	3.39	0.426	0.809	0.345	0.27911	0.01737	25.0	2435
RM12/ILP	11.9	34.0	6.1	4.20	0.439	1.250	0.549	0.68625	0.05625	37.8	3087
RM14/ILP	19.5	55.0	7.1	5.09	0.463	1.680	0.777	1.30536	0.12355	52.5	3652

* This AL value has been normalized for a permeability of 1K. For a close approximation of AL for other values of permeability, multiply this AL value by the new permeability in kilo-perm. If the new permeability is 2500, then use 2.5.

© 2011 by Taylor and Francis Group, LLC

Design and Dimensional Data for DS, Ferrite Cores

The DS ferrite cores are similar to standard Pot Cores. These cores have a large opening to bring out many strands of wire, which is convenient for high power and multiple outputs. The dimensional outline for DS ferrite cores is shown in Figure 3-44. Dimensional data for DS ferrite cores is given in Table 3-46; design data is given in Table 3-47.

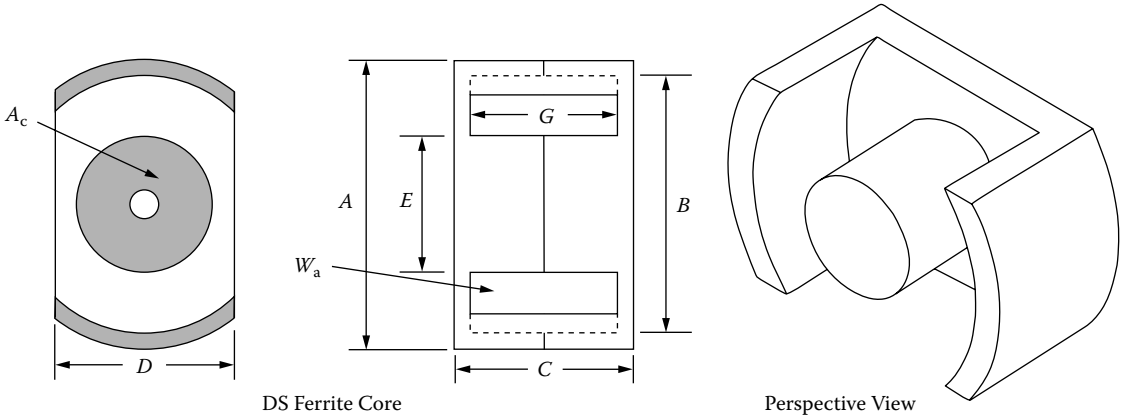

Figure 3-44. Dimension Outline for DS Ferrite Cores.

Table 3-46. Dimensional Data for DS Ferrite Cores

DS, Ferrite Cores (Magnetics)						
Part No.	A cm	B cm	C cm	D cm	E cm	G cm
DS-42311	2.286	1.793	1.108	1.524	0.990	0.726
DS-42318	2.286	1.793	1.800	1.524	0.990	1.386
DS-42616	2.550	2.121	1.610	1.709	1.148	1.102
DS-43019	3.000	2.500	1.880	2.032	1.351	1.300
DS-43622	3.561	2.990	2.170	2.385	1.610	1.458
DS-44229	4.240	3.561	2.960	2.840	1.770	2.042

Table 3-47. Design Data for DS Ferrite Cores

DS, Ferrite Cores (Magnetics)											
Part No.	W_{tcu} grams	W_{tfe} grams	MLT cm	MPL cm	$\frac{W_a}{A_c}$	A_c cm^2	W_a cm^2	A_p cm^4	K_g cm^5	A_t cm^2	*AL mh/1K
DS-42311	4.7	10.0	4.5	2.68	0.568	0.512	0.291	0.149	0.00678	16.2	1496
DS-42318	9.1	13.0	4.6	3.99	0.959	0.580	0.556	0.322	0.01626	21.1	1264
DS-42616	10.1	15.0	5.3	3.89	0.696	0.770	0.536	0.413	0.02398	23.1	1664
DS-43019	16.7	22.0	6.3	4.62	0.638	1.170	0.747	0.874	0.06492	31.9	1930
DS-43622	26.6	37.0	7.5	5.69	0.619	1.620	1.002	1.623	0.14025	44.2	2348
DS-44229	56.0	78.0	8.6	7.60	0.788	2.320	1.829	4.243	0.45788	67.7	2827

* This AL value has been normalized for a permeability of 1K. For a close approximation of AL for other values of permeability, multiply this AL value by the new permeability in kilo-perm. If the new permeability is 2500, then use 2.5.

© 2011 by Taylor and Francis Group, LLC

Design and Dimensional Data for UUR, Ferrite Cores

The UUR ferrite cores feature round legs with rather small cross sections. The round legs allow easy winding with either wire or foil. U cores are used for power, pulse and high-voltage transformers. The dimensional outline for UUR ferrite cores is shown in Figure 3-45. Dimensional data for UUR ferrite cores is given in Table 3-48; design data is given in Table 3-49.

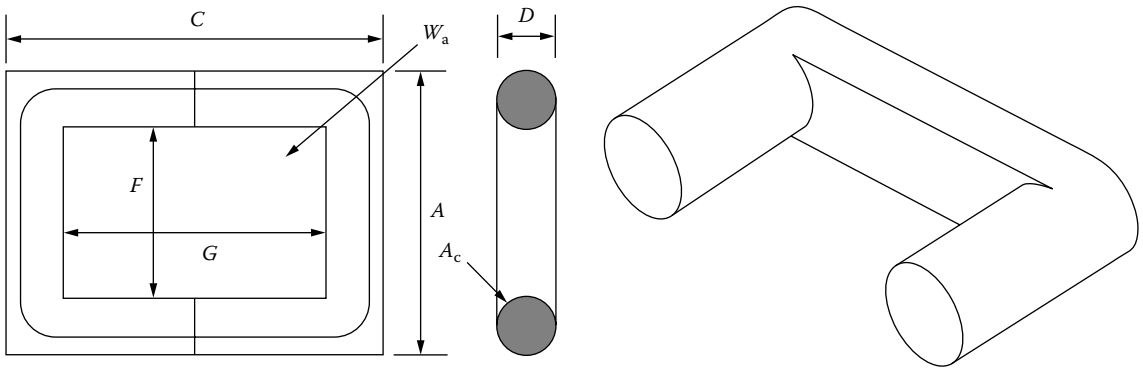

Figure 3-45. Dimension Outline for UUR Ferrite Cores.

Table 3-48. Dimensional Data for UUR Ferrite Cores

UUR, Ferrite Cores (Magnetics)					
Part No.	A cm	C cm	D cm	F cm	G cm
UUR-44121	4.178	5.080	1.194	1.880	3.180
UUR-44119	4.178	4.120	1.194	1.880	2.200
UUR-44125	4.178	5.080	1.194	1.880	3.180
UUR-44130	4.178	6.100	1.194	1.880	4.160

Table 3-49. Design Data for UUR Ferrite Cores

UUR, Ferrite Cores (Magnetics)											
Part No.	W_{tcu} grams	W_{tfe} grams	MLT cm	MPL cm	$\frac{W_a}{A_c}$	A_c cm^2	W_a cm^2	A_p cm^4	K_g cm^5	A_t cm^2	*AL mh/1K
UUR-44121	119.0	55.0	8.0	11.5	3.643	1.143	4.164	4.759	0.272	98.5	817
UUR-44119	146.2	54.0	8.0	12.1	5.619	0.911	5.119	4.663	0.212	102.9	707
UUR-44125	171.3	64.0	8.0	13.4	5.302	1.131	5.997	6.783	0.384	116.1	606
UUR-44130	227.0	75.0	8.0	15.5	7.095	1.120	7.946	8.900	0.498	134.9	609

* This AL value has been normalized for a permeability of 1K. For a close approximation of AL for other values of permeability, multiply this AL value by the new permeability in kilo-perm. If the new permeability is 2500, then use 2.5.

© 2011 by Taylor and Francis Group, LLC

Design and Dimensional Data for UUS, Ferrite Cores

The UUS ferrite cores feature square or rectangular legs. U cores are used for power, pulse and high-voltage transformers. The dimensional outline for UUS ferrite cores is shown in Figure 3-46. Dimensional data for UUS ferrite cores is given in Table 3-50; design data is given in Table 3-51.

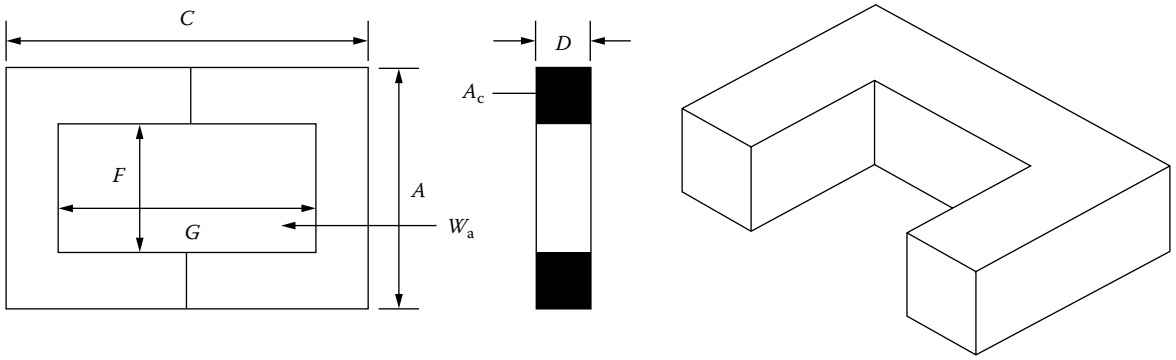

Figure 3-46. Dimension Outline for UUS Ferrite Cores.

Table 3-50. Dimensional Data for UUS Ferrite Cores

UUS, Ferrite Cores (Ferroxcube)					
Part No.	A cm	C cm	D cm	F cm	G cm
U10-08-03	1.000	1.640	0.290	0.435	1.000
U20-16-07	2.080	3.120	0.750	0.640	1.660
U25-20-13	2.480	3.920	1.270	0.840	2.280
U30-25-16	3.130	5.060	1.600	1.050	2.980
U67-27-14	6.730	5.400	1.430	3.880	2.540
U93-76-16	9.300	15.200	1.600	3.620	9.600

Table 3-51. Design Data for UUS Ferrite Cores

UUS, Ferrite Cores (Ferroxcube)											
Part No.	W_{tcu} grams	W_{tfe} grams	MLT cm	MPL cm	W_a/A_c	A_c cm^2	W_a cm^2	A_p cm^4	K_g cm^5	A_t cm^2	*AL mh/1K
U10-08-03	3.5	1.8	2.2	3.8	5.370	0.081	0.435	0.0352	0.000519	8.1	213
U20-16-07	16.4	19.0	4.4	6.8	1.896	0.560	1.062	0.5947	0.030277	29.5	826
U25-20-13	41.6	47.0	6.1	8.8	1.841	1.040	1.915	1.9916	0.135821	51.1	1261
U30-25-16	83.9	86.0	7.5	11.1	1.943	1.610	3.129	5.0377	0.432570	82.5	1609
U67-27-14	435.0	170.0	12.4	17.3	4.831	2.040	9.855	20.1042	1.322986	240.2	1652
U93-76-16	1875.2	800.0	15.2	35.4	7.757	4.480	34.752	155.6890	18.354909	605.3	1478

* This AL value has been normalized for a permeability of 1K. For a close approximation of AL for other values of permeability, multiply this AL value by the new permeability in kilo-perm. If the new permeability is 2500, then use 2.5.

© 2011 by Taylor and Francis Group, LLC

Design and Dimensional Data for Toroidal, Ferrite Cores

The toroidal ferrite core has the best possible shape from the magnetic point of view. The magnetic flux path is completely enclosed within the magnetic structure. The toroidal structure fully exploits the capabilities of a ferrite material. The dimensional outline for toroidal ferrite cores is shown in Figure 3-47. Dimensional data for toroidal ferrite cores is given in Table 3-52; design data is given in Table 3-53.

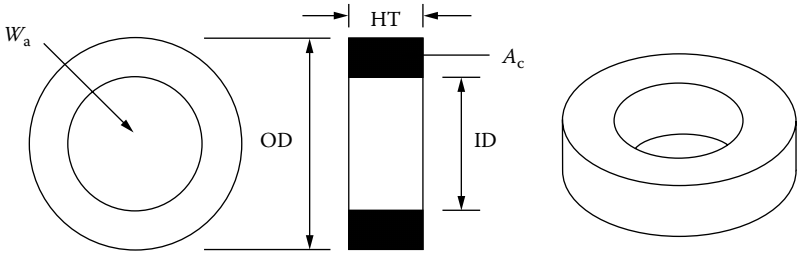

Figure 3-47. Dimension Outline for Toroidal Ferrite Cores.

Table 3-52. Dimensional Data for Toroidal Ferrite Cores

Toroidal, Ferrite Z Coated Cores (Magnetics)							
Part No.	OD cm	ID cm	HT cm	Part No.	OD cm	ID cm	HT cm
TC-40907	1.017	0.504	0.766	TC-42206	2.286	1.295	0.691
TC-41005	1.017	0.420	0.533	TC-42908	2.990	1.811	0.806
TC-41206	1.334	0.452	0.691	TC-43806	3.925	1.790	0.691
TC-41306	1.334	0.729	0.691	TC-43610	3.715	2.205	1.065
TC-41605	1.664	0.812	0.521	TC-43813	3.925	1.790	1.334
TC-42106	2.134	1.193	0.691	TC-48613	8.738	5.389	1.334

Table 3-53. Design Data for Toroidal Ferrite Cores

Toroidal, Ferrite Cores (Magnetics)											
Part No.	W_{tcu} grams	W_{tfe} grams	MLT cm	MPL cm	$\frac{W_a}{A_c}$	A_c cm^2	W_a cm^2	A_p cm^4	K_g cm^5	A_t cm^2	*AL mh/1K
TC-41005	0.8	1.2	1.7	2.07	1.220	0.109	0.133	0.014497	0.000372	5.3	661
TC-40907	1.4	1.6	2.0	2.27	1.401	0.137	0.192	0.026304	0.000721	6.6	754
TC-41206	1.2	3.3	2.2	2.50	0.727	0.220	0.160	0.035200	0.001408	8.6	1130
TC-41306	3.2	2.4	2.2	3.17	2.937	0.142	0.417	0.059214	0.001529	10.2	591
TC-41605	4.0	2.8	2.2	3.72	3.321	0.156	0.518	0.080808	0.002292	12.8	530
TC-42106	11.2	5.4	2.8	5.03	4.819	0.232	1.118	0.259376	0.008596	22.7	600
TC-42206	13.7	6.4	2.9	5.41	5.105	0.258	1.317	0.339786	0.012092	25.8	604
TC-42908	33.7	12.9	3.7	7.32	7.000	0.368	2.576	0.947968	0.037714	44.6	634
TC-43806	38.0	29.4	4.2	8.28	4.323	0.582	2.516	1.464312	0.081165	61.2	878
TC-43610	63.6	26.4	4.7	8.96	6.139	0.626	3.843	2.405718	0.128168	68.5	883
TC-43813	47.2	51.7	5.3	8.29	2.203	1.142	2.516	2.873272	0.247644	71.0	1674
TC-48613	740.1	203.0	9.1	21.50	12.068	1.890	22.809	43.109010	3.581364	348.0	1091

* This AL value has been normalized for a permeability of 1K. For a close approximation of AL for other values of permeability, multiply this AL value by the new permeability in kilo-perm. If the new permeability is 2500, then use 2.5.

© 2011 by Taylor and Francis Group, LLC

Design and Dimensional Data for Toroidal, MPP Powder Cores

The dimensional outline for MPP powder cores is shown in Figure 3-48. Dimensional data for MPP powder cores is given in Table 3-54; design data is given in Table 3-55. See Chapter 2 for more information.

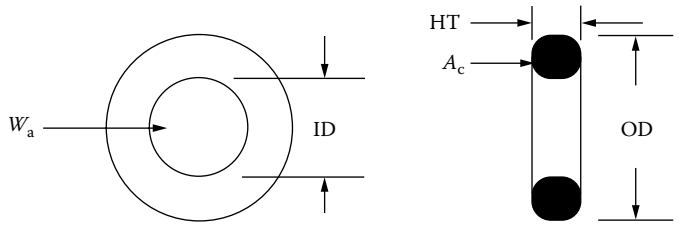

Figure 3-48. Dimension Outline for Toroidal MPP Powder Cores.

Table 3-54. Dimensional Data for Toroidal MPP Powder Cores

MPP Powder Cores, Magnetics 60 mu (coated)											
Part No.	OD cm	ID cm	HT cm	Part No.	OD cm	ID cm	HT cm	Part No.	OD cm	ID cm	HT cm
55021	0.699	0.229	0.343	55381	1.803	0.902	0.711	55076	3.670	2.150	1.135
55281	1.029	0.427	0.381	55848	2.110	1.207	0.711	55083	4.080	2.330	1.537
55291	1.029	0.427	0.460	55059	2.360	1.334	0.838	55439	4.760	2.330	1.892
55041	1.080	0.457	0.460	55351	2.430	1.377	0.965	55090	4.760	2.790	1.613
55131	1.181	0.584	0.460	55894	2.770	1.410	1.194	55716	5.170	3.090	1.435
55051	1.346	0.699	0.551	55071	3.380	1.930	1.143	55110	5.800	3.470	1.486
55121	1.740	0.953	0.711	55586	3.520	2.260	0.978				

Table 3-55. Design Data for Toroidal MPP Powder Cores

MPP Powder Cores, Magnetics 60 mu (coated)											
Part No.	W_{tcu} grams	W_{tfe} grams	MLT cm	MPL cm	$\frac{W_a}{A_c}$	A_c cm^2	W_a cm^2	A_p cm^4	K_g cm^5	A_t cm^2	AL mh/1K
55021	0.10	0.553	1.10	1.36	0.723	0.047	0.034	0.001598	0.000027	2.30	24
55281	0.70	1.307	1.40	2.18	1.729	0.075	0.130	0.009776	0.000210	4.80	25
55291	0.70	1.645	1.60	2.18	1.376	0.095	0.130	0.012285	0.000290	5.10	32
55041	0.90	1.795	1.60	2.38	1.500	0.100	0.150	0.015000	0.000375	5.60	32
55131	1.50	1.993	1.70	2.69	2.759	0.091	0.250	0.022650	0.000483	6.90	26
55051	2.50	2.886	2.00	3.12	3.175	0.114	0.362	0.041268	0.000941	9.30	27
55121	6.10	6.373	2.50	4.11	3.563	0.192	0.684	0.131328	0.004034	16.00	35
55381	5.60	7.670	2.60	4.14	2.634	0.232	0.611	0.141752	0.005059	16.30	43
55848	11.10	8.836	2.80	5.09	4.898	0.226	1.107	0.250182	0.008077	22.70	32
55059	15.20	14.993	3.20	5.67	4.097	0.331	1.356	0.448836	0.018571	28.60	43
55351	17.90	18.706	3.50	5.88	3.727	0.388	1.446	0.561048	0.024878	31.40	51
55894	22.30	33.652	4.10	6.35	2.320	0.654	1.517	0.992118	0.063302	39.80	75
55071	46.20	44.086	4.50	8.15	4.263	0.672	2.865	1.925280	0.115003	58.30	61
55586	61.40	34.900	4.40	8.95	8.681	0.454	3.941	1.789214	0.073846	64.40	38
55076	60.20	48.692	4.80	8.98	5.255	0.678	3.563	2.415714	0.136488	68.00	56
55083	85.30	86.198	5.70	9.84	3.910	1.072	4.191	4.492752	0.337981	87.50	81
55439	101.90	170.140	6.80	10.74	2.106	1.990	4.191	8.340090	0.976281	112.60	135
55090	136.90	122.576	6.40	11.63	4.497	1.340	6.026	8.074840	0.676268	117.20	86
55716	169.30	132.540	6.40	12.73	5.917	1.251	7.402	9.259902	0.724009	133.10	73
55110	233.30	164.500	7.00	14.300	6.474	1.444	9.348	13.498512	1.113820	164.70	75

© 2011 by Taylor and Francis Group, LLC

Design and Dimensional Data for Toroidal, Iron Powder Cores

The dimensional outline for Iron powder cores is shown in Figure 3-49. Dimensional data for Iron powder cores is given in Table 3-56; design data is given in Table 3-57. See Chapter 2 for more information.

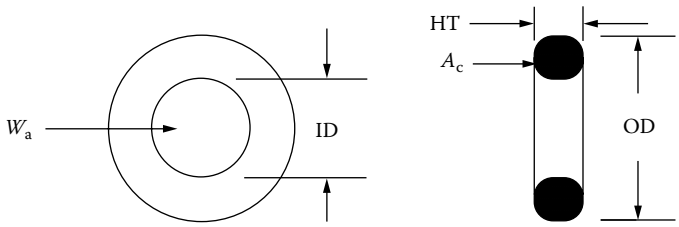

Figure 3-49. Dimension Outline for Toroidal Iron Powder Cores.

Table 3-56. Dimensional Data for Toroidal Iron Powder Cores

Iron Powder Cores, Micrometals 75 mu (coated)											
Part No.	OD cm	ID cm	HT cm	Part No.	OD cm	ID cm	HT cm	Part No.	OD cm	ID cm	HT cm
T20-26	0.508	0.224	0.178	T50-26	1.270	0.770	0.483	T130-26	3.300	1.980	1.110
T25-26	0.648	0.305	0.244	T60-26	1.520	0.853	0.594	T132-26	3.300	1.780	1.110
T26-26	0.673	0.267	0.483	T68-26	1.750	0.940	0.483	T131-26	3.300	1.630	1.110
T30-26	0.780	0.384	0.325	T80-26	2.020	1.260	0.635	T141-26	3.590	2.240	1.050
T37-26	0.953	0.521	0.325	T94-26	2.390	1.420	0.792	T150-26	3.840	2.150	1.110
T38-26	0.953	0.445	0.483	T90-26	2.290	1.400	0.953	T175-26	4.450	2.720	1.650
T44-26	1.120	0.582	0.404	T106-26	2.690	1.450	1.110				

Table 3-57. Design Data for Toroidal Iron Powder Cores

Iron Powder Cores, Micrometals 75 mu (coated)											
Part No.	W_{tcu} grams	W_{tfe} grams	MLT cm	MPL cm	$\frac{W_a}{A_c}$	A_c cm^2	W_a cm^2	A_p cm^4	K_g cm^5	A_t cm^2	AL mh/1K
T20-26	0.10	0.19	0.70	1.15	1.713	0.023	0.039	0.000906	0.000012	1.2	18.5
T25-26	0.24	0.39	0.90	1.50	1.973	0.037	0.073	0.002701	0.000044	2.0	24.5
T26-26	0.26	0.93	1.30	1.47	0.644	0.090	0.058	0.005220	0.000145	2.6	57
T30-26	0.47	0.77	1.14	1.84	1.933	0.060	0.116	0.006960	0.000147	3.1	33.5
T37-26	0.97	1.04	1.28	2.31	3.328	0.064	0.213	0.013632	0.000273	4.5	28.5
T38-26	0.85	1.74	1.50	2.18	1.360	0.114	0.155	0.017670	0.000537	4.8	49
T44-26	1.46	1.86	1.50	2.68	2.687	0.099	0.266	0.026334	0.000695	6.2	37
T50-26	2.96	2.50	1.80	3.19	4.071	0.112	0.456	0.051072	0.001271	8.8	33
T60-26	4.40	4.89	2.20	3.74	3.053	0.187	0.571	0.106777	0.003630	12.2	50
T68-26	5.36	5.30	2.17	4.23	3.877	0.179	0.694	0.124226	0.004099	14.4	43.5
T80-26	11.66	8.31	2.63	5.14	5.394	0.231	1.246	0.287826	0.010112	21.4	46
T94-26	17.44	15.13	3.10	5.97	4.373	0.362	1.583	0.573046	0.026767	29.6	60
T90-26	18.37	15.98	3.40	5.78	3.894	0.395	1.538	0.607510	0.028231	29.4	70
T106-26	23.05	29.94	3.93	6.49	2.504	0.659	1.650	1.087350	0.072970	38.0	93
T130-26	48.33	40.46	4.40	8.28	4.408	0.698	3.077	2.147746	0.136284	56.9	81
T132-26	39.05	44.85	4.40	7.96	3.089	0.805	2.487	2.002035	0.146513	53.9	103
T131-26	32.75	47.83	4.40	7.72	2.357	0.885	2.086	1.845818	0.148504	51.7	116
T141-26	62.70	45.70	4.60	9.14	5.743	0.674	3.871	2.609054	0.152913	66.6	75
T150-26	62.55	58.24	4.85	9.38	4.091	0.887	3.629	3.218923	0.235479	71.6	96
T175-26	128.04	105.05	6.20	11.20	4.334	1.340	5.808	7.782318	0.672794	107.4	105

© 2011 by Taylor and Francis Group, LLC

Design and Dimensional Data for Toroidal, Sendust Powder Cores

The dimensional outline for Sendust powder cores is shown in Figure 3-50. Dimensional data for Sendust powder cores is given in Table 3-58; design data is given in Table 3-59. See Chapter 2 for more information.

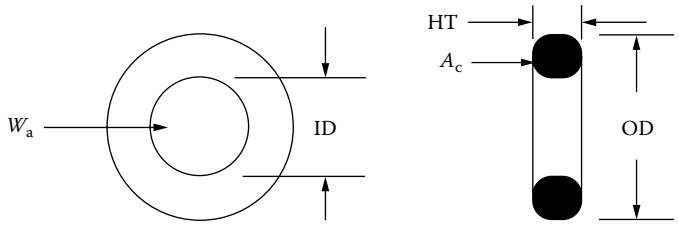

Figure 3-50. Dimension Outline for Toroidal Sendust Powder Cores.

Table 3-58. Dimensional Data for Toroidal Sendust Powder Cores

Sendust Powder Cores, Magnetics 60 mu (coated)											
Part No.	OD cm	ID cm	HT cm	Part No.	OD cm	ID cm	HT cm	Part No.	OD cm	ID cm	HT cm
77021	0.699	0.229	0.343	77381	1.803	0.902	0.711	77076	3.670	2.150	1.135
77281	1.029	0.427	0.381	77848	2.110	1.207	0.711	77083	4.080	2.330	1.537
77291	1.029	0.427	0.460	77059	2.360	1.334	0.838	77439	4.760	2.330	1.892
77041	1.080	0.457	0.460	77351	2.430	1.377	0.965	77090	4.760	2.790	1.613
77131	1.181	0.584	0.460	77894	2.770	1.410	1.194	77716	5.170	3.090	1.435
77051	1.346	0.699	0.551	77071	3.380	1.930	1.143	77110	5.800	3.470	1.486
77121	1.740	0.953	0.711	77586	3.520	2.260	0.978				

Table 3-59. Design Data for Toroidal Sendust Powder Cores

Sendust Powder Cores, Magnetics 60 mu (coated)											
Part No.	W_{tcu} grams	W_{tfe} grams	MLT cm	MPL cm	$\frac{W_a}{A_c}$	A_c cm^2	W_a cm^2	A_p cm^4	K_g cm^5	A_t cm^2	AL mh/1K
77021	0.10	0.448	1.10	1.36	0.723	0.047	0.034	0.001598	0.000027	2.30	24
77281	0.70	1.148	1.40	2.18	1.729	0.075	0.130	0.009776	0.000210	4.80	25
77291	0.70	1.442	1.60	2.18	1.376	0.095	0.130	0.012285	0.000290	5.10	32
77041	0.90	1.666	1.60	2.38	1.500	0.100	0.150	0.015000	0.000375	5.60	32
77131	1.50	1.706	1.70	2.69	2.759	0.091	0.250	0.022650	0.000483	6.90	26
77051	2.50	2.490	2.00	3.12	3.175	0.114	0.362	0.041268	0.000941	9.30	27
77121	6.10	5.524	2.50	4.11	3.563	0.192	0.684	0.131328	0.004034	16.00	35
77381	5.60	6.723	2.60	4.14	2.634	0.232	0.611	0.141752	0.005059	16.30	43
77848	11.10	8.052	2.80	5.09	4.898	0.226	1.107	0.250182	0.008077	22.70	32
77059	15.20	13.137	3.20	5.67	4.097	0.331	1.356	0.448836	0.018571	28.60	43
77351	17.90	15.970	3.50	5.88	3.727	0.388	1.446	0.561048	0.024878	31.40	51
77894	22.30	29.070	4.10	6.35	2.320	0.654	1.517	0.992118	0.063302	39.80	75
77071	46.20	38.338	4.50	8.15	4.263	0.672	2.865	1.925280	0.115003	58.30	61
77586	61.40	28.443	4.40	8.95	8.681	0.454	3.941	1.789214	0.073846	64.40	38
77076	60.20	42.619	4.80	8.98	5.255	0.678	3.563	2.415714	0.136488	68.00	56
77083	85.30	73.839	5.70	9.84	3.910	1.072	4.191	4.492752	0.337981	87.50	81
77439	101.90	149.608	6.80	10.74	2.106	1.990	4.191	8.340090	0.976281	112.60	135
77090	136.90	109.089	6.40	11.63	4.497	1.340	6.026	8.074840	0.676268	117.20	86
77716	169.30	111.477	6.40	12.73	5.917	1.251	7.402	9.259902	0.724009	133.10	73
77110	233.30	144.544	7.00	14.300	6.474	1.444	9.348	13.498512	1.113820	164.70	75

© 2011 by Taylor and Francis Group, LLC

Design and Dimensional Data for Toroidal, High Flux Powder Cores

The dimensional outline for High Flux powder cores is shown in Figure 3-51. Dimensional data for High Flux powder cores is given in Table 3-60; design data is given in Table 3-61. See Chapter 2 for more information.

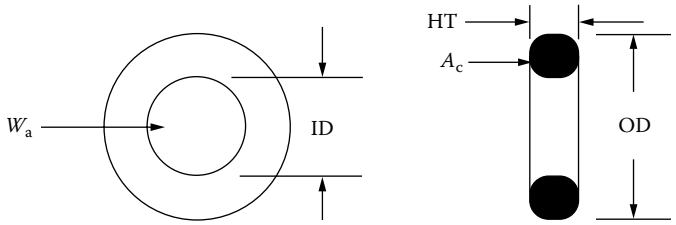

Figure 3-51. Dimension Outline for Toroidal High Flux Powder Cores.

Table 3-60. Dimensional Data for Toroidal High Flux Powder Cores

High Flux Powder Cores, Magnetics 60 mu (coated)											
Part No.	OD cm	ID cm	HT cm	Part No.	OD cm	ID cm	HT cm	Part No.	OD cm	ID cm	HT cm
58021	0.699	0.229	0.343	58381	1.803	0.902	0.711	58076	3.670	2.150	1.135
58281	1.029	0.427	0.381	58848	2.110	1.207	0.711	58083	4.080	2.330	1.537
58291	1.029	0.427	0.460	58059	2.360	1.334	0.838	58439	4.760	2.330	1.892
58041	1.080	0.457	0.460	58351	2.430	1.377	0.965	58090	4.760	2.790	1.613
58131	1.181	0.584	0.460	58894	2.770	1.410	1.194	58716	5.170	3.090	1.435
58051	1.346	0.699	0.551	58071	3.380	1.930	1.143	58110	5.800	3.470	1.486
58121	1.740	0.953	0.711	58586	3.520	2.260	0.978				

Table 3-61. Design Data for Toroidal High Flux Powder Cores

High Flux Powder Cores, Magnetics 60 mu (coated)											
Part No.	W_{tcu} grams	W_{tfe} grams	MLT cm	MPL cm	$\frac{W_a}{A_c}$	A_c cm^2	W_a cm^2	A_p cm^4	K_g cm^5	A_t cm^2	AL mh/1K
58021	0.10	0.519	1.10	1.36	0.723	0.047	0.034	0.001598	0.000027	2.30	24
58281	0.70	1.222	1.40	2.18	1.729	0.075	0.130	0.009776	0.000210	4.80	25
58291	0.70	1.598	1.60	2.18	1.376	0.095	0.130	0.012285	0.000290	5.10	32
58041	0.90	1.692	1.60	2.38	1.500	0.100	0.150	0.015000	0.000375	5.60	32
58131	1.50	1.870	1.70	2.69	2.759	0.091	0.250	0.022650	0.000483	6.90	26
58051	2.50	2.726	2.00	3.12	3.175	0.114	0.362	0.041268	0.000941	9.30	27
58121	6.10	5.960	2.50	4.11	3.563	0.192	0.684	0.131328	0.004034	16.00	35
58381	5.60	7.238	2.60	4.14	2.634	0.232	0.611	0.141752	0.005059	16.30	43
58848	11.10	8.366	2.80	5.09	4.898	0.226	1.107	0.250182	0.008077	22.70	32
58059	15.20	14.100	3.20	5.67	4.097	0.331	1.356	0.448836	0.018571	28.60	43
58351	17.90	17.672	3.50	5.88	3.727	0.388	1.446	0.561048	0.024878	31.40	51
58894	22.30	31.772	4.10	6.35	2.320	0.654	1.517	0.992118	0.063302	39.80	75
58071	46.20	41.548	4.50	8.15	4.263	0.672	2.865	1.925280	0.115003	58.30	61
58586	61.40	30.926	4.40	8.95	8.681	0.454	3.941	1.789214	0.073846	64.40	38
58076	60.20	45.966	4.80	8.98	5.255	0.678	3.563	2.415714	0.136488	68.00	56
58083	85.30	81.310	5.70	9.84	3.910	1.072	4.191	4.492752	0.337981	87.50	81
58439	101.90	160.740	6.80	10.74	2.106	1.990	4.191	8.340090	0.976281	112.60	135
58090	136.90	115.620	6.40	11.63	4.497	1.340	6.026	8.074840	0.676268	117.20	86
58716	169.30	125.020	6.40	12.73	5.917	1.251	7.402	9.259902	0.724009	133.10	73
58110	233.30	155.100	7.00	14.300	6.474	1.444	9.348	13.498512	1.113820	164.70	75

© 2011 by Taylor and Francis Group, LLC

Design and Dimensional Data for EE, Iron Powder Cores

The dimensional outline for EE iron powder cores is shown in Figure 3-52. Dimensional data for EE iron powder cores is given in Table 3-62; design data is given in Table 3-63. See Chapter 2 for more information.

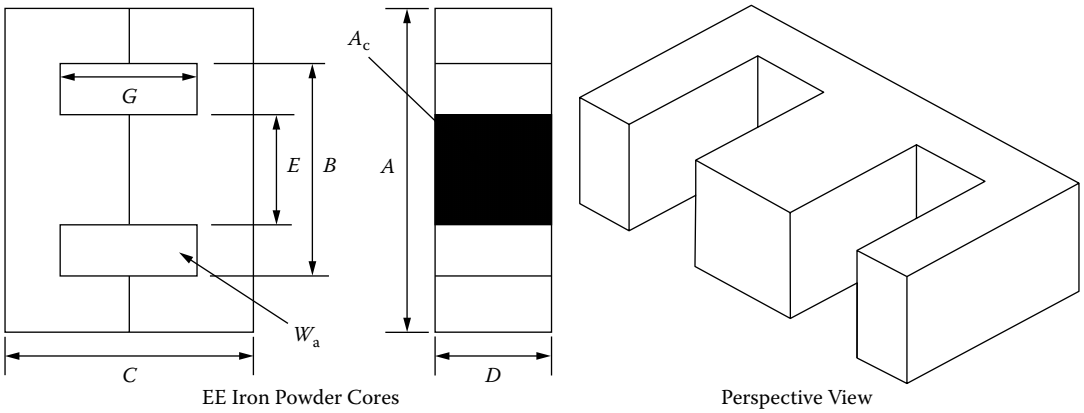

Figure 3-52. Dimension Outline for EE Iron Powder Cores.

Table 3-62. Dimensional Data for EE Iron Powder Cores

EE, Iron Powder Cores (Micrometals) 75 mu Mix-26													
Part No.	A cm	B cm	C cm	D cm	E cm	G cm	Part No.	A cm	B cm	C cm	D cm	E cm	G cm
DIN-16-5	1.640	1.130	1.630	0.462	0.462	1.200	DIN-42-15	4.280	3.070	4.220	1.500	1.200	3.070
EI-187	1.910	1.430	1.610	0.475	0.475	1.160	DIN-42-20	4.280	3.070	4.220	2.000	1.200	3.070
EE-24-25	2.540	1.910	1.910	0.635	0.635	1.270	EI-625	4.740	3.180	3.940	1.570	1.570	2.420
EI-375	3.490	2.540	2.910	0.953	0.953	1.960	DIN-55-21	5.610	3.860	5.540	2.080	1.730	3.830
EI-21	4.130	2.860	3.410	1.270	1.270	2.140	EI-75	5.690	3.810	4.760	1.890	1.890	2.900

Table 3-63. Design Data for EE Iron Powder Cores

EE, Iron Powder Cores (Micrometals) 75 mu Mix-26											
Part No.	W_{tcu} grams	W_{tfe} grams	MLT cm	MPL cm	W_a/A_c	A_c cm^2	W_a cm^2	A_p cm^4	K_g cm^5	A_t cm^2	AL mh/1K
DIN-16-5	4.7	5.3	3.3	3.98	1.790	0.224	0.401	0.090	0.00243	11.5	58
EI-187	7.5	5.5	3.8	4.10	2.451	0.226	0.554	0.125	0.00298	14.4	64
E1-24-25	14.3	12.2	5.0	5.10	2.010	0.403	0.810	0.326	0.01052	23.5	92
EI-375	37.1	40.1	6.7	7.40	1.714	0.907	1.555	1.410	0.07637	46.8	134
EI-21	50.2	80.8	8.2	8.40	1.071	1.610	1.725	2.777	0.21812	63.3	210
DIN-42-15	91.3	112.4	8.9	10.40	1.586	1.810	2.870	5.195	0.42258	84.4	195
DIN-42-20	101.5	149.6	9.9	10.40	1.191	2.410	2.870	6.917	0.67350	92.9	232
EI-625	65.2	141.1	9.4	9.5	0.785	2.480	1.948	4.831	0.50983	82.4	265
DIN-55-21	167.9	283.7	11.6	13.2	1.133	3.600	4.079	14.684	1.82289	141.3	275
EI-75	110.7	245.8	11.2	11.5	0.778	3.580	2.784	9.967	1.27432	119.3	325

© 2011 by Taylor and Francis Group, LLC

Design and Dimensional Data for EE, Sendust Powder Cores

The dimensional outline for EE Sendust cores is shown in Figure 3-53. Dimensional data for EE Sendust powder cores is given in Table 3-64; design data is given in Table 3-65. See Chapter 2 for more information.

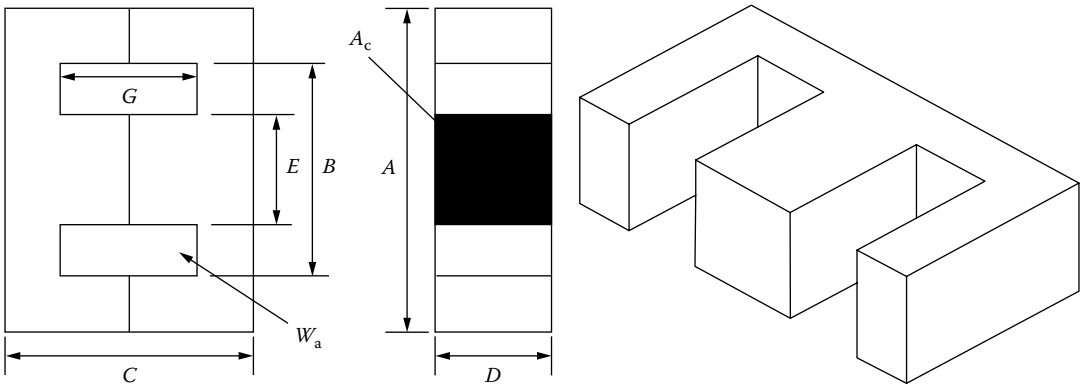

Figure 3-53. Dimension Outline for EE Sendust Powder Cores.

Table 3-64. Dimensional Data for EE Sendust Powder Cores

EE, Sendust Powder Cores (Magnetics) 60 mu													
Part No.	A cm	B cm	C cm	D cm	E cm	G cm	Part No.	A cm	B cm	C cm	D cm	E cm	G cm
EI-187	1.910	1.430	1.610	0.475	0.475	1.160	DIN-42-15	4.280	3.070	4.220	1.500	1.200	3.070
EE-24-25	2.540	1.910	1.910	0.635	0.635	1.270	DIN-42-20	4.280	3.070	4.220	2.000	1.200	3.070
EI-375	3.490	2.540	2.910	0.953	0.953	1.960	DIN-55-21	5.610	3.860	5.540	2.080	1.730	3.830
EI-21	4.130	2.860	3.410	1.270	1.270	2.140							

Table 3-65. Design Data for EE Sendust Powder Cores

EE, Sendust Powder Cores (Magnetics) 60 mu											
Part No.	W_{tcu} grams	W_{tfe} grams	MLT cm	MPL cm	$\frac{W_a}{A_c}$	A_c cm^2	W_a cm^2	A_p cm^4	K_g cm^5	A_t cm^2	AL mh/1K
EI-187	7.5	6.4	3.8	4.01	2.451	0.226	0.554	0.125	0.00298	14.4	48
E1-24-25	14.3	13.1	5.0	4.85	2.010	0.403	0.810	0.326	0.01052	23.5	70
EI-375	37.1	40.8	6.7	6.94	1.714	0.907	1.555	1.410	0.07637	46.8	102
EI-21	50.2	82.6	8.2	7.75	1.071	1.610	1.725	2.777	0.21812	63.3	163
DIN-42-15	91.3	126.0	8.9	9.84	1.586	1.810	2.870	5.195	0.42258	84.4	150
DIN-42-20	101.5	163.0	9.9	9.84	1.191	2.410	2.870	6.917	0.67350	92.9	194
DIN-55-21	167.9	302.0	11.6	12.3	1.133	3.600	4.079	14.684	1.82289	141.3	219

© 2011 by Taylor and Francis Group, LLC

Manufacturers' Material Product List

Table 3-66 has been put together to show a product list of the leading manufacturers for ferrites, powder cores, nickel-iron tape cores, amorphous tape cores, and laminations. Listed in the references are the manufacturers and their web-page address.

Table 3-66

Manufacturers Material Product List				
Ferrites Cores				
Manufacturers	Mn-Zn	Ni-Zn	Special Machining	
Ferroxcube	X			
TDK	X			
Magnetics	X		X	
EPCOS, Inc.	X			
TSC Ferrite Int.	X			
Fair-Rite	X	X	X	
MMG	X	X		
Ceramic Magnetics, Inc.	X	X	X	
Powder Cores				
Manufacturers	MPP	Hi-Flux	Sendust	Iron Powder
Magnetics	X	X	X	X
Micrometals	X	X	X	X
MMG	X	X	X	X
Tape Toroids and C Cores				
Manufacturers	Silicon	Supermendur	50-50 NiFe	80-20 NiFe
Magnetics	X	X	X	X
Magnetic Metals	X	X	X	X
Electro-Core, Inc.	X			
Amorphous Tape Toroids and C Cores				
Manufacturers	2605SC	2714A	Nanocrystalline	Special
Magnetic Metals	X	X	X	
Metglas	X	X		
VAC	X	X	X	
MK Magnetics, Inc.	X	X	X	Only
Laminations				
Manufacturers	Silicon	Supermendur	50-50 NiFe	80-20 NiFe
Thomas & Skinner, Inc.	X			
Magnetic Metals	X	X	X	X
Tempel Steel Co.	X			

© 2011 by Taylor and Francis Group, LLC

References

Ceramic Magnetics, Inc. www.cmi-ferrite.com

Electro-Core Inc. www.electro-core.com

EPCOS www.usa.epcos.com

Fair Rite www.fair-rite.com

Ferroxcube www.ferroxcube.com

Magnetics www.mag-inc.com

Magnetic Metals Corp. www.magmet.com

Metglas www.metglas.com

Micrometals www.micrometals.com

MK Magnetics www.mkmagnetics.com

MMG www.mmgca.com

TDK www.tdk.com

Tempel Steel Co. www.tempel.com

Thomas and Skinner, Inc. www.thomas-skinner.com

TSC Ferrite International www.tscinternational.com

VAC www.vaccorp.com

© 2011 by Taylor and Francis Group, LLC

Chapter 4

Window Utilization, Magnet Wire and Insulation

© 2011 by Taylor and Francis Group, LLC

Table of Contents

1. Window Utilization Factor, K_u 4-4
2. S_1, Wire Insulation 4-5
3. S_2, Fill Factor 4-6
4. S_3, Effective Window 4-9
5. S_4, Insulation Factor 4-12
6. Summary 4-12
7. Window Utilization Factor, K_u for Bobbin Ferrites 4-13
8. Circular mil and Square mil 4-14
9. Magnet Wire 4-15
10. Magnet Wire, Film Insulation 4-16
11. Wire Table 4-16
12. Solderable Insulation 4-19
13. Bondable Magnet Wire 4-20
14. Base Film Insulation 4-20
15. Bonding Methods 4-21
16. Miniature Square Magnet Wire 4-21
17. Multistrand Wire and Skin Effect 4-22
18. Reduce Skin Effect in Transformers 4-23
19. Calculating Skin Effect in Inductors 4-24
20. Multistrand Litz Wire 4-27
21. Proximity Effect 4-28
22. Proximity Effect in Transformers 4-29
23. Multiple Layer High Frequency Transformers and High Loss 4-29
24. Proximity Effect Using Dowell Curves 4-31
25. Specialty Wire 4-33
26. Triple Insulated Wire 4-33
27. Triple Insulated Litz 4-34
28. Polyfilar Magnetic Wire 4-35
29. Standard Foils 4-36
30. The Use of Foils 4-37
31. Calculating, MLT 4-40
32. Calculating, MLT (toroid) 4-40

© 2011 by Taylor and Francis Group, LLC

33. Copper Resistance 4-41
34. Copper Weight 4-41
35. Electrical Insulating Materials 4-41
36. References 4-42

© 2011 by Taylor and Francis Group, LLC

Window Utilization Factor, K_u

The window utilization factor is the amount of copper that appears in the window area of the transformer or inductor. The window utilization factor is influenced by five main factors:

1. Wire insulation, S_1.
2. Wire lay fill factor, layer or random wound, S_2.
3. Effective window area (or when using a toroid, the clearance hole for passage of the shuttle), S_3.
4. Insulation required for multiplayer windings, or between windings, S_4.
5. Workmanship, (quality).

These factors, multiplied together, will give a normalized window utilization of $K_u = 0.4$, as shown in Figure 4-1.

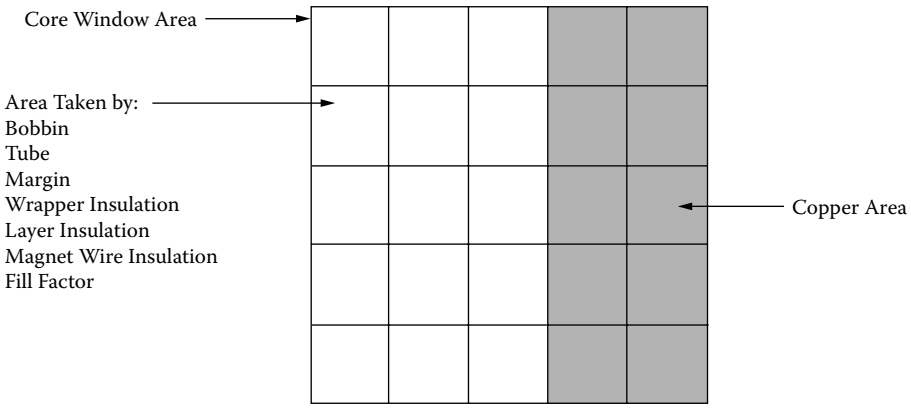

Figure 4-1. Window Area Occupied by Copper.

The window utilization factor, K_u, of the available core window is that space occupied by the winding (copper), and is calculated from areas S_1, S_2, S_3, and S_4:

$$K_u = S_1 S_2 S_3 S_4 \qquad [4\text{-}1]$$

Where:

S_1 = conductor area/wire area

S_2 = wound area/usable window area

S_3 = usable window area/window area

S_4 = usable window area/usable window area + insulation

© 2011 by Taylor and Francis Group, LLC

In which:

Conductor area, $A_{w(B)}$ = copper area.

Wire area, A_w = copper area + insulation area.

Wound area = number of turns × wire area of one turn.

Usable window area = available window area − residual area, that results from the particular winding technique used.

Window area = available window area.

Insulation area = area used for winding insulation.

S_1, Wire Insulation

In the design of high-current or low-current transformers, the ratio of the conductor area to the total wire area can vary from 0.941 to 0.673, depending on the wire size. In Figure 4-2, the thickness of the insulation has been exaggerated to show how the insulation impacts the overall area of the wire.

It can be seen, in Figure 4-2, that, by using multi-strands of fine wire to reduce the skin effect, it will have a significant impact on the window utilization factor, K_u. S_1 is not only dependent upon wire size, but it is also dependent upon insulation coating. Table 4-1 shows the ratio of bare magnet wire to the magnet wire with insulation for single, heavy, triple, and quad insulation. When designing low-current transformers, it is advisable to re-evaluate, S_1, because of the increased amount of insulating material.

$$S_1 = \frac{A_{w(B)}}{A_w} \qquad [4\text{-}2]$$

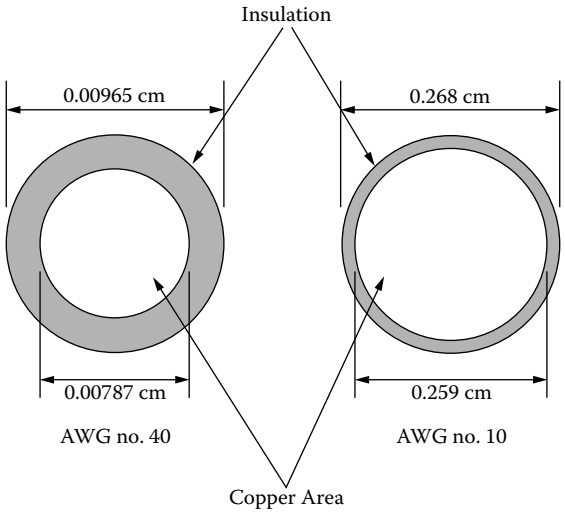

Figure 4-2. Comparing Insulation with Different Wire Gauges.

© 2011 by Taylor and Francis Group, LLC

Table 4-1. Magnetic Wire Data (Nominal)

Magnetic Wire Data (Nominal)					
Size AWG	Bare Area (cm^2)	Ratio Bare/Single	Ratio Bare/Heavy	Ratio Bare/Triple	Ratio Bare/Quad
10	0.1019	0.961	0.930	0.910	0.880
15	0.0571	0.939	0.899	0.867	0.826
20	0.0320	0.917	0.855	0.812	0.756
25	0.0179	0.878	0.793	0.733	0.662
30	0.0100	0.842	0.743	0.661	0.574
35	0.0056	0.815	0.698	0.588	0.502
40	0.0031	0.784	0.665	0.544	0.474

S_2, Fill Factor

S_2 is the fill factor, or the wire lay, for the usable window area. When winding a large number of turns tightly on a smooth surface, the winding length exceeds the calculated value from the wire diameter by 10 to 15%, depending on the wire gauge. See Figure 4-3. The wire lay is subjected to wire tension, and wire quality, such as continuous wire diameter and the winding technique depending on the skill of the operator. The wire lay factor relationship for various wire sizes for layer wound coils is shown in Table 4-2, and for random wound coils in Table 4-3. These two Tables list the outside diameter for heavy film magnetic wire, 10–44 AWG.

Table 4-2. Wire Lay Factors For Layer Wound Coils

Wire Lay Factors For Layer Wound Coils			
AWG	Insulated Wire OD (inch)	Insulated Wire OD (cm)	Wire Lay Factor
10 to 25	0.1051-0.0199	0.2670-0.0505	0.90
26 to 30	0.0178-0.0116	0.0452-0.0294	0.89
31 to 35	0.0105-0.0067	0.0267-0.0170	0.88
36 to 38	0.0060-0.0049	0.0152-0.0124	0.87
39 to 40	0.0043-0.0038	0.0109-0.0096	0.86
41 to 44	0.0034-0.0025	0.00863-0.00635	0.85
Heavy film magnetic wire.			

Table 4-3. Wire Lay Factor For Random Wound Coils

Wire Lay Factor For Random Wound Coils			
AWG	Insulated Wire OD (inch)	Insulated Wire OD (cm)	Wire Lay Factor
10 to 22	0.1051-0.0276	0.267-0.0701	0.90
23 to 39	0.0623-0.0109	0.0249-0.0043	0.85
40 to 44	0.0038-0.0025	0.0096-0.00635	0.75
Heavy film magnet wire.			

© 2011 by Taylor and Francis Group, LLC

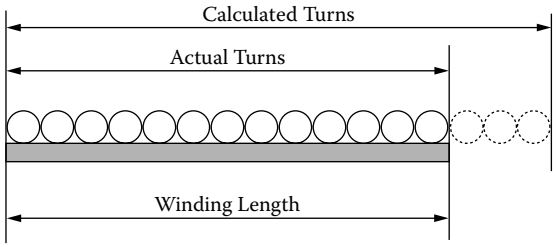

Figure 4-3. Capable Turns per Unit Length.

There are two ideal winding arrangements shown in Figure 4-4 and Figure 4-5. The square winding is shown in Figure 4-4 and the hexagonal winding is shown in Figure 4-5. The simplest form of winding is done by a coil being wound, turn-by-turn and layer-upon-layer, as shown in Figure 4-4. The square winding pattern has a theoretical, fill factor of 0.785.

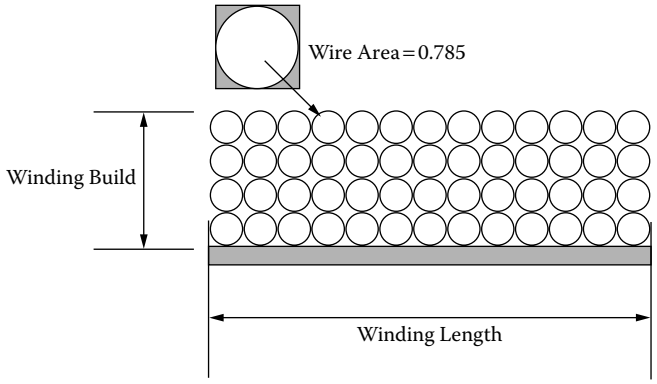

Figure 4-4. Theoretically, the Square Winding Pattern Fill Factor 0.785.

A seemingly, better fill factor can be achieved by using the hexagonal winding in Figure 4-5, compared to the square winding in Figure 4-4. In this type of winding, the individual wires do not lie exactly above each other, as in the square winding pattern. Instead, the wires lie in the grooves of the lower layer, as shown in Figure 4-5.

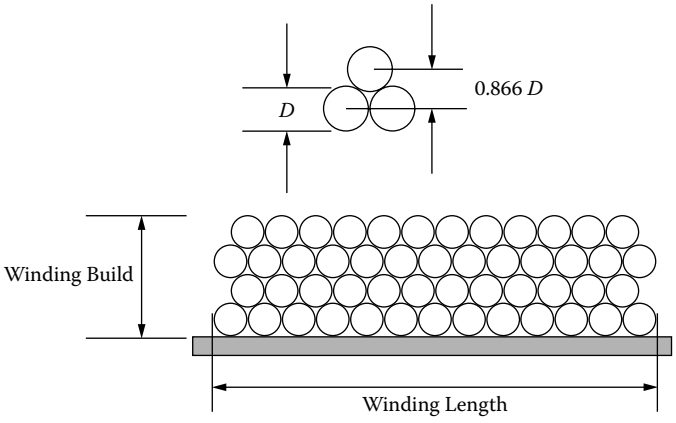

Figure 4-5. Theoretically, the Hexagonal Winding Pattern Fill Factor 0.907.

© 2011 by Taylor and Francis Group, LLC

This style of winding produces the tightest possible packing of the wire. The hexagonal style of winding will yield a theoretical, fill factor of 0.907.

The fill factor, using the square-winding pattern of 0.785, would be nearly impossible to achieve by hand winding without some layer insulation. Any layer insulation will reduce the fill factor even further. The fill factor, using the hexagonal winding pattern of 0.907, is just as hard to get. Hand-winding, using the hexagonal technique, will result in the following: The first layer goes down with almost complete order. In the second layer, some disordering has occurred. With the third and fourth layer, disordering really sets in and the winding goes completely awry. This type of winding performs well with a small number of turns, but, with a large number of turns, it becomes randomly wound.

The ideal winding on a rectangular bobbin is shown in Figure 4-6. Then, when winding rectangular bobbins or tubes, the actual winding height in the region covered by the core will be greater than the calculated winding height or build, due to the bowing of the windings. See Figure 4-7. The amount of bowing depends on the proportions of the winding and the height of the winding. Usually, the available winding build should be reduced by 15 to 20%, or 0.85 times the winding build. When winding on a round bobbin or tube, this bowing effect is negligible.

The conclusion is, when comparing the square winding pattern used in the layer wound coil with its insulation with the hexagonal winding pattern and its awry winding pattern, both seem to have a fill factor of about 0.61. But there is always the hundred to one exception, such as, when a design happens to have the right bobbin, the right number of turns, and the right wire size. This normally only happens when the design is not critical.

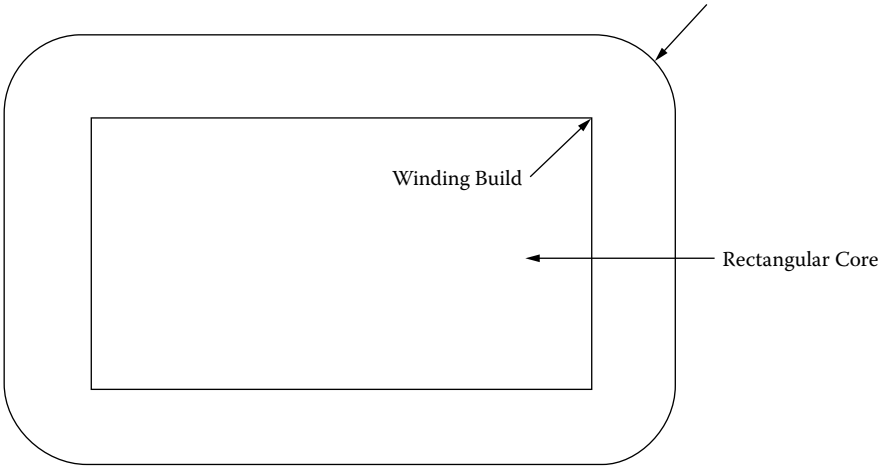

Figure 4-6. Ideal Winding on a Rectangular Bobbin.

© 2011 by Taylor and Francis Group, LLC

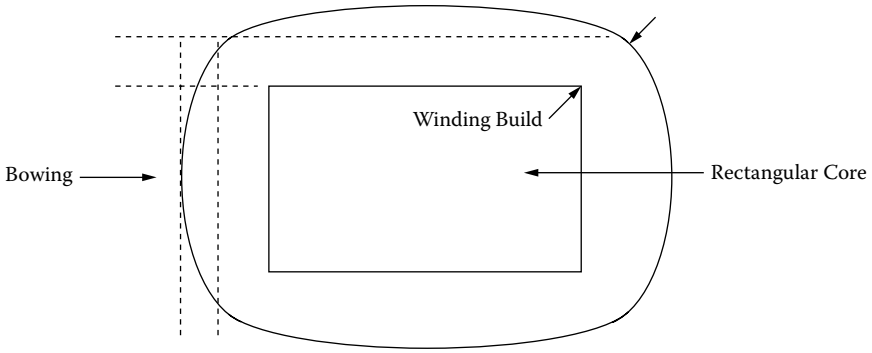

Figure 4-7. Bowing in Transformer Windings.

To minimize this bowing effect and to insure a minimum build for either random or layer winding, the round bobbin, shown in Figure 4-8, will provide the most compact design. It can be seen, in Figure 4-8, that the round bobbin provides a uniform tension, all 360 degrees around the bobbin, for both layer and random windings. The other benefit, in using a round bobbin, is the reduction and minimizing of the leakage inductance caused from the bowing.

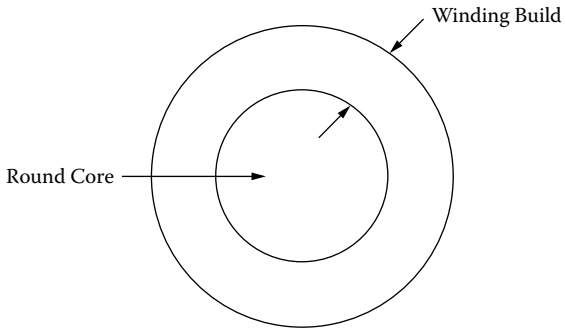

Figure 4-8. A Round Bobbin Insures Minimum Bowing.

S_3, Effective Window

The effective window, S_3, defines how much of the available window space may actually be used for the winding. The winding area available to the designer depends on the bobbin or tube configuration. Designing a layer winding that uses a tube will require a margin, as shown in Figure 4-9. The margin dimensions will vary with wire size. See Table 4-4. It can be seen, in Figure 4-9 and Table 4-4, how the margin reduces the effective window area. When transformers are constructed, using the layer winding technique, there is an industry standard for layer insulation thickness. This thickness is based on the diameter of the wire, as shown in Table 4-5.

© 2011 by Taylor and Francis Group, LLC

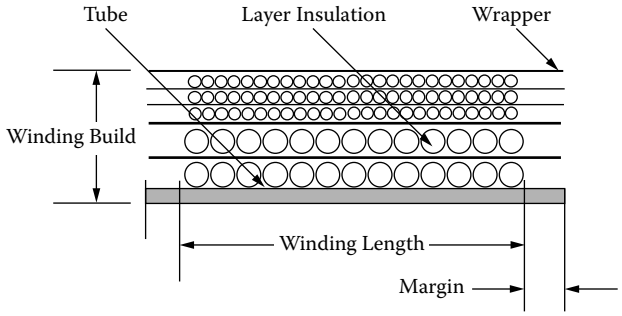

Figure 4-9. Transformer Windings with Margins.

Table 4-4. Winding Margins Versus AWG

Winding Margins Versus AWG		
	Margin	
AWG	cm	inch
10-15	0.635	0.25
16-18	0.475	0.187
19-21	0.396	0.156
22-31	0.318	0.125
32-37	0.236	0.093
38-up	0.157	0.062

Table 4-5. Layer Insulation Thickness

Layer Insulation Thickness		
	Insulation Thickness	
AWG	cm	inch
10 - 16	0.02540	0.01000
17 - 19	0.01780	0.00700
20 - 21	0.01270	0.00500
22 - 23	0.00760	0.00300
24 - 27	0.00510	0.00200
28 - 33	0.00381	0.00150
34 - 41	0.00254	0.00100
42 - 46	0.00127	0.00050

A single bobbin design, as shown in Figure 4-10, offers an effective area, W_a, between 0.835 to 0.929 for laminations, and 0.55 to 0.75 for ferrites; a two bobbin configuration, as shown in Figure 4-11, offers an effective area, W_a, between 0.687 to 0.873 for the tape C cores.

© 2011 by Taylor and Francis Group, LLC

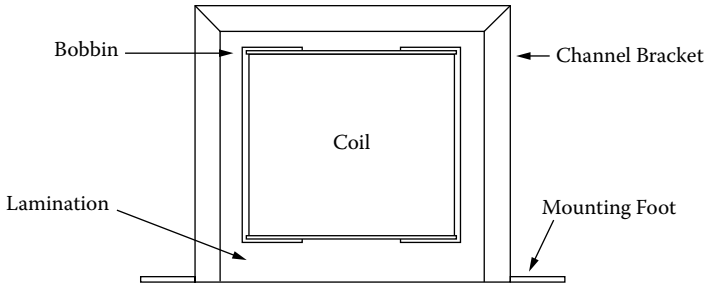

Figure 4-10. Transformer Construction with Single Bobbin.

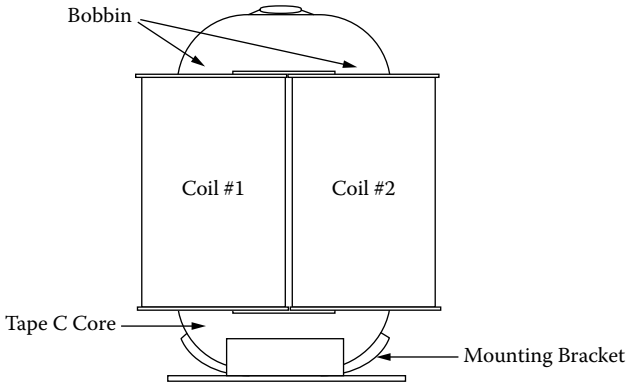

Figure 4-11. Transformer Construction with Dual Bobbins.

The toroid is a little different. The term, S_3, defines how much of the available window space can actually be used for the winding. In order to wind the toroidal core, there has to be room to allow free passage of the shuttle. If half of the inside diameter is set aside for the shuttle, then, there will be 75% of the window area, (W_a), left for the design which is a good value for the effective window area factor, $S_3 = 0.75$, as shown in Figure 4-12. The toroid would fall within its limits, into all of the above categories.

Effective Window area $W_{a(eff)} = (0.75)(\pi)(ID)^2/4$

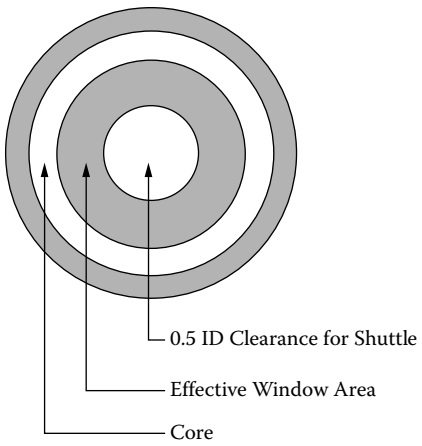

Figure 4-12. Effective Winding Area of a Toroidal Core.

© 2011 by Taylor and Francis Group, LLC

S_4, Insulation Factor

The insulation factor, S_4, defines how much of the usable window space is actually being used for insulation. If the transformer has multiple secondaries with significant amounts of insulation, S_4, should be reduced by 5 to 10% for each additional secondary winding, partly because of the added space occupied by insulation and partly because of the poorer space factor.

The insulation factor, S_4, is not taken into account in Figure 4-12. The insulation factor, S_4, is to be 1.0. The window utilization factor, K_u, is highly influenced by insulation factor, S_4, because of the rapid buildup of insulation in the toroid, as shown in Figure 4-13.

In Figure 4-13, it can be seen that the insulation buildup is greater on the inside, than on the outside. For example, in Figure 4-13, if 1.27 cm (1/2″) wide tape was used with an overlap of 0.32 cm (1/8″) on the outside diameter, the overlap thickness would be four times the thickness of the tape. It should be noted that the amount of overlap depends greatly on the size of the toroid and the required tape. In the design of toroidal components, and using the 0.5 ID remaining for passage of the shuttle, there is normally enough room for the wrapper.

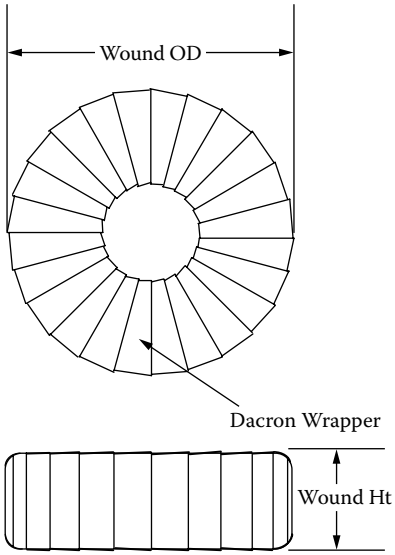

Figure 4-13. Wrapped Toroid.

Summary

The author hopes to have cleared up some of the mystery of how the window utilization factor, K_u, was derived and that the magic of 0.4 is now clear. All the different parts making up window utilization, have been explained, hopefully eliminating confusion and simplifying the complexity of the subject.

© 2011 by Taylor and Francis Group, LLC

As stated at the beginning of this chapter, a good approximation for the window utilization factor is $K_u = 0.4$.

S_1 = conductor area/wire area = 0.855, #20 AWG

S_2 = wound area/usable window area = 0.61

S_3 = usable window area/windo.w area = 0.75

S_4 = usable window area/usable window area + insulation = 1

$$K_u = S_1 S_2 S_3 S_4$$
$$K_u = (0.855)(0.61)(0.75)(1.0) = 0.391 \approx 0.4 \quad [4\text{-}3]$$

Being a very conservative number, it can be used in most designs. It is an important factor in all designs of magnetic components.

Window Utilization Factor, K_u for Bobbin Ferrites

In high frequency power electronics, the majority of the designs will use some kind of bobbin ferrite. The main reasons for using ferrites is its high frequency performance and cost. The window utilization factor, K_u, for bobbin ferrites is not as high as it is for iron alloy materials, such as laminations and C cores. Design engineers, who have been using bobbin ferrite materials, know the drawback in the window utilization factor, K_u. Once this problem is understood, then, the problem should go away.

Ferrite materials are fired in kilns like ceramic pottery. There is a certain amount of shrinkage after firing, and the amount varies from one manufacturer's process to another. The amount of shrinkage could vary as much as 15 to 30%, as shown in Figure 4-14. The ferrite manufacturers try to keep a tight control on the amount of shrinkage, because these cores must meet a dimensional tolerance after firing. Even though the shrinkage is under tight control, the tolerances on the end product are much larger than the iron alloy, stamped laminations. The end result is the bobbin has to slip on and meet all of the minimum and maximum dimensional tolerances.

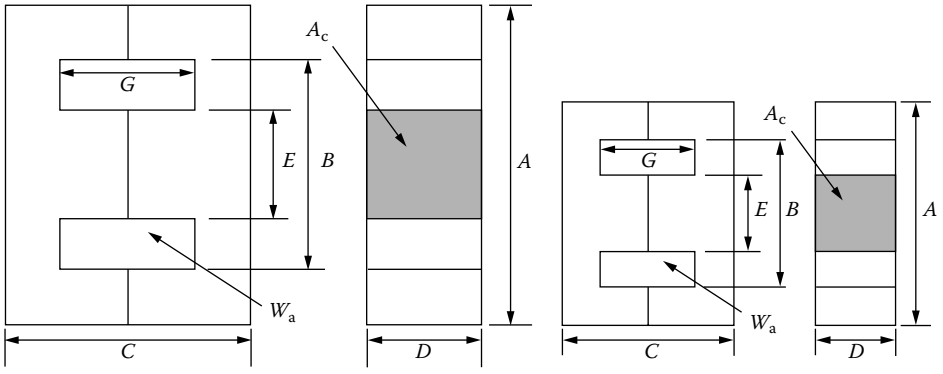

EE Ferrite Cores Before Firing EE Ferrite Cores After Firing

Figure 4-14. Ferrite EE Core Before and After Firing.

© 2011 by Taylor and Francis Group, LLC

This dimensional tolerance has an impact on the winding area of the bobbin, clearly shown in Table 4-6. This smaller winding area reduces the power handling capability of the core. Operating at high frequency will also reduce the power handling capability of the core because of the skin effect. The skin effect requires the use of multistrands of fine wire in place of a large single strand. The selection of the correct wire size to minimize the skin effect at a given frequency is shown in Equations [4-5] through [4-9]. Also shown is an example of the largest wire size that should be used when operating at 100kHz. Reevaluate the, K_u, Equation [4-3] so that it can operate at 100kHz, using a #26 wire, and using a cut ferrite core.

S_1 = conductor area/wire area = 0.79, #26 AWG (Transformers)

S_1 = conductor area/wire area = 0.855, #20 AWG (DC Inductors)

S_2 = wound area/usable window area = 0.61

S_3 = usable window area/window area = 0.6

S_4 = usable window area/usable window area + insulation = 1

$$K_u = S_1 S_2 S_3 S_4$$
$$K_u = (0.79)(0.61)(0.6)(1.0) = 0.289, \text{ [Transformers]} \quad [4\text{-}4]$$
$$K_u = (0.855)(0.61)(0.6)(1.0) = 0.313, \text{ [DC Inductors]}$$

Table 4-6. Effective Window Area

Effective Window Area			
Core	Window cm^2	Bobbin cm^2	Ratio B/W
RM-6	0.260	0.150	0.577
RM-8	0.449	0.303	0.675
RM-12	1.103	0.730	0.662
PQ-20/16	0.474	0.256	0.540
PQ-26/25	0.845	0.502	0.594
PQ-35/35	2.206	1.590	0.721
EFD-10	0.116	0.042	0.362
EFD-15	0.314	0.148	0.471
EFD-25	0.679	0.402	0.592
EC-35	1.571	0.971	0.618
EC-41	2.082	1.375	0.660
EC-70	6.177	4.650	0.753
Laminations			
EI-187	0.529	0.368	0.696
EI-375	1.512	1.170	0.774
EI-21	1.638	1.240	0.757

Circular mil and Square mil

There are engineers that use Circular mils (CM)/amp or square mils/amp. This is the reciprocal current density. The norm is to use amps/cm^2, which is a true current density. There have been some requests to define circular mils and square mils. First, let's define a mil, which is .001 inch. Figure 4-15 shows the area of a square mil, and the area of a circular mil.

© 2011 by Taylor and Francis Group, LLC

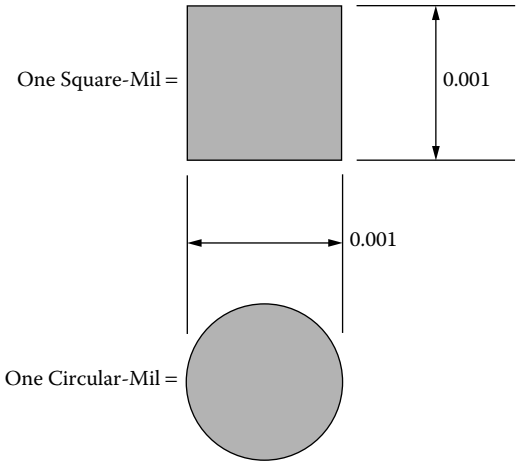

Figure 4-15. Comparing Circular-Mils and Square-Mils.

To convert Square mils to Circular mils, multiply by 1.2732.

To convert Circular mils to Square mils, multiply by 0.7854.

To convert Circular mils to Square centimeters, multiply by 5.066×10^{-6}.

To convert Square mils to Square centimeters, multiply by 6.45×10^{-6}.

Note: Designers have used this rule of thumb for many years:

$$500\text{CM/Amp} \approx 400\,\text{Amps/cm}^2$$
$$1000\text{CM/Amp} \approx 200\,\text{Amps/cm}^2$$

Magnet Wire

Standard magnet wire is available in three different materials, shown in Table 4-7. The most common material is copper, but aluminum and silver are available. Aluminum magnet wire is one-third the weight of copper for the same size conductor and one-half the weight for the same conductivity. Aluminum magnet wire is a little more difficult to terminate, but it can be done. Silver magnet wire has the highest conductivity, is easy to solder to, and weighs 20% more than copper.

Table 4-7. Magnet Wire Material Properties

Magnet Wire Material Properties						
Material	Symbol	Density grams/cm^3	Resistivity μΩ/cm	Weight Factor	Resistance Factor	Temperature Coefficient
Copper	Cu	8.89	1.72	1	1	0.00393
Silver	Ag	10.49	1.59	1.18	0.95	0.00380
Aluminum	Al	2.703	2.83	0.3	1.64	0.00410

© 2011 by Taylor and Francis Group, LLC

Magnet Wire, Film Insulation

It is the design engineer's responsibility to ensure that the selected magnet wire used in the design is compatible with the environmental and design specification. The environmental specification will set the ambient temperature. The maximum operating temperature of the magnet wire is obtained by summing the maximum ambient temperature, plus the temperature rise of the magnetic component. After the maximum temperature has been obtained, see Table 4-8 for the Temperature Class. The magnet wire insulation guide listing in Table 4-7, is only a partial list from NEMA, Standard MW 1000.

The maximum operating temperature is the "Achilles Heel" to the magnet wire. Standard magnet wire is rated by temperature. The range is from 105°C to 220°C, as shown in Table 4-8. The insulation film of the magnet wire is on the surface of the copper wire. This insulation film is the most vulnerable to thermal overloads, so the selection of the insulation film is very critical for long life. When magnet wire is subjected to thermal overloads, or a high ambient temperature above its rated temperature, the life of the magnet wire is greatly reduced, as shown in Figures 4-16 and 4-17. The engineer must be very careful of hot spots so as not to degrade the service life of the magnetic component.

Table 4-8. Magnet Wire Insulation Guide

Magnet Wire Insulation Guide			
Temperature Class	Insulation Type	Dielectric Constant	NEMA Standard MW 1000
105°C	Polyurethane*	6.20	MW-2-C
105°C	Formvar	3.71	MW-15-C
130°C	Polyurethane-Nylon*	6.20	MW-28-C
155°C	Polyurethane-155	6.20	MW-79-C
180°C	Polyester Solderable*	3.95	MW-77-C
200°C	Polyester-amid-imide	4.55	MW-35-C
220°C	Polyimide (ML)	3.90	MW-16-C
* Solderable insulations.			

Wire Table

Table 4-9 is the Wire Table for AWG, 10 to 44, heavy film wire. The bare wire areas are given in cm^2 in column 2, and the circular mils are given in column 3 for each wire size. The equivalent resistance in micro-ohms per centimeter ($\mu\Omega$/cm or 10^{-6} Ω/cm) is given in column 4 for each wire size. Columns 5 through 13 relate to the heavy, insulated film coating. The weight of the magnet wire is found in column 13, in grams, per centimeter.

Table 4-10 provides the maximum outside diameter for magnet wire with single, heavy, triple, and quad film insulation. The dimensional data is in centimeters and inches, for AWG 10 through 44.

© 2011 by Taylor and Francis Group, LLC

Table 4-9. Wire Table

Wire Table												
	Bare Area		Resistance μΩ/cm	Heavy Synthetics								
				Area		Diameter		Turns-Per		Turns-Per		Weight
AWG	$cm^2(10^{-3})$	cir-mil	20°C	$cm^2(10^{-3})$	cir-mil	cm	Inch	cm	Inch	cm^2	$Inch^2$	gm/cm
1	2	3	4	5	6	7	8	9	10	11	12	13
10	52.6100	10384.00	32.7	55.9000	11046.00	0.2670	0.105	3.9	10	11	69	0.46800
11	41.6800	8226.00	41.4	44.5000	8798.00	0.2380	0.094	4.4	11	13	90	0.37500
12	33.0800	6529.00	52.1	35.6400	7022.00	0.2130	0.084	4.9	12	17	108	0.29770
13	26.2600	5184.00	65.6	28.3600	5610.00	0.1900	0.075	5.5	13	21	136	0.23670
14	20.8200	4109.00	82.8	22.9500	4556.00	0.1710	0.068	6.0	45	26	169	0.18790
15	16.5100	3260.00	104.3	18.3700	3624.00	0.1530	0.060	6.8	17	33	211	0.14920
16	13.0700	2581.00	131.8	14.7300	2905.00	0.1370	0.054	7.3	19	41	263	0.11840
17	10.3900	2052.00	165.8	11.6800	2323.00	0.1220	0.048	8.2	21	51	331	0.09430
18	8.2280	1624.00	209.5	9.3260	1857.00	0.1090	0.043	9.1	23	64	415	0.07474
19	6.5310	1289.00	263.9	7.5390	1490.00	0.0980	0.039	10.2	26	80	515	0.05940
20	5.1880	1024.00	332.3	6.0650	1197.00	0.0879	0.035	11.4	29	99	638	0.04726
21	4.1160	812.30	418.9	4.8370	954.80	0.0785	0.031	12.8	32	124	800	0.03757
22	3.2430	640.10	531.4	3.8570	761.70	0.0701	0.028	14.3	36	156	1003	0.02965
23	2.5880	510.80	666.0	3.1350	620.00	0.0632	0.025	15.8	40	191	1234	0.02372
24	2.0470	404.00	842.1	2.5140	497.30	0.0566	0.022	17.6	45	239	1539	0.01884
25	1.6230	320.40	1062.0	2.0020	396.00	0.0505	0.020	19.8	50	300	1933	0.01498
26	1.2800	252.80	1345.0	1.6030	316.80	0.0452	0.018	22.1	56	374	2414	0.01185
27	1.0210	201.60	1687.0	1.3130	259.20	0.0409	0.016	24.4	62	457	2947	0.00945
28	0.8046	158.80	2142.0	1.0515	207.30	0.0366	0.014	27.3	69	571	3680	0.00747
29	0.6470	127.70	2664.0	0.8548	169.00	0.0330	0.013	30.3	77	702	4527	0.00602
30	0.5067	100.00	3402.0	0.6785	134.50	0.0294	0.012	33.9	86	884	5703	0.00472
31	0.4013	79.21	4294.0	0.5596	110.20	0.0267	0.011	37.5	95	1072	6914	0.00372
32	0.3242	64.00	5315.0	0.4559	90.25	0.0241	0.010	41.5	105	1316	8488	0.00305
33	0.2554	50.41	6748.0	0.3662	72.25	0.0216	0.009	46.3	118	1638	10565	0.00241
34	0.2011	39.69	8572.0	0.2863	56.25	0.0191	0.008	52.5	133	2095	13512	0.00189
35	0.1589	31.36	10849.0	0.2268	44.89	0.0170	0.007	58.8	149	2645	17060	0.00150
36	0.1266	25.00	13608.0	0.1813	36.00	0.0152	0.006	62.5	167	3309	21343	0.00119
37	0.1026	20.25	16801.0	0.1538	30.25	0.0140	0.006	71.6	182	3901	25161	0.00098
38	0.0811	16.00	21266.0	0.1207	24.01	0.0124	0.005	80.4	204	4971	32062	0.00077
39	0.0621	12.25	27775.0	0.0932	18.49	0.0109	0.004	91.6	233	6437	41518	0.00059
40	0.0487	9.61	35400.0	0.0723	14.44	0.0096	0.004	103.6	263	8298	53522	0.00046
41	0.0397	7.84	43405.0	0.0584	11.56	0.0086	0.003	115.7	294	10273	66260	0.00038
42	0.0317	6.25	54429.0	0.0456	9.00	0.0076	0.003	131.2	333	13163	84901	0.00030
43	0.0245	4.84	70308.0	0.0368	7.29	0.0069	0.003	145.8	370	16291	105076	0.00023
44	0.0202	4.00	85072.0	0.0316	6.25	0.0064	0.003	157.4	400	18957	122272	0.00020

© 2011 by Taylor and Francis Group, LLC

Table 4-10. Dimensional Data for Film Insulated Magnetic Wire

Dimensional Data for Film Insulated Magnetic Wire								
Wire Size AWG	Maximum Diameter							
	Single-Insulation		Heavy-Insulation		Triple-Insulation		Quad-Insulation	
	Inches	Centimeters	Inches	Centimeters	Inches	Centimeters	Inches	Centimeters
10	0.1054	0.2677	0.1071	0.2720	0.1084	0.2753	0.1106	0.2809
11	0.9410	2.3901	0.0957	0.2431	0.0969	0.2461	0.0991	0.2517
12	0.0840	0.2134	0.0855	0.2172	0.0867	0.2202	0.0888	0.2256
13	0.0750	0.1905	0.0765	0.1943	0.0776	0.1971	0.0796	0.2022
14	0.0670	0.1702	0.0684	0.1737	0.0695	0.1765	0.0715	0.1816
15	0.0599	0.1521	0.0613	0.1557	0.0624	0.1585	0.0644	0.1636
16	0.0534	0.1356	0.0548	0.1392	0.0558	0.1417	0.0577	0.1466
17	0.0478	0.1214	0.0492	0.1250	0.0502	0.1275	0.0520	0.1321
18	0.0426	0.1082	0.0440	0.1118	0.0450	0.1143	0.0468	0.1189
19	0.0382	0.0970	0.0395	0.1003	0.0404	0.1026	0.0422	0.1072
20	0.0341	0.0866	0.0353	0.0897	0.0362	0.0919	0.0379	0.0963
21	0.0306	0.0777	0.0317	0.0805	0.0326	0.0828	0.0342	0.0869
22	0.0273	0.0693	0.0284	0.0721	0.0292	0.0742	0.0308	0.0782
23	0.0244	0.0620	0.0255	0.0648	0.0263	0.0668	0.0279	0.0709
24	0.0218	0.0554	0.0229	0.0582	0.0237	0.0602	0.2520	0.6401
25	0.0195	0.0495	0.0206	0.0523	0.0214	0.0544	0.0228	0.0579
26	0.0174	0.0442	0.0185	0.0470	0.0192	0.0488	0.0206	0.0523
27	0.0156	0.0396	0.0165	0.0419	0.0172	0.0437	0.0185	0.0470
28	0.0139	0.0353	0.0148	0.0376	0.0155	0.0394	0.0166	0.0422
29	0.0126	0.0320	0.0134	0.0340	0.0141	0.0358	0.0152	0.0386
30	0.0112	0.0284	0.0120	0.0305	0.0127	0.0323	0.0137	0.0348
31	0.0100	0.0254	0.0108	0.0274	0.0115	0.0292	0.0124	0.0315
32	0.0091	0.0231	0.0098	0.0249	0.0105	0.0267	0.0113	0.0287
33	0.0081	0.0206	0.0088	0.0224	0.0095	0.0241	0.0102	0.0259
34	0.0072	0.0183	0.0078	0.0198	0.0084	0.0213	0.0091	0.0231
35	0.0064	0.0163	0.0070	0.0178	0.0076	0.0193	0.0082	0.0208
36	0.0058	0.0147	0.0063	0.0160	0.0069	0.0175	0.0074	0.0188
37	0.0052	0.0132	0.0057	0.0145	0.0062	0.0157	0.0067	0.0170
38	0.0047	0.0119	0.0051	0.0130	0.0056	0.0142	0.0060	0.0152
39	0.0041	0.0104	0.0045	0.0114	0.0050	0.0127	0.0053	0.0135
40	0.0037	0.0094	0.0040	0.0102	0.0044	0.0112	0.0047	0.0119
41	0.0033	0.0084	0.0036	0.0091	0.0040	0.0102	0.0043	0.0109
42	0.0030	0.0076	0.0032	0.0081	0.0037	0.0094	0.0038	0.0097
43	0.0026	0.0066	0.0029	0.0074	0.0033	0.0084	0.0035	0.0089
44	0.0024	0.0061	0.0027	0.0069	0.0030	0.0076	0.0032	0.0081

© 2011 by Taylor and Francis Group, LLC

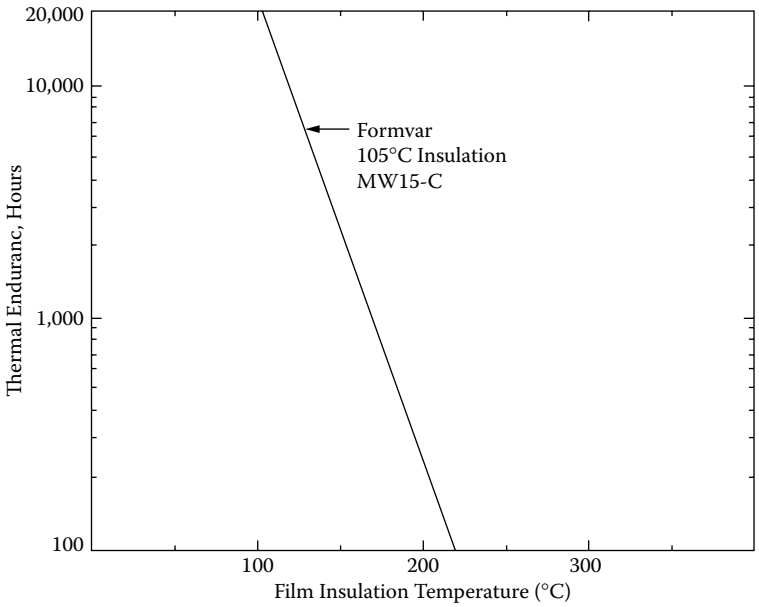

Figure 4-16. Thermal Endurance, for 105°C Formvar Insulation.

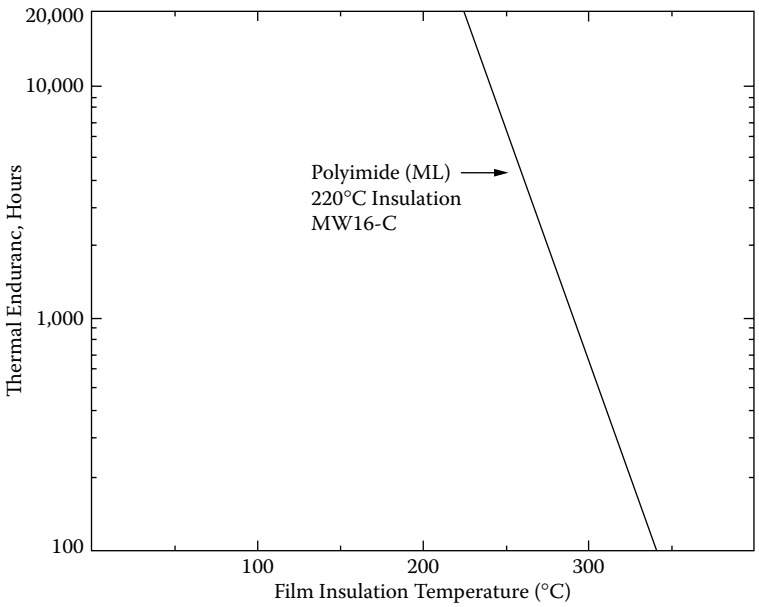

Figure 4-17. Thermal Endurance for 220°C Polyimide Insulation (ML).

Solderable Insulation

Solderable insulation is a special film insulation that is used on magnet wire in low cost, high volume applications. The magnet wire, with this solderable insulation, is wrapped around the terminal or pin, as shown in Figure 4-18. Then the terminal can be dip-soldered at the prescribed temperature without prior stripping. The ambient temperature range for this type of film insulation is 105°C to 180°C.

© 2011 by Taylor and Francis Group, LLC

There are drawbacks in using some of the solderable insulation magnet wire. Prior to using, check your application with the wire manufacturer. Some solderable film insulation is not recommended where severe overloads may occur. Some solderable film insulations are susceptible to softening, due to prolonged exposure to strong solvents, such as alcohol, acetone, and methylethylketone.

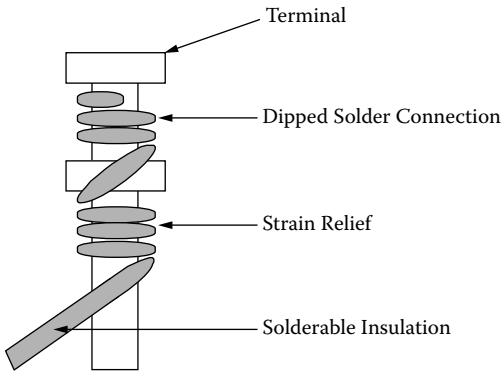

Figure 4-18. Solderable Insulation on a Dip Solder Terminal.

Bondable Magnet Wire

Bondable, magnet wires are a film-coated, copper or aluminum, with an additional coating of a thermoplastic adhesive. See Figure 4-19. They are used in applications where it is desirable to have the bonding agent, such as a solvent, which will hold the coil form until it is oven-baked. Most adhesive coatings can be softened with solvents or heat. If a coil is wound with an irregular shape, held in a form, and then raised to the appropriate temperature, the coil will retain its shape. Bondable magnet wires have applications such as armatures, field coils, and self-supporting coils.

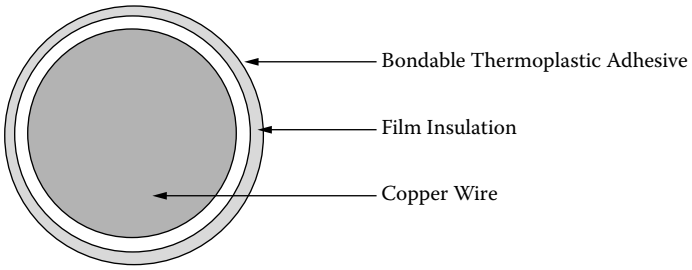

Figure 4-19. Typical Cross-Section of a Bondable Magnet Wire.

Base Film Insulation

All conventional film insulations may be adhesive-coated to achieve a bondable wire. However, care should be taken in selecting wires, which are insulated with high temperature films, since the adhesive coating may not withstand the equally high temperatures. See Table 4-11. The temperatures, in Table 4-11, are for reference

© 2011 by Taylor and Francis Group, LLC

only. It is wise to always check with the manufacturer for the latest in materials and application notes. The addition of the adhesive coating over the film insulation will result in an increase in the finished diameter, by the same magnitude, as if going from a single to a heavy insulation.

Table 4-11. Bondable Overcoats

Bondable Overcoats			
Type	Operating Temperature	Heat Activation Temperature	Solvents Activating Agents
Polyvinyl Butryal	105°C	120° - 140°C	Alcohol
Epoxy	130°C	130° - 150°C	Methylethylketone Acetone
Polyester	130°C	130° - 150°C	Methylethylketone
Nylon	155°C	180° - 220°C	None

Bonding Methods

Heat Bonding may be accomplished by the use of a temperature-controlled oven. Small components can use a controlled hot air blower to bond the wires. In either case, caution should be used when handling the coil while it is still hot, since deformation can take place.

Resistance Bonding is a method where a current is passed through the winding to achieve the desired bonding temperature. This method generates a very even, heat distribution resulting in a good bonding throughout the winding. Many coils can be resistance-bonded at the same time. The current required for one coil, will be the same current required when many are connected in series. Just solder the coils in series then adjust the applied voltage until the same current is reached.

Solvent Bonding is a method where the solvent activates the bonding material. This can be done, by passing the wire through a solvent-saturated felt pad or a light spray application. There are many activating solvents that can be used: denatured ethyl alcohol, isopropyl alcohol, methylethylketone and acetone. The solvents should always be checked on with the manufacturer for the latest in materials and for application notes.

Miniature Square Magnet Wire

When product miniaturization calls for more copper in a given area, MWS Microsquare film, insulated magnet wire allows the design of compact coils to deliver more power in less space. See Table 4-12. Microsquare magnet wire is available in both copper and aluminum. It is also available in a range of solderable and high temperature film insulation. A cross-section of a Number 26, heavy-build, microsquare magnet wire is shown in Figure 4-20.

© 2011 by Taylor and Francis Group, LLC

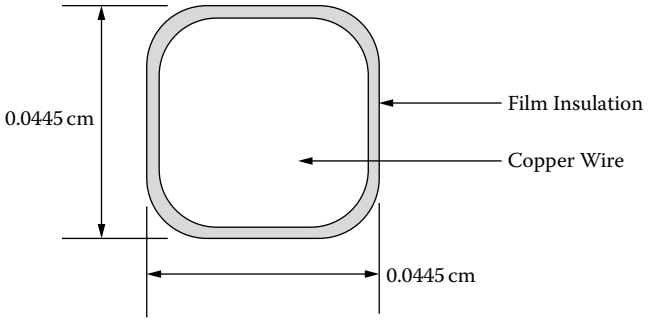

Figure 4-20. Cross-Section of a #26, Heavy-build, Microsquare Magnet Wire.

Table 4-12. Micro-Square Magnetic Wire (Nominal Dimension)

Micro-Square Magnetic Wire (Nominal Dimension)								
Wire Size AWG	Bare Width cm	Bare Width Inch	Wire Area cm^2	Wire Area sq-mils	Copper Resistance Ω/cm	Aluminum Resistance Ω/cm	Single Width cm	Heavy Width cm
15	0.1450	0.0571	0.019614	3041	0.0000879	0.000144	0.1483	0.1514
16	0.1290	0.0508	0.015228	2361	0.0001132	0.000186	0.1323	0.1354
17	0.1151	0.0453	0.011816	1832	0.0001459	0.000239	0.1184	0.1212
18	0.1024	0.0403	0.009675	1500	0.0001782	0.000293	0.1054	0.1080
19	0.0912	0.0359	0.007514	1165	0.0002294	0.000377	0.0940	0.0968
20	0.0813	0.0320	0.006153	954	0.0002802	0.000460	0.0841	0.0866
21	0.0724	0.0285	0.004786	742	0.0003602	0.000591	0.0749	0.0772
22	0.0643	0.0253	0.003935	610	0.0004382	0.000719	0.0668	0.0688
23	0.0574	0.0226	0.003096	480	0.0005568	0.000914	0.0599	0.0620
24	0.0511	0.0201	0.002412	374	0.0007147	0.001173	0.0536	0.0556
25	0.0455	0.0179	0.002038	316	0.0008458	0.001388	0.0480	0.0498
26	0.0404	0.0159	0.001496	232	0.0011521	0.001891	0.0427	0.0445
27	0.0361	0.0142	0.001271	197	0.0013568	0.002227	0.0389	0.0409
28	0.0320	0.0126	0.001006	156	0.0017134	0.002813	0.0348	0.0366
29	0.0287	0.0113	0.000787	122	0.0021909	0.003596	0.0312	0.0330
30	0.0254	0.0100	0.000587	91	0.0029372	0.004822	0.0277	0.0295

Multistrand Wire and Skin Effect

Electronic equipment now operates at higher frequencies. With direct current and low frequencies the efficiency can be predicted. The current carried by the conductor is distributed uniformly across the cross-section of the conductor. The flux generated by the magnet wire is shown in Figure 4-21. There is a concentration of current near the wire surface at higher frequencies, which is termed the skin effect. This is the result of magnetic flux lines that generate eddy currents in the magnet wire, as shown in Figure 4-22.

© 2011 by Taylor and Francis Group, LLC

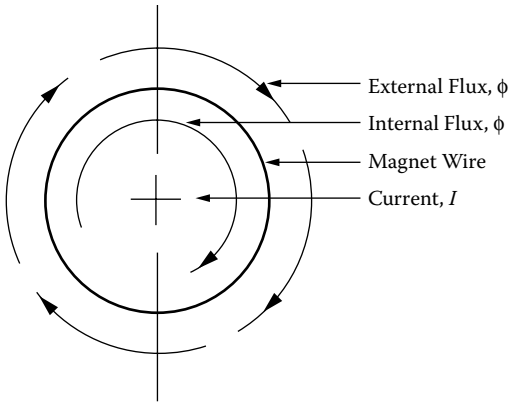

Figure 4-21. Flux Distribution in a Magnet Wire.

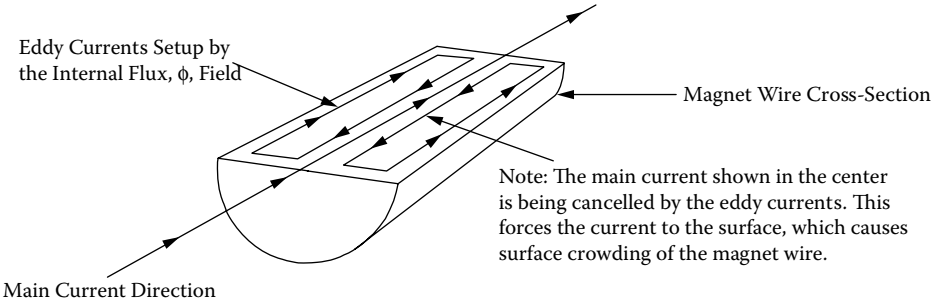

Figure 4-22. Eddy Currents Generated in a Magnet Wire.

Reduce Skin Effect in Transformers

Skin effect accounts for the fact that the ratio of effective alternating current resistance to direct current is greater than unity. The magnitude of this effect, at high frequency on conductivity, magnetic permeability, and inductance, is sufficient to require further evaluation of conductor size, during design. The skin depth is defined as the distance below the surface, where the current density has fallen to 1/ε or 37 percent of its value at the surface.

$$\varepsilon = \left(\frac{6.62}{\sqrt{f}}\right)K, \quad \text{[cm]}$$

ε, is the skin depth [4-5]

f, is frequency in hertz

K, is equal to 1 for copper

When selecting the wire for high frequency, select a wire where the relationship between the ac resistance and the dc resistance is 1.

$$R_R = \frac{R_{ac}}{R_{dc}} = 1 \qquad [4\text{-}6]$$

© 2011 by Taylor and Francis Group, LLC

Using this approach, select the largest wire, operating at 100 kHz.

$$\varepsilon = \left(\frac{6.62}{\sqrt{f}}\right)K, \quad [\text{cm}]$$
$$\varepsilon = \left(\frac{6.62}{\sqrt{100{,}000}}\right)(1), \quad [\text{cm}] \qquad [4\text{-}7]$$
$$\varepsilon = 0.0209, \quad [\text{cm}]$$

The wire diameter is:

$$D_{AWG} = 2(\varepsilon), \quad [\text{cm}]$$
$$D_{AWG} = 2(0.0209), \quad [\text{cm}] \qquad [4\text{-}8]$$
$$D_{AWG} = 0.0418, \quad [\text{cm}]$$

The bare wire area $A_{w(B)}$ is:

$$A_{w(B)} = \frac{\pi D_{AWG}^2}{4}, \quad [\text{cm}^2]$$
$$A_{w(B)} = \frac{(3.14)(0.0418)}{4}, \quad [\text{cm}^2] \qquad [4\text{-}9]$$
$$A_{w(B)} = 0.00137, \quad [\text{cm}^2]$$

The wire size closest to this area of 0.00137 is AWG #26 with 0.00128 cm^2. (See Table 4-9.)

Calculating Skin Effect in Inductors

Inductors have skin effect problems just like transformers. The skin effect depends on the amount of ac current ΔI in the inductor. The high frequency inductor current has two components: the dc current, I_{dc}, and the ac current, ΔI. The dc current travels in the center of the conductor, and the ac travels on the surface of the conductor, as shown in Figure 4-23.

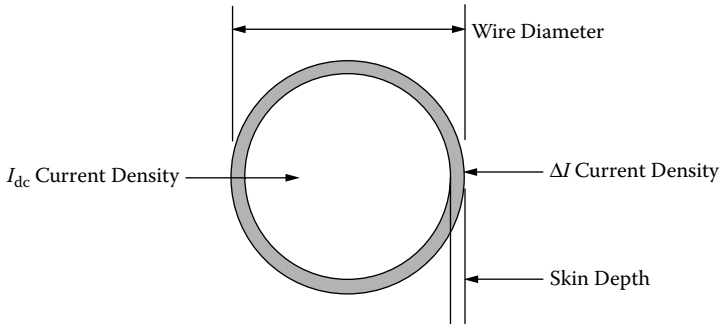

Figure 4-23. DC Inductor High Frequency Current Distribution.

The following procedure is used to calculate the high frequency current density, ΔI, while using Figure 4-23, as a reference.

© 2011 by Taylor and Francis Group, LLC

The skin depth Equation is:

$$\varepsilon = \left(\frac{6.62}{\sqrt{f}}\right)K, \quad [\text{cm}] \tag{4-10}$$

Calculate the diameter of the copper conductor:

$$D_{AWG} = \sqrt{\frac{4\left(A_{w(B)}\right)}{\pi}}, \quad [\text{cm}] \tag{4-11}$$

Subtract two times the skin depth, ε, from the diameter, D_{AWG}.

$$D_n = D_{AWG} - 2\varepsilon, \quad [\text{cm}] \tag{4-12}$$

Calculate the new wire area, A_n.

$$A_n = \frac{\pi\left(D_n\right)^2}{4}, \quad [\text{cm}^2] \tag{4-13}$$

The high frequency wire area, $A_{w(\Delta I)}$, is the difference between the wire area, $A_{w(B)}$, and the new area, A_n.

$$A_{w(\Delta I)} = A_{w(B)} - A_n, \quad [\text{cm}^2] \tag{4-14}$$

The ac current, ΔI, in an inductor is a triangular waveform. The, ΔI_{rms}, current is:

$$\Delta I_{rms} = I_{pk}\sqrt{\frac{1}{3}}, \quad [\text{amps}] \tag{4-15}$$

Calculate the current density for the delta rms current, ΔI_{rms}.

$$J = \frac{\Delta I_{rms}}{A_{w(\Delta I)}}, \quad [\text{amps-per-cm}^2] \tag{4-16}$$

The delta rms current, ΔI_{rms}, current density, J, should be:

$$\Delta I_{rms} \text{ current density } \leq I_{dc} \text{ current density}$$

© 2011 by Taylor and Francis Group, LLC

A graph of Skin Depth, as a function of frequency, is shown in Figure 4-24. The relationship of Skin Depth to AWG radius is shown in Figure 4-25, where $R_{ac}/R_{dc} = 1$, is plotted on a graph of AWG versus frequency.

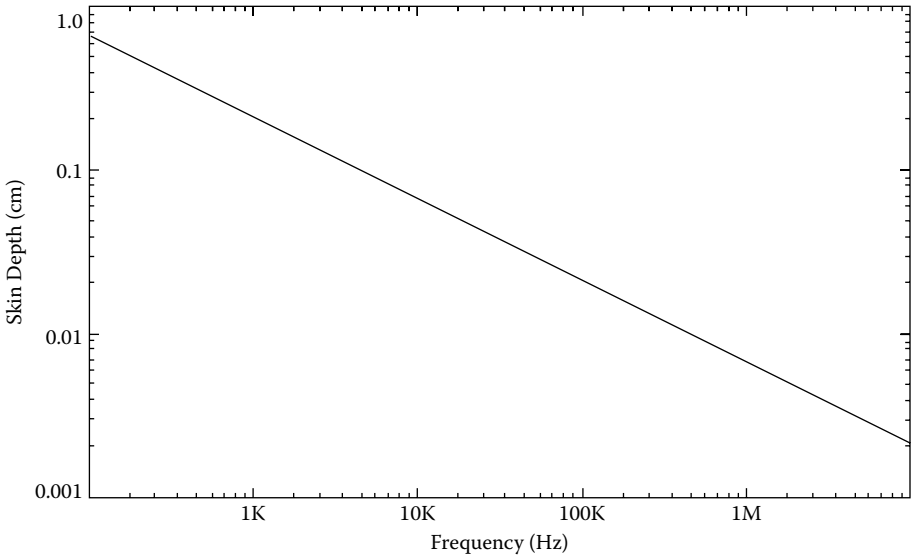

Figure 4-24. Skin Depth Versus Frequency.

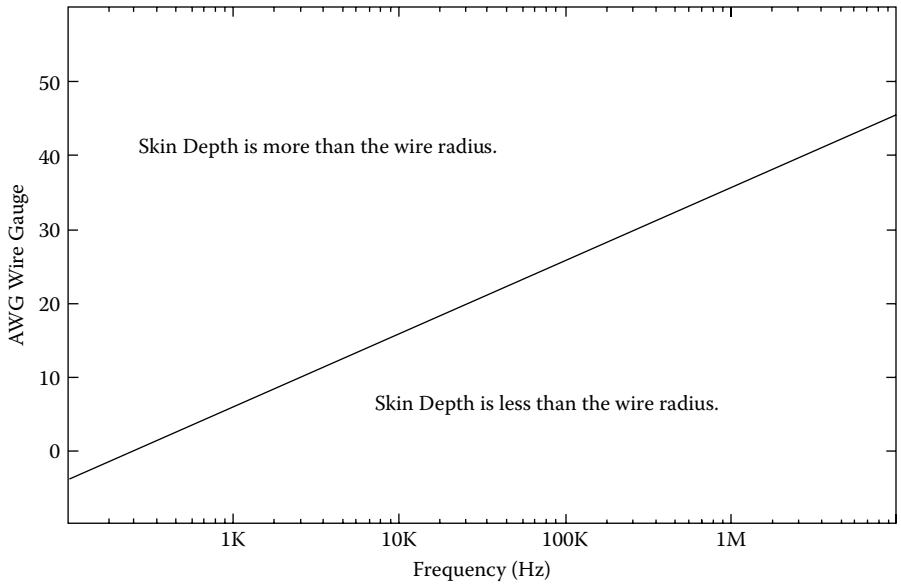

Figure 4-25. AWG Versus Frequency at Which Skin Depth Equals the Radius.

To illustrate how the AWG ac/dc resistance ratio changes with frequency, see Table 4-13. In Table 4-13, it can be seen that when a converter operates at 100 kHz, the largest wire that should be used is a Number 26, with an ac/dc resistance ratio of 1.001.

© 2011 by Taylor and Francis Group, LLC

Table 4-13. AWG ac/dc Resistance Ratio at Common Converter Frequencies

AWG ac/dc Resistance Ratio at Common Converter Frequencies									
AWG	$D_{(AWG)}$ cm	25 kHz		50 kHz		100 kHz		200 kHz	
		ε cm	$\frac{R_{ac}}{R_{dc}}$	ε cm	$\frac{R_{ac}}{R_{dc}}$	ε cm	$\frac{R_{ac}}{R_{dc}}$	ε cm	$\frac{R_{ac}}{R_{dc}}$
12	0.20309	0.041868	1.527	0.029606	2.007	0.020934	2.704	0.014802	3.699
14	0.16132	0.041868	1.300	0.029606	1.668	0.020934	2.214	0.014802	2.999
16	0.12814	0.041868	1.136	0.029606	1.407	0.020934	1.829	0.014802	2.447
18	0.10178	0.041868	1.032	0.029606	1.211	0.020934	1.530	0.014802	2.011
20	0.08085	0.041868	1.001	0.029606	1.077	0.020934	1.303	0.014802	1.672
22	0.06422	0.041868	1.000	0.029606	1.006	0.020934	1.137	0.014802	1.410
24	0.05101	0.041868	1.000	0.029606	1.000	0.020934	1.033	0.014802	1.214
26	0.04052	0.041868	1.000	0.029606	1.000	0.020934	1.001	0.014802	1.078
28	0.03219	0.041868	1.000	0.029606	1.000	0.020934	1.000	0.014802	1.006
30	0.02557	0.041868	1.000	0.029606	1.000	0.020934	1.000	0.014802	1.000
AWG Copper, skin depth is at 20°C.									

Multistrand Litz Wire

The term litz wire is extracted from the German word, meaning woven wire. Litz wire is generally defined, as a wire constructed of individually, film insulated wires, braided together in a uniform pattern of twists and length of lay. This multistrand configuration minimizes the power losses, otherwise encountered, in a solid conductor, due to the skin effect. The minimum and maximum number of strand for standard litz wire is shown in Table 4-14. Magnet wire suppliers will supply larger, twisted magnet wire, on request.

Table 4-14. Standard Litz Wire

Standard Litz Wire				
AWG	Minimum Strands	Approximate AWG	Maximum Strands	Approximate AWG
30	3	25	20	17.0
32	3	27	20	19.0
34	3	29	20	21.0
36	3	31	60	18.5
38	3	33	60	20.5
40	3	35	175	18.0
41	3	36	175	18.5
42	3	37	175	19.5
43	3	38	175	21.0
44	3	39	175	21.5
45	3	40	175	22.5
46	3	41	175	23.5
47	3	42	175	25.0
48	3	43	175	25.5

© 2011 by Taylor and Francis Group, LLC

Proximity Effect

The operating frequency for power supplies is now in the range of 50 to 500 kHz. With it came along some new tasks for the engineer to address, skin effect and proximity effect. They are quite similar in that they both generate eddy currents in the magnet wire. The eddy currents produced by these effects have the same solution, keeping the ratio of the ac resistance, R_{ac}, to the dc resistance, R_{dc} down:

$$R_R = \frac{R_{ac}}{R_{dc}} \qquad [4\text{-}17]$$

The information provided here on proximity effect is taken from the five References provided at the end of this Chapter. The references are excellent, providing an in-depth analysis of the losses due to proximity effect, which is beyond the intent of this effort.

Proximity effect is caused by eddy currents induced in a wire due to the alternating magnetic field of other conductors in the vicinity. The flux generated by the magnet wire is shown in Figure 4-26. The eddy currents cause a distortion of the current density. This distortion is the result of magnetic flux lines that generate eddy currents in the magnet wire, therefore enhancing the main current, I, on one side and subtracting from the main current on the other, as shown in Figure 4-27. A magnet wire with its distorted current density is shown in Figure 4-28.

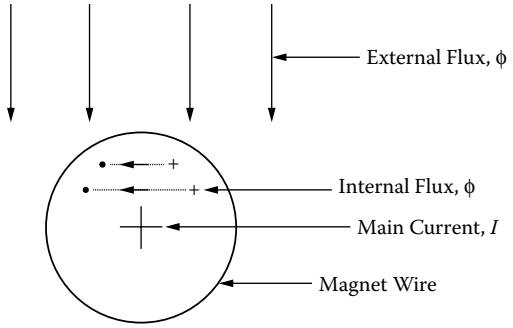

Figure 4-26. Flux Distribution in a Magnet Wire.

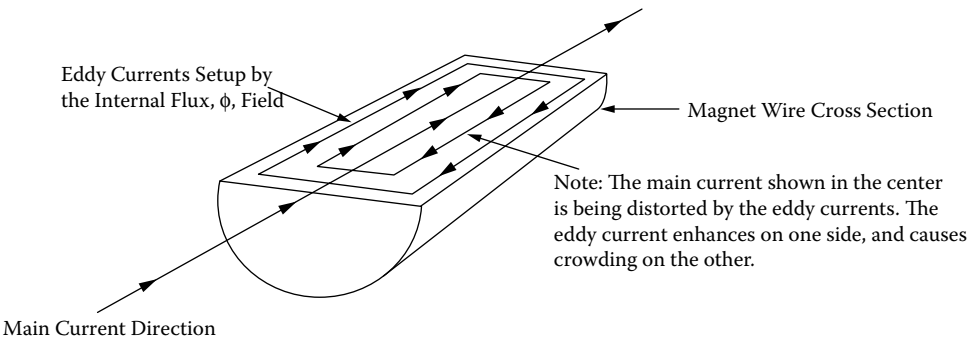

Figure 4-27. Eddy Currents Generated in a Magnet Wire.

© 2011 by Taylor and Francis Group, LLC

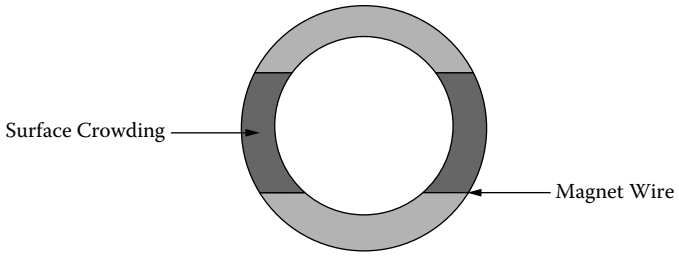

Figure 4-28. Magnet Wire, Showing Distorted Surface Crowding.

Proximity Effect in Transformers

Proximity effect has a minimum of impact on a transformer with a single layer secondary, as shown in Figure 4-29 along with its low frequency magneto-motive force (mmf) diagram. Keeping the proximity effect to a minimum requires the transformer to be designed with a minimum of layers. The selection of a core with a long narrow window will produce a design with a minimum of layers, in the same way as picking a core for a minimum of leakage inductance.

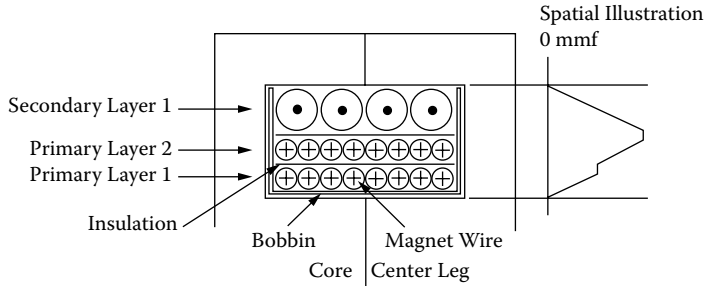

Figure 4-29. Simple Transformer Showing mmf.

Multiple Layer High Frequency Transformers and High Loss

The proximity effect is outlined for a transformer having a secondary with three layers, evenly spaced, as shown in Figure 4-30. A schematic diagram version of the transformer is shown in Figure 4-31, showing the different magneto-motive force (mmf = F_m) potentials. It is assumed that the high frequency penetration depth

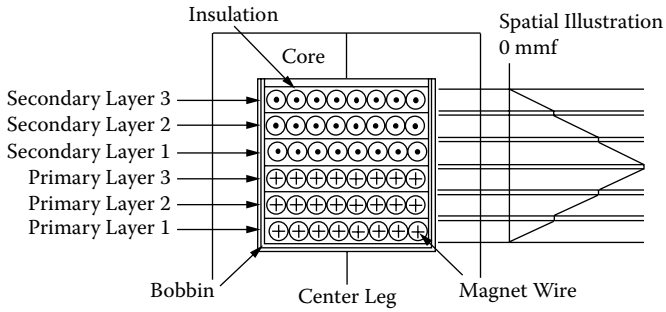

Figure 4-30. A Simple Transformer, Showing the Magneto-Motive Force, mmf.

© 2011 by Taylor and Francis Group, LLC

is twenty-five percent. The transformer has a 24 turn primary and a 24 turn secondary at 1 ampere. The transformer, A-T or magneto-motive force, (mmf) or F_m, is equal to 24.

$$F_m = NI, \quad \text{[magneto-motive force, mmf]}$$
$$\text{cgs, } F_m = 0.8NI, \quad \text{[magneto-motive force, mmf]} \qquad [4\text{-}18]$$

The schematic diagram as shown in Figure 4-31, is used as a guide to show how the proximity effect impacts the layer wound transformers. The load current, I_o, equals 1 amp, and the secondary will have three identical layers, with each layer having eight turns. Due to the skin effect or penetration depth, each wire uses only 25% of the available area. Therefore, the current will be crowded into 25% of the available copper wire.

To the right of S3, the mmf is 0. At the left of S3, $F_m = 8$ A-T.

1. The magnet field, ϕ_3, set up by the load current, I_o, of 1 amp in layer S3 will generate a current, $1I_g$, in the winding layer, S2. It is in the opposite direction to the normal current flow and cancels the load current, I_o. The magneto-motive force, F_m, will generate 16 A-T or $I_c = 2$ amps to preserve the original load current, I_o, of 1 amp.
2. The magnet field, ϕ_2, set up by the load current, I_o, plus the difference between, I_c and I_g, in S2 will generate, $2I_g$, in the winding layer, S1. This is in the opposite direction to the normal current flow that cancels the load current, I_o, out. The magneto-motive force, F_m, will generate, 24 A-T or $I_c = 3$ amps, to preserve the original load current, I_o, equals 1 amp.

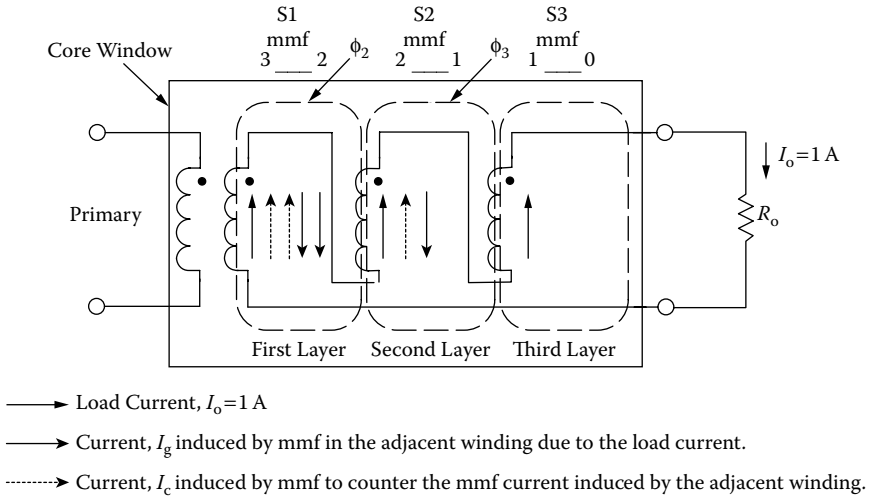

Figure 4-31. Transformer Schematic Diagram Showing mmf.

If the current in each layer is just the 1 amp, and limited in penetration, due to skin effect of only 25% of the conductor's thickness, the ac to dc resistance ratio, R_R, would be 4:1. The surface currents successive layers become much larger, as discussed above. The winding currents are tabulated in Table 4-15. The summation of the currents is given in Table 4-15. The current, I_g, is the adjacent winding induced current. The current, I_c, is the counter-current induced by the magneto-motive force, mmf.

© 2011 by Taylor and Francis Group, LLC

Table 4-15. Secondary Current Levels

Secondary Current Levels						
Winding	I_o	I_c	$I_o + I_c$	$I_o + I_c$	I_g	Total Wire Current
	amps	amps	amps	amps^2	amps	amps^2
S3	1	0	1	1	0	$(I_o + I_c)^2 = 1$
S2	1	1	2	4	1	$(I_o + I_c)^2 + (I_g)^2 = 5$
S1	1	2	3	9	2	$(I_o + I_c)^2 + (I_g)^2 = 13$

It can be seen, from the data in Table 4-15 that transformers with multiple layers operating at high frequency could be a real problem with proximity effect. The eddy current losses caused by the proximity effect go up exponentially as the number of layers. The selection of a core with a long winding length to a winding height ratio, will reduce the number of layers to a minimum, as shown in Figure 4-32.

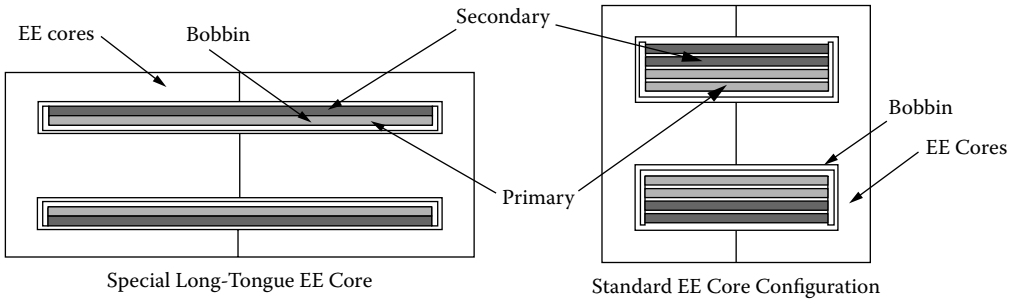

Figure 4-32. Comparing the Standard and the Special Long Tongue EE Cores.

Proximity Effect Using Dowell Curves

Dowell curves on proximity effect are shown in Figure 4-33. The vertical scale is, R_R, the ratio of, R_{ac}, to R_{dc}. The horizontal scale, K, is the ratio of the effective conductor height, or layer thickness, to the penetration depth, ε. On the right side of the curve it is labeled Number of Layers. These are segmented layers. Segmented layers are when the secondary is interleaved with the primary, then, each separation is a segment. The equation for K is:

$$K = \frac{h\sqrt{F_l}}{\varepsilon} \qquad h = 0.866 D_{AWG} \qquad [4\text{-}19]$$

Where:

$$F_l = \frac{N D_{AWG}}{l_w} \qquad [4\text{-}20]$$

© 2011 by Taylor and Francis Group, LLC

The variables in Equation 4-20 are described in Figure 4-34. It can be seen that if the number of turns, N, times the wire diameter, D_{AWG}, are equal to the winding length, l_w, then, Equation 4-21 is simplified to:

$$K = \frac{h}{\varepsilon} \qquad [4\text{-}21]$$
$$h = 0.866 D_{AWG}$$

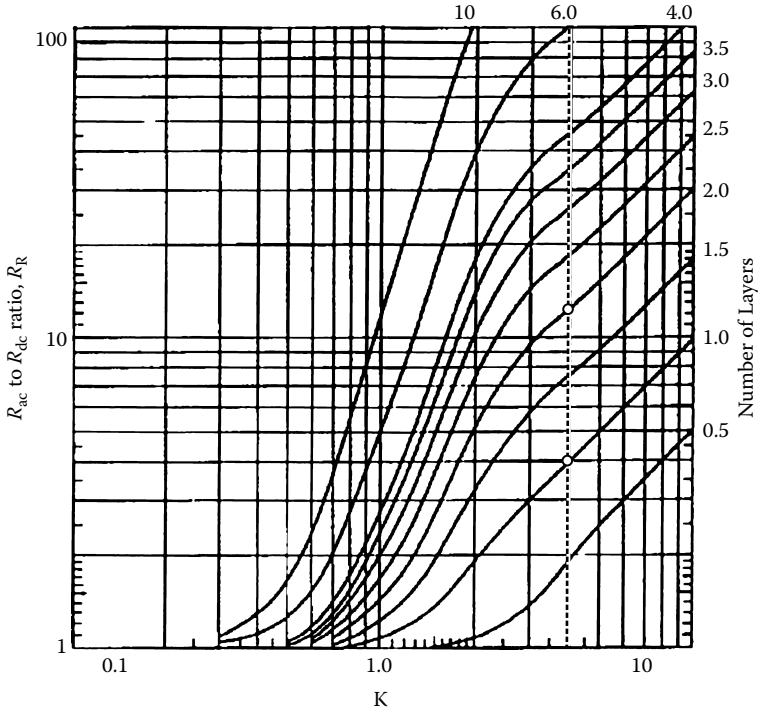

Figure 4-33. Ratio of ac/dc Resistance Due to Proximity Effect.

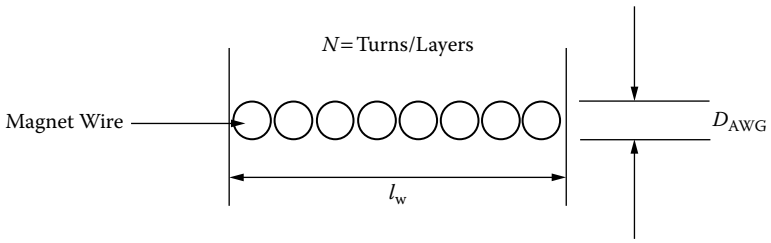

Figure 4-34. Winding Layer Parameters.

Use the Dowell curves, as shown in Figure 4-33. As shown in Figure 4-35, compare the loss ratio between the transformer in configuration A with two layers and transformer B that has the secondary interleaved with the primary. With a skin effect penetration depth of 25%, it will yield a, K, factor of 4. Both transformers, A and B, have the same A-T, but since the windings on transformer B are interleaved. It has only half the low frequency magneto-motive force (mmf).

© 2011 by Taylor and Francis Group, LLC

There is a vertical dotted line shown in Figure 4-33, where K = 4. Follow the dotted line up to where it intersects 1 layer, then read the vertical column on the left, $R_R = 4$. Now, follow the dotted line up to where it intersects 2 layers, then read the vertical column on the left, $R_R = 13$. Transformer B, with its interleaved windings, has a lower ac to dc resistance ratio, R_R, by a factor 3.25.

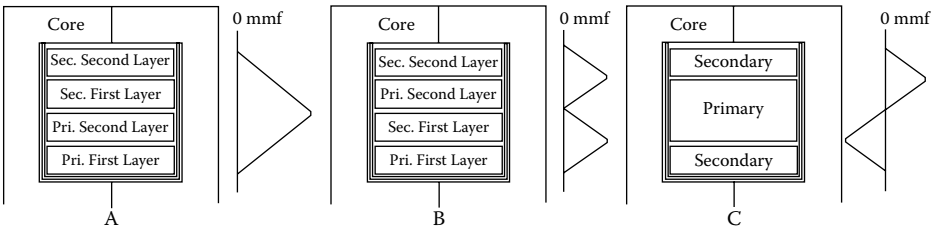

Figure 4-35. Transformers Wound with Different Primary and Secondary Configurations.

The proximity effect, with its exponentially losses tends to be the dominant conductor loss mechanism in high frequency magnetic components, particularly when windings are multi-layered.

Specialty Wire

There are a lot of new ideas out in the wire industry, if only the engineer had the time to evaluate these new concepts to build confidence and apply them.

Triple Insulated Wire

Transformers designed to meet the IEC/VDE safety specification requirements for creepage and clearance must adhere to one of the following specifications:

1. VDE0805
2. IEC950
3. EN60950
4. UL1950-3e
5. CSA 950-95

The engineer must be aware that one specification does not encompass all applications. For example, the IEC has specifications for office machines, data-processing equipment, electromedical equipment, appliances, and others.

Originally these IEC specifications were developed around linear 50 and 60 Hz transformers, and were not, always, conducive to optimal designs for high frequency, such as switching power transformers. The complexity of a standard, high frequency, switching type transformer, designed to the IEC/VDE safety specification, is shown in Figure 4-36. In any switching transformer, coupling has the highest priority because of the leakage flux.

© 2011 by Taylor and Francis Group, LLC

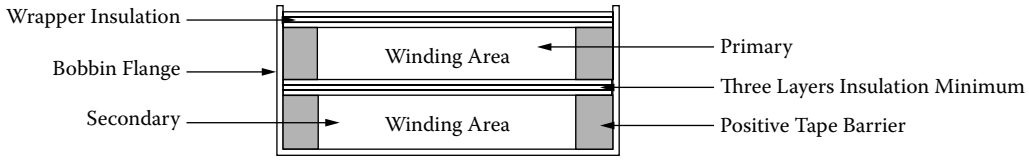

Figure 4-36. Bobbin Cross-Section Design to Meet IEC/VDE Specifications.

The triple, insulated wire was developed to meet the above specification and eliminate the need for three layers of insulating tape between primary and secondary. Also, the triple, insulated wire eliminates the need for the creepage margin, and now, the whole bobbin can be used for winding. This wire can also be used as hook-up wire, from the primary or secondary, to the circuits, without the use of sleeving or tubing.

The construction of the triple, insulated wire is shown in Figure 4-37. The temperature range for this type of wire is from 105°C to 180°C. The dimensions for triple, insulated wire are shown in Table 4-16, using a 0.002 inch coat per layer. Other thicknesses are available. The manufacturer, Rubadue Wire Company, is listed in the Reference Section of this chapter.

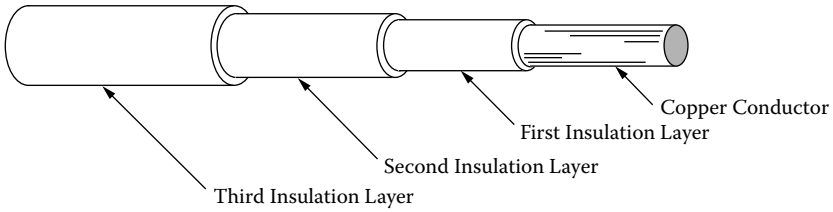

Figure 4-37. Triple, Insulated Wire Construction.

Triple Insulated Litz

High frequency litz wire, shown in Figure 4-38, is also available as a triple insulated wire from manufacturers. The insulation layers' thickness for litz wire comes in 0.002 and 0.003 inches.

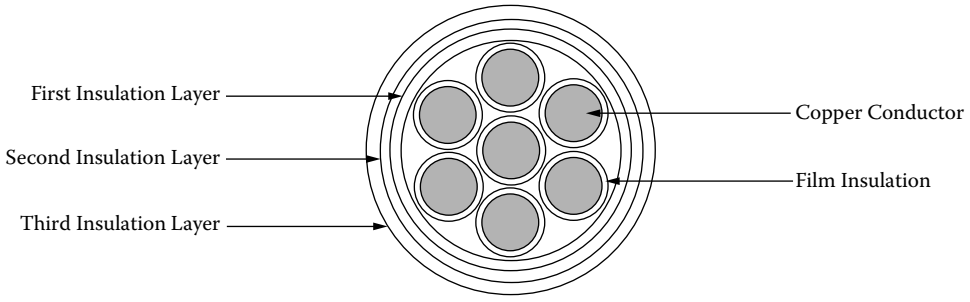

Figure 4-38. Triple, Insulated Litz Wire.

© 2011 by Taylor and Francis Group, LLC

Table 4-16. Triple Insulated Wire (.002) Material

Triple Insulated Wire (.002) Material						
	Bare Wire				With Insulation	
AWG	Area $cm^2(10^{-3})$	Diameter inch	Diameter mm	Resistance μΩ/cm	Diameter inch	Diameter mm
16	13.0700	0.0508	1.2903	132	0.0628	1.5951
18	8.2280	0.0403	1.0236	166	0.0523	1.3284
19	6.5310	0.0359	0.9119	264	0.0479	1.2167
20	5.1880	0.0320	0.8128	332	0.0440	1.1176
21	4.1160	0.0285	0.7239	419	0.0405	1.0287
22	3.2430	0.0253	0.6426	531	0.0373	0.9474
23	2.5880	0.0226	0.5740	666	0.0346	0.8788
24	2.0470	0.0201	0.5105	842	0.0321	0.8153
25	1.6230	0.0179	0.4547	1062	0.0299	0.7595
26	1.2800	0.0159	0.4039	1345	0.0279	0.7087
27	1.0210	0.0142	0.3607	1687	0.0262	0.6655
28	0.8046	0.0126	0.3200	2142	0.0246	0.6248
29	0.6470	0.0113	0.2870	2664	0.0233	0.5918
30	0.5067	0.0100	0.2540	3402	0.0220	0.5588
32	0.3242	0.0080	0.2032	5315	0.0200	0.5080
34	0.2011	0.0063	0.1600	8572	0.0183	0.4648
36	0.1266	0.0050	0.1270	13608	0.0170	0.4318
38	0.0811	0.0040	0.1016	21266	0.0160	0.4064

Polyfilar Magnetic Wire

Poly or multiple strands of magnet wire, bonded together, can be used in many high frequency transformer and inductor applications. Round polyfilar magnet wire is shown in Figure 4-39, and square polyfilar is shown in Figure 4-40. Both can be used in place of foil in some applications. Polyfilar magnet wire can be used as a foil type winding, such as a low voltage, high current, or even a Faraday shield. The polyfilar, magnet wire strip width can be easily increased or decreased by adding or removing wires to provide the proper strip width to fit a bobbin. It is relatively easy to wind. Polyfilar wire has complete insulation, and it does not have the sharp edge problem that could cut insulation in the way foil does. It is not recommended to wind a transformer with polyfilar magnet wire in order to have an exact center tap, unless it is just a few turns, because of the penalty in capacitance. If the use of polyfilar is necessary, then use a magnet wire with a film insulation that has a low dielectric constant. See Table 4-8.

© 2011 by Taylor and Francis Group, LLC

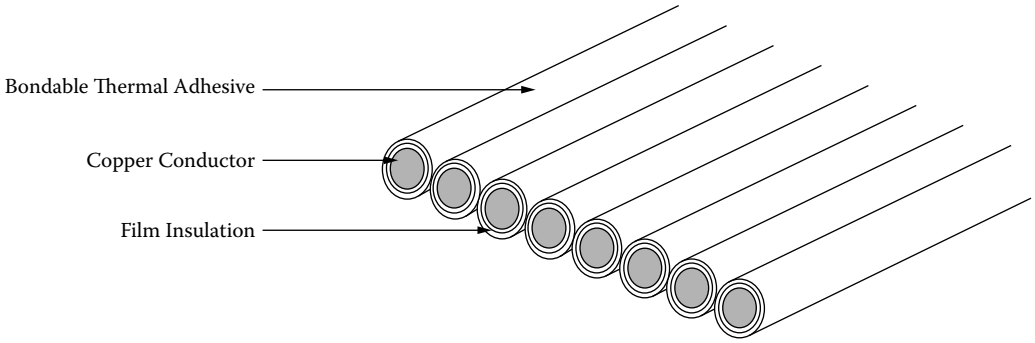

Figure 4-39. Polyfilar, Strip-Bonded, Round Magnet Wire.

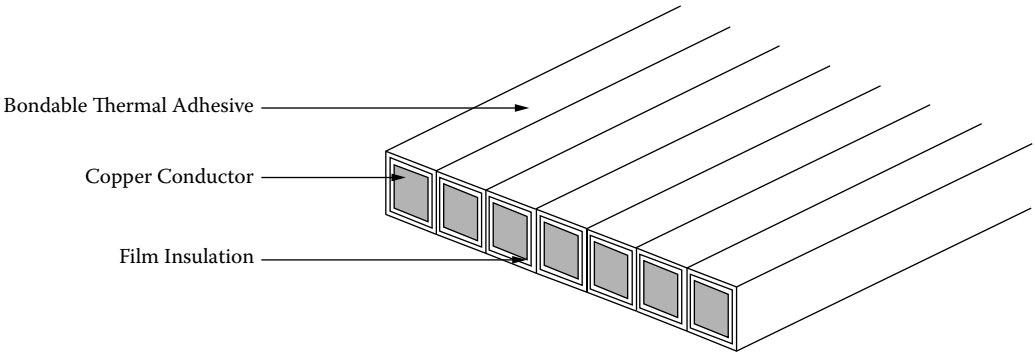

Figure 4-40. Polyfilar, Strip-Bonded, Square Magnet Wire.

Standard Foils

The biggest advantage for using foil over magnet wire is the fill factor. The design of a high current, high frequency, dc to dc converter is common place. The main reason for going to high frequency is the reduction in size. The power transformer is the largest component in the design. When designing high frequency transformers, the design equations relate to a very small transformer. When operating transformers at high frequencies, the skin effect becomes more and more dominate, and requires the use of smaller wire. If larger wire is required, because of the required current density, then, more parallel strands of wire will have to be used (litz wire). The use of small wire has a large effect on the fill factor.

When using foil, the gain in the fill factor is the biggest improvement over litz. To make a comparison, a litz design is shown in Figure 4-41, and a foil design is shown in Figure 4-42. In the litz design, there is a percentage of the winding area which cannot be used for the conductors. This lost area is made up of voids, space between the wires, and the insulation film on the wire. The foil wound coil, shown in Figure 4-42, can be designed to make optimum use of the available winding area. Each turn of the foil can extend, within limits, edge-to-edge of the bobbin or tube. The insulation required between layers is at a minimum, as long as the foil has been rolled to remove the sharp burr, as shown in Figure 4-46.

© 2011 by Taylor and Francis Group, LLC

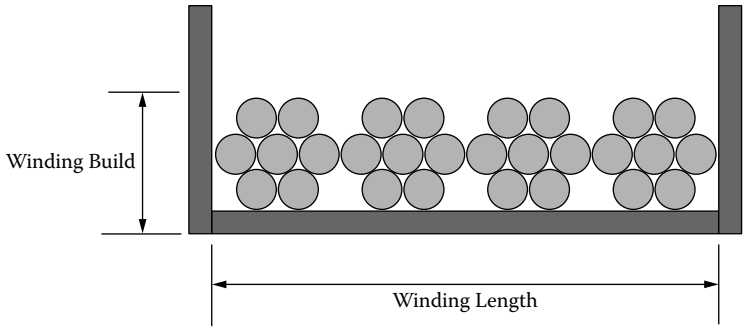

Figure 4-41. Layer Winding, Using Litz Magnet Wire.

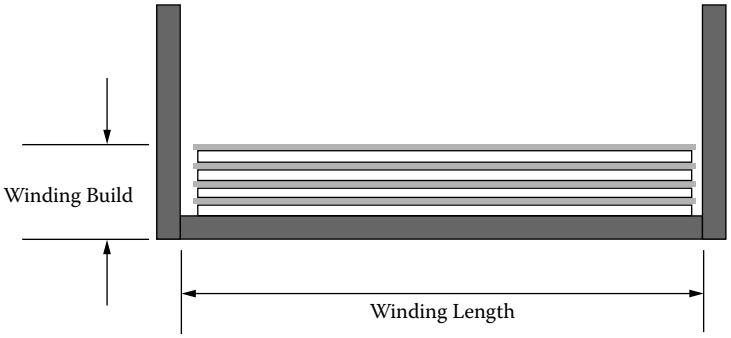

Figure 4-42. Layer Winding, Using Foil with Insulation.

The Use of Foils

Designing transformers and inductors, with foil, is a very laborious task, especially if the engineer only does it now and then. A monumental job, in itself, is finding out where to get the materials. Foil has its advantages, mainly, in high current, high frequency, and a high density environment.

The window utilization factor, K_u, can be greater than 0.6, under the right conditions, without a lot of force. The standard foil materials used, by transformer engineers, are copper and aluminum. The engineer has a good selection of standard thicknesses as shown:

1.0 mil, 1.4 mil, 2.0 mil, 5.0 mil, and 10 mil

The engineer will find other thicknesses available, but standard thicknesses should be considered first. Be careful of using a nonstandard thickness. What the engineer might be using could be from an overrun, and definitely could create problems for him. Foil comes in standard widths, in inches, as shown:

0.25, 0.375, 0.50, 0.625, 0.75, 1.0, 1.25, 1.50, 2.00, 2.50, 3.00, 4.00 (inches)

Standard widths are the widths that are most readily available. There are also different styles of pre-fab foils, as shown in Figures 4-43, 4-44, and 4-45.

© 2011 by Taylor and Francis Group, LLC

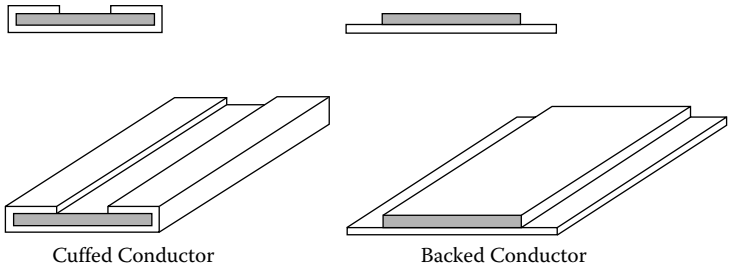

Figure 4-43. Pre-fab Foils.

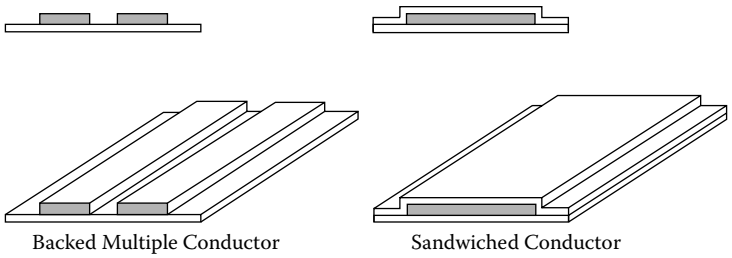

Figure 4-44. Pre-fab Foils.

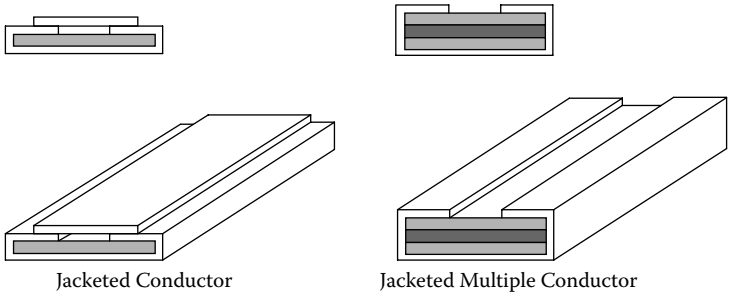

Figure 4-45. Pre-fab Foils.

Although special slitting is done all the time, there is normally a minimum buy. When slitting is done, special care must be attended to, with the sharp edges, as shown in Figure 4-46. The cut edge should be rolled after slitting it, at least two times, to remove the sharp burrs that could cut through the insulation. Therefore, it is wise not to use insulation between layers of less than 1 mil.

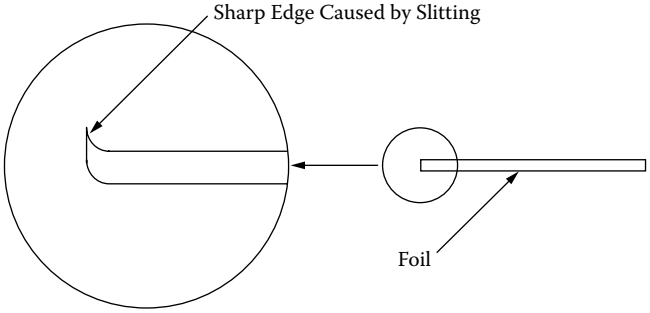

Figure 4-46. Foil with Sharp Edge Burrs, after Slitting.

© 2011 by Taylor and Francis Group, LLC

When winding transformers or inductors with foil, special care must be taken with lead finishing. One of the biggest problems about using foil is solder wicking. This wicking will puncture the insulation, resulting in a shorted turn. The normal insulation used for foil is very thin. Winding with foil, the coil is still subjected to bowing, only more so, as shown in Figure 4-7.

Foil used for winding transformers and inductors should be dead soft. There is another shortcoming about using foil, and that is, the inherit capacitance build-up, as shown in Figure 4-47.

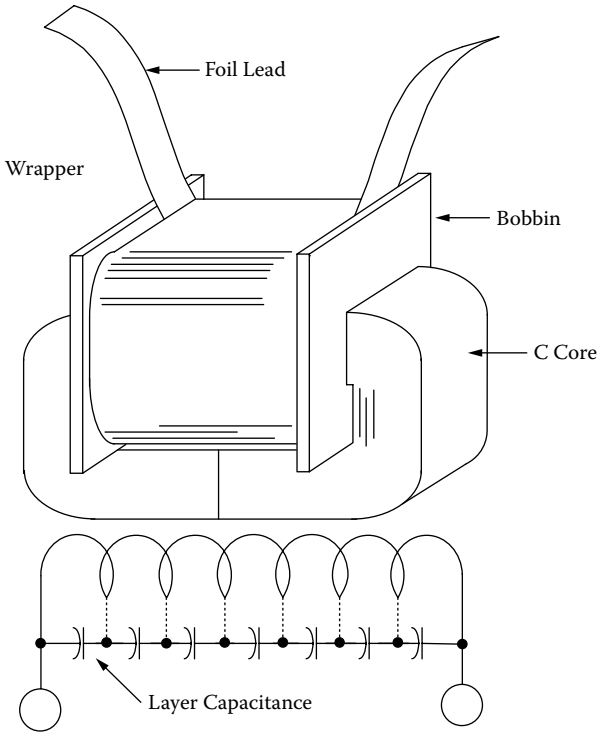

Figure 4-47. Foil Capacitance Equation.

The capacitance build-up is expressed:

$$C = 0.0885\left(\frac{K(N-1)(\text{MLT})(G)}{d}\right), \quad [pfd] \qquad [4\text{-}22]$$

K = Dielectric Constant
MLT = Mean Length Turn
N = Number of Turns
G = Foil Width, cm
d = Layer Insulation Thickness, cm

The dielectric constant K for different materials can be found in Table 4-17.

© 2011 by Taylor and Francis Group, LLC

Table 4-17. Dielectric Constants

Dielectric Constants	
Material	K
Kapton	3.2-3.5
Mylar	3-3.5
Kraft Paper	1.5-3.0
Fish Paper	1.5-3.0
Nomex	1.6-2.9

Calculating, MLT

The Mean Length Turn, (MLT), is required to calculate the winding resistance and weight for any given winding. The winding dimensions, relating to the Mean Length Turn, (MLT) for a tube or bobbin coil, are shown in Figure 4-48.

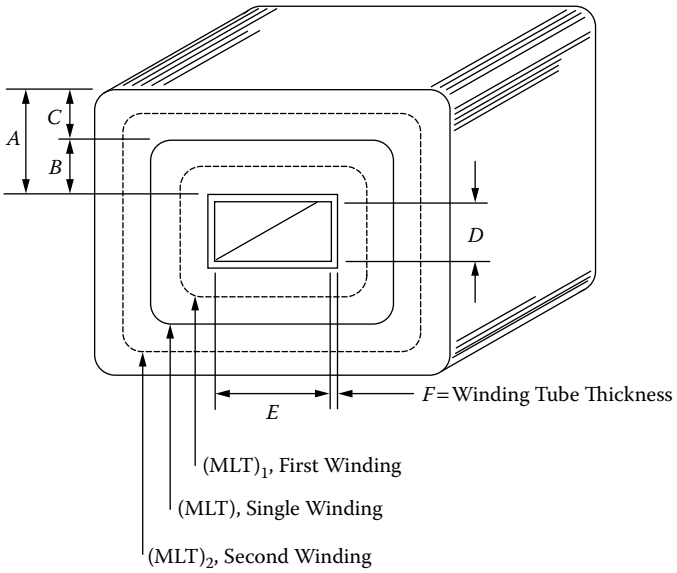

Figure 4-48. Dimensions, Relating to the Winding Mean Length Turn, (MLT).

$$\begin{aligned} \text{MLT} &= 2(D+2F)+2(E+2F)+\pi A, \quad \text{single winding} \\ \text{MLT}_1 &= 2(D+2F)+2(E+2F)+\pi B, \quad \text{first winding} \\ \text{MLT}_2 &= 2(D+2F)+2(E+2F)+\pi(2B+C), \quad \text{second winding} \end{aligned} \qquad [4\text{-}23]$$

Calculating, MLT (toroid)

It is very difficult to calculate the Mean Length Turn (MLT) for a toroidal core that would satisfy all conditions. There are just too many ways to wind a toroid. If the toroid was designed to be wound by machine, then that would require a special clearance for a wire shuttle. If the toroid was designed to be

© 2011 by Taylor and Francis Group, LLC

hand-wound, the inside wound diameter would be different. The fabrication of a toroidal design depends heavily on the skill of the winder. A good approximation for a toroidal core, Mean Length Turn (MLT), is shown in Figure 4-49.

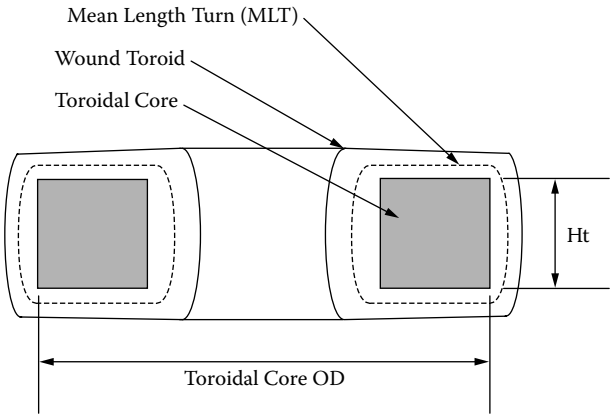

Figure 4-49. Toroidal Mean Length Turn (MLT), is an Approximation.

$$\text{MLT} = 0.8\left(OD + 2\left(Ht\right)\right), \quad \text{approximation} \qquad [4\text{-}24]$$

Copper Resistance

The dc resistance calculation of a winding requires knowing the total length, l, of the conductor, the cross-sectional area, A_w, of the conductor, and the resistivity, ρ, of the conductor material. The value for the resistivity, ρ, in μΩ per cm for three different conductor materials can be found in Table 4-7.

$$R_{dc} = \left(\frac{\rho l}{A_w}\right), \quad [\Omega] \qquad [4\text{-}25]$$

Copper Weight

The weight calculation of a winding requires knowing the total length, l, of the conductor, the cross-sectional area, A_w, of the conductor, and the density, λ, of the conductor material. The value for the density, λ, in grams per cm^3 for three different conductor materials, can be found in Table 4-7.

$$W_t = \lambda l A_w, \quad [\text{grams}] \qquad [4\text{-}26]$$

Electrical Insulating Materials

The reliability and life span of a magnetic component depends on the stress level put upon the insulating materials. If the design or workmanship is not incorporated, then, insulation will not help the engineer.

© 2011 by Taylor and Francis Group, LLC

References

1. P.L. Dowell, "Effects of Eddy Currents in Transformer Windings," *Proceedings IEE* (UK), Vol. 113, No.8, August, 1966, pp. 1387–1394.

2. B. Carsten, "High Frequency Conductor Losses in Switch Mode Magnetics," High Frequency Power Converter Conference, 1986, pp. 155–176.

3. L. Dixon, Eddy Current Losses in Transformer Windings and Circuit Wiring, Unitrode Corp. Power Supply Seminar Handbook, Unitrode Corp., Watertown MA, 1988.

4. E. Snelling, *Soft Ferrites,* pp. 341–348, Iliffe, London, 1969.

5. A.I. Pressman, *Switching Power Supply Design,* pp. 298–317, McGraw-Hill, Inc., New York 1991.

6. E.C. Snelling, *Soft Ferrites*, CRC Press, Iliffe Books Ltd., 42 Russell Square, London, W.C.I, 1969.

7. Werner Osterland, "The Influence of Wire Characteristics on the Winding Factor and Winding Method," *WIRE*, Coburg, Germany. Issue 97, October, 1968.

8. H.A. George, "Orthocyclic Winding of Magnet Wire Without Interleaving Materials," Insulation/Circuits, August, 1976.

9. MWS Wire Industries, "Wire Catalog," Revised June, 1992, 31200 Cedar Valley Drive, Westlake Village, CA 91362.

10. Alpha-Core Inc. (Special Foils), 915 Pembroke Street, Bridgeport, CT 06608.

11. Industrial Dielectrics West, Inc., (Special Foils), 455 East 9th Street, San Bernardino, CA 92410.

12. Rubadue Wire Company, Inc., (Triple Insulated Wire), 5150 E. LaPalma Avenue, Suite 108, Anaheim Hills, CA 92807 Email: www.rubaduewire.com.

© 2011 by Taylor and Francis Group, LLC

Chapter 5

Transformer Design Trade-Offs

© 2011 by Taylor and Francis Group, LLC

Table of Contents

1. Introduction....5-3
2. The Design Problem Generally....5-3
3. Power Handling Ability....5-4
4. Relationship, A_p, to Transformer Power Handling Capability....5-4
5. Relationship, K_g, to Transformer Regulation and Power Handling Capability....5-5
6. Transformer Area Product, A_p....5-6
7. Transformer Volume and the Area Product, A_p....5-6
8. Transformer Weight and the Area Product, A_p....5-9
9. Transformer Surface Area and the Area Product, A_p....5-11
10. Transformer Current Density, J, and the Area Product, A_p....5-15
11. Transformer Core Geometry, K_g, and the Area Product, A_p....5-18
12. Weight Versus Transformer Regulation....5-20
13. References....5-21

© 2011 by Taylor and Francis Group, LLC

Introduction

The conversion process in power electronics requires the use of transformer components that are frequently the heaviest and bulkiest item in the conversion circuit. They also have a significant effect upon the overall performance and efficiency of the system. Accordingly, the design of such transformers has an important influence on the overall system weight, power conversion efficiency, and cost. Because of the interdependence and interaction of these parameters, judicious trade-offs are necessary to achieve design optimization.

The Design Problem Generally

The designer is faced with a set of constraints that must be observed in the design on any transformer. One of these constraints is the output power, P_o, (operating voltage multiplied by maximum current demand) in that the secondary winding must be capable of delivering to the load within specified regulation limits. Another constraint relates to the minimum efficiency of the operation, which is dependent upon the maximum power loss that can be allowed in the transformer. Still another constraint defines the maximum permissible temperature rise for the transformer when it is used in a specified temperature environment.

One of the basic steps in transformer design is the selection of proper a core material. Magnetic materials used to design low and high frequency transformers are shown in Table 5-1. Each one of these materials has its own optimum point in the cost, size, frequency and efficiency spectrum. The designer should be aware of the cost difference between silicon-iron, nickel-iron, amorphous and ferrite materials. Other constraints relate to volume occupied by the transformer and, particularly in aerospace applications, weight minimization is an important goal. Finally, cost effectiveness is always an important consideration.

Depending upon the application, some of these constraints will dominate. Parameters affecting others may then be traded-off, as necessary, to achieve the most desirable design. It is not possible to optimize all parameters in a single design because of their interaction and interdependence. For example, if volume and weight are of great significance, reductions in both can often be affected, by operating the transformer at a higher frequency, but with the penalty being in efficiency. When, the frequency cannot be increased, reduction in weight and volume may still be possible by selecting a more efficient core material, but there would be the penalty of increased cost. Thus, judicious trade-offs must be affected to achieve the design goals.

Transformer designers have used various approaches in arriving at suitable designs. For example, in many cases, a rule of thumb is used for dealing with current density. Typically, an assumption is made that a good working level is 200 amps-per-cm^2 (1000 circular mils-per-ampere). This rule of thumb will work in many instances, but the wire size needed to meet this requirement may produce a heavier and bulkier transformer than desired or required. The information presented in this Chapter makes it possible to develop a more economical design with great accuracy, therefore avoiding the above assumption and other rules of thumb.

© 2011 by Taylor and Francis Group, LLC

Table 5-1. Magnetic Materials and Their Characteristics

Magnetic Core Material Characteristics					
Material Name	Initial Permeability μ_i	Flux Density Teslas B_s	Curie Temperature °C	dc, Coercive Force, Hc Oersteds	Operating Frequency f
Iron Alloys					
Magnesil	1.5K	1.5-1.8	750	0.4-0.6	<2 kHz
Supermendur*	0.8K	1.9-2.2	940	0.15-0.35	<1 kHz
Orthonol	2K	1.42-1.58	500	0.1-0.2	<2 kHz
Sq. permalloy	12K-100K	0.66-0.82	460	0.02-0.04	<25 kHz
Supermalloy	10K-50K	0.65-0.82	460	0.003-0.008	<25 kHz
Amorphous					
2605-SC	3K	1.5-1.6	370	0.03-0.08	<250 kHz
2714A	20K	0.5-0.58	>200	0.008-0.02	<250 kHz
Vitro perm 500	30K	1.0-1.2	>200	<0.05	<250 kHz
Ferrite					
MnZn	0.75-15K	0.3-0.5	100-300	0.04-0.25	<2 MHz
NiZn	15-1500	0.3-0.5	150-450	0.3-0.5	<100 MHz
*Field Anneal.					

Power Handling Ability

For years, manufacturers have assigned numeric codes to their cores to indicate their power-handling ability. This method assigns to each core a number called the area product, A_p. That is the product of the window area, W_a, and the core cross-section, A_c. The core suppliers use these numbers to summarize dimensional and electrical properties in their catalogs. They are available for laminations, C cores, ferrite cores, powder cores, and toroidal tape wound cores.

Relationship, A_p, to Transformer Power Handling Capability

Transformers

According to the newly developed approach, the power handling capability of a core is related to its area product, A_p, by an Equation, which may be stated as:

$$A_p = \frac{P_t\left(10^4\right)}{K_f K_u B_m J f}, \quad [\text{cm}^4] \qquad [5\text{-}1]$$

© 2011 by Taylor and Francis Group, LLC

Where:

K_f = waveform coefficient

4.0 square wave

4.44 sine wave

From the above, it can be seen that the factors, such as flux density, frequency of operation, and window utilization factor K_u, define the maximum space which may be occupied by the copper in the window.

Relationship, K_g, to Transformer Regulation and Power Handling Capability

Although most transformers are designed for a given temperature rise, they can also be designed for a given regulation. The regulation and power-handling ability of a core is related to two constants:

$$\alpha = \frac{P_t}{2K_g K_e}, \quad [\%] \tag{5-2}$$

$$\alpha = \text{Regulation } (\%) \tag{5-3}$$

The constant, K_g, (See Chapter 7) is determined by the core geometry, which may be related by the following equations:

$$K_g = \frac{W_a A_c^2 K_u}{\text{MLT}}, \quad [\text{cm}^5] \tag{5-4}$$

The constant, K_e, is determined by the magnetic and electric operating conditions, which may be related by the following Equation:

$$K_e = 0.145 K_f^2 f^2 B_m^2 \left(10^{-4}\right) \tag{5-5}$$

Where:

K_f = waveform coefficient

4.0 square wave

4.44 sine wave

From the above, it can be seen that the factors, such as flux density, frequency of operation, and waveform coefficient, have an influence on the transformer size. Because of their significance, the area product, A_p, and the core geometry, K_g, are treated extensively in this handbook. A great deal of other information is also presented for the convenience of the designer. Much of the information is in tabular form to assist designers in making the trade-offs best suited for the particular application, in a minimum amount of time.

© 2011 by Taylor and Francis Group, LLC

Transformer Area Product, A_p

The author has developed additional relationships between, A_p, numbers and current density, J, for given regulation and temperature rise. The area product, A_p, is a length dimension to the fourth power, (l^4), as shown in Figure 5-1.

$$W_a = FG, \quad [\text{cm}^2]$$
$$A_c = DE, \quad [\text{cm}^2] \qquad [5\text{-}6]$$
$$A_p = W_a A_c, \quad [\text{cm}^4]$$

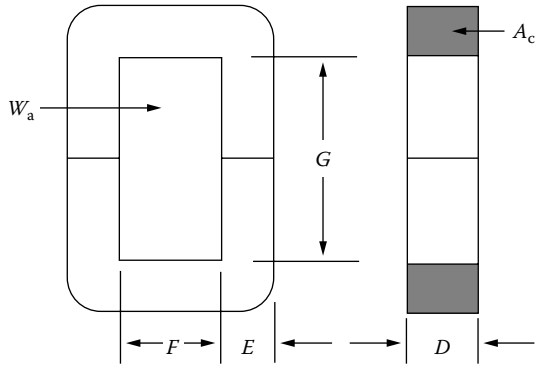

Figure 5-1. C Core Outline Showing the Window Area, W_a and Iron Area, A_c.

It should be noted that the constants for tape-wound cores, such as: K_{vol}, K_w, K_s, K_j and K_p will have a tendency to jump around and not be consistent. This inconsistency has to do with the core being in a housing, without true proportions.

Transformer Volume and the Area Product, A_p

The volume of a transformer can be related to the area product, A_p of a transformer, treating the volume, as shown in Figures 5-2 to 5-4, as a solid quantity without any subtraction for the core window. The relationship is derived according to the following reasoning: Volume varies in accordance with the cube of any linear dimension, (l), whereas area product, A_p, varies as the fourth power:

$$\text{Volume} = K_1 l^3, \quad [\text{cm}^3] \qquad [5\text{-}7]$$

$$A_p = K_2 l^4, \quad [\text{cm}^4] \qquad [5\text{-}8]$$

$$l^4 = \frac{A_p}{K_2} \qquad [5\text{-}9]$$

© 2011 by Taylor and Francis Group, LLC

$$l = \left(\frac{A_p}{K_2} \right)^{(0.25)} \quad [5\text{-}10]$$

$$l^3 = \left[\left(\frac{A_p}{K_2} \right)^{0.25} \right]^3 = \left(\frac{A_p}{K_2} \right)^{0.75} \quad [5\text{-}11]$$

$$\text{Volume} = K_1 \left(\frac{A_p}{K_2} \right)^{0.75} \quad [5\text{-}12]$$

$$K_{vol} = \frac{K_1}{K_2^{(0.75)}} \quad [5\text{-}13]$$

The volume-area product, A_p, relationship is therefore:

$$\text{Volume} = K_{vol} A_p^{(0.75)}, \quad [\text{cm}^3] \quad [5\text{-}14]$$

In which, K_{vol}, is a constant related to core configuration whose values are given in Table 5-2. These values were obtained by averaging the values from the data taken from Tables 3-1 through Tables 3-64 in Chapter 3.

Table 5-2. Volume-Area Product Relationship

Volume-Area Product Relationship	
Core Type	K_{vol}
Pot Core	14.5
Powder Core	13.1
Laminations	19.7
C Core	17.9
Single-coil C Core	25.6
Tape-wound Core	25.0

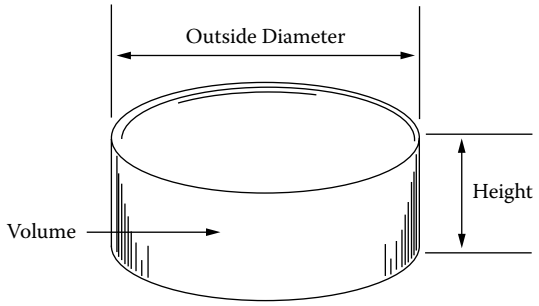

Figure 5-2. Toroidal Transformer Outline, Showing the Volume.

© 2011 by Taylor and Francis Group, LLC

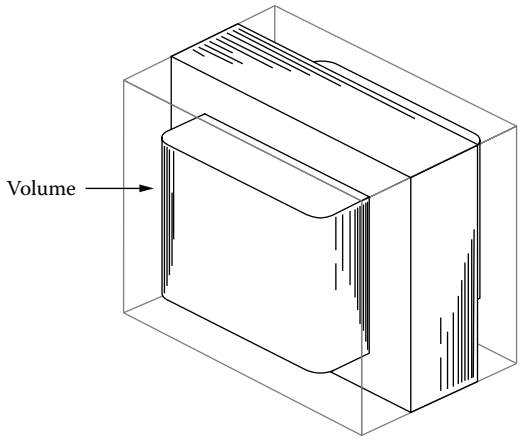

Figure 5-3. EI Core Transformer Outline, Showing the Volume.

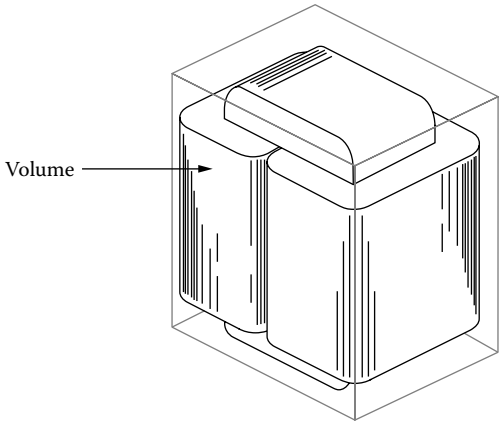

Figure 5-4. C Core Transformer Outline, Showing the Volume.

The relationship between volume and area product, A_p, for various core types is graphed in Figures 5-5 through 5-7. The data for these Figures has been taken from Tables in Chapter 3.

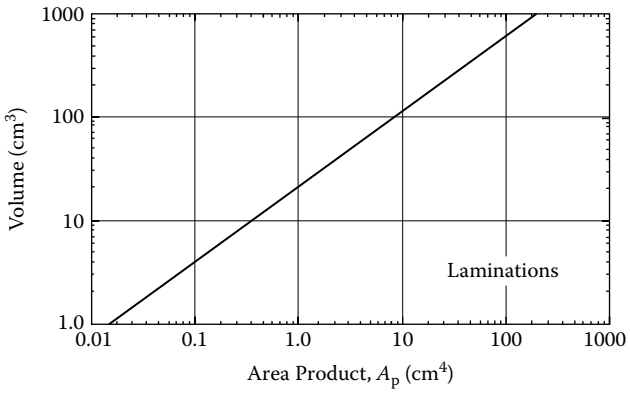

Figure 5-5. Volume Versus Area Product, A_p for EI Laminations.

© 2011 by Taylor and Francis Group, LLC

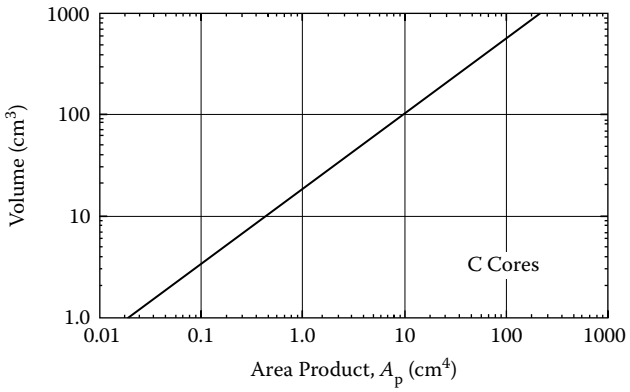

Figure 5-6. Volume Versus Area Product, A_p for C Cores.

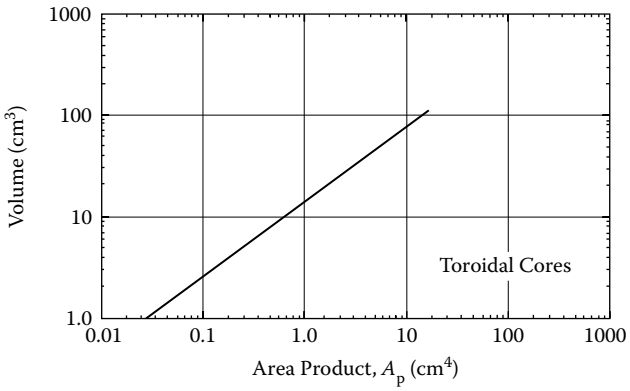

Figure 5-7. Volume Versus Area Product, A_p, for Toroidal MPP Cores.

Transformer Weight and the Area Product, A_p

The total weight of a transformer can also be related to the area product, A_p, of a transformer. The relationship is derived according to the following reasoning: weight, W_t, varies, in accordance with the cube of any linear dimension, (l), whereas area product, A_p, varies, as the fourth power:

$$W_t = K_3 l^3, \quad \text{[grams]} \tag{5-15}$$

$$A_p = K_2 l^4, \quad [\text{cm}^4] \tag{5-16}$$

$$l^4 = \frac{A_p}{K_2} \tag{5-17}$$

$$l^4 = \left(\frac{A_p}{K_2}\right)^{(0.25)} \tag{5-18}$$

$$l^3 = \left[\left(\frac{A_p}{K_2}\right)^{0.25}\right]^3 = \left(\frac{A_p}{K_2}\right)^{0.75} \tag{5-19}$$

© 2011 by Taylor and Francis Group, LLC

$$W_t = K_3 \left(\frac{A_p}{K_2} \right)^{0.75} \quad [5\text{-}20]$$

$$K_w = \frac{K_3}{K_2^{(0.75)}} \quad [5\text{-}21]$$

The weight-area product, A_p, relationship is therefore:

$$W_t = K_w A_p^{(0.75)} \quad [5\text{-}22]$$

In which, K_w, is a constant related to core configuration, whose values are given in Table 5-3, These values were obtained by averaging the values from the data taken from the Tables 3-1 through Tables 3-64 in Chapter 3.

Table 5-3. Weight-Area Product Relationship

Weight-Area Product Relationship	
Core Type	K_w
Pot Core	48.0
Powder Core	58.8
Laminations	68.2
C Core	66.6
Single-coil C Core	76.6
Tape-wound Core	82.3

The relationship between weight and area product, A_p, for various core types is graphed in Figures 5-8 through 5-10. The data for Figures 5-8 through 5-10 has been taken from Tables in Chapter 3.

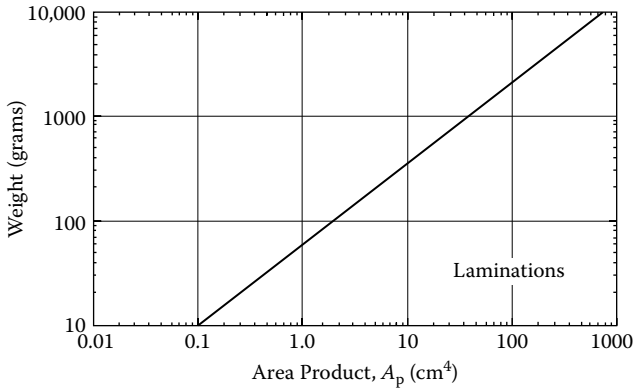

Figure 5-8. Total Weight Versus Area Product, A_p, for EI Laminations.

© 2011 by Taylor and Francis Group, LLC

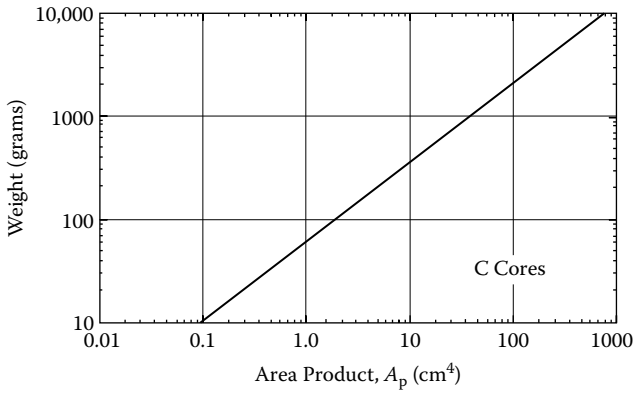

Figure 5-9. Total Weight Versus Area Product, A_p, for C Cores.

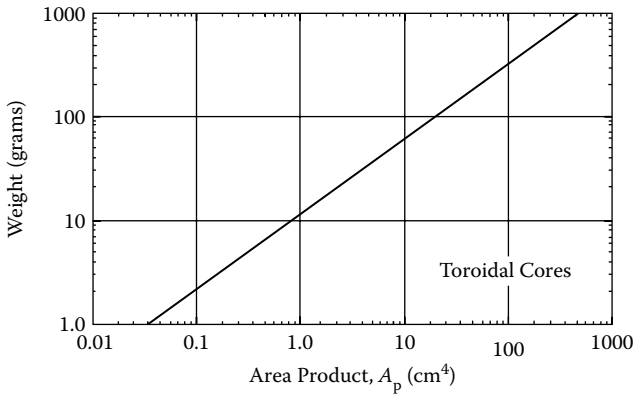

Figure 5-10. Total Weight Versus Area Product, A_p, for Toroidal MPP Cores.

Transformer Surface Area and the Area Product, A_p

The surface area of a transformer can be related to the area product, A_p, of a transformer, treating the surface area, as shown in Figure 5-11 through 5-13. The relationship is derived in accordance with the following reasoning: the surface area varies with the square of any linear dimension (l), whereas the area product, A_p, varies as the fourth power.

$$A_t = K_4 l^2, \quad [\text{cm}^2] \tag{5-23}$$

$$A_p = K_2 l^4, \quad [\text{cm}^4] \tag{5-24}$$

$$l^4 = \frac{A_p}{K_2} \tag{5-25}$$

$$l = \left(\frac{A_p}{K_2} \right)^{(0.25)} \tag{5-26}$$

© 2011 by Taylor and Francis Group, LLC

$$l^2 = \left[\left(\frac{A_p}{K_2}\right)^{0.25}\right]^2 = \left(\frac{A_p}{K_2}\right)^{0.5} \quad [5\text{-}27]$$

$$A_t = K_4\left(\frac{A_p}{K_2}\right)^{0.5} \quad [5\text{-}28]$$

$$K_s = \frac{K_4}{K_2^{(0.5)}} \quad [5\text{-}29]$$

The relationship between surface area, A_t and area product, A_p can be expressed as:

$$A_t = K_s A_p^{(0.5)} \quad [5\text{-}30]$$

In which, K_s, is a constant related to core configuration, whose values are given in Table 5-4. These values were obtained by averaging the values from the data taken from the Tables 3-1 through Tables 3-64 in Chapter 3.

Table 5-4. Surface Area-Area Product Relationship

Surface Area-Area Product Relationship	
Core Type	K_s
Pot Core	33.8
Powder Core	32.5
Laminations	41.3
C Core	39.2
Single-coil C Core	44.5
Tape-wound Core	50.9

The surface area for toroidal type transformers is calculated, as shown below.

$$\text{Top and Bottom Surface} = 2\left(\frac{\pi(OD)^2}{4}\right), \quad [\text{cm}^2]$$

$$\text{Periphery Surface} = \left(\pi(OD)\right)\left(\text{Height}\right), \quad [\text{cm}^2] \quad [5\text{-}31]$$

$$A_t = \frac{\pi(OD)^2}{2} + \left(\pi(OD)\right)\left(\text{Height}\right), \quad [\text{cm}^2]$$

© 2011 by Taylor and Francis Group, LLC

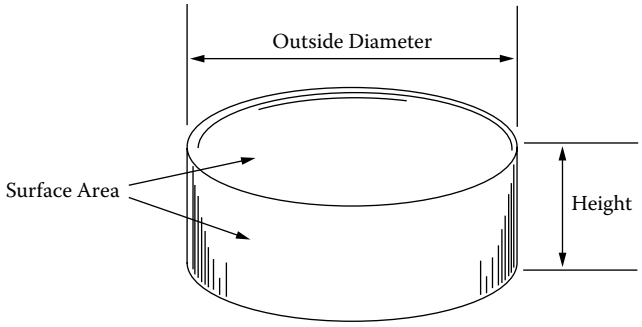

Figure 5-11. Toroidal Transformer Outline Showing the Surface Area.

The surface areas for C cores, Laminations and similar configurations are calculated as shown below. There is a small amount of area that is deducted because the sides and the ends are not a complete square.

$$\begin{aligned}
\text{End} &= (\text{Height})(\text{Length}), \quad [\text{cm}^2] \\
\text{Top} &= (\text{Length})(\text{Width}), \quad [\text{cm}^2] \\
\text{Side} &= (\text{Height})(\text{Width}), \quad [\text{cm}^2] \\
\text{Surface Area} &= 2(\text{End}) + 2(\text{Top}) + 2(\text{Side}), \quad [\text{cm}^2]
\end{aligned} \tag{5-32}$$

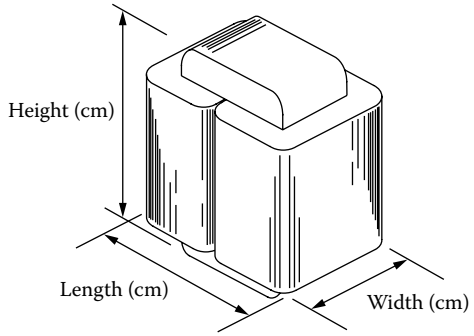

Figure 5-12. C Core Transformer Outline, Showing the Surface Area.

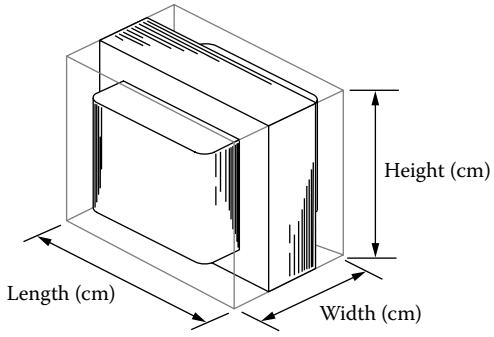

Figure 5-13. Typical EE or EI Transformer Outline, Showing the Surface Area.

© 2011 by Taylor and Francis Group, LLC

The relationship between surface area and area product, A_p, for various core types is graphed in Figures 5-14 through 5-16. The data for these Figures has been taken from Tables in Chapter 3.

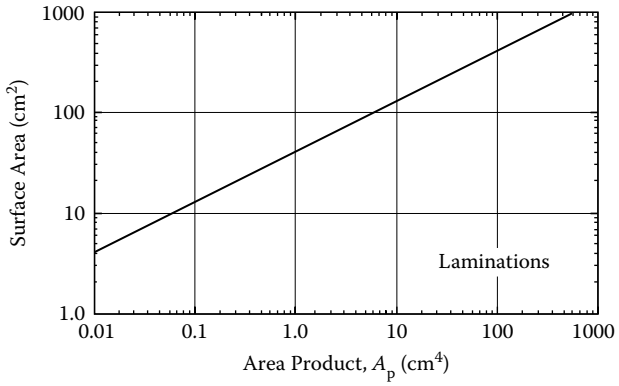

Figure 5-14. Surface Area, A_t, Versus Area Product, A_p, for EI Laminations.

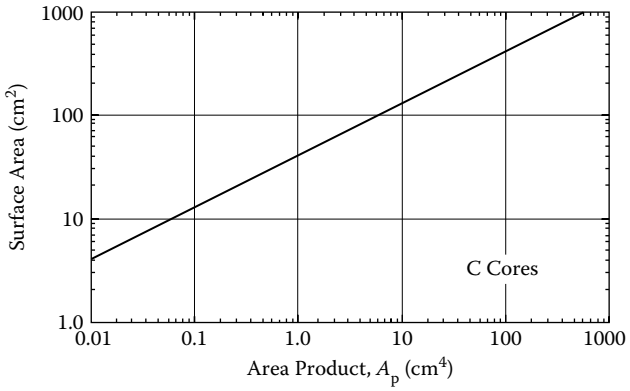

Figure 5-15. Surface Area, A_t, Versus Area Product, A_p, for C Cores.

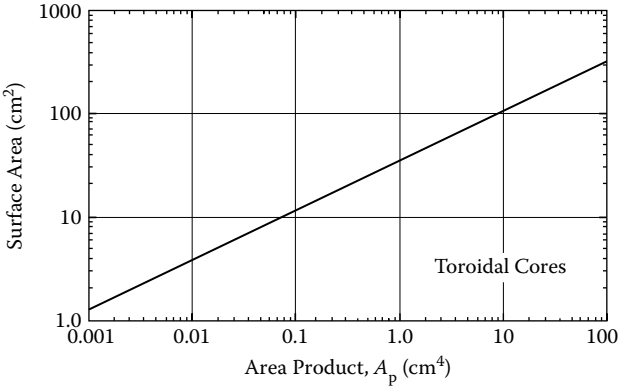

Figure 5-16. Surface Area, A_t, Versus Area Product, A_p, for Toroidal MPP Cores.

© 2011 by Taylor and Francis Group, LLC

Transformer Current Density, J, and the Area Product, A_p

The current density, J, of a transformer can be related to the area product, A_p, of a transformer for a given temperature rise. The relationship can be derived as follows:

$$A_t = K_s A_p^{(0.5)}, \quad [\text{cm}^2] \tag{5-33}$$

$$P_{cu} = I^2 R, \quad [\text{watts}] \tag{5-34}$$

$$I = A_w J, \quad [\text{amps}] \tag{5-35}$$

Therefore,

$$P_{cu} = A_w^2 J^2 R \tag{5-36}$$

And since,

$$R = \frac{\text{MLT}}{A_w} N\rho, \quad [\text{ohms}] \tag{5-37}$$

We have:

$$P_{cu} = A_w^2 J^2 \frac{\text{MLT}}{A_w} N\rho \tag{5-38}$$

$$P_{cu} = A_w J^2 (\text{MLT}) N\rho \tag{5-39}$$

Since MLT has a dimension of length,

$$\text{MLT} = K_5 A_p^{(0.25)} \tag{5-40}$$

$$P_{cu} = A_w J^2 \left(K_5 A_p^{(0.25)}\right) N\rho \tag{5-41}$$

$$A_w N = K_3 W_a = K_6 A_p^{(0.5)} \tag{5-42}$$

$$P_{cu} = \left(K_6 A_p^{(0.5)}\right)\left(K_5 A_p^{(0.25)}\right) J^2 \rho \tag{5-43}$$

Let:

$$K_7 = K_6 K_5 \rho \tag{5-44}$$

© 2011 by Taylor and Francis Group, LLC

Then assuming the core loss is the same as the copper loss for optimized transformer operation: (See Chapter 6),

$$P_{cu} = K_7 A_p^{(0.75)} J^2 = P_{fe} \quad [5\text{-}45]$$

$$P_\Sigma = P_{cu} + P_{fe} \quad [5\text{-}46]$$

$$\Delta T = K_8 \frac{P_\Sigma}{A_t} \quad [5\text{-}47]$$

$$\Delta T = \frac{2K_8 K_7 J^2 A_p^{(0.75)}}{K_s A_p^{(0.5)}} \quad [5\text{-}48]$$

To simplify, let:

$$K_9 = \frac{2K_8 K_7}{K_s} \quad [5\text{-}49]$$

Then,

$$\Delta T = K_9 J^2 A_p^{(0.25)} \quad [5\text{-}50]$$

$$J^2 = \frac{\Delta T}{K_9 A_p^{(0.25)}} \quad [5\text{-}51]$$

Then, letting:

$$K_{10} = \frac{\Delta T}{K_9} \quad [5\text{-}52]$$

We have:

$$J^2 = K_{10} A_p^{(0.25)} \quad [5\text{-}53]$$

The relationship between current density, J, and area product, A_p, can, therefore, be expressed as:

$$J = K_j A_p^{(0.125)} \quad [5\text{-}54]$$

The constant, K_j, is related to the core configuration, whose values are given in Table 5-5. These values have been derived by averaging the values from the data taken from Tables 3-1 through Tables 3-64 in Chapter 3.

© 2011 by Taylor and Francis Group, LLC

Table 5-5. Constant, K_j, for Temperature Increases of 25°C and 50°C

Temperature Constant, K_j		
Core Type	K_j (Δ25°)	K_j (Δ50°)
Pot Core	433	632
Powder Core	403	590
Laminations	366	534
C Core	322	468
Single-coil C Core	395	569
Tape-wound Core	250	365

The relationship between current density, J, and area product, A_p, for temperature increases of 25°C and 50°C is graphed in Figures 5-17 through 5-19 from data calculated of Tables 3-1 through 3-64 in Chapter 3.

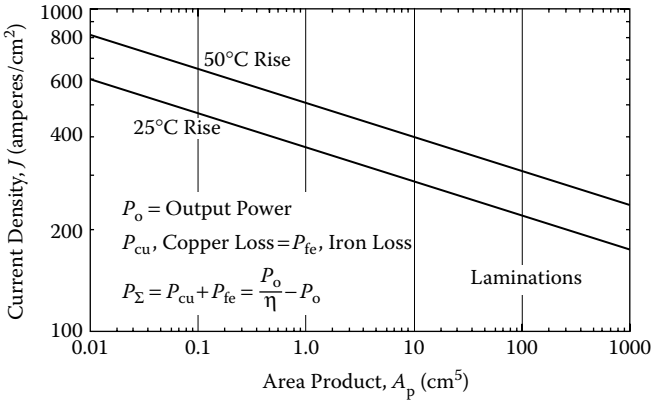

Figure 5-17. Current Density, J, Versus Area Product, A_p, for EI Laminations.

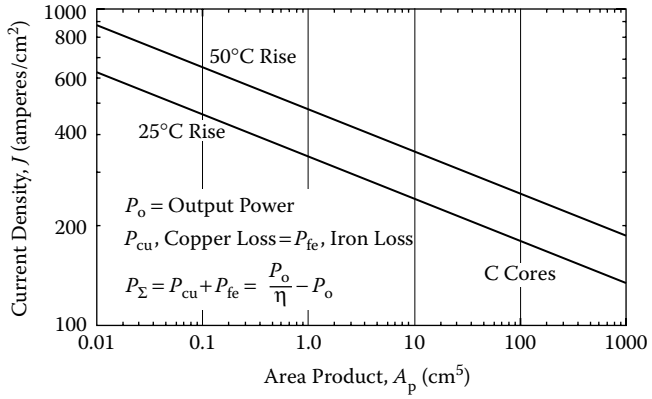

Figure 5-18. Current Density, J, Versus Area Product, A_p, for C Cores.

© 2011 by Taylor and Francis Group, LLC

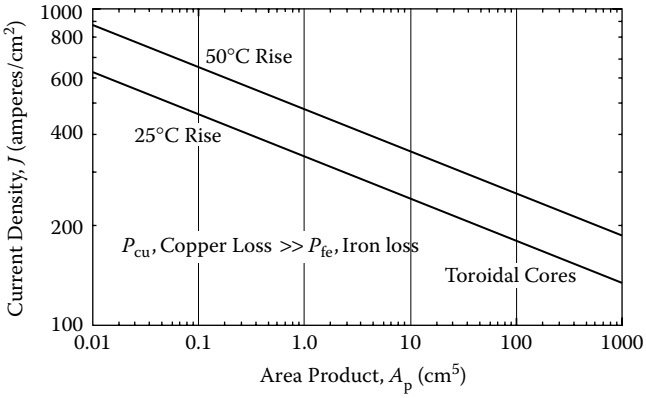

Figure 5-19. Current Density, J, Versus Area Product, A_p, for MPP Cores.

Transformer Core Geometry, K_g, and the Area Product, A_p

The core geometry, K_g, of a transformer can be related to the area product, A_p. The relationship is according to the following: the core geometry, K_g, varies in accordance with the fifth power of any linear dimension, (l), whereas area product, A_p, varies as the fourth power.

$$K_g = \frac{W_a A_c^2 K_u}{\text{MLT}}, \quad [\text{cm}^5] \tag{5-55}$$

$$K_g = K_{10} l^5 \tag{5-56}$$

$$A_p = K_2 l^4 \tag{5-57}$$

From Equation 5-56,

$$l = \left(\frac{K_g}{K_{10}} \right)^{(0.2)} \tag{5-58}$$

Then,

$$l^4 = \left[\left(\frac{K_g}{K_{10}} \right)^{(0.2)} \right]^4 = \left(\frac{K_g}{K_{10}} \right)^{(0.8)} \tag{5-59}$$

Substituting Equation 5-59 into Equation 5-57,

$$A_p = K_2 \left(\frac{K_g}{K_{10}} \right)^{(0.8)} \tag{5-60}$$

© 2011 by Taylor and Francis Group, LLC

Let:

$$K_p = \frac{K_2}{K_{10}^{(0.8)}} \quad [5\text{-}61]$$

Then,

$$A_p = K_p K_g^{(0.8)} \quad [5\text{-}62]$$

The constant, K_p, is related to the core configuration, whose values are given in Table 5-6. These values have been derived by averaging the values from the data taken from Tables 3-1 through Tables 3-64 in Chapter 3.

Table 5-6. Configuration Constant, K_p, for Area Product, A_p, and Core geometry, K_g

Constant, K_p	
Core Type	K_p
Pot Core	8.9
Powder Core	11.8
Laminations	8.3
C Core	12.5
Tape-wound Core	14.0

The relationship between area product, A_p, and core geometry, K_g, is graphed in Figures 5-20 through 5-22, from the data taken from Tables 3-1 through Tables 3-64 in Chapter 3.

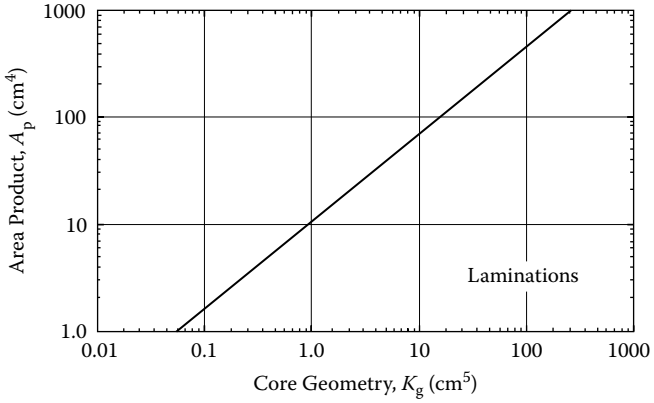

Figure 5-20. Area Product, A_p, Versus Core Geometry, K_g, for EI Laminations.

© 2011 by Taylor and Francis Group, LLC

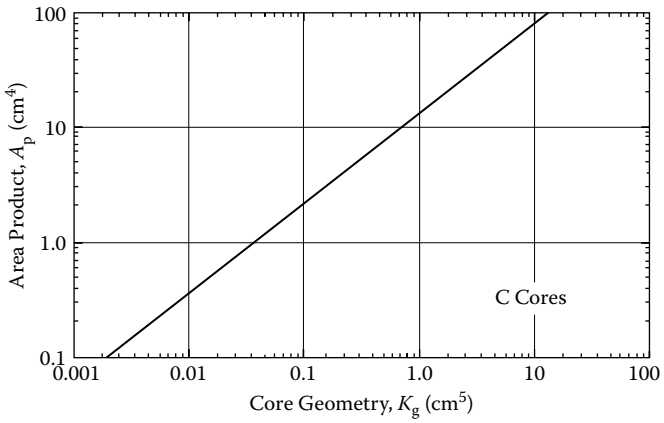

Figure 5-21. Area Product, A_p, Versus Core Geometry, K_g, for C Cores.

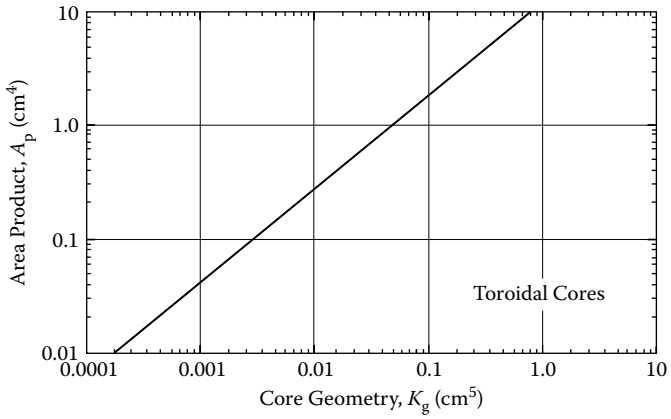

Figure 5-22. Area Product, A_p, Versus Core Geometry, K_g, for MPP Powder Cores.

Weight Versus Transformer Regulation

There are many design tasks where the transformer weight is very important in meeting the design specification. The engineer will raise the operating frequency in order to reduce the size and weight. The magnetic materials will be reviewed for performance at the operating frequency, and at the minimum and maximum temperatures. When the idealized magnetic material has been found and the weight of the transformer is still too high, then the only solution is to change the regulation. The regulation of a transformer versus the weight is shown in Figure 5-23. There are times when the engineer would like to know what the weight impact would be, if the regulation were to be increased or decreased.

© 2011 by Taylor and Francis Group, LLC

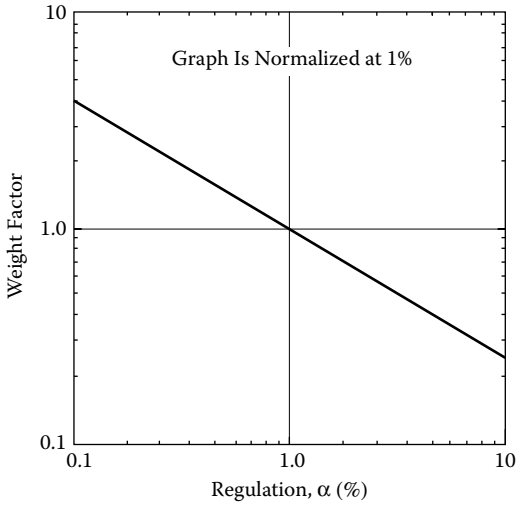

Figure 5-23. Weight Versus Regulation.

References

1. C. McLyman, Transformer Design Trade-offs, Technical Memorandum 33-767 Rev. 1, Jet Propulsion Laboratory, Pasadena, CA.

2. W. J. Muldoon, High Frequency Transformer Optimization, HAC Trade Study Report 2228/1130, May, 1970

3. R. G. Klimo, A. B. Larson, and J. E. Murray, Optimization Study of High Power Static Inverters and Converters, Quarterly report No. 2 NASA-CR-54021, April 20, 1964, Contract NAS 3-2785.

4. F. F. Judd and D. R. Kessler, Design Optimization of Power Transformers, Bell Laboratories, Whippany, New Jersey IEEE Applied Magnetics Workshop, June 5–6, 1975

© 2011 by Taylor and Francis Group, LLC

Chapter 6

Transformer-Inductor Efficiency, Regulation, and Temperature Rise

© 2011 by Taylor and Francis Group, LLC

Table of Contents

1. Introduction....6-3
2. Transformer Efficiency....6-3
3. Maximum Efficiency....6-3
4. Transformer Dissipation, by Radiation and Convection....6-5
5. Temperature Rise Versus Surface Area, A_t, Dissipation....6-6
6. Surface Area, A_t, Required for Heat Dissipation....6-7
7. Required Surface Area, A_t....6-8
8. Regulation as a Function of Efficiency....6-9
9. References....6-11

© 2011 by Taylor and Francis Group, LLC

Introduction

Transformer efficiency, regulation, and temperature rise are all interrelated. Not all of the input power to the transformer is delivered to the load. The difference between input power and output power is converted into heat. This power loss can be broken down into two components: core loss, P_{fe}, and copper loss, P_{cu}. The core loss is a fixed loss, and the copper loss is a variable loss that is related to the current demand of the load. The copper loss increases by the square of the current and also is termed a quadratic loss. Maximum efficiency is achieved when the fixed loss is equal to the quadratic loss at rated load. Transformer, regulation, α is the copper loss, P_{cu}, divided by the output power, P_o, as shown in Equation [6-1].

$$\alpha = \frac{P_{cu}}{P_o}(100), \quad [\%] \tag{6-1}$$

Transformer Efficiency

The efficiency of a transformer is a good way to measure the effectiveness of the design. Efficiency is defined as the ratio of the output power, P_o, to the input power, P_{in}. The difference between, P_o, and, P_{in}, is due to losses. The total power loss, P_Σ, in the transformer is determined by the fixed losses in the core and the quadratic losses in the windings or copper, as shown in Equation [6-2].

$$P_\Sigma = P_{fe} + P_{cu}, \quad [\text{watts}] \tag{6-2}$$

Where, P_{fe}, is the core loss, and P_{cu}, is the copper loss.

Maximum Efficiency

Maximum efficiency is achieved when the fixed loss is made equal to the quadratic loss, as shown by Equation 6-12. A graph of transformer loss versus output load current is shown in Figure 6-1.

The copper loss increases as the square of the output power, P_o, is multiplied by a constant, K_c:

$$P_{cu} = K_c P_o^2 \tag{6-3}$$

Which may be rewritten as:

$$P_\Sigma = P_{fe} + K_c P_o^2 \tag{6-4}$$

Since:

$$P_{in} = P_o + P_\Sigma \tag{6-5}$$

© 2011 by Taylor and Francis Group, LLC

The efficiency can be expressed as:

$$\eta = \frac{P_o}{P_o + P_\Sigma} \quad [6\text{-}6]$$

Then, substituting Equation 6-4 into 6-6 gives:

$$\eta = \frac{P_o}{P_o + P_{fe} + KP_o^2} = \frac{P_o}{P_{fe} + P_o + KP_o^2} \quad [6\text{-}7]$$

And, differentiating with respect to P_o:

$$\frac{d\eta}{dP_o} = \frac{P_{fe} + P_o + KP_o^2 - P_o(1 + 2KP_o)}{\left(P_{fe} + P_o + KP_o^2\right)^2} \quad [6\text{-}8]$$

Then, to solve for the maximum, equate Equation 6-8 to 0.

$$\frac{P_{fe} + P_o + KP_o^2 - P_o(1 + 2KP_o)}{\left(P_{fe} + P_o + KP_o^2\right)^2} = 0 \quad [6\text{-}9]$$

$$-P_o(1 + 2KP_o) + \left(P_{fe} + P_o + KP_o^2\right) = 0 \quad [6\text{-}10]$$

$$-P_o - 2KP_o^2 + P_{fe} + P_o + KP_o^2 = 0 \quad [6\text{-}11]$$

Therefore,

$$P_{fe} = KP_o^2 = P_{cu} \quad [6\text{-}12]$$

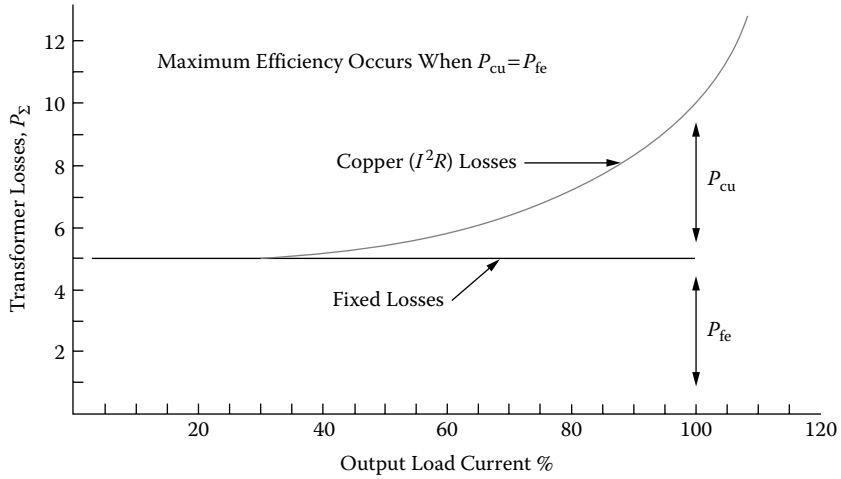

Figure 6-1. Transformer Losses Versus Output Load Current.

© 2011 by Taylor and Francis Group, LLC

Transformer Dissipation, by Radiation and Convection

Temperature rise in a transformer winding cannot be predicted with complete precision, despite the fact that many techniques are described in the literature for its calculation. One reasonable accurate method for open core and winding construction is based upon the assumption that core and winding losses may be lumped together as:

$$P_{\Sigma} = P_{cu} + P_{fe}, \quad \text{[watts]} \tag{6-13}$$

And the assumption is made that thermal energy is dissipated uniformly throughout the surface area of the core and winding assembly.

Transfer of heat by thermal radiation occurs when a body is raised to a temperature above its surroundings, and emits radiant energy in the form of waves. In accordance with Stefan-Boltzmann Law, (in Ref. 1) this transfer of heat may be expressed as:

$$W_r = K_r \varepsilon \left(T_2^4 - T_1^4 \right) \tag{6-14}$$

Where:

W_r, is watts per square centimeter of surface

$K_r = 5.70(10^{-12})W/(\text{cm}^2/K^4)$

ε, is the emissivity factor

T_2, is the hot body temperature, K (kelvin)

T_1, is the ambient or surrounding temperature, K (kelvin)

Transfer of heat by convection occurs when a body is hotter than the surrounding medium, which is usually air. The layer of air in contact with the hot body that is heated by conduction expands and rises, taking the absorbed heat with it. The next layer, being colder, replaces the risen layer and, in turn, on being heated, also rises. This transfer continues as long as the air, or other medium surrounding the body, is at a lower temperature. The transfer of heat by convection is stated mathematically as:

$$W_c = K_c F \theta^{(\eta)} \sqrt{P} \tag{6-15}$$

Where:

W_c, is the watts loss per square centimeter

$K_c = 2.17\,(10^{-4})$

F, is the air friction factor (unity for a vertical surface)

θ, is the temperature rise, °C

© 2011 by Taylor and Francis Group, LLC

P, is the relative barometic pressure (unity at sea level)

η, is the exponential value, which ranges from 1.0 to 1.25,

depending on the shape and position of the surface being cooled

The total heat dissipated from a plane vertical surface is expressed by Equations 6-13 and 6-15:

$$W = 5.70\left(10^{-12}\right)\varepsilon\left(T_2^4 - T_1^4\right) + 1.4\left(10^{-3}\right)F\theta^{(1.25)}\sqrt{P} \qquad [6\text{-}16]$$

Temperature Rise Versus Surface Area, A_t, Dissipation

The temperature rise that can be expected for various levels of power loss is shown in the monograph of Figure 6-2. It is based on Equation 6-16, relying on data obtained from Blume (1938) (Ref. 1) for heat transfer affected by the combination of 55% radiation and 45% convection, from a surface having an emissivity of 0.95, in an ambient temperature of 25°C, at sea level. Power loss (heat dissipation) is expressed in watts per square centimeter of the total surface area. Heat dissipation, by convection from the upper side of a horizontal flat surface, is on the order of 15-20% more than from vertical surface. Heat dissipation, from the underside of a horizontal flat surface, depends upon area and conductivity.

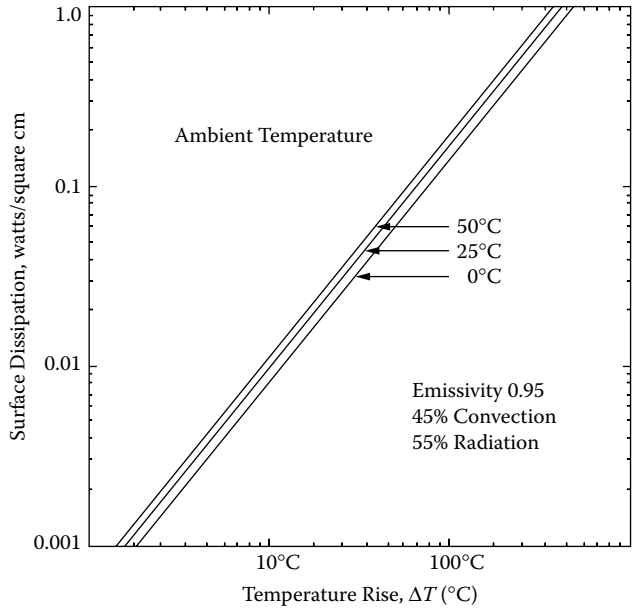

Figure 6-2. Temperature Rise Versus Surface Dissipation. (Adapted from L. F. Blume, *Transformers Engineering*, Wiley, New York, 1938, Figure 7.)

© 2011 by Taylor and Francis Group, LLC

Surface Area, A_t, Required for Heat Dissipation

The effective surface area, A_t, required to dissipate heat, (expressed as watts dissipated per unit area), is:

$$A_t = \frac{P_\Sigma}{\psi}, \quad [\text{cm}^2] \tag{6-17}$$

In which ψ is the power density or the average power dissipated per unit area from the surface of the transformer and, P_Σ is the total power lost or dissipated.

The surface area, A_t, of a transformer can be related to the area product, A_p, of a transformer. The straight-line logarithmic relationship, shown in Figure 6-3, has been plotted from the data in Chapter 3. The derivation for the surface area, A_t, and the area product, A_p, is in Chapter 5.

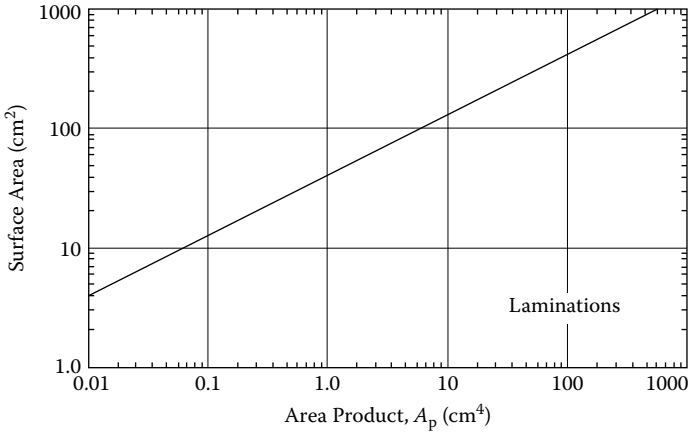

Figure 6-3. Surface Area, A_t Versus Area Product, A_p.

From this surface area, A_t, the following relationship evolves:

$$A_t = K_s \left(A_p\right)^{(0.5)} = \frac{P_\Sigma}{\psi}, \quad [\text{cm}^2] \tag{6-18}$$

And from Figure 6-3:

$$\psi = 0.03, \quad [\text{watts-per-cm}^2 \text{ at } 25°\text{C}]$$

$$\psi = 0.07, \quad [\text{watts-per-cm}^2 \text{ at } 50°\text{C}]$$

The temperature rise, T_r, in Equation [6-19] in °C is:

$$T_r = 450\left(\psi\right)^{(0.826)}, \quad [°\text{C}] \tag{6-19}$$

© 2011 by Taylor and Francis Group, LLC

Required Surface Area, A_t

There are two common allowable temperature rises for transformers above the ambient temperature. These temperatures are shown in Figure 6-4. The surface area, A_t, required for a 25°C and 50°C rise above the ambient temperature for the total watts, dissipated. The presented data is used as basis for determining the needed transformer surface area, A_t, in cm^2.

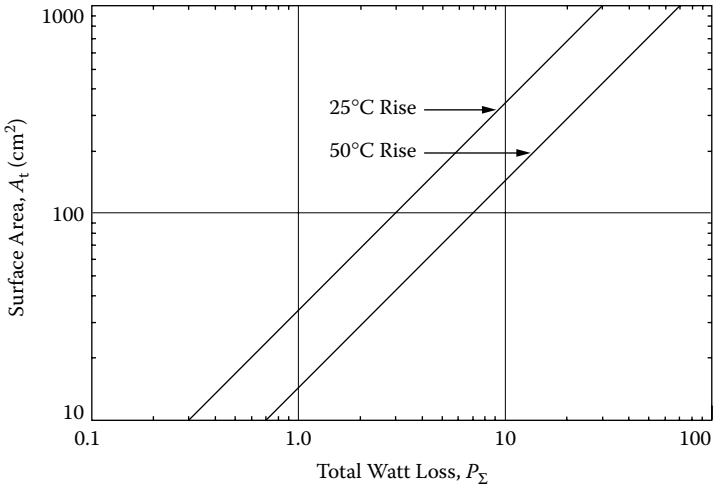

Figure 6-4. Surface Area, A_t Versus Total Watts Loss for Temperature Increases of 25°C and 50°C.

If the transformer is said to be homogeneous, and the thermal energy is dissipated uniformly throughout the surface area of the core and winding assembly, then Figure 6-5 will give a good approximation for the required time constant for a transformer to reach 63% of the final temperature. The temperature rise of a typical transformer is shown in Figure 6-6.

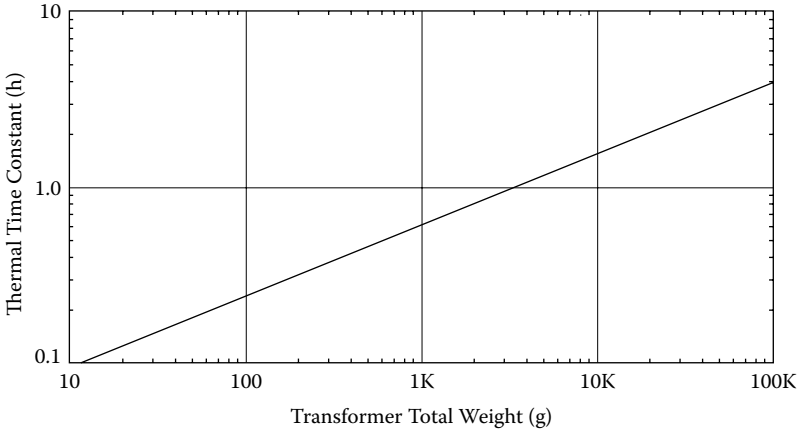

Figure 6-5. Time Required to Reach 63% of Final Temperature.

© 2011 by Taylor and Francis Group, LLC

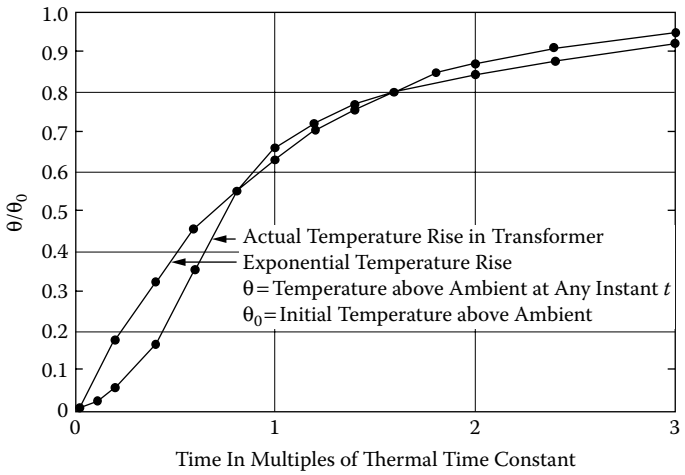

Figure 6-6. Transformer Temperature Rise Time.

Regulation as a Function of Efficiency

The minimum size of a transformer is usually determined either by a temperature rise limit, or by allowable voltage regulation, assuming that size and weight are to be minimized. Figure 6-7 shows a circuit diagram of a transformer with one secondary. Note that α = regulation (%).

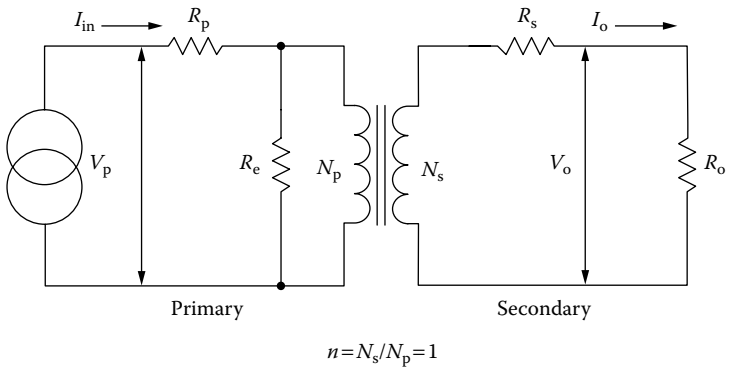

Figure 6-7. Transformer Circuit Diagram.

The assumption is that distributed capacitance in the secondary can be neglected because the frequency and secondary voltage are not excessively high. Also, the winding geometry is designed to limit the leakage inductance to a level, low enough, to be neglected under most operating conditions. The transformer window allocation is shown in Figure 6-8.

$$\frac{W_a}{2} = \text{Primary} = \text{Secondary} \qquad [6\text{-}20]$$

© 2011 by Taylor and Francis Group, LLC

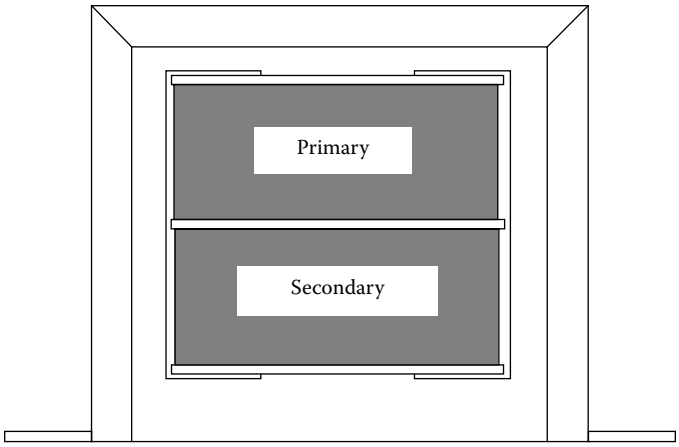

Figure 6-8. Transformer Window Allocation.

Transformer voltage regulation can now be expressed as:

$$\alpha = \frac{V_o\,(\text{N.L.}) - V_o\,(\text{F.L.})}{V_o\,(\text{F.L.})}(100), \quad [\%] \tag{6-21}$$

in which, V_o(N.L.), is the no load voltage and, V_o(F.L.), is the full load voltage. For the sake of simplicity, assume the transformer, in Figure 6-5, is an isolation transformer, with a 1:1 turns ratio, and the core impedance, R_e, is infinite.

If the transformer has a 1:1 turns ratio, and the core impedance is infinite, then:

$$\begin{aligned} I_{in} &= I_o, \quad [\text{amps}] \\ R_p &= R_s, \quad [\text{ohms}] \end{aligned} \tag{6-22}$$

With equal window areas allocated for the primary and secondary windings, and using the same current density, J:

$$\Delta V_p = I_{in} R_p = \Delta V_s = I_o R_s, \quad [\text{volts}] \tag{6-23}$$

Then Regulation is:

$$\alpha = \frac{\Delta V_p}{V_p}(100) + \frac{\Delta V_s}{V_s}(100), \quad [\%] \tag{6-24}$$

Multiply the Equation [6-24] by currents, I:

$$\alpha = \frac{\Delta V_p I_{in}}{V_p I_{in}}(100) + \frac{\Delta V_s I_o}{V_s I_o}(100), \quad [\%] \tag{6-25}$$

© 2011 by Taylor and Francis Group, LLC

Primary copper loss is:

$$P_p = \Delta V_p I_{in}, \quad \text{[watts]} \qquad \text{[6-26]}$$

Secondary copper loss is:

$$P_s = \Delta V_s I_o, \quad \text{[watts]} \qquad \text{[6-27]}$$

Total copper loss is:

$$P_{cu} = P_p + P_s, \quad \text{[watts]} \qquad \text{[6-28]}$$

Then, the regulation equation can be rewritten to:

$$\alpha = \frac{P_{cu}}{P_o}(100), \quad [\%] \qquad \text{[6-29]}$$

References

1. Blume, L. F., *Transformer Engineering*, John Wiley & Sons Inc. New York, 1938, pp. 272–282.

2. Terman, F. E., *Radio Engineers Handbook*, McGraw-Hill Book Co., Inc., New York, 1943, pp. 28–37.

© 2011 by Taylor and Francis Group, LLC

Chapter 7

Power Transformer Design

© 2011 by Taylor and Francis Group, LLC

Table of Contents

1. Introduction 7-3
2. The Design Problem Generally 7-3
3. Power-Handling Ability 7-4
4. Output Power, P_o, Versus Apparent Power, P_t, Capability 7-5
5. Transformers with Multiple Outputs 7-8
6. Regulation 7-10
7. Relationship, K_g, to Power Transformer Regulation Capability 7-12
8. Relationship, A_p, to Transformer Power Handling Capability 7-13
9. Different Cores, Same Area Product 7-13
10. 250 Watt Isolation Transformer Design, Using the Core Geometry, K_g, Approach 7-15
11. 38 Watt 100kHz Transformer Design, Using the Core Geometry, K_g, Approach 7-20

© 2011 by Taylor and Francis Group, LLC

Introduction

The conversion process in power electronics requires the use of transformers and components that are frequently the heaviest and bulkiest item in the conversion circuit. They also have a significant effect upon the overall performance and efficiency of the system. Accordingly, the design of such transformers has an important influence on the overall system weight, power conversion efficiency and cost. Because of the interdependence and interaction of parameters, judicious trade-offs are necessary to achieve design optimization.

The Design Problem Generally

The designer is faced with a set of constraints that must be observed in the design on any transformer. One of these constraints is the output power, P_o, (operating voltage multiplied by maximum current demand). The secondary winding must be capable of delivering to the load within specified regulation limits. Another constraint relates to the minimum efficiency of operation, which is dependent upon the maximum power loss that can be allowed in the transformer. Still another defines the maximum permissible temperature rise for the transformer when it is used in a specified temperature environment.

One of the basic steps in transformer design is the selection of proper core material. Magnetic materials used to design low and high frequency transformers are shown in Table 7-1. Each one of these materials has its own optimum point in the cost, size, frequency and efficiency spectrum. The designer should be aware of the cost difference between silicon-iron, nickel-iron, amorphous and ferrite materials. Other constraints relate to the volume occupied by the transformer and, particularly in aerospace applications, the weight, since weight minimization is an important goal in today's electronics. Finally, cost effectiveness is always an important consideration.

Depending upon the application, certain ones of these constraints will dominate. Parameters affecting others may then be a trade-off, as necessary, to achieve the most desirable design. It is not possible to optimize all parameters in a single design because of their interaction and interdependence. For example, if volume and weight are of greater significance, reductions in both can often be affected, by operating the transformer at a higher frequency, but at a penalty in efficiency. When, the frequency cannot be increased, reduction in weight and volume may still be possible by selecting a more efficient core material, but, at the penalty of increased cost. Thus, judicious trade-offs must be affected to achieve the design goals.

Transformer designers have used various approaches in arriving at suitable designs. For example, in many cases, a rule of thumb is used for dealing with current density. Typically, an assumption is made that a good working level is 200 amps-per-cm^2 (1000 circular mils-per-ampere). This will work in many instances, but

© 2011 by Taylor and Francis Group, LLC

Table 7-1. Magnetic Materials

Magnetic Material Properties				
Material Name	Trade Name Composition	Initial Permeability μ_i	Flux Density Teslas B_s	Typical Operating Frequency
Silicon	3-97 SiFe	1500	1.5-1.8	50-2k
Orthonol	50-50 NiFe	2000	1.42-1.58	50-2k
Permalloy	80-20 NiFe	25000	0.66-0.82	1k-25k
Amorphous	2605SC	1500	1.5-1.6	250k
Amorphous	2714A	20,000	0.5-6.5	250k
Amorphous	Nanocrystalline	30,000	1.0-1.2	250k
Ferrite	MnZn	0.75-15k	0.3-0.5	10k-2M
Ferrite	NiZn	0.20-1.5k	0.3-0.4	0.2M-100M

the wire size needed to meet this requirement may produce a heavier and bulkier transformer than desired or required. The information presented in this chapter makes it possible to avoid the use of this assumption and other rules of thumb, and to develop a more economical design with greater accuracy.

Power-Handling Ability

For years manufacturers have assigned numeric codes to their cores; these codes represent the power-handling ability. This method assigns to each core a number that is the product of its window area, W_a, and core cross-section area, A_c, and is called the area product, A_p.

These numbers are used by core suppliers to summarize dimensional and electrical properties in their catalogs. They are available for laminations, C-cores, pot cores, powder cores, ferrite toroids, and toroidal tape-wound cores.

The regulation and power-handling ability of a core is related to the core geometry, K_g. Every core has its own inherent, K_g. The core geometry is relatively new, and magnetic core manufacturers do not list this coefficient.

Because of their significance, the area product, A_p, and core geometry, K_g, are treated extensively in this book. A great deal of other information is also presented for the convenience of the designer. Much of the material is in tabular form to assist the designer in making trade-offs, best-suited for his particular application in a minimum amount of time.

© 2011 by Taylor and Francis Group, LLC

These relationships can now be used as new tools to simplify and standardize the process of transformer design. They make it possible to design transformers of lighter weight and smaller volume, or to optimize efficiency, without going through a cut-and-try, design procedure. While developed especially for aerospace applications, the information has wider utility, and can be used for the design of non-aerospace, as well.

Output Power, P_o, Versus Apparent Power, P_t, Capability

Output power, P_o, is of the greatest interest to the user. To the transformer designer, the apparent power, P_t, which is associated with the geometry of the transformer, is of greater importance. Assume, for the sake of simplicity, that the core of an isolation transformer has only two windings in the window area, a primary and a secondary. Also, assume that the window area, W_a, is divided up in proportion to the power-handling capability of the windings, using equal current density. The primary winding handles, P_{in}, and the secondary handles, P_o, to the load. Since the power transformer has to be designed to accommodate the primary, P_{in}, and, P_o, then,

By definition:

$$P_t = P_{in} + P_o, \quad \text{[watts]}$$
$$P_{in} = \frac{P_o}{\eta}, \quad \text{[watts]} \qquad [7\text{-}1]$$

The primary turns can be expressed using Faraday's Law:

$$N_p = \frac{V_p\left(10^4\right)}{A_c B_{ac} f K_f}, \quad \text{[turns]} \qquad [7\text{-}2]$$

The winding area of a transformer is fully utilized when:

$$K_u W_a = N_p A_{wp} + N_s A_{ws} \qquad [7\text{-}3]$$

By definition the wire area is:

$$A_w = \frac{I}{J}, \quad [\text{cm}^2] \qquad [7\text{-}4]$$

Rearranging the Equation shows:

$$K_u W_a = N_p\left(\frac{I_p}{J}\right) + N_s\left(\frac{I_s}{J}\right) \qquad [7\text{-}5]$$

© 2011 by Taylor and Francis Group, LLC

Now, substitute in Faraday's Equation:

$$K_u W_a = \frac{V_p\left(10^4\right)}{A_c B_{ac} f K_f}\left(\frac{I_p}{J}\right) + \frac{V_s\left(10^4\right)}{A_c B_{ac} f K_f}\left(\frac{I_s}{J}\right) \quad [7\text{-}6]$$

Rearranging shows:

$$W_a A_c = \frac{\left[\left(V_p I_p\right) + \left(V_s I_s\right)\right]\left(10^4\right)}{B_{ac} f J K_f K_u}, \quad [\text{cm}^4] \quad [7\text{-}7]$$

The output power, P_o, is:

$$P_o = V_s I_s, \quad [\text{watts}] \quad [7\text{-}8]$$

The input power, P_{in}, is:

$$P_{in} = V_p I_p, \quad [\text{watts}] \quad [7\text{-}9]$$

Then:

$$P_t = P_{in} + P_o, \quad [\text{watts}] \quad [7\text{-}10]$$

Substitute in, P_t:

$$W_a A_c = \frac{P_t\left(10^4\right)}{B_{ac} f J K_f K_u}, \quad [\text{cm}^4] \quad [7\text{-}11]$$

By definition, A_p, equals:

$$A_p = W_a A_c, \quad [\text{cm}^4] \quad [7\text{-}12]$$

Then:

$$A_p = \frac{P_t\left(10^4\right)}{B_{ac} f J K_f K_u}, \quad [\text{cm}^4] \quad [7\text{-}13]$$

© 2011 by Taylor and Francis Group, LLC

The designer must be concerned with the apparent power, P_t, and power handling capability of the transformer core and windings. P_t may vary by a factor, ranging from 2 to 2.828 times the input power, P_{in}, depending upon the type of circuit in which the transformer is used. If the current in the rectifier transformer becomes interrupted, its effective RMS value changes. Thus, transformer size is not only determined by the load demand, but also, by application, because of the different copper losses incurred, due to the current waveform.

For example, for a load of one watt, compare the power handling capabilities required for each winding, (neglecting transformer and diode losses, so that $P_{in} = P_o$). For the full-wave bridge circuit of Figure 7-1, the full-wave center-tapped secondary circuit of Figure 7-2, and the push-pull, center-tapped full-wave circuit in Figure 7-3, all the windings have the same number of turns, (N).

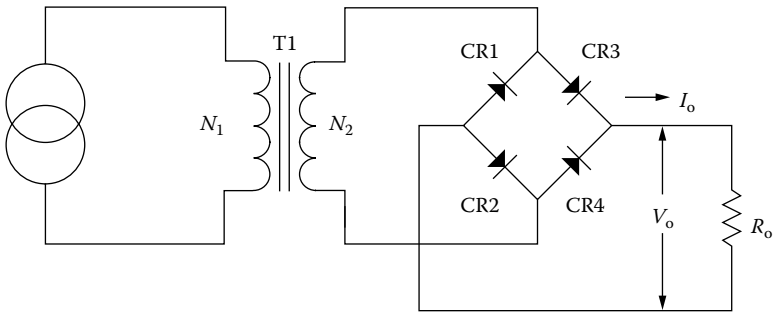

Figure 7-1. Full-Wave Bridge Secondary.

The total apparent power, P_t, for the circuit shown in Figure 7-1 is 2 watts.

This is shown in the following Equation:

$$P_t = P_{in} + P_o, \quad \text{[watts]} \qquad \text{[7-14]}$$

$$P_t = 2P_{in}, \quad \text{[watts]} \qquad \text{[7-15]}$$

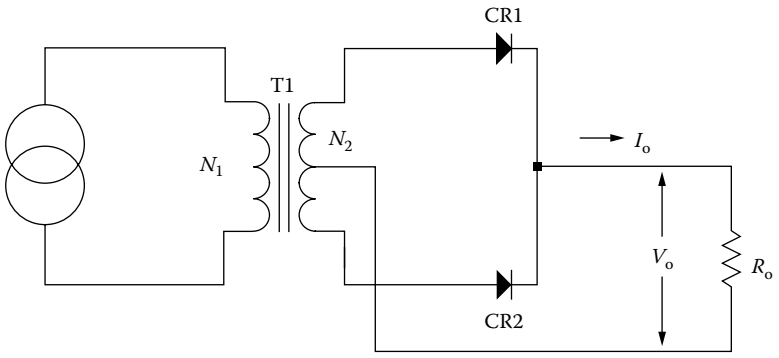

Figure 7-2. Full-Wave, Center-Tapped Secondary.

© 2011 by Taylor and Francis Group, LLC

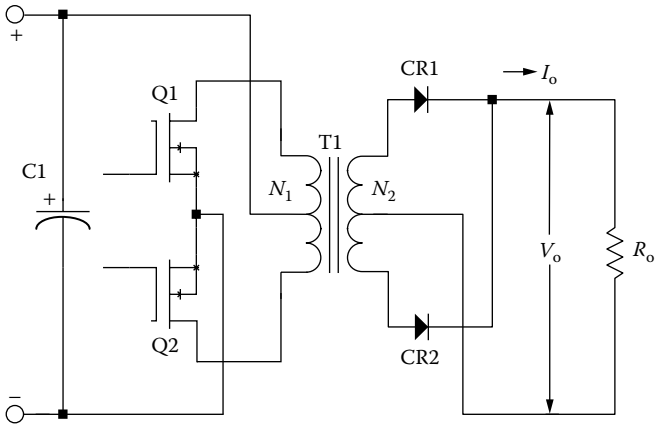

Figure 7-3. Push-Pull Primary, Full-Wave, Center-Tapped Secondary.

The total power, P_t, for the circuit shown in Figure 7-2, increased 20.7%, due to the distorted wave form of the interrupted current flowing in the secondary winding. This is shown in the following Equation:

$$P_t = P_{in} + P_o\sqrt{2}, \quad \text{[watts]} \qquad \text{[7-16]}$$

$$P_t = P_{in}\left(1+\sqrt{2}\right), \quad \text{[watts]} \qquad \text{[7-17]}$$

The total power, P_t, for the circuit is shown in Figure 7-3, which is typical of a dc to dc converter. It increases to 2.828 times, P_{in}, because of the interrupted current flowing in both the primary and secondary windings.

$$P_t = P_{in}\sqrt{2} + P_o\sqrt{2}, \quad \text{[watts]} \qquad \text{[7-18]}$$

$$P_t = 2P_{in}\sqrt{2}, \quad \text{[watts]} \qquad \text{[7-19]}$$

Transformers with Multiple Outputs

This example shows how the apparent power, P_t, changes with a multiple output transformers.

Output	Circuit
5 V @ 10A	center-tapped V_d = diode drop = 1 V
15 V @ 1A	full-wave bridge V_d = diode drop = 2 V
Efficiency = 0.95	

© 2011 by Taylor and Francis Group, LLC

The output power seen by the transformer in Figure 7-4 is:

$$\begin{aligned} P_{o1} &= (V_{o1} + V_d)(I_{o1}), \quad \text{[watts]} \\ P_{o1} &= (5+1)(10), \quad \text{[watts]} \\ P_{o1} &= 60, \quad \text{[watts]} \end{aligned} \tag{7-20}$$

And:

$$\begin{aligned} P_{o2} &= (V_{o2} + V_d)(I_{o2}), \quad \text{[watts]} \\ P_{o2} &= (15+2)(1.0), \quad \text{[watts]} \\ P_{o2} &= 17, \quad \text{[watts]} \end{aligned} \tag{7-21}$$

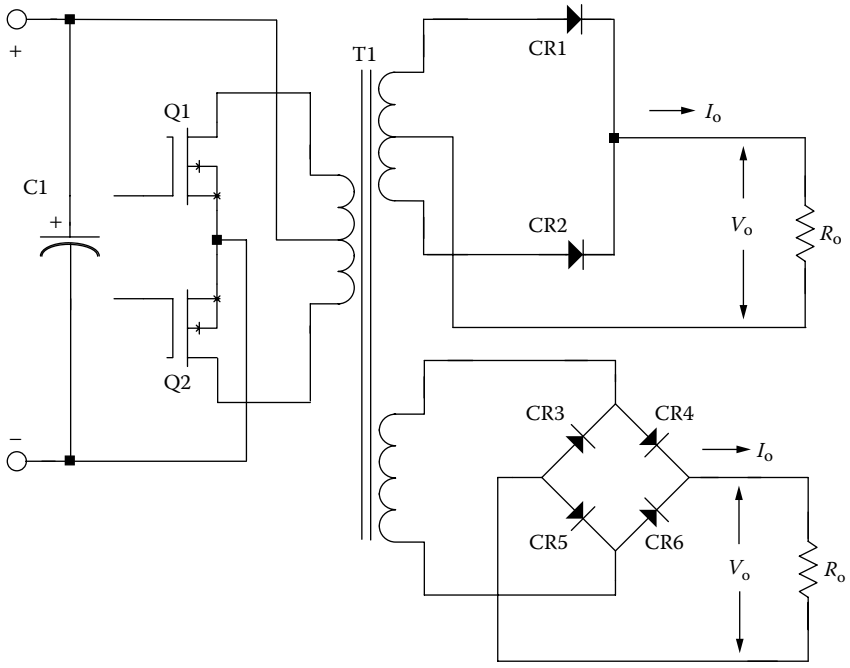

Figure 7-4. Multiple Output Converter.

Because of the different winding configurations, the apparent power, P_t, the transformer outputs will have to be summed to reflect this. When a winding has a center-tap and produces a discontinuous current, then, the power in that winding, be it primary or secondary, has to be multiplied by the factor, U. The factor, U, corrects for the rms current in that winding. If the winding has a center-tap, then the factor, U, is equal to 1.41. If not, the factor, U, is equal to 1.

For an example, summing up the output power of a multiple output transformer, would be:

$$P_\Sigma = P_{o1}(U) + P_{o2}(U) + P_n(U) + \cdots \tag{7-22}$$

© 2011 by Taylor and Francis Group, LLC

Then:

$$P_{\Sigma} = P_{o1}(U) + P_{o2}(U), \quad \text{[watts]}$$
$$P_{\Sigma} = 60(1.41) + 17(1), \quad \text{[watts]} \qquad \text{[7-23]}$$
$$P_{\Sigma} = 101.6, \quad \text{[watts]}$$

After the secondary has been totaled, then the primary power can be calculated.

$$P_{in} = \frac{P_{o1} + P_{o2}}{\eta}, \quad \text{[watts]}$$
$$P_{in} = \frac{(60) + (17)}{(0.95)}, \quad \text{[watts]} \qquad \text{[7-24]}$$
$$P_{in} = 81, \quad \text{[watts]}$$

Then, the apparent power, P_t, equals:

$$P_t = P_{in}(U) + P_{\Sigma}, \quad \text{[watts]}$$
$$P_t = (81)(1.41) + (101.6), \quad \text{[watts]} \qquad \text{[7-25]}$$
$$P_t = 215.8, \quad \text{[watts]}$$

Regulation

The minimum size of a transformer is usually determined either by a temperature rise limit, or by allowable voltage regulation, assuming that size and weight are to be minimized. Figure 7-5 shows a circuit diagram of a transformer with one secondary.

Note that α = regulation (%).

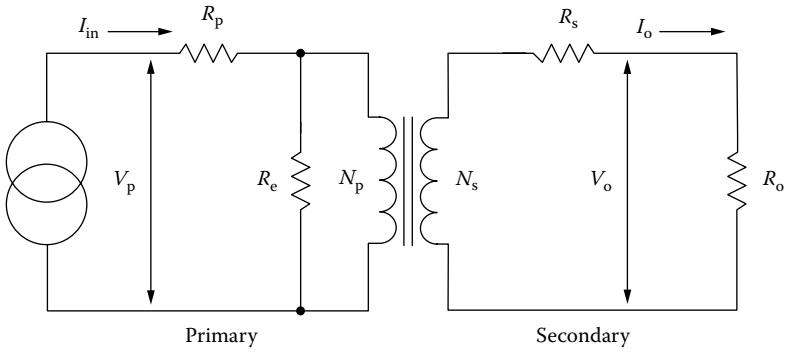

Figure 7-5. Transformer Circuit Diagram.

© 2011 by Taylor and Francis Group, LLC

The assumption is that distributed capacitance in the secondary can be neglected because the frequency and secondary voltage are not excessively high. Also, the winding geometry is designed to limit the leakage inductance to a level, low enough, to be neglected under most operating conditions.

Transformer voltage regulation can now be expressed as:

$$\alpha = \frac{V_o(\text{N.L.}) - V_o(\text{F.L.})}{V_o(\text{F.L.})}(100), \quad [\%] \tag{7-26}$$

In which, V_o(N.L.), is the no load voltage and, V_o(F.L.), is the full load voltage. For the sake of simplicity, assume the transformer in Figure 7-5, is an isolation transformer, with a 1:1 turns ratio, and the core impedance, R_e, is infinite.

If the transformer has a 1:1 turns ratio, and the core impedance is infinite, then:

$$\begin{aligned} I_{in} &= I_o, \quad [\text{amps}] \\ R_p &= R_s, \quad [\text{ohms}] \end{aligned} \tag{7-27}$$

With equal window areas allocated for the primary and secondary windings, and using the same current density, J:

$$\Delta V_p = I_{in} R_p = \Delta V_s = I_o R_s, \quad [\text{volts}] \tag{7-28}$$

Regulation is then:

$$\alpha = \frac{\Delta V_p}{V_p}(100) + \frac{\Delta V_s}{V_s}(100), \quad [\%] \tag{7-29}$$

Multiply the Equation by currents, I:

$$\alpha = \frac{\Delta V_p I_{in}}{V_p I_{in}}(100) + \frac{\Delta V_s I_o}{V_s I_o}(100), \quad [\%] \tag{7-30}$$

Primary copper loss is:

$$P_p = \Delta V_p I_{in}, \quad [\text{watts}] \tag{7-31}$$

Secondary copper loss is:

$$P_s = \Delta V_s I_o, \quad [\text{watts}] \tag{7-32}$$

© 2011 by Taylor and Francis Group, LLC

Total copper loss is:

$$P_{cu} = P_p + P_s, \quad \text{[watts]} \tag{7-33}$$

Then, the regulation Equation can be rewritten to:

$$\alpha = \frac{P_{cu}}{P_o}(100), \quad [\%] \tag{7-34}$$

Regulation can be expressed as the power lost in the copper. A transformer, with an output power of 100 watts and a regulation of 2%, will have a 2 watt loss in the copper:

$$P_{cu} = \frac{P_o \alpha}{100}, \quad \text{[watts]} \tag{7-35}$$

$$P_{cu} = \frac{(100)(2)}{100}, \quad \text{[watts]} \tag{7-36}$$

$$P_{cu} = 2, \quad \text{[watts]} \tag{7-37}$$

Relationship, Kg, to Power Transformer Regulation Capability

Although most transformers are designed for a given temperature rise, they can also be designed for a given regulation. The regulation and power-handling ability of a core is related to two constants:

$$\alpha = \frac{P_t}{2K_g K_e}, \quad [\%] \tag{7-38}$$

$$\alpha = \text{Regulation } (\%) \tag{7-39}$$

The constant, K_g, is determined by the core geometry, which may be related by the following Equations:

$$K_g = \frac{W_a A_c^2 K_u}{\text{MLT}}, \quad [\text{cm}^5] \tag{7-40}$$

© 2011 by Taylor and Francis Group, LLC

The constant, K_e, is determined by the magnetic and electric operating conditions, which may be related by the following Equation:

$$K_e = 0.145 K_f^2 f^2 B_m^2 \left(10^{-4}\right) \quad [7\text{-}41]$$

Where:

K_f = waveform coefficient

4.0 square wave

4.44 sine wave

From the above, it can be seen that factors such as flux density, frequency of operation, and the waveform coefficient have an influence on the transformer size.

Relationship, Ap, to Transformer Power Handling Capability

Transformers

According to the newly developed approach, the power handling capability of a core is related to its area product, A_p, by an equation which may be stated as:

$$A_p = \frac{P_t\left(10^4\right)}{K_f K_u B_m J f}, \quad [\text{cm}^4] \quad [7\text{-}42]$$

Where:

K_f = waveform coefficient

4.0 square wave

4.44 sine wave

From the above, it can be seen that factors, such as flux density, frequency of operation, and the window utilization factor, K_u, define the maximum space which may be occupied by the copper in the window.

Different Cores, Same Area Product

The area product, A_p, of a core is the product of the available window area, W_a, of the core in square centimeters, (cm^2), multiplied by the effective, cross-sectional area, A_c, in square centimeters, (cm^2), which may be stated as:

$$A_p = W_a A_c, \quad [\text{cm}^4] \quad [7\text{-}43]$$

© 2011 by Taylor and Francis Group, LLC

Figures 7-6 through Figure 7-9 show, in outline form, three transformer core types that are typical of those shown in the catalogs of suppliers.

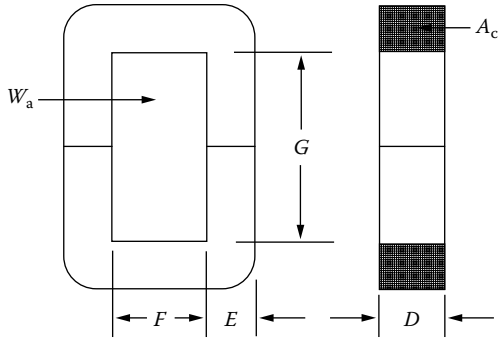

Figure 7-6. Dimensional Outline of a C Core.

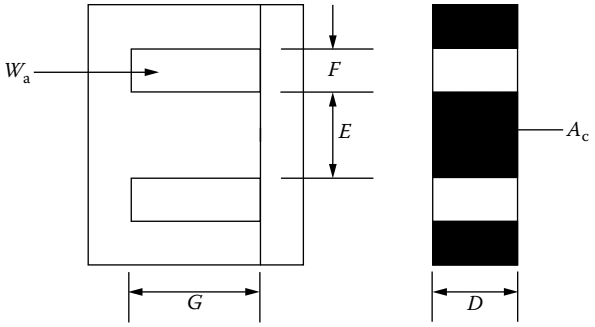

Figure 7-7. Dimensional Outline of a EI Lamination.

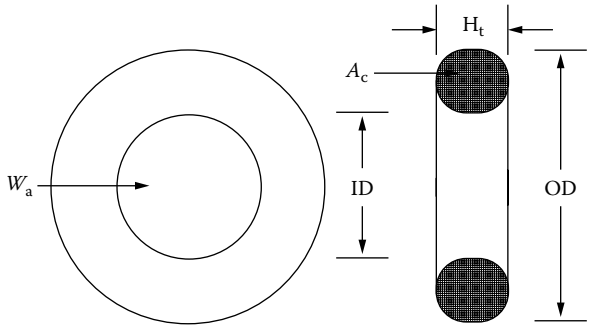

Figure 7-8. Dimensional Outline of a Toroidal Core.

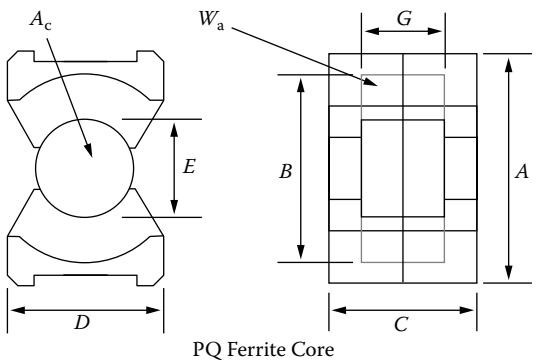

Figure 7-9. Dimensional Outline of a PQ Ferrite Core.

© 2011 by Taylor and Francis Group, LLC

250 Watt Isolation Transformer Design, Using the Core Geometry, K_g, Approach

The following information is the Design specification for a 250 watt isolation transformer, operating at 47 Hz, using the, K_g, core geometry approach. For a typical design example, assume with the following specification:

1. Input voltage, V_{in} = 115 volts
2. Output voltage, V_o = 115 volts
3. Output current, I_o = 2.17 amps
4. Output power, P_o = 250 watts
5. Frequency, f = 47 Hz
6. Efficiency, η = 95%
7. Regulation, α = 5%
8. Operating flux density, B_{ac} = 1.6 teslas
9. Core Material = Silicon M6X
10. Window utilization, K_u = 0.4
11. Temperature rise goal, T_r = 30°C

Step No. 1: Calculate the transformer apparent power, P_t.

$$P_t = P_o\left(\frac{1}{\eta}+1\right), \quad \text{[watts]}$$

$$P_t = 250\left(\frac{1}{0.95}+1\right), \quad \text{[watts]}$$

$$P_t = 513, \quad \text{[watts]}$$

Step No. 2: Calculate the electrical conditions, K_e.

$$K_e = 0.145\left(K_f\right)^2\left(f\right)^2\left(B_m\right)^2\left(10^{-4}\right)$$

$$K_f = 4.44, \quad \text{[sine wave]}$$

$$K_e = 0.145(4.44)^2(47)^2(1.6)^2\left(10^{-4}\right)$$

$$K_e = 1.62$$

Step No. 3: Calculate the core geometry, K_g.

$$K_g = \frac{P_t}{2K_e\alpha}, \quad [\text{cm}^5]$$

$$K_g = \frac{(513)}{2(1.62)(5)}, \quad [\text{cm}^5]$$

$$K_g = 31.7, \quad [\text{cm}^5]$$

© 2011 by Taylor and Francis Group, LLC

Step No. 4: Select a lamination from Chapter 3, comparable in core geometry, K_g.

Lamination number = EI-150

Manufacturer = Thomas and Skinner

Magnetic path length, MPL = 22.9 cm

Core weight, W_{tfe} = 2.334 kilograms

Copper weight, $W_{tcu,}$ = 853 grams

Mean length turn, MLT = 22 cm

Iron area, A_c = 13.8 cm^2

Window area, W_a = 10.89 cm^2

Area product, $A_{p,}$ = 150 cm^4

Core geometry, K_g = 37.6 cm^5

Surface area, A_t = 479 cm^2

Step No. 5: Calculate the number of primary turns, N_p using Faraday's Law.

$$N_p = \frac{V_{in}\left(10^4\right)}{K_f B_{ac} f A_c}, \quad \text{[turns]}$$

$$N_p = \frac{(115)\left(10^4\right)}{(4.44)(1.6)(47)(13.8)}, \quad \text{[turns]}$$

$$N_p = 250, \quad \text{[turns]}$$

Step No. 6: Calculate the current density, J.

$$J = \frac{P_t\left(10^4\right)}{K_f K_u B_{ac} f A_p}, \quad \text{[amps/cm}^2\text{]}$$

$$J = \frac{513\left(10^4\right)}{(4.44)(0.4)(1.6)(47)(150)}, \quad \text{[amps/cm}^2\text{]}$$

$$J = 256, \quad \text{[amps/cm}^2\text{]}$$

Step No. 7: Calculate the input current, I_{in}.

$$I_{in} = \frac{P_o}{V_{in}\eta}, \quad \text{[amps]}$$

$$I_{in} = \frac{250}{(115)(0.95)}, \quad \text{[amps]}$$

$$I_{in} = 2.28, \quad \text{[amps]}$$

© 2011 by Taylor and Francis Group, LLC

Step No. 8: Calculate the primary bare wire area, $A_{wp(B)}$.

$$A_{wp(B)} = \frac{I_{in}}{J}, \quad [\text{cm}^2]$$

$$A_{wp(B)} = \frac{(2.28)}{256}, \quad [\text{cm}^2]$$

$$A_{wp(B)} = 0.0089, \quad [\text{cm}^2]$$

Step No. 9: Select the wire from the Wire Table, in Chapter 4.

$$AWG = \#18$$

$$A_{wp(B)} = 0.00822, \quad [\text{cm}^2]$$

$$A_{wp} = 0.00933, \quad [\text{cm}^2]$$

$$\left(\frac{\mu\Omega}{\text{cm}}\right) = 209, \quad [\text{micro-ohm/cm}]$$

Step No. 10: Calculate the primary resistance, R_p.

$$R_p = \text{MLT}(N_p)\left(\frac{\mu\Omega}{\text{cm}}\right)\left(10^{-6}\right), \quad [\text{ohms}]$$

$$R_p = (22)(250)(209)\left(10^{-6}\right), \quad [\text{ohms}]$$

$$R_p = 1.15, \quad [\text{ohms}]$$

Step No. 11: Calculate the primary copper loss, P_p.

$$P_p = I_p^2 R_p, \quad [\text{watts}]$$

$$P_p = (2.28)^2(1.15), \quad [\text{watts}]$$

$$P_p = 5.98, \quad [\text{watts}]$$

Step No. 12: Calculate the secondary turns, N_s.

$$N_s = \frac{N_p V_s}{V_{in}}\left(1 + \frac{\alpha}{100}\right), \quad [\text{turns}]$$

$$N_s = \frac{(250)(115)}{(115)}\left(1 + \frac{5}{100}\right), \quad [\text{turns}]$$

$$N_s = 262.5 \text{ use } 263, \quad [\text{turns}]$$

© 2011 by Taylor and Francis Group, LLC

Step No. 13: Calculate the secondary bare wire area, $A_{ws(B)}$.

$$A_{ws(B)} = \frac{I_o}{J}, \quad [\text{cm}^2]$$

$$A_{ws(B)} = \frac{(2.17)}{256}, \quad [\text{cm}^2]$$

$$A_{ws(B)} = 0.00804, \quad [\text{cm}^2]$$

Step No. 14: Select the wire from the Wire Table, in Chapter 4.

$$AWG = \#18$$

$$A_{wp(B)} = 0.00822, \quad [\text{cm}^2]$$

$$A_{wp} = 0.00933, \quad [\text{cm}^2]$$

$$\left(\frac{\mu\Omega}{\text{cm}}\right) = 209, \quad [\text{micro-ohm/cm}]$$

Step No. 15: Calculate the secondary winding resistance, R_s.

$$R_s = \text{MLT}(N_s)\left(\frac{\mu\Omega}{\text{cm}}\right)\left(10^{-6}\right), \quad [\text{ohms}]$$

$$R_s = (22)(263)(209)\left(10^{-6}\right), \quad [\text{ohms}]$$

$$R_s = 1.21, \quad [\text{ohms}]$$

Step No. 16: Calculate the secondary copper loss, P_s.

$$P_s = I_o^2 R_s, \quad [\text{watts}]$$

$$P_s = (2.17)^2(1.21), \quad [\text{watts}]$$

$$P_s = 5.70, \quad [\text{watts}]$$

Step No. 17: Calculate the total primary and secondary copper loss, P_{cu}.

$$P_{cu} = P_p + P_s, \quad [\text{watts}]$$

$$P_{cu} = 5.98 + 5.7, \quad [\text{watts}]$$

$$P_{cu} = 11.68, \quad [\text{watts}]$$

© 2011 by Taylor and Francis Group, LLC

Step No. 18: Calculate the transformer regulation, α.

$$\alpha = \frac{P_{cu}}{P_o}(100), \quad [\%]$$

$$\alpha = \frac{(11.68)}{(250)}(100), \quad [\%]$$

$$\alpha = 4.67, \quad [\%]$$

Step No. 19: Calculate the watts per kilogram, W/K. Use the Equation for this material in Chapter 2.

$$W/K = 0.000557(f)^{1.68}(B_{ac})^{1.86}$$

$$W/K = 0.000557(47)^{1.68}(1.6)^{1.86}$$

$$W/K = 0.860$$

Step No. 20: Calculate the core loss, P_{fe}.

$$P_{fe} = (W/K)(W_{tfe})(10^{-3}), \quad [\text{watts}]$$

$$P_{fe} = (0.860)(2.33), \quad [\text{watts}]$$

$$P_{fe} = 2.00, \quad [\text{watts}]$$

Step No. 21: Calculate the total loss, P_Σ.

$$P_\Sigma = P_{cu} + P_{fe}, \quad [\text{watts}]$$

$$P_\Sigma = (11.68) + (2.00), \quad [\text{watts}]$$

$$P_\Sigma = 13.68, \quad [\text{watts}]$$

Step No. 22: Calculate the watts per unit area, ψ.

$$\psi = \frac{P_\Sigma}{A_t}, \quad [\text{watts/cm}^2]$$

$$\psi = \frac{(13.68)}{(479)}, \quad [\text{watts/cm}^2]$$

$$\psi = 0.0286, \quad [\text{watts/cm}^2]$$

© 2011 by Taylor and Francis Group, LLC

Step No. 23: Calculate the temperature rise, T_r.

$$T_r = 450(\psi)^{(0.826)}, \quad [°C]$$

$$T_r = 450(0.0286)^{(0.826)}, \quad [°C]$$

$$T_r = 23.9, \quad [°C]$$

Step No. 24: Calculate the total window utilization, K_u.

$$K_u = K_{up} + K_{us}$$

$$K_{us} = \frac{N_s A_{ws(B)}}{W_a}$$

$$K_{us} = \frac{(263)(0.00822)}{(10.89)} = 0.199$$

$$K_{up} = \frac{N_p A_{wp(B)}}{W_a}$$

$$K_{up} = \frac{(250)(0.00822)}{(10.89)} = 0.189$$

$$K_u = (0.189) + (0.199)$$

$$K_u = 0.388$$

38 Watt 100kHz Transformer Design, Using the Core Geometry, K_g, Approach

The following information is the design specification for a 38 watt push-pull transformer, operating at 100kHz, using the K_g core geometry approach. For a typical design example, assume a push-pull, full-wave, center-tapped circuit, as shown in Figure 7-4, with the following specification:

1. Input voltage, $V_{(min)} = 24$ volts
2. Output voltage #1, $V_{(o1)} = 5.0$ volts
3. Output current #1, $I_{(o1)} = 4.0$ amps
4. Output voltage #2, $V_{(o2)} = 12.0$ volts
5. Output current #2, $I_{(o2)} = 1.0$ amps
6. Frequency, $f = 100$kHz
7. Efficiency, $\eta = 98\%$
8. Regulation, $\alpha = 0.5\%$

© 2011 by Taylor and Francis Group, LLC

9. Diode voltage drop, $V_d = 1.0$ volt
10. Operating flux density, $B_{ac} = 0.05$ teslas
11. Core Material = ferrite
12. Window utilization, $K_u = 0.4$
13. Temperature rise goal, $T_r = 30°C$
14. Maximum duty ratio, $D_{max} = 0.5$
15. Notes:

    Using a center-tapped winding, U = 1.41

    Using a single winding, U = 1.0

At this point, select a wire so that the relationship between the ac resistance and the dc resistance is 1:

$$\frac{R_{ac}}{R_{dc}} = 1$$

The skin depth, ε in centimeters, is:

$$\varepsilon = \frac{6.62}{\sqrt{f}}, \quad [\text{cm}]$$

$$\varepsilon = \frac{6.62}{\sqrt{100,000}}, \quad [\text{cm}]$$

$$\varepsilon = 0.0209, \quad [\text{cm}]$$

Then, the wire diameter, D_{AWG}, is:

$$D_{AWG} = 2(\varepsilon), \quad [\text{cm}]$$

$$D_{AWG} = 2(0.0209), \quad [\text{cm}]$$

$$D_{AWG} = 0.0418, \quad [\text{cm}]$$

Then, the bare wire area, A_w, is:

$$A_w = \frac{\pi(D_{AWG})^2}{4}, \quad [\text{cm}^2]$$

$$A_w = \frac{(3.1416)(0.0418)^2}{4}, \quad [\text{cm}^2]$$

$$A_w = 0.00137, \quad [\text{cm}^2]$$

From the Wire Table 4-9, in Chapter 4, Number 27 has a bare wire area of 0.001021 centimeters. This will be the minimum wire size used in this design. If the design requires more wire area to meet the specification,

© 2011 by Taylor and Francis Group, LLC

then the design will use a multifilar of #26. Listed Below are #27 and #28, just in case #26 requires too much rounding off.

Wire AWG	Bare Area	Area Ins.	Bare/Ins.	μΩ/cm
#26	0.001280	0.001603	0.798	1345
#27	0.001021	0.001313	0.778	1687
#28	0.0008046	0.0010515	0.765	2142

Step No. 1: Calculate the transformer output power, P_o.

$$P_o = P_{o1} + P_{o2}, \quad \text{[watts]}$$
$$P_{o1} = I_{o1}(V_{o1} + V_d), \quad \text{[watts]}$$
$$P_{o1} = 4(5+1), \quad \text{[watts]}$$
$$P_{o1} = 24, \quad \text{[watts]}$$
$$P_{o2} = I_{o2}(V_{o2} + V_d), \quad \text{[watts]}$$
$$P_{o2} = 1(12+2), \quad \text{[watts]}$$
$$P_{o2} = 14, \quad \text{[watts]}$$
$$P_o = (24+14), \quad \text{[watts]}$$
$$P_o = 38, \quad \text{[watts]}$$

Step No. 2: Calculate the total secondary apparent power, P_{ts}.

$$P_{ts} = P_{tso1} + P_{tso2}, \quad \text{[watts]}$$
$$P_{tso1} = P_{o1}(U), \quad \text{[watts]}$$
$$P_{tso1} = 24(1.41), \quad \text{[watts]}$$
$$P_{tso1} = 33.8, \quad \text{[watts]}$$
$$P_{tso2} = P_{o2}(U), \quad \text{[watts]}$$
$$P_{tso2} = 14(1), \quad \text{[watts]}$$
$$P_{tso2} = 14, \quad \text{[watts]}$$
$$P_{ts} = (33.8+14), \quad \text{[watts]}$$
$$P_{ts} = 47.8, \quad \text{[watts]}$$

© 2011 by Taylor and Francis Group, LLC

Step No. 3: Calculate the total apparent power, P_t.

$$P_{in} = \left(\frac{P_o}{\eta}\right), \quad \text{[watts]}$$

$$P_{tp} = P_{in}P_a, \quad \text{[watts]}$$

$$P_t = P_{tp} + P_{ts}, \quad \text{[watts]}$$

$$P_t = \left(\frac{38}{0.98}\right)(1.41) + 47.8, \quad \text{[watts]}$$

$$P_t = 102.5, \quad \text{[watts]}$$

Step No. 4: Calculate the electrical conditions, K_e.

$$K_e = 0.145\left(K_f\right)^2\left(f\right)^2\left(B_m\right)^2\left(10^{-4}\right)$$

$$K_f = 4.0, \quad \text{[square wave]}$$

$$K_e = 0.145(4.0)^2(100000)^2(0.05)^2\left(10^{-4}\right)$$

$$K_e = 5800$$

Step No. 5: Calculate the core geometry, K_g.

$$K_g = \frac{P_t}{2K_e\alpha}, \quad [\text{cm}^5]$$

$$K_g = \frac{(102.5)}{2(5800)0.5}, \quad [\text{cm}^5]$$

$$K_g = 0.0177, \quad [\text{cm}^5]$$

When operating at high frequencies, the engineer has to review the window utilization factor, K_u, in Chapter 4. When using small bobbin ferrites, use the ratio of the bobbin winding area to the core window area which is only about 0.6. Operating at 100kHz and having to use a #26 wire, because of the skin effect, the ratio of the bare copper area to the total area is 0.78. Therefore, the overall window utilization, K_u, is reduced. To return the design back to the norm, the core geometry, K_g, is to be multiplied by 1.35, and then, the current density, J, is calculated, using a window utilization factor of 0.29.

$$K_g = 0.0177(1.35), \quad [\text{cm}^5]$$

$$K_g = 0.0239, \quad [\text{cm}^5]$$

© 2011 by Taylor and Francis Group, LLC

Step No. 6: Select a PQ core from Chapter 3, comparable in core geometry K_g.

Core number = PQ-2020

Manufacturer = TDK

Magnetic material, 2000 um = PC44

Magnetic path length, MPL = 4.5 cm

Window height, G = 1.43 cm

Core weight, W_{tfe} = 15 grams

Copper weight, W_{tcu} = 10.4 grams

Mean length turn, MLT = 4.4 cm

Iron area, A_c = 0.62 cm^2

Window area, W_a = 0.658 cm^2

Area product, A_p = 0.408 cm^4

Core geometry, K_g = 0.0227 cm^5

Surface area, A_t = 19.7 cm^2

Millihenrys per 1000 turns, AL = 3150

Step No. 7: Calculate the number of primary turns, N_p, using Faraday's Law.

$$N_p = \frac{V_p\left(10^4\right)}{K_f B_{ac} f A_c}, \quad \text{[turns]}$$

$$N_p = \frac{(24)\left(10^4\right)}{(4.0)(0.05)(100000)(0.62)}, \quad \text{[turns]}$$

$$N_p = 19, \quad \text{[turns]}$$

Step No. 8: Calculate the current density, J, using a window utilization, K_u = 0.29.

$$J = \frac{P_t\left(10^4\right)}{K_f K_u B_{ac} f A_p}, \quad \text{[amps/cm}^2\text{]}$$

$$J = \frac{102.5\left(10^4\right)}{(4.0)(0.29)(0.05)(100000)(0.408)}, \quad \text{[amps/cm}^2\text{]}$$

$$J = 433, \quad \text{[amps/cm}^2\text{]}$$

Step No. 9: Calculate the input current, I_{in}.

$$I_{in} = \frac{P_o}{V_{in}\eta}, \quad \text{[amps]}$$

$$I_{in} = \frac{38}{(24)(0.98)}, \quad \text{[amps]}$$

$$I_{in} = 1.61, \quad \text{[amps]}$$

© 2011 by Taylor and Francis Group, LLC

Step No. 10: Calculate the primary bare wire area, $A_{wp(B)}$.

$$A_{wp(B)} = \frac{I_{in}\sqrt{D_{\max}}}{J}, \quad [\text{cm}^2]$$

$$A_{wp(B)} = \frac{(1.61)(0.707)}{433}, \quad [\text{cm}^2]$$

$$A_{wp(B)} = 0.00263, \quad [\text{cm}^2]$$

Step No. 11: Calculate the required number of primary strands, S_{np}.

$$S_{np} = \frac{A_{wp(B)}}{\#26}$$

$$S_{np} = \frac{0.00263}{0.00128}$$

$$S_{np} = 2.05 \text{ use } 2$$

Step No. 12: Calculate the primary new μΩ per centimeter.

$$(\text{new})\mu\Omega/\text{cm} = \frac{\mu\Omega/\text{cm}}{S_{np}}$$

$$(\text{new})\mu\Omega/\text{cm} = \frac{1345}{2}$$

$$(\text{new})\mu\Omega/\text{cm} = 673$$

Step No. 13: Calculate the primary resistance, R_p.

$$R_p = \text{MLT}(N_p)\left(\frac{\mu\Omega}{\text{cm}}\right)(10^{-6}), \quad [\text{ohms}]$$

$$R_p = (4.4)(19)(673)(10^{-6}), \quad [\text{ohms}]$$

$$R_p = 0.0563, \quad [\text{ohms}]$$

Step No. 14: Calculate the primary copper loss, P_p.

$$P_p = I_p^2 R_p, \quad [\text{watts}]$$

$$P_p = (1.61)^2(0.0563), \quad [\text{watts}]$$

$$P_p = 0.146, \quad [\text{watts}]$$

© 2011 by Taylor and Francis Group, LLC

Step No. 15: Calculate the secondary turns, N_{s1}.

$$N_{s1} = \frac{N_p V_{s1}}{V_{in}}\left(1 + \frac{\alpha}{100}\right), \quad [\text{turns}]$$

$$V_{s1} = V_o + V_d, \quad [\text{volts}]$$

$$V_{s1} = 5 + 1, \quad [\text{volts}]$$

$$V_{s1} = 6, \quad [\text{volts}]$$

$$N_{s1} = \frac{(19)(6)}{(24)}\left(1 + \frac{0.5}{100}\right), \quad [\text{turns}]$$

$$N_{s1} = 4.77 \text{ use } 5, \quad [\text{turns}]$$

Step No. 16: Calculate the secondary turns, N_{s2}.

$$N_{s2} = \frac{N_p V_{s1}}{V_{in}}\left(1 + \frac{\alpha}{100}\right), \quad [\text{turns}]$$

$$V_{s2} = V_o + 2V_d, \quad [\text{volts}]$$

$$V_{s2} = 12 + 2, \quad [\text{volts}]$$

$$V_{s2} = 14, \quad [\text{volts}]$$

$$N_{s2} = \frac{(19)(14)}{(24)}\left(1 + \frac{0.5}{100}\right), \quad [\text{turns}]$$

$$N_{s2} = 11.1 \text{ use } 11, \quad [\text{turns}]$$

Step No. 17: Calculate the secondary bare wire area, A_{ws1}.

$$A_{ws1} = \frac{I_o\sqrt{D_{\max}}}{J}, \quad [\text{cm}^2]$$

$$A_{ws1} = \frac{(4)(0.707)}{433}, \quad [\text{cm}^2]$$

$$A_{ws1} = 0.00653, \quad [\text{cm}^2]$$

Step No. 18: Calculate the required number of secondary strands, S_{ns1}.

$$S_{ns1} = \frac{A_{ws1(B)}}{\#26}$$

$$S_{ns1} = \frac{0.00653}{0.00128}$$

$$S_{ns1} = 5.1 \text{ use } 5$$

© 2011 by Taylor and Francis Group, LLC

Step No. 19: Calculate the secondary, S_1 new μΩ per centimeter.

$$(\text{new})\mu\Omega/\text{cm} = \frac{\mu\Omega/\text{cm}}{S_{ns1}}$$

$$(\text{new})\mu\Omega/\text{cm} = \frac{1345}{5}$$

$$(\text{new})\mu\Omega/\text{cm} = 269$$

Step No. 20: Calculate the secondary S_1 resistance, R_{s1}.

$$R_{s1} = \text{MLT}(N_{s1})\left(\frac{\mu\Omega}{\text{cm}}\right)\left(10^{-6}\right), \quad [\text{ohms}]$$

$$R_{s1} = (4.4)(5)(269)\left(10^{-6}\right), \quad [\text{ohms}]$$

$$R_{s1} = 0.0059, \quad [\text{ohms}]$$

Step No. 21: Calculate the secondary copper loss, P_{s1}.

$$P_{s1} = I_{s1}^2 R_{s1}, \quad [\text{watts}]$$

$$P_{s1} = (4.0)^2(0.0059), \quad [\text{watts}]$$

$$P_{s1} = 0.0944, \quad [\text{watts}]$$

Step No. 22: Calculate the secondary bare wire area, A_{ws2}.

$$A_{ws2} = \frac{I_o}{J}, \quad [\text{cm}^2]$$

$$A_{ws2} = \frac{(1)}{433}, \quad [\text{cm}^2]$$

$$A_{ws2} = 0.00231, \quad [\text{cm}^2]$$

Step No. 23: Calculate the required number of secondary strands, S_{ns2}.

$$S_{ns2} = \frac{A_{ws2(B)}}{\#26}$$

$$S_{ns2} = \frac{0.00231}{0.00128}$$

$$S_{ns2} = 1.8 \text{ use } 2$$

© 2011 by Taylor and Francis Group, LLC

Step No. 24: Calculate the secondary, S_2 new μΩ per centimeter.

$$(\text{new})\mu\Omega/\text{cm} = \frac{\mu\Omega/\text{cm}}{S_{ns2}}$$

$$(\text{new})\mu\Omega/\text{cm} = \frac{1345}{2}$$

$$(\text{new})\mu\Omega/\text{cm} = 673$$

Step No. 25: Calculate the secondary, S_2 resistance, R_{s2}.

$$R_{s2} = \text{MLT}(N_{s1})\left(\frac{\mu\Omega}{\text{cm}}\right)\left(10^{-6}\right), \quad [\text{ohms}]$$

$$R_{s2} = (4.4)(11)(673)\left(10^{-6}\right), \quad [\text{ohms}]$$

$$R_{s2} = 0.0326, \quad [\text{ohms}]$$

Step No. 26: Calculate the secondary, S_2 copper loss, P_{s2}.

$$P_{s2} = I_{s2}^2 R_{s2}, \quad [\text{watts}]$$

$$P_{s2} = (1.0)^2(0.0326), \quad [\text{watts}]$$

$$P_{s2} = 0.0326, \quad [\text{watts}]$$

Step No. 27: Calculate the total secondary copper loss, P_s.

$$P_s = P_{s1} + P_{s2}, \quad [\text{watts}]$$

$$P_s = 0.0944 + 0.0326, \quad [\text{watts}]$$

$$P_s = 0.127, \quad [\text{watts}]$$

Step No. 28: Calculate the total primary and secondary copper loss, P_{cu}.

$$P_{cu} = P_p + P_s, \quad [\text{watts}]$$

$$P_{cu} = 0.146 + 0.127, \quad [\text{watts}]$$

$$P_{cu} = 0.273, \quad [\text{watts}]$$

Step No. 29: Calculate the transformer regulation, α.

$$\alpha = \frac{P_{cu}}{P_o}(100), \quad [\%]$$

$$\alpha = \frac{(0.273)}{(38)}(100), \quad [\%]$$

$$\alpha = 0.718, \quad [\%]$$

© 2011 by Taylor and Francis Group, LLC

Step No. 30: Calculate the milliwatts per gram, mW/g. Use the Equation for this material in Chapter 2.

$$mW/g = 0.000318\left(f\right)^{1.51}\left(B_{ac}\right)^{2.747}$$
$$mW/g = 0.000318\left(100000\right)^{1.51}\left(0.05\right)^{2.747}$$
$$mW/g = 3.01$$

Step No. 31: Calculate the core loss, P_{fe}.

$$P_{fe} = \left(mW/g\right)\left(W_{tfe}\right)\left(10^{-3}\right), \quad \text{[watts]}$$
$$P_{fe} = \left(3.01\right)\left(15\right)\left(10^{-3}\right), \quad \text{[watts]}$$
$$P_{fe} = 0.045, \quad \text{[watts]}$$

Step No. 32: Calculate the total loss, P_{Σ}.

$$P_{\Sigma} = P_{cu} + P_{fe}, \quad \text{[watts]}$$
$$P_{\Sigma} = \left(0.273\right) + \left(0.045\right), \quad \text{[watts]}$$
$$P_{\Sigma} = 0.318, \quad \text{[watts]}$$

Step No. 33: Calculate the watts per unit area, ψ.

$$\psi = \frac{P_{\Sigma}}{A_t}, \quad \text{[watts/cm}^2\text{]}$$
$$\psi = \frac{\left(0.318\right)}{\left(19.7\right)}, \quad \text{[watts/cm}^2\text{]}$$
$$\psi = 0.0161, \quad \text{[watts/cm}^2\text{]}$$

Step No. 34: Calculate the temperature rise, T_r.

$$T_r = 450\left(\psi\right)^{(0.826)}, \quad [°\text{C}]$$
$$T_r = 450\left(0.0161\right)^{(0.826)}, \quad [°\text{C}]$$
$$T_r = 14.9, \quad [°\text{C}]$$

© 2011 by Taylor and Francis Group, LLC

Step No. 35: Calculate the total window utilization, K_u.

$$K_u = K_{up} + K_{us}$$

$$K_{us} = K_{us1} + K_{us2}$$

$$K_{us1} = \frac{N_{s1} S_{n1} A_{ws1(B)}}{W_a}$$

$$K_{us1} = \frac{(10)(5)(0.00128)}{(0.658)} = 0.0973$$

$$K_{us2} = \frac{(11)(2)(0.00128)}{(0.658)} = 0.0428$$

$$K_{up} = \frac{N_p S_{np} A_{wp(B)}}{W_a}$$

$$K_{up} = \frac{(38)(2)(0.00128)}{(0.658)} = 0.148$$

$$K_u = (0.148) + (0.0973 + 0.0428)$$

$$K_u = 0.288$$

© 2011 by Taylor and Francis Group, LLC

Chapter 8

DC Inductor Design, Using Gapped Cores

© 2011 by Taylor and Francis Group, LLC

Table of Contents

1. Introduction....8-3
2. Critical Inductance for Sine Wave Rectification....8-3
3. Critical Inductance for Buck Type Converters....8-5
4. Core Materials, Used in PWM Converters....8-8
5. Fundamental Considerations....8-9
6. Fringing Flux....8-11
7. Inductors....8-12
8. Relationship of, A_p, to Inductor's Energy-Handling Capability....8-13
9. Relationship of, K_g, to Inductor's Energy-Handling Capability....8-14
10. Gapped Inductor Design Example Using the Core Geometry, K_g, Approach....8-15
11. Gapped Inductor Design Example Using the Area Product, A_p, Approach....8-21

© 2011 by Taylor and Francis Group, LLC

Introduction

Designers have used various approaches in arriving at suitable inductor designs. For example, in many cases, a rule of thumb used for dealing with current density is that a good working level is 200 amps-per-cm^2 (1000 Cir-Mils-per-amp). This rule is satisfactory in many instances. However, the wire size used to meet this requirement may produce a heavier and bulkier inductor than desired or required. The information presented, herein, will make it possible to avoid the use of this rule and other rules of thumb, and will help to develop an economical and a better design.

Critical Inductance for Sine Wave Rectification

The LC filter is the basic method of reducing ripple levels. The two basic rectifier circuits are the full-wave center-tap, as shown in Figure 8-1, and the full-wave bridge, as shown in Figure 8-2. To achieve normal inductor operation, it is necessary that there be a continuous flow of current through the input inductor, L1.

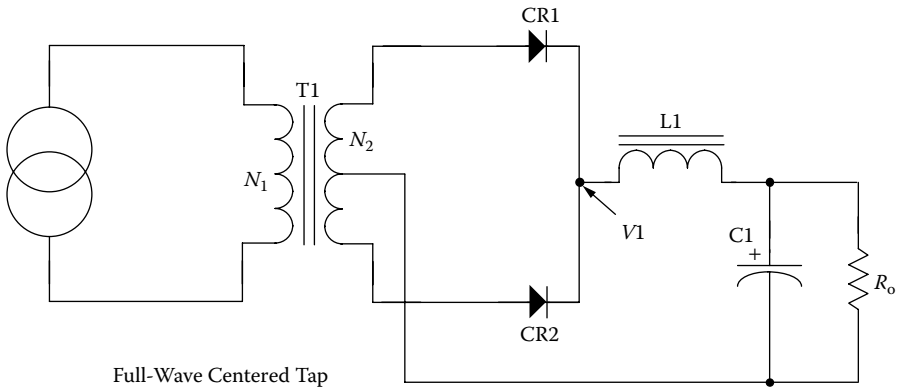

Figure 8-1. Full-Wave Center Tap with an LC filter.

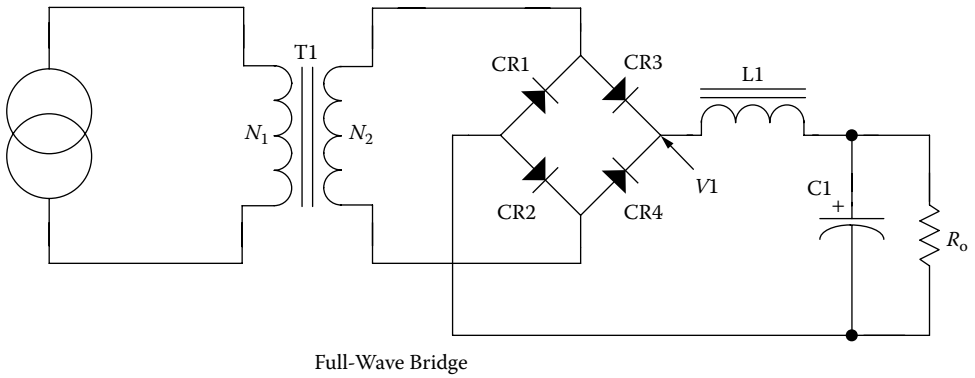

Figure 8-2. Full-Wave Bridge with an LC filter.

© 2011 by Taylor and Francis Group, LLC

The value for minimum inductance called critical inductance, $L_{(crt)}$ is:

$$L_{(crt)} = \frac{R_{o(\max)}}{3\omega}, \quad \text{[henrys]} \qquad \text{[8-1]}$$

Where:

$\omega = 2\pi f$

$f =$ line frequency

The higher the load resistance, R_o, (i.e., the lower the dc load current), the more difficult it is to maintain a continuous flow of current. The filter inductor operates in the following manner: When, R_o, approaches infinity, under an unloaded condition, (no bleeder resistor), $I_o = 0$, the filter capacitor will charge to, $V1_{pk}$, the peak voltage. Therefore, the output voltage will be equal to the peak value of the input voltage, as shown in Figure 8-3.

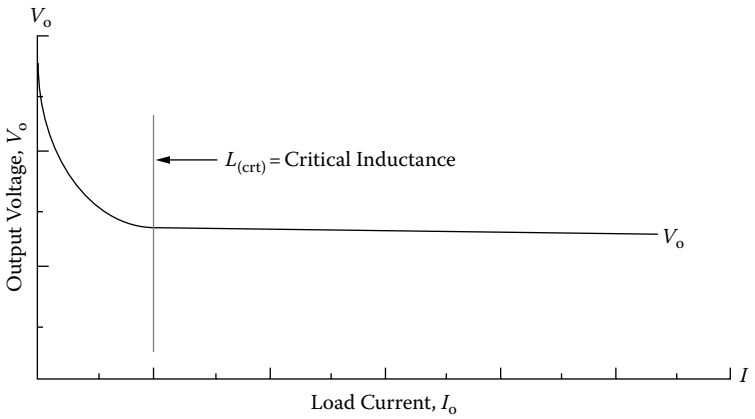

Figure 8-3. Critical Inductance Point.

The ripple reduction from a single stage LC filter can be calculated, using Equation [8-2] and Figure 8-4.

$$V_{r(pk)} = V_{in(pk)}\left(\frac{1}{(2\pi f)^2 L1C1}\right), \quad \text{[volts-peak]} \qquad \text{[8-2]}$$

Where:

L = henrys

C = micro-farads

© 2011 by Taylor and Francis Group, LLC

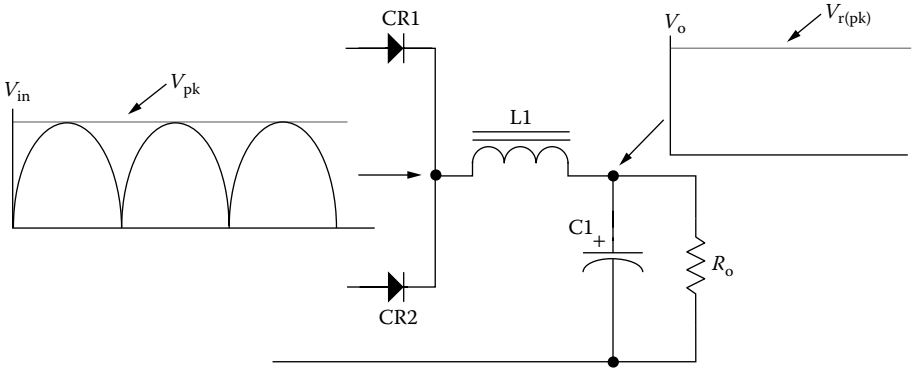

Figure 8-4. LC Filter Ripple Reduction.

Critical Inductance for Buck Type Converters

The buck type converter schematic is shown in Figure 8-5, and the buck type dc-to-dc converter is shown in Figure 8.6. The buck regulator filter circuit shown in Figure 8-5 has three current probes. These current probes monitor the three basic currents in a switch mode, buck output filter. Current probe A monitors the power

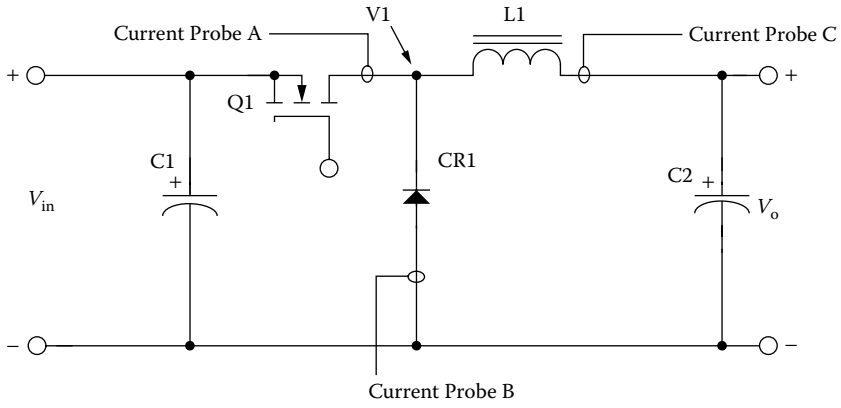

Figure 8-5. Buck Regulator Converter.

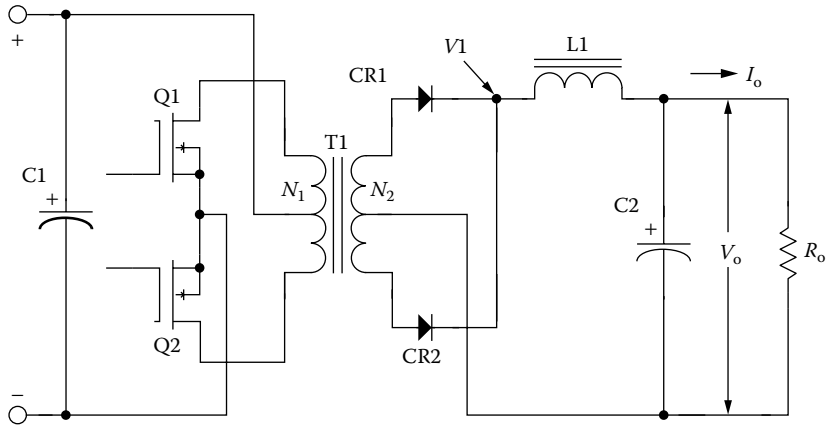

Figure 8-6. Push-Pull Buck Type Converter.

© 2011 by Taylor and Francis Group, LLC

MOSFET, Q1, switching current. Current probe B monitors the commutating current through CR1. Current probe C monitors the current through the output inductor, L1.

The typical filter waveforms of the buck converter are shown in Figure 8-7. The waveforms are shown with the converter operating at a 0.5 duty ratio. The applied voltage, V1, to the filter, is shown in Figure 8-7A. The power MOSFET, Q1, current is shown in Figure 8-7B. The commutating current flowing through CR1 is shown in Figure 8-7C. The commutating current is the result of, Q1, being turned off, and the field in L1 collapsing, producing the commutating current. The current flowing through, L1, is shown in Figure 8-7D. The current flowing through, L1, is the sum of the currents in Figure 8-7B and 8-7C.

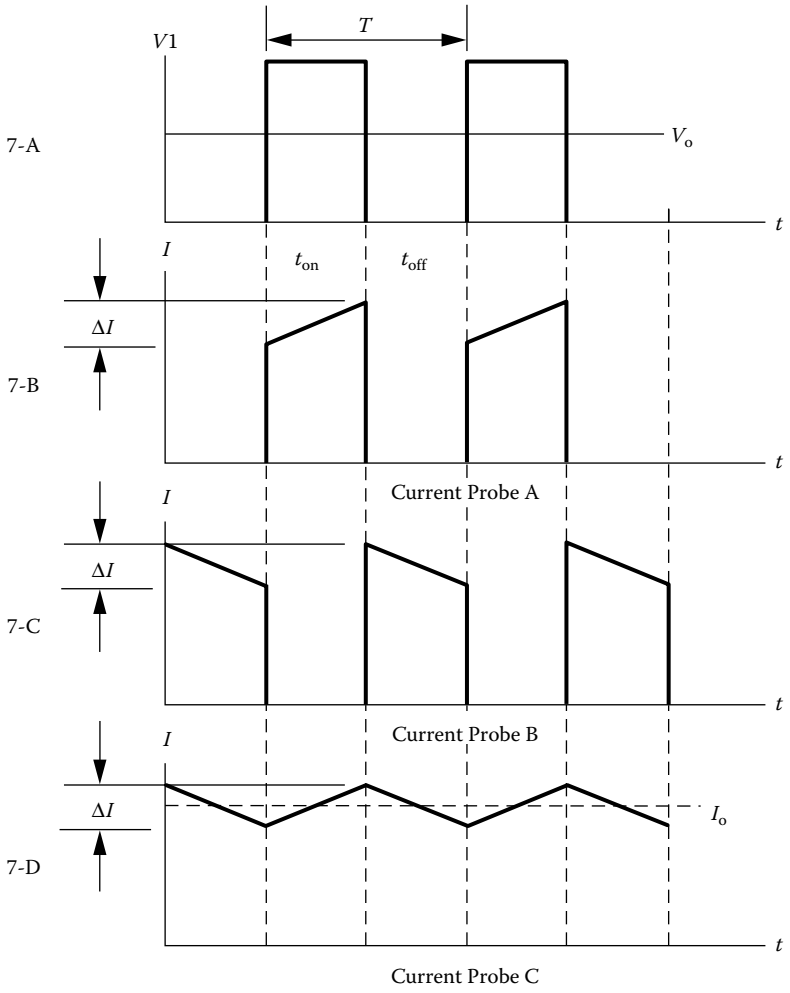

Figure 8-7. Typical Buck Converter Waveforms, Operating at a 0.5 Duty Ratio.

The critical inductance current is shown in Figure 8-8, 8-B and is realized in Equation 8-3. The critical inductance current is when the ratio of the delta current to the output load current is equal to $2 = \Delta I / I_o$. If the output load current is allowed to go beyond this point, the current will become discontinuous, as shown in Figure 8-8,

© 2011 by Taylor and Francis Group, LLC

8-D. The applied voltage, V1, will have ringing at the level of the output voltage, as shown in Figure 8-8, 8-C. When the current in the output inductor becomes discontinuous, as shown in Figure 8-8, 8-D, the response time for a step load becomes very poor.

$$L_{(critical)} = \frac{V_o T\left(1 - D_{(\min)}\right)}{2I_{o(\min)}}, \quad \text{[henrys]} \qquad [8\text{-}3]$$

$$D_{(\min)} = \frac{V_o}{\left(\eta V_{in(\max)}\right)} \qquad [8\text{-}4]$$

When designing multiple output converters similar to Figure 8-6, the slaved outputs should never have the current in the inductor go discontinuous or to zero. If the current goes to zero, a slaved output voltage will rise to the value of, V1. If the current is allowed to go to zero, then, there is no potential difference between the input and output voltage of the filter. Then the output voltage will rise to equal the peak input voltage.

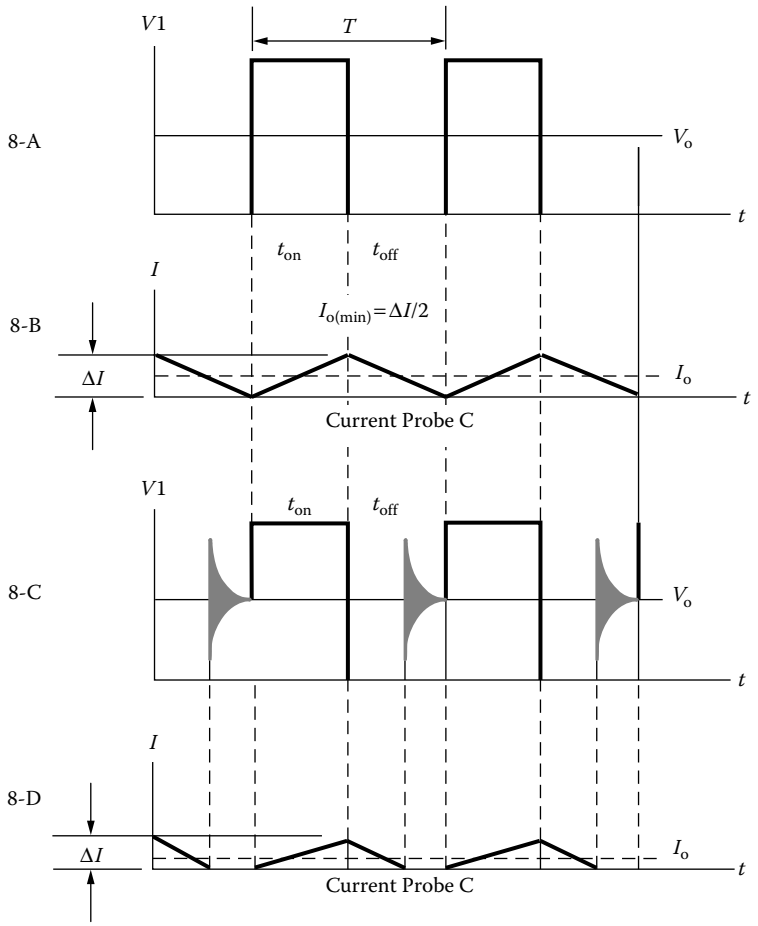

Figure 8-8. Buck Converter, Output Filter Inductor Goes from Critical to Discontinuous Operation.

© 2011 by Taylor and Francis Group, LLC

Core Materials, Used in PWM Converters

Designers have routinely tended to specify Molypermalloy powder materials for filter inductors used in high-frequency, power converters and pulse-width-modulators (PWM) switched regulators, because of the availability of manufacturers' literature containing tables, graphs, and examples that simplify the design task. Use of these cores may result in an inductor design, not optimized for size and weight. For example, as shown in Figure 8-9, Molypermalloy powder cores, operating with a dc bias of 0.3T, have only about 80% of the original inductance, with very rapid falloff at higher flux densities. When size is of greatest concern then, magnetic materials with high flux saturation, B_s, would be the first choice. Materials, such as silicon or some amorphous materials, have approximately four times the useful flux density compared to Molypermalloy powder cores. Iron alloys retain 90% of their original inductance, at greater than 1.2T. Iron alloys when designed correctly and used in the right application, will perform well at frequencies up to 100kHz. When operating above 100kHz, then the only material is a ferrite. Ferrite materials have a negative temperature coefficient regarding flux density. The operating temperature and temperature rise should be used to calculate the maximum flux density.

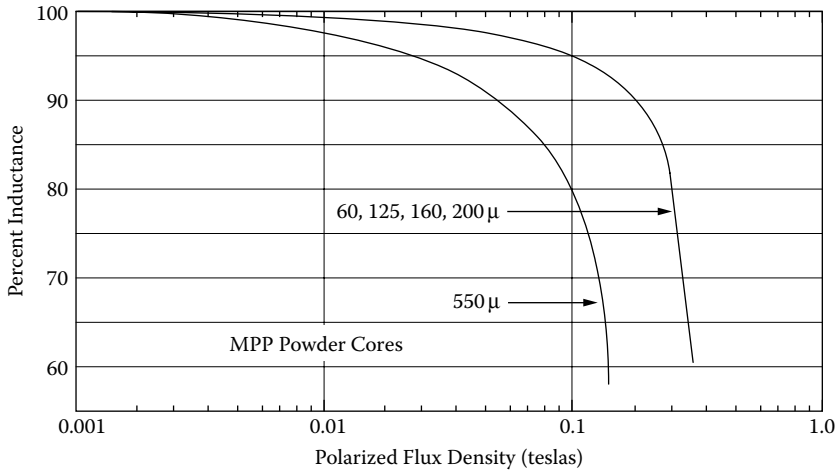

Figure 8-9. Inductance Versus dc Bias.

To get optimum performance, together with size, the engineer must evaluate the materials for both, B_s, and, B_{ac}. See Table 8-1. The operating dc flux has only to do with I^2R losses, (copper). The ac flux, B_{ac}, has to do with core loss. This loss depends directly on the material. There are many factors that impact a design: cost, size, temperature rise and material availability.

There are significant advantages to be gained by the use of iron alloys and ferrites in the design of power inductors, despite certain disadvantages, such as the need for banding and gapping materials, banding tools, mounting brackets, and winding mandrels.

© 2011 by Taylor and Francis Group, LLC

Table 8-1. Magnetic Material Properties

Magnetic Material Properties					
Material Name	Composition	Initial Permeability μ_i	Flux Density Teslas B_s	Curie Temp. °C	Density grams/cm^3 δ
Silicon	3-97 SiFe	1500	1.5-1.8	750	7.63
Orthonol	50-50 NiFe	2000	1.42-1.58	500	8.24
Permalloy	80-20 NiFe	25000	0.66-0.82	460	8.73
Amorphous	81-3.5 FeSi	1500	1.5-1.6	370	7.32
Amorphous	66-4 CoFe	800	0.57	250	7.59
Amorphous(μ)	73-15 FeSi	30000	1.0-1.2	460	7.73
Ferrite	MnZn	2500	0.5	>230	4.8

Iron alloys and ferrites provide greater flexibility in the design of high frequency power inductors, because the air gap can be adjusted to any desired length, and because the relative permeability is high, even at high, dc flux density.

Fundamental Considerations

The design of a linear reactor depends upon four related factors:

1. Desired inductance, L
2. Direct current, I_{dc}
3. Alternating current, ΔI
4. Power loss and temperature, T_r

With these requirements established, the designer must determine the maximum values for, B_{dc}, and, B_{ac}, that will not produce magnetic saturation. The designer must make trade-offs that will yield the highest inductance for a given volume. It should be remembered the peak operating flux, B_{pk}, depends upon, $B_{dc} + B_{ac}$, in the manner in Figure 8-10.

$$B_{pk} = B_{dc} + \frac{B_{ac}}{2}, \quad \text{[teslas]} \qquad [8\text{-}5]$$

$$B_{dc} = \frac{0.4\pi N I_{dc}\left(10^{-4}\right)}{l_g + \left(\frac{\text{MPL}}{\mu_m}\right)}, \quad \text{[teslas]} \qquad [8\text{-}6]$$

© 2011 by Taylor and Francis Group, LLC

$$B_{ac} = \frac{0.4\pi N\left(\frac{\Delta I}{2}\right)\left(10^{-4}\right)}{l_g + \left(\frac{\text{MPL}}{\mu_m}\right)}, \quad \text{[teslas]} \qquad [8\text{-}7]$$

$$B_{pk} = \frac{0.4\pi N\left(I_{dc} + \frac{\Delta I}{2}\right)\left(10^{-4}\right)}{l_g + \left(\frac{\text{MPL}}{\mu_m}\right)}, \quad \text{[teslas]} \qquad [8\text{-}8]$$

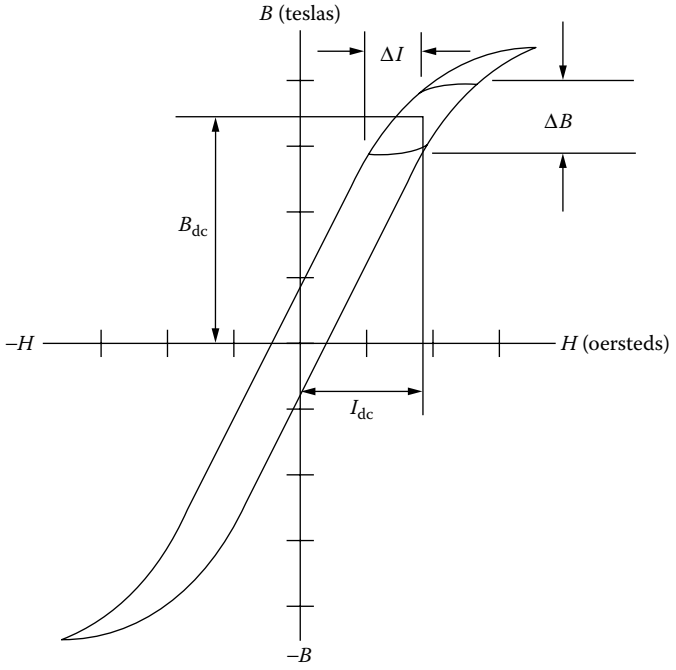

Figure 8-10. Inductor Flux Density Versus $I_{dc} + \Delta I$ Current.

The inductance of an iron-core inductor carrying direct current and having an air gap may be expressed as:

$$L = \frac{0.4\pi N^2 A_c\left(10^{-8}\right)}{l_g + \left(\frac{\text{MPL}}{\mu_m}\right)}, \quad \text{[henrys]} \qquad [8\text{-}9]$$

This equation shows that inductance is dependent on the effective length of the magnetic path, which is the sum of the air gap length, l_g, and the ratio of the core mean length to the material permeability, MPL/μ_m. When the core air gap, l_g, is large compared to the ratio, MPL/μ_m, because of material permeability, μ_m, variations in,

© 2011 by Taylor and Francis Group, LLC

μ_m, do not substantially affect the total effective Magnetic Path Length or the inductance. Then the inductance Equation [8-9] reduces to:

$$L = \frac{0.4\pi N^2 A_c\left(10^{-8}\right)}{l_g}, \quad \text{[henrys]} \qquad \text{[8-10]}$$

Final determination of the air gap size requires consideration of the effect of fringing flux, which is a function of gap dimension, the shape of the pole faces, and the shape, size, and location of the winding. Its net effect is to shorten the air gap. Because of the fringing flux it is wise to lower the initial operating flux density, 10 to 20%.

Fringing Flux

Fringing flux decreases the total reluctance of the magnetic path and therefore, increases the inductance by a factor, F, to a value greater than that calculated from Equation [8-10]. Fringing flux is a larger percentage of the total for the larger gaps.

The fringing factor is:

$$F = 1 + \frac{l_g}{\sqrt{A_c}} \ln\left(\frac{2G}{l_g}\right) \qquad \text{[8-11]}$$

Where G is the winding length, defined in Chapter 3. This equation is valid for laminations, C cores and cut ferrites. Equation [8-11] is plotted in Figure 8-11.

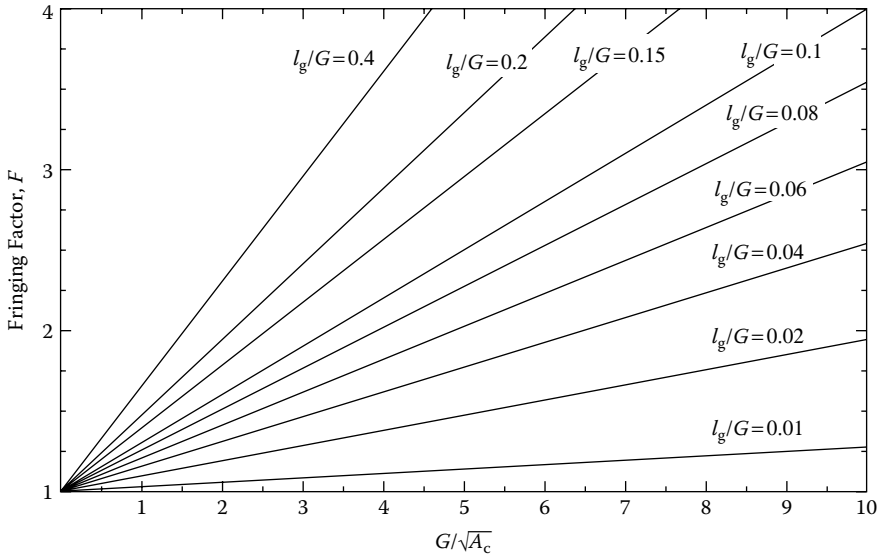

Figure 8-11. Increase of Inductance with Fringing Flux at the Gap.

© 2011 by Taylor and Francis Group, LLC

As the air gap increases, the flux across the gap fringes more and more. Some of the fringing flux strikes the core, perpendicular to the strip or tape, and sets up eddy currents, which cause additional losses in the core. If the gap dimension gets too large, the fringing flux will strike the copper winding and produce eddy currents, generating heat, just like an induction heater. The fringing flux will jump the gap and produce eddy currents, in both the core and winding, as shown in Figure 8-12.

The inductance, L, computed in Equation [8-10], does not include the effect of the fringing flux. The value of inductance, L´, corrected for fringing flux is:

$$L' = \frac{0.4\pi N^2 F A_c \left(10^{-8}\right)}{l_g}, \quad \text{[henrys]} \qquad [8\text{-}12]$$

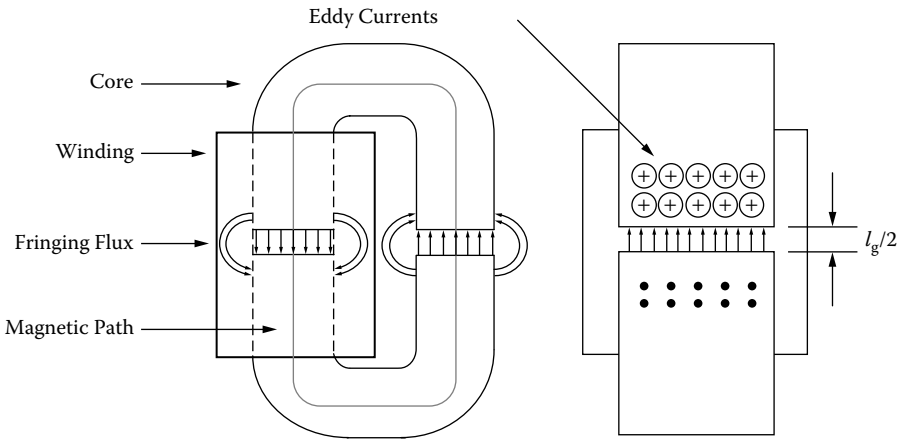

Figure 8-12. Fringing Flux Around the Gap of an Inductor.

The effect permeability may be calculated from the following Equation:

$$\mu_e = \frac{\mu_m}{1 + \left(\frac{l_g}{\text{MPL}}\right)\mu_m} \qquad [8\text{-}13]$$

Where, μ_m, is the material permeability.

Inductors

Inductors that carry direct current are used frequently in a wide variety of ground, air, and space applications. Selection of the best magnetic core for an inductor frequently involves a trial-and-error type of calculation.

© 2011 by Taylor and Francis Group, LLC

The author has developed a simplified method of designing optimum, dc carrying inductors with gapped cores. This method allows the engineer to select the proper core that will provide correct copper loss, and make allowances for fringing flux, without relying on trial-and-error and the use of the cumbersome Hanna's curves.

Rather than discuss the various methods used by transformer designers, the author believes it is more useful to consider typical design problems, and to work out solutions using the approach based upon newly formulated relationships. Two gapped core designs will be compared. To compare their merits, the first design example will use the core geometry, K_g, and the second design will use the area product, A_p.

Inductors, designed in this handbook, are banded together with phosphor bronze banding material, or held together with aluminum brackets. The use of steel banding material, or brackets that bridge the gap are not recommended, because the use of steel across the gap is called shorting the gap. When the gap is shorted, the inductance will increase from the calculated value.

Relationship of, A_p, to Inductor's Energy-Handling Capability

The energy-handling capability of a core is related to its area product, A_p, by the Equation:

$$A_p = \frac{2(\text{Energy})(10^4)}{B_m J K_u}, \quad [\text{cm}^4] \qquad [8\text{-}14]$$

Where: Energy is in watt-seconds.

B_m is the flux density, teslas.

J is the current density, amps-per-cm^2.

K_u is the window utilization factor. (See Chapter 4)

From the above, it can be seen that factors, such as flux density, B_m, window utilization factor, K_u, (which defines the maximum space that may be used by the copper in the window), and the current density, J, which controls the copper loss, all impact the area product, A_p. The energy-handling capability of a core is derived from:

$$\text{Energy} = \frac{LI^2}{2}, \quad [\text{watt-seconds}] \qquad [8\text{-}15]$$

© 2011 by Taylor and Francis Group, LLC

Relationship of, K_g, to Inductor's Energy-Handling Capability

Inductors, like transformers, are designed for a given temperature rise. They can also be designed for a given regulation. The regulation and energy handling ability of a core is related to two constants:

$$\alpha = \frac{(\text{Energy})^2}{K_g K_e}, \quad [\%] \tag{8-16}$$

Where, α, is the regulation, %:
The constant, K_g, is determined by the core geometry:

$$K_g = \frac{W_a A_c^2 K_u}{\text{MLT}}, \quad [\text{cm}^5] \tag{8-17}$$

The constant, K_e, is determined by the magnetic and electrical operating conditions:

$$K_e = 0.145 P_o B_{pk}^2 \left(10^{-4}\right) \tag{8-18}$$

The peak operating flux density, B_{pk}, is:

$$B_{pk} = B_{dc} + \frac{B_{ac}}{2}, \quad [\text{teslas}] \tag{8-19}$$

From the above, it can be seen that the flux density, B_{pk}, is the predominant factor governing size.

The output power, P_o, is defined in Figure 8-13.

$$P_{o(L1)} = V_{(01)} I_{(01)} \quad P_{o(L2)} = V_{(02)} I_{(02)} \tag{8-20}$$

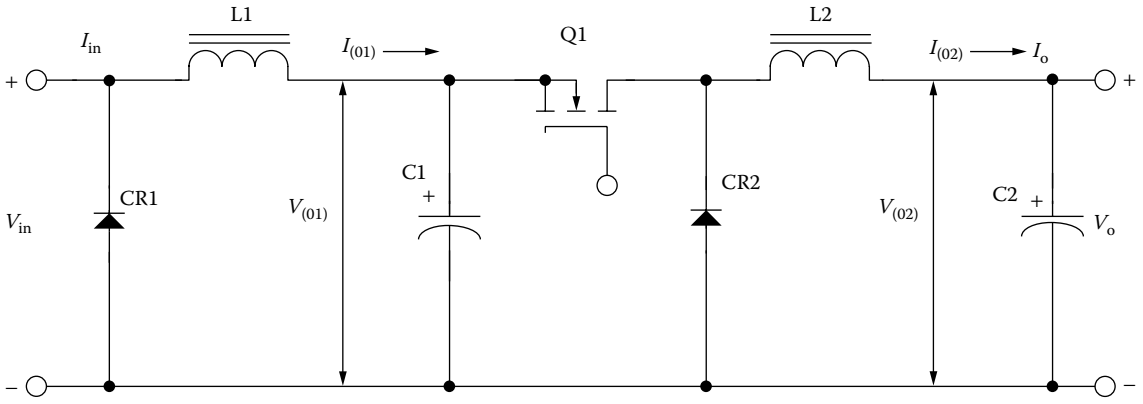

Figure 8-13. Defining the Inductor Output Power.

© 2011 by Taylor and Francis Group, LLC

Gapped Inductor Design Example Using the Core Geometry, K_g, Approach

Step No. 1: Design a linear dc inductor with the following specifications:

1. Inductance, L = 0.0025 henrys
2. dc current, I_o = 1.5 amps
3. ac current, ΔI = 0.2 amps
4. Output power, P_o = 100 watts
5. Regulation, α = 1.0 %
6. Ripple Frequency = 200kHz
7. Operating flux density, B_m = 0.22 tesla
8. Core Material = ferrite
9. Window utilization, K_u = 0.4
10. Temperature rise goal, T_r = 25°C

Step No. 2: Calculate the peak current, I_{pk}.

$$I_{pk} = I_o + \frac{\Delta I}{2}, \quad \text{[amps]}$$

$$I_{pk} = (1.5) + \frac{(0.2)}{2}, \quad \text{[amps]}$$

$$I_{pk} = 1.6, \quad \text{[amps]}$$

Step No. 3: Calculate the energy-handling capability.

$$\text{Energy} = \frac{LI_{pk}^2}{2}, \quad \text{[watt-seconds]}$$

$$\text{Energy} = \frac{(0.0025)(1.6)^2}{2}, \quad \text{[watt-seconds]}$$

$$\text{Energy} = 0.0032, \quad \text{[watt-seconds]}$$

Step No. 4: Calculate the electrical conditions coefficient, K_e.

$$K_e = 0.145 P_o B_m^2 \left(10^{-4}\right)$$

$$K_e = 0.145(100)(0.22)^2 \left(10^{-4}\right)$$

$$K_e = 0.0000702$$

© 2011 by Taylor and Francis Group, LLC

Step No. 5: Calculate the core geometry coefficient, K_g.

$$K_g = \frac{(\text{Energy})^2}{K_e \alpha}, \quad [\text{cm}^5]$$

$$K_g = \frac{(0.0032)^2}{(0.0000702)(1.0)}, \quad [\text{cm}^5]$$

$$K_g = 0.146, \quad [\text{cm}^5]$$

Step No. 6: Select an ETD ferrite core from Chapter 3. The data listed is the closest core to the calculated core geometry, K_g.

1. Core Number = ETD-39
2. Magnetic Path Length, MPL = 9.22 cm
3. Core Weight, W_{tfe} = 60 grams
4. Mean Length Turn, MLT = 8.3 cm
5. Iron Area, A_c = 1.252 cm^2
6. Window Area, W_a = 2.34 cm^2
7. Area Product, A_p = 2.93 cm^4
8. Core Geometry, K_g = 0.177 cm^5
9. Surface Area, A_t = 69.9 cm^2
10. Material, P = 2500μ
11. Millihenrys-per-1000 Turns, AL = 3295 mh
12. Winding Length, G = 2.84 cm

Step No. 7: Calculate the current density, J, using the area product Equation, A_p.

$$J = \frac{2(Energy)(10^4)}{B_m A_p K_u}, \quad [\text{amps-per-cm}^2]$$

$$J = \frac{2(0.0032)(10^4)}{(0.22)(2.93)(0.4)}, \quad [\text{amps-per-cm}^2]$$

$$J = 248, \quad [\text{amps-per-cm}^2]$$

Step No. 8: Calculate the rms current, I_{rms}.

$$I_{rms} = \sqrt{I_o^2 + \Delta I^2}, \quad [\text{amps}]$$

$$I_{rms} = \sqrt{(1.5)^2 + (0.2)^2}, \quad [\text{amps}]$$

$$I_{rms} = 1.51, \quad [\text{amps}]$$

© 2011 by Taylor and Francis Group, LLC

Step No. 9: Calculate the required bare wire area, $A_{w(B)}$.

$$A_{W(B)} = \frac{I_{rms}}{J}, \quad [\text{cm}^2]$$

$$A_{W(B)} = \frac{(1.51)}{(248)}, \quad [\text{cm}^2]$$

$$A_{W(B)} = 0.00609, \quad [\text{cm}^2]$$

Step No. 10: Select a wire from the Wire Table in Chapter 4. If the area is not within 10%, take the next smallest size. Also, record the micro-ohms per centimeter.

$$\text{AWG} = \#19$$

$$\text{Bare, } A_{W(B)} = 0.00653, \quad [\text{cm}^2]$$

$$\text{Insulated, } A_W = 0.00754, \quad [\text{cm}^2]$$

$$\left(\frac{\mu\Omega}{\text{cm}}\right) = 264, \quad [\text{micro-ohm/cm}]$$

Step No. 11: Calculate the effective window area, $W_{a(eff)}$, using the window area found in Step 6. A typical value for, S_3, is 0.75, as shown in Chapter 4.

$$W_{a(eff)} = W_a S_3, \quad [\text{cm}^2]$$

$$W_{a(eff)} = (2.34)(0.75), \quad [\text{cm}^2]$$

$$W_{a(eff)} = 1.76, \quad [\text{cm}^2]$$

Step No. 12: Calculate the number turns possible, N, using the insulated wire area, A_w, found in Step 10. A typical value for, S_2, is 0.6, as shown in Chapter 4.

$$N = \frac{W_{a(eff)} S_2}{A_W}, \quad [\text{turns}]$$

$$N = \frac{(1.76)(0.60)}{(0.00754)}, \quad [\text{turns}]$$

$$N = 140, \quad [\text{turns}]$$

© 2011 by Taylor and Francis Group, LLC

Step No. 13: Calculate the required gap, l_g.

$$l_g = \frac{0.4\pi N^2 A_c\left(10^{-8}\right)}{L} - \left(\frac{\text{MPL}}{\mu_m}\right), \quad \text{[cm]}$$

$$l_g = \frac{(1.26)(140)^2(1.25)\left(10^{-8}\right)}{(0.0025)} - \left(\frac{9.22}{2500}\right), \quad \text{[cm]}$$

$$l_g = 0.120, \quad \text{[cm]}$$

Step No. 14: Calculate the equivalent gap in mils.

$$\text{mils} = cm(393.7)$$

$$\text{mils} = (0.120)(393.7)$$

$$\text{mils} = 47.2 \text{ use } 50$$

Step No. 15: Calculate the fringing flux factor, F.

$$F = 1 + \frac{l_g}{\sqrt{A_c}} \ln\left(\frac{2G}{l_g}\right)$$

$$F = 1 + \frac{(0.120)}{\sqrt{1.25}} \ln\left(\frac{2(2.84)}{0.120}\right)$$

$$F = 1.41$$

Step No. 16: Calculate the new number of turns, N_n, by inserting the fringing flux, F.

$$N_n = \sqrt{\frac{l_g L}{0.4\pi A_c F\left(10^{-8}\right)}}, \quad \text{[turns]}$$

$$N_n = \sqrt{\frac{(0.120)(0.0025)}{(1.26)(1.25)(1.41)\left(10^{-8}\right)}}, \quad \text{[turns]}$$

$$N_n = 116, \quad \text{[turns]}$$

Step No. 17: Calculate the winding resistance, R_L. Use the MLT, from Step 6, and the micro-ohm per centimeter from Step 10.

$$R_L = (\text{MLT})(N_n)\left(\frac{\mu\Omega}{\text{cm}}\right)\left(10^{-6}\right), \quad \text{[ohms]}$$

$$R_L = (8.3)(116)(264)\left(10^{-6}\right), \quad \text{[ohms]}$$

$$R_L = 0.254, \quad \text{[ohms]}$$

© 2011 by Taylor and Francis Group, LLC

Step No. 18: Calculate the copper loss, P_{cu}.

$$P_{cu} = I_{rms}^2 R_L, \quad \text{[watts]}$$

$$P_{cu} = (1.51)^2 (0.254), \quad \text{[watts]}$$

$$P_{cu} = 0.579, \quad \text{[watts]}$$

Step No. 19: Calculate the regulation, α.

$$\alpha = \frac{P_{cu}}{P_o}(100), \quad [\%]$$

$$\alpha = \frac{(0.579)}{(100)}(100), \quad [\%]$$

$$\alpha = 0.579, \quad [\%]$$

Step No. 20: Calculate the ac flux density, B_{ac}.

$$B_{ac} = \frac{0.4\pi N_n F\left(\frac{\Delta I}{2}\right)\left(10^{-4}\right)}{l_g + \left(\frac{\text{MPL}}{\mu_m}\right)}, \quad \text{[teslas]}$$

$$B_{ac} = \frac{(1.26)(116)(1.41)\left(\frac{0.2}{2}\right)\left(10^{-4}\right)}{(0.120) + \left(\frac{9.22}{2500}\right)}, \quad \text{[teslas]}$$

$$B_{ac} = 0.0167, \quad \text{[teslas]}$$

Step No. 21: Calculate the watts per kilogram for ferrite, P, material in Chapter 2. Watts per kilogram can be written in milliwatts per gram.

$$\text{mW/g} = k f^{(m)} B_{ac}^{(n)}$$

$$\text{mW/g} = (0.00004855)(200000)^{(1.63)} (0.0167)^{(2.62)}$$

$$\text{mW/g} = 0.468$$

Step No. 22: Calculate the core loss, P_{fe}.

$$P_{fe} = (\text{mW/g})(W_{tfe})\left(10^{-3}\right), \quad \text{[watts]}$$

$$P_{fe} = (0.468)(60)\left(10^{-3}\right), \quad \text{[watts]}$$

$$P_{fe} = 0.0281, \quad \text{[watts]}$$

© 2011 by Taylor and Francis Group, LLC

Step No. 23: Calculate the total loss, copper plus iron, P_Σ.

$$P_\Sigma = P_{fe} + P_{cu}, \quad \text{[watts]}$$
$$P_\Sigma = (0.0281) + (0.579), \quad \text{[watts]}$$
$$P_\Sigma = 0.607, \quad \text{[watts]}$$

Step No. 24: Calculate the watt density, ψ. The surface area, A_t, can be found in Step 6.

$$\psi = \frac{P_\Sigma}{A_t}, \quad \text{[watts/cm}^2\text{]}$$
$$\psi = \frac{(0.607)}{(69.9)}, \quad \text{[watts/cm}^2\text{]}$$
$$\psi = 0.00868, \quad \text{[watts/cm}^2\text{]}$$

Step No. 25: Calculate the temperature rise, T_r.

$$T_r = 450(\psi)^{(0.826)}, \quad [°\text{C}]$$
$$T_r = 450(0.00868)^{(0.826)}, \quad [°\text{C}]$$
$$T_r = 8.92, \quad [°\text{C}]$$

Step No. 26: Calculate the peak flux density, B_{pk}.

$$B_{pk} = \frac{0.4\pi N_n F\left(I_{dc} + \frac{\Delta I}{2}\right)(10^{-4})}{l_g + \left(\frac{\text{MPL}}{\mu_m}\right)}, \quad \text{[teslas]}$$
$$B_{pk} = \frac{(1.26)(116)(1.41)(1.6)(10^{-4})}{(0.127) + \left(\frac{9.22}{2500}\right)}, \quad \text{[teslas]}$$
$$B_{pk} = 0.252, \quad \text{[teslas]}$$

Note: The big advantage in using the core geometry design procedure is that the wire current density is calculated. When using the area product design procedure, the current density is an estimate, at best. In this next design the same current density will be used as in the core geometry design.

© 2011 by Taylor and Francis Group, LLC

Gapped Inductor Design Example Using the Area Product, A_p, Approach

Step No. 1: Design a linear dc inductor with the following specifications:

1. Inductance, L = 0.0025 henrys
2. dc current, I_o = 1.5 amps
3. ac current, ΔI = 0.2 amps
4. Output power, P_o = 100 watts
5. Current Density, J = 250 amps-per-cm^2
6. Ripple Frequency = 200kHz
7. Operating flux density, B_m = 0.22 tesla
8. Core Material = ferrite
9. Window utilization, K_u = 0.4
10. Temperature rise goal, T_r = 25°C

Step No. 2: Calculate the peak current, I_{pk}.

$$I_{pk} = I_o + \frac{\Delta I}{2}, \quad [\text{amps}]$$

$$I_{pk} = (1.5) + \frac{(0.2)}{2}, \quad [\text{amps}]$$

$$I_{pk} = 1.6, \quad [\text{amps}]$$

Step No. 3: Calculate the energy-handling capability.

$$\text{Energy} = \frac{L I_{pk}^2}{2}, \quad [\text{watt-seconds}]$$

$$\text{Energy} = \frac{(0.0025)(1.6)^2}{2}, \quad [\text{watt-seconds}]$$

$$\text{Energy} = 0.0032, \quad [\text{watt-seconds}]$$

Step No. 4: Calculate the area product, A_p.

$$A_p = \frac{2(\text{Energy})(10^4)}{B_m J K_u}, \quad [\text{cm}^4]$$

$$A_p = \frac{2(0.0032)(10^4)}{(0.22)(248)(0.4)}, \quad [\text{cm}^4]$$

$$A_p = 2.93, \quad [\text{cm}^4]$$

© 2011 by Taylor and Francis Group, LLC

Step No. 5: Select an ETD ferrite core from Chapter 3. The data listed is the closest core to the calculated area product, A_p.

1. Core Number = ETD-39
2. Magnetic Path Length, MPL = 9.22 cm
3. Core Weight, W_{tfe} = 60 grams
4. Mean Length Turn, MLT = 8.3 cm
5. Iron Area, A_c = 1.252 cm^2
6. Window Area, W_a = 2.34 cm^2
7. Area Product, A_p = 2.93 cm^4
8. Core Geometry, K_g = 0.177 cm^5
9. Surface Area, A_t = 69.9 cm^2
10. Material, P = 2500μ
11. Millihenrys-per-1k, AL = 3295 mh
12. Winding Length, G = 2.84 cm

Step No. 6: Calculate the rms current, I_{rms}.

$$I_{rms} = \sqrt{I_o^2 + \Delta I^2}, \quad [\text{amps}]$$

$$I_{rms} = \sqrt{(1.5)^2 + (0.2)^2}, \quad [\text{amps}]$$

$$I_{rms} = 1.51, \quad [\text{amps}]$$

Step No. 7: Calculate the required bare wire area, $A_{w(B)}$.

$$A_{W(B)} = \frac{I_{rms}}{J}, \quad [\text{cm}^2]$$

$$A_{W(B)} = \frac{(1.51)}{(248)}, \quad [\text{cm}^2]$$

$$A_{W(B)} = 0.00609, \quad [\text{cm}^2]$$

Step No. 8: Select a wire from the Wire Table in Chapter 4. If the area is not within 10%, take the next smallest size. Also, record micro-ohms per centimeter.

AWG = #19

Bare, $A_{W(B)} = 0.00653, \quad [\text{cm}^2]$

Insulated, $A_W = 0.00754, \quad [\text{cm}^2]$

$$\left(\frac{\mu\Omega}{\text{cm}}\right) = 264, \quad [\text{micro-ohm/cm}]$$

© 2011 by Taylor and Francis Group, LLC

Step No. 9: Calculate the effective window area, $W_{a(eff)}$. Use the window area found in Step 6. A typical value for, S_3, is 0.75, as shown in Chapter 4.

$$W_{a(eff)} = W_a S_3, \quad [\text{cm}^2]$$

$$W_{a(eff)} = (2.34)(0.75), \quad [\text{cm}^2]$$

$$W_{a(eff)} = 1.76, \quad [\text{cm}^2]$$

Step No. 10: Calculate the number turns possible, N, using the insulated wire area, A_w, found in Step 8. A typical value for, S_2, is 0.6, as shown in Chapter 4.

$$N = \frac{W_{a(eff)} S_2}{A_W}, \quad [\text{turns}]$$

$$N = \frac{(1.76)(0.60)}{(0.00754)}, \quad [\text{turns}]$$

$$N = 140, \quad [\text{turns}]$$

Step No. 11: Calculate the required gap, l_g.

$$l_g = \frac{0.4\pi N^2 A_c (10^{-8})}{L} - \left(\frac{\text{MPL}}{\mu_m}\right), \quad [\text{cm}]$$

$$l_g = \frac{(1.26)(140)^2(1.25)(10^{-8})}{(0.0025)} - \left(\frac{9.22}{2500}\right), \quad [\text{cm}]$$

$$l_g = 0.120, \quad [\text{cm}]$$

Step No. 12: Calculate the equivalent gap in mils.

$$\text{mils} = cm(393.7)$$

$$\text{mils} = (0.120)(393.7)$$

$$\text{mils} = 47.2 \text{ use } 50$$

Step No. 13: Calculate the fringing flux factor, F.

$$F = 1 + \frac{l_g}{\sqrt{A_c}} \ln\left(\frac{2G}{l_g}\right)$$

$$F = 1 + \frac{(0.120)}{\sqrt{1.25}} \ln\left(\frac{2(2.84)}{0.120}\right)$$

$$F = 1.41$$

© 2011 by Taylor and Francis Group, LLC

Step No. 14: Calculate the new number of turns, N_n, by inserting the fringing flux, F.

$$N_n = \sqrt{\frac{l_g L}{0.4\pi A_c F\left(10^{-8}\right)}}, \quad [\text{turns}]$$

$$N_n = \sqrt{\frac{(0.120)(0.0025)}{(1.26)(1.25)(1.41)\left(10^{-8}\right)}}, \quad [\text{turns}]$$

$$N_n = 116, \quad [\text{turns}]$$

Step No. 15: Calculate the winding resistance, R_L. Use the, MLT, from Step 5, and the micro-ohm per centimeter, from Step 10.

$$R_L = (\text{MLT})(N_n)\left(\frac{\mu\Omega}{\text{cm}}\right)\left(10^{-6}\right), \quad [\text{ohms}]$$

$$R_L = (8.3)(116)(264)\left(10^{-6}\right), \quad [\text{ohms}]$$

$$R_L = 0.254, \quad [\text{ohms}]$$

Step No. 16: Calculate the copper loss, P_{cu}.

$$P_{cu} = I_{rms}^2 R_L, \quad [\text{watts}]$$

$$P_{cu} = (1.51)^2(0.254), \quad [\text{watts}]$$

$$P_{cu} = 0.579, \quad [\text{watts}]$$

Step No. 17: Calculate the regulation, α.

$$\alpha = \frac{P_{cu}}{P_o}(100), \quad [\%]$$

$$\alpha = \frac{(0.579)}{(100)}(100), \quad [\%]$$

$$\alpha = 0.579, \quad [\%]$$

Step No. 18: Calculate the ac flux density, B_{ac}.

$$B_{ac} = \frac{0.4\pi N_n F\left(\frac{\Delta I}{2}\right)\left(10^{-4}\right)}{l_g + \left(\frac{\text{MPL}}{\mu_m}\right)}, \quad [\text{teslas}]$$

$$B_{ac} = \frac{(1.26)(116)(1.41)\left(\frac{0.2}{2}\right)\left(10^{-4}\right)}{(0.120) + \left(\frac{9.22}{2500}\right)}, \quad [\text{teslas}]$$

$$B_{ac} = 0.0167, \quad [\text{teslas}]$$

© 2011 by Taylor and Francis Group, LLC

Step No. 19: Calculate the watts per kilogram for ferrite, P, material in Chapter 2. Watts per kilogram can be written in milliwatts per gram.

$$\text{mW/g} = k\, f^{(m)} B_{ac}^{(n)}$$

$$\text{mW/g} = (0.00004855)(200000)^{(1.63)}\,(0.0167)^{(2.62)}$$

$$\text{mW/g} = 0.468$$

Step No. 20: Calculate the core loss, P_{fe}.

$$P_{fe} = (\text{mW/g})(W_{tfe})(10^{-3}), \quad [\text{watts}]$$

$$P_{fe} = (0.468)(60)(10^{-3}), \quad [\text{watts}]$$

$$P_{fe} = 0.0281, \quad [\text{watts}]$$

Step No. 21: Calculate the total loss copper plus iron, P_{Σ}.

$$P_{\Sigma} = P_{fe} + P_{cu}, \quad [\text{watts}]$$

$$P_{\Sigma} = (0.0281) + (0.579), \quad [\text{watts}]$$

$$P_{\Sigma} = 0.607, \quad [\text{watts}]$$

Step No. 22: Calculate the watt density, ψ. The surface area, A_t, can be found in Step 5.

$$\psi = \frac{P_{\Sigma}}{A_t}, \quad [\text{watts/cm}^2]$$

$$\psi = \frac{(0.607)}{(69.9)}, \quad [\text{watts/cm}^2]$$

$$\psi = 0.00868, \quad [\text{watts/cm}^2]$$

Step No. 23: Calculate the temperature rise, T_r.

$$T_r = 450(\psi)^{(0.826)}, \quad [°\text{C}]$$

$$T_r = 450(0.00868)^{(0.826)}, \quad [°\text{C}]$$

$$T_r = 8.92, \quad [°\text{C}]$$

© 2011 by Taylor and Francis Group, LLC

Step No. 24: Calculate the peak flux density, B_{pk}.

$$B_{pk} = \frac{0.4\pi N_n F\left(I_{dc} + \frac{\Delta I}{2}\right)\left(10^{-4}\right)}{l_g + \left(\frac{\text{MPL}}{\mu_m}\right)}, \quad \text{[teslas]}$$

$$B_{pk} = \frac{(1.26)(116)(1.41)(1.6)\left(10^{-4}\right)}{(0.127) + \left(\frac{9.22}{2500}\right)}, \quad \text{[teslas]}$$

$$B_{pk} = 0.252, \quad \text{[teslas]}$$

Step No. 25: Calculate the effective permeability, μ_e. Knowing the effective permeability, the ETD-39 ferrite core can be ordered with a built-in gap.

$$\mu_e = \frac{\mu_m}{1 + \left(\frac{l_g}{\text{MPL}}\right)\mu_m}$$

$$\mu_e = \frac{(2500)}{1 + \left(\frac{(0.120)}{9.22}\right)(2500)}$$

$$\mu_e = 74.5 \text{ use } 75$$

Step No. 26: Calculate the window utilization, K_u.

$$K_u = \frac{N_n A_{w(B)}}{W_a}$$

$$K_u = \frac{(116)(0.00653)}{(2.34)}$$

$$K_u = 0.324$$

© 2011 by Taylor and Francis Group, LLC

Chapter 9

DC Inductor Design, Using Powder Cores

© 2011 by Taylor and Francis Group, LLC

Table of Contents

1. Introduction....9-3
2. Molybdenum Permalloy Powder Cores (MPP)....9-3
3. High Flux Powder Cores (HF)....9-3
4. Sendust Powder Cores (Magnetics Kool Mμ)....9-4
5. Iron Powder Cores....9-4
6. Inductors....9-5
7. Relationship of, A_p, to Inductor's Energy-Handling Capability....9-5
8. Relationship of, K_g, to Inductor's Energy-Handling Capability....9-6
9. Fundamental Considerations....9-7
10. Toroidal Powder Core Design Using the Core Geometry, K_g, Approach....9-9
11. Toroidal Powder Core Inductor Design, Using the Area Product, A_p, Approach....9-15

© 2011 by Taylor and Francis Group, LLC

Introduction

Powder cores are manufactured from very fine particles of magnetic materials. The powder is coated with an inert insulation to minimize eddy current losses and to introduce a distributed air gap into the core structure. The insulated powder is then compacted into toroidal and EE cores. The magnetic flux in a toroidal powder core can be contained inside the core more readily than in a lamination or C core, as the winding covers the core along the entire Magnetic Path Length. The design of an inductor also frequently involves consideration of the effect of its magnetic field on devices near where it is placed. This is especially true in the design of high-current inductors for converters and switching regulators used in spacecraft.

Toroidal powder cores are widely used in high-reliability military and space applications because of their good stability over wide temperature ranges, and their ability to withstand high levels of shock, vibration, and nuclear radiation without degradation. Other applications for these cores are:

1. Stable, high-Q filters operating in the frequency range of 1kHz to 1MHz.
2. Loading coils used to cancel out the distributed capacitance in telephone cables.
3. Pulse transformers.
4. Differential mode EMI noise filters.
5. Flyback transformers.
6. Energy storage, or output inductors, in circuits with large amounts of dc current flowing.

Molybdenum Permalloy Powder Cores (MPP)

Molybdenum Permalloy Powder Cores (MPP) are manufactured from very fine particles of an 81% nickel, 17% iron, and a 2% molybdenum alloy. The insulated powder is then compacted into, EE, and toroidal cores. The toroidal cores range in size from 0.1 inch (0.254 cm) to 5 inches (12.7 cm) in the outside diameter. MPP cores are available in permeabilities ranging from 14 up to 550. See Table 9-1.

High Flux Powder Cores (HF)

High Flux Powder Cores (HF) are manufactured from very fine particles of a 50% nickel, and 50% iron. The insulated powder is then compacted into, EE, and toroidal cores. The toroidal cores range in size from 0.25 inch (0.635 cm) to 3 inches (7.62 cm) in the outside diameter. HF cores are available in permeabilities ranging from 14 up to 160. See Table 9-1.

© 2011 by Taylor and Francis Group, LLC

Sendust Powder Cores (Magnetics Kool Mμ)

Sendust powder cores are manufactured from very fine particles of an 85% iron, 9% silicon, and 6% aluminum. The insulated powder is then compacted into EE and toroidal cores. The toroidal cores range in size from 0.14 inch (0.35 cm) to 3 inches (7.62 cm) in the outside diameter. Sendust cores are available in permeabilities ranging from 26 up to 125. See Table 9-1.

Iron Powder Cores

The low cost iron powder cores are typically used in today's low and high frequency power switching conversion applications for differential-mode, input and output, power inductors. The distributed air gap characteristic of iron powder produces a core with permeability ranging from 10 to 100. This feature, in conjunction with the inherent high saturation point of iron, makes it very difficult to saturate. While iron powder cores may be limited in their use because of low permeability, or rather high core loss at high frequency, they have become a very popular choice in either, EE, or toroidal as a core material for high-volume commercial applications. They are popular due to their low cost compared with other core materials. The toroidal cores range in size from 0.3 inch (0.76 cm) to 6.5 inches (16.5 cm) in the outside diameter. See Table 9-1.

Table 9-1. Standard Powder Core Permeability

Standard Powder Core Permeabilities				
Powder Material	MPP	High Flux	Sendust (Kool Mμ)	Iron Powder
Initial Permeability, μ_i				
10				X
14	X	X		
26	X	X	X	
35				X
40			X	
55				X
60	X	X	X	X
75			X	X
90			X	
100				X
125	X	X	X	
147	X	X		
160	X	X		
173	X			
200	X			
300	X			
550	X			

© 2011 by Taylor and Francis Group, LLC

Inductors

Inductors that carry direct current are used frequently in a wide variety of ground, air, and space applications. Selection of the best magnetic core for an inductor frequently involves a trial-and-error type of calculation.

The design of an inductor also frequently involves consideration of the effect of its magnetic field on other devices in the immediate vicinity. This is especially true in the design of high-current inductors for converters and switching regulators used in spacecraft, which may also employ sensitive magnetic field detectors. For this type of design problem, it is frequently imperative that a toroidal core be used. The magnetic flux in a powder core can be contained inside the core more readily than in a lamination or C core, as the winding covers the core along the entire Magnetic Path Length. The author has developed a simplified method of designing optimum, dc carrying inductors with powder cores. This method allows the correct core permeability to be determined without relying on the trial and error method.

Relationship of, A_p, to Inductor's Energy-Handling Capability

The energy-handling capability of a core is related to its area product, A_p, by the Equation:

$$A_p = \frac{2(\text{Energy})(10^4)}{B_m J K_u}, \quad [\text{cm}^4] \tag{9-1}$$

Where: Energy is in watt-seconds.

B_m is the flux density, teslas.

J is the current density, amps-per-cm^2.

K_u is the window utilization factor. (See Chapter 4)

From the above factors, such as flux density, B_m, window utilization factor, K_u, (which defines the maximum space that may be used by the copper in the window), and the current density, J, which controls the copper loss can be seen. The energy-handling capability of a core is derived from:

$$\text{Energy} = \frac{LI^2}{2}, \quad [\text{watt-seconds}] \tag{9-2}$$

© 2011 by Taylor and Francis Group, LLC

Relationship of, K_g, to Inductor's Energy-Handling Capability

Inductors, like transformers, are designed for a given temperature rise. They can also be designed for a given regulation. The regulation and energy handling ability of a core is related to two constants:

$$\alpha = \frac{(\text{Energy})^2}{K_g K_e}, \quad [\%] \tag{9-3}$$

Where, α, is the regulation in, %.

The constant, K_g, is determined by the core geometry:

$$K_g = \frac{W_a A_c^2 K_u}{\text{MLT}}, \quad [\text{cm}^5] \tag{9-4}$$

The constant, K_e, is determined by the magnetic and electrical operating conditions:

$$K_e = 0.145 P_o B_m^2 \left(10^{-4}\right) \tag{9-5}$$

The output power, P_o, is defined in Figure 9-1.

$$P_{o(L1)} = V_{(01)} I_{(01)} \quad P_{o(L2)} = V_{(02)} I_{(02)} \tag{9-6}$$

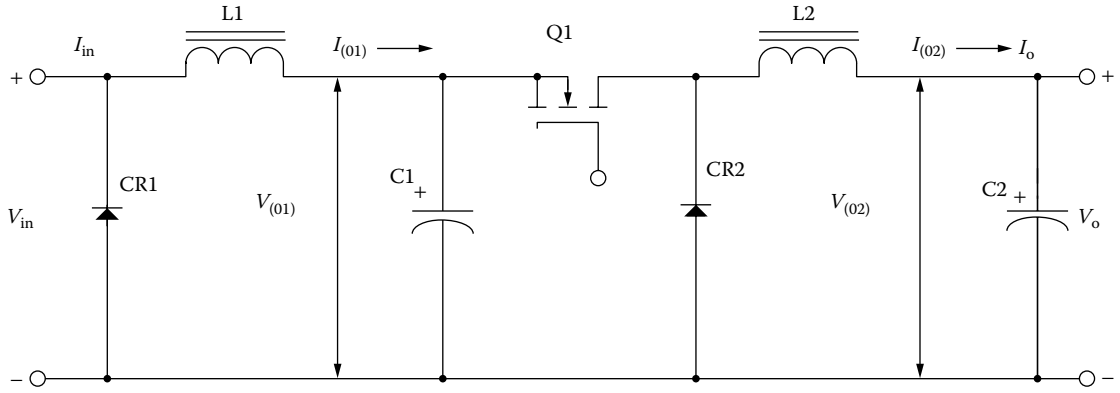

Figure 9-1. Defining the Inductor Output Power.

The operating flux density, B_m, is:

$$B_m = B_{dc} + \frac{B_{ac}}{2}, \quad [\text{teslas}] \tag{9-7}$$

From the above, it can be seen that the flux density, B_m, is the predominant factor in governing size.

© 2011 by Taylor and Francis Group, LLC

Fundamental Considerations

The design of a linear reactor depends upon four related factors:

1. Desired inductance, L.
2. Direct current, I_{dc}.
3. Alternating current, ΔI.
4. Power loss and temperature, T_r.

With these requirements established, the designer must determine the maximum values for, B_{dc}, and B_{ac}, that will not produce magnetic saturation and must make trade-offs that will yield the highest inductance for a given volume. The core permeability chosen dictates the maximum dc flux density that can be tolerated for a given design.

If an inductance is to be constant with the increasing direct current, there must be a negligible drop in inductance over the operating current range. The maximum, H, (magnetizing force) then is an indication of a core's capability, as shown in Figure 9-2.

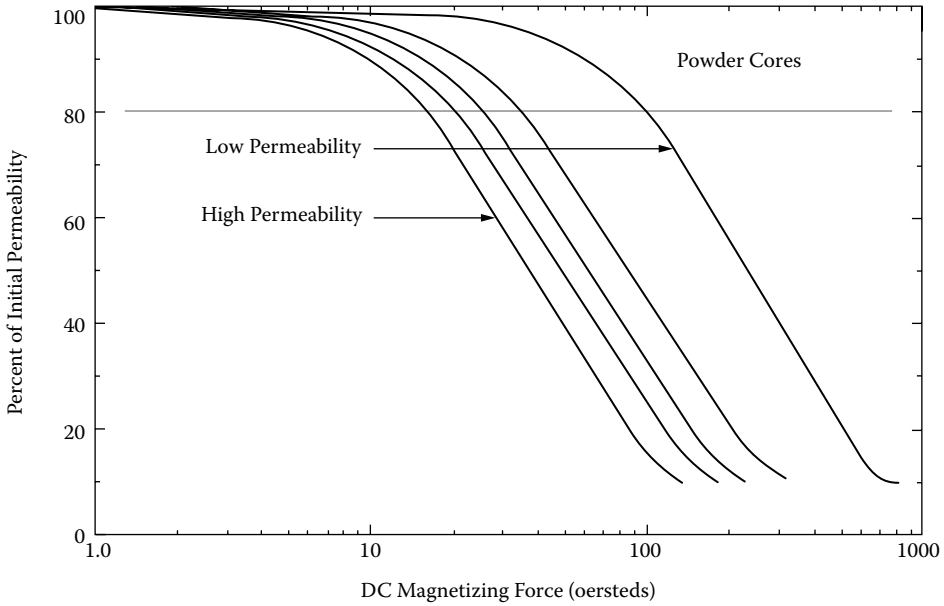

Figure 9-2. Typical Permeability Versus dc Bias Curves for Powder Cores.

Most manufacturers give the dc magnetizing force, H in oersteds:

$$H = \frac{0.4\pi NI}{\text{MPL}}, \quad \text{[oersteds]} \qquad [9\text{-}8]$$

© 2011 by Taylor and Francis Group, LLC

Some engineers prefer amp-turns:

$$NI = 0.8H(\text{MPL}), \quad \text{[amp-turns]} \tag{9-9}$$

Inductance decreases with increasing flux density, B, and magnetizing force, H, for various materials of different values of permeability. The selection of the correct permeability for a given design is made using Equation [9-10].

$$\mu_{\Delta} = \frac{B_m(\text{MPL})\left(10^4\right)}{0.4\pi W_a J K_u} \tag{9-10}$$

It should be remembered that the maximum flux, B_m, depends upon, $B_{dc} + B_{ac}$, in the manner shown in Figure 9-3.

$$B_m = B_{dc} + \frac{B_{ac}}{2}, \quad \text{[teslas]} \tag{9-11}$$

$$B_{dc} = \frac{0.4\pi N I_{dc}\mu\left(10^{-4}\right)}{\text{MPL}}, \quad \text{[teslas]} \tag{9-12}$$

$$B_{ac} = \frac{0.4\pi N\left(\frac{\Delta I}{2}\right)\mu\left(10^{-4}\right)}{\text{MPL}}, \quad \text{[teslas]} \tag{9-13}$$

$$B_{pk} = \frac{0.4\pi N\left(I_{dc} + \frac{\Delta I}{2}\right)\mu\left(10^{-4}\right)}{\text{MPL}}, \quad \text{[teslas]} \tag{9-14}$$

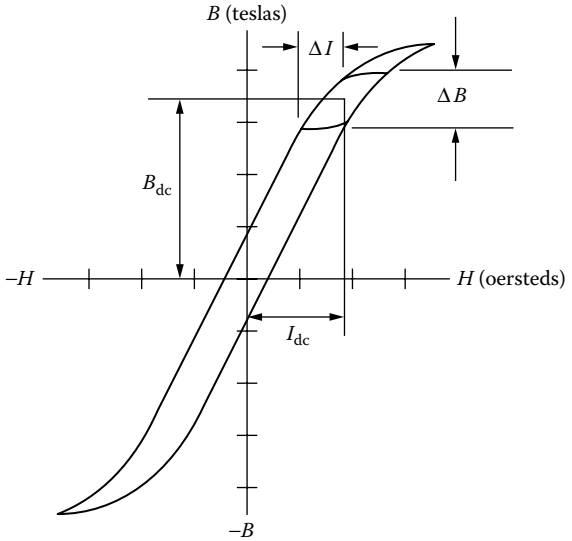

Figure 9-3. Inductor Flux Density Versus, $I_{dc} + \Delta I$ Current.

© 2011 by Taylor and Francis Group, LLC

The flux density for the initial design for Molypermalloy powder cores should be limited to 0.3T maximum for, $B_{dc} + B_{ac}$, as shown in Figure 9-4.

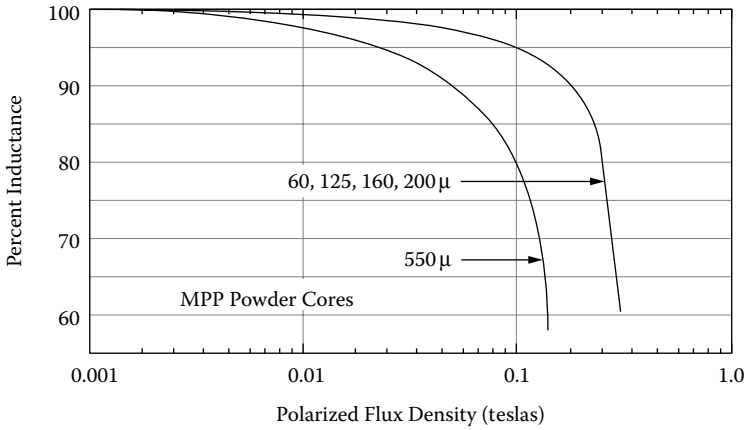

Figure 9-4. Inductance Versus dc Bias.

Toroidal Powder Core Design Using the Core Geometry, K_g, Approach

This design procedure will work with all powder cores.

Step No. 1: Design a linear dc inductor with the following specifications:

1. Inductance, L = 0.0025 henrys
2. dc current, I_o = 1.5 amps
3. ac current, ΔI = 0.2 amps
4. Output power, P_o = 100 watts
5. Regulation, α = 1.0 %
6. Ripple Frequency = 20kHz
7. Operating flux density, B_m = 0.3 tesla
8. Core Material = MPP
9. Window utilization, K_u = 0.4
10. Temperature rise goal, T_r = 25°C

Step No. 2: Calculate the peak current, I_{pk}.

$$I_{pk} = I_o + \frac{\Delta I}{2}, \quad \text{[amps]}$$

$$I_{pk} = (1.5) + \frac{(0.2)}{2}, \quad \text{[amps]}$$

$$I_{pk} = 1.6, \quad \text{[amps]}$$

© 2011 by Taylor and Francis Group, LLC

Step No. 3: Calculate the energy-handling capability.

$$\text{Energy} = \frac{LI_{pk}^2}{2}, \quad \text{[watt-seconds]}$$

$$\text{Energy} = \frac{(0.0025)(1.6)^2}{2}, \quad \text{[watt-seconds]}$$

$$\text{Energy} = 0.0032, \quad \text{[watt-seconds]}$$

Step No. 4: Calculate the electrical conditions coefficient, K_e.

$$K_e = 0.145 P_o B_m^2 \left(10^{-4}\right)$$

$$K_e = 0.145(100)(0.3)^2\left(10^{-4}\right)$$

$$K_e = 0.0001305$$

Step No. 5: Calculate the core geometry coefficient, K_g.

$$K_g = \frac{(\text{Energy})^2}{K_e \alpha}, \quad [\text{cm}^5]$$

$$K_g = \frac{(0.0032)^2}{(0.0001305)(1.0)}, \quad [\text{cm}^5]$$

$$K_g = 0.0785, \quad [\text{cm}^5]$$

Step No. 6: Select a MPP powder core from Chapter 3. The data listed is the closest core to the calculated core geometry, K_g.

1. Core Number = 55586
2. Magnetic Path Length, MPL = 8.95 cm
3. Core Weight, W_{tfe} = 34.9 grams
4. Mean Length Turn, MLT = 4.40 cm
5. Iron Area, A_c = 0.454 cm^2
6. Window Area, W_a = 3.94 cm^2
7. Area Product, A_p = 1.79 cm^4
8. Core Geometry, K_g = 0.0738 cm^5
9. Surface Area, A_t = 64.4 cm^2
10. Permeability, μ = 60
11. Millihenrys-per-1k, AL = 38 mh

© 2011 by Taylor and Francis Group, LLC

Step No. 7: Calculate the current density, J, using the area product Equation, A_p.

$$J = \frac{2(Energy)(10^4)}{B_m A_p K_u}, \quad [\text{amps-per-cm}^2]$$

$$J = \frac{2(0.0032)(10^4)}{(0.3)(1.79)(0.4)}, \quad [\text{amps-per-cm}^2]$$

$$J = 298, \quad [\text{amps-per-cm}^2]$$

Step No. 8: Calculate the rms current, I_{rms}.

$$I_{rms} = \sqrt{I_o^2 + \Delta I^2}, \quad [\text{amps}]$$

$$I_{rms} = \sqrt{(1.5)^2 + (0.2)^2}, \quad [\text{amps}]$$

$$I_{rms} = 1.51, \quad [\text{amps}]$$

Step No. 9: Calculate the required bare wire area, $A_{w(B)}$.

$$A_{W(B)} = \frac{I_{rms}}{J}, \quad [\text{cm}^2]$$

$$A_{W(B)} = \frac{(1.51)}{(298)}, \quad [\text{cm}^2]$$

$$A_{W(B)} = 0.00507, \quad [\text{cm}^2]$$

Step No. 10: Select a wire from the Wire Table in Chapter 4. If the area is not within 10%, take the next smallest size. Also, record the micro-ohms per centimeter.

$$\text{AWG} = \#20$$

$$\text{Bare}, A_{W(B)} = 0.00519, \quad [\text{cm}^2]$$

$$\text{Insulated}, A_W = 0.00606, \quad [\text{cm}^2]$$

$$\left(\frac{\mu\Omega}{\text{cm}}\right) = 332, \quad [\text{micro-ohm/cm}]$$

Step No. 11: Calculate the effective window area, $W_{a(eff)}$. Use the window area found in Step 6. A typical value for, S_3, is 0.75, as shown in Chapter 4.

$$W_{a(eff)} = W_a S_3, \quad [\text{cm}^2]$$

$$W_{a(eff)} = (3.94)(0.75), \quad [\text{cm}^2]$$

$$W_{a(eff)} = 2.96, \quad [\text{cm}^2]$$

© 2011 by Taylor and Francis Group, LLC

Step No. 12: Calculate the number turns possible for, N. Use the insulated wire area, A_w, found in Step 10. A typical value for, S_2, is 0.6, as shown in Chapter 4.

$$N = \frac{W_{a(eff)} S_2}{A_W}, \quad \text{[turns]}$$

$$N = \frac{(2.96)(0.60)}{(0.00606)}, \quad \text{[turns]}$$

$$N = 293, \quad \text{[turns]}$$

Step No. 13: Calculate the required core permeability, μ.

$$\mu_\Delta = \frac{B_m\,(\text{MPL})\left(10^4\right)}{0.4\pi W_a J K_u}$$

$$\mu_\Delta = \frac{(0.30)(8.95)\left(10^4\right)}{(1.26)(3.94)(298)(0.4)}$$

$$\mu_\Delta = 45.4$$

Note: The permeability of 45.4 is close enough to use a 60μ core. Also note that there are other permeabilities available, See Table 9-1. Because of size, Chapter 3 has listed only 60μ Tables for MPP, High Flux, Sendust and a 75μ Table for Iron powder. For cores, with other than 60μ, use the manufacturer's catalog.

Step No. 14: Calculate the number of turns, N_L, required.

$$N_L = 1000\sqrt{\frac{L}{L_{(1000)}}}, \quad \text{[turns]}$$

$$N_L = 1000\sqrt{\left(\frac{2.5}{38}\right)}, \quad \text{[turns]}$$

$$N_L = 256, \quad \text{[turns]}$$

Step No. 15: Calculate the winding resistance, R_L. Use the MLT from Step 6 and the micro-ohm per centimeter from Step 10.

$$R_L = (\text{MLT})(N_L)\left(\frac{\mu\Omega}{\text{cm}}\right)\left(10^{-6}\right), \quad \text{[ohms]}$$

$$R_L = (4.4)(256)(332)\left(10^{-6}\right), \quad \text{[ohms]}$$

$$R_L = 0.374, \quad \text{[ohms]}$$

Step No. 16: Calculate the copper loss, P_{cu}.

$$P_{cu} = I_{rms}^2 R_L, \quad \text{[watts]}$$

$$P_{cu} = (1.51)^2(0.374), \quad \text{[watts]}$$

$$P_{cu} = 0.853, \quad \text{[watts]}$$

© 2011 by Taylor and Francis Group, LLC

Step No. 17: Calculate the regulation, α.

$$\alpha = \frac{P_{cu}}{P_o}(100), \quad [\%]$$

$$\alpha = \frac{(0.853)}{(100)}(100), \quad [\%]$$

$$\alpha = 0.853, \quad [\%]$$

Step No. 18: Calculate the ac flux density, B_{ac}.

$$B_{ac} = \frac{0.4\pi N_L\left(\frac{\Delta I}{2}\right)\mu\left(10^{-4}\right)}{\text{MPL}}, \quad [\text{teslas}]$$

$$B_{ac} = \frac{(1.25)(256)\left(\frac{0.2}{2}\right)(60)\left(10^{-4}\right)}{(8.95)}, \quad [\text{teslas}]$$

$$B_{ac} = 0.0215, \quad [\text{teslas}]$$

Step No. 19: Calculate the watts per kilogram for the appropriate MPP powder core material in Chapter 2.

Watts per kilogram can be written in milliwatts per gram.

$$\text{mW/g} = k f^{(m)} B_{ac}^{(n)}$$

$$\text{mW/g} = (0.000788)(20000)^{(1.41)}(0.0215)^{(2.24)}$$

$$\text{mW/g} = 0.168$$

Step No. 20: Calculate the core loss, P_{fe}.

$$P_{fe} = (\text{mW/g})(W_{tfe})\left(10^{-3}\right), \quad [\text{watts}]$$

$$P_{fe} = (0.168)(34.9)\left(10^{-3}\right), \quad [\text{watts}]$$

$$P_{fe} = 0.00586, \quad [\text{watts}]$$

Step No. 21: Calculate the total loss copper plus iron, P_Σ.

$$P_\Sigma = P_{fe} + P_{cu}, \quad [\text{watts}]$$

$$P_\Sigma = (0.00586) + (0.853), \quad [\text{watts}]$$

$$P_\Sigma = 0.859, \quad [\text{watts}]$$

© 2011 by Taylor and Francis Group, LLC

Step No. 22: Calculate the watt density, ψ. The surface area, A_t can be found in Step 6.

$$\psi = \frac{P_\Sigma}{A_t}, \quad [\text{watts/cm}^2]$$

$$\psi = \frac{(0.859)}{(64.4)}, \quad [\text{watts/cm}^2]$$

$$\psi = 0.0133, \quad [\text{watts/cm}^2]$$

Step No. 23: Calculate the temperature rise, T_r.

$$T_r = 450(\psi)^{(0.826)}, \quad [^\circ\text{C}]$$

$$T_r = 450(0.0133)^{(0.826)}, \quad [^\circ\text{C}]$$

$$T_r = 12.7, \quad [^\circ\text{C}]$$

Step No. 24: Calculate the dc magnetizing force, H.

$$H = \frac{0.4\pi N_L I_{pk}}{\text{MPL}}, \quad [\text{oersteds}]$$

$$H = \frac{(1.26)(256)(1.6)}{(8.95)}, \quad [\text{oersteds}]$$

$$H = 57.7, \quad [\text{oersteds}]$$

Step No. 25: Calculate the window utilization, K_u.

$$K_u = \frac{N_{L(new)} A_{w(B)\#20}}{W_a}$$

$$K_u = \frac{((256)(0.00519))}{(3.94)}$$

$$K_u = 0.337$$

Note: The big advantage in using the core geometry design procedure is that the current density is calculated. Using the area product design procedure, the current density is an estimate, at best. In this next design the same current density will be used as in core geometry.

© 2011 by Taylor and Francis Group, LLC

Toroidal Powder Core Inductor Design, Using the Area Product, A_p, Approach

Step No. 1: Design a linear dc inductor with the following specifications:

1. Inductance, L = 0.0025 henrys.
2. dc current, I_o = 1.5 amps
3. ac current, ΔI = 0.2 amps
4. Output power, P_o = 100 watts
5. Current Density, J = 300 amps-per-cm^2
6. Ripple Frequency = 20kHz
7. Operating flux density, B_m = 0.3 tesla
8. Core Material = MPP
9. Window utilization, K_u = 0.4
10. Temperature rise goal, T_r = 25°C

Step No. 2: Calculate the peak current, I_{pk}.

$$I_{pk} = I_o + \frac{\Delta I}{2}, \quad \text{[amps]}$$

$$I_{pk} = (1.5) + \frac{(0.2)}{2}, \quad \text{[amps]}$$

$$I_{pk} = 1.6, \quad \text{[amps]}$$

Step No. 3: Calculate the energy-handling capability.

$$\text{Energy} = \frac{LI_{pk}^2}{2}, \quad \text{[watt-seconds]}$$

$$\text{Energy} = \frac{(0.0025)(1.6)^2}{2}, \quad \text{[watt-seconds]}$$

$$\text{Energy} = 0.0032, \quad \text{[watt-seconds]}$$

Step No. 4: Calculate the area product, A_p.

$$A_p = \frac{2(\text{Energy})(10^4)}{B_m J K_u}, \quad [\text{cm}^4]$$

$$A_p = \frac{2(0.0032)(10^4)}{(0.3)(300)(0.4)}, \quad [\text{cm}^4]$$

$$A_p = 1.78, \quad [\text{cm}^4]$$

© 2011 by Taylor and Francis Group, LLC

Step No. 5: Select a MPP powder core from Chapter 3. The data listed is the closest core to the calculated core geometry, K_g.

1. Core Number = 55586
2. Magnetic Path Length, MPL = 8.95 cm
3. Core Weight, W_{tfe} = 34.9 grams
4. Mean Length Turn, MLT = 4.40 cm
5. Iron Area, A_c = 0.454 cm^2
6. Window Area, W_a = 3.94 cm^2
7. Area Product, A_p = 1.79 cm^4
8. Core Geometry, K_g = 0.0742 cm^5
9. Surface Area, A_t = 64.4 cm^2
10. Permeability, μ = 60
11. Millihenrys-per-1k, AL = 38 mh

Step No. 6: Calculate the rms current, I_{rms}.

$$I_{rms} = \sqrt{I_o^2 + \Delta I^2}, \quad [\text{amps}]$$

$$I_{rms} = \sqrt{(1.5)^2 + (0.2)^2}, \quad [\text{amps}]$$

$$I_{rms} = 1.51, \quad [\text{amps}]$$

Step No. 7: Calculate the required bare wire area, $A_{w(B)}$.

$$A_{W(B)} = \frac{I_{rms}}{J}, \quad [\text{cm}^2]$$

$$A_{W(B)} = \frac{(1.51)}{(298)}, \quad [\text{cm}^2]$$

$$A_{W(B)} = 0.00507, \quad [\text{cm}^2]$$

Step No. 8: Select a wire from the Wire Table in Chapter 4. If the area is not within 10%, take the next smallest size. Also, record the micro-ohms per centimeter.

AWG = # 20

Bare, $A_{W(B)} = 0.00519, \quad [\text{cm}^2]$

Insulated, $A_W = 0.00606, \quad [\text{cm}^2]$

$$\left(\frac{\mu\Omega}{\text{cm}}\right) = 332, \quad [\text{micro-ohm/cm}]$$

© 2011 by Taylor and Francis Group, LLC

Step No. 9: Calculate the effective window area, $W_{a(eff)}$. Use the window area found in Step 5. A typical value for, S_3, is 0.75, as shown in Chapter 4.

$$W_{a(eff)} = W_a S_3, \quad [\text{cm}^2]$$
$$W_{a(eff)} = (3.94)(0.75), \quad [\text{cm}^2]$$
$$W_{a(eff)} = 2.96, \quad [\text{cm}^2]$$

Step No. 10: Calculate the number turns possible, N. Use the insulated wire area, A_w, found in Step 8. A typical value for, S_2, is 0.6, as shown in Chapter 4.

$$N = \frac{W_{a(eff)} S_2}{A_W}, \quad [\text{turns}]$$
$$N = \frac{(2.96)(0.60)}{(0.00606)}, \quad [\text{turns}]$$
$$N = 293, \quad [\text{turns}]$$

Step No. 11: Calculate the required core permeability, μ.

$$\mu_\Delta = \frac{B_m (\text{MPL})\left(10^4\right)}{0.4\pi W_a J K_u}$$
$$\mu_\Delta = \frac{(0.30)(8.95)\left(10^4\right)}{(1.26)(3.94)(298)(0.4)}$$
$$\mu_\Delta = 45.4$$

Note: The permeability of 45.4 is close enough to use a 60μ core. Also note, there are other permeabilities available. See Table 9-1. Because of size, Chapter 3 has listed only 60μ tables for MPP, High Flux, Sendust and 75μ table for Iron powder. For cores, with other than 60μ, use the manufacturer's catalog.

Step No. 12: Calculate the number of turns, N_L, required.

$$N_L = 1000\sqrt{\frac{L}{L_{(1000)}}}, \quad [\text{turns}]$$
$$N_L = 1000\sqrt{\left(\frac{2.5}{38}\right)}, \quad [\text{turns}]$$
$$N_L = 256, \quad [\text{turns}]$$

© 2011 by Taylor and Francis Group, LLC

Step No. 13: Calculate the winding resistance, R_L. Use the MLT, from Step 5, and the micro-ohm per centimeter, from Step 8.

$$R_L = (\text{MLT})(N_L)\left(\frac{\mu\Omega}{\text{cm}}\right)\left(10^{-6}\right), \quad [\text{ohms}]$$

$$R_L = (4.4)(256)(332)\left(10^{-6}\right), \quad [\text{ohms}]$$

$$R_L = 0.374, \quad [\text{ohms}]$$

Step No. 14: Calculate the copper loss, P_{cu}.

$$P_{cu} = I_{rms}^2 R_L, \quad [\text{watts}]$$

$$P_{cu} = (1.51)^2(0.374), \quad [\text{watts}]$$

$$P_{cu} = 0.853, \quad [\text{watts}]$$

Step No. 15: Calculate the ac flux density, B_{ac}.

$$B_{ac} = \frac{0.4\pi N_L\left(\frac{\Delta I}{2}\right)\mu\left(10^{-4}\right)}{\text{MPL}}, \quad [\text{teslas}]$$

$$B_{ac} = \frac{(1.25)(256)\left(\frac{0.2}{2}\right)(60)\left(10^{-4}\right)}{(8.95)}, \quad [\text{teslas}]$$

$$B_{ac} = 0.0215, \quad [\text{teslas}]$$

Step No. 16: Calculate the watts per kilogram for the appropriate MPP powder core material in Chapter 2. Watts per kilogram can be written in milliwatts per gram.

$$\text{mW/g} = k\, f^{(m)} B_{ac}^{(n)}$$

$$\text{mW/g} = (0.000788)(20000)^{(1.41)}(0.0215)^{(2.24)}$$

$$\text{mW/g} = 0.168$$

Step No. 17: Calculate the core loss, P_{fe}.

$$P_{fe} = (\text{mW/g})\left(W_{tfe}\right)\left(10^{-3}\right), \quad [\text{watts}]$$

$$P_{fe} = (0.168)(34.9)\left(10^{-3}\right), \quad [\text{watts}]$$

$$P_{fe} = 0.00586, \quad [\text{watts}]$$

© 2011 by Taylor and Francis Group, LLC

Step No. 18: Calculate the total copper loss plus iron, P_Σ.

$$P_\Sigma = P_{fe} + P_{cu}, \quad \text{[watts]}$$
$$P_\Sigma = (0.00586) + (0.853), \quad \text{[watts]}$$
$$P_\Sigma = 0.859, \quad \text{[watts]}$$

Step No. 19: Calculate the watt density, ψ. The surface area, A_t can be found in Step 5.

$$\psi = \frac{P_\Sigma}{A_t}, \quad \text{[watts/cm}^2\text{]}$$
$$\psi = \frac{(0.859)}{(64.4)}, \quad \text{[watts/cm}^2\text{]}$$
$$\psi = 0.0133, \quad \text{[watts/cm}^2\text{]}$$

Step No. 20: Calculate the temperature rise, T_r.

$$T_r = 450(\psi)^{(0.826)}, \quad [°\text{C}]$$
$$T_r = 450(0.0133)^{(0.826)}, \quad [°\text{C}]$$
$$T_r = 12.7, \quad [°\text{C}]$$

Step No. 21: Calculate the dc magnetizing force, H.

$$H = \frac{0.4\pi N_L I_{pk}}{\text{MPL}}, \quad \text{[oersteds]}$$
$$H = \frac{(1.26)(256)(1.6)}{(8.95)}, \quad \text{[oersteds]}$$
$$H = 57.7, \quad \text{[oersteds]}$$

Step No. 22: Calculate the window utilization, K_u.

$$K_u = \frac{N_{L(new)} A_{w(B)\#20}}{W_a}$$
$$K_u = \frac{((256)(0.00519))}{(3.94)}$$
$$K_u = 0.337$$

© 2011 by Taylor and Francis Group, LLC

Chapter 10

AC Inductor Design

© 2011 by Taylor and Francis Group, LLC

Table of Contents

1. Introduction....10-3
2. Requirements....10-3
3. Relationship of, A_p, to the Inductor Volt-Amp Capability....10-3
4. Relationship of, K_g, to the Inductor Volt-Amp Capability....10-4
5. Fundamental Considerations....10-4
6. Fringing Flux....10-5
7. AC Inductor Design Example....10-9
8. Reference....10-13

© 2011 by Taylor and Francis Group, LLC

Introduction

The design of an ac inductor is quite similar to that of a transformer. If there is no dc flux in the core, the design calculations are straightforward. The apparent power, P_t, of an inductor is the VA of the inductor. As shown in Equation [10-1] it is the product of the excitation voltage and the current through the inductor.

$$P_t = VA, \quad \text{[watts]} \tag{10-1}$$

Requirements

The design of the ac inductor requires the calculation of the volt-amp (VA) capability. In some applications the inductance is specified, and in others, the current is specified. If the inductance is specified, then, the current has to be calculated. If the current is specified, then the inductance has to be calculated. A series, ac inductor, L1, being used in a Ferroresonant Voltage Stabilizer is shown in Figure 10-1.

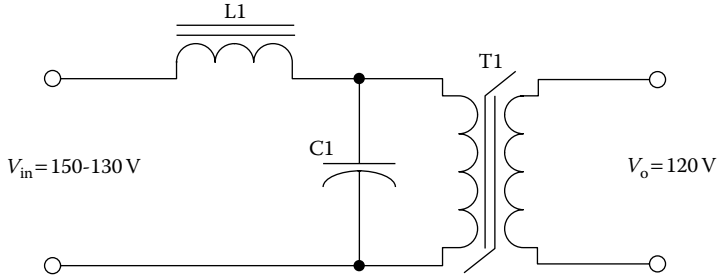

Figure 10-1. Series ac Inductor, L1, as used in a Ferroresonant Voltage Stabilizer.

Relationship of, A_p, to the Inductor Volt-Amp Capability

The volt-amp capability of a core is related to its area product, A_p, as shown in Equation [10-2].

$$A_p = \frac{VA\left(10^4\right)}{K_f K_u B_{ac} f J}, \quad [\text{cm}^4] \tag{10-2}$$

Where:

K_f = wave form factor.

K_u = window utilization factor.

B_{ac} = operating flux density, T, teslas

f = operating frequency, Hz

J = current density, amps/cm^2

© 2011 by Taylor and Francis Group, LLC

From the above, it can be seen that factors such as flux density, B_{ac}, the window utilization factor, K_u, (which defines the maximum space occupied by the copper in the window), and the current density, J, all have an influence on the inductor area product, A_p.

Relationship, K_g, to the Inductor Volt-Amp Capability

Although most inductors are designed for a given temperature rise, they can also be designed for a given regulation. The regulation and volt-amp ability of a core is related to two constants, as shown in Equation [10-3].

$$\alpha = \frac{VA}{K_g K_e}, \quad [\%] \tag{10-3}$$

$$\alpha = \text{Regulation } (\%) \tag{10-4}$$

The constant, K_g, is determined by the core geometry, which may be related, as shown in Equation [10-5].

$$K_g = \frac{W_a A_c^2 K_u}{\text{MLT}}, \quad [\text{cm}^5] \tag{10-5}$$

The constant, K_e, is determined by the magnetic and electric operating conditions, which may be related, as shown in Equation [10-6].

$$K_e = 0.145 K_f^2 f^2 B_m^2 \left(10^{-4}\right) \tag{10-6}$$

Where:

K_f = waveform coefficient

4.0 square wave

4.44 sine wave

From the above, it can be seen that factors such as flux density, frequency of operation, and the waveform coefficient have an influence on the transformer size.

Fundamental Considerations

The design of a linear ac inductor depends upon five related factors:

1. Desired inductance
2. Applied voltage, (across inductor)
3. Frequency
4. Operating Flux density
5. Temperature Rise

© 2011 by Taylor and Francis Group, LLC

With these requirements established, the designer must determine the maximum values for, B_{ac}, which will not produce magnetic saturation, and then make trade-offs that will yield the highest inductance for a given volume. The core material selected determines the maximum flux density that can be tolerated for a given design. Magnetic materials and their operating flux levels are given in Chapter 2.

The ac inductor like a transformer, must support the applied voltage, V_{ac}. The number of turns is calculated from Faraday's Law, as shown in Equation [10-7].

$$N = \frac{V_{ac}\left(10^4\right)}{K_f B_{ac} f A_c}, \quad \text{[turns]} \qquad [10\text{-}7]$$

The inductance of an iron-core inductor, with an air gap, may be expressed, as shown in Equation [10-8].

$$L = \frac{0.4\pi N^2 A_c \left(10^{-8}\right)}{l_g + \left(\frac{\text{MPL}}{\mu_m}\right)}, \quad \text{[henrys]} \qquad [10\text{-}8]$$

Inductance is seen to be inversely dependent on the effective Magnetic Path Length, MPL, which is the sum of the air gap length, l_g, and the ratio of the Magnetic Path Length, MPL, to material permeability, μ_m.

When the core air gap, l_g, is larger compared to the ratio, MPL/μ_m, because of the high material permeability, μ_m, variations in, μ_m, do not substantially affect the total effective Magnetic Path Length, MPL, or the inductance, L. The inductance Equation then reduces to Equation [10-9].

$$L = \frac{0.4\pi N^2 A_c \left(10^{-8}\right)}{l_g}, \quad \text{[henrys]} \qquad [10\text{-}9]$$

Rearranging the Equation to solve for the gap is shown in Equation [10-10].

$$l_g = \frac{0.4\pi N^2 A_c \left(10^{-8}\right)}{L}, \quad \text{[cm]} \qquad [10\text{-}10]$$

Fringing Flux

Final determination of the air gap requires consideration of the effect of fringing flux, which is a function of gap dimension, the shape of the pole faces, and the shape, size, and location of the winding, as shown in Figure 10-2 and Figure 10-3. Its net effect is to make the effective air gap less than its physical dimension.

© 2011 by Taylor and Francis Group, LLC

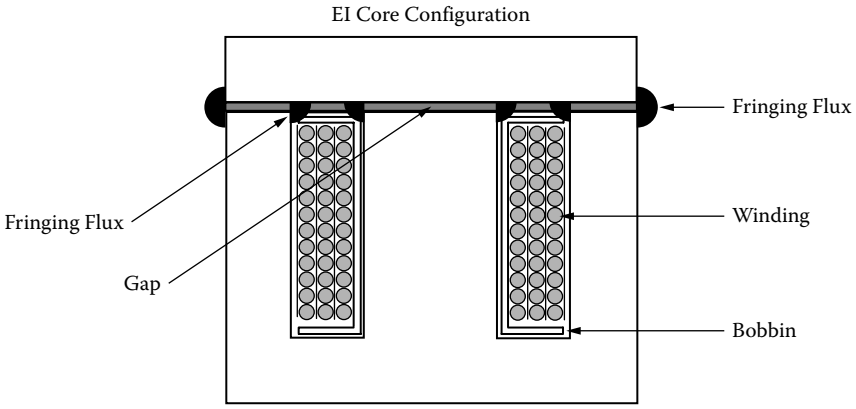

Figure 10-2. Fringing Flux Location on an EI Core Configuration.

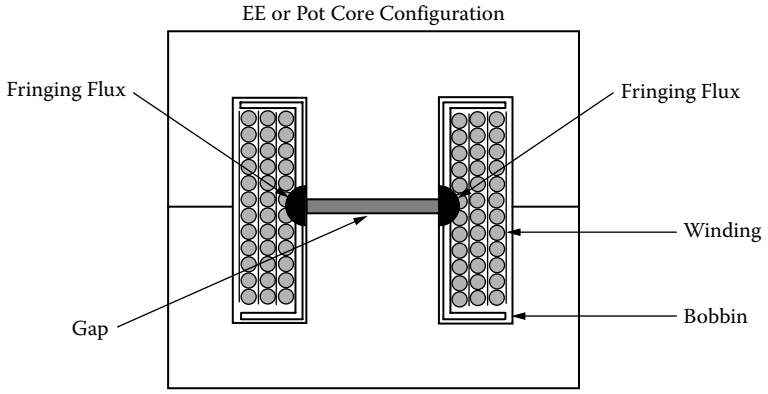

Figure 10-3. Fringing Flux Location on an EE or Pot Core Configuration.

Fringing flux decreases the total reluctance of the magnetic path, and therefore increases the inductance by a factor, F, to a value greater than that calculated from Equation [10-9]. Fringing flux is a larger percentage of the total for larger gaps. The fringing flux factor is shown in Equation [10-11].

$$F = \left(1 + \frac{l_g}{\sqrt{A_c}} \ln\left(\frac{2G}{l_g}\right)\right) \qquad [10\text{-}11]$$

G is the winding length as defined in Chapter 3. Equation [10-11] is valid for cut C cores, laminations and cut ferrite cores.

The inductance, L, computed in Equation [10-9] does not include the effect of fringing flux, F. The value of inductance, L', in Equation [10-12] does correct for fringing flux:

$$L' = \frac{0.4\pi N^2 A_c F\left(10^{-8}\right)}{l_g}, \quad \text{[henrys]} \qquad [10\text{-}12]$$

© 2011 by Taylor and Francis Group, LLC

Now that the fringing flux, F, has been calculated, it is necessary to recalculate the number of turns using the fringing flux, Factor F, as shown in Equation [10-13].

$$N_{(new)} = \sqrt{\frac{Ll_g}{0.4\pi A_c F\left(10^{-8}\right)}}, \quad \text{[turns]} \qquad \text{[10-13]}$$

After the new turns, $N_{(new)}$, have been calculated, then, use Equation [10-13] with the new turns, $N_{(new)}$, and solve for B_{ac}. This check will provide the operating flux density, in order to calculate the core loss, P_{fe}, and will also provide a check on core saturation margin, as shown in Equation [10-14].

$$B_{ac} = \frac{V_{ac}\left(10^4\right)}{K_f N_{(new)} f A_c}, \quad \text{[teslas]} \qquad \text{[10-14]}$$

The losses in an ac inductor are made up of three components:

1. Copper loss, P_{cu}
2. Iron loss, P_{fe}
3. Gap loss, P_g

The copper loss, P_{cu}, is I^2R and is straightforward, if the skin effect is minimal. The iron loss, P_{fe}, is calculated from core manufacturers' data. Gap loss, P_g, is independent of core material strip thickness and permeability. Maximum efficiency is reached in an inductor, as in a transformer, when the copper loss, P_{cu}, and the iron loss, P_{fe}, are equal, but only when the gap of the core is zero. The gap loss does not occur in the air gap, itself, but is caused by magnetic flux, fringing around the gap, and reentering the core in a direction of high loss. As the air gap increases, the flux across the gap fringes more and more, and some of the fringing flux strikes the core, perpendicular to the laminations, and sets up eddy currents which cause additional losses called gap loss, P_g. Also distribution of the fringing flux is affected by other aspects of the core geometry, the proximity of the coils turns to the core, and whether there are turns on both legs. (See Table 10-1). Accurate prediction of the gap loss depends on the amount of fringing flux. The gap loss Equation [10-15] is from an article written by Ruben, L., and Stephens, D. (See the Reference at the end of this Chapter.)

$$P_g = K_i E l_g f B_{ac}^2, \quad \text{[watt]} \qquad \text{[10-15]}$$

Where, E (as defined in Chapter 3) is the strip or tongue width, in cm.

Table 10-1. Gap Loss Coefficient

Configuration	K_i
Two-coil C core	0.0388
Single-coil C core	0.0775
Lamination	0.1550

© 2011 by Taylor and Francis Group, LLC

When designing inductors where there is a choice of cores, always pick the core with the smallest ratio between window area, W_a and iron area, A_c, as shown in Equation [10-16].

$$\frac{W_a}{A_c} = \text{ [smallest ratio]} \qquad [10\text{-}16]$$

Comparing two cores with identical area products, A_p, for the same design specification, the core with a minimum of window area will generate a minimum of fringing flux. If there is a design change and it requires the use of the next larger core, it would be far more beneficial to double up on the core being used, than to pick a larger core, as shown in Figure 10-4.

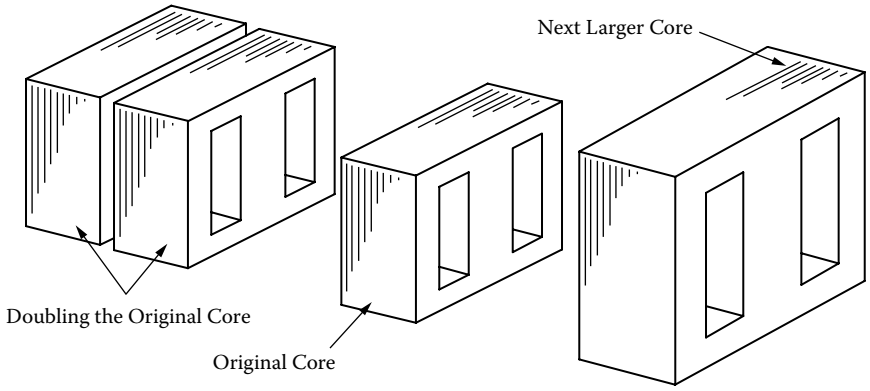

Figure 10-4. Comparing Core Configurations.

For example, if the next larger core was selected, normally all of the core proportions will increase. This means, the window, W_a, and the iron cross-section, A_c, would have both increased. (A larger core should not be used, as the fringing flux would also increase.) If you want to keep the fringing flux to a minimum, then double up on the original core. Therefore the iron area, A_c, would double, but the window area, W_a, will remain the same. This will reduce the, W_a/A_c, ratio, as shown in Equation 10-16. With an increase in iron cross-section, A_c, the turns would have to decrease for the same window area, W_a. With a decrease in turns, the gap would also decrease, resulting in less fringing flux.

When designing a transformer, the engineer will push the flux density as far he can without saturating the core. That cannot be done with an ac inductor because you must leave a margin for the fringing flux factor. One of the biggest problems in designing ac inductors is keeping the gap to a minimum. This problem becomes acute when designing high frequency ac inductors. The problem in designing high frequency inductors is the required turns to support the applied voltage, then gapping to provide the proper inductance. This problem is minimized when using powder cores if the right permeability can be found.

© 2011 by Taylor and Francis Group, LLC

AC Inductor Design Example

Step No. 1: Design a linear ac inductor with the following specifications.

1. Applied voltage, V_L= 120 volts
2. Line current, I_L = 1.0 amps
3. Line frequency = 60 hertz.
4. Current density, J = 300 amp/cm^2
5. Efficiency goal, η(100) = 90%
6. Magnetic material = Silicon
7. Magnetic material permeability, μ_m = 1500
8. Flux density, B_{ac} = 1.4 teslas
9. Window utilization, K_u = 0.4
10. Waveform factor, K_f = 4.44
11. Temperature rise goal, T_r = 50°C

Step No. 2: Calculate the apparent power, P_t or VA of the inductor, L.

$$VA = V_L I_L, \quad \text{[watts]}$$

$$VA = (120)(1.0), \quad \text{[watts]}$$

$$VA = 120, \quad \text{[watts]}$$

Step No. 3: Calculate the area product, A_p.

$$A_p = \frac{VA\left(10^4\right)}{K_f K_u f B_{ac} J}, \quad [\text{cm}^4]$$

$$A_p = \frac{(120)\left(10^4\right)}{(4.44)(0.4)(60)(1.4)(300)}, \quad [\text{cm}^4]$$

$$A_p = 26.8, \quad [\text{cm}^4]$$

Step No. 4: Select an EI lamination from Chapter 3. The closest lamination to the calculated area product, A_p, is the EI-100.

1. Core Number = EI-100
2. Magnetic Path Length, MPL = 15.2 cm
3. Core Weight, W_{tfe} = 676 grams
4. Mean Length Turn, MLT = 14.8 cm
5. Iron Area, A_c = 6.13 cm^2

© 2011 by Taylor and Francis Group, LLC

6. Window Area, $W_a = 4.84$ cm^2
7. Area Product, $A_p = 29.7$ cm^4
8. Core Geometry, $K_g = 4.93$ cm^5
9. Surface Area, $A_t = 213$ cm^2
10. Winding length, G = 3.81 cm
11. Lamination tongue, E = 2.54 cm

Step No. 5: Calculate the number of inductor turns, N_L.

$$N_L = \frac{V_L\left(10^4\right)}{K_f B_{ac} f A_c}, \quad \text{[turns]}$$

$$N_L = \frac{(120)\left(10^4\right)}{(4.44)(1.4)(60)(6.13)}, \quad \text{[turns]}$$

$$N_L = 525, \quad \text{[turns]}$$

Step No. 6: Calculate the inductive reactance, X_L.

$$X_L = \frac{V_L}{I_L}, \quad \text{[ohms]}$$

$$X_L = \frac{(120)}{(1.0)}, \quad \text{[ohms]}$$

$$X_L = 120, \quad \text{[ohms]}$$

Step No. 7: Calculate the required inductance, L.

$$L = \frac{X_L}{2\pi f}, \quad \text{[henrys]}$$

$$L = \frac{120}{2(3.14)(60)}, \quad \text{[henrys]}$$

$$L = 0.318, \quad \text{[henrys]}$$

Step No. 8: Calculate the required gap, l_g.

$$l_g = \left(\frac{0.4\pi N_L^2 A_c\left(10^{-8}\right)}{L}\right) - \left(\frac{\text{MPL}}{\mu_m}\right), \quad \text{[cm]}$$

$$l_g = \left(\frac{(1.26)(525)^2(6.13)\left(10^{-8}\right)}{0.318}\right) - \left(\frac{15.2}{1500}\right), \quad \text{[cm]}$$

$l_g = 0.0568$, [cm] or $l_g = 22.4$, [mils]: This would be in 10 mils each leg.

© 2011 by Taylor and Francis Group, LLC

Step No. 9: Calculate the fringing flux, F.

$$F = \left(1 + \frac{l_g}{\sqrt{A_c}} \ln \frac{2(G)}{l_g}\right)$$

$$F = \left(1 + \frac{0.0568}{\sqrt{6.13}} \ln \frac{2(3.81)}{0.0568}\right)$$

$$F = 1.112$$

Step No. 10: Using the fringing flux, recalculate the series inductor turns, $N_{L(new)}$.

$$N_{L(new)} = \sqrt{\frac{l_g L}{0.4\pi A_c F\left(10^{-8}\right)}}, \quad [\text{turns}]$$

$$N_{L(new)} = \sqrt{\frac{(0.0568)(0.318)}{(1.26)(6.13)(1.112)\left(10^{-8}\right)}}, \quad [\text{turns}]$$

$$N_{L(new)} = 459, \quad [\text{turns}]$$

Step No. 11: Using the new turns, recalculate the flux density, B_{ac}.

$$B_{ac} = \frac{V_L\left(10^4\right)}{K_f N_{L(new)} A_c f}, \quad [\text{teslas}]$$

$$B_{ac} = \frac{(120)\left(10^4\right)}{(4.44)(459)(6.13)(60)}, \quad [\text{teslas}]$$

$$B_{ac} = 1.6, \quad [\text{teslas}]$$

Step No. 12: Calculate the inductor bare wire area, $A_{wL(B)}$.

$$A_{wL(B)} = \frac{I_L}{J}, \quad [\text{cm}^2]$$

$$A_{wL(B)} = \frac{(1.0)}{(300)}, \quad [\text{cm}^2]$$

$$A_{wL(B)} = 0.00333, \quad [\text{cm}^2]$$

Step No. 13: Select a wire from the Wire Table in Chapter 4.

$$AWG = \#22$$

$$A_{w(B)} = 0.00324, \quad [\text{cm}^2]$$

$$\left(\frac{\mu\Omega}{\text{cm}}\right) = 531, \quad [\text{micro-ohm/cm}]$$

© 2011 by Taylor and Francis Group, LLC

Step No. 14: Calculate the inductor winding resistance, R_L. Use the MLT from the core data found in Step 4 and the micro-ohm per centimeter, found in Step 13.

$$R_L = (\text{MLT})(N_s)\left(\frac{\mu\Omega}{\text{cm}}\right)\left(10^{-6}\right), \quad [\text{ohms}]$$

$$R_L = (14.8)(459)(531)\left(10^{-6}\right), \quad [\text{ohms}]$$

$$R_L = 3.61, \quad [\text{ohms}]$$

Step No. 15: Calculate the inductor winding copper loss, P_L.

$$P_L = (I_L)^2 R_L, \quad [\text{watts}]$$

$$P_L = (1.0)^2 (3.61), \quad [\text{watts}]$$

$$P_L = 3.61, \quad [\text{watts}]$$

Step No. 16: Calculate the watts-per-kilograms, W/K, for the appropriate core material. See Chapter 2.

$$W/K = 0.000557 f^{(1.68)} B_s^{(1.86)}, \quad [\text{watts-per-kilogram}]$$

$$W/K = 0.000557(60)^{(1.68)}(1.6)^{(1.86)}, \quad [\text{watts-per-kilogram}]$$

$$W/K = 1.30, \quad [\text{watts-per-kilogram}]$$

Step No. 17: Calculate the core loss in watts, P_{fe}.

$$P_{fe} = (W/K)W_{tfe}, \quad [\text{watts}]$$

$$P_{fe} = (1.30)(0.676), \quad [\text{watts}]$$

$$P_{fe} = 0.878, \quad [\text{watts}]$$

Step No. 18: Calculate the gap loss, P_g.

$$P_g = K_i E l_g f B_{ac}^2, \quad [\text{watts}]$$

$$P_g = (0.155)(2.54)(0.0568)(60)(1.6)^2, \quad [\text{watts}]$$

$$P_g = 3.43, \quad [\text{watts}]$$

Step No. 19: Calculate the total inductor losses, P_Σ.

$$P_\Sigma = P_{cu} + P_{fe} + P_g, \quad [\text{watts}]$$

$$P_\Sigma = (3.61) + (0.878) + (3.43), \quad [\text{watts}]$$

$$P_\Sigma = 7.92, \quad [\text{watts}]$$

© 2011 by Taylor and Francis Group, LLC

Step No. 20: Calculate the inductor surface area watt density, ψ.

$$\psi = \frac{P_{\Sigma}}{A_t}, \quad [\text{watts-per-cm}^2]$$

$$\psi = \frac{(7.92)}{(213)}, \quad [\text{watts-per-cm}^2]$$

$$\psi = 0.0372, \quad [\text{watts-per-cm}^2]$$

Step No. 21: Calculate the temperature rise, T_r.

$$T_r = 450(\psi)^{(0.826)}, \quad [^{o}\text{C}]$$

$$T_r = 450(0.0372)^{(0.826)}, \quad [^{o}C]$$

$$T_r = 29.7, \quad [^{o}\text{C}]$$

Step No. 22: Calculate the window utilization, K_u.

$$K_u = \frac{N_{L(new)} A_{w(B)\#22}}{W_a}$$

$$K_u = \frac{((459)(0.00324))}{(4.84)}$$

$$K_u = 0.307$$

Reference

1. Ruben, L., and Stephens, D. Gap Loss in Current-Limiting Transformer. *Electromechanical Design*, April, 1973, pp. 24–126.

© 2011 by Taylor and Francis Group, LLC

Chapter 11

Constant Voltage Transformer (CVT)

© 2011 by Taylor and Francis Group, LLC

Table of Contents

1. Introduction 11-3
2. Constant-Voltage Transformer, Regulating Characteristics 11-3
3. Electrical Parameters of a CVT Line Regulator 11-4
4. Constant-Voltage Transformer, Design Equations 11-5
5. Constant-Voltage Transformer, Design Example 11-8
6. Series AC Inductor, Design Example 11-15
7. References 11-20

© 2011 by Taylor and Francis Group, LLC

Introduction

The Constant-Voltage Transformer (CVT) has a wide application, particularly where reliability and inherent regulating ability against line voltage changes are of prime importance. The output of a Constant-Voltage Transformer is essentially a square wave, which is desirable for rectifier output applications while, also having good circuit characteristics. The main disadvantage to a Constant-Voltage Transformer is efficiency and regulation for frequency and load. The equations presented here for designing a Constant-Voltage Transformers at line frequency have been used at 400Hz on aircraft, and as high as 20kHz.

Constant-Voltage Transformer, Regulating Characteristics

The basic two-component (CVT) Ferroresonant regulator is shown in Figure 11-1. The inductor, L1, is a linear inductor and is in series with, C1, across the input line. The voltage across capacitor, C1, would be considerably greater than the line voltage, because of the resonant condition between L1 and C1.

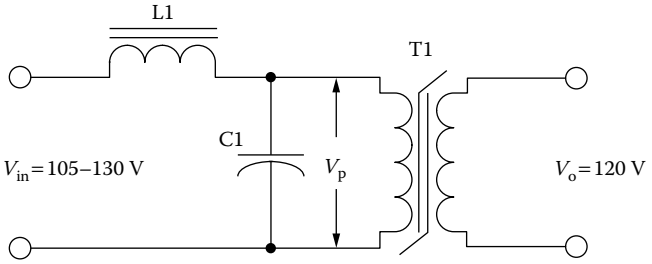

Figure 11-1. Two Component Ferroresonant Voltage Stabilizer.

The voltage, V_p, can be limited to a predetermined amplitude by using a self-saturating transformer, T1, which has high impedance, until a certain level of flux density is reached. At that flux density, the transformer saturates and becomes a low-impedance path, which prevents further voltage buildup across the capacitor. This limiting action produces a voltage waveform that has a fairly flat top characteristic, as shown in Figure 11-2 on each half-cycle.

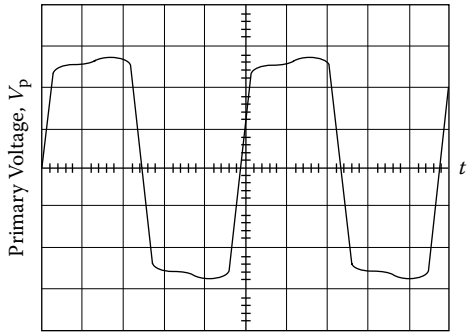

Figure 11-2. Primary Voltage Waveform of a Constant Voltage Transformer.

© 2011 by Taylor and Francis Group, LLC

Electrical Parameters of a CVT Line Regulator

When the Constant-Voltage Transformer is operating as a line regulator, the output voltage will vary as a function of the input voltage, as shown in Figure 11-3. The magnetic material used to design transformer, T1, has an impact on line regulation. Transformers designed with a square B-H loop will result in better line regulation. If the output of the line regulator is subjected to a load power factor (lagging) with less than unity, the output will change, as shown in Figure 11-4.

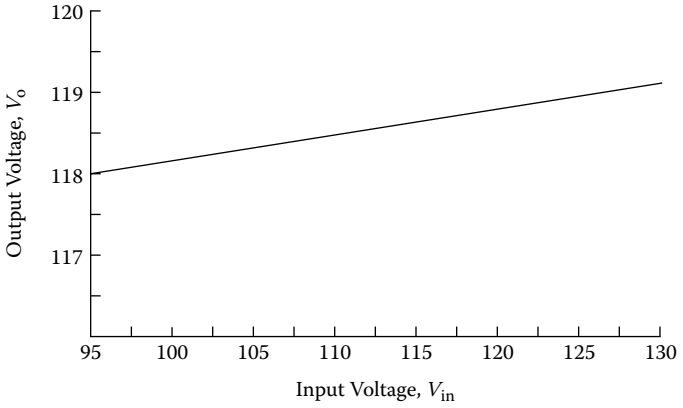

Figure 11-3. Output Voltage Variation, as a Function of Input Voltage.

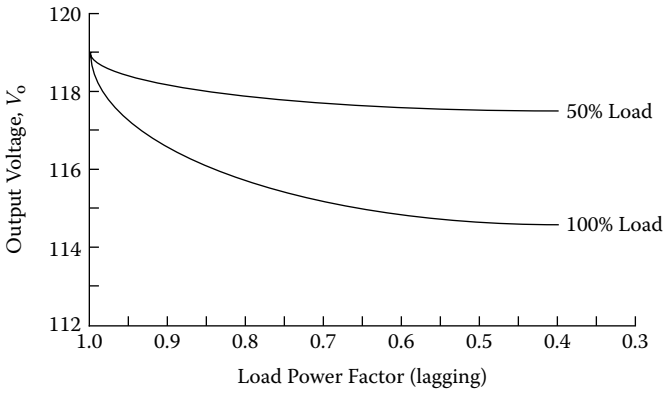

Figure 11-4. Output Voltage Variation, as a Function of Load Power Factor.

If the Constant-Voltage Transformer is subjected to a line voltage frequency change, the output voltage will vary, as shown in Figure 11-5. The regulation of a Constant-Voltage Transformer can be designed to be better than a few percent. Capability for handling a short circuit is an inherent feature of a Constant-Voltage Transformer. The short-circuit current is limited and set by the series inductance, L. The regulation characteristics, at various lines and loads, are shown in Figure 11-6. It should be noted that a dead short, corresponding to zero output voltage, does not greatly increase the load current; whereas for most transformers, this dead short would be destructive.

© 2011 by Taylor and Francis Group, LLC

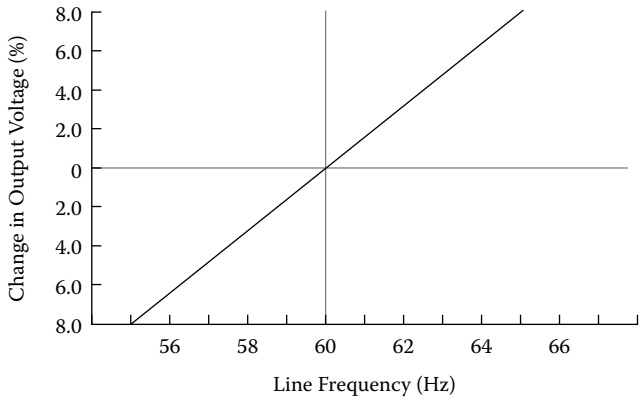

Figure 11-5. Output Voltage Variation, as a Function of Line Frequency Change.

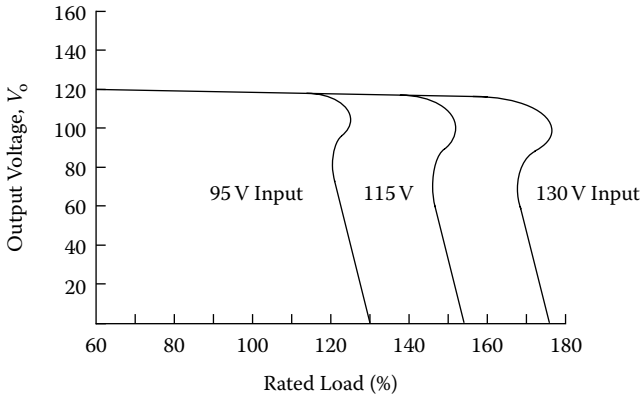

Figure 11-6. Output Voltage Variation, as a Function of Output Voltage vs. Load.

Constant-Voltage Transformer, Design Equations

Proper operation and power capacity of a Constant-Voltage Transformer (CVT) depends on components, L1 and C1, as shown in Figure 11-7. Experience has shown that the, LC, relationship is shown in Equation [11-1].

$$LC\omega^2 = 1.5 \qquad [11\text{-}1]$$

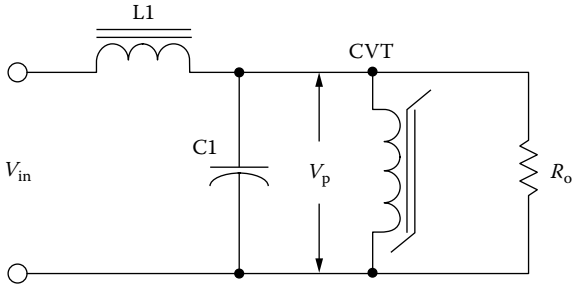

Figure 11-7. Basic, Constant Voltage Transformer Circuit.

© 2011 by Taylor and Francis Group, LLC

The inductance can be expressed, as shown in Equation [11-2].

$$L = \frac{R_{o(R)}}{2\omega}, \quad \text{[henrys]} \tag{11-2}$$

The capacitance can be expressed, as shown in Equation [11-3].

$$C = \frac{1}{0.33\omega R_{o(R)}}, \quad \text{[farads]} \tag{11-3}$$

Referring to Figure 11-7, assume there is a sinusoidal input voltage, an ideal input inductor, L1, and a series capacitor, C1. All voltage and currents are rms values. V_{in} is the voltage value just before the circuit starts to regulate at full load; $R_{o(R)}$, is the reflected resistance back to the primary, including efficiency; η is the efficiency, and, P_o, is the output power, as shown in Equations [11-4] and [11-5].

$$P_o = \frac{V_s^2}{R_o}, \quad \text{[watts]} \tag{11-4}$$

$$R_{o(R)} = \frac{\left(V_p\right)^2 \eta}{P_o}, \quad \text{[ohms]} \tag{11-5}$$

It is common practice for the output to be isolated from the input and to connect C1 to a step-up winding on the Constant-Voltage Transformer (CVT). In order to use smaller capacitor values, a step-up winding must be added, as shown in Figure 11-8. The penalty for using a smaller capacitor requires the use of a step-up winding. This step-up winding increases the, VA, or size of the transformer. This can be seen in Equation [11-6]. The energy in a capacitor is:

$$\begin{aligned} \text{Energy} &= \frac{CV^2}{2}, \quad \text{[watt-seconds]} \\ C &= \frac{2(\text{Energy})}{V^2}, \quad \text{[farads]} \end{aligned} \tag{11-6}$$

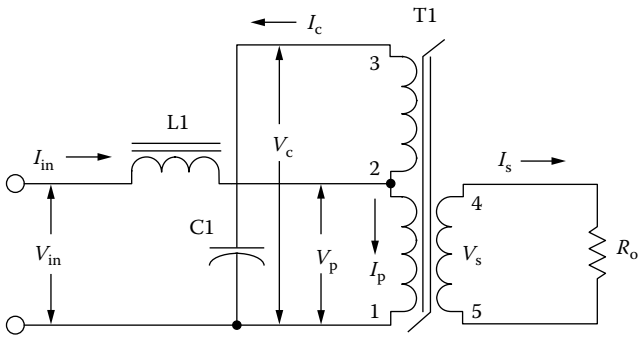

Figure 11-8. CVT, with a Capacitor Step-up Winding.

© 2011 by Taylor and Francis Group, LLC

The secondary current, I_s, can be expressed, as shown in Equation [11-7].

$$I_s = \frac{P_o}{V_s}, \quad \text{[amps]} \tag{11-7}$$

With the step-up winding, the primary current, I_p, is related to the secondary current by the following Equation [11-8] [Ref. 4].

$$I_p = \frac{I_s\left(V_{s(4-5)}\right)}{\eta\left(V_{p(1-2)}\right)}\left(1+\sqrt{\frac{V_{p(1-2)}}{V_{c(1-3)}}}\right), \quad \text{[amps]} \tag{11-8}$$

The current, I_c, through the capacitor, is increased by, K_c, because of the effective higher frequency. Due to the quasi-voltage waveform, as shown in Figure 11-2, the equivalent ac impedance of the resonant capacitor is reduced to some value lower than its normal sine wave value. This is due to an increase in odd harmonics, as shown in Equation [11-9].

$$I_c = K_c V_c \omega C, \quad \text{[amps]} \tag{11-9}$$

Where, K_c, can vary from 1.0 to 1.5.

Empirically, it has been shown that, for good performance, the primary operating voltage should be as shown in Equation [11-10].

$$V_p = V_{in}(0.95), \quad \text{[volts]} \tag{11-10}$$

When the resonating capacitor is connected across a step-up winding, as is Figure 11-8, both the value of the capacitor and the volume can be reduced. C_n, is the new capacitance value, and, V_n, is the new voltage across the capacitor.

$$C_n V_n^2 = C_{(1-2)} V_{(1-2)}^2 \tag{11-11}$$

The apparent power, P_t, is the sum of each winding, VA, as shown in Equation [11-12].

$$P_t = \left(VA_{(1-2)}\right) + \left(VA_{(2-3)}\right) + \left(VA_{(4-5)}\right), \quad \text{[watts]} \tag{11-12}$$

The line voltage regulation of a constant-voltage transformer is shown in Equation [11-13].

$$\Delta V_p = 4.44 \Delta B_s A_c f N_p \left(10^4\right), \quad \text{[volts]} \tag{11-13}$$

The output voltage regulation of a constant-voltage transformer, for a change in line voltage, is a function of the squareness of the B-H loop, as shown in Figure 11-9. The saturation flux density, B_s, is dependent on the

© 2011 by Taylor and Francis Group, LLC

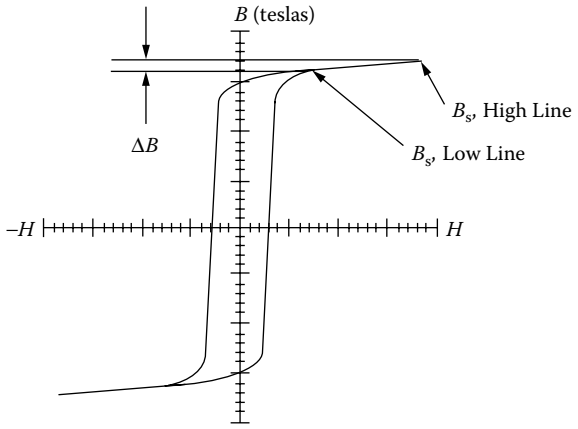

Figure 11-9. B-H Loop of a CVT at High and Low Line.

annealing process of the magnetic material. It seems that each manufacturer has his own annealing process, which has an impact on the saturation flux density, B_s.

Constant-Voltage Transformer, Design Example

Design a Constant-Voltage Transformer (CVT) line regulator with the following specifications:

1. Input voltage = 105-129 volts
2. Line frequency = 60 hertz.
3. Output voltage, V_s = 120 volts
4. Output VA = 250 watts.
5. Transformer current density, J = 300 amps/cm^2
6. Capacitor voltage, V_c = 440 volts
7. Capacitor coefficient, K_c = 1.5
8. Efficiency goal, $\eta(100)$ = 85%
9. Magnetic Material = Silicon
10. Saturating flux density, B_s = 1.95 teslas
11. Window utilization, K_u = 0.4
12. Temperature rise goal, T_r = 50°C

Step No. 1: Calculate the primary voltage, V_p.

$$V_p = V_{in(\min)}(0.95), \quad \text{[volts]}$$

$$V_p = (105)(0.95), \quad \text{[volts]}$$

$$V_p = 99.75, \quad \text{[volts]}$$

© 2011 by Taylor and Francis Group, LLC

Step No. 2: Calculate the reflected resistance, $R_{o(R)}$ back to the primary, including efficiency η.

$$R_{o(R)} = \frac{(V_p)^2 \eta}{P_o}, \quad \text{[ohms]}$$

$$R_{o(R)} = \frac{(99.75)^2 (0.85)}{250}, \quad \text{[ohms]}$$

$$R_{o(R)} = 33.8, \quad \text{[ohms]}$$

Step No. 3: Calculate the required capacitance, C1.

$$C = \frac{1}{0.33\omega R_{o(R)}}, \quad \text{[farads]}$$

$$C = \frac{1}{0.33(377)(33.8)}, \quad \text{[farads]}$$

$$C = 238\left(10^{-6}\right), \quad \text{[farads]}$$

Step No. 4: Calculate the new capacitance value, using the higher voltage, V_c.

$$C_{(1-3)} = \frac{C_{(1-2)} \left(V_{(1-2)}\right)^2}{\left(V_{(1-3)}\right)^2}, \quad \text{[farads]}$$

$$C_{(1-3)} = \frac{\left(238\left(10^{-6}\right)\right)(99.75)^2}{(440)^2}, \quad \text{[farads]}$$

$$C_{(1-3)} = 12.3\left(10^{-6}\right), \quad \text{[farads]}$$

A standard motor run capacitor is a 12.5 μf/440v.

Step No. 5: Calculate the capacitor current, I_c.

$$I_c = 1.5 V_c \omega C, \quad \text{[amps]}$$

$$I_c = 1.5(440)(377)\left(12.5\left(10^{-6}\right)\right), \quad \text{[amps]}$$

$$I_c = 3.11, \quad \text{[amps]}$$

Step No. 6: Calculate the secondary current, I_s.

$$I_s = \frac{P_o}{V_s}, \quad \text{[amps]}$$

$$I_s = \frac{250}{120}, \quad \text{[amps]}$$

$$I_s = 2.08, \quad \text{[amps]}$$

© 2011 by Taylor and Francis Group, LLC

Step No. 7: Calculate the primary current, I_p.

$$I_p = \frac{I_s\left(V_{s(4-5)}\right)}{\eta\left(V_{p(1-2)}\right)}\left(1+\sqrt{\frac{V_{p(1-2)}}{V_{c(1-3)}}}\right), \quad \text{[amps]}$$

$$I_p = \frac{2.08(120)}{(0.85)(99.75)}\left(1+\sqrt{\frac{99.75}{440}}\right), \quad \text{[amps]}$$

$$I_p = 4.35, \quad \text{[amps]}$$

Step No. 8: Calculate the apparent power P_t.

$$P_t = \left(VA_{(1-2)}\right)+\left(VA_{(2-3)}\right)+\left(VA_{(4-5)}\right), \quad \text{[watts]}$$

$$VA_{(1-2)} = V_p I_p = (99.75)(4.35) = 434, \quad \text{[watts]}$$

$$VA_{(2-3)} = \left(V_c - V_p\right)I_c = (340)(3.11) = 1057, \quad \text{[watts]}$$

$$VA_{(4-5)} = V_s I_s = (120)(2.08) = 250, \quad \text{[watts]}$$

$$P_t = (434)+(1057)+(250), \quad \text{[watts]}$$

$$P_t = 1741, \quad \text{[watts]}$$

Step No. 9: Calculate the area product, A_p.

$$A_p = \frac{P_t\left(10^4\right)}{K_f K_u f B_s J}, \quad [\text{cm}^4]$$

$$A_p = \frac{(1742)\left(10^4\right)}{(4.44)(0.4)(60)(1.95)(300)}, \quad [\text{cm}^4]$$

$$A_p = 279, \quad [\text{cm}^4]$$

Step No. 10: Select an, EI, lamination from Chapter Three. The closest lamination to the calculated area product, A_p, is the EI-175.

1. Core Number = EI-175
2. Magnetic Path Length, MPL = 26.7 cm
3. Core Weight, W_{tfe} = 3.71 kilograms
4. Mean Length Turn, MLT = 25.6 cm
5. Iron Area, A_c = 18.8 cm^2
6. Window Area, W_a = 14.8 cm^2
7. Area Product, A_p = 278 cm^4
8. Core Geometry, K_g = 81.7 cm^5
9. Surface Area, A_t = 652 cm^2

© 2011 by Taylor and Francis Group, LLC

Step No. 11: Calculate the number of primary turns, N_p.

$$N_p = \frac{V_p\left(10^4\right)}{K_f B_s f A_c}, \quad \text{[turns]}$$

$$N_p = \frac{(99.75)\left(10^4\right)}{(4.44)(1.95)(60)(18.8)}, \quad \text{[turns]}$$

$$N_p = 102, \quad \text{[turns]}$$

Step No. 12: Calculate the primary bare wire area, $A_{wp(B)}$.

$$A_{wp(B)} = \frac{I_p}{J}, \quad [\text{cm}^2]$$

$$A_{wp(B)} = \frac{(4.35)}{(300)}, \quad [\text{cm}^2]$$

$$A_{wp(B)} = 0.0145, \quad [\text{cm}^2]$$

Step No. 13: Select a wire from the Wire Table in Chapter 4.

$$AWG = \#16$$

$$A_{w(B)} = 0.0131, \quad [\text{cm}^2]$$

$$\left(\frac{\mu\Omega}{\text{cm}}\right) = 132, \quad \text{[micro-ohm/cm]}$$

Step No. 14: Calculate the primary resistance, R_p. Use the MLT from the core data and the micro-ohm per centimeter found in Step 13.

$$R_p = (\text{MLT})\left(N_p\right)\left(\frac{\mu\Omega}{\text{cm}}\right)\left(10^{-6}\right), \quad \text{[ohms]}$$

$$R_p = (25.6)(102)(132)\left(10^{-6}\right), \quad \text{[ohms]}$$

$$R_p = 0.345, \quad \text{[ohms]}$$

Step No. 15: Calculate the primary copper loss, P_p.

$$P_p = \left(I_p\right)^2 R_p, \quad \text{[watts]}$$

$$P_p = (4.35)^2(0.345), \quad \text{[watts]}$$

$$P_p = 6.53, \quad \text{[watts]}$$

© 2011 by Taylor and Francis Group, LLC

Step No. 16: Calculate the required turns for the step-up capacitor winding, N_c.

$$N_c = \frac{N_p\left(V_c - V_p\right)}{V_p}, \quad [\text{turns}]$$

$$N_c = \frac{(102)(440 - 99.75)}{99.75}, \quad [\text{turns}]$$

$$N_c = 348, \quad [\text{turns}]$$

Step No. 17: Calculate the capacitor step-up winding bare wire area, $A_{wc(B)}$.

$$A_{wc(B)} = \frac{I_c}{J}, \quad [\text{cm}^2]$$

$$A_{wc(B)} = \frac{(3.11)}{(300)}, \quad [\text{cm}^2]$$

$$A_{wc(B)} = 0.0104, \quad [\text{cm}^2]$$

Step No. 18: Select a wire from the Wire Table in Chapter 4.

$$AWG = \#17$$

$$A_{w(B)} = 0.0104, \quad [\text{cm}^2]$$

$$\left(\frac{\mu\Omega}{\text{cm}}\right) = 166, \quad [\text{micro-ohm/cm}]$$

Step No. 19: Calculate the capacitor winding resistance, R_c. Use the MLT from the core data and the micro-ohm per centimeter found in Step 18.

$$R_c = (\text{MLT})(N_c)\left(\frac{\mu\Omega}{\text{cm}}\right)\left(10^{-6}\right), \quad [\text{ohms}]$$

$$R_c = (25.6)(348)(166)\left(10^{-6}\right), \quad [\text{ohms}]$$

$$R_c = 1.48, \quad [\text{ohms}]$$

Step No. 20: Calculate the capacitor step-up winding copper loss, P_c.

$$P_c = \left(I_c\right)^2 R_c, \quad [\text{watts}]$$

$$P_c = (3.11)^2(1.48), \quad [\text{watts}]$$

$$P_c = 14.3, \quad [\text{watts}]$$

© 2011 by Taylor and Francis Group, LLC

Step No. 21: Calculate the turns for the secondary, N_s.

$$N_s = \frac{N_p V_s}{V_p}, \quad [\text{turns}]$$

$$N_s = \frac{(102)(120)}{99.75}, \quad [\text{turns}]$$

$$N_s = 123, \quad [\text{turns}]$$

Step No. 22: Calculate the secondary bare wire area, $A_{ws(B)}$.

$$A_{ws(B)} = \frac{I_s}{J}, \quad [\text{cm}^2]$$

$$A_{ws(B)} = \frac{(2.08)}{(300)}, \quad [\text{cm}^2]$$

$$A_{ws(B)} = 0.00693, \quad [\text{cm}^2]$$

Step No. 23: Select a wire from the Wire Table in Chapter 4.

$$AWG = \#19$$

$$A_{w(B)} = 0.00653, \quad [\text{cm}^2]$$

$$\left(\frac{\mu\Omega}{\text{cm}}\right) = 264, \quad [\text{micro-ohm/cm}]$$

Step No. 24: Calculate the secondary winding resistance, R_s. Use the MLT from the core data and the micro-ohm per centimeter found in Step 23.

$$R_s = (\text{MLT})(N_s)\left(\frac{\mu\Omega}{\text{cm}}\right)\left(10^{-6}\right), \quad [\text{ohms}]$$

$$R_s = (25.6)(123)(264)\left(10^{-6}\right), \quad [\text{ohms}]$$

$$R_s = 0.831, \quad [\text{ohms}]$$

Step No. 25: Calculate the secondary winding copper loss, P_s.

$$P_s = (I_s)^2 R_s, \quad [\text{watts}]$$

$$P_s = (2.08)^2(0.831), \quad [\text{watts}]$$

$$P_s = 3.59, \quad [\text{watts}]$$

© 2011 by Taylor and Francis Group, LLC

Step No. 26: Calculate the total copper loss, P_{cu}.

$$P_{cu} = P_p + P_s + P_c, \quad \text{[watts]}$$
$$P_{cu} = (6.53) + (3.59) + (14.3), \quad \text{[watts]}$$
$$P_{cu} = 24.4, \quad \text{[watts]}$$

Step No. 27: Calculate the watts-per-kilogram, W/K, for the appropriate core material. See Chapter 2.

$$W/K = 0.000557 f^{(1.68)} B_s^{(1.86)}, \quad \text{[watts-per-kilogram]}$$
$$W/K = 0.000557(60)^{(1.68)}(1.95)^{(1.86)}, \quad \text{[watts-per-kilogram]}$$
$$W/K = 1.87, \quad \text{[watts-per-kilogram]}$$

Step No. 28: Calculate the core loss in watts, P_{fe}.

$$P_{fe} = (W/K) W_{tfe}, \quad \text{[watts]}$$
$$P_{fe} = (1.87)(3.71), \quad \text{[watts]}$$
$$P_{fe} = 6.94, \quad \text{[watts]}$$

Step No. 29: Calculate the total losses, P_Σ

$$P_\Sigma = P_{cu} + P_{fe}, \quad \text{[watts]}$$
$$P_\Sigma = (24.4) + (6.94), \quad \text{[watts]}$$
$$P_\Sigma = 31.34, \quad \text{[watts]}$$

Step No. 30: Calculate the transformer surface watt density, ψ.

$$\psi = \frac{P_\Sigma}{A_t}, \quad \text{[watts-per-cm}^2\text{]}$$
$$\psi = \frac{(31.34)}{(652)}, \quad \text{[watts-per-cm}^2\text{]}$$
$$\psi = 0.0481, \quad \text{[watts-per-cm}^2\text{]}$$

Step No. 31: Calculate the temperature rise, T_r.

$$T_r = 450(\psi)^{(0.826)}, \quad [°\text{C}]$$
$$T_r = 450(0.0481)^{(0.826)}, \quad [°\text{C}]$$
$$T_r = 36.7, \quad [°\text{C}]$$

© 2011 by Taylor and Francis Group, LLC

Step No. 32: Calculate the transformer efficiency, η

$$\eta = \frac{P_o}{(P_o + P_\Sigma)}(100), \quad [\%]$$

$$\eta = \frac{(250)}{(250 + 31.3)}(100), \quad [\%]$$

$$\eta = 88.9, \quad [\%]$$

Step No. 33: Calculate the window utilization, K_u.

$$K_u = \frac{N_p A_{wp(B)\#16} + N_c A_{wc(B)\#17} + N_s A_{ws(B)\#19}}{W_a}$$

$$K_u = \frac{((102)(0.0131)) + ((348)(0.0104)) + ((123)(0.00653))}{(14.6)}$$

$$K_u = 0.394$$

Series AC Inductor, Design Example

(Also, see Chapter 9.)

Step No. 34: Design a series, linear ac inductor with the following specifications:

1. Applied voltage = 129 volts
2. Line frequency = 60 hertz
3. Current density, J = 300 amp/cm^2
4. Efficiency goal, η(100) = 85%
5. Magnetic material = Silicon
6. Magnetic material permeability, $\mu_m = 1500$
7. Flux density, $B_{ac} = 1.4$ teslas
8. Window utilization, $K_u = 0.4$
9. Waveform factor, $K_f = 4.44$
10. Temperature rise goal, $T_r = 50°C$

Step No. 35: Calculate the required series inductance, L1. See Figure 11-8.

$$L1 = \frac{R_{o(R)}}{2\omega}, \quad [\text{henrys}]$$

$$L1 = \frac{(33.8)}{2(377)}, \quad [\text{henrys}]$$

$$L1 = 0.0448, \quad [\text{henrys}]$$

© 2011 by Taylor and Francis Group, LLC

Step No. 36: Calculate the inductor reactance, X_L.

$$X_L = 2\pi f L1, \quad [\text{ohms}]$$

$$X_L = (6.28)(60)(0.0448), \quad [\text{ohms}]$$

$$X_L = 16.9, \quad [\text{ohms}]$$

Step No. 37: Calculate the short-circuit current, I_L.

$$I_L = \frac{V_{in(\max)}}{X_L}, \quad [\text{amps}]$$

$$I_L = \frac{(129)}{(16.9)}, \quad [\text{amps}]$$

$$I_L = 7.63, \quad [\text{amps}]$$

Step No. 38: Calculate the apparent power, P_t or VA, of the input series inductor, L1. Use the high line voltage of 129 volts and the normal running current, I_p, from Step 7.

$$VA = V_{in(\max)} I_{L(n)}, \quad [\text{watts}]$$

$$VA = (129)(4.35), \quad [\text{watts}]$$

$$VA = 561, \quad [\text{watts}]$$

Step No. 39: Calculate the area product, A_p.

$$A_p = \frac{VA\left(10^4\right)}{K_f K_u f B_{ac} J}, \quad [\text{cm}^4]$$

$$A_p = \frac{(561)\left(10^4\right)}{(4.44)(0.4)(60)(1.4)(300)}, \quad [\text{cm}^4]$$

$$A_p = 125, \quad [\text{cm}^4]$$

Step No. 40: Select an EI lamination from Chapter Three with the closest calculated area product, A_p.

1. Core Number = EI-138
2. Magnetic Path Length, MPL = 21 cm
3. Core Weight, W_{tfe} = 1.79 kilograms
4. Mean Length Turn, MLT = 20.1 cm
5. Iron Area, A_c = 11.6 cm^2
6. Window Area, W_a = 9.15 cm^2
7. Area Product, A_p = 106 cm^4
8. Core Geometry, K_g = 24.5 cm^5
9. Surface Area, A_t = 403 cm^2
10. Winding length, G = 5.24 cm
11. Lamination tongue, E = 3.49 cm

© 2011 by Taylor and Francis Group, LLC

Step No. 41: Calculate the number of inductor turns, N_L.

$$N_L = \frac{V_{in(\max)}\left(10^4\right)}{K_f B_{ac} f A_c}, \quad [\text{turns}]$$

$$N_L = \frac{(129)\left(10^4\right)}{(4.44)(1.4)(60)(11.6)}, \quad [\text{turns}]$$

$$N_L = 298, \quad [\text{turns}]$$

Step No. 42: Calculate the required gap, L_g.

$$l_g = \left(\frac{0.4\pi N_L^2 A_c\left(10^{-8}\right)}{L}\right) - \left(\frac{\text{MPL}}{\mu_m}\right), \quad [\text{cm}]$$

$$l_g = \left(\frac{(1.26)(298)^2(11.6)\left(10^{-8}\right)}{0.0448}\right) - \left(\frac{21}{1500}\right), \quad [\text{cm}]$$

$l_g = 0.276$, [cm] or $l_g = 0.109$, [mils]: This would be 50 mils in each leg.

Step No. 43: Calculate the fringing flux, F.

$$F = \left(1 + \frac{l_g}{\sqrt{A_c}} \ln \frac{2(G)}{l_g}\right)$$

$$F = \left(1 + \frac{0.276}{\sqrt{11.6}} \ln \frac{2(5.24)}{0.276}\right)$$

$$F = 1.29$$

Step No. 44: Using the fringing flux, recalculate the series inductor turns, $N_{L(new)}$.

$$N_{L(new)} = \sqrt{\frac{l_g L}{0.4\pi A_c F\left(10^{-8}\right)}}, \quad [\text{turns}]$$

$$N_{L(new)} = \sqrt{\frac{(0.276)(0.0448)}{(1.26)(11.6)(1.29)\left(10^{-8}\right)}}, \quad [\text{turns}]$$

$$N_{L(new)} = 256, \quad [\text{turns}]$$

Step No. 45: Using the new turns, recalculate the flux density, B_{ac}.

$$B_{ac} = \frac{V_{in(\max)}\left(10^4\right)}{K_f N_{L(new)} A_c f}, \quad [\text{teslas}]$$

$$B_{ac} = \frac{(129)\left(10^4\right)}{(4.44)(256)(11.6)(60)}, \quad [\text{teslas}]$$

$$B_{ac} = 1.63, \quad [\text{teslas}]$$

© 2011 by Taylor and Francis Group, LLC

Step No. 46: Calculate the inductor bare wire area, $A_{wL(B)}$.

$$A_{wL(B)} = \frac{I_{L(n)}}{J}, \quad [\text{cm}^2]$$

$$A_{wL(B)} = \frac{(4.35)}{(300)}, \quad [\text{cm}^2]$$

$$A_{wL(B)} = 0.0145, \quad [\text{cm}^2]$$

Step No. 47: Select a wire from the Wire Table in Chapter 4.

$$AWG = \#16$$

$$A_{w(B)} = 0.01307, \quad [\text{cm}^2]$$

$$\left(\frac{\mu\Omega}{\text{cm}}\right) = 132, \quad [\text{micro-ohm/cm}]$$

Step No. 48: Calculate the inductor winding resistance, R_L. Use the MLT from the core data and the micro-ohm per centimeter found in Step 40.

$$R_L = (\text{MLT})(N_s)\left(\frac{\mu\Omega}{\text{cm}}\right)\left(10^{-6}\right), \quad [\text{ohms}]$$

$$R_L = (20.1)(256)(132)\left(10^{-6}\right), \quad [\text{ohms}]$$

$$R_L = 0.679, \quad [\text{ohms}]$$

Step No. 49: Calculate the inductor winding copper loss, P_L.

$$P_L = (I_L)^2 R_L, \quad [\text{watts}]$$

$$P_L = (4.35)^2(0.679), \quad [\text{watts}]$$

$$P_L = 12.8, \quad [\text{watts}]$$

Step No. 50: Calculate the watts-per-kilogram, W/K, for the appropriate core material. See Chapter 2.

$$W/K = 0.000557 f^{(1.68)} B_s^{(1.86)}, \quad [\text{watts-per-kilogram}]$$

$$W/K = 0.000557(60)^{(1.68)}(1.63)^{(1.86)}, \quad [\text{watts-per-kilogram}]$$

$$W/K = 1.34, \quad [\text{watts-per-kilogram}]$$

© 2011 by Taylor and Francis Group, LLC

Step No. 51: Calculate the core loss in watts, P_{fe}.

$$P_{fe} = \left(W/K\right)W_{tfe}, \quad \text{[watts]}$$
$$P_{fe} = (1.34)(1.79), \quad \text{[watts]}$$
$$P_{fe} = 2.4, \quad \text{[watts]}$$

Step No. 52: Calculate the gap loss, P_g.

$$P_g = K_i E l_g f B_{ac}^2, \quad \text{[watts]}$$
$$P_g = (0.155)(3.49)(0.276)(60)(1.63)^2, \quad \text{[watts]}$$
$$P_g = 23.8, \quad \text{[watts]}$$

Step No. 53: Calculate the total losses, P_Σ

$$P_\Sigma = P_{cu} + P_{fe} + P_g, \quad \text{[watts]}$$
$$P_\Sigma = (12.8) + (2.4) + (23.8), \quad \text{[watts]}$$
$$P_\Sigma = 39, \quad \text{[watts]}$$

Step No. 54: Calculate the inductor surface area watt density, ψ.

$$\psi = \frac{P_\Sigma}{A_t}, \quad \text{[watts-per-cm}^2\text{]}$$
$$\psi = \frac{(39)}{(403)}, \quad \text{[watts-per-cm}^2\text{]}$$
$$\psi = 0.0968, \quad \text{[watts-per-cm}^2\text{]}$$

Step No. 55: Calculate the temperature rise, T_r.

$$T_r = 450\left(\psi\right)^{(0.826)}, \quad [^\circ\text{C}]$$
$$T_r = 450(0.0968)^{(0.826)}, \quad [^\circ\text{C}]$$
$$T_r = 65, \quad [^\circ\text{C}]$$

Step No. 56: Calculate the window utilization, K_u.

$$K_u = \frac{N_{L(new)} A_{w(B)\#16}}{W_a}$$
$$K_u = \frac{\left((256)(0.0131)\right)}{(9.15)}$$
$$K_u = 0.367$$

© 2011 by Taylor and Francis Group, LLC

References

1. Ruben, L., and Stephens, D. Gap Loss in Current-Limiting Transformer. *Electromechanical Design*, April, 1973, pp. 24–126.

2. H. P. Hart and R. J. Kakalec, "The Derivation and Application of Design Equations for Ferroresonant Voltage Regulators and Regulated Rectifiers," *IEEE Trans. Magnetics*, vol. Mag-7, No.1, March, 1971, pp. 205–211.

3. I. B. Friedman, "The Analysis and Design of Constant Voltage Regulators," *IRE Trans. Component Parts*, vol. CP-3, March, 1956, pp. 11–14.

4. S. Lendena, "Design of a Magnetic Voltage Stabilizer." *Electronics Technology*, May, 1961, pp. 154–155.

© 2011 by Taylor and Francis Group, LLC

Chapter 12

Three-Phase Transformer Design

© 2011 by Taylor and Francis Group, LLC

Table of Contents

1. Introduction....12-3
2. Primary Circuit....12-3
3. Comparing Transformer, Physical Size....12-4
4. Phase Current, Line Current, and Voltage in a Delta System....12-6
5. Phase Voltage, Line Voltage, and Current in a Wye System....12-6
6. Comparing Multiphase and Single-Phase Power....12-7
7. Multiphase Rectifier Circuits....12-8
8. Area Product, A_p, and Core Geometry, K_g, for Three Phase Transformers....12-10
9. Output Power Versus Apparent Power, P_t, Capability....12-11
10. Relationship, K_g, to Power Transformer Regulation Capability....12-12
11. Relationship, A_p, to Transformer Power Handling Capability....12-13
12. Three-Phase, Transformer Design Example....12-13

© 2011 by Taylor and Francis Group, LLC

Introduction

Three-phase power is used almost exclusively for generation, transmission, and distribution, as well as for all industrial uses. It is also used on aircraft, both commercial and military. It has many advantages over single-phase power. The transformer can be made smaller and lighter for the same power handling capability, because the copper and iron are used more effectively. In circuitry, for conversion from ac to dc, the output contains a much lower ripple amplitude, and a higher frequency component, which is 3 times and 6 times the line frequency, and which, in turn, requires less filtering.

Primary Circuit

The two most commonly used primary circuits for three-phase transformers are the Star, or Y connection, as shown in Figure 12-1, and the other being known as the Delta (Δ) connection, as shown in Figure 12-2. The design requirement for each particular job dictates which method of connection will be used.

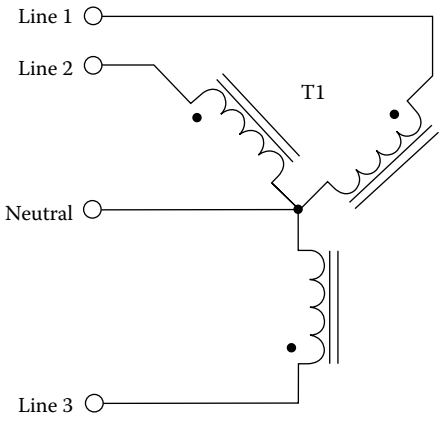

Figure 12-1. Three-Phase Transformer, Connected in Star.

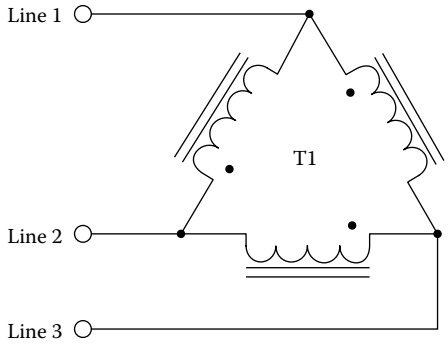

Figure 12-2. Three-Phase Transformer, Connected in Delta.

© 2011 by Taylor and Francis Group, LLC

Comparing Transformer, Physical Size

The schematic diagram in Figure 12-3, shows the connection of three single-phase transformers: (a) Operating from a three-phase power source and a single three-phase transformer; and (b) Operating from a three-phase power source connected in a delta-delta configuration. The single three-phase transformer, T4, would be lighter and smaller than a bank of three single-phase transformers of the same total rating. Since the windings of the three-phase transformer are placed on a common magnetic core, rather than on three independent cores, the consolidation results in an appreciable savings in the copper, the core, and the insulating materials.

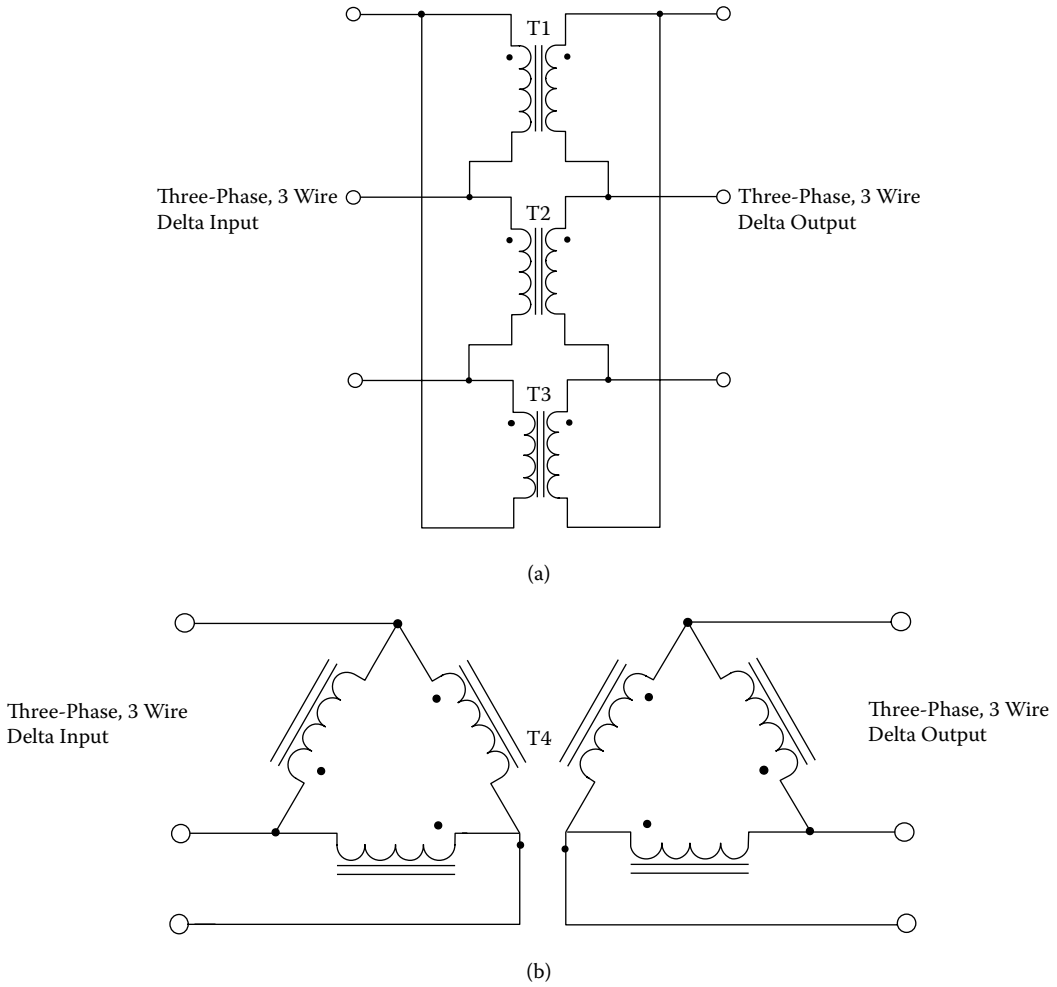

Figure 12-3. Comparing Three Single-Phase Transformers Connected in Three-Phase Delta.

A cutaway view of a single-phase transformer, showing the window area and iron area of two types of core configuration, is shown in Figure 12-4 and Figure 12-5. The EI lamination, shown in Figure 12-4, is known as a shell type, because it looks like the core surrounds the coil. The C core, shown in Figure 12-5, is known as a core type, because it looks like the coil surrounds the core.

© 2011 by Taylor and Francis Group, LLC

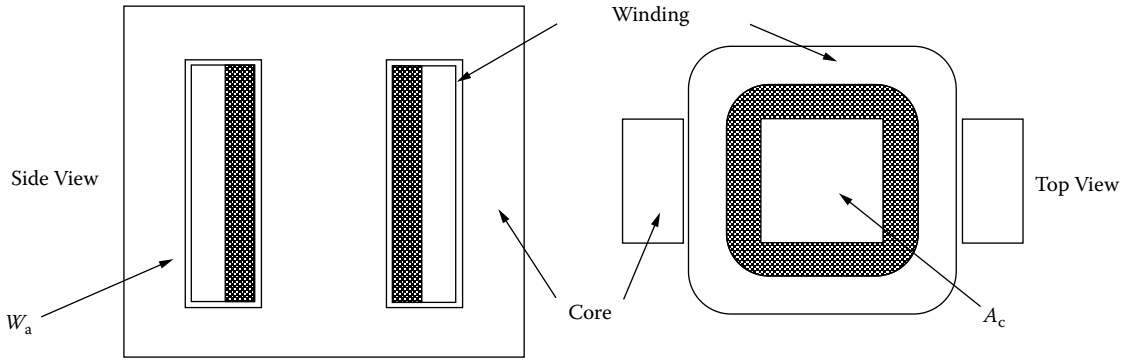

Figure 12-4. Illustrating a Shell Type Transformer.

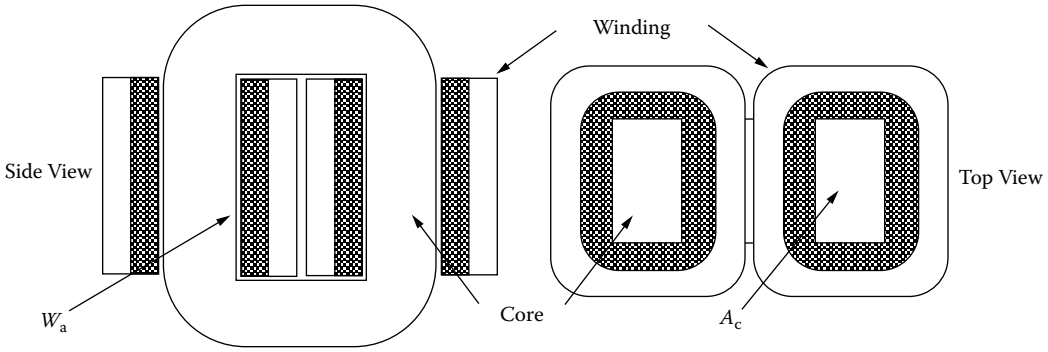

Figure 12-5. Illustrating a Core Type Transformer.

Cutaway views of a three-phase transformer are shown in Figure 12-6. These cross-sectional views show the window and iron areas. The three-legged core is designed to take advantage of the fact that, with balanced voltages impressed, the flux in each phase leg, adds up to zero. Therefore, no return leg is needed under normal conditions. When the transformer is subjected to unbalanced loads, or unbalanced line voltages, it may be best to use three single-phase transformers, because of the high-circulating currents.

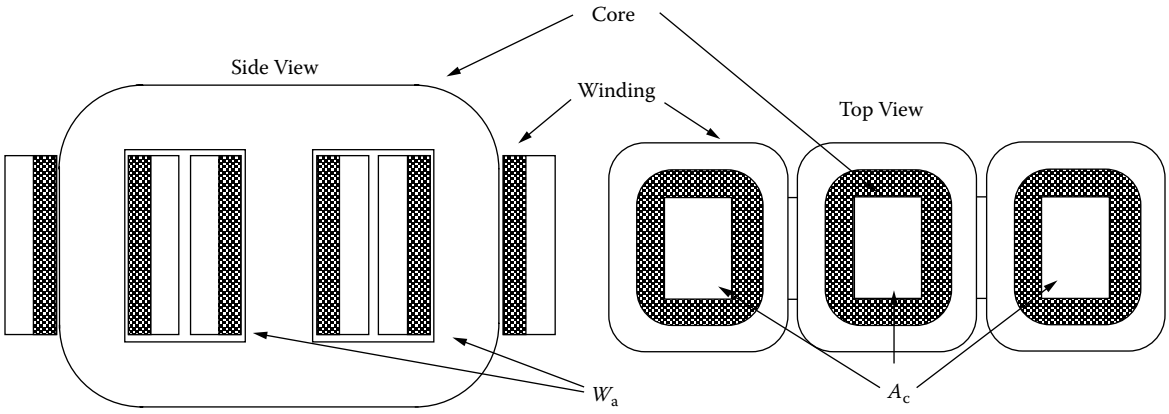

Figure 12-6. Cutaway View of a Three-Phase Transformer.

© 2011 by Taylor and Francis Group, LLC

Phase Current, Line Current, and Voltage in a Delta System

In a Three-Phase Delta Circuit, such as the one shown in Figure 12-7, the line voltage and line current are commonly called phase voltage and phase current. The line voltage, $E_{(Line)}$, will be the same as the actual winding voltage of the transformer. However, the line current, $I_{(Line)}$, is equal to the phase current, $I_{(Phase)}$, times the square root of 3, as shown in Equation [12-1].

$$I_{(line)} = I_{(phase)}\sqrt{3}, \quad \text{[amps]} \tag{12-1}$$

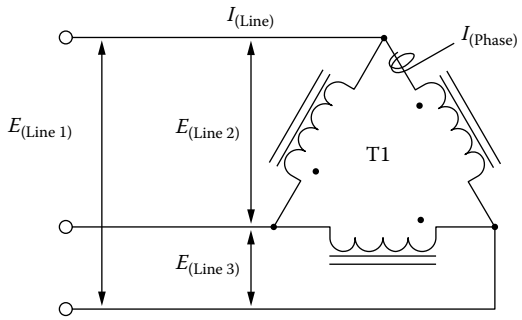

Figure 12-7. Voltage and Current Relationship of a Three-Phase Delta Circuit.

Phase Voltage, Line Voltage, and Current in a Wye System

The relationship between the Line voltage, Line current and the winding, or Phase voltage and Phase current, in a Three-Phase Wye Circuit can be seen in Figure 12-8. In a Wye System, the voltage between any two wires in the line will always be the square root of three times the phase voltage, $E_{(Phase)}$, between the neutral, and any one of the lines, as shown in Equation [12-2].

$$E_{(phase)} = \frac{E_{(line)}}{\sqrt{3}}, \quad \text{[volts]} \tag{12-2}$$

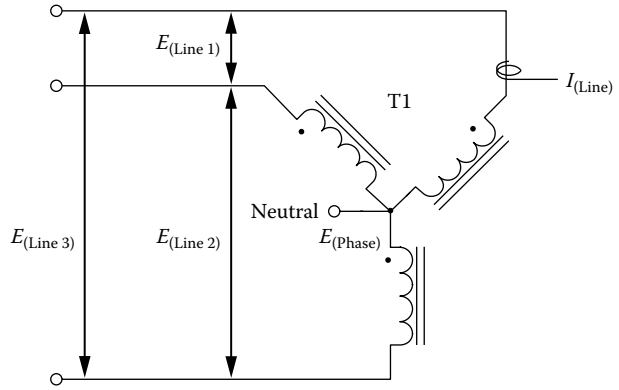

Figure 12-8. Voltage and Current Relationship for a Three-Phase Wye Circuit.

© 2011 by Taylor and Francis Group, LLC

Comparing Multiphase and Single-Phase Power

Three-phase power distribution has a significant advantage over the single-phase. Most high power equipment and industrial complexes will use three-phase power. One of the biggest advantages in using three-phase power distribution has to do with smaller magnetic components handling the same power as single-phase. This can be seen in aircraft and shipboard equipment, as well as fixed ground installations. One of the basic reasons for selecting three-phase is the transformer size. Another reason is, if dc is a requirement, the capacitor and inductor filtering components are both smaller. The odd shape of a three-phase transformer could be troublesome, as well as the keeping of balanced loads to minimize circulating currents.

The single-phase, full wave bridge circuit is shown in Figure 12-9. The ripple voltage frequency is always twice the line frequency. Only 50% of the total current flows through each rectifier. The three-phase, Delta full wave bridge circuit is shown in Figure 12-10. The ripple voltage frequency is always 6 times the line frequency. Only 33% of the total current flows through each rectifier. Looking at the ripple in Figure 12-10, it is obvious the LC components will be smaller.

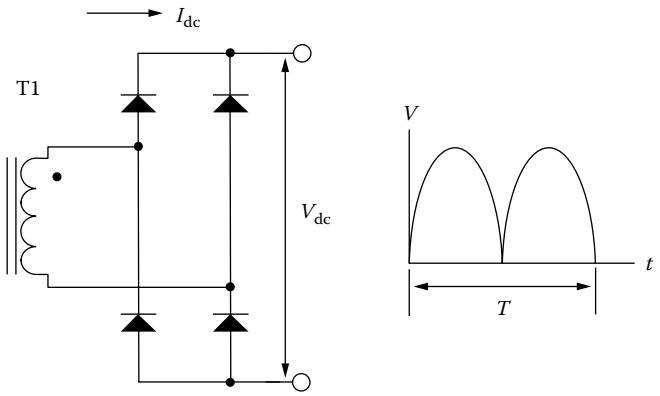

Figure 12-9. Single-Phase Full Wave Bridge.

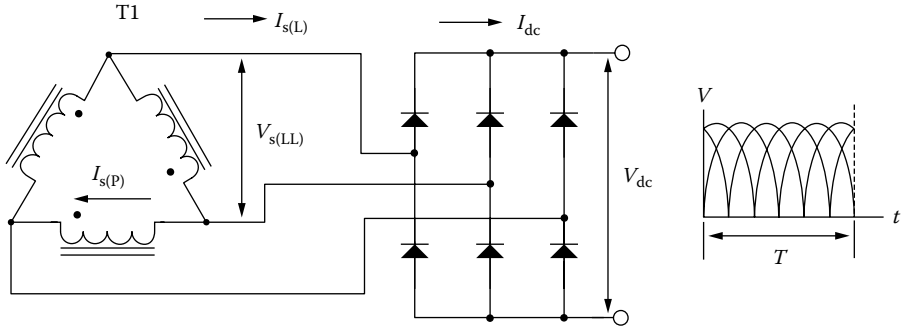

Figure 12-10. Three-Phase, "Delta" Full Wave Bridge.

© 2011 by Taylor and Francis Group, LLC

Multiphase Rectifier Circuits

Table 12-1 lists voltage and current ratios for the circuits, shown in Figures 12-11 through Figures 12-14 for inductive output filters. These ratios apply for sinusoidal ac input voltages. The values that are shown do not take into consideration voltage drops, which occur in the power transformer or rectifier diodes.

Table 12-1. Three-Phase Voltage and Current Ratios for Rectifier Circuits

Three Phase Rectifier Circuit Data			
Delta-Delta Full Wave, Figure 12-11			
Item	Factor		
Primary VA	1.050	×	dc watts output
Secondary V/leg	0.740	×	average dc output voltage
Secondary I/leg	0.471	×	average dc output current
Secondary VA	1.050	×	dc watts output
Ripple Voltage %	4.200		
Ripple Frequency	6f		
Delta-Wye Full Wave, Figure 12-12			
Item	Factor		
Primary VA	1.050	×	dc watts output
Secondary Line to Line	0.740	×	average dc output voltage
Secondary V/leg	0.428 to Neutral	×	average dc output voltage
Secondary I/leg	0.817	×	average dc output current
Secondary VA	1.050	×	dc watts output
Ripple Voltage %	4.200		
Ripple Frequency	6f		
Delta-Wye Half Wave, Figure 12-13			
Item	Factor		
Primary VA	1.210	×	dc watts output
Secondary Line to Line	0.740	×	average dc output voltage
Secondary V/leg	0.855 to Neutral	×	average dc output voltage
Secondary I/leg	0.577	×	average dc output current
Secondary VA	1.480	×	dc watts output
Ripple Voltage %	18.000		
Ripple Frequency	3f		
Delta-Wye 6 Phase Half Wave, Figure 12-14			
Item	Factor		
Primary VA	1.280	×	dc watts output
Secondary Line to Line	1.480	×	average dc output voltage
Secondary V/leg	0.740 to Neutral	×	average dc output voltage
Secondary I/leg	0.408	×	average dc output current
Secondary VA	1.810	×	dc watts output
Ripple Voltage %	4.200		
Ripple Frequency	6f		
Root mean square values to the average dc. Sine-wave, infinite inductance, no transformer or rectifier losses.			

© 2011 by Taylor and Francis Group, LLC

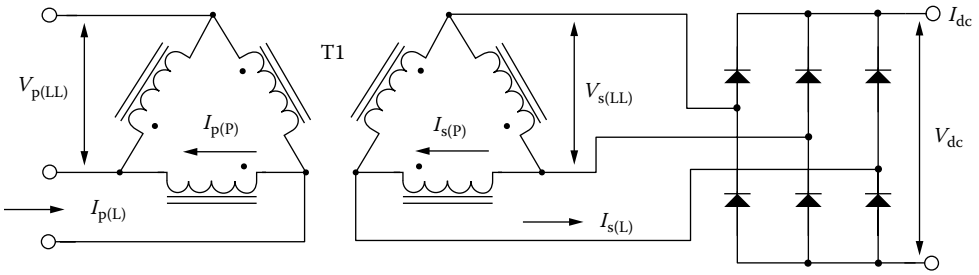

Figure 12-11. Three-Phase, "Delta-Delta" Full Wave Bridge.

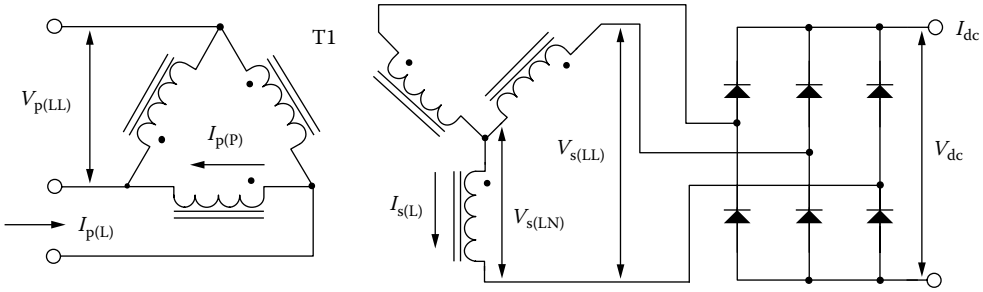

Figure 12-12. Three-Phase, "Delta-Wye" Full Wave Circuit.

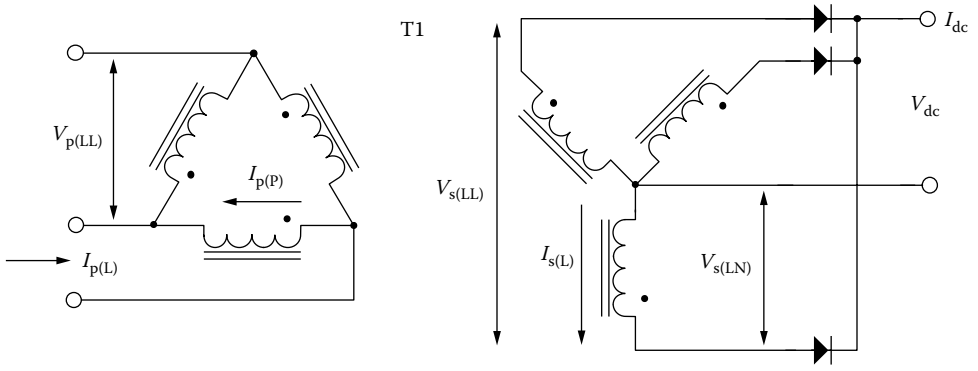

Figure 12-13. Three-Phase, "Delta-Wye" Half Wave Bridge.

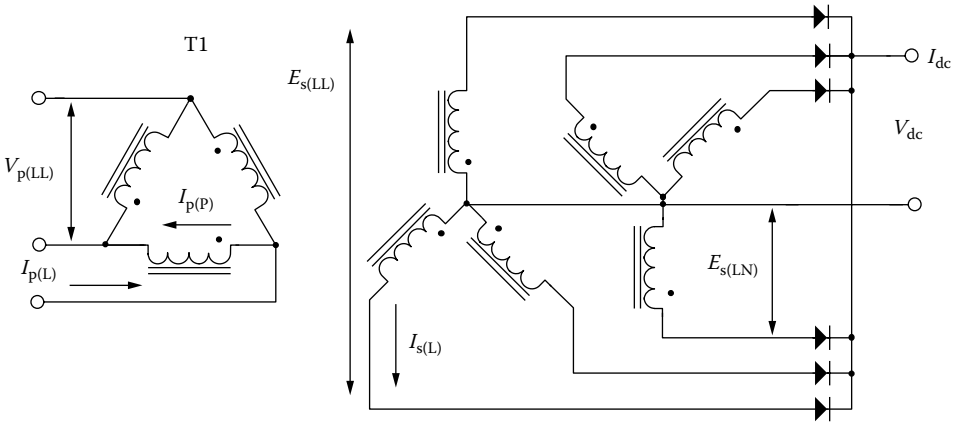

Figure 12-14. Three-Phase, "Delta-Wye" Six Phase Star.

© 2011 by Taylor and Francis Group, LLC

Area Product, A_p, and Core Geometry, K_g, for Three Phase Transformers

The area product, A_p, of a three-phase core is defined differently than that for a single-phase core. The window area, W_a, and iron area, A_c, for a single-phase transformer are shown in Figure 12-4 and 12-5. The window area, W_a, and iron area, A_c, for a three-phase transformer are shown in Figure 12-6. The area product, A_p, of a core is the product of the available window area, W_a, of the core in square centimeters, (cm^2), multiplied by the effective, cross-section area, A_c, in square centimeters, (cm^2), which may be stated as shown, in Equation [12-3].

$$\text{Single-phase}: \; A_p = W_a A_c, \quad [\text{cm}^4] \tag{12-3}$$

This is correct for a single-phase transformer. For three-phase transformers, because there are basically two window areas, W_a, and three iron areas, A_c, the window utilization is different, and the area product, A_p, changes to the Equation [12-4].

$$\text{Three-phase}: \; A_p = 3\left(\frac{W_a}{2} A_c\right), \quad [\text{cm}^4] \tag{12-4}$$

This reduces to Equation [12-5].

$$A_p = 1.5\left(W_a A_c\right), \quad [\text{cm}^4] \tag{12-5}$$

It is basically the same thing for the core geometry, K_g, for a single-phase transformer and the core geometry, K_g, for a three-phase transformer. The core geometry, K_g, for a single-phase transformer is shown in Equation [12-6].

$$\text{Single-phase}: \; K_g = \left(\frac{W_a A_c^2 K_u}{\text{MLT}}\right), \quad [\text{cm}^5] \tag{12-6}$$

In the three-phase transformer, core geometry, K_g, is shown in Equation [12-7].

$$\text{Three-phase}: \; K_g = 3\left(\left(\frac{W_a}{2}\right)\frac{A_c^2 K_u}{\text{MLT}}\right), \quad [\text{cm}^5] \tag{12-7}$$

This reduces to Equation [12-8].

$$K_g = 1.5\left(\frac{W_a A_c^2 K_u}{\text{MLT}}\right), \quad [\text{cm}^5] \tag{12-8}$$

© 2011 by Taylor and Francis Group, LLC

Output Power Versus Apparent Power, P_t, Capability

The apparent power, P_t, is described in detail in Chapter 7. The apparent power, P_t, of a transformer is the combined power of the primary and secondary windings, which handle, P_{in} and P_o, to the load, respectively. Since the power transformer has to be designed to accommodate the primary, P_{in}, and the secondary, P_o the apparent power is shown in Equation [12-9].

$$P_t = P_{in} + P_o, \quad \text{[watts]} \tag{12-9}$$

$$P_{in} = \frac{P_o}{\eta}, \quad \text{[watts]} \tag{12-10}$$

Substituting:

$$P_t = \frac{P_o}{\eta} + P_o, \quad \text{[watts]} \tag{12-11}$$

$$P_t = P_o\left(\frac{1}{\eta} + 1\right), \quad \text{[watts]} \tag{12-12}$$

The designer must be concerned with the apparent power handling capability, P_t, of the transformer core and winding. The apparent power, P_t, varies with the type of circuit in which the transformer is used. If the current in the rectifier is interrupted, its effective rms value changes. Transformer size is thus determined, not only by the load demand, but also by current wave shape. An example of the primary and secondary, VA, is shown to compare the power-handling capability required by each three-phase rectifier circuit in Table 12-1 and Figures 12-11 through 12-14. This comparison will negate transformer and diode losses so that $P_{in} = P_o$ ($\eta = 1$) for all three-phase rectifier circuits.

1. The apparent power, P_t, for a Delta-Delta, Full Wave, from Figure 12-11 is shown in Equation [12-13].

$$\begin{aligned} P_t &= P_o\left(\frac{P_{VA}}{\eta} + S_{VA}\right), \quad \text{[watts]} \\ P_t &= P_o\left(\frac{1.05}{1} + 1.05\right), \quad \text{[watts]} \\ P_t &= P_o(2.1), \quad \text{[watts]} \end{aligned} \tag{12-13}$$

2. The apparent power, P_t, for a Delta-Wye, Full Wave, from Figure 12-12 is shown in Equation [12-14].

$$\begin{aligned} P_t &= P_o\left(\frac{P_{VA}}{\eta} + S_{VA}\right), \quad \text{[watts]} \\ P_t &= P_o\left(\frac{1.05}{1} + 1.05\right), \quad \text{[watts]} \\ P_t &= P_o(2.1), \quad \text{[watts]} \end{aligned} \tag{12-14}$$

© 2011 by Taylor and Francis Group, LLC

3. The apparent power, P_t, for a Delta-Wye, Half Wave, from Figure 12-13 is shown in Equation [12-15].

$$\begin{aligned} P_t &= P_o\left(\frac{P_{VA}}{\eta} + S_{VA}\right), \quad \text{[watts]} \\ P_t &= P_o\left(\frac{1.21}{1} + 1.48\right), \quad \text{[watts]} \\ P_t &= P_o(2.69), \quad \text{[watts]} \end{aligned} \tag{12-15}$$

4. The apparent power, P_t, for a Delta-Wye, 6 Phase Wave, from Figure 12-14 is shown in Equation [12-16].

$$\begin{aligned} P_t &= P_o\left(\frac{P_{VA}}{\eta} + S_{VA}\right), \quad \text{[watts]} \\ P_t &= P_o\left(\frac{1.28}{1} + 1.81\right), \quad \text{[watts]} \\ P_t &= P_o(3.09), \quad \text{[watts]} \end{aligned} \tag{12-16}$$

Relationship, K_g, to Power Transformer Regulation Capability

Although most transformers are designed for a given temperature rise, they can also be designed for a given regulation. The regulation and power-handling ability of a core are related to two constants:

$$\alpha = \frac{P_t}{2K_g K_e}, \quad [\%] \tag{12-17}$$

$$\alpha = \text{Regulation } (\%) \tag{12-18}$$

The constant, K_g, is determined by the core geometry, which is shown in Equation [12-19].

$$K_g = 1.5\left(\frac{W_a A_c^2 K_u}{\text{MLT}}\right) = \frac{P_t}{2K_e\alpha}, \quad [\text{cm}^5] \tag{12-19}$$

The constant, K_e, is determined by the magnetic and electric operating conditions, which is shown in Equation [12-20].

$$K_e = 2.86 f^2 B^2 \left(10^{-4}\right) \tag{12-20}$$

From the above, it can be seen that factors, such as flux density, frequency of operation, and waveform coefficient, have an influence on the transformer size.

© 2011 by Taylor and Francis Group, LLC

Relationship, A_p, to Transformer Power Handling Capability

According to the newly developed approach, the power handling capability of a core is related to its area product, A_p, for a single phase as shown in Equation [12-21], and a three phase as shown in Equation [12-22].

$$A_p = \frac{P_t\left(10^4\right)}{K_f K_u B_m J f}, \quad [\text{cm}^4] \qquad [12\text{-}21]$$

$$A_p = 1.5\left(W_a A_c\right) = \frac{P_t\left(10^4\right)}{K_f K_u B_m J f}, \quad [\text{cm}^4] \qquad [12\text{-}22]$$

Where:

K_f = waveform coefficient

K_f = 4.0 square wave

K_f = 4.44 sine wave

From the above, it can be seen that factors such as flux density, frequency of operation, and window utilization factor, K_u, define the maximum space, which may be occupied by the copper in the window.

Three-Phase, Transformer Design Example

The following information is the Design specification for a three-phase, isolation transformer, using the K_g, core geometry approach.

Design specification:

1. Input voltage, V_{in} = 208 V, 3 Wire
2. Output voltage, V_o = 28 V
3. Output Current, I_o = 10 amps
4. Output Circuit = Full Bridge
5. Input / Output = Delta / Delta
6. Frequency, Three Phase, f = 60 hertz
7. Efficiency, $\eta(100)$ = 95 %
8. Regulation, α = 5 %
9. Flux Density, B_{ac} = 1.4 teslas
10. Magnetic Material = Silicon M6X
11. Window Utilization $K_u = (K_{up} + K_{us})$ = 0.4
12. Diode Drop, V_d = 1.0 volt

© 2011 by Taylor and Francis Group, LLC

Step No. 1: Calculate the apparent power, P_t.

$$P_t = P_o\left(\frac{1.05}{\eta} + 1.05\right), \quad [\text{watts}]$$

$$P_o = I_o\left(V_o + 2V_d\right) = (10)(30) = 300, \quad [\text{watts}]$$

$$P_t = 300\left(\frac{1.05}{0.95} + 1.05\right), \quad [\text{watts}]$$

$$P_t = 647, \quad [\text{watts}]$$

Step No. 2: Calculate the electrical conditions, K_e.

$$K_e = 2.86 f^2 B^2 \left(10^{-4}\right)$$

$$K_e = 2.86(60)^2(1.4)^2 \left(10^{-4}\right)$$

$$K_e = 2.02$$

Step No. 3: Calculate the core geometry, K_g.

$$K_g = \frac{P_t}{2K_e \alpha}, \quad [\text{cm}^5]$$

$$K_g = \frac{647}{2(2.02)(5)}, \quad [\text{cm}^5]$$

$$K_g = 32, \quad [\text{cm}^5]$$

Step No. 4: This data is taken from Chapter 3. The section is on, EI, Three-Phase Laminations.

Core number = 100EI-3P

Iron weight, W_{tfe} = 2.751 kilograms

Mean length turn, MLT = 16.7 cm

Iron area, A_c = 6.129 cm^2

Window area, W_a = 29.0 cm^2

Area product, A_p = 267cm^4

Core geometry, K_g = 39 cm^5

Surface area, A_t = 730 cm^2

Step No. 5: Calculate the number of primary turns, N_p, using Faraday's Law.

$$N_p = \frac{V_{p(Line)}\left(10^4\right)}{4.44 B_{ac} A_c f}, \quad [\text{turns}]$$

$$N_p = \frac{208\left(10^4\right)}{4.44(1.4)(6.129)(60)}, \quad [\text{turns}]$$

$$N_p = 910, \quad [\text{turns}]$$

© 2011 by Taylor and Francis Group, LLC

Step No. 6: Calculate the primary line current, $I_{p(Line)}$.

$$I_{p(Line)} = \frac{P_o}{3V_{p(Line)}\eta}, \quad [\text{amps}]$$

$$I_{p(Line)} = \frac{300}{3(208)(0.95)}, \quad [\text{amps}]$$

$$I_{p(Line)} = 0.506, \quad [\text{amps}]$$

Step No. 7: Calculate the primary phase current, $I_{p(phase)}$.

$$I_{p(Phase)} = \frac{I_{p(Line)}}{\sqrt{3}}, \quad [\text{amps}]$$

$$I_{p(Phase)} = \frac{0.506}{1.73}, \quad [\text{amps}]$$

$$I_{p(Phase)} = 0.292, \quad [\text{amps}]$$

Step No. 8: Calculate the primary bare wire area, $A_{wp(B)}$. The window area available for the primary is, W_a / 4. The primary window utilization is, $K_{up} = 0.2$.

$$A_{wp(B)} = \left(\frac{K_{u(p)}W_a}{4N_p}\right), \quad [\text{cm}^2]$$

$$A_{wp(B)} = \left(\frac{(0.2)(29.0)}{4(910)}\right), \quad [\text{cm}^2]$$

$$A_{wp(B)} = 0.00159, \quad [\text{cm}^2]$$

Step No. 9: The selection of the wire would be from the Wire Table, in Chapter 4.

$$AWG \ \#25$$

$$A_{w(B)} = 0.001623, \quad [\text{cm}^2]$$

$$A_{w(Ins)} = 0.002002, \quad [\text{cm}^2]$$

$$\frac{\mu\Omega}{\text{cm}} = 1062$$

Step No. 10: Calculate the primary winding resistance. Use the MLT, from Step 4, and the micro-ohm, per centimeter, found in Step 9.

$$R_p = \text{MLT}(N_p)\left(\frac{\mu\Omega}{\text{cm}}\right)\left(10^{-6}\right), \quad [\text{ohms}]$$

$$R_p = (16.7)(910)(1062)\left(10^{-6}\right), \quad [\text{ohms}]$$

$$R_p = 16.1, \quad [\text{ohms}]$$

© 2011 by Taylor and Francis Group, LLC

Step No. 11: Calculate the total primary copper loss, P_p.

$$P_p = 3\left(I_{p(phase)}\right)^2 R_p, \quad \text{[watts]}$$

$$P_p = 3(0.292)^2(16.1), \quad \text{[watts]}$$

$$P_p = 4.12, \quad \text{[watts]}$$

Step No. 12: Calculate the secondary turns, N_s.

$$N_s = \frac{N_p V_s}{V_p}\left(1 + \frac{\alpha}{100}\right), \quad \text{[turns]}$$

$$V_s = (0.740)(V_o + 2V_d) = (0.740)(28 + 2) = 22.2$$

$$N_s = \frac{(910)(22.2)}{(208)}\left(1 + \frac{5}{100}\right), \quad \text{[turns]}$$

$$N_s = 102, \quad \text{[turns]}$$

Step No. 13: Calculate the secondary bare wire area, $A_{ws(B)}$.

$$A_{ws(B)} = \left(\frac{K_{u(s)} W_a}{4N_s}\right), \quad [\text{cm}^2]$$

$$A_{ws(B)} = \left(\frac{(0.2)(29.0)}{4(102)}\right), \quad [\text{cm}^2]$$

$$A_{ws(B)} = 0.0142, \quad [\text{cm}^2]$$

Step No. 14: The selection of the wire will be from the Wire Table in Chapter 4.

$$AWG\ \#16$$

$$A_{w(B)} = 0.01307, \quad [\text{cm}^2]$$

$$A_{w(Ins)} = 0.01473, \quad [\text{cm}^2]$$

$$\frac{\mu\Omega}{\text{cm}} = 132$$

Step No. 15: Calculate the secondary winding resistance, R_s. Use the MLT, from Step 4, and the micro-ohm per centimeter, found in Step 14.

$$R_s = \text{MLT}(N_s)\left(\frac{\mu\Omega}{\text{cm}}\right)\left(10^{-6}\right), \quad \text{[ohms]}$$

$$R_s = (16.7)(102)(132)\left(10^{-6}\right), \quad \text{[ohms]}$$

$$R_s = 0.225, \quad \text{[ohms]}$$

© 2011 by Taylor and Francis Group, LLC

Step No. 16: Calculate the secondary line current, $I_{s(line)}$.

$$I_{s(line)} = (0.471) I_o, \quad [\text{amps}]$$
$$I_{s(line)} = (0.471)(10), \quad [\text{amps}]$$
$$I_{s(line)} = 4.71, \quad [\text{amps}]$$

Step No. 17: Calculate the secondary phase current, $I_{s(phase)}$.

$$I_{s(phase)} = \frac{I_{s(line)}}{\sqrt{3}}, \quad [\text{amps}]$$
$$I_{s(phase)} = \frac{4.71}{1.73}, \quad [\text{amps}]$$
$$I_{s(phase)} = 2.72, \quad [\text{amps}]$$

Step No. 18: Calculate the total secondary copper loss, P_s.

$$P_s = 3\left(I_{s(phase)}\right)^2 R_s, \quad [\text{watts}]$$
$$P_s = 3(2.72)^2 (0.225), \quad [\text{watts}]$$
$$P_s = 4.99, \quad [\text{watts}]$$

Step No. 19: Calculate the transformer regulation, α.

$$\alpha = \frac{P_{cu}}{P_o}(100), \quad [\%]$$
$$P_{cu} = P_p + P_s, \quad [\text{watts}]$$
$$P_{cu} = 4.12 + 4.99, \quad [\text{watts}]$$
$$P_{cu} = 9.11, \quad [\text{watts}]$$
$$\alpha = \left(\frac{9.11}{300}\right)(100), \quad [\%]$$
$$\alpha = 3.03, \quad [\%]$$

Step No. 20: Calculate the watts per kilogram.

$$\text{Watts/kilogram} = K f^{(m)} B_{ac}^{(n)}$$
$$\text{Watts/kilogram} = 0.000557(60)^{(1.68)} (1.40)^{(1.86)}$$
$$\text{Watts/kilogram} = 1.01$$

© 2011 by Taylor and Francis Group, LLC

Step No. 21: Calculate the core loss, P_{fe}. Core weight, W_{tfe}, is found in Step 4.

$$P_{fe} = \text{Watts/Kilogram}\left(W_{tfe}\right), \quad [\text{watts}]$$
$$P_{fe} = 1.01(2.751), \quad [\text{watts}]$$
$$P_{fe} = 2.78, \quad [\text{watts}]$$

Step No. 22: Summarize the total transformer losses, P_{Σ}.

$$P_{\Sigma} = P_p + P_s + P_{fe}, \quad [\text{watts}]$$
$$P_{\Sigma} = 4.12 + 4.99 + 2.78, \quad [\text{watts}]$$
$$P_{\Sigma} = 11.89, \quad [\text{watts}]$$

Step No. 23: Calculate the transformer efficiency, η.

$$\eta = \frac{P_o}{P_o + P_{\Sigma}}(100), \quad [\%]$$
$$\eta = \frac{300}{300 + 11.89}(100), \quad [\%]$$
$$\eta = 96.2, \quad [\%]$$

Step No. 24: Calculate the watts per unit area, ψ. The surface area, A_t, is found in Step 4.

$$\psi = \frac{P_{\Sigma}}{A_t}, \quad [\text{watts per cm}^2]$$
$$\psi = \frac{(11.89)}{(730)}, \quad [\text{watts per cm}^2]$$
$$\psi = 0.0163, \quad [\text{watts per cm}^2]$$

Step No. 25: Calculate the temperature rise, T_r. The watts per unit area ψ is found in Step 24.

$$T_r = 450\left(\psi\right)^{0.826}, \quad [^{\circ}\text{C}]$$
$$T_r = 450\left(0.0163\right)^{0.826}, \quad [^{\circ}\text{C}]$$
$$T_r = 15, \quad [^{\circ}\text{C}]$$

© 2011 by Taylor and Francis Group, LLC

Step No. 26: Calculate the total window utilization, K_u. The window area is found in Step 4.

$$K_u = K_{up} + K_{us}$$

$$K_u = \frac{4N_p A_{wp(B)(25)}}{W_a} + \frac{4N_s A_{ws(B)(16)}}{W_a}$$

$$K_u = \frac{4(910)(0.001623)}{29} + \frac{4(102)(0.01307)}{29}$$

$$K_u = (0.204) + (0.184)$$

$$K_u = 0.388$$

© 2011 by Taylor and Francis Group, LLC

Chapter 13

Flyback Converters, Transformer Design

© 2011 by Taylor and Francis Group, LLC

Table of Contents

1. Introduction....13-3
2. Energy Transfer....13-3
3. Discontinuous Current Mode....13-4
4. Continuous Current Mode....13-4
5. Continuous and Discontinuous Boundary....13-5
6. The Buck Converter....13-5
7. Discontinuous Current, Buck Converter Design Equations....13-5
8. Continuous Current, Buck Converter Design Equations....13-6
9. The Boost Converter....13-8
10. Discontinuous Current, Boost Converter Design Equations....13-8
11. Continuous Current, Boost Converter Design Equations....13-9
12. The Inverting Buck-Boost Converter....13-10
13. Discontinuous Current, Inverting Buck-Boost Design Equations....13-11
14. Continuous Current, Inverting Buck-Boost Design Equations....13-12
15. The Isolated, Buck-Boost Converter....13-13
16. Discontinuous Current, Isolated Buck-Boost Design Equations....13-14
17. Continuous Current, Isolated Buck-Boost Design Equations....13-15
18. Design Example, Buck-Boost Isolated Converter Discontinuous Current....13-17
19. Design Example, Boost Converter, Discontinuous Current....13-29
20. Designing Boost Inductors for Power Factor Correction (PFC)....13-37
21. Standard Boost Flyback Converter....13-39
22. Boost, PFC Converter....13-39
23. Design Example, (PFC) Boost Converter, Continuous Current....13-40
24. Skin Effect....13-40
25. Recognitions....13-47
26. References....13-47

© 2011 by Taylor and Francis Group, LLC

Introduction

The principle behind Flyback converters is based on the storage of energy in the inductor during the charging, or the "on period", t_{on}, and the discharge of the energy to the load during the "off period", t_{off}. There are four basic types that are the most common, energy storage, inductor type converter circuits:

1. Step down, or buck converter.
2. Step up, or boost converter.
3. Inverting, buck-boost converter.
4. Isolated, buck-boost converter.

Energy Transfer

Two distinct modes of operation are possible for the Flyback switching converters, shown in Figure 13-1:

Discontinuous Mode All energy stored in the inductor is transferred to an output capacitor and load circuit before another charging period occurs. This topology results in a smaller inductor size, but puts a larger stress on the capacitor and switching device.

Continuous Mode Energy stored in the inductor is not completely transferred to the output capacitor and load circuit before another charging period occurs.

The total period is shown in Equation [13-1].

$$T = \frac{1}{f} \qquad [13\text{-}1]$$

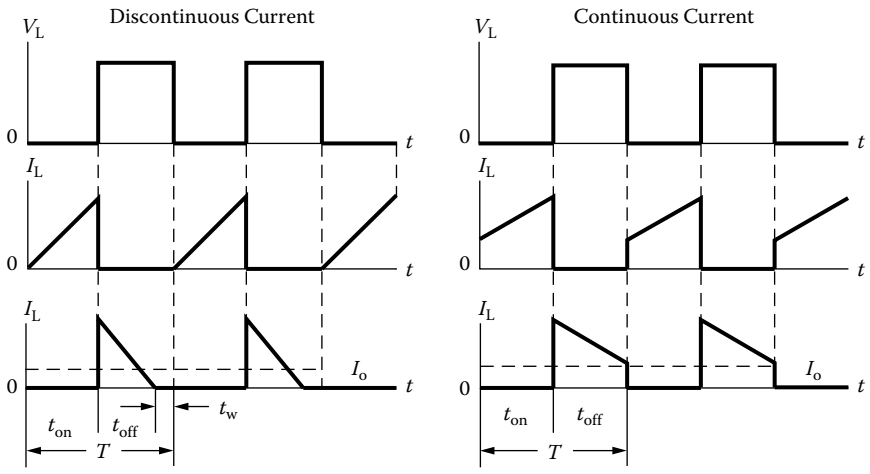

Figure 13-1. Comparing Discontinuous and Continuous Current Waveforms.

© 2011 by Taylor and Francis Group, LLC

Discontinuous Current Mode

In the Discontinuous Mode, a smaller inductance is required, but the penalty results in higher peak currents in the switching transistor. As a consequence, the winding losses are increased because of the higher rms values, due to the higher peak currents. This also results in a higher ripple current and ripple voltage in the input and output capacitor, and gives added stress to the switching transistor. The advantage of this circuit, other than having a smaller inductor, is that when the switching device is turned on, the initial current is zero. A zero current means the output diode has completely recovered, and the switching device does not momentarily turn on into a short. This diode recovery reduces the EMI radiation. The discontinuous mode converter does not exhibit the right half plane zero. Without the right half plane zero, the loop is easy to stabilize.

Continuous Current Mode

In the Continuous Mode, a larger inductor is required; this results in a lower peak current at the end of the cycle than in a discontinuous system of equivalent output power. The Continuous Mode demands a high current flowing through the switch during turn-on, and can lead to high switch dissipation. The continuous mode converter does exhibit the right half-plane zero. With the right half-plane zero, the loop becomes very difficult to stabilize for a wide range of input voltage. The relationship between the B-H loops for continuous and discontinuous operation is shown in Figure 13-2.

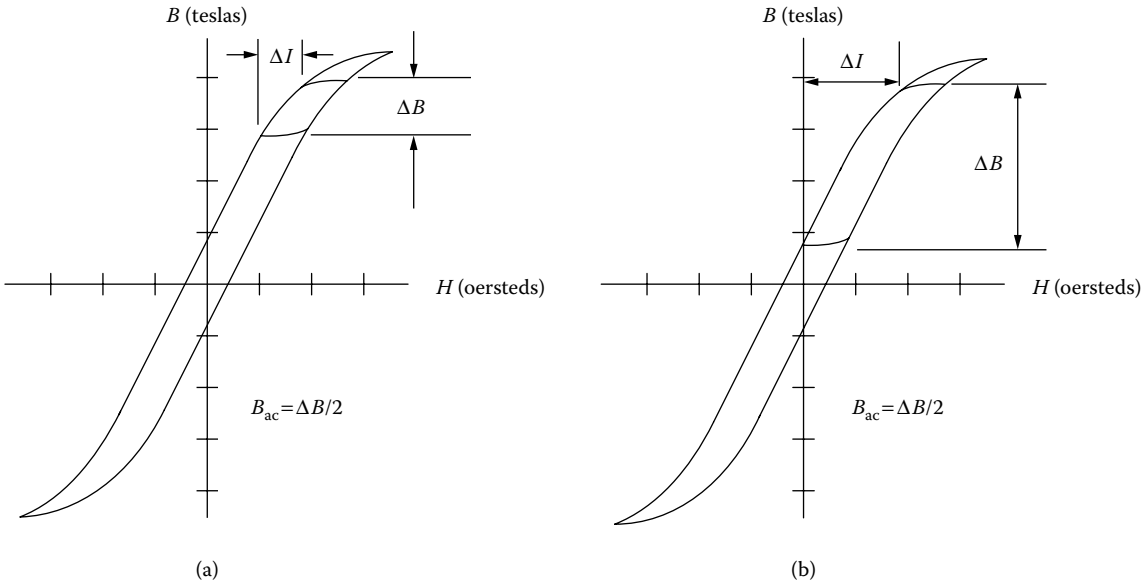

Figure 13-2. Continuous (A) and Discontinuous (B), B-H Loops, Showing ΔB and ΔI.

© 2011 by Taylor and Francis Group, LLC

Continuous and Discontinuous Boundary

When the load current increases, the control circuit causes the transistor to increase the "on time", t_{on}. The peak current in the inductor will increase, resulting in a steady reduction in the dwell time, t_w. When the load current increases to a critical level, t_w becomes zero, and the discontinuous boundary is reached. If the load current is further increased, the inductor current will no longer discharge to zero on every cycle, and continuous current operation results.

The Buck Converter

The Buck Converter is shown in Figure 13-3. The output voltage of this converter is always less than the input voltage. In the buck circuit, the transistor switch, Q1, is placed in series with the dc input voltage. The transistor, Q1, interrupts the dc input voltage, providing a variable-width pulse, (duty ratio), to a simple averaging, LC, filter. When the transistor switch, Q1, is closed, the dc input voltage is applied across the output filter inductor, L1, and the current flows through the inductor to the load. When the switch is open, the energy, stored in the field of the inductor, L1, maintains the current through the load. The discontinuous voltage and current waveforms are shown in Figure 13-4, and the continuous waveforms in Figure 13-5.

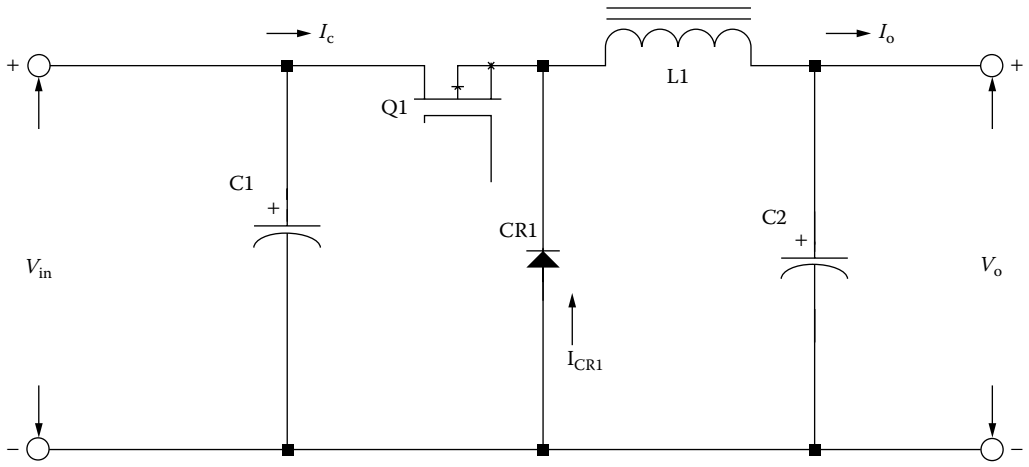

Figure 13-3. Schematic of a Buck Switching Converter.

Discontinuous Current, Buck Converter Design Equations

The maximum Inductance, L_{max}, is shown in Equation [13-2].

$$L_{\max} = \frac{(V_o + V_d)T(1 - D_{\max} - D_w)}{2I_{o(\max)}}, \quad \text{[henrys]} \qquad \text{[13-2]}$$

© 2011 by Taylor and Francis Group, LLC

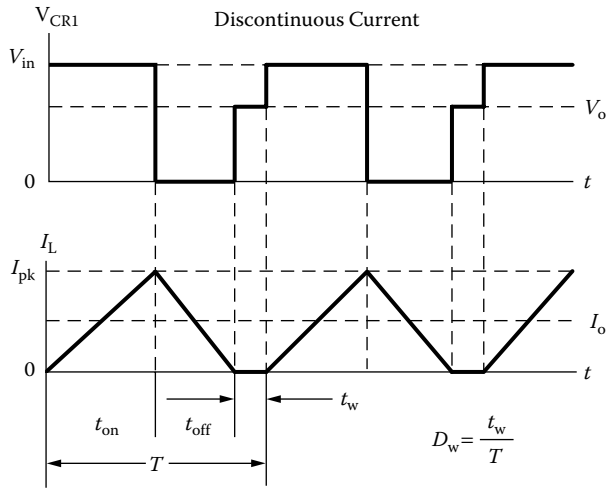

Figure 13-4. Discontinuous Current, Buck Converter Waveforms.

Maximum duty ratio, $D_{(max)}$ is shown in Equation [13-3].

$$D_{(\max)} = \frac{V_o(1 - D_w)}{\left(\eta V_{in(\min)}\right)} \quad [13\text{-}3]$$

Maximum on time, $t_{on(max)}$, is shown in Equation [13-4].

$$t_{on(\max)} = T D_{\max} \quad [13\text{-}4]$$

Maximum off time, $t_{off(max)}$, is shown in Equation [13-5].

$$t_{off\,(\max)} = T(1 - D_{\min}) \quad [13\text{-}5]$$

The inductor peak current, $I_{(pk)}$ is shown in Equation [13-6].

$$I_{(pk)} = \frac{2I_{o(\max)}}{(1 - D_w)} \quad [13\text{-}6]$$

Continuous Current, Buck Converter Design Equations

Inductance, L, is shown in Equation [13-7].

$$L = \frac{V_o T(1 - D_{\min})}{2I_{o(\min)}}, \quad \text{[henrys]} \quad [13\text{-}7]$$

© 2011 by Taylor and Francis Group, LLC

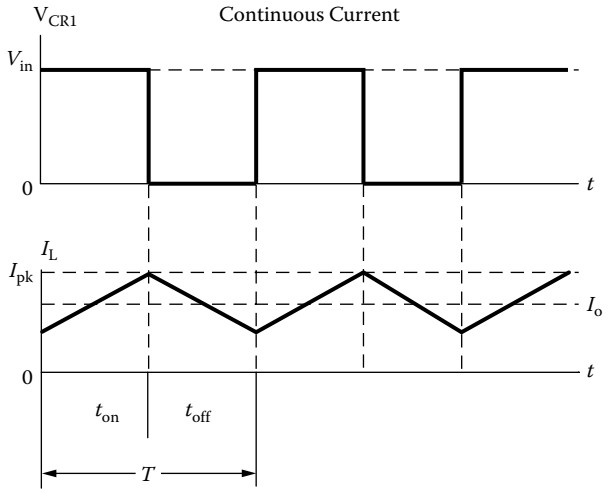

Figure 13-5. Continuous Current, Buck Converter Waveforms.

Maximum duty ratio, $D_{(max)}$, is shown in Equation [13-8].

$$D_{(\max)} = \frac{V_o}{\left(\eta V_{in(\min)}\right)} \quad [13\text{-}8]$$

Minimum duty ratio, $D_{(min)}$, is shown in Equation [13-9].

$$D_{(\min)} = \frac{V_o}{\left(\eta V_{in(\max)}\right)} \quad [13\text{-}9]$$

Maximum on time, $t_{on(max)}$ is shown in Equation [13-10].

$$t_{on(\max)} = T\,D_{\max} \quad [13\text{-}10]$$

Maximum off time, $t_{off(max)}$ is shown in Equation [13-11].

$$t_{off\,(\max)} = T\left(1 - D_{\max}\right) \quad [13\text{-}11]$$

The inductor delta current, ΔI, is shown in Equation [13-12].

$$\Delta I = \frac{\left(TV_{in(\max)}D_{(\min)}\right)\left(1 - D_{(\min)}\right)}{L} \quad [13\text{-}12]$$

The inductor peak current, $I_{(pk)}$, is shown in Equation [13-13].

$$I_{(pk)} = I_{o(\max)} + \frac{\Delta I}{2} \quad [13\text{-}13]$$

© 2011 by Taylor and Francis Group, LLC

The Boost Converter

The Boost Converter is shown in Figure 13-6. The output voltage of this converter is always greater than the input voltage. The boost converter stores energy in the inductor, L1, and then, delivers the stored energy along with the energy from the dc source to the load. When the transistor switch, Q1, is closed, current flows through inductor, L1, and the transistor switch, Q1, charging inductor, L1, but does not deliver any current to the load. When the switch is open, the voltage across the load equals the dc input voltage plus the energy stored in inductor, L1. The energy is stored in, L1, then discharges, delivering current to the load. The discontinuous voltage and current waveforms are shown in Figure 13-7, and the continuous waveforms in Figure 13-8.

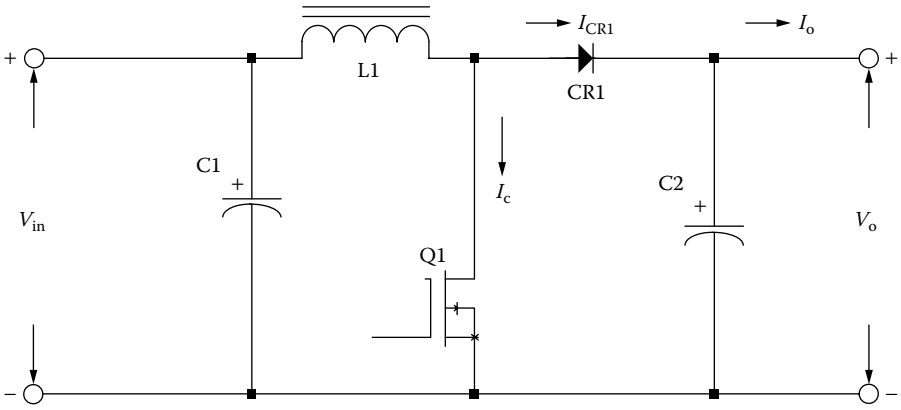

Figure 13-6. Schematic of a Boost Switching Converter.

Discontinuous Current, Boost Converter Design Equations

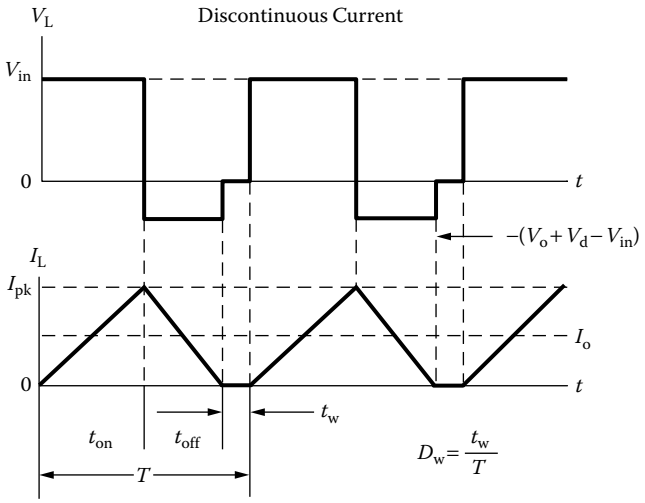

Figure 13-7. Discontinuous Current, Boost Converter Waveforms.

© 2011 by Taylor and Francis Group, LLC

The maximum inductance, L_{max}, is shown in Equation [13-14].

$$L_{\max} = \frac{(V_o + V_d)\,T\,D_{(\max)}\,(1 - D_{\max} - D_w)^2}{2I_{o(\max)}}, \quad \text{[henrys]} \qquad \text{[13-14]}$$

Maximum duty ratio, $D_{(max)}$, is shown in Equation [13-15].

$$D_{(\max)} = (1 - D_w)\left(\frac{V_o - V_{in(\min)} + V_d}{V_o}\right) \qquad \text{[13-15]}$$

Minimum duty ratio, $D_{(min)}$, is shown in Equation [13-16].

$$D_{(\min)} = (1 - D_w)\left(\frac{V_o - V_{in(\max)} + V_d}{V_o}\right) \qquad \text{[13-16]}$$

Maximum on time, $t_{on(max)}$, is shown in Equation [13-17].

$$t_{on(\max)} = T\,D_{\max} \qquad \text{[13-17]}$$

Maximum off time, $t_{off(max)}$, is shown in Equation [13-18].

$$t_{off\,(\max)} = T(1 - D_{\min}) \qquad \text{[13-18]}$$

The inductor peak current, $I_{(pk)}$, is shown in Equation [13-19].

$$I_{(pk)} = \frac{2P_{o(\max)}}{\eta V_{in}\,(1 - D_w)} \qquad \text{[13-19]}$$

Continuous Current, Boost Converter Design Equations

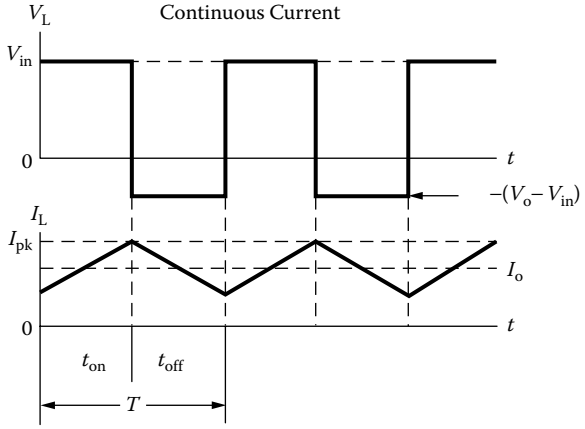

Figure 13-8. Continuous Current, Boost Converter Waveforms.

© 2011 by Taylor and Francis Group, LLC

Inductance, L, is shown in Equation [13-20].

$$L = \frac{(V_o + V_d)\,T\,D_{(\min)}\,(1 - D_{\min})^2}{2I_{o(\min)}}, \quad \text{[henrys]} \qquad [13\text{-}20]$$

Maximum duty ratio, $D_{(max)}$ is shown in Equation [13-21].

$$D_{(\max)} = 1 - \left(\frac{V_{in(\min)}\eta}{V_o}\right) \qquad [13\text{-}21]$$

Minimum duty ratio, $D_{(min)}$, is shown in Equation [13-22].

$$D_{(\min)} = 1 - \left(\frac{V_{in(\max)}\eta}{V_o}\right) \qquad [13\text{-}22]$$

Maximum on time, $t_{on(max)}$, is shown in Equation [13-23].

$$t_{on(\max)} = T\,D_{\max} \qquad [13\text{-}23]$$

Maximum off time, $t_{off(max)}$, is shown in Equation [13-24].

$$t_{off\,(\max)} = T(1 - D_{\min}) \qquad [13\text{-}24]$$

The inductor delta current, ΔI, is shown in Equation [13-25].

$$\Delta I = \frac{\left(TV_{in(\max)}D_{(\min)}\right)}{L} \qquad [13\text{-}25]$$

The inductor peak current, $I_{(pk)}$, is shown in Equation [13-26].

$$I_{(pk)} = \left(\frac{I_{o(\max)}}{1 - D_{(\max)}}\right) + \left(\frac{\Delta I}{2}\right) \qquad [13\text{-}26]$$

The Inverting Buck-Boost Converter

The inverting buck boost converter is shown in Figure 13-9. It is a variation of the boost circuit. The inverting converter delivers only the energy stored by the inductor, L1, to the load. The output voltage of the inverting converter can be greater, or less than, the input voltage. When the transistor switch, Q1, is closed, the inductor is storing energy, but no current is delivered to the load because diode, CR1, is back-biased. When the transistor switch, Q1, is open, the blocking diode is forward-biased and the energy stored in the inductor, L1, is

© 2011 by Taylor and Francis Group, LLC

transferred to the load. The discontinuous voltage and current waveforms are shown in Figure 13-10 and the continuous waveforms in Figure 13-11.

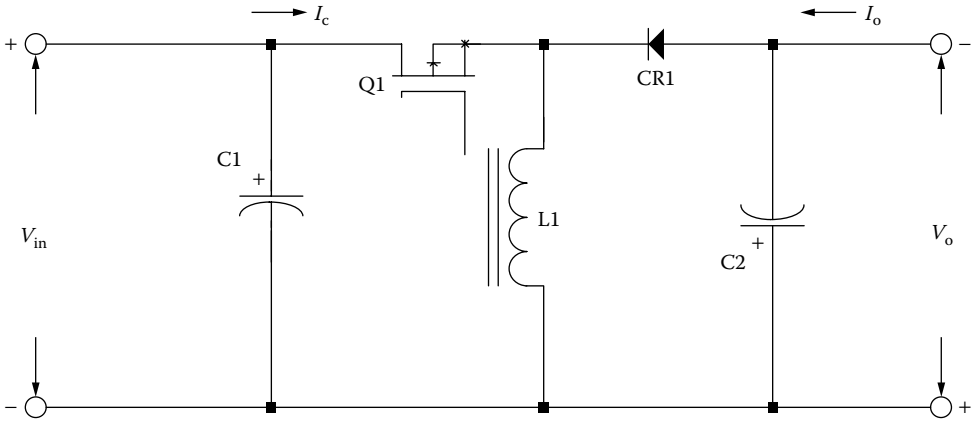

Figure 13-9. Schematic of an Inverting Buck-Boost Switching Converter.

Discontinuous Current, Inverting Buck-Boost Design Equations

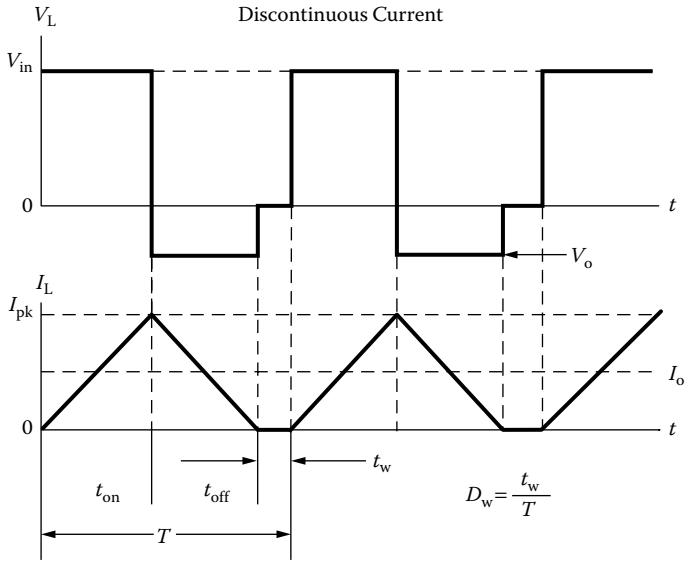

Figure 13-10. Discontinuous Current, Inverting, Buck-Boost Converter Waveforms.

The maximum inductance, L_{max}, is shown in Equation [13-27].

$$L_{max} = \frac{(V_o + V_d)T(1 - D_{max} - D_w)^2}{2I_{o(max)}}, \quad \text{[henrys]} \qquad \text{[13-27]}$$

© 2011 by Taylor and Francis Group, LLC

Maximum duty ratio, D_{max}, is shown in Equation [13-28].

$$D_{\max} = \frac{(V_o + V_d)(1 - D_w)}{(V_o + V_d + V_{in(\min)})} \quad [13\text{-}28]$$

Minimum duty ratio, D_{min}, is shown in Equation [13-29].

$$D_{\min} = \frac{(V_o + V_d)(1 - D_w)}{V_o + V_d + V_{in(\max)}} \quad [13\text{-}29]$$

Maximum on time, $t_{on(max)}$, is shown in Equation [13-30].

$$t_{on(\max)} = T D_{\max} \quad [13\text{-}30]$$

Maximum off time, $t_{off(max)}$, is shown in Equation [13-31].

$$t_{off(\max)} = T(1 - D_{\min} - D_w) \quad [13\text{-}31]$$

The inductor peak current, $I_{(pk)}$, is shown in Equation [13-32].

$$I_{(pk)} = \frac{2P_{o(\max)}}{(D_{(\max)} V_{in(\min)} \eta)} \quad [13\text{-}32]$$

Continuous Current, Inverting Buck-Boost Design Equations

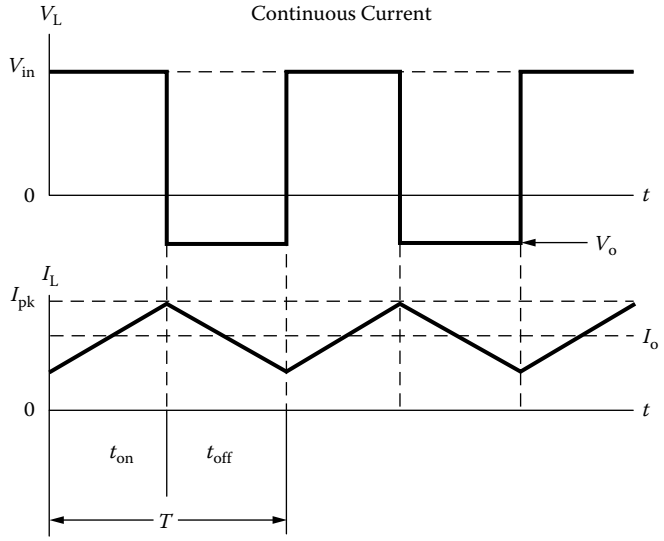

Figure 13-11. Continuous Current, Inverting, Buck-Boost Converter Waveforms.

© 2011 by Taylor and Francis Group, LLC

Inductance, L, is shown in Equation [13-33].

$$L = \frac{(V_o + V_d)T(1 - D_{\min})^2}{2I_{o(\min)}}, \quad \text{[henrys]} \qquad [13\text{-}33]$$

Maximum duty ratio, D_{max}, is shown in Equation [13-34].

$$D_{\max} = \frac{V_o}{V_o + (\eta V_{in(\min)})} \qquad [13\text{-}34]$$

Minimum duty ratio, D_{min}, is shown in Equation [13-35].

$$D_{\min} = \frac{V_o}{V_o + (\eta V_{in(\max)})} \qquad [13\text{-}35]$$

Maximum on time, $t_{on(max)}$, is shown in Equation [13-36].

$$t_{on(\max)} = T D_{\max} \qquad [13\text{-}36]$$

Maximum off time, $t_{off(max)}$, is shown in Equation [13-37].

$$t_{off(\max)} = T(1 - D_{\min}) \qquad [13\text{-}37]$$

The inductor delta current, ΔI, is shown in Equation [13-38].

$$\Delta I = \frac{(T V_{in(\max)} D_{(\min)})}{L} \qquad [13\text{-}38]$$

The inductor peak current, $I_{(pk)}$, is shown in Equation [13-39].

$$I_{(pk)} = \left(\frac{I_{o(\max)}}{1 - D_{\max}}\right) + \left(\frac{\Delta I}{2}\right) \qquad [13\text{-}39]$$

The Isolated, Buck-Boost Converter

The Isolated Buck-Boost Converter is shown in Figure 13-12. This converter can provide line isolation, and also has the capability of multiple outputs, which require only a diode and a capacitor; the filter inductor is built-in. The isolated buck-boost converter is quite popular in low power applications because of simplicity and

© 2011 by Taylor and Francis Group, LLC

low cost. This converter does not lend itself to the VDE specification because of the required voltage insulation between primary and secondary. Care must be taken because this leakage inductance could generate high voltage spikes on the primary. The discontinuous voltage and current waveforms are shown in Figure 13-13, and the continuous waveforms in Figure 13-14.

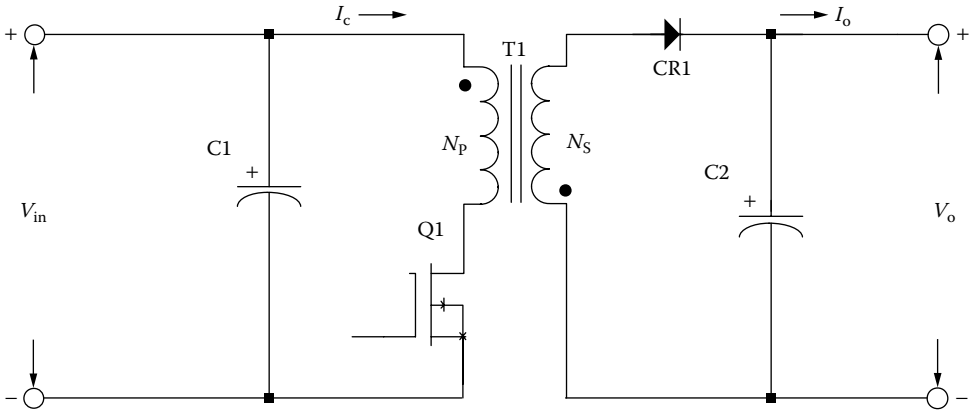

Figure 13-12. Schematic of an Isolated Buck-Boost Switching Converter.

Discontinuous Current, Isolated Buck-Boost Design Equations

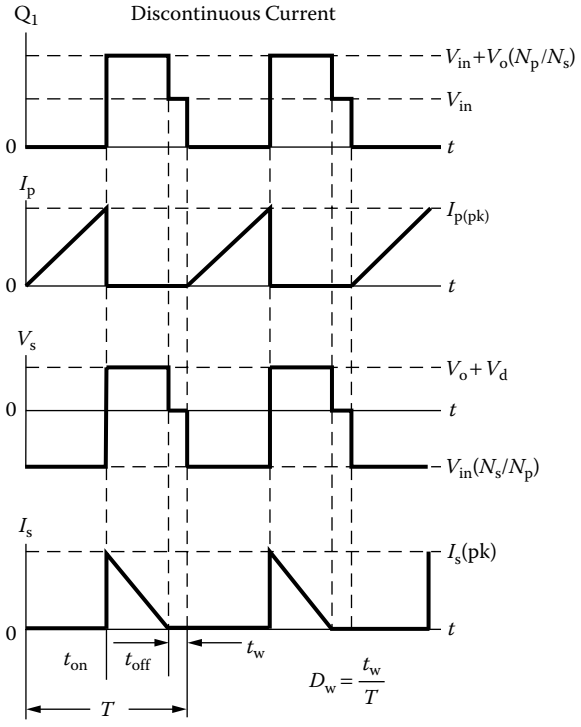

Figure 13-13. Discontinuous Current, Isolated Buck-Boost Converter Waveforms.

© 2011 by Taylor and Francis Group, LLC

Primary maximum inductance, $L_{p(max)}$, is shown in Equation [13-40].

$$L_{p(\max)} = \frac{\left(R_{in(equiv.)}\right) T \left(D_{\max}\right)^2}{2}, \quad \text{[henrys]} \qquad \text{[13-40]}$$

Maximum on time, $t_{on(max)}$, is shown in Equation [13-41].

$$t_{on(\max)} = T D_{\max} \qquad \text{[13-41]}$$

Maximum off time, $t_{off(max)}$, is shown in Equation [13-42].

$$t_{off(\max)} = T\left(1 - D_{\min} - D_w\right) \qquad \text{[13-42]}$$

Total output power, $P_{o(max)}$ is shown in Equation [13-43].

$$P_{o(\max)} = I_{o1(\max)}\left(V_{o1} + V_d\right) + I_{o2(\max)}\left(V_{o2} + V_d\right) + \ldots\ldots\ldots \qquad \text{[13-43]}$$

Maximum input power, $P_{in(max)}$ is shown in Equation [13-44].

$$P_{in(\max)} = \frac{P_{o(\max)}}{\eta} \qquad \text{[13-44]}$$

Equivalent input resistance, $R_{in(equiv)}$, is shown in Equation [13-45].

$$R_{in(equv.)} = \frac{\left(V_{in(\min)}\right)^2}{P_{in(\max)}} \qquad \text{[13-45]}$$

The primary peak current, $I_{p(pk)}$ is shown in Equation [13-46].

$$I_{p(pk)} = \frac{2P_{in(\max)} T}{T_{on(\max)} V_{in(\min)}} \qquad \text{[13-46]}$$

Continuous Current, Isolated Buck-Boost Design Equations

Inductance, L, is shown in Equation [13-47].

$$L = \frac{\left(V_{in(\max)} D_{(\min)}\right)^2 T}{2P_{in(\min)}}, \quad \text{[henrys]} \qquad \text{[13-47]}$$

Minimum duty ratio, D_{min}, is shown in Equation [13-48].

$$D_{\min} = \left(\frac{V_{in(\min)}}{V_{in(\max)}}\right) D_{(\max)} \qquad \text{[13-48]}$$

© 2011 by Taylor and Francis Group, LLC

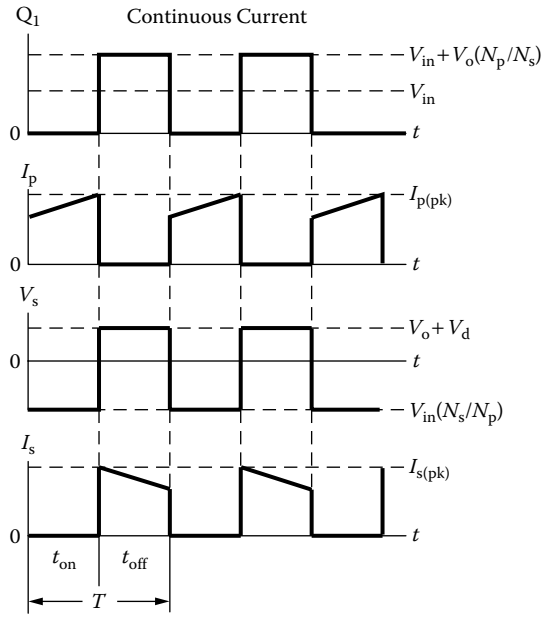

Figure 13-14. Continuous Current, Isolated Buck-Boost Converter Waveforms.

Maximum on time, $t_{on(max)}$, is shown in Equation [13-49].

$$t_{on(\max)} = T\,D_{\max} \qquad [13\text{-}49]$$

Maximum off time, $t_{off(max)}$, is shown in Equation [13-50].

$$t_{off\,(\max)} = T\left(1 - D_{\min}\right) \qquad [13\text{-}50]$$

Minimum output power, $P_{o(min)}$, is shown in Equation [13-51].

$$P_{o(\min)} = I_{o1(\min)}\left(V_{o1} + V_d\right) + I_{o2(\min)}\left(V_{o2} + V_d\right) + \ldots\ldots\ldots \qquad [13\text{-}51]$$

Minimum input power, $P_{in(min)}$, is shown in Equation [13-52].

$$P_{in(\min)} = \frac{P_{o(\min)}}{\eta} \qquad [13\text{-}52]$$

The inductor delta current, ΔI, is shown in Equation [13-53].

$$\Delta I = \frac{\left(T V_{in(\min)} D_{(\max)}\right)}{L} \qquad [13\text{-}53]$$

The inductor peak current, $I_{(pk)}$, is shown in Equation [13-54].

$$I_{(pk)} = \left(\frac{I_{in(\max)}}{D_{\max}}\right) + \left(\frac{\Delta I}{2}\right) \qquad [13\text{-}54]$$

© 2011 by Taylor and Francis Group, LLC

Design Example, Buck-Boost Isolated Converter Discontinuous Current

1. Input voltage nominal, V_{in} = 28 volts
2. Input voltage minimum, $V_{in(min)}$ = 24 volts
3. Input voltage maximum, $V_{in(max)}$ = 32 volts
4. Output voltage, V_{o1} = 5 volts
5. Output current, I_{o1} = 2 amps
6. Output voltage, V_{o2} = 12 volts
7. Output current, I_{o2} = 0.5 amps
8. *Window utilization, K_u = 0.29
9. Frequency, f = 100kHz
10. Converter efficiency, η = 90%
11. Maximum duty ratio, $D_{(max)}$ = 0.5
12. Dwell time duty ratio, $D_{(w)}$ = 0.1
13. Regulation, α = 1.0%
14. Operating flux density, B_m = 0.25 tesla
15. Diode voltage, V_d = 1.0 volt

*When operating at high frequencies, the engineer has to review the window utilization factor, K_u. When using a small bobbin ferrite, the ratio of the bobbin winding area to the core window area is only about 0.6. Operating at 100kHz and having to use a #26 wire, because of the skin effect, the ratio of the bare copper area is 0.78. Therefore, the overall window utilization, K_u, is reduced. The core geometries, K_g, in Chapter 3 have been calculated with a window utilization, K_u, of 0.4. To return the design back to the norm, the core geometry, K_g is to be multiplied by 1.35, and then, the current density, J, is calculated, using a window utilization factor of 0.29. See Chapter 4.

Skin Effect

The skin effect on an inductor is the same as a transformer. In the normal dc inductor, the ac current (ac flux), is much lower, and does not require the use of the same, maximum wire size. This is not the case in the discontinuous, current type, flyback converter, where all of the flux is ac and without dc. In the discontinuous, flyback design, the skin effect has to be treated just like a high frequency transformer.

There are times when the larger wire is just too difficult to wind. Large wire is not only hard to handle, but it does not give the proper lay. It is easier to wind with bi-filar or quad-filar wire, with the equivalent cross-section.

Select a wire so that the relationship between the ac resistance and the dc resistance is 1 is shown in Equation [13-55].

$$\frac{R_{ac}}{R_{dc}} = 1 \qquad [13\text{-}55]$$

© 2011 by Taylor and Francis Group, LLC

The skin depth in centimeters is:

$$\varepsilon = \frac{6.62}{\sqrt{f}}, \quad [\text{cm}]$$

$$\varepsilon = \frac{6.62}{\sqrt{100,000}}, \quad [\text{cm}]$$

$$\varepsilon = 0.0209, \quad [\text{cm}]$$

Then, the wire diameter is:

$$\text{Wire Diameter} = 2(\varepsilon), \quad [\text{cm}]$$

$$\text{Wire Diameter} = 2(0.0209), \quad [\text{cm}]$$

$$\text{Wire Diameter} = 0.0418, \quad [\text{cm}]$$

Then, the bare wire area A_w is:

$$A_w = \frac{\pi D^2}{4}, \quad [\text{cm}^2]$$

$$A_w = \frac{(3.1416)(0.0418)^2}{4}, \quad [\text{cm}^2]$$

$$A_w = 0.00137, \quad [\text{cm}^2]$$

From the Wire Table in Chapter 4, Number 26 has a bare wire area of 0.00128 centimeters. This will be the minimum wire size used in this design. If the design requires more wire area to meet the specification, then the design will use a multifilar of #26. Listed below are #27 and #28, just in case #26 requires too much rounding off.

Wire AWG	Bare Area	Area Ins.	Bare/Ins.	μΩ/cm
#26	0.001280	0.001603	0.798	1345
#27	0.001021	0.001313	0.778	1687
#28	0.0008046	0.0010515	0.765	2142

Step No. 1: Calculate the total period, T.

$$T = \frac{1}{f} \quad [\text{seconds}]$$

$$T = \frac{1}{100000} \quad [\text{seconds}]$$

$$T = 10 \quad [\mu\text{sec}]$$

© 2011 by Taylor and Francis Group, LLC

Step No. 2: Calculate the maximum transistor on time, t_{on}.

$$t_{on} = TD_{\max} \quad [\mu\text{sec}]$$
$$t_{on} = \left(10 \times 10^{-6}\right)\left(0.5\right) \quad [\mu\text{sec}]$$
$$t_{on} = 5.0 \quad [\mu\text{sec}]$$

Step No. 3: Calculate the secondary load power, P_{o1}.

$$P_{o1} = I_{o1}\left(V_{o1} + V_d\right) \quad [\text{watts}]$$
$$P_{o1} = (2)(5+1) \quad [\text{watts}]$$
$$P_{o1} = 12 \quad [\text{watts}]$$

Step No. 4: Calculate the secondary load power, P_{o2}.

$$P_{o2} = I_{o2}\left(V_{o2} + V_d\right) \quad [\text{watts}]$$
$$P_{o2} = (0.5)(12+1) \quad [\text{watts}]$$
$$P_{o2} = 6.5 \quad [\text{watts}]$$

Step No. 5: Calculate the total secondary load power, $P_{o(max)}$.

$$P_{o(\max)} = P_{o1} + P_{o2} \quad [\text{watts}]$$
$$P_{o(\max)} = 12 + 6.5 \quad [\text{watts}]$$
$$P_{o(\max)} = 18.5 \quad [\text{watts}]$$

Step No. 6: Calculate the maximum input current, $I_{in(max)}$.

$$I_{in(\max)} = \frac{P_{o(\max)}}{V_{in(\min)}\eta} \quad [\text{amps}]$$
$$I_{in(\max)} = \frac{18.5}{(24)(0.9)} \quad [\text{amps}]$$
$$I_{in(\max)} = 0.856 \quad [\text{amps}]$$

Step No. 7: Calculate the primary peak current, $I_{p(pk)}$.

$$I_{p(pk)} = \frac{2\,P_{o(\max)}T}{\eta V_{in(\min)}t_{on(\max)}} \quad [\text{amps peak}]$$
$$I_{p(pk)} = \frac{2\left(18.5\right)\left(10 \times 10^{-6}\right)}{\left(0.9\right)\left(24\right)\left(5 \times 10^{-6}\right)} \quad [\text{amps peak}]$$
$$I_{p(pk)} = 3.43 \quad [\text{amps peak}]$$

© 2011 by Taylor and Francis Group, LLC

Step No. 8: Calculate the primary rms current, $I_{p(pk)}$.

$$I_{p(rms)} = I_{p(pk)}\sqrt{\frac{t_{on}}{3T}} \quad \text{[amps]}$$

$$I_{p(rms)} = 3.43\sqrt{\frac{5}{3(10)}} \quad \text{[amps]}$$

$$I_{p(rms)} = 1.40 \quad \text{[amps]}$$

Step No. 9: Calculate the maximum input power, $P_{in(max)}$.

$$P_{in(\max)} = \frac{P_{o(\max)}}{\eta} \quad \text{[watts]}$$

$$P_{in(\max)} = \frac{18.5}{0.9} \quad \text{[watts]}$$

$$P_{in(\max)} = 20.6 \quad \text{[watts]}$$

Step No. 10: Calculate the equivalent input resistance, $R_{in(equiv)}$.

$$R_{in(equiv)} = \frac{\left(V_{in(\min)}\right)^2}{P_{in(\max)}}, \quad \text{[ohms]}$$

$$R_{in(equiv)} = \frac{(24)^2}{20.6}, \quad \text{[ohms]}$$

$$R_{in(equiv)} = 28, \quad \text{[ohms]}$$

Step No. 11: Calculate the required primary inductance, L.

$$L = \frac{\left(R_{in(equiv)}\right)T\left(D_{\max}\right)^2}{2} \quad \text{[henry]}$$

$$L = \frac{\left(28\right)\left(10\times10^{-6}\right)\left(0.5\right)^2}{2} \quad \text{[henry]}$$

$$L = 35 \quad \text{[µh]}$$

Step No. 12: Calculate the energy-handling capability in watt-seconds, w-s.

$$\text{Energy} = \frac{LI_{p(pk)}^2}{2} \quad \text{[w-s]}$$

$$\text{Energy} = \frac{\left(35\times10^{-6}\right)\left(3.43\right)^2}{2} \quad \text{[w-s]}$$

$$\text{Energy} = 0.000206 \quad \text{[w-s]}$$

© 2011 by Taylor and Francis Group, LLC

Step No. 13: Calculate the electrical conditions, K_e.

$$K_e = 0.145 P_o B_m^2 \times 10^{-4}$$

$$K_e = (0.145)(18.5)(0.25)^2 \times 10^{-4}$$

$$K_e = 0.0000168$$

Step No. 14: Calculate the core geometry, K_g. See the design specification for, window utilization factor, K_u.

$$K_g = \frac{(\text{Energy})^2}{K_e \alpha} \quad [\text{cm}^5]$$

$$K_g = \frac{(0.000206)^2}{(16.8(10^{-6}))(1.0)} \quad [\text{cm}^5]$$

$$K_g = 0.00253 \quad [\text{cm}^5]$$

$$K_g = 0.00253(1.35), \quad [\text{cm}^5]$$

$$K_g = 0.00342, \quad [\text{cm}^5]$$

Step No. 15: Select, from Chapter 3, an EFD core comparable in core geometry, K_g.

Core number = EFD-20

Manufacturer = Ferroxcube

Material = 3C85

Magnetic path length, MPL = 4.7 cm

Core weight, W_{tfe} = 7.0 grams

Copper weight, W_{tcu} = 6.8 grams

Mean length turn, MLT = 3.80 cm

Iron area, A_c = 0.31 cm^2

Window Area, W_a = 0.501 cm^2

Area Product, A_p = 0.155 cm^4

Core geometry, K_g = 0.00507 cm^5

Surface area, A_t = 13.3 cm^2

Core Permeability = 2500

Winding Length, G = 1.54 cm

Step No. 16: Calculate the current density, J, using a window utilization, K_u = 0.29.

$$J = \frac{2(\text{Energy})(10^4)}{B_m A_p K_u}, \quad [\text{amps/cm}^2]$$

$$J = \frac{2(0.000206)(10^4)}{(0.25)(0.155)(0.29)}, \quad [\text{amps/cm}^2]$$

$$J = 367, \quad [\text{amps/cm}^2]$$

© 2011 by Taylor and Francis Group, LLC

Step No. 17: Calculate the primary wire area, $A_{pw(B)}$.

$$A_{pw(B)} = \frac{I_{prms}}{J} \quad [\text{cm}^2]$$

$$A_{pw(B)} = \frac{1.4}{367} \quad [\text{cm}^2]$$

$$A_{pw(B)} = 0.00381 \quad [\text{cm}^2]$$

Step No. 18: Calculate the required number of primary strands, S_{np}.

$$S_{np} = \frac{A_{wp(B)}}{\#26 \ (\text{bare area})}$$

$$S_{np} = \frac{(0.00381)}{(0.00128)}$$

$$S_{np} = 2.97 \ \text{ use } 3$$

Step No. 19: Calculate the number of primary turns, N_p. Half of the available window is primary, $W_{ap}/2$. Use the number of strands, S_{np}, and the area for #26.

$$W_{ap} = \frac{W_a}{2} = \frac{0.501}{2} = 0.250, \quad [\text{cm}^2]$$

$$N_p = \frac{K_u W_{ap}}{3(\#26(\text{Bare Area}))}, \quad [\text{turns}]$$

$$N_p = \frac{(0.29)(0.25)}{3(0.00128)}, \quad [\text{turns}]$$

$$N_p = 18.9 \text{ use } 19, \quad [\text{turns}]$$

Step No. 20: Calculate the required gap, l_g.

$$l_g = \frac{0.4\pi N^2 A_c (10^{-8})}{L} - \left(\frac{\text{MPL}}{\mu_m}\right), \quad [\text{cm}]$$

$$l_g = \frac{(1.26)(19)^2(0.31)(10^{-8})}{(0.000035)} - \left(\frac{4.7}{2500}\right), \quad [\text{cm}]$$

$$l_g = 0.0384, \quad [\text{cm}]$$

© 2011 by Taylor and Francis Group, LLC

Step No. 21: Calculate the equivalent gap in mils.

$$\text{mils} = \text{cm}(393.7)$$

$$\text{mils} = (0.0384)(393.7)$$

$$\text{mils} = 15$$

Step No. 22: Calculate the fringing flux factor, F.

$$F = 1 + \frac{l_g}{\sqrt{A_c}} \ln\left(\frac{2G}{l_g}\right)$$

$$F = 1 + \frac{(0.0384)}{\sqrt{0.31}} \ln\left(\frac{2(1.54)}{0.0384}\right)$$

$$F = 1.30$$

Step No. 23: Calculate the new number of turns, N_{np}, by inserting the fringing flux, F.

$$N_{np} = \sqrt{\frac{l_g L}{0.4\pi A_c F\left(10^{-8}\right)}}, \quad \text{[turns]}$$

$$N_{np} = \sqrt{\frac{(0.0384)(0.000035)}{(1.26)(0.31)(1.3)\left(10^{-8}\right)}}, \quad \text{[turns]}$$

$$N_{np} = 16, \quad \text{[turns]}$$

Step No. 24: Calculate the peak flux density, B_{pk}.

$$B_{pk} = \frac{0.4\pi N_{np} F\left(I_{p(pk)}\right)\left(10^{-4}\right)}{l_g + \left(\frac{\text{MPL}}{\mu_m}\right)}, \quad \text{[teslas]}$$

$$B_{pk} = \frac{(1.26)(16)(1.3)(3.43)\left(10^{-4}\right)}{(0.0384) + \left(\frac{4.7}{2500}\right)}, \quad \text{[teslas]}$$

$$B_{pk} = 0.223, \quad \text{[teslas]}$$

Step No. 25: Calculate the primary, the new μΩ/cm.

$$(\text{new})\mu\Omega / cm = \frac{\mu\Omega / cm}{S_{np}}$$

$$(\text{new})\mu\Omega / cm = \frac{1345}{3}$$

$$(\text{new})\mu\Omega / cm = 448$$

© 2011 by Taylor and Francis Group, LLC

Step No. 26: Calculate the primary winding resistance, R_p.

$$R_p = MLT\left(N_{np}\right)\left(\frac{\mu\Omega}{cm}\right)\times 10^{-6} \quad \text{[ohms]}$$

$$R_p = \left(3.8\right)\left(16\right)\left(448\right)\times 10^{-6} \quad \text{[ohms]}$$

$$R_p = 0.0272 \quad \text{[ohms]}$$

Step No. 27: Calculate the primary copper loss, P_p.

$$P_p = I_p^2 R_p \quad \text{[watts]}$$

$$P_p = (1.4)^2\,(.0272) \quad \text{[watts]}$$

$$P_p = 0.0533 \text{ [watts]}$$

Step No. 28: Calculate the secondary turns, N_{s01}.

$$N_{s01} = \frac{N_{np}\left(V_{01}+V_d\right)\left(1-D_{\max}-D_w\right)}{\left(V_p D_{\max}\right)} \quad \text{[turns]}$$

$$N_{s01} = \frac{16(5+1)(1-0.5-0.1)}{(24)(0.5)} \quad \text{[turns]}$$

$$N_{s01} = 3.2 \text{ use } 3 \text{ [turns]}$$

Step No. 29: Calculate the secondary peak current, $I_{s01(pk)}$.

$$I_{s01(pk)} = \frac{2I_{01}}{\left(1-D_{\max}-D_w\right)} \quad \text{[amps]}$$

$$I_{s01(pk)} = \frac{2(2.0)}{(1-0.5-0.1)} \quad \text{[amps]}$$

$$I_{s01(pk)} = 10 \quad \text{[amps]}$$

Step No. 30: Calculate the secondary rms current, $I_{s0(rms)}$.

$$I_{s01(rms)} = I_{s01(pk)}\sqrt{\frac{\left(1-D_{\max}-D_w\right)}{3}} \quad \text{[amps]}$$

$$I_{s01(rms)} = (10)\sqrt{\frac{(1-0.5-0.1)}{3}} \quad \text{[amps]}$$

$$I_{s01(rms)} = 3.65 \quad \text{[amps]}$$

© 2011 by Taylor and Francis Group, LLC

Step No. 31: Calculate the secondary wire area, $A_{sw01(B)}$.

$$A_{sw01(B)} = \frac{I_{s01(rms)}}{J} \quad [\text{cm}^2]$$

$$A_{sw01(B)} = \frac{3.65}{367} \quad [\text{cm}^2]$$

$$A_{sw01(B)} = 0.00995 \quad [\text{cm}^2]$$

Step No. 32: Calculate the required number of secondary strands, S_{ns01}.

$$S_{ns01} = \frac{A_{sw01(B)}}{\text{wire}_A}$$

$$S_{ns01} = \frac{(0.00995)}{(0.00128)}$$

$$S_{ns01} = 7.8 \text{ use } 8$$

Step No. 33: Calculate the, S_{01}, secondary, μΩ/cm.

$$(S_{01})\mu\Omega / cm = \frac{\mu\Omega / cm}{S_{ns01}}$$

$$(S_{01})\mu\Omega / cm = \frac{1345}{8}$$

$$(S_{01})\mu\Omega / cm = 168$$

Step No. 34: Calculate the winding resistance, R_{s01}.

$$R_{s01} = MLT(N_{s01})\left(\frac{\mu\Omega}{cm}\right)\times 10^{-6} \quad [\text{ohms}]$$

$$R_{s01} = 3.8(3)(168)\times 10^{-6} \quad [\text{ohms}]$$

$$R_{s01} = 0.00192 \quad [\text{ohms}]$$

Step No. 35: Calculate the secondary copper loss, P_{s01}.

$$P_{s01} = I_{s01}^2 R_{s01} \quad [\text{watts}]$$

$$P_{s01} = (3.65)^2 (.00192) \quad [\text{watts}]$$

$$P_{s01} = 0.0256 \text{ [watts]}$$

© 2011 by Taylor and Francis Group, LLC

Step No. 36: Calculate the secondary turns, N_{s02}.

$$N_{s02} = \frac{N_{np}\left(V_{02} + V_d\right)\left(1 - D_{\max} - D_w\right)}{\left(V_p D_{\max}\right)} \quad \text{[turns]}$$

$$N_{s02} = \frac{16(12+1)(1-0.5-0.1)}{(24)(0.5)} \quad \text{[turns]}$$

$$N_{s02} = 6.9 \text{ use } 7 \quad \text{[turns]}$$

Step No. 37: Calculate the secondary peak current, $I_{s02(pk)}$.

$$I_{s02(pk)} = \frac{2I_{02}}{\left(1 - D_{\max} - D_w\right)} \quad \text{[amps]}$$

$$I_{s02(pk)} = \frac{2(0.5)}{(1-0.5-0.1)} \quad \text{[amps]}$$

$$I_{s02(pk)} = 2.5 \quad \text{[amps]}$$

Step No. 38: Calculate the secondary rms current, $I_{s02(rms)}$.

$$I_{s02(rms)} = I_{s02(pk)}\sqrt{\frac{\left(1 - D_{\max} - D_w\right)}{3}} \quad \text{[amps]}$$

$$I_{s02(rms)} = (2.5)\sqrt{\frac{(1-0.5-0.1)}{3}} \quad \text{[amps]}$$

$$I_{s02(rms)} = 0.913 \quad \text{[amps]}$$

Step No. 39: Calculate the secondary wire area, $A_{sw02(B)}$.

$$A_{sw02(B)} = \frac{I_{s02(rms)}}{J} \quad [\text{cm}^2]$$

$$A_{sw02(B)} = \frac{0.913}{367} \quad [\text{cm}^2]$$

$$A_{sw02(B)} = 0.00249 \quad [\text{cm}^2]$$

Step No. 40: Calculate the required number of secondary strands, S_{ns02}.

$$S_{ns02} = \frac{A_{sw02(B)}}{wire_A}$$

$$S_{ns02} = \frac{(0.00249)}{(0.00128)}$$

$$S_{ns02} = 1.95 \text{ use } 2$$

© 2011 by Taylor and Francis Group, LLC

Step No. 41: Calculate the, S_{02}, secondary, μΩ/cm.

$$(S_{02})\mu\Omega / cm = \frac{\mu\Omega / cm}{S_{ns02}}$$

$$(S_{02})\mu\Omega / cm = \frac{1345}{2}$$

$$(S_{02})\mu\Omega / cm = 672$$

Step No. 42: Calculate the winding resistance, R_{s02}.

$$R_{s02} = MLT(N_{s02})\left(\frac{\mu\Omega}{cm}\right)\times 10^{-6} \quad \text{[ohms]}$$

$$R_{s02} = 3.8(7)(672)\times 10^{-6} \quad \text{[ohms]}$$

$$R_{s02} = 0.0179 \quad \text{[ohms]}$$

Step No. 43: Calculate the secondary copper loss, P_{s02}.

$$P_{s02} = I_{s02}^2 R_{s02} \quad \text{[watts]}$$

$$P_{s2} = (0.913)^2 (.0179) \quad \text{[watts]}$$

$$P_{s2} = 0.0149 \text{ [watts]}$$

Step No. 44: Calculate the window utilization, K_u.

$$\text{[turns]} = (N_p S_{np}) \quad \text{[primary]}$$

$$\text{[turns]} = (16)(3) = 48 \quad \text{[primary]}$$

$$\text{[turns]} = (N_{s01} S_{ns01}) \quad \text{[secondary]}$$

$$\text{[turns]} = (3)(8) = 24 \quad \text{[secondary]}$$

$$\text{[turns]} = (N_{s02} S_{ns02}) \quad \text{[secondary]}$$

$$\text{[turns]} = (7)(2) = 14 \quad \text{[secondary]}$$

$$N_t = 86 \text{ turns \#26}$$

$$K_u = \frac{N_t A_w}{W_a} = \frac{(86)(0.00128)}{(0.501)}$$

$$K_u = 0.220$$

Step No. 45: Calculate the total copper loss, P_{cu}.

$$P_{cu} = P_p + P_{s01} + P_{s02} \quad \text{[watts]}$$

$$P_{cu} = (0.0533) + (0.0256) + (0.0149) \quad \text{[watts]}$$

$$P_{cu} = 0.0938 \quad \text{[watts]}$$

© 2011 by Taylor and Francis Group, LLC

Step No. 46: Calculate the regulation, α, for this design.

$$\alpha = \frac{P_{cu}}{P_o} \times 100 \quad [\%]$$

$$\alpha = \frac{\left(0.0938\right)}{\left(18.5\right)} \times 100 \quad [\%]$$

$$\alpha = 0.507 \quad [\%]$$

Step No. 47: Calculate the ac flux density, B_{ac}.

$$B_{ac} = \frac{0.4\pi N_{np} F \left(\frac{I_{p(pk)}}{2} \right) \left(10^{-4}\right)}{l_g + \left(\frac{\text{MPL}}{\mu_m} \right)}, \quad [\text{teslas}]$$

$$B_{ac} = \frac{(1.26)(16)(1.3)(1.72)\left(10^{-4}\right)}{(0.0384) + \left(\frac{4.7}{2500} \right)}, \quad [\text{teslas}]$$

$$B_{ac} = 0.111, \quad [\text{teslas}]$$

Step No. 48: Calculate the watts per kilogram, WK.

$$WK = 4.855\left(10^{-5}\right)\left(f\right)^{(1.63)}\left(B_{ac}\right)^{(2.62)} \quad [\text{watts/kilogram}]$$

$$WK = 4.855\left(10^{-5}\right)(100000)^{(1.63)}\left(0.111\right)^{(2.62)} \quad [\text{watts/kilogram}]$$

$$WK = 21.6 \quad [\text{watts/kilogram}] \text{ or } [\text{milliwatts/gram}]$$

Step No. 49: Calculate the core loss, P_{fe}.

$$P_{fe} = \left(\frac{\text{milliwatts}}{\text{gram}} \right) W_{tfe} \times 10^{-3} \quad [\text{watts}]$$

$$P_{fe} = \left(21.6\right)\left(7\right) \times 10^{-3} \quad [\text{watts}]$$

$$P_{fe} = 0.151 \quad [\text{watts}]$$

Step No. 50: Calculate the total loss, core P_{fe} and copper P_{cu}, in watts, P_{Σ}.

$$P_{\Sigma} = P_{fe} + P_{cu} \quad [\text{watts}]$$

$$P_{\Sigma} = \left(0.151\right) + \left(0.0938\right) \quad [\text{watts}]$$

$$P_{\Sigma} = 0.245 \quad [\text{watts}]$$

© 2011 by Taylor and Francis Group, LLC

Step No. 51: Calculate the watt density, ψ

$$\psi = \frac{P_{\Sigma}}{A_t} \quad [\text{watts/cm}^2]$$

$$\psi = \frac{0.245}{13.3} \quad [\text{watts/cm}^2]$$

$$\psi = 0.0184 \quad [\text{watts/cm}^2]$$

Step No. 52: Calculate the temperature rise, T_r, in, °C.

$$T_r = 450(\psi)^{(0.826)} \quad [°\text{C}]$$

$$T_r = 450(0.0184)^{(0.826)} \quad [°\text{C}]$$

$$T_r = 16.6 \quad [°\text{C}]$$

Design Example, Boost Converter, Discontinuous Current

1. Input voltage nominal, $V_{in} = 28$ volts
2. Input voltage minimum, $V_{in(min)} = 26$ volts
3. Input voltage maximum, $V_{in(max)} = 32$ volts
4. Output voltage, $V_{o1} = 50$ volts
5. Output current, $I_{o1} = 1$ amps
6. *Window utilization, $K_u = 0.29$
7. Frequency, f = 100kHz
8. Converter efficiency, $\eta = 92$ %
9. Dwell time duty ratio, $D_{(w)} = 0.1$
10. Regulation, $\alpha = 1.0\%$
11. Operating flux density, $B_m = 0.25$ tesla
12. Diode voltage, $V_d = 1.0$ volts

*When operating at high frequencies, the engineer has to review the window utilization factor, K_u. When using a small bobbin ferrite, the ratio of the bobbin winding area to the core window area is only about 0.6. Operating at 100kHz and having to use a #26 wire, because of the skin effect, the ratio of the bare copper area is 0.78. Therefore, the overall window utilization, K_u, is reduced. The core geometries, K_g, in Chapter 3 have been calculated with a window utilization, K_u, of 0.4. To return the design back to the norm, the core geometry, K_g is to be multiplied by 1.35, and then, the current density, J, is calculated, using a window utilization factor of 0.29. See Chapter 4.

© 2011 by Taylor and Francis Group, LLC

Skin Effect

The skin effect on an inductor is the same as a transformer. In the normal dc inductor, the ac current, (ac flux), is much lower and does not require the use of the same maximum wire size. This is not the case in the discontinuous, current type, flyback converter, where all of the flux is ac and without dc. In the discontinuous, flyback design, the skin effect has to be treated just like a high frequency transformer.

There are times when the larger wire is just too difficult to wind. Large wire is not only hard to handle, but it does not give the proper lay. It is easier to wind with bi-filar or quad-filar, wire with the equivalent cross-section.

At this point, select a wire so that the relationship between the ac resistance and the dc resistance is 1, as is shown in Equation [13-56].

$$\frac{R_{ac}}{R_{dc}} = 1 \qquad [13\text{-}56]$$

The skin depth in centimeters is:

$$\varepsilon = \frac{6.62}{\sqrt{f}}, \quad [\text{cm}]$$

$$\varepsilon = \frac{6.62}{\sqrt{100,000}}, \quad [\text{cm}]$$

$$\varepsilon = 0.0209, \quad [\text{cm}]$$

Then, the wire diameter is:

$$\text{Wire Diameter} = 2(\varepsilon), \quad [\text{cm}]$$

$$\text{Wire Diameter} = 2(0.0209), \quad [\text{cm}]$$

$$\text{Wire Diameter} = 0.0418, \quad [\text{cm}]$$

Then, the bare wire area A_w is:

$$A_w = \frac{\pi D^2}{4}, \quad [\text{cm}^2]$$

$$A_w = \frac{(3.1416)(0.0418)^2}{4}, \quad [\text{cm}^2]$$

$$A_w = 0.00137, \quad [\text{cm}^2]$$

From the Wire Table in Chapter 4, Number 26 has a bare wire area of 0.001028 centimeters. This will be the minimum wire size used in this design. If the design requires more wire area to meet the specification, then the design will use a multifilar of #26. Listed Below are #27 and #28, just in case #26 requires too much rounding off.

© 2011 by Taylor and Francis Group, LLC

Wire AWG	Bare Area	Area Ins.	Bare/Ins.	μΩ/cm
#26	0.001280	0.001603	0.798	1345
#27	0.001021	0.001313	0.778	1687
#28	0.0008046	0.0010515	0.765	2142

Step No. 1: Calculate the total period, T.

$$T = \frac{1}{f}, \quad \text{[seconds]}$$

$$T = \frac{1}{100,000}, \quad \text{[seconds]}$$

$$T = 10, \quad \text{[μsec]}$$

Step No. 2: Calculate the maximum output power, P_o.

$$P_o = (V_o + V_d)(I_o), \quad \text{[watts]}$$

$$P_o = (50 + 1.0)(1.0), \quad \text{[watts]}$$

$$P_o = 51, \quad \text{[watts]}$$

Step No. 3: Calculate the maximum input current, $I_{in(max)}$.

$$I_{in(\max)} = \frac{P_o}{V_{in(\min)}\eta}, \quad \text{[amps]}$$

$$I_{in(\max)} = \frac{(51)}{(26)(0.92)}, \quad \text{[amps]}$$

$$I_{in(\max)} = 2.13, \quad \text{[amps]}$$

Step No. 4: Calculate the maximum duty ratio, $D_{(max)}$.

$$D_{(\max)} = (1 - D_w)\left(\frac{V_o - V_{in(\min)} + V_d}{V_o}\right)$$

$$D_{(\max)} = (1 - 0.1)\left(\frac{(50) - (26) + (1.0)}{50}\right)$$

$$D_{(\max)} = 0.45$$

© 2011 by Taylor and Francis Group, LLC

Step No. 5: Calculate the minimum duty ratio, $D_{(min)}$.

$$D_{(\min)} = (1 - D_w)\left(\frac{V_o - V_{in(\max)} + V_d}{V_o}\right)$$

$$D_{(\min)} = (1 - 0.1)\left(\frac{(50) - (32) + (1.0)}{50}\right)$$

$$D_{(\min)} = 0.342$$

Step No. 6: Calculate the required inductance, L_{max}.

$$L_{\max} = \frac{(V_o + V_d)T\,D_{(\max)}(1 - D_{\max} - D_w)^2}{2I_{o(\max)}}, \quad \text{[henrys]}$$

$$L_{\max} = \frac{(50 + 1.0)\left(10\left(10^{-6}\right)\right)(0.45)(1 - 0.45 - 0.1)^2}{2(1.0)}, \quad \text{[henrys]}$$

$$L_{\max} = 23.2 \text{ use } 23, \quad [\mu h]$$

Step No. 7: Calculate the peak current, I_{pk}. In a discontinuous current boost the peak current is, $I_{(pk)} = \Delta I$.

$$I_{(pk)} = \frac{2P_{o(\max)}}{\eta\left(V_o D_{(\min)}\right)}, \quad \text{[amps]}$$

$$I_{(pk)} = \frac{2(51)}{(0.92)\left((50)(0.342)\right)}, \quad \text{[amps]}$$

$$I_{(pk)} = 6.48, \quad \text{[amps]}$$

Step No. 8: Calculate the rms current, $I_{(rms)}$.

$$I_{(rms)} = I_{pk}\sqrt{\frac{TD_{(\max)}}{3T}}, \quad \text{[amps]}$$

$$I_{(rms)} = (6.48)\sqrt{\frac{\left(10 \times 10^{-6}\right)(0.45)}{3\left(10 \times 10^{-6}\right)}}, \quad \text{[amps]}$$

$$I_{(rms)} = 2.51, \quad \text{[amps]}$$

© 2011 by Taylor and Francis Group, LLC

Step No. 9: Calculate the total energy-handling capability in watt-seconds, w-s.

$$\text{Energy} = \frac{LI_{pk}^2}{2}, \quad \text{[w-s]}$$

$$\text{Energy} = \frac{\left(23\times10^{-6}\right)\left(6.48\right)^2}{2}, \quad \text{[w-s]}$$

$$\text{Energy} = 0.000483, \quad \text{[w-s]}$$

Step No. 10: Calculate the electrical conditions, K_e.

$$K_e = 0.145P_oB_m^2\left(10^{-4}\right)$$

$$K_e = 0.145(51)(0.25)^2\left(10^{-4}\right)$$

$$K_e = 0.0000462$$

Step No. 11: Calculate the core geometry, K_g.

$$K_g = \frac{(\text{Energy})^2}{K_e\alpha}, \quad [\text{cm}^5]$$

$$K_g = \frac{(0.000483)^2}{(0.0000462)(1.0)}, \quad [\text{cm}^5]$$

$$K_g = 0.00505, \quad [\text{cm}^5]$$

$$K_g = 0.00505(1.35), \quad [\text{cm}^5]$$

$$K_g = 0.00682, \quad [\text{cm}^5]$$

Step No. 12: From Chapter 3, select a core that is comparable in core geometry, K_g.

Core number = RM-6

Manufacturer = TDK

Magnetic path length, MPL = 2.86 cm

Core weight, W_{tfe} = 5.5 grams

Copper weight, W_{tcu} = 2.9 grams

Mean length turn, MLT = 3.1 cm

Iron area, A_c = 0.366 cm^2

Window Area, W_a = 0.260 cm^2

Area Product, A_p = 0.0952 cm^4

Core geometry, K_g = 0.0044 cm^5

Surface area, A_t = 11.3 cm^2

Permeability, μ_m = 2500

Winding Length, G = 0.82

© 2011 by Taylor and Francis Group, LLC

Step No. 13: Calculate the current density, J, using a window utilization, $K_u = 0.29$.

$$J = \frac{2(Energy)(10^4)}{B_m A_p K_u}, \quad [\text{amps/cm}^2]$$

$$J = \frac{2(0.000483)(10^4)}{(0.25)(0.0952)(0.29)}, \quad [\text{amps/cm}^2]$$

$$J = 1398, \quad [\text{amps/cm}^2]$$

Step No. 14: Calculate the wire area, $A_{w(B)}$.

$$A_{w(B)} = \frac{I_{rms}}{J} \quad [\text{cm}^2]$$

$$A_{w(B)} = \frac{2.51}{1398} \quad [\text{cm}^2]$$

$$A_{w(B)} = 0.00179 \quad [\text{cm}^2]$$

Step No. 15: Calculate the required number of strands, S_n.

$$S_n = \frac{A_{w(B)}}{\#26 \text{ (bare area)}}$$

$$S_n = \frac{(0.00180)}{(0.00128)}$$

$$S_n = 1.41 \text{ use } 2$$

Step No. 16: Calculate the number of turns, N, using the number of strands, S_n, and the area for #26.

$$N = \frac{K_u W_a}{S_n \#26}, \quad [\text{turns}]$$

$$N = \frac{(0.29)(0.26)}{2(0.00128)}, \quad [\text{turns}]$$

$$N = 29.5 \text{ use } 30, \quad [\text{turns}]$$

Step No. 17: Calculate the required gap, l_g.

$$l_g = \frac{0.4\pi N^2 A_c (10^{-8})}{L} - \left(\frac{\text{MPL}}{\mu_m}\right), \quad [\text{cm}]$$

$$l_g = \frac{(1.26)(30)^2(0.366)(10^{-8})}{(0.000023)} - \left(\frac{2.86}{2500}\right), \quad [\text{cm}]$$

$$l_g = 0.179, \quad [\text{cm}]$$

© 2011 by Taylor and Francis Group, LLC

Step No. 19: Calculate the equivalent gap in mils.

$$\text{mils} = \text{cm}(393.7)$$

$$\text{mils} = (0.179)(393.7)$$

$$\text{mils} = 70$$

Step No. 20: Calculate the fringing flux factor, F.

$$F = 1 + \frac{l_g}{\sqrt{A_c}} \ln\left(\frac{2G}{l_g}\right)$$

$$F = 1 + \frac{(0.179)}{\sqrt{0.366}} \ln\left(\frac{2(0.82)}{0.179}\right)$$

$$F = 1.66$$

Step No. 21: Calculate the new number of turns, N_{np}, by inserting the fringing flux, F.

$$N_{np} = \sqrt{\frac{l_g L}{0.4\pi A_c F\left(10^{-8}\right)}}, \quad \text{[turns]}$$

$$N_{np} = \sqrt{\frac{(0.179)(0.000023)}{(1.26)(0.366)(1.66)\left(10^{-8}\right)}}, \quad \text{[turns]}$$

$$N_{np} = 23, \quad \text{[turns]}$$

Step No. 22: Calculate the peak flux density, B_{pk}.

$$B_{pk} = \frac{0.4\pi N_n F\left(I_{(pk)}\right)\left(10^{-4}\right)}{l_g + \left(\frac{\text{MPL}}{\mu_m}\right)}, \quad \text{[teslas]}$$

$$B_{pk} = \frac{(1.26)(23)(1.66)(6.48)\left(10^{-4}\right)}{(0.179) + \left(\frac{2.86}{2500}\right)}, \quad \text{[teslas]}$$

$$B_{pk} = 0.177, \quad \text{[teslas]}$$

Step No. 23: Calculate the new, μΩ/cm.

$$(\text{new})\mu\Omega / \text{cm} = \frac{\mu\Omega / \text{cm}}{S_n}$$

$$(\text{new})\mu\Omega / \text{cm} = \frac{1345}{2}$$

$$(\text{new})\mu\Omega / \text{cm} = 673$$

© 2011 by Taylor and Francis Group, LLC

Step No. 24: Calculate the primary winding resistance, R.

$$R = MLT\left(N_n\right)\left(\frac{\mu\Omega}{cm}\right)\times 10^{-6} \quad \text{[ohms]}$$

$$R = \left(3.1\right)\left(23\right)\left(673\right)\times 10^{-6} \quad \text{[ohms]}$$

$$R = 0.0480 \quad \text{[ohms]}$$

Step No. 25: Calculate the copper loss, P_{cu}.

$$P_{cu} = I_{rms}^2 R \quad \text{[watts]}$$

$$P_{cu} = \left(2.51\right)^2\left(.0480\right) \quad \text{[watts]}$$

$$P_{cu} = 0.302 \text{ [watts]}$$

Step No. 26: Calculate the regulation, α, for this design.

$$\alpha = \frac{P_{cu}}{P_o}\times 100, \quad [\%]$$

$$\alpha = \frac{\left(0.302\right)}{\left(50\right)}\times 100, \quad [\%]$$

$$\alpha = 0.604, \quad [\%]$$

Step No. 27: Calculate the ac flux density in teslas, B_{ac}.

$$B_{ac} = \frac{0.4\pi N_n F\left(\frac{\Delta I}{2}\right)\left(10^{-4}\right)}{l_g + \left(\frac{\text{MPL}}{\mu_m}\right)}, \quad \text{[teslas]}$$

$$B_{ac} = \frac{(1.26)(23)(1.66)(3.24)\left(10^{-4}\right)}{(0.179) + \left(\frac{2.86}{2500}\right)}, \quad \text{[teslas]}$$

$$B_{ac} = 0.0869, \quad \text{[teslas]}$$

Step No. 28: Calculate the watts per kilogram, WK.

$$WK = 4.855\left(10^{-5}\right)\left(f\right)^{(1.63)}\left(B_{ac}\right)^{(2.62)}, \quad \text{[watts/kilogram]}$$

$$WK = 4.855\left(10^{-5}\right)(100000)^{(1.63)}\left(0.0869\right)^{(2.62)}, \quad \text{[watts/kilogram]}$$

$$WK = 11.39, \quad \text{[watts/kilogram] or [milliwatts/gram]}$$

© 2011 by Taylor and Francis Group, LLC

Step No. 29: Calculate the core loss, P_{fe}.

$$P_{fe} = \left(\frac{\text{milliwatts}}{\text{gram}}\right) W_{tfe} \times 10^{-3}, \quad [\text{watts}]$$

$$P_{fe} = \left(11.39\right)\left(5.5\right) \times 10^{-3}, \quad [\text{watts}]$$

$$P_{fe} = 0.0626, \quad [\text{watts}]$$

Step No. 30: Calculate the total loss, P_{Σ}, core, P_{fe}, and copper, P_{cu}.

$$P_{\Sigma} = P_{fe} + P_{cu}, \quad [\text{watts}]$$

$$P_{\Sigma} = \left(0.0626\right) + \left(0.302\right), \quad [\text{watts}]$$

$$P_{\Sigma} = 0.365, \quad [\text{watts}]$$

Step No. 31: Calculate the watt density, ψ.

$$\psi = \frac{P_{\Sigma}}{A_t}, \quad [\text{watts/cm}^2]$$

$$\psi = \frac{0.365}{11.3}, \quad [\text{watts/cm}^2]$$

$$\psi = 0.0323, \quad [\text{watts/cm}^2]$$

Step No. 32: Calculate the temperature rise, T_r, in, °C.

$$T_r = 450\left(\psi\right)^{(0.826)}, \quad [°\text{C}]$$

$$T_r = 450\left(0.0323\right)^{(0.826)}, \quad [°\text{C}]$$

$$T_r = 26.4, \quad [°\text{C}]$$

Designing Boost Inductors for Power Factor Correction (PFC)

Historically, the standard power supplies designed for electronic equipment have had a notoriously poor power factor in the area of (0.5-0.6), and a correspondingly, high, harmonic current content. This design approach utilizes a simple rectifier capacitor input filter that results in large current pulses drawn from the line, that cause distorting of the line voltage and create large amounts of EMI and noise.

The regulating bodies, IEC in Europe and IEEE in the United States, have been working to develop a standard for limiting harmonic current, in off-line equipment. The German standardization bodies have established IEC 1000-2, and it is generally accepted as the standard for limiting harmonic currents in off-line equipment.

© 2011 by Taylor and Francis Group, LLC

Many new electronic products are required to have a near unity power factor and a distortion free, current input waveform. The conventional ac-dc converters usually employ a full wave, rectifier-bridge, with a simple filter to draw power from the ac line. The typical, rectifier capacitor, input bridge filter and associated waveforms, as shown in Figure 13-15, are no longer good enough.

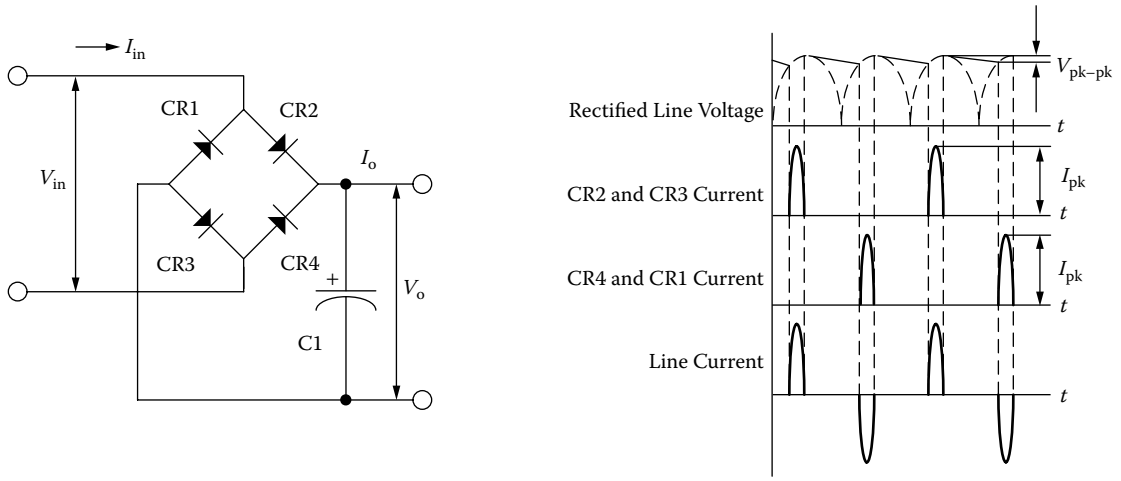

Figure 13-15. Typical, Capacitor Input Bridge Rectifier Filter.

The line current waveform for equipment that utilizes off-line rectifier capacitor input filter, is shown in Figure 13-15. The line current is supplied in narrow pulses. Consequently, the power factor is poor (0.5 – 0.6), due to a high harmonic distortion of the current waveform. The power supply can be designed with a power factor approaching unity, by the addition of an input inductor, as shown in Figure 13-16. The reasons why the input inductors are not designed into power supplies is very simple: cost, weight and bulk. The inductance Equation for, L1, is shown in Equation [13-57].

$$L1 = \frac{V_o}{3\omega I_{o(\min)}}, \quad \text{[henrys]} \qquad \text{[13-57]}$$

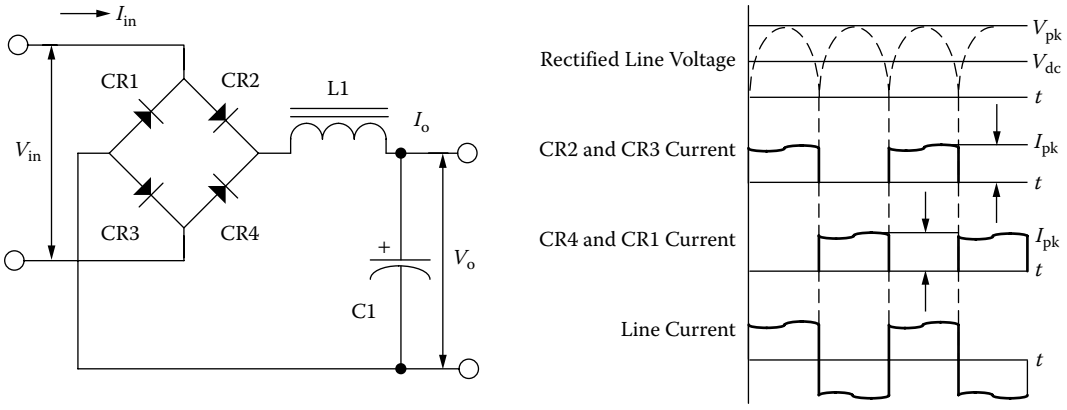

Figure 13-16. A Typical, Inductor Input Bridge Rectifier Filter.

© 2011 by Taylor and Francis Group, LLC

Standard Boost Flyback Converter

The standard dc-to-dc boost flyback converter is shown in Figure 13-6, along with the voltage and current waveforms, shown in Figures 13-7 and 13-8. The boost converter has become the choice of many engineers as the power stage in the active power factor corrector design. The basic circuit can be operated in either the continuous or discontinuous mode.

Boost PFC Converter

The boost Power Factor Correction (PFC) converter is shown in Figure 13-17. The boost converter is the most popular of the power factor pre-regulators. The boost converter can operate in two modes, continuous and discontinuous. The current through the inductor, L1, is shown in Figure 13-18, for both continuous and discontinuous operation. After examining the schematic, the advantages and disadvantages of the boost converter can readily be seen. The disadvantage is the high output voltage to the load circuit and therefore the current limit cannot be implemented. The advantage is that the circuit requires a minimum of parts and the gate drive to, Q1, is referenced to ground.

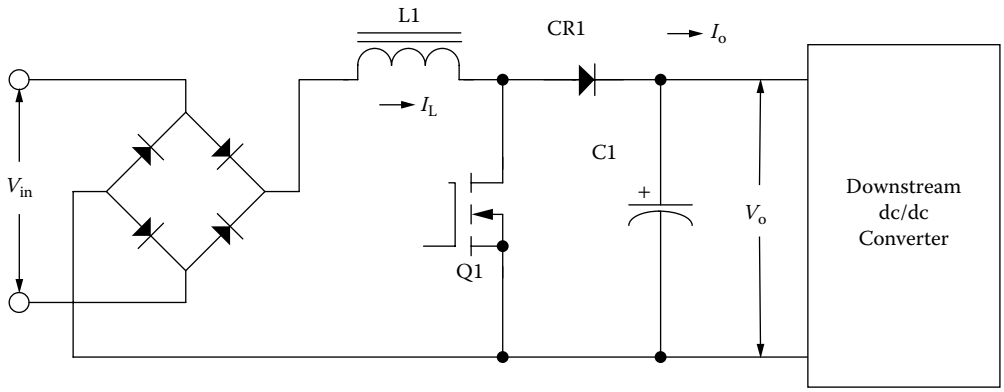

Figure 13-17. Boost PFC Converter.

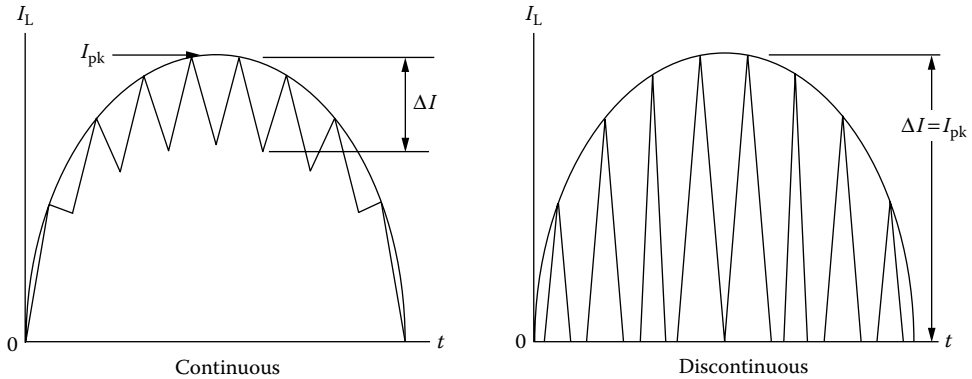

Figure 13-18. Current Through Inductor L1.

© 2011 by Taylor and Francis Group, LLC

Design Example, (PFC) Boost Converter, Continuous Current

The following pages describe a step-by-step procedure for designing a continuous current boost inductor for a Power Factor Correction (PFC) converter, as shown in Figure 13-17, with the following specifications:

1. Output power, $P_o = 250$ watts
2. Input voltage range, $V_{in} = 90 – 270$ volts
3. Line frequency, $f_{(line)} = 47 – 65$ Hz
4. Output voltage, $V_o = 400$ volts
5. Switching frequency, f = 100kHz
6. Inductor ripple current, $\Delta I = 20\%$ of I_{pk}
7. Magnetic core = ETD
8. Magnetic material = R
9. Converter efficiency, $\eta = 95\%$
10. Inductor regulation, $\alpha = 1\%$
11. *Window utilization, $K_u = 0.29$
12. Operating Flux, $B_m = 0.25$ tesla

*When operating at high frequencies, the engineer has to review the window utilization factor, K_u. When using a small bobbin ferrite, the ratio of the bobbin winding area to the core window area is only about 0.6. Operating at 100kHz and having to use a #26 wire, because of the skin effect, the ratio of the bare copper area is 0.78. Therefore, the overall window utilization, K_u, is reduced. The core geometries, K_g, in Chapter 3 have been calculated with a window utilization, K_u, of 0.4. To return the design back to the norm, the core geometry, K_g, is to be multiplied by 1.35, and then, the current density, J, is calculated, using a window utilization factor of 0.29. See Chapter 4.

Skin Effect

The skin effect on an inductor is the same as a transformer. In the normal dc inductor, the ac current (ac flux), is much lower, and does not require the use of the same, maximum wire size. This is not the case in the discontinuous, current type, flyback converter, where all of the flux is ac and no dc. In the discontinuous, flyback design, the skin effect has to be treated just like a high frequency transformer.

There are times when the larger wire is just too difficult to wind. Large wire is not only hard to handle, but it does not give the proper lay. It is easier to wind with bi-filar or quad-filar wire, with the equivalent cross-section.

Select a wire so that the relationship between the ac resistance and the dc resistance is 1:

$$\frac{R_{ac}}{R_{dc}} = 1$$

© 2011 by Taylor and Francis Group, LLC

The skin depth in centimeters is:

$$\varepsilon = \frac{6.62}{\sqrt{f}}, \quad [\text{cm}]$$

$$\varepsilon = \frac{6.62}{\sqrt{100,000}}, \quad [\text{cm}]$$

$$\varepsilon = 0.0209, \quad [\text{cm}]$$

Then, the wire diameter is:

$$\text{Wire Diameter} = 2(\varepsilon), \quad [\text{cm}]$$

$$\text{Wire Diameter} = 2(0.0209), \quad [\text{cm}]$$

$$\text{Wire Diameter} = 0.0418, \quad [\text{cm}]$$

Then, the bare wire area, A_w, is:

$$A_w = \frac{\pi D^2}{4}, \quad [\text{cm}^2]$$

$$A_w = \frac{(3.1416)(0.0418)^2}{4}, \quad [\text{cm}^2]$$

$$A_w = 0.00137, \quad [\text{cm}^2]$$

From the Wire Table in Chapter 4, Number 26 has a bare wire area of 0.00128 centimeters. This will be the minimum wire size used in this design. If the design requires more wire area to meet the specification, then, the design will use a multifilar of #26.

Wire AWG	Bare Area	Area Ins.	Bare/Ins.	μΩ/cm
#26	0.001280	0.001603	0.798	1345

Step No. 1: Calculate the input power, P_{in}.

$$P_{in} = \frac{P_o}{\eta}, \quad [\text{watts}]$$

$$P_{in} = \frac{250}{0.95}, \quad [\text{watts}]$$

$$P_{in} = 263, \quad [\text{watts}]$$

Step No. 2: Calculate the peak input current, I_{pk}.

$$I_{pk} = \frac{P_{in}\sqrt{2}}{V_{in(\min)}}, \quad [\text{amps}]$$

$$I_{pk} = \frac{(263)(1.41)}{90}, \quad [\text{amps}]$$

$$I_{pk} = 4.12, \quad [\text{amps}]$$

© 2011 by Taylor and Francis Group, LLC

Step No. 3: Calculate the input ripple current, ΔI.

$$\Delta I = 0.2 I_{pk}, \quad \text{[amps]}$$

$$\Delta I = 0.2\left(4.12\right), \quad \text{[amps]}$$

$$\Delta I = 0.824, \quad \text{[amps]}$$

Step No. 4: Calculate the maximum duty ratio, $D_{(max)}$.

$$D_{(\max)} = \frac{\left(V_o - \left(V_{in(\min)}\sqrt{2}\right)\right)}{V_o}$$

$$D_{(\max)} = \frac{\left(400 - \left(90\sqrt{2}\right)\right)}{400}$$

$$D_{(\max)} = 0.683$$

Step No. 5: Calculate the required boost inductance, L.

$$L = \frac{\left(V_{in(\min)}\sqrt{2}\right) D_{(\max)}}{\Delta I\, f}, \quad \text{[henrys]}$$

$$L = \frac{(126.9)(0.683)}{(0.824)(100000)}, \quad \text{[henrys]}$$

$$L = 0.00105, \quad \text{[henrys]}$$

Step No. 6: Calculate the Energy required, Eng.

$$\text{Eng} = \frac{L I_{pk}^2}{2}, \quad \text{[watt-seconds]}$$

$$\text{Eng} = \frac{(0.00105)(4.12)^2}{2}, \quad \text{[watt-seconds]}$$

$$\text{Eng} = 0.00891, \quad \text{[watt-seconds]}$$

Step No. 7: Calculate the electrical coefficient, K_e.

$$K_e = 0.145 P_o B_m^2 \left(10^{-4}\right)$$

$$K_e = 0.145(250)(0.25)^2 \left(10^{-4}\right)$$

$$K_e = 0.000227$$

© 2011 by Taylor and Francis Group, LLC

Step No. 8: Calculate the core geometry coefficient, K_g.

$$K_g = \frac{(\text{Eng})^2}{K_e \alpha}, \quad [\text{cm}^5]$$

$$K_g = \frac{(0.00891)^2}{(0.000227)(1)}, \quad [\text{cm}^5]$$

$$K_g = 0.35, \quad [\text{cm}^5]$$

$$K_g = 0.35(1.35), \quad [\text{cm}^5] \text{ Corrected}$$

$$K_g = 0.47, \quad [\text{cm}^5]$$

Step No. 9: From Chapter 3, select an ETD ferrite core, comparable in core geometry, K_g.

Core number = ETD-44

Manufacturer = Ferroxcube

Magnetic path length, MPL = 10.3 cm

Core weight, W_{tfe} = 94 grams

Copper weight, W_{tcu} = 93.2 grams

Mean length turn, MLT = 9.4 cm

Iron area, A_c = 1.74 cm^2

Window Area, W_a = 2.79 cm^2

Area Product, A_p = 4.85 cm^4

Core geometry, K_g = 0.360 cm^5

Surface area, A_t = 87.9 cm^2

Material 3F3, μ_m = 2000

Millihenrys per 1000 turns, AL = 3364

Winding Length, G = 3.22

Step No. 10: Calculate the current density, J.

$$J = \frac{2(\text{Eng})(10^4)}{B_m A_p K_u}, \quad [\text{amps/cm}^2]$$

$$J = \frac{2(0.00891)(10^4)}{(0.25)(4.85)(0.29)}, \quad [\text{amps/cm}^2]$$

$$J = 507, \quad [\text{amps/cm}^2]$$

Step No. 11: Calculate the rms current, I_{rms}.

$$I_{rms} = \frac{I_{pk}}{\sqrt{2}}, \quad [\text{amps}]$$

$$I_{rms} = \frac{4.12}{\sqrt{2}}, \quad [\text{amps}]$$

$$I_{rms} = 2.91, \quad [\text{amps}]$$

© 2011 by Taylor and Francis Group, LLC

Step No. 12: Calculate the required bare wire area, $A_{w(B)}$.

$$A_{w(B)} = \frac{I_{rms}}{J}, \quad [\text{cm}^2]$$

$$A_{w(B)} = \frac{2.91}{507}, \quad [\text{cm}^2]$$

$$A_{w(B)} = 0.00574, \quad [\text{cm}^2]$$

Step No. 13: Calculate the required number of strands, S_n.

$$S_n = \frac{A_{w(B)}}{\#26(\text{bare area})}, \quad [\text{cm}^2]$$

$$S_n = \frac{(0.00574)}{(0.00128)}, \quad [\text{cm}^2]$$

$$S_n = 4.48 \text{ use } 5, \quad [\text{cm}^2]$$

Step No. 14: Calculate the required number of turns, N, using the number of strands, S_n, and the area for #26.

$$N = \frac{W_a K_u}{S_n \#26}, \quad [\text{turns}]$$

$$N = \frac{(2.79)(0.29)}{5(0.00128)}, \quad [\text{turns}]$$

$$N = 126, \quad [\text{turns}]$$

Step No. 15: Calculate the required gap, l_g.

$$l_g = \left(\frac{0.4\pi N^2 A_c \left(10^{-8}\right)}{L} \right), \quad [\text{cm}]$$

$$l_g = \left(\frac{(1.257)(126)^2 (1.74)\left(10^{-8}\right)}{0.00105} \right), \quad [\text{cm}]$$

$$l_g = 0.331, \quad [\text{cm}]$$

Change the gap to mils: $0.331 \times 393.7 = 130$ mils center or 65 mils per each outer leg.

Step No. 16: Calculate the fringing flux factor, F.

$$F = \left(1 + \left(\frac{l_g}{\sqrt{A_c}} \right) \ln \left(\frac{2G}{l_g} \right) \right)$$

$$F = \left(1 + \left(\frac{0.331}{1.32} \right) \ln \left(\frac{6.44}{0.331} \right) \right)$$

$$F = 1.74$$

© 2011 by Taylor and Francis Group, LLC

Step No. 17: Calculate the new turns using the fringing flux.

$$N = \sqrt{\frac{l_g L}{0.4\pi A_c F\left(10^{-8}\right)}}, \quad \text{[turns]}$$

$$N = \sqrt{\frac{(0.331)(0.00105)}{(1.257)(1.74)(1.74)\left(10^{-8}\right)}}, \quad \text{[turns]}$$

$$N = 96, \quad \text{[turns]}$$

Step No. 18: Calculate the peak flux, B_{pk}.

$$B_{pk} = F\left(\frac{0.4\pi N I_{pk}\left(10^{-4}\right)}{l_g}\right), \quad \text{[teslas]}$$

$$B_{pk} = 1.74\left(\frac{(1.257)(96)(4.12)\left(10^{-4}\right)}{0.331}\right), \quad \text{[teslas]}$$

$$B_{pk} = 0.261, \quad \text{[teslas]}$$

Step No. 19: Calculate the new, μΩ/cm.

$$(\text{new})\mu\Omega / \text{cm} = \frac{\mu\Omega / \text{cm}}{S_n}$$

$$(\text{new})\mu\Omega / \text{cm} = \frac{1345}{5}$$

$$(\text{new})\mu\Omega / \text{cm} = 269$$

Step No. 20: Calculate the winding resistance, R.

$$R = (\text{MLT}) N\left(\frac{\mu\Omega}{\text{cm}}\right)\left(10^{-6}\right), \quad \text{[ohms]}$$

$$R = (9.4)(96)(269)\left(10^{-6}\right), \quad \text{[ohms]}$$

$$R = 0.243, \quad \text{[ohms]}$$

Step No. 21: Calculate the winding copper loss, P_{cu}.

$$P_{cu} = I_{rms}^2 R, \quad \text{[watts]}$$

$$P_{cu} = (2.91)^2 (0.243), \quad \text{[watts]}$$

$$P_{cu} = 2.06, \quad \text{[watts]}$$

© 2011 by Taylor and Francis Group, LLC

Step No. 22: Calculate the regulation, α.

$$\alpha = \frac{P_{cu}}{P_o}100, \quad [\%]$$

$$\alpha = \frac{(2.06)}{(250)}100, \quad [\%]$$

$$\alpha = 0.824, \quad [\%]$$

Step No. 23: Calculate the ac flux density, B_{ac}.

$$B_{ac} = \frac{0.4\pi N\left(\frac{\Delta I}{2}\right)\left(10^{-4}\right)}{l_g}, \quad [\text{teslas}]$$

$$B_{ac} = \frac{(1.257)(96)(0.412)\left(10^{-4}\right)}{0.331}, \quad [\text{teslas}]$$

$$B_{ac} = 0.0150, \quad [\text{teslas}]$$

Step No. 24: Calculate the watts per kilogram, W/K, using R material in Chapter 2.

$$W/K = 4.316\left(10^{-5}\right)(f)^{1.64}\left(B_{ac}\right)^{2.68}, \quad [\text{watts per kilogram}]$$

$$W/K = 4.316\left(10^{-5}\right)(100000)^{1.64}(0.0150)^{2.68}, \quad [\text{watts per kilogram}]$$

$$W/K = 0.0885, \quad [\text{watts per kilogram}]$$

Step No. 25: Calculate the core loss, P_{fe}.

$$P_{fe} = W_{tfe}\left(10^{-3}\right)(W/K), \quad [\text{watts}]$$

$$P_{fe} = (94)\left(10^{-3}\right)(0.0885), \quad [\text{watts}]$$

$$P_{fe} = 0.0083, \quad [\text{watts}]$$

Step No. 26: Calculate the total loss core loss, P_{fe} and copper loss, P_{cu}.

$$P = P_{cu} + P_{fe}, \quad [\text{watts}]$$

$$P = (2.03) + (0.0083), \quad [\text{watts}]$$

$$P = 2.04, \quad [\text{watts}]$$

© 2011 by Taylor and Francis Group, LLC

Step No. 27: Calculate the watt density, ψ.

$$\psi = \frac{P}{A_t}, \quad [\text{watts per cm}^2]$$

$$\psi = \frac{2.04}{87.9}, \quad [\text{watts per cm}^2]$$

$$\psi = 0.023, \quad [\text{watts per cm}^2]$$

Step No. 28: Calculate the temperature rise, T_r.

$$T_r = 450(\psi)^{0.826}, \quad [°\text{C}]$$

$$T_r = 450(0.023)^{0.826}, \quad [°\text{C}]$$

$$T_r = 19.9, \quad [°\text{C}]$$

Step No. 29: Calculate the window utilization, K_u.

$$K_u = \frac{N S_n A_{w(B)}}{W_a}$$

$$K_u = \frac{(95)(5)(0.00128)}{(2.79)}$$

$$K_u = 0.218$$

Recognitions

The author would like to thank **Dr. V. Vorperian**, Senior Engineer, of the Power and Sensor Electronics Group, Jet Propulsion Laboratory (JPL), **Richard Ozenbaugh** of Linear Magnetics and **Kit Sum**, Senior Consultant, for their help with the Flyback Design Equations.

References

1. Unitode Application Note U-132, Power Factor Correction Using The UC3852 Controller on-time zero current Switching Technique.

2. Unitode Application Note U-134, UC3854 Controlled Power Factor Correction Circuit Design.

3. AlliedSignal Application Guide: Power Factor Correction Inductor Design for Switch Mode Power Supplies using Powerlite C Cores.

© 2011 by Taylor and Francis Group, LLC

4. PCIM August, 1990, Active Power Factor Correction Using a Flyback Topology, James LoCascio and Mehmet Nalbant/Micor Linear Corporation.

5. Silicon General Application SG3561A Power Factor Controller.

6. SGS Thomson Application Note AN628/0593 Designing a High Power Factor Pre-regulator with the L4981 Continuous Current.

7. IEEE, A Comparison Between Hysteretic and Fixed Frequency Boost Converter Used for Power Factor Correction, James J. Spanger Motorola and Anup K. Behera Illinois Institute Technology.

© 2011 by Taylor and Francis Group, LLC

Chapter 14

Forward Converter, Transformer Design, and Output Inductor Design

© 2011 by Taylor and Francis Group, LLC

Table of Contents

1. Introduction 14-3
2. Circuit Operation 14-3
3. Comparing the Dynamic B-H Loops 14-4
4. Forward Converter Waveforms 14-4
5. Transformer Design Using the Core Geometry, K_g, Approach 14-7
6. Forward Converter Output Inductor Design 14-15
7. Output Inductor Design Using the Core Geometry, K_g, Approach 14-18
8. Recognition 14-24

© 2011 by Taylor and Francis Group, LLC

Introduction

When speaking of a forward converter, the circuit that comes to mind is the single-ended, forward converter circuit, as shown in Figure 14-1. This single-ended, forward converter was developed about 1974 and has become one of the most popular and widely-used topology for powers under 200 W. The single-ended, forward converter gets its name from a family of converters. A description of a forward converter is that when current is flowing in the primary, there is current flowing in the secondary, and in the load. The push-pull converter, full-bridge converter, and half-bridge converter are all, basically, forward converters. The voltage stress on the single-forward converter is the same as it is on the push-pull converter, $2V_{in}$. This circuit's main advantage, that is so appealing to engineers is its simplicity and parts' count.

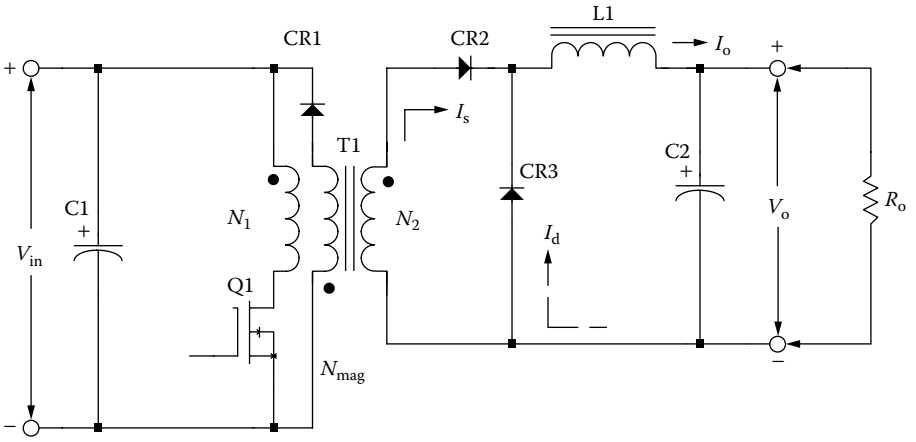

Figure 14-1. Schematic of a Single-Ended Forward Converter.

Circuit Operation

The basic circuit operation of this single-ended, forward converter is as follows: When the drive is applied to, Q1, the secondary current, I_s, will flow through, CR2, and, L1, and into the load. This process is due to transformer action, (T1). At the same time, the magnetizing current begins to build up in the transformer primary. When the base-drive to, Q1, is removed, then, Q1, turns off the magnetizing current that has built up in the primary. The magnetizing current continues to flow through the demagnetizing winding, N_{mag} and CR1. The demagnetizing winding, N_{mag}, has the same number of turns as the primary winding. So, when the magnetizing field collapses, when, Q1, is turned off, diode, CR1, is clamped to the same voltage as the applied voltage during the, t_{on}, time. This means the transistor on time, t_{on}, divided by the total time, T, must not exceed 0.5 or 50%. Otherwise, the forward volt-seconds will exceed the reset volt-second capability and the transformer will saturate. To ensure smooth transfer of the magnetizing current, the primary and demagnetizing winding must be tightly coupled (bifilar). In a push-pull converter, the reset of the core occurs naturally on each alternate half cycle.

© 2011 by Taylor and Francis Group, LLC

Comparing the Dynamic B-H Loops

One of the main reasons for engineers to use the single-ended, forward converter circuit is the problem they have with the push-pull converter, core saturating. The core saturation can be due to an imbalance of the primary or secondary. The dynamic BH loops for the single-ended, forward converter and the push-pull converter are shown in Figure 14-2.

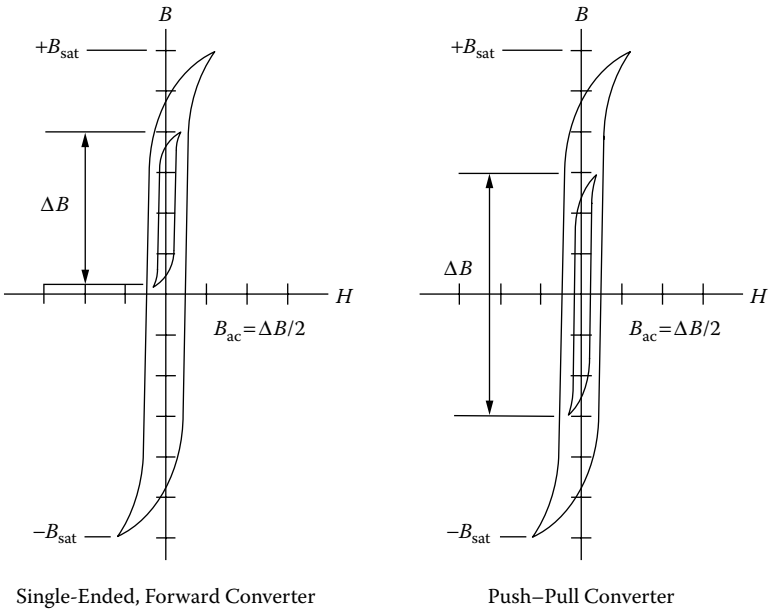

Figure 14-2. The Dynamic BH Loop Comparison.

The average input current for the single-ended, forward converter is about the same as the push-pull converter, but the peak current is always greater than twice the average current. Operating the single-ended, forward converter at low input voltages, the high peak currents could be a component problem. The input filter and output filter for the single-ended, forward converter are always larger than the push-pull converter, because it is operating at the fundamental frequency.

Forward Converter Waveforms

The waveforms, shown in Figure 14-3, are typical waveforms of the single-ended forward converter. The collector current, I_c, is shown in Figure (14-3-A), and the magnetizing current, I_m, is shown in the Figure (14-3-B). The inductor, L1, current, I_L, made up from the rectifier, CR2, and the commutating rectifier, CR3, are shown in Figure (14-3-C). The collector voltage, V_c, is shown in Figure (14-3-D).

© 2011 by Taylor and Francis Group, LLC

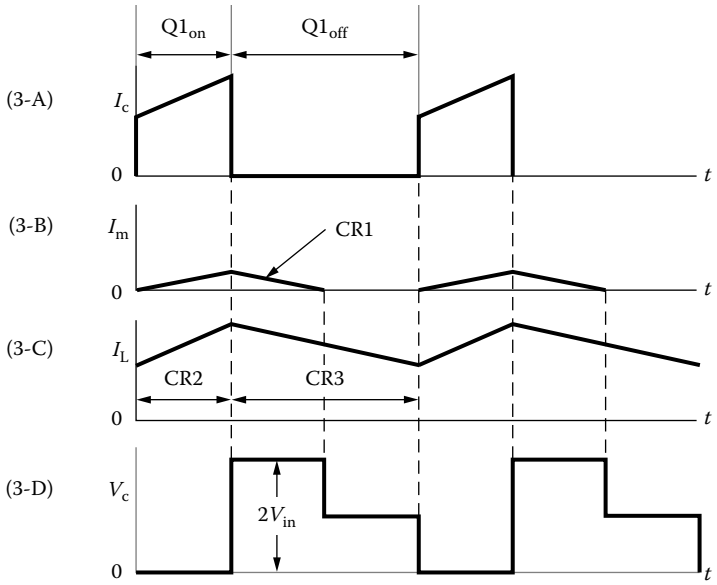

Figure 14-3. Typical Single-Ended Forward, Converter Waveforms.

Another version of the classic, forward converter is the double-ended, forward converter, shown in Figure 14-4. The double-ended, forward converter has two transistors rather than one, compared to the single-ended, forward converter, shown in Figure 14-1. The double-ended forward converter is more complicated than the single-ended forward converter because one of the transistors is on the high side of the input voltage, but it has some significant advantages. The series switching transistors are subjected to only the input voltage, (V_{in}), rather than twice the input voltage, ($2V_{in}$). It also removes the need for a demagnetizing winding. The demagnetizing current now flows through the primary, through, CR1, and CR2, and back to the source, as shown in Figure 14-5. This demagnetizing path also provides a path for the energy stored in the leakage inductance. The resulting spiking voltage, caused from the leakage inductance, is now clamped to the input voltage, plus the two diode drops ($V_{in} + 2V_d$).

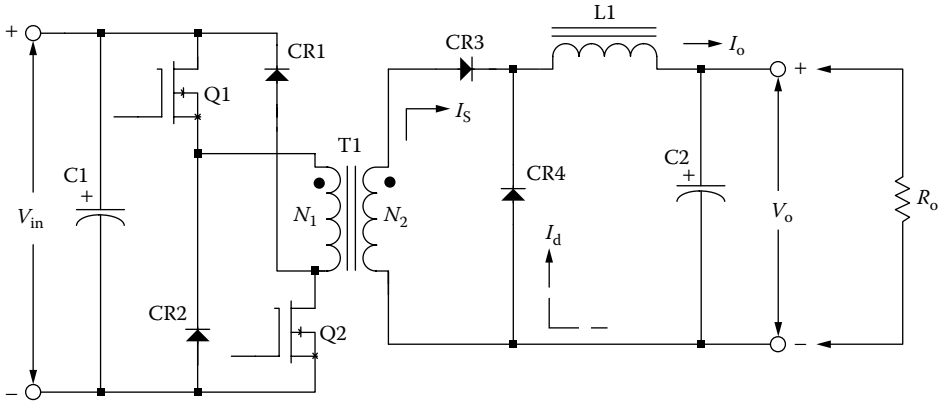

Figure 14-4. Schematic of a Double-Ended Forward Converter.

© 2011 by Taylor and Francis Group, LLC

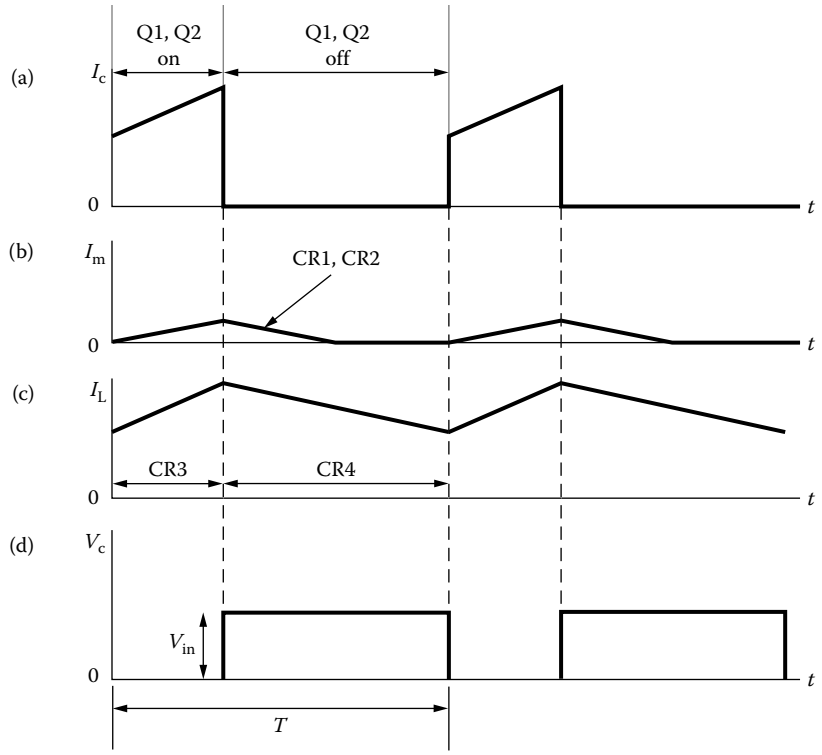

Figure 14-5. Typical Double-Ended Forward, Converter Waveforms.

Note: The Design Equations are from communication and work with the late Dr. J. K. Watson, Professor of Electrical Engineering at the University of Florida.

Electrical coefficient, K_e, is shown in Equation [14-1].

$$K_e = 0.145 f^2 \Delta B^2 \left(10^{-4}\right) \qquad [14\text{-}1]$$

Core geometry, K_g, is shown in Equation [14-2].

$$K_g = \frac{P_{in} D_{(\max)}}{\alpha K_e}, \quad [\text{cm}^5] \qquad [14\text{-}2]$$

Current density, J, is shown in Equation [14-3].

$$J = \frac{2P_{in}\sqrt{D_{(\max)}}\left(10^4\right)}{f \Delta B A_c W_a K_u}, \quad [\text{amps per cm}^2] \qquad [14\text{-}3]$$

Primary current, I_p, is shown in Equation [14-4].

$$I_p = \frac{P_{in}}{V_{in(\min)}\sqrt{D_{(\max)}}}, \quad [\text{amps}] \qquad [14\text{-}4]$$

© 2011 by Taylor and Francis Group, LLC

Transformer Design Using the Core Geometry, K_g, Approach

The following information is the Design specification for a 30 watts, single-ended transformer, operating at 100kHz, using the, K_g, core geometry approach. For a typical design example, assume a single-ended converter circuit, as shown in Figure 14-1, with the following specification:

1. Input voltage, $V_{(min)} = 22$ volts
2. Input voltage, $V_{(nom)} = 28$ volts
3. Input voltage, $V_{(max)} = 35$ volts
4. Output voltage, $V_o = 5.0$ volts
5. Output current, $I_o = 5.0$ amps
6. Frequency, f = 100kHz
7. Efficiency, $\eta = 98\%$
8. Regulation, $\alpha = 0.5\%$
9. Diode voltage drop, $V_d = 1.0$ volt
10. Operating flux density, ΔB, $(B_{ac} = \Delta B/2) = 0.1$ teslas
11. Core Material = ferrite
12. Window utilization, $K_u = 0.3$
13. Temperature rise goal, $T_r = 30°C$
14. Maximum duty ratio, $D_{max} = 0.5$
15. Notes:
    Demag turns ratio, $N_{mag}/N_p = 1$
    Demag power, $P_{mag} = (0.1)P_o$

Select a wire so that the relationship between the ac resistance and the dc resistance is 1:

$$\frac{R_{ac}}{R_{dc}} = 1$$

The skin depth in centimeters is:

$$\varepsilon = \frac{6.62}{\sqrt{f}}, \quad [\text{cm}]$$

$$\varepsilon = \frac{6.62}{\sqrt{100,000}}, \quad [\text{cm}]$$

$$\varepsilon = 0.0209, \quad [\text{cm}]$$

Then, the wire diameter is:

$$\text{Wire Diameter} = 2(\varepsilon), \quad [\text{cm}]$$

$$\text{Wire Diameter} = 2(0.0209), \quad [\text{cm}]$$

$$\text{Wire Diameter} = 0.0418, \quad [\text{cm}]$$

© 2011 by Taylor and Francis Group, LLC

Then, the bare wire area, A_w, is:

$$A_w = \frac{\pi D^2}{4}, \quad [\text{cm}^2]$$

$$A_w = \frac{(3.1416)(0.0418)^2}{4}, \quad [\text{cm}^2]$$

$$A_w = 0.00137, \quad [\text{cm}^2]$$

From the Wire Table, in Chapter 4, Number 26 has a bare wire area of 0.001280 centimeters. This will be the minimum wire size used in this design. If the design requires more wire area to meet the specification, then, the design will use a multifilar of #26. Listed Below are #27 and #28, just in case #26 requires too much rounding off.

Wire AWG	Bare Area	Area Ins.	Bare/Ins.	μΩ/cm
#26	0.001280	0.001603	0.798	1345
#27	0.001021	0.001313	0.778	1687
#28	0.0008046	0.0010515	0.765	2142

Step No. 1: Calculate the transformer output power, P_o.

$$P_o = I_o (V_o + V_d), \quad [\text{watts}]$$

$$P_o = 5(5+1), \quad [\text{watts}]$$

$$P_o = 30, \quad [\text{watts}]$$

Step No. 2: Calculate the input power, P_{in}.

$$P_{in} = \frac{P_o (1.1)}{\eta}, \quad [\text{watts}]$$

$$P_{in} = \frac{30(1.1)}{(0.98)}, \quad [\text{watts}]$$

$$P_{in} = 33.67, \quad [\text{watts}]$$

Step No. 3: Calculate the electrical coefficient, K_e.

$$K_e = 0.145 f^2 \Delta B^2 \left(10^{-4}\right)$$

$$K_e = 0.145(100,000)^2 (0.1)^2 \left(10^{-4}\right)$$

$$K_e = 1450$$

© 2011 by Taylor and Francis Group, LLC

Step No. 4: Calculate the core geometry, K_g.

$$K_g = \frac{P_{in} D_{\max}}{\alpha K_e}, \quad [\text{cm}^5]$$

$$K_g = \frac{(33.67)(0.5)}{(0.5)(1450)}, \quad [\text{cm}^5]$$

$$K_g = 0.0232, \quad [\text{cm}^5]$$

When operating at high frequencies, the engineer has to review the window utilization factor, K_u. When using small bobbin ferrites, the ratio of the bobbin winding area to the core window area is only about 0.6. Operating at 100kHz and having to use a #26 wire, because of the skin effect, the ratio of the bare copper area to the total area is 0.78. Therefore, the overall window utilization, K_u, is reduced. To return the design back to the norm, the core geometry, K_g, is to be multiplied by 1.35, and then, the current density, J, is calculated, using a window utilization factor of 0.29.

$$K_g = 0.0232(1.35), \quad [\text{cm}^5]$$

$$K_g = 0.0313, \quad [\text{cm}^5]$$

Step No. 5: Select a EPC core from Chapter 3, comparable in core geometry K_g.

Core number = EPC-30

Manufacturer = TDK

Magnetic material = PC44

Magnetic path length, MPL = 8.2 cm

Window height, G = 2.6 cm

Core weight, W_{tfe} = 23 grams

Copper weight, W_{tcu} = 22 grams

Mean length turn, MLT = 5.5 cm

Iron area, A_c = 0.61 cm^2

Window area, W_a = 1.118 cm^2

Area product, A_p = 0.682 cm^4

Core geometry, K_g = 0.0301 cm^5

Surface area, A_t = 31.5 cm^2

Millihenrys per 1000 turns, AL = 1570

Step No. 6: Calculate the number of primary turns, N_p.

$$N_p = \frac{V_{in(\min)} D_{(\max)} \left(10^4\right)}{f A_c \Delta B}, \quad [\text{turns}]$$

$$N_p = \frac{(22)(0.5)\left(10^4\right)}{(100,000)(0.61)(0.1)}, \quad [\text{turns}]$$

$$N_p = 18.0, \quad [\text{turns}]$$

© 2011 by Taylor and Francis Group, LLC

Step No. 7: Calculate the current density, J, using a window utilization, $K_u = 0.29$.

$$J = \frac{2P_{in}\sqrt{D_{(\max)}}\left(10^4\right)}{f\,A_c\,\Delta B W_a\,K_u}, \quad [\text{amps/cm}^2]$$

$$J = \frac{2(33.67)(0.707)\left(10^4\right)}{(100,000)(0.61)(0.1)(1.118)(0.29)}, \quad [\text{amps/cm}^2]$$

$$J = 241, \quad [\text{amps/cm}^2]$$

Step No. 8: Calculate the primary rms current, I_p.

$$I_p = \frac{P_{in}}{V_{in(\min)}\sqrt{D_{(\max)}}}, \quad [\text{amps}]$$

$$I_p = \frac{(33.67)}{(22)(0.707)}, \quad [\text{amps}]$$

$$I_p = 2.16, \quad [\text{amps}]$$

Step No. 9: Calculate the primary bare wire area, $A_{wp(B)}$.

$$A_{wp(B)} = \frac{I_p}{J}, \quad [\text{cm}^2]$$

$$A_{wp(B)} = \frac{2.16}{241}, \quad [\text{cm}^2]$$

$$A_{wp(B)} = 0.00896, \quad [\text{cm}^2]$$

Step No. 10: Calculate the required number of primary strands, NS_p.

$$NS_p = \frac{A_{wp(B)}}{\#\,26}$$

$$NS_p = \frac{0.00896}{0.00128}$$

$$NS_p = 7$$

Step No. 11: Calculate the primary new μΩ per centimeter.

$$(\text{new})\,\mu\Omega/\text{cm} = \frac{\mu\Omega/\text{cm}}{NS_p}$$

$$(\text{new})\,\mu\Omega/\text{cm} = \frac{1345}{7}$$

$$(\text{new})\,\mu\Omega/\text{cm} = 192$$

© 2011 by Taylor and Francis Group, LLC

Step No. 12: Calculate the primary resistance, R_p.

$$R_p = \text{MLT}(N_p)\left(\frac{\mu\Omega}{\text{cm}}\right)\left(10^{-6}\right), \quad [\text{ohms}]$$

$$R_p = (5.5)(18)(192)\left(10^{-6}\right), \quad [\text{ohms}]$$

$$R_p = 0.0190, \quad [\text{ohms}]$$

Step No. 13: Calculate the primary copper loss, P_p.

$$P_p = I_p^2 R_p, \quad [\text{watts}]$$

$$P_p = (2.16)^2(0.019), \quad [\text{watts}]$$

$$P_p = 0.0886, \quad [\text{watts}]$$

Step No. 14: Calculate the secondary turns, N_s.

$$N_s = \frac{N_p(V_o + V_d)}{D_{(\max)}V_{in(\min)}}\left(1 + \frac{\alpha}{100}\right), \quad [\text{turns}]$$

$$N_s = \frac{(18)(5+1)}{(0.5)(22)}\left(1 + \frac{0.5}{100}\right), \quad [\text{turns}]$$

$$N_s = 9.87 \text{ use } 10, \quad [\text{turns}]$$

Step No. 15: Calculate the secondary rms current, I_s.

$$I_s = \frac{I_o}{\sqrt{2}}, \quad [\text{amps}]$$

$$I_s = \frac{5}{1.41}, \quad [\text{amps}]$$

$$I_s = 3.55, \quad [\text{amps}]$$

Step No. 16: Calculate the secondary bare wire area, $A_{ws(B)}$.

$$A_{ws(B)} = \frac{I_s}{J}, \quad [\text{cm}^2]$$

$$A_{ws(B)} = \frac{3.55}{241}, \quad [\text{cm}^2]$$

$$A_{ws(B)} = 0.0147, \quad [\text{cm}^2]$$

Step No. 17: Calculate the required number of secondary strands, NS_s.

$$NS_s = \frac{A_{ws(B)}}{\#26}$$

$$NS_s = \frac{0.0147}{0.00128}$$

$$NS_s = 11.48 \text{ use } 11$$

© 2011 by Taylor and Francis Group, LLC

Step No. 18: Calculate the secondary, new μΩ per centimeter.

$$(\text{new})\mu\Omega / \text{cm} = \frac{\mu\Omega / \text{cm}}{NS_s}$$

$$(\text{new})\mu\Omega / \text{cm} = \frac{1345}{11}$$

$$(\text{new})\mu\Omega / \text{cm} = 122$$

Step No. 19: Calculate the secondary winding resistance, R_s.

$$R_s = \text{MLT}(N_s)\left(\frac{\mu\Omega}{\text{cm}}\right)\left(10^{-6}\right), \quad [\text{ohms}]$$

$$R_s = (5.5)(10)(122)\left(10^{-6}\right), \quad [\text{ohms}]$$

$$R_s = 0.00671, \quad [\text{ohms}]$$

Step No. 20: Calculate the secondary copper loss, P_s.

$$P_s = I_s^2 R_s, \quad [\text{watts}]$$

$$P_s = (3.55)^2(0.00671), \quad [\text{watts}]$$

$$P_s = 0.0846, \quad [\text{watts}]$$

Step No. 21: Calculate the total primary and secondary copper loss, P_{cu}.

$$P_{cu} = P_p + P_s, \quad [\text{watts}]$$

$$P_{cu} = 0.0886 + 0.0846, \quad [\text{watts}]$$

$$P_{cu} = 0.173, \quad [\text{watts}]$$

Step No. 22: Calculate the transformer regulation, α.

$$\alpha = \frac{P_{cu}}{P_o}(100), \quad [\%]$$

$$\alpha = \frac{(0.173)}{(30)}(100), \quad [\%]$$

$$\alpha = 0.576, \quad [\%]$$

Step No. 23: Calculate the demag winding inductance, L_{demag}.

$$L_{demag} = L_{1000}N_{demag}^2\left(10^{-6}\right), \quad [\text{mh}]$$

$$L_{demag} = (1570)(18)^2\left(10^{-6}\right), \quad [\text{mh}]$$

$$L_{demag} = 0.509, \quad [\text{mh}]$$

© 2011 by Taylor and Francis Group, LLC

Step No. 24: Calculate the time of, Δt. See Figure 14-6.

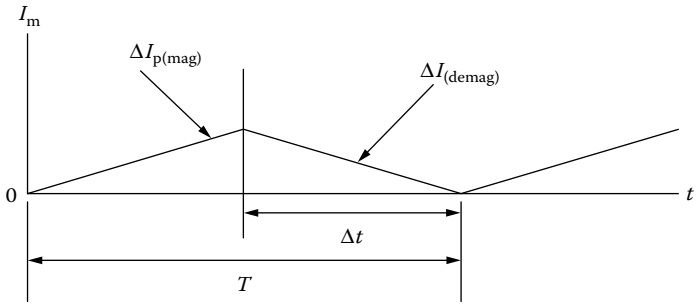

Figure 14-6. Magnetizing Current Waveform.

$$\Delta t = T D_{(\max)}, \quad \text{[seconds]}$$

$$T = \frac{1}{f}, \quad \text{[seconds]}$$

$$T = \frac{1}{100,000}, \quad \text{[seconds]}$$

$$T = 10\left(10^{-6}\right), \quad \text{[seconds]}$$

$$\Delta t = \left(10\left(10^{-6}\right)\right)(0.5), \quad \text{[seconds]}$$

$$\Delta t = 5\left(10^{-6}\right), \quad \text{[seconds]}$$

Step No. 25: Calculate the demag, winding delta current, ΔI_{demag}.

$$\Delta I_{demag} = \frac{V_{in}\,\Delta t}{L_{demag}}, \quad \text{[amps]}$$

$$\Delta I_{demag} = \frac{(22)\left(5\left(10^{-6}\right)\right)}{\left(509\left(10^{-6}\right)\right)}, \quad \text{[amps]}$$

$$\Delta I_{demag} = 0.217, \quad \text{[amps]}$$

Step No. 26: Calculate the demag, winding rms current, I_{demag}. This is the rms equation for a saw tooth current.

$$I_{demag} = \Delta I \sqrt{\frac{D_{(\max)}}{3}}, \quad \text{[amps]}$$

$$I_{demag} = (0.217)(0.408), \quad \text{[amps]}$$

$$I_{demag} = 0.089, \quad \text{[amps]}$$

© 2011 by Taylor and Francis Group, LLC

Step No. 27: Calculate the required demag, wire area, $A_{w(demag)}$.

$$A_{w(demag)} = \frac{I_{demag}}{J}, \quad [\text{cm}^2]$$

$$A_{w(demag)} = \frac{0.089}{241}, \quad [\text{cm}^2]$$

$$A_{w(demag)} = 0.000369, \quad \approx \#31 \text{ use a } \#26$$

Step No. 28: Calculate the window utilization, K_u.

$$K_u = \frac{N A_{w(B)(\#26)}}{W_a}$$

$$N = \left(N_p NS_p\right) + \left(N_s NS_s\right) + \left(N_{demag} NS_{demag}\right)$$

$$N = (18)(7) + (10)(11) + (18)(1)$$

$$N = 254$$

$$K_u = \frac{(254)(0.00128)}{1.118}$$

$$K_u = 0.291$$

Step No. 29: Calculate the milliwatts per gram, mW/g.

$$\text{mW/g} = 0.000318\left(f\right)^{1.51}\left(B_{ac}\right)^{2.747}$$

$$\text{mW/g} = 0.000318\left(100000\right)^{1.51}\left(0.05\right)^{2.747}$$

$$\text{mW/g} = 3.01$$

Step No. 30: Calculate the core loss, P_{fe}.

$$P_{fe} = \left(mW/g\right)\left(W_{tfe}\right)\left(10^{-3}\right), \quad [\text{watts}]$$

$$P_{fe} = (3.01)(23)\left(10^{-3}\right), \quad [\text{watts}]$$

$$P_{fe} = 0.069, \quad [\text{watts}]$$

Step No. 31: Calculate the total loss, P_Σ.

$$P_\Sigma = P_{cu} + P_{fe}, \quad [\text{watts}]$$

$$P_\Sigma = (0.173) + (0.069), \quad [\text{watts}]$$

$$P_\Sigma = 0.242, \quad [\text{watts}]$$

Step No. 32: Calculate the watts per unit area, ψ.

$$\psi = \frac{P_\Sigma}{A_t}, \quad [\text{watts/cm}^2]$$

$$\psi = \frac{(0.242)}{(31.5)}, \quad [\text{watts/cm}^2]$$

$$\psi = 0.0077, \quad [\text{watts/cm}^2]$$

© 2011 by Taylor and Francis Group, LLC

Step No. 33: Calculate the temperature rise, T_r.

$$T_r = 450(\psi)^{(0.826)}, \quad [°C]$$

$$T_r = 450(0.0077)^{(0.826)}, \quad [°C]$$

$$T_r = 8.08, \quad [°C]$$

Forward Converter Output Inductor Design

Part 2 is designing the output inductor, L1, as shown in Figure 14-7. The output filter inductor for Switch-Mode Power Supplies, (SMPS), probably has been designed more times than any other single component. Presented here is a straight-forward approach for selecting the core and the proper wire size to meet the specification.

The losses in the magnetic material will increase significantly when the converter is operating at a higher frequency. However, the core loss in the output inductor of a switching regulator is much lower compared to the core loss in the main converter transformer. The core loss in the output inductor is caused by the change in current or ΔI, which induces a change in flux, as shown in Figure 14-7.

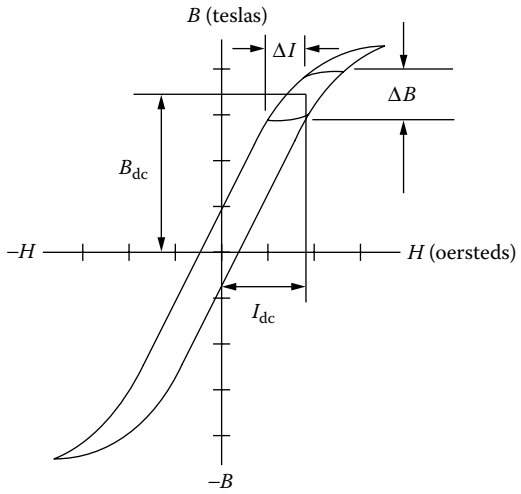

Figure 14-7. Typical Output Inductor BH Loop.

The single-ended, forward converter schematic is shown in Figure 14-8. This topology is appealing to engineers for it simplicity and parts' count. The output filter circuit, shown in Figure 14-8, has three current probes. These current probes monitor the three basic currents in a switch mode, converter output filter. Current probe

© 2011 by Taylor and Francis Group, LLC

A monitors the transformer's secondary current. Current probe B monitors the commutating current through, CR3. Current probe, C, monitors the current through the output inductor, L1.

The typical secondary and filter waveforms of the forward converter are shown in Figure 14-8. The waveforms are shown with the converter operating at a 0.5 duty ratio. The applied voltage, V_1, to the filter, is shown in Figure (14-9-A). The transformer's secondary current is shown in Figure (14-9-B). The commutating current

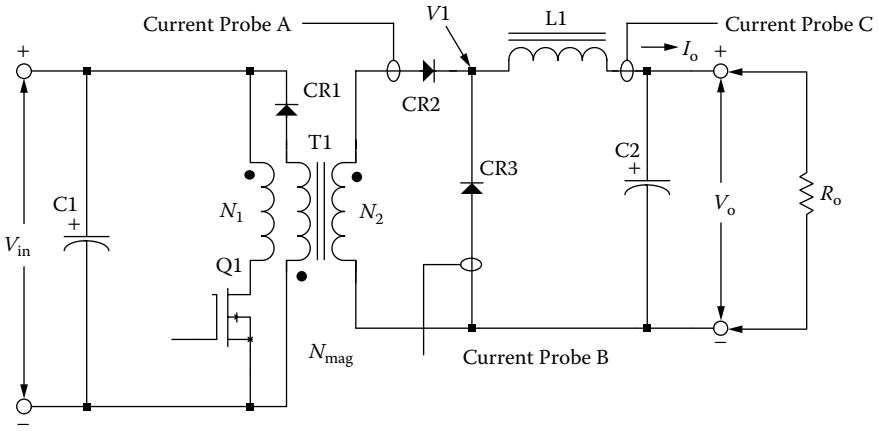

Figure 14-8. Typical Single-ended, Forward Converter.

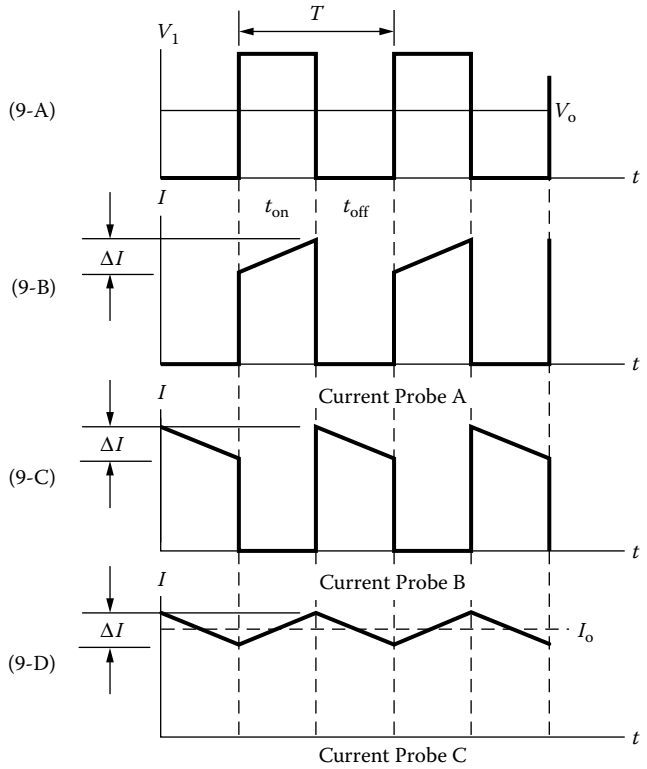

Figure 14-9. Typical Forward Converter Waveforms, Operating at a 0.5 Duty Ratio.

© 2011 by Taylor and Francis Group, LLC

flowing through, CR3, is shown in Figure (14-9-C). The commutating current is the result of, Q1, being turned off, and the field in, L1, collapsing, producing the commutating current. The current flowing through, L1, is shown in Figure (14-9-D). The current flowing through, L1, is the sum of the currents in Figure (14-9-B) and (14-9-C).

The critical inductance current is shown in Figure (14-10-B). The critical inductance current is when the ratio of the delta current to the output load current is equal to $2 = \Delta I / I_o$. If the output load current is allowed to go beyond this point, the current will become discontinuous, as shown in Figure (14-10-D). The applied voltage, V_1, will have ringing at the level of the output voltage, as shown in Figure (14-10-C). When the current in the output inductor becomes discontinuous, as shown in Figure (14-10-D), the response time for a step load becomes very poor.

When designing multiple output converters, the slaved outputs should never have the current in the inductor go discontinuous, or to zero. If the current goes to zero, a slaved output voltage will rise to the value of, V_1. If the current is allowed to go to zero, then, there is not any potential difference between the input and output voltage of the filter. Then the output voltage will rise to equal the peak input voltage.

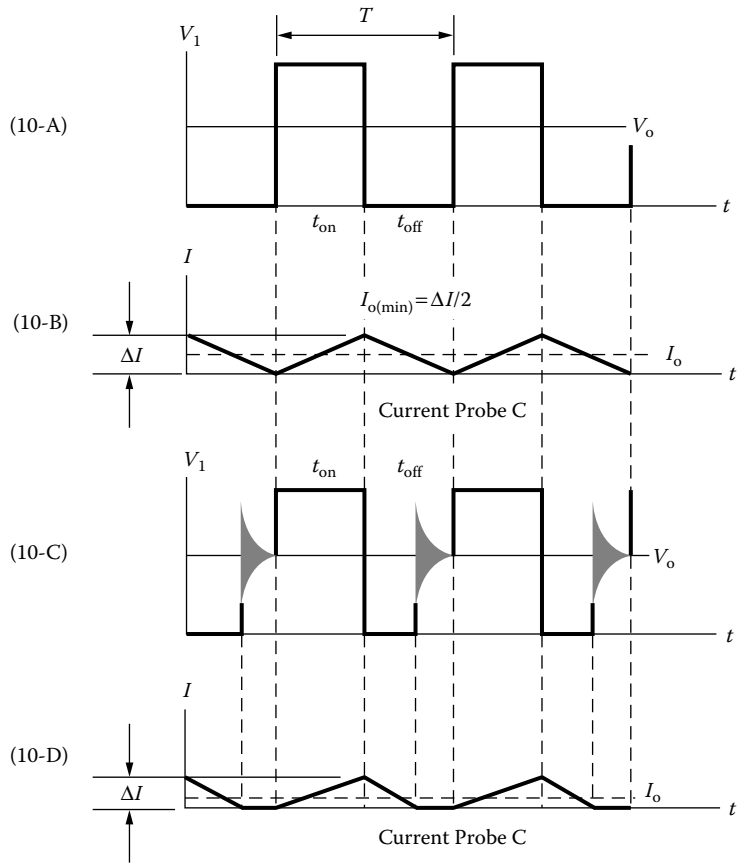

Figure 14-10. Forward Converter; Output Filter Inductor goes from Critical to Discontinuous Operation.

© 2011 by Taylor and Francis Group, LLC

Output Inductor Design Using the Core Geometry, K_g, Approach

The following information is the design specification for a forward converter, 30watt output filter design, operating at 100kHz, using the Kg core geometry approach. For a typical design example, assume an Output Filter Circuit, as shown in Figure 14-1, with the following specifications:

1. Frequency, f = 100kHz
2. Output voltage, $V_o = 5$ volts
3. Output current, $I_{o(max)} = 5.0$ amps
4. Output current, $I_{o(min)} = 0.5$ amps
5. Delta current, $\Delta I = 1.0$ amps
6. Input voltage, $V_{I(max)} = 19$ volts
7. Input voltage, $V_{I(min)} = 12$ volts
8. Regulation, $\alpha = 1.0\%$
9. Output power $(V_o + V_d)\ (I_{o(max)})$, $P_o = 30$ watts
10. Operating flux density, $B_{pk} = 0.3$ teslas
11. Window utilization, $K_u = 0.4$
12. Diode voltage drop, $V_d = 1.0$ volt

This design procedure will work equally well with all of the various powder cores. Care must be taken regarding maximum flux density with different materials and core loss.

The skin effect on an inductor is the same as a transformer. The main difference is that the ac flux is much lower and does not require the use of the same maximum wire size. The ac flux is caused by the delta current, ΔI, and is normally only a fraction of the dc flux. In this design the ac current and the dc current will be treated the same.

At this point, select a wire so that the relationship between the ac resistance and the dc resistance is 1:

$$\frac{R_{ac}}{R_{dc}} = 1$$

The skin depth, ε, in centimeters, is:

$$\varepsilon = \frac{6.62}{\sqrt{f}}, \quad [\text{cm}]$$

$$\varepsilon = \frac{6.62}{\sqrt{100,000}}, \quad [\text{cm}]$$

$$\varepsilon = 0.0209, \quad [\text{cm}]$$

© 2011 by Taylor and Francis Group, LLC

Then, the wire diameter, D_w, is:

$$D_w = 2(\varepsilon), \quad [\text{cm}]$$
$$D_w = 2(0.0209), \quad [\text{cm}]$$
$$D_w = 0.0418, \quad [\text{cm}]$$

Then, the bare wire area, A_w, is:

$$A_w = \frac{\pi(D_w)^2}{4}, \quad [\text{cm}^2]$$
$$A_w = \frac{(3.1416)(0.0418)^2}{4}, \quad [\text{cm}^2]$$
$$A_w = 0.00137, \quad [\text{cm}^2]$$

From the Wire Table in Chapter 4, Number 27 has a bare wire area of 0.001021 centimeters. This will be the minimum wire size used in this design. If the design requires more wire area to meet the specification, then the design will use a multifilar of #26. Listed Below are #27 and #28, just, in case #26 requires too much rounding off.

Wire AWG	Bare Area	Area Ins.	Bare/Ins.	μΩ/cm
#26	0.001280	0.001603	0.798	1345
#27	0.001021	0.001313	0.778	1687
#28	0.0008046	0.0010515	0.765	2142

Step No. 1: Calculate the total period, T.

$$T = \frac{1}{f}, \quad [\text{seconds}]$$
$$T = \frac{1}{100,000}, \quad [\text{seconds}]$$
$$T = 10, \quad [\mu\text{sec}]$$

Step No. 2: Calculate the minimum duty ratio, D_{min}.

$$D_{\min} = \frac{V_o}{V_{1\max}}$$
$$D_{\min} = \frac{5}{19}$$
$$D_{\min} = 0.263$$

© 2011 by Taylor and Francis Group, LLC

Step No. 3: Calculate the required inductance, L.

$$L = \frac{T(V_o + V_d)(1 - D_{\min})}{\Delta I}, \quad \text{[henrys]}$$

$$L = \frac{\left(10 \times 10^{-6}\right)(5.0 + 1.0)(1 - 0.263)}{(1.0)}, \quad \text{[henrys]}$$

$$L = 44.2, \quad [\mu\text{h}]$$

Step No. 4: Calculate the peak current, I_{pk}.

$$I_{pk} = I_{o(\max)} + \left(\frac{\Delta I}{2}\right), \quad \text{[amps]}$$

$$I_{pk} = (5.0) + \left(\frac{1.0}{2}\right), \quad \text{[amps]}$$

$$I_{pk} = 5.5, \quad \text{[amps]}$$

Step No. 5: Calculate the energy-handling capability in, watt-seconds.

$$\text{Energy} = \frac{LI_{pk}^2}{2}, \quad \text{[watt-seconds]}$$

$$\text{Energy} = \frac{\left(44.2x10^{-6}\right)(5.5)^2}{2}, \quad \text{[watt-seconds]}$$

$$\text{Energy} = 0.000668, \quad \text{[watt-seconds]}$$

Step No. 6: Calculate the electrical conditions, K_e.

$$K_e = 0.145 P_o B_m^2 \times 10^{-4}$$

$$K_e = (0.145)(30)(0.3)^2 \times 10^{-4}$$

$$K_e = 0.0000392$$

Step No. 7: Calculate the core geometry, K_g.

$$K_g = \frac{(\text{Energy})^2}{K_e \alpha} \quad [\text{cm}^5]$$

$$K_g = \frac{(0.000668)^2}{(0.0000392)(1.0)} \quad [\text{cm}^5]$$

$$K_g = 0.01138 \quad [\text{cm}^5]$$

Step No. 8: Select, from Chapter 4, a MPP powder core, comparable in core geometry, K_g.

Core number = MP-55059-A2

Manufacturer = Magnetics

Magnetic path length, MPL = 5.7 cm

Core weight, W_{tfe} = 16.0 grams

Copper weight, W_{tcu} = 15.2 grams

Mean length turn, MLT = 3.2 cm

© 2011 by Taylor and Francis Group, LLC

Iron area, $A_c = 0.331$ cm^2

Window Area, $W_a = 1.356$ cm^2

Area Product, $A_p = 0.449$ cm^4

Core geometry, $K_g = 0.0184$ cm^5

Surface area, $A_t = 28.6$ cm^2

Permeability, $\mu = 60$

Millihenrys per 1000 turns, AL = 43

Step No. 9: Calculate the number of turns, N.

$$N = 1000\sqrt{\frac{L_{(new)}}{L_{(1000)}}}, \quad \text{[turns]}$$

$$N = 1000\sqrt{\frac{0.0442}{43}}, \quad \text{[turns]}$$

$$N = 32, \quad \text{[turns]}$$

Step No. 10: Calculate the rms current, I_{rms}.

$$I_{rms} = \sqrt{I_{o(\max)}^2 + \Delta I^2}, \quad \text{[amps]}$$

$$I_{rms} = \sqrt{(5.0)^2 + (1.0)^2}, \quad \text{[amps]}$$

$$I_{rms} = 5.1, \quad \text{[amps]}$$

Step No. 11: Calculate the current density, J, using a window utilization, $K_u = 0.4$.

$$J = \frac{NI}{W_a K_u}, \quad \text{[amps-per-cm}^2\text{]}$$

$$J = \frac{(32)(5.1)}{(1.36)(0.4)}, \quad \text{[amps-per-cm}^2\text{]}$$

$$J = 300, \quad \text{[amps-per-cm}^2\text{]}$$

Step No. 12: Calculate the required permeability, $\Delta\mu$.

$$\Delta\mu = \frac{B_{pk}\,(\text{MPL})\left(10^4\right)}{0.4\pi W_a J K_u}, \quad \text{[perm]}$$

$$\Delta\mu = \frac{(0.3)(5.7)\left(10^4\right)}{(1.26)(1.36)(300)(0.4)}, \quad \text{[perm]}$$

$$\Delta\mu = 83.1, \quad \text{use } 60 \quad \text{[perm]}$$

© 2011 by Taylor and Francis Group, LLC

Step No. 13: Calculate the peak flux density, B_{pk}.

$$B_{pk} = \frac{0.4\pi N I_{pk} \mu_r \left(10^{-4}\right)}{(\text{MPL})}, \quad [\text{teslas}]$$

$$B_{pk} = \frac{(1.26)(32)(5.5)(60)\left(10^{-4}\right)}{(5.7)}, \quad [\text{teslas}]$$

$$B_{pk} = 0.233, \quad [\text{teslas}]$$

Step No. 14: Calculate the required bare wire area, $A_{w(B)}$.

$$A_{w(B)} = \frac{I_{rms}}{J}, \quad [\text{cm}^2]$$

$$A_{w(B)} = \frac{5.1}{300}, \quad [\text{cm}^2]$$

$$A_{w(B)} = 0.017, \quad [\text{cm}^2]$$

Step No. 15: Calculate the required number of strands, S_n.

$$S_n = \frac{A_{w(B)}}{\#26}, \quad [\text{strands}]$$

$$S_n = \frac{0.017}{0.00128}, \quad [\text{strands}]$$

$$S_n = 13, \quad [\text{strands}]$$

Step No. 16: Calculate the new, μΩ, per centimeter.

$$(\text{new})\mu\Omega / \text{cm} = \frac{\mu\Omega / \text{cm}}{S_n}$$

$$(\text{new})\mu\Omega / \text{cm} = \frac{1345}{13}$$

$$(\text{new})\mu\Omega / \text{cm} = 103$$

Step No. 17: Calculate the winding resistance, R.

$$R = (\text{MLT})N\left(\frac{\mu\Omega}{\text{cm}}\right)\left(10^{-6}\right), \quad [\text{ohms}]$$

$$R = (3.2)(32)(103)\left(10^{-6}\right), \quad [\text{ohms}]$$

$$R = 0.0105, \quad [\text{ohms}]$$

Step No. 18: Calculate the winding copper loss, P_{cu}.

$$P_{cu} = I_{rms}^2 R, \quad [\text{watts}]$$

$$P_{cu} = (5.1)^2(0.0105), \quad [\text{watts}]$$

$$P_{cu} = 0.273, \quad [\text{watts}]$$

© 2011 by Taylor and Francis Group, LLC

Step No. 19: Calculate the magnetizing force in oersteds, H.

$$H = \frac{0.4\pi N I_{pk}}{\text{MPL}}, \quad \text{[oersteds]}$$

$$H = \frac{(1.26)(32)(5.5)}{5.7}, \quad \text{[oersteds]}$$

$$H = 38.9, \quad \text{[oersteds]}$$

Step No. 20: Calculate the ac flux density in teslas, B_{ac}.

$$B_{ac} = \frac{0.4\pi N\left(\frac{\Delta I}{2}\right)\mu_r\left(10^{-4}\right)}{\text{MPL}}, \quad \text{[teslas]}$$

$$B_{ac} = \frac{(1.26)(32)(0.5)(60)\left(10^{-4}\right)}{(5.7)}, \quad \text{[teslas]}$$

$$B_{ac} = 0.0212, \quad \text{[teslas]}$$

Step No. 21: Calculate the regulation, α, for this design.

$$\alpha = \frac{P_{cu}}{P_o}(100), \quad [\%]$$

$$\alpha = \frac{(0.273)}{(30)}(100), \quad [\%]$$

$$\alpha = 0.91, \quad [\%]$$

Step No. 22: Calculate the watts per kilogram, WK, using MPP 60 perm powder cores coefficients, shown in Chapter 2.

$$WK = 0.551\left(10^{-2}\right) f^{(1.23)} B_{ac}^{(2.12)}, \quad \text{[watts-per-kilogram]}$$

$$WK = 0.551\left(10^{-2}\right)(100000)^{(1.23)}(0.0212)^{(2.12)}, \quad \text{[watts-per-kilogram]}$$

$$WK = 2.203, \quad \text{[watts-per-kilogram]}$$

Step No. 23: Calculate the core loss, P_{fe}.

$$P_{fe} = \left(\frac{\text{milliwatts}}{\text{gram}}\right) W_{tfe}\left(10^{-3}\right), \quad \text{[watts]}$$

$$P_{fe} = (2.203)(16)\left(10^{-3}\right), \quad \text{[watts]}$$

$$P_{fe} = 0.0352, \quad \text{[watts]}$$

© 2011 by Taylor and Francis Group, LLC

Step No. 24: Calculate the total loss, P_Σ, core, P_{fe}, and copper, P_{cu}, in watts.

$$P_\Sigma = P_{fe} + P_{cu}, \quad [\text{watts}]$$

$$P_\Sigma = (0.0352) + (0.273), \quad [\text{watts}]$$

$$P_\Sigma = 0.308, \quad [\text{watts}]$$

Step No. 25: Calculate the watt density, ψ.

$$\psi = \frac{P_\Sigma}{A_t}, \quad [\text{watts-per-cm}^2]$$

$$\psi = \frac{(0.308)}{(28.6)}, \quad [\text{watts-per-cm}^2]$$

$$\psi = 0.0108, \quad [\text{watts-per-cm}^2]$$

Step No. 26: Calculate the temperature rise, in, °C.

$$T_r = 450(\psi)^{(0.826)}, \quad [°\text{C}]$$

$$T_r = 450(0.0108)^{(0.826)}, \quad [°\text{C}]$$

$$T_r = 10.7, \quad [°\text{C}]$$

Step No. 27: Calculate the window utilization, K_u.

$$K_u = \frac{N S_n A_{w(B)}}{W_a}$$

$$K_u = \frac{(32)(13)(0.00128)}{(1.356)}$$

$$K_u = 0.393$$

Recognition

The author would like to thank the late **Dr. J. K. Watson**, Professor of Electrical Engineering at the University of Florida for his help with the Forward Converter design equations.

© 2011 by Taylor and Francis Group, LLC

Chapter 15

Input Filter Design

© 2011 by Taylor and Francis Group, LLC

Table of Contents

1. Introduction....15-3
2. Capacitor....15-3
3. Inductor....15-5
4. Oscillation....15-5
5. Applying Power....15-6
6. Resonant Charge....15-8
7. Input Filter Inductor Design Procedure....15-9
8. Input Filter Design Specification....15-11
9. Recognition....15-16
10. References....15-16

© 2011 by Taylor and Francis Group, LLC

Introduction

Today, almost all modern equipment uses some sort of power conditioning. There are a lot of different circuit topologies used. When you get to the bottom line, all power conditioning requires some kind of an input filter. The input, LC, filter has become very critical in its design and must be designed not only for EMI, but also for system stability, and for the amount of ac ripple current drawn from the source.

The input voltage supplied to the equipment is also supplied to other users. For this reason, there is a specification requirement regarding the amount of ripple current seen at the source, as shown in Figure 15-1. Ripple currents generated by the user induce a ripple voltage, V_z, across the source impedance. This ripple voltage could impede the performance of other equipment connected to the same bus.

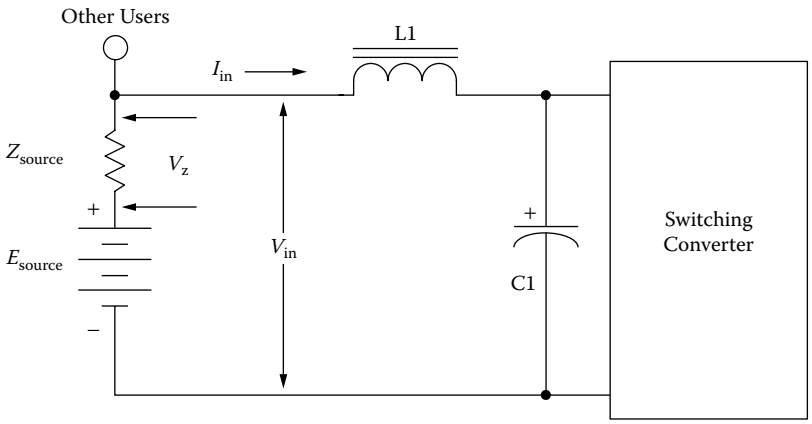

Figure 15-1. Simple, LC, Input Filter.

Capacitor

Switching regulators have required the engineer to put a significantly more analytical effort into the design of the input filter. The current pulse, induced by the switching regulator, has had the most impact on the input capacitor. These current pulses required the use of high quality capacitors with low ESR. The waveforms, induced by the switching regulator, are shown in Figure 15-2. In the input inductor, L1, peak-peak ripple current is, I_L. In the capacitor, C1, peak-peak, ripple current is, I_c. In the capacitor, C1, peak-peak, ripple voltage is, ΔV_c. The equivalent circuit for the capacitor is shown in Figure 15-3. The voltage, ΔV_c, developed across the capacitor, is the sum of two components, the Equivalent Series Resistance, (ESR), and the reactance of the capacitor.

© 2011 by Taylor and Francis Group, LLC

The voltage, V_{CR}, developed across the Equivalent Series Resistance, (ESR), is shown in Equation [15-1].

$$V_{CR} = I_C(\text{ESR}), \quad \text{[volts]} \tag{15-1}$$

The voltage, ΔV_{CC}, developed across the capacitance is shown in Equation [15-2].

$$\Delta V_{CC} = I_C\left(\frac{(t_{on})(t_{off})}{(C1)(T)}\right), \quad \text{[volts]} \tag{15-2}$$

The sum of the two voltages, ΔV_{CR} and ΔV_{CC}, is shown in Equation [15-3].

$$\Delta V_C = \Delta V_{CR} + \Delta V_{CC}, \quad \text{[volts]} \tag{15-3}$$

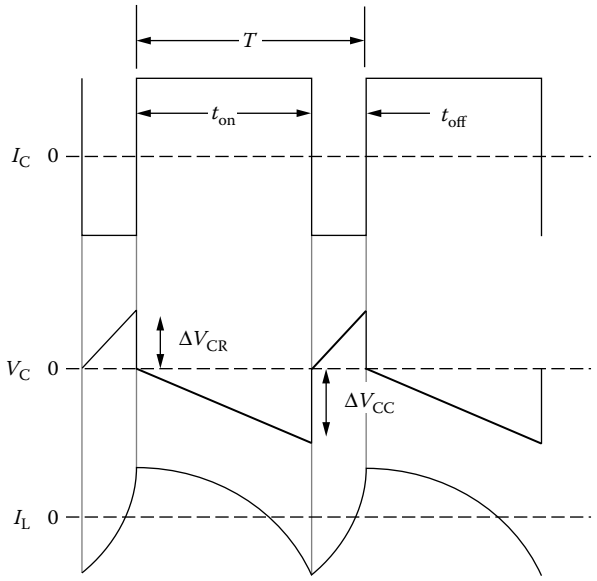

Figure 15-2. Typical Voltage, Current Waveforms.

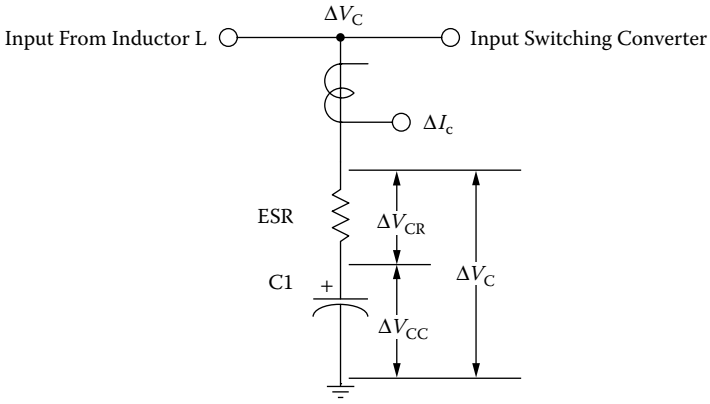

Figure 15-3. Capacitor, Individual Ripple, Components.

© 2011 by Taylor and Francis Group, LLC

Inductor

The input filter inductor is basically a straightforward design. There are four parameters required to achieve a good design: (1) required inductance, (2) dc current, (3) dc resistance, and (4) temperature rise. The requirement for the input inductor is to provide a low ac ripple current to the source. The low ac ripple current in the inductor produces an ac flux at a magnitude of about 0.025 teslas. This resulting low ac flux will keep the core loss to a minimum. The input inductor losses will normally be 80 to 90% copper. A high flux magnetic material is ideally suited in this application. Operating with a high dc flux and a low ac flux, silicon, with its high flux density of 1.6 teslas, will produce the smallest size, as shown in Table 15-1.

Table 15-1. Most Commonly Used Input Filter Material

Magnetic Material Properties		
Material	Operating Flux, B, teslas	Permeability μ_i
Silicon	1.5-1.8	1.5K
Permalloy Powder	0.3	14-550
Iron Power	1.2-1.4	35-90
Ferrite	0.3	1K-15K

Oscillation

The input filter can affect the stability of the associated switching converter. The stability problem results from an interaction between the output impedance of the input filter and the input impedance of the switching converter. Oscillation occurs when the combined positive resistance of the LC filter, and power source exceed the negative dynamic resistance of the regulator's dc input. To prevent oscillation, the capacitor's ESR, and the inductor's resistance must provide sufficient damping. Oscillation will not occur when the conditions are, as shown in Equation [15-4].

$$\left(\frac{\eta(V_{in})^2}{P_o}\right) > \left(\frac{L}{\frac{C+(R_L+R_s)(\text{ESR})}{(R_L+R_s)+(\text{ESR})}}\right) \qquad [15\text{-}4]$$

Where, η, is the switching converter efficiency, $V_{in(max)}$, is the input voltage; P_o, is the output power in watts; L, is the input inductor in henrys; where, C, is the filter capacitor in farads, R_L, is inductor series resistance in ohms; R_s, is the source resistance in ohms, and, R_d (ESR), is the equivalent series resistance in ohms. If additional damping, is required, it can be done, by increasing the, R_d (ESR), and/or, R_L. See Figure 15-4. The series resistance, R_d, lowers the, Q, of the filter and kills the potential oscillation.

© 2011 by Taylor and Francis Group, LLC

Applying Power

The inrush current has always been a problem with this simple, LC, input filter. When a step input is applied, such as a relay or switch, S1, as shown in Figure 15-5, there is always a high inrush current.

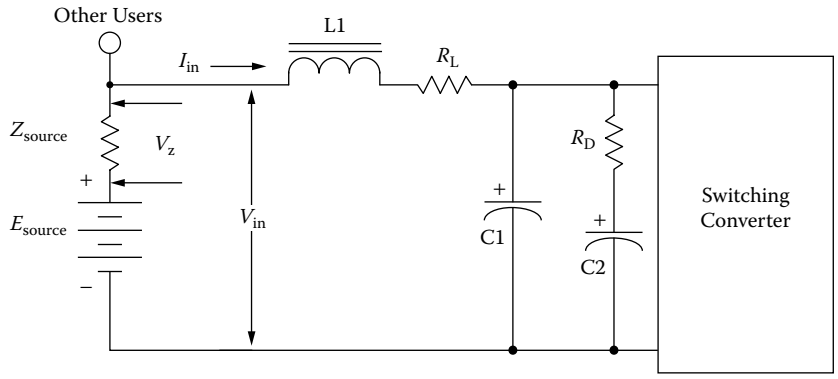

Figure 15-4. Input Filter, with Additional Damping.

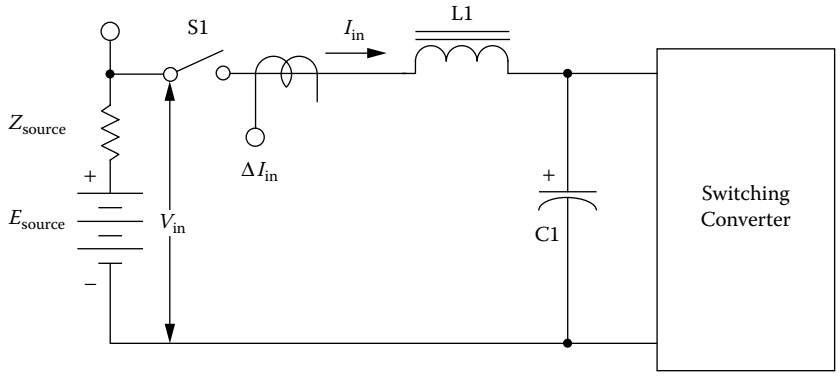

Figure 15-5. Input Filter Inrush Current Measurement.

When, S1, is closed, the full input voltage, V_{in}, is applied directly across the input inductor, L1, because, C1, is discharged. The applied input voltage, V_{in}, (volt-seconds), to the input inductor, L1, and the dc current, (amp-turns), flowing through it is enough to saturate the core. The inductor, L1, is normally designed, using the upper limits of the flux density for minimum size. There are two types of core configurations commonly used for input inductor design: powder cores and gapped cores. Some engineers prefer to design around powder cores because they are simple and less of a hassle, while others design using gapped cores. It is strictly a game of trade-offs. Tests were performed using three different core materials: (1) powder core, (2) ferrite core, and (3) iron alloy. All three materials were designed to have the same inductance and the same dc resistance. The three-inductor designs were tested to compare the inrush current under the same conditions. The inrush current, ΔI, for all three materials is shown in Figure 15-6, using the test circuit, shown in Figure 15-5.

© 2011 by Taylor and Francis Group, LLC

As, shown in Figure 15-6, the inrush current for all three test inductors has about the same general shape and amplitude. The changes in permeability, with dc bias, for both gapped and powder cores are shown in Figure 15-7. Gapped cores have a definitely sharper knee while the powder cores roll off more gradually. The advantage in using a gapped core over the powder core is the ability to use the full flux capacity of the core up to the knee, before the permeability starts to droop.

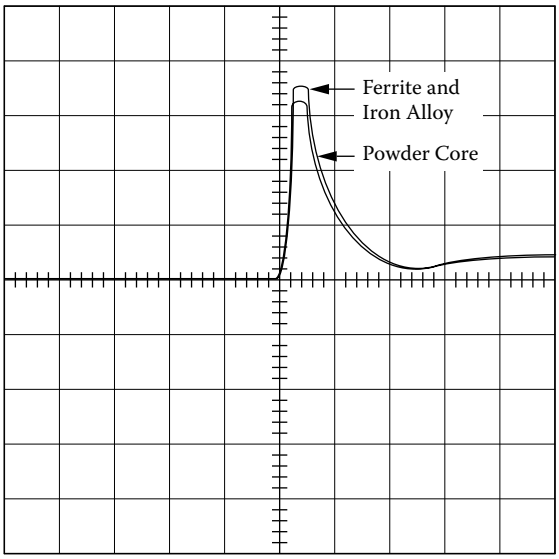

Vertical 2 amps/Div., Horizontal 500 µsec/Div.

Figure 15-6. Typical, Inrush Current for a Simple Input.

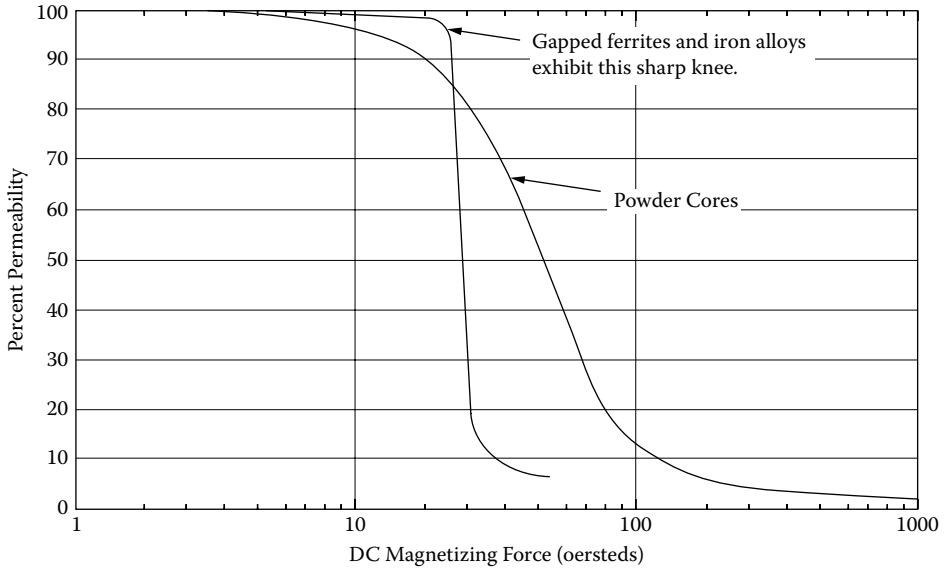

Figure 15-7. Comparing Gapped and Powder Cores, Permeability Change with DC Bias.

© 2011 by Taylor and Francis Group, LLC

Resonant Charge

Most all types of electronic equipment are energized by either a switch or relay. This type of turn-on goes for spacecraft, aircraft, computer, medical equipment, and automobiles. There are some power sources that require some type of current limiting that do not follow the general rule. If the input voltage is applied via a switch or relay to an input filter, as shown in Figure 15-8, a resonant charge condition will develop with, L1 and C1. The resulting resonant charge, with L1 and C1, could put a potential on, C1, which could be as much as twice the applied input voltage, as shown in Figure 15-9. The voltage rating of, C1, must be high enough to sustain this peak voltage without damage. The oscillating voltage is applied to the switching converter.

A simple way to dampen this oscillation is to place one or two diodes across the input choke, as shown in Figure 15-10. The reason for two diodes is the ripple voltage, V_c, might be greater than the threshold voltage of the diode. As the voltage across, C1, rises above the input voltage, V_{in}, due to the oscillation diodes, CR1 and CR2, will become forward-biased, clamping the voltage across, C1, to two diode drops above the input voltage, V_{in}, as shown in Figure 15-11.

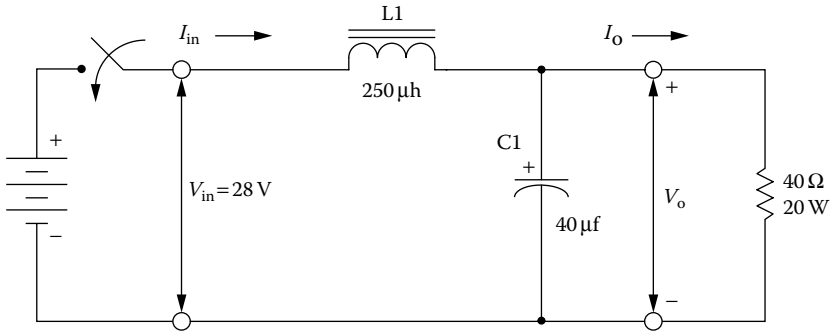

Figure 15-8. Typical, Simple LC, Input Filter.

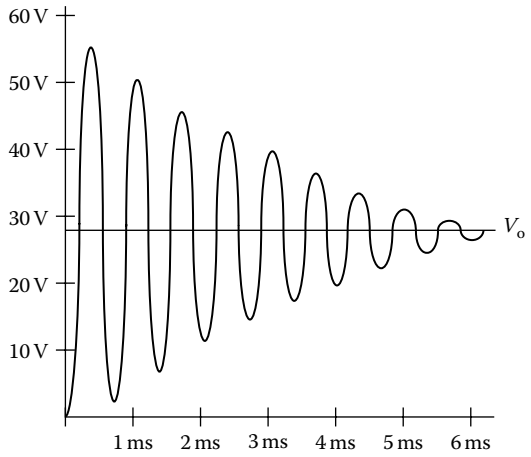

Figure 15-9. Resonating Voltage, across Capacitor, C1.

© 2011 by Taylor and Francis Group, LLC

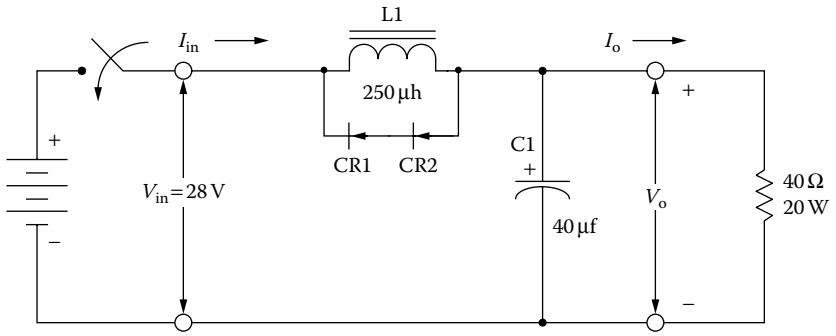

Figure 15-10. Input Inductor with Clamp Diodes.

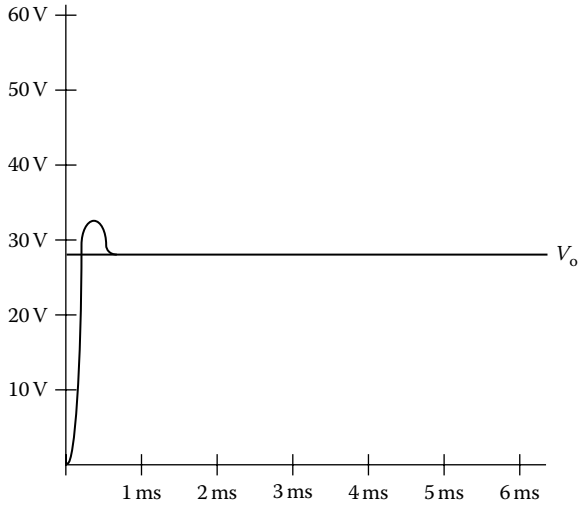

Figure 15-11. DC Voltage Across C1, with the Clamp Diodes.

Input Filter Inductor Design Procedure

The input filter inductor, L1, for this design is shown in Figure 15-12.

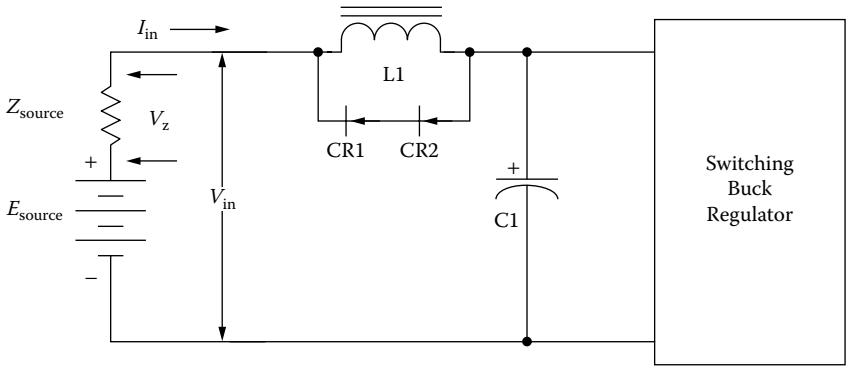

Figure 15-12. Input Filter Circuit.

© 2011 by Taylor and Francis Group, LLC

The ac voltages and currents associated with the input capacitor, C1, are shown in Figure 15-13.

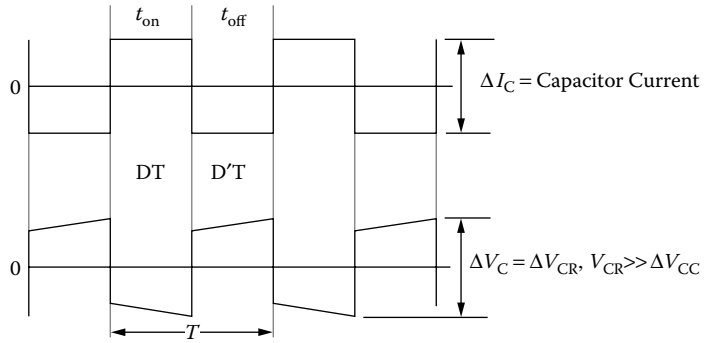

Figure 15-13. Input Capacitor Voltage and Current Ripple.

The ac voltages and currents impressed on the input capacitor, C1, are defined in Figure 15-14.

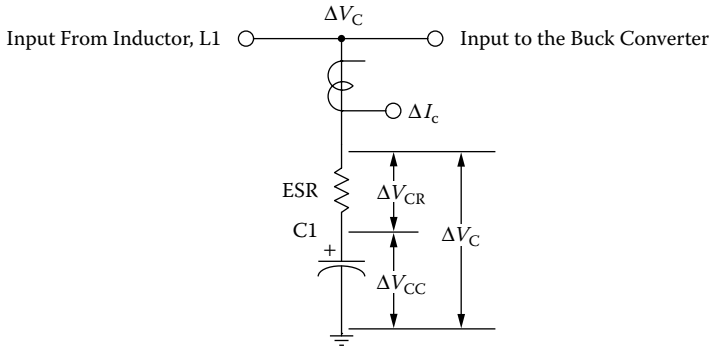

Figure 15-14. Defining the Input Capacitor Voltage and Current Ripple.

The components of the inductor current, due to, ΔV_{CR}, and ΔV_{CC}, are:

ΔV_{CR} = Peak to Peak component due to capacitor, ESR.

ΔV_{CC} = Peak to Peak component due to capacitor.

ΔI_{LR} = Component of the inductor ripple current developed by, ΔV_{CR}.

ΔI_{LC} = Component of the inductor ripple current developed by, ΔV_{CC}.

$$\Delta I_{LR} = \left(\frac{\Delta V_{CR}}{L}\right)\left(DD'T\right), \quad \text{[amps]}$$
$$\Delta I_{LC} = \left(\frac{\Delta V_{CC}}{2L}\right)\left(\frac{T}{4}\right), \quad \text{[amps]} \qquad \text{[15-5]}$$

It will be considered that, ΔI_{LR}, dominates because of the capacitor, ESR, so:

$$\Delta I_{LR} = \left(\frac{\Delta V_{CR}}{L}\right)\left(DD'T\right), \quad \text{[amps]} \qquad \text{[15-6]}$$

© 2011 by Taylor and Francis Group, LLC

Input Filter Design Specification

1. Peak-Peak ripple voltage, $\Delta V_{cr} = 0.5$ volts
2. Peak-Peak ripple current to the source, $\Delta I_L = 0.010$ amps
3. Period, T = 10 μsec
4. *Converter on-time duty cycle, $D = t_{on}/T = 0.5$
5. *Converter off-time duty cycle, $D' = t_{off}/T = 0.5$
6. Regulation, $\alpha = 0.5\%$
7. Output power drawn from the filter network, $P_o = 50$ watts
8. Maximum current to the load, $\Delta I_c = 4$ amps
9. Average input current, $I_{in} = I_{av} = \Delta I_c\, D = 2$ amps
10. The ripple frequency, f = 100kHz
11. The core RM ferrite, gapped, $B_{max} = 0.25$ teslas

Step No. 1: Calculate the required inductance, L.

$$L = \frac{\Delta V_{CR}}{\Delta I_L}\left(DD'T\right), \quad \text{[henrys]}$$

$$L = \frac{0.5}{0.01}(0.5)(0.5)\left(10\left(10^{-6}\right)\right), \quad \text{[henrys]}$$

$$L = 0.000125, \quad \text{[henrys]}$$

Step No. 2: Calculate the energy-handling capability.

$$\text{Energy} = \frac{L\left(I_{av}\right)^2}{2}, \quad \text{[watt-second]}$$

$$\text{Energy} = \frac{125\left(10^{-6}\right)(2.0)^2}{2}, \quad \text{[watt-second]}$$

$$\text{Energy} = 0.000250, \quad \text{[watt-second]}$$

Step No. 3: Calculate the electrical coefficient, K_e.

$$K_e = 0.145 P_o B_m^2 \left(10^{-4}\right)$$

$$K_e = 0.145(50)(0.25)^2 \left(10^{-4}\right)$$

$$K_e = 0.0000453$$

* The worse case time domain is where, D and D′ = 0.5

© 2011 by Taylor and Francis Group, LLC

Step No. 4: Calculate the core geometry, K_g.

$$K_g = \frac{(\text{Energy})^2}{K_e \alpha}, \quad [\text{cm}^5]$$

$$K_g = \frac{(0.00025)^2}{(0.0000453)(0.5)}, \quad [\text{cm}^5]$$

$$K_g = 0.00275, \quad [\text{cm}^5]$$

Step No. 5: Select the comparable core geometry from the RM ferrite cores.

1. Core part number = RM-6
2. Core geometry, $K_g = 0.0044$ cm^5
3. Core cross-section, $A_c = 0.366$ cm^2
4. Window area, $W_a = 0.260$ cm^2
5. Area product, $A_p = 0.0953$ cm^4
6. Mean length turn, MLT = 3.1 cm
7. Magnetic path length, MPL = 2.86 cm
8. Core weight, $W_{tfe} = 5.5$ grams
9. Surface area, $A_t = 11.3$ cm^2
10. Winding Length, G = 0.82 cm
11. Material, P, $\mu_m = 2500$

Step No. 6: Calculate the current density, J, using the area product equation, A_p.

$$J = \frac{2(\text{Energy})(10^4)}{B_m A_p K_u}, \quad [\text{amps-per-cm}^2]$$

$$J = \frac{2(0.00025)(10^4)}{(0.25)(0.0952)(0.4)}, \quad [\text{amps-per-cm}^2]$$

$$J = 525, \quad [\text{amps-per-cm}^2]$$

Step No. 7: Calculate the required bare wire area, $A_{w(B)}$.

$$A_{W(B)} = \frac{I_{avg}}{J}, \quad [\text{cm}^2]$$

$$A_{W(B)} = \frac{(2.0)}{(525)}, \quad [\text{cm}^2]$$

$$A_{W(B)} = 0.00381, \quad [\text{cm}^2]$$

© 2011 by Taylor and Francis Group, LLC

Step No. 8: Select a wire from the Wire Table in Chapter 4. If the area is not within 10%, take the next smallest size. Also record micro-ohms per centimeter.

$$\text{AWG} = \#21$$

$$\text{Bare, } A_{W(B)} = 0.00411, \quad [\text{cm}^2]$$

$$\text{Insulated, } A_W = 0.00484, \quad [\text{cm}^2]$$

$$\left(\frac{\mu\Omega}{\text{cm}}\right) = 419, \quad [\text{micro-ohm/cm}]$$

Step No. 9: Calculate the effective window area, $W_{a(eff)}$. Use the window area found in Step 5. A typical value for, S_3 is 0.75, as shown in Chapter 4.

$$W_{a(eff)} = W_a S_3, \quad [\text{cm}^2]$$

$$W_{a(eff)} = (0.260)(0.75), \quad [\text{cm}^2]$$

$$W_{a(eff)} = 0.195, \quad [\text{cm}^2]$$

Step No. 10: Calculate the number turns possible, N. Use the insulated wire area, A_w, found in Step 8. A typical value for, S_2, is 0.6, as shown in Chapter 4.

$$N = \frac{W_{a(eff)} S_2}{A_W}, \quad [\text{turns}]$$

$$N = \frac{(0.195)(0.60)}{(0.00484)}, \quad [\text{turns}]$$

$$N = 24, \quad [\text{turns}]$$

Step No. 11: Calculate the required gap, l_g.

$$l_g = \frac{0.4\pi N^2 A_c\left(10^{-8}\right)}{L} - \left(\frac{\text{MPL}}{\mu_m}\right), \quad [\text{cm}]$$

$$l_g = \frac{(1.26)(24)^2(0.366)\left(10^{-8}\right)}{(0.000125)} - \left(\frac{2.86}{2500}\right), \quad [\text{cm}]$$

$$l_g = 0.0201, \quad [\text{cm}]$$

Step No. 12: Calculate the equivalent gap in mils.

$$\text{mils} = \text{cm}(393.7)$$

$$\text{mils} = (0.0197)(393.7)$$

$$\text{mils} = 7.91 \text{ use } 8$$

© 2011 by Taylor and Francis Group, LLC

Step No. 13: Calculate the fringing flux factor, F.

$$F = 1 + \frac{l_g}{\sqrt{A_c}} \ln\left(\frac{2G}{l_g}\right)$$

$$F = 1 + \frac{(0.0201)}{\sqrt{0.366}} \ln\left(\frac{2(0.82)}{0.0201}\right)$$

$$F = 1.146$$

Step No. 14: Calculate the new number of turns, N_n, by inserting the fringing flux, F.

$$N_n = \sqrt{\frac{l_g L}{0.4\pi A_c F\left(10^{-8}\right)}}, \quad \text{[turns]}$$

$$N_n = \sqrt{\frac{(0.0201)(0.000125)}{(1.26)(0.366)(1.146)\left(10^{-8}\right)}}, \quad \text{[turns]}$$

$$N_n = 22, \quad \text{[turns]}$$

Step No. 15: Calculate the winding resistance, R_L. Use the, MLT, from Step 5 and the micro-ohm per centimeter, from Step 8.

$$R_L = (\text{MLT})(N_n)\left(\frac{\mu\Omega}{\text{cm}}\right)\left(10^{-6}\right), \quad \text{[ohms]}$$

$$R_L = (3.1)(22)(419)\left(10^{-6}\right), \quad \text{[ohms]}$$

$$R_L = 0.0286, \quad \text{[ohms]}$$

Step No. 16: Calculate the copper loss, P_{cu}.

$$P_{cu} = I_{avg}^2 R_L, \quad \text{[watts]}$$

$$P_{cu} = (2.0)^2 (0.0286), \quad \text{[watts]}$$

$$P_{cu} = 0.114, \quad \text{[watts]}$$

Step No. 17: Calculate the regulation, α.

$$\alpha = \frac{P_{cu}}{P_o}(100), \quad [\%]$$

$$\alpha = \frac{(0.114)}{(50)}(100), \quad [\%]$$

$$\alpha = 0.228, \quad [\%]$$

© 2011 by Taylor and Francis Group, LLC

Step No. 18: Calculate the ac flux density, B_{ac}.

$$B_{ac} = \frac{0.4\pi N_n F\left(\frac{\Delta I}{2}\right)\left(10^{-4}\right)}{l_g + \left(\frac{\text{MPL}}{\mu_m}\right)}, \quad \text{[teslas]}$$

$$B_{ac} = \frac{(1.26)(22)(1.14)\left(\frac{0.01}{2}\right)\left(10^{-4}\right)}{(0.0197) + \left(\frac{2.86}{2500}\right)}, \quad \text{[teslas]}$$

$$B_{ac} = 0.000758, \quad \text{[teslas]}$$

Step No. 19: Calculate the watts-per-kilogram, for ferrite, P, material in Chapter 2. Watts per kilogram can be written in milliwatts-per-gram.

$$\text{mW/g} = k f^{(m)} B_{ac}^{(n)}$$

$$\text{mW/g} = (0.00198)(100000)^{(1.36)}(0.000758)^{(2.86)}$$

$$\text{mW/g} = 0.0000149$$

Step No. 20: Calculate the core loss, P_{fe}.

$$P_{fe} = (\text{mW/g})\left(W_{tfe}\right)\left(10^{-3}\right), \quad \text{[watts]}$$

$$P_{fe} = (0.0000149)(5.5)\left(10^{-3}\right), \quad \text{[watts]}$$

$$P_{fe} = 0.082\left(10^{-6}\right), \quad \text{[watts]}$$

Step No. 21: Calculate the total loss copper plus iron, P_{Σ}.

$$P_{\Sigma} = P_{fe} + P_{cu}, \quad \text{[watts]}$$

$$P_{\Sigma} = (0.000) + (0.114), \quad \text{[watts]}$$

$$P_{\Sigma} = 0.114, \quad \text{[watts]}$$

Step No. 22: Calculate the watt density, ψ. The surface area, A_t, can be found in Step 5.

$$\psi = \frac{P_{\Sigma}}{A_t}, \quad \text{[watts/cm}^2\text{]}$$

$$\psi = \frac{(0.114)}{(11.3)}, \quad \text{[watts/cm}^2\text{]}$$

$$\psi = 0.010, \quad \text{[watts/cm}^2\text{]}$$

© 2011 by Taylor and Francis Group, LLC

Step No. 23: Calculate the temperature rise, T_r.

$$T_r = 450(\psi)^{(0.826)}, \quad [°C]$$

$$T_r = 450(0.010)^{(0.826)}, \quad [°C]$$

$$T_r = 10.0, \quad [°C]$$

Step No. 24: Calculate the peak flux density, B_{pk}.

$$B_{pk} = \frac{0.4\pi N_n F\left(I_{dc} + \frac{\Delta I}{2}\right)\left(10^{-4}\right)}{l_g + \left(\frac{\text{MPL}}{\mu_m}\right)}, \quad [\text{teslas}]$$

$$B_{pk} = \frac{(1.26)(22)(1.14)(2.005)\left(10^{-4}\right)}{(0.0197) + \left(\frac{2.86}{2500}\right)}, \quad [\text{teslas}]$$

$$B_{pk} = 0.304, \quad [\text{teslas}]$$

Step No. 25: Calculate the window utilization, K_u.

$$K_u = \frac{A_{w(B)} N_n}{W_a}$$

$$K_u = \frac{(0.00411)(22)}{(0.260)}$$

$$K_u = 0.348$$

Recognition

I would like to thank Jerry Fridenberg, for modeling the circuits in Figure 15-8 and 15-10, on his SPICE program. The modeling results are shown in Figures 15-9 and 15-11.

References

1. T. K. Phelps and W. S. Tate, “Optimizing Passive Input Filter Design,” (no source).

2. David Silber, “Simplifying the Switching Regulator Input Filter,” *Solid-State Power Conversion*, May/June 1975.

3. Dan Sheehan, “Designing a Regulator’s LC Input Filter: ‘Ripple’ Method Prevents Oscillation Woes,” *Electronic Design* 16, August 2, 1979.

© 2011 by Taylor and Francis Group, LLC

Chapter 16

Current Transformer Design

© 2011 by Taylor and Francis Group, LLC

Table of Contents

1. Introduction....16-3
2. Analysis of the Input Current Component....16-4
3. Uniqueness of a Current Transformer....16-5
4. Current Transformer Circuit Applications....16-7
5. Current Transformer Design Example....16-9
6. Design Performance....16-13

© 2011 by Taylor and Francis Group, LLC

Introduction

Current transformers are used to measure, or monitor, the current in the lead of an ac power circuit. They are very useful in high-power circuits, where the current is large, i.e., higher than the ratings of so-called self-contained current meters. Other applications relate to overcurrent and undercurrent relaying for power circuit protection, such as, in the power lead of an inverter or converter. Multiturn secondaries then provide a reduced current for detecting overcurrent, undercurrent, peak current, and average current, as shown in Figure 16-1.

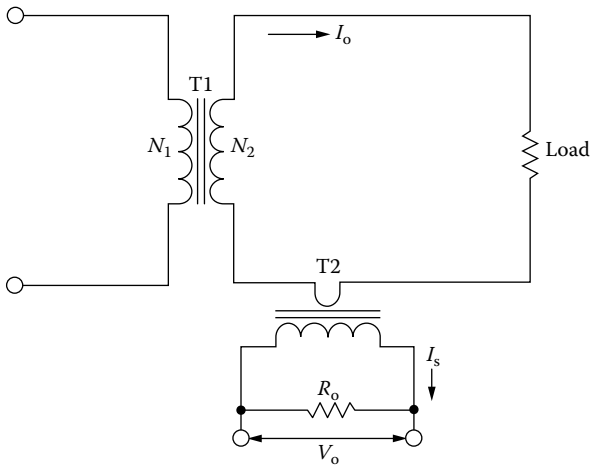

Figure 16-1. Simple, Secondary AC Current Monitor.

In current transformer designs, the core characteristics must be carefully selected because excitation current, I_m, essentially subtracts from the metered current and effects the true ratio and phase angle of the output current.

The simplified equivalent circuit of a current transformer, as shown in Figure 16-2, represents the important elements of a current transformer, where the ratio of primary to secondary turns is shown in the Equation [16-1].

$$n = \frac{N_s}{N_p}, \quad \text{[turns ratio]} \qquad \text{[16-1]}$$

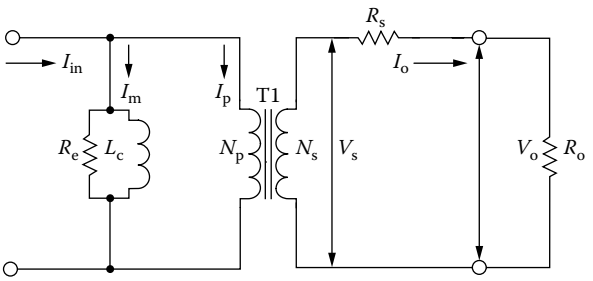

Figure 16-2. Simplified, Equivalent Circuit for a Current Transformer.

© 2011 by Taylor and Francis Group, LLC

Analysis of the Input Current Component

A better understanding of the current transformer behavior may be achieved by considering the applied input current to the primary winding, in terms of various components. Only the ampere-turn component, $I_{in}N_p$, drives the magnetic flux around the core. The ampere-turn, I_mN_p, provides the core loss. The secondary ampere-turns, I_sN_p, balance the remainder of the primary ampere-turns.

The exciting current, I_m, in Figure 16-2, determines the maximum accuracy that can be achieved with a current transformer. Exciting current, I_m, may be defined as the portion of the primary current that satisfies the hysteresis and eddy current losses of the core. If the values of L_c and R_e, in Figure 16-2, are too low because the permeability of the core material is low and the core loss is high, only a part of the current, (I_p/n), will flow in the output load resistor, R_o. The relationship of the exciting current, I_m, to the load current, I_o, is shown in Figure 16-3.

The exciting current, I_m, is equal to:

$$I_m = \frac{H(\text{MPL})}{0.4\pi N}, \quad \text{[amps]} \qquad \text{[16-2]}$$

Where H is the magnetizing force and material dependent, and MPL is the Magnetic Path Length.

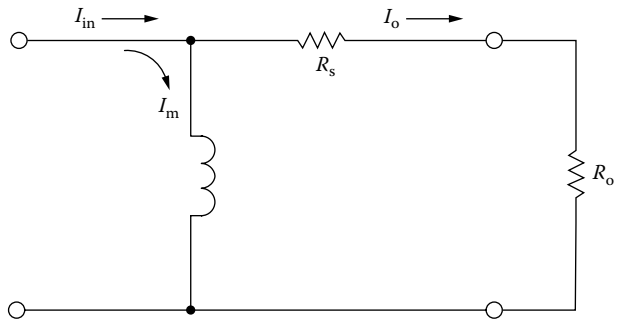

Figure 16-3. Input Current-Output Current Relationship.

The input current is comprised of two components: exciting current, I_m, and the load current, I_o.

$$I_{in}^2 = I_m^2 + I_o^2, \quad \text{[amps]} \qquad \text{[16-3]}$$

Then:

$$I_m^2 = I_{in}^2 - I_o^2, \quad \text{[amps]} \qquad \text{[16-4]}$$

© 2011 by Taylor and Francis Group, LLC

$$I_m = I_{in}\left[1-\left(\frac{I_o}{I_{in}}\right)^2\right]^{1/2}, \quad \text{[amps]} \qquad \text{[16-5]}$$

The above Equation has shown graphically, as in Figure 16-4, that the higher the exciting current, I_m, or core loss, the larger the error. The magnetizing impedance, R_e, determines accuracy, because it shunts part of the input current, I_{in}, away from the primary and thus, produces an error, as shown in Figure 16-4. Core material with the lowest value of, H, achieves the highest accuracy.

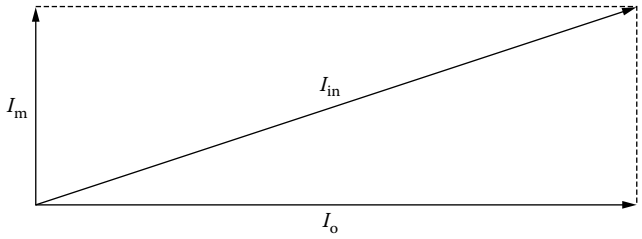

Figure 16-4. Input Current I_{in} Phase Relationship Diagram.

Uniqueness of a Current Transformer

The current transformer function is different than that of a voltage transformer. A current transformer operates with a set primary current and will try to output a constant current to the load, independent of the load. The current transformer will operate into either a short circuit or a resistive load until the voltage induced is enough to saturate the core or cause voltage breakdown. For this reason a current transformer should never operate into an open circuit, as a voltage transformer should never operate into a short circuit. The primary current of a current transformer is not dependent of the secondary load current. The current is really injected into the primary by an external load current, I_{in}. If the load current, I_o, on the current transformer is removed from the secondary winding, while the external load current, I_{in}, is still applied, the flux in the core will rise to a high level, because there is not an opposing current in the secondary winding to prevent this. A very high voltage will appear across the secondary. A current transformer, like any other transformer, must satisfy the amp-turn equation, as shown in Equation [16-6].

$$\frac{I_p}{I_s} = \frac{N_s}{N_p} \qquad \text{[16-6]}$$

The secondary load, R_o, secondary winding resistance, R_s, and secondary load current, I_o, determine the induced voltage of the current transformer, as shown in Equation [16-7].

$$V_s = I_o\left(R_s + R_o\right), \quad \text{[volts]} \qquad \text{[16-7]}$$

© 2011 by Taylor and Francis Group, LLC

If the secondary is designed for dc, then the diode drop must be taken into account, as shown in Equation [16-8].

$$V_s = I_o\left(R_s + R_o\right) + V_d, \quad \text{[volts]} \tag{16-8}$$

Simple form:

$$V_s = V_o + V_d, \quad \text{[volts]} \tag{16-9}$$

The current ratio will set the turns ratio. The secondary, R_o, load will determine the secondary voltage, V_s. The engineer would use Equation 16-10, to select the required core cross-section, A_c. It is now up to the engineer to pick a core material that would provide the highest permeability at the operating flux density, B_{ac}.

$$A_c = \frac{I_{in}\left(R_s + R_o\right)\left(10^4\right)}{K_f B_{ac} f N_s}, \quad \text{[cm}^2\text{]} \tag{16-10}$$

The design requirements would dictate choosing a core material and operating flux density, B_{ac}, that would result in values of, L_c and R_e, as shown in Figure 16-2, values which would be large enough to reduce the current flowing in these elements to satisfy the ratio and phase requirements.

The inductance is calculated from the Equation:

$$L_c = \frac{0.4\pi N_p^2 A_c \Delta\mu\left(10^{-8}\right)}{\text{MPL}}, \quad \text{[henrys]} \tag{16-11}$$

R_e is the equivalent core loss, (shunt), resistance. The current is, in phase, with the voltage.

$$R_e = \frac{V_s/n}{P_{fe}}, \quad \text{[ohms]} \tag{16-12}$$

Where:

$$\frac{R_e}{n^2} \gg R_s + R_o \tag{16-13}$$

And:

$$\frac{2\pi f L_c}{n^2} \gg R_s + R_o \tag{16-14}$$

© 2011 by Taylor and Francis Group, LLC

Then:

$$I_p = nI_s \quad [16\text{-}15]$$

Or:

$$I_p N_p = I_s N_s \quad [16\text{-}16]$$

Except for relatively low-accuracy industrial types, current transformers are wound on toroidal cores, which virtually eliminate errors due to leakage inductance. Some errors may be compensated for by adjusting the number of secondary turns.

Current Transformer Circuit Applications

Typical current transformer applications are shown in Figures 16-5 through 16-8.

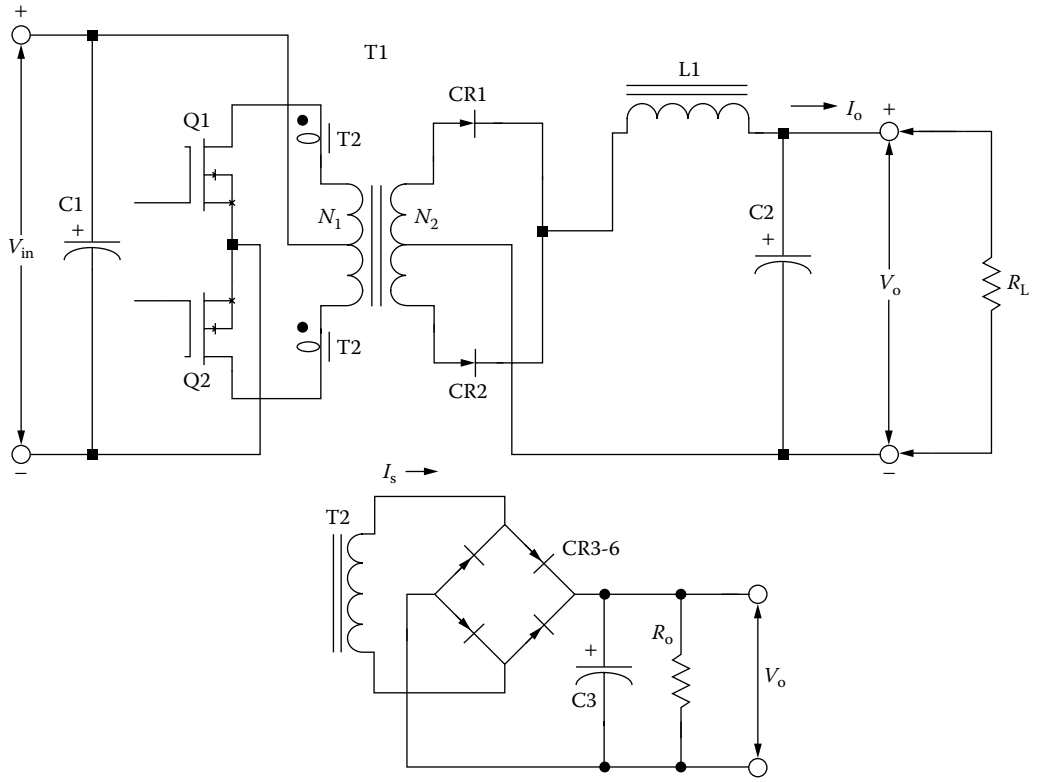

Figure 16-5. Current Transformer, T2, used to Monitor, Q1 and Q2, Drain Current.

© 2011 by Taylor and Francis Group, LLC

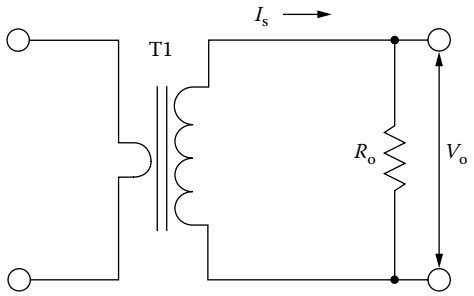

Figure 16-6. Current Transformer, T1, used to Monitor Line Current.

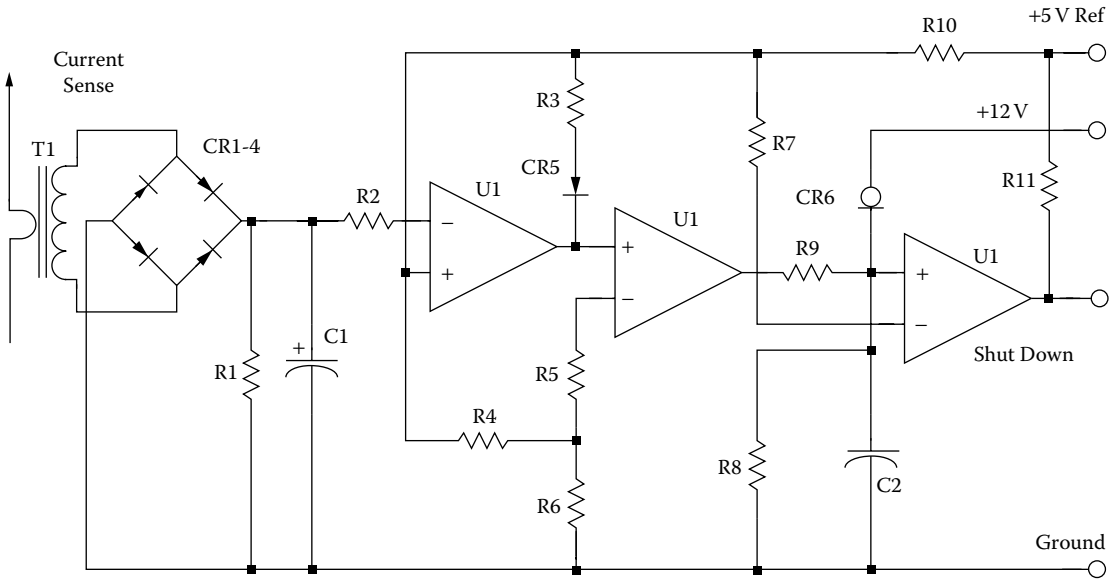

Figure 16-7. Current Transformer, T1, is used as a Level Detector.

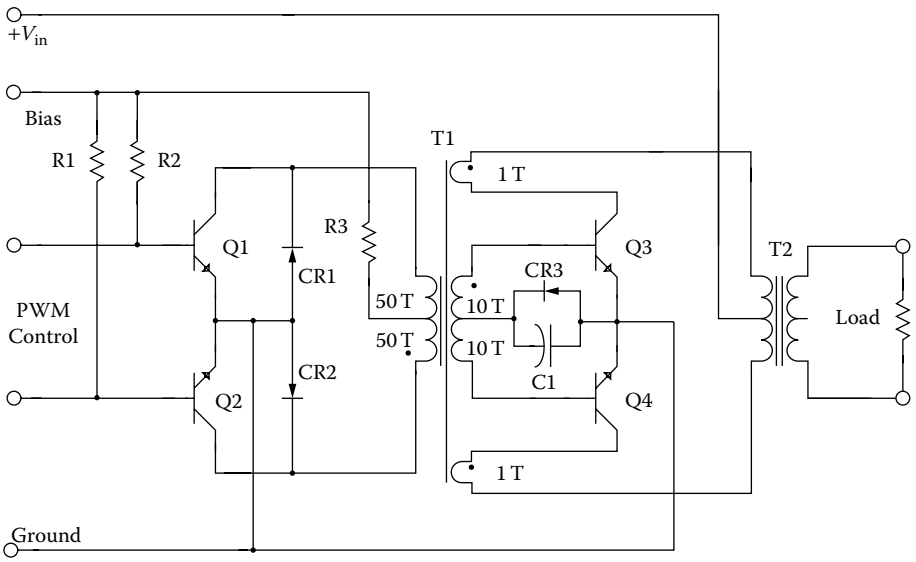

Figure 16-8. Current Transformer, T1, is used for Regenerative Drive.

© 2011 by Taylor and Francis Group, LLC

Current Transformer Design Example

The following information is the design specification for a Current Transformer, as shown in Figure 16-9.

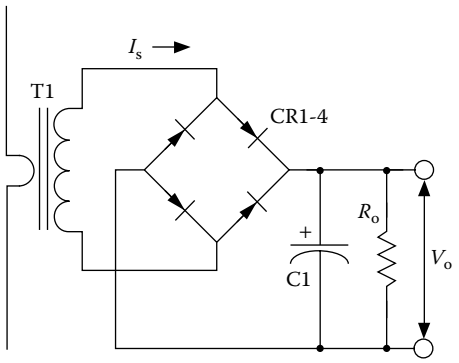

Figure 16-9. Current Monitoring Transformer with dc Output.

1. Primary = 1 turn
2. Input current, $I_{in} = 0 - 5$ amps
3. Output voltage, $V_o = 0 - 5$ volts
4. Output load resistance, $R_o = 500$ ohms
5. Operating frequency, f (square wave) = 2500 hertz
6. Operating flux density, $B_{ac} = 0.2$ tesla
7. Core loss less than = 3% (error)
8. Diode drop, $V_d = 1$ volt
9. Magnetic material = Supermalloy 2 mil
10. Waveform factor, $K_f = 4.0$

Step 1: Calculate the secondary current, I_s.

$$I_s = \frac{V_o}{R_o}, \quad \text{[amps]}$$

$$I_s = \frac{5.0}{500}, \quad \text{[amps]}$$

$$I_s = 0.01, \quad \text{[amps]}$$

Step 2: Calculate the secondary turns, N_s.

$$N_s = \frac{I_p N_p}{I_s}, \quad \text{[turns]}$$

$$N_s = \frac{(5.0)(1.0)}{(0.01)}, \quad \text{[turns]}$$

$$N_s = 500, \quad \text{[turns]}$$

© 2011 by Taylor and Francis Group, LLC

Step 3: Calculate the secondary voltage, V_s.

$$V_s = V_o + 2V_d, \quad [\text{volts}]$$

$$V_s = 5.0 + 2(1.0), \quad [\text{volts}]$$

$$V_s = 7.0, \quad [\text{volts}]$$

Step 4: Calculate the required core iron cross-section, A_c, using Faraday's Equation.

$$A_c = \frac{V_s\left(10^4\right)}{\left(K_f\right)B_{ac}\,f\,N_s}, \quad [\text{cm}^2]$$

$$A_c = \frac{(7.0)\left(10^4\right)}{(4.0)(0.2)(2500)(500)}, \quad [\text{cm}^2]$$

$$A_c = 0.070, \quad [\text{cm}^2]$$

Step 5: Select a 2mil tape, toroidal core from Chapter 3 with an iron cross-section, A_c, closest to the value calculated.

Toroid = 52000-2F
Manufacturer = Magnetics
Magnetic material = 2mil Supermalloy
Magnetic path length, MPL = 4.99 cm
Core weight, W_{tfe} = 3.3 grams
Copper weight, W_{tcu} = 8.1 grams
Mean length turn, MLT = 2.7 cm
Iron area, A_c = 0.086 cm^2
Window area, W_a = 0.851 cm^2
Area product, A_p = 0.0732 cm^4
Core geometry, K_g = 0.000938 cm^5
Surface area, A_t = 20.6 cm^2

Step 6: Calculate the effective window area, $W_{a\,(eff)}$. A typical value for, S_3, is 0.75, as shown in Chapter 4.

$$W_{a(eff)} = W_a S_3, \quad [\text{cm}^2]$$

$$W_{a(eff)} = (0.851)(0.75), \quad [\text{cm}^2]$$

$$W_{a(eff)} = 0.638, \quad [\text{cm}^2]$$

© 2011 by Taylor and Francis Group, LLC

Step 7: Calculate the secondary window area, $W_{a\,(sec)}$.

$$W_{a(\sec)} = \frac{W_{a(eff)}}{2}, \quad [\text{cm}^2]$$

$$W_{a(\sec)} = \frac{0.638}{2}, \quad [\text{cm}^2]$$

$$W_{a(\sec)} = 0.319, \quad [\text{cm}^2]$$

Step 8: Calculate the wire area, A_w, with insulation, using a fill factor, S_2 of 0.6.

$$A_w = \frac{W_{a(\sec)} S_2}{N_s}, \quad [\text{cm}^2]$$

$$A_w = \frac{(0.319)(0.6)}{(500)}, \quad [\text{cm}^2]$$

$$A_w = 0.000383, \quad [\text{cm}^2]$$

Step 9: Select a wire area, A_w, with insulation from Wire Table in Chapter 4 for an equivalent AWG wire size. The rule is that when the calculated wire area does not fall within 10% of those listed in the Wire Table, then, the next smaller size should be selected.

AWG No. 33

$$A_w = 0.0003662, \quad [\text{cm}^2]$$

Step 10: Calculate the secondary winding resistance, R_s using the Wire Table in Chapter 4, for μΩ/cm; and Step 5 for the MLT.

$$R_s = \text{MLT}(N_s)\left(\frac{\mu\Omega}{\text{cm}}\right)\left(10^{-6}\right), \quad [\text{ohms}]$$

$$R_s = (2.7)(500)(6748)\left(10^{-6}\right), \quad [\text{ohms}]$$

$$R_s = 9.11, \quad [\text{ohms}]$$

Step 11: Calculate the secondary output power, P_o.

$$P_o = I_s\left(V_o + 2V_d\right), \quad [\text{watts}]$$

$$P_o = (0.01)\left(5.0 + 2(1.0)\right), \quad [\text{watts}]$$

$$P_o = 0.070, \quad [\text{watts}]$$

Step 12: Calculate the acceptable core loss, P_{fe}.

$$P_{fe} = P_o\left(\frac{\text{core loss \%}}{100}\right), \quad [\text{watts}]$$

$$P_{fe} = (0.07)\left(\frac{3}{100}\right), \quad [\text{watts}]$$

$$P_{fe} = 0.0021, \quad [\text{watts}]$$

© 2011 by Taylor and Francis Group, LLC

Step 13: Calculate the effective core weight, $W_{tfe(eff)}$. Select the core weight correction factor, K_w, in Chapter 2, for Supermalloy.

$$W_{tfe(eff)} = W_{tfe} K_w, \quad \text{[grams]}$$
$$W_{tfe(eff)} = (3.3)(1.148), \quad \text{[grams]}$$
$$W_{tfe(eff)} = 3.79, \quad \text{[grams]}$$

Step 14: Calculate the allowable core loss, P_{fe}, in milliwatts per gram, mW/g.

$$\text{mW/g} = \frac{P_{fe}}{W_{tfe}}\left(10^3\right), \quad \text{[milliwatts per gram]}$$
$$\text{mW/g} = \frac{(0.0021)}{(3.79)}\left(10^3\right), \quad \text{[milliwatts per gram]}$$
$$\text{mW/g} = 0.554, \quad \text{[milliwatts per gram]}$$

Step 15: Calculate the new flux density using the new core iron, cross-section, A_c.

$$B_{ac} = \frac{V_s\left(10^4\right)}{\left(K_f\right)A_c f N_s}, \quad \text{[teslas]}$$
$$B_{ac} = \frac{(7.0)\left(10^4\right)}{(4.0)(0.086)(2500)(500)}, \quad \text{[teslas]}$$
$$B_{ac} = 0.162, \quad \text{[teslas]}$$

Step 16: Calculate the core loss, P_{fe}, in milliwatts per gram, mW/g.

$$\text{mW/g} = 0.000179\left(f\right)^{(1.48)}\left(B_{ac}\right)^{(2.15)}, \quad \text{[milliwatts per gram]}$$
$$\text{mW/g} = 0.000179(2500)^{(1.48)}(0.162)^{(2.15)}, \quad \text{[milliwatts per gram]}$$
$$\text{mW/g} = 0.382, \quad \text{[milliwatts per gram]}$$

Step 17: Calculate the core loss, P_{fe}, in watts.

$$P_{fe} = W_{tfe}\left(\frac{mW}{g}\right)\left(10^{-3}\right), \quad \text{[watts]}$$
$$P_{fe} = 3.79(0.382)\left(10^{-3}\right), \quad \text{[watts]}$$
$$P_{fe} = 0.00145, \quad \text{[watts]}$$

© 2011 by Taylor and Francis Group, LLC

Step 18: Calculate the induced core error in, %.

$$\text{Core loss induced error} = \frac{P_{fe}}{P_o}(100), \quad [\%]$$

$$\text{Core loss induced error} = \frac{0.00145}{.07}(100), \quad [\%]$$

$$\text{Core loss induced error} = 2.07, \quad [\%]$$

Design Performance

A current transformer was built and the data recorded in Table 16-1. It was plotted in Figure 16-10, with an error of 3.4 %. The secondary winding resistance was 6.5 ohms.

Table 16-1.

Current Transformer Electrical Data					
I_{in} amps	I_o volts	I_{in} amps	I_o volts	I_{in} amps	I_o volts
0.250	0.227	1.441	1.377	3.625	3.488
0.500	0.480	2.010	1.929	3.942	3.791
0.746	0.722	2.400	2.310	4.500	4.339
1.008	0.978	2.693	2.593	5.014	4.831
1.262	1.219	3.312	3.181	5.806	5.606

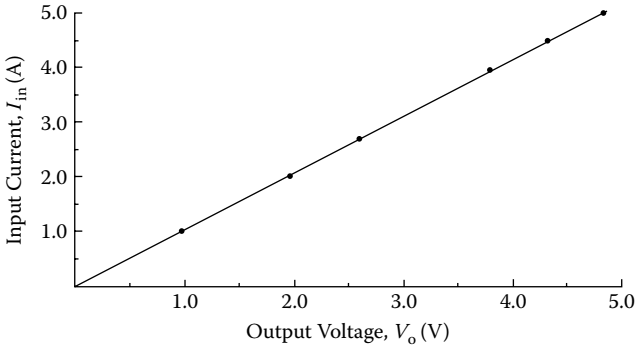

Figure 16-10. Current Transformer, Input Current versus Output Voltage.

© 2011 by Taylor and Francis Group, LLC

Chapter 17

Winding Capacitance and Leakage Inductance

© 2011 by Taylor and Francis Group, LLC

Table of Contents

1. Introduction 17-3
2. Parasitic Effects 17-3
3. Leakage Flux 17-4
4. Minimizing Leakage Inductance 17-7
5. Winding Capacitance 17-8
6. Winding Capacitance Turn-to-Turn 17-10
7. Winding Capacitance Layer-to-Layer 17-10
8. Capacitance Winding-to-Winding 17-11
9. Stray Capacitance 17-12
10. References 17-14

© 2011 by Taylor and Francis Group, LLC

Introduction

Operation of transformers at high frequencies presents unique design problems due to the increased importance of core loss, leakage inductance, and winding capacitance. The design of high frequency power converters is far less stringent than designing high frequency, wide-band audio transformers. Operating at a single frequency requires fewer turns, and consequently, there is less leakage inductance and less capacitance with which to deal. The equivalent circuit for a two-winding transformer is shown in Figure 17-1.

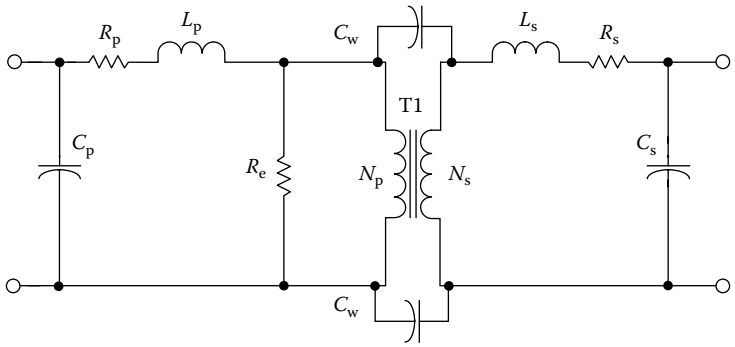

Figure 17-1. Equivalent Transformer Circuit.

High frequency designs require considerably more care in specifying the winding specification. This is because physical orientation and spacing of the windings determine leakage inductance and winding capacitance. Leakage inductance and capacitance are actually distributed throughout the winding in the transformer. However, for simplicity, they are shown as lumped constants, in Figure 17-1. The leakage inductance is represented by L_p for the primary, and L_s for the secondary. The equivalent lumped capacitance is represented by C_p, and, C_s, for the primary and secondary windings. The dc winding resistance is R_p, and, R_s, is for the equivalent resistance for the primary and secondary windings. C_w, is the equivalent lumped, winding-to-winding capacitance. R_e is the equivalent core-loss shunt resistance.

Parasitic Effects

The effects of leakage inductance on switching power supply circuits are shown in Figure 17-2. The voltage spikes, shown in Figure 17-2, are caused by the stored energy in the leakage flux and will increase with load, as shown in Equation 17-1. These spikes will always appear on the leading edge of the voltage switching waveform.

$$Energy = \frac{L_{(Leakage)}\left(I_{(pk)}\right)^2}{2}, \quad \text{[watt-seconds]} \qquad \text{[17-1]}$$

© 2011 by Taylor and Francis Group, LLC

Transformers designed for switching applications are normally designed to have minimum leakage inductance, in order to minimize the voltage spikes, as shown in Figure 17-2. Also, leakage inductance can be observed by the leading edge slope of the trapezoidal current waveform.

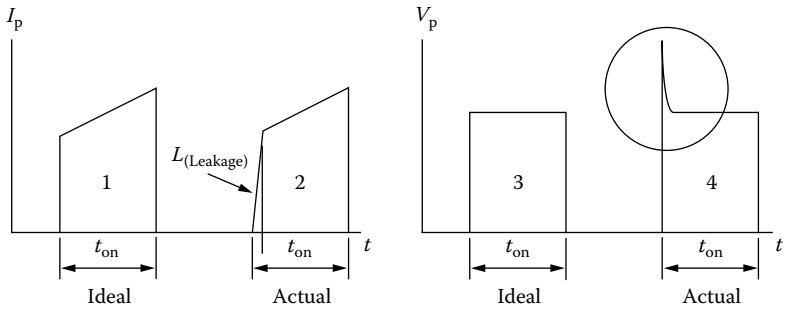

Figure 17-2. Switching Transistor Voltage and Current Waveforms.

Transformers designed for power conversion are normally being driven with a square wave, characterized by fast rise and fall times. This fast transition will generate high current spikes in the primary winding, due to the parasitic capacitance in the transformer. These current spikes, shown in Figure 17-3, are caused by the capacitance in the transformer; they will always appear on the lead edge of the current waveform and always with the same amplitude, regardless of the load. This parasitic capacitance will be charged and discharged every half cycle. Transformer leakage inductance and capacitance have an inverse relationship: if you decrease the leakage inductance, you will increase the capacitance; if you decrease the capacitance, you increase the leakage inductance. These are trade-offs that the power conversion engineer must make to design the best transformer for the application.

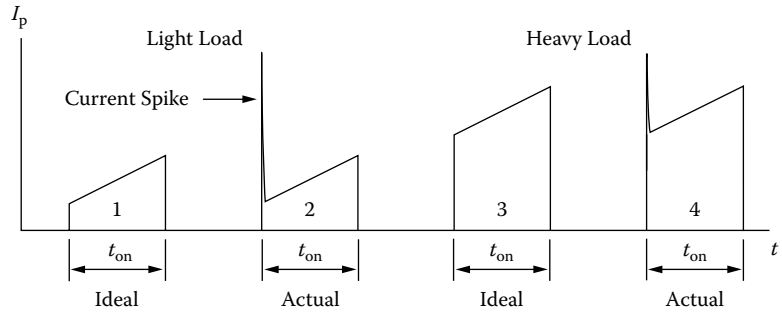

Figure 17-3. Transformer Capacitance Induced Current spike.

Leakage Flux

Leakage inductance is actually distributed throughout the windings of a transformer because of the flux set-up by the primary winding, which does not link the secondary, thus giving rise to leakage inductance in each winding without contributing to the mutual flux, as shown in Figure 17-4.

© 2011 by Taylor and Francis Group, LLC

However, for simplicity, leakage inductance is shown as a lumped constant in Figure 17-1, where the leakage inductance is represented by L_p.

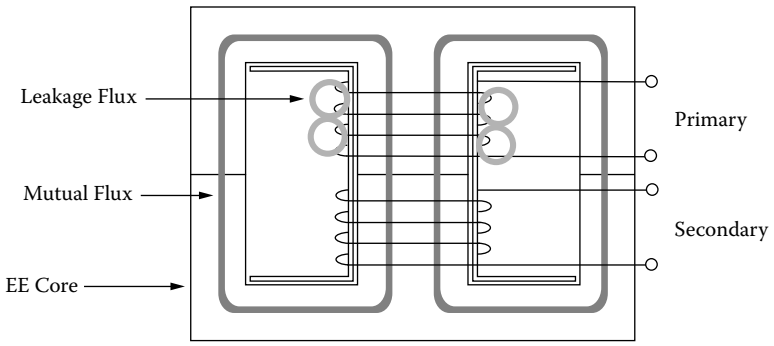

Figure 17-4. Leakage Flux.

In the layer-wound coil, a substantial reduction in leakage inductance, L_p and L_s, is obtained by interweaving the primary and secondary windings. The standard transformer, with a single primary and secondary winding, is shown in Figure 17-5, along with its leakage inductance, Equation [17-2]. Taking the same transformer and splitting the secondary on either side of the primary will reduce the leakage inductance, as shown in Figure 17-6, along with its leakage inductance, Equation [17-3]. The leakage inductance can be reduced even more, by interleaving the primary and secondary, as shown in Figure 17-7, along with its leakage inductance, Equation [17-4]. Transformers can also be constructed using the side-by-side, sectionalized bobbin as shown in Figure 17-8, along with its leakage inductance, Equation [17-5]. The modified three section, side-by-side bobbin is shown in Figure 17-9, along with its leakage inductance Equation [17-6].

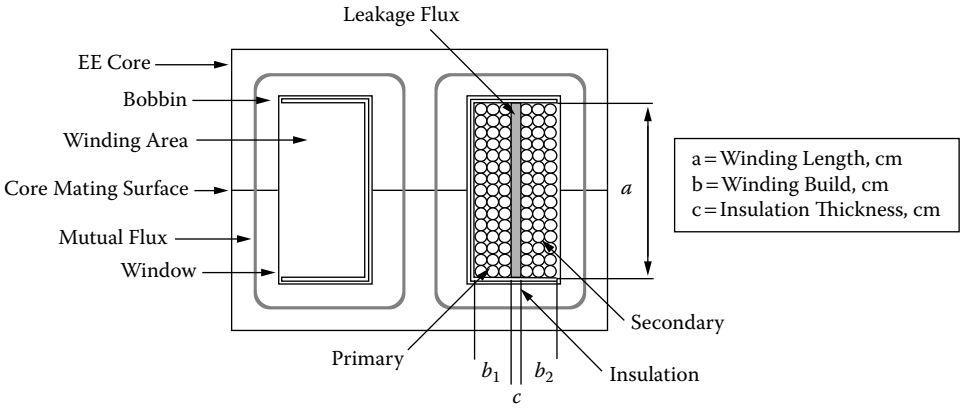

Figure 17-5. Conventional Transformer Configuration.

$$L_p = \frac{4\pi(MLT)N_p^2}{a}\left(c + \frac{b_1 + b_2}{3}\right)\left(10^{-9}\right), \quad \text{[henrys]} \qquad \text{[17-2]}$$

© 2011 by Taylor and Francis Group, LLC

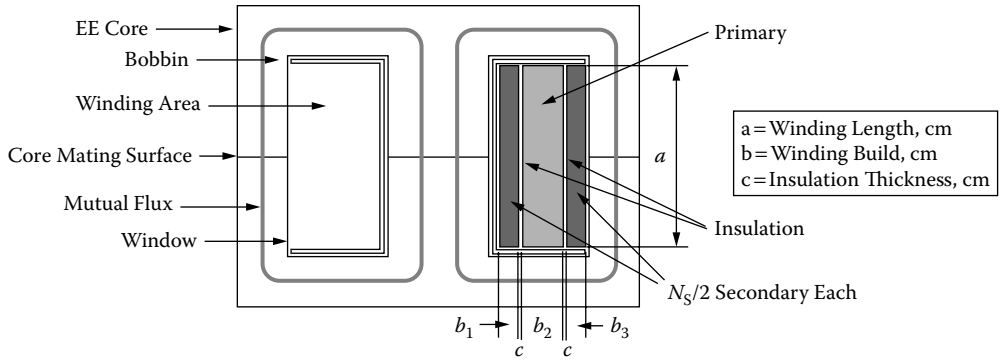

Figure 17-6. Conventional, Transformer Configuration with Simple Interleave.

$$L_p = \frac{\pi(MLT)N_p^2}{a}\left(\Sigma c + \frac{\Sigma b}{3}\right)\left(10^{-9}\right), \quad \text{[henrys]} \qquad \text{[17-3]}$$

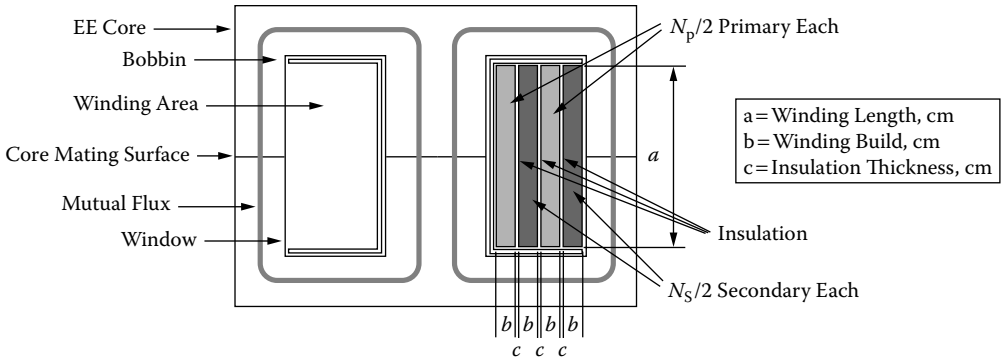

Figure 17-7. Sectionalized, Transformer Configuration Primary and Secondary Interleave.

$$L_p = \frac{\pi(MLT)N_p^2}{a}\left(\Sigma c + \frac{\Sigma b}{3}\right)\left(10^{-9}\right), \quad \text{[henrys]} \qquad \text{[17-4]}$$

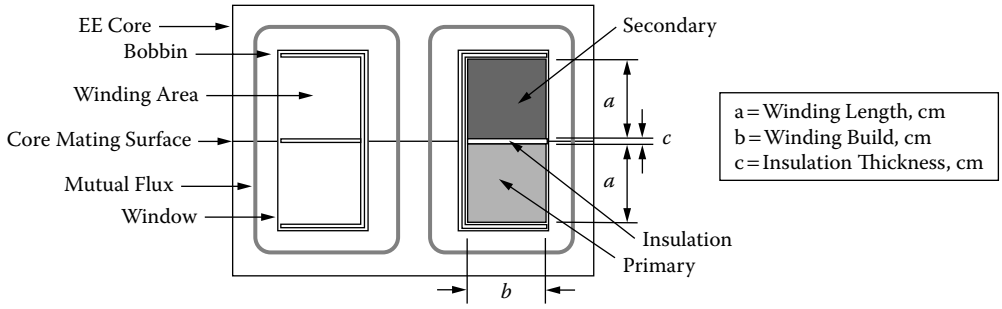

Figure 17-8. Pot Core, Sectionalized Transformer Configuration.

$$L_p = \frac{4\pi(MLT)N_p^2}{b}\left(c + \frac{\Sigma a}{3}\right)\left(10^{-9}\right), \quad \text{[henrys]} \qquad \text{[17-5]}$$

© 2011 by Taylor and Francis Group, LLC

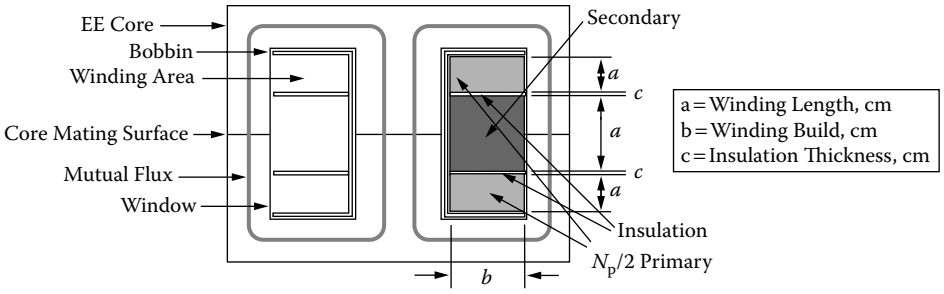

Figure 17-9. Modified, Pot Core Sectionalized, Transformer Configuration.

$$L_p = \frac{\pi (MLT) N_p^2}{b} \left(\Sigma c + \frac{\Sigma a}{3} \right) \left(10^{-9} \right), \quad \text{[henrys]} \qquad \text{[17-6]}$$

Minimizing Leakage Inductance

Magnetic core geometry has a big influence on leakage inductance. To minimize leakage inductance, the primary winding should be wound on a long bobbin, or tube, with the secondary wound as close as possible, using a minimum of insulation. Magnetic cores can have identical rating, but one core will provide a lower leakage inductance than the other. A simple comparison would be two cores with the same window area, but one core has twice the winding length. Only half the winding build is shown in Figure 17-10.

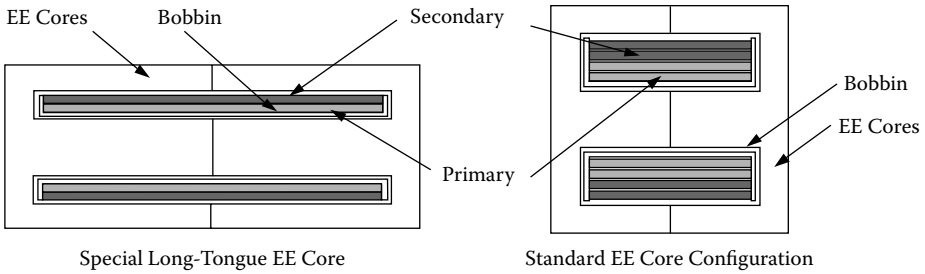

Figure 17-10. Comparing a Standard EE Core and a Special Long Tongue Core.

If layers must be used, the only way to reduce the leakage inductance is to divide the primary winding into sections, and then to sandwich the secondary winding between them, as shown in Figure 17-7. This can pose a real problem when designing around the European VDE specification, because of the required creepage distance and the minimum insulation requirements between the primary and secondary. Minimizing the leakage inductance on a push-pull converter design could be a big problem. A special consideration is required symmetry in both the leakage inductance and dc resistance; this is in order to get a balanced winding for the primary switching circuit to function properly.

© 2011 by Taylor and Francis Group, LLC

The best way to minimize the leakage inductance, and to have a balanced dc resistance in a push-pull or center-tapped winding, is to wind bifilar. Bifilar windings will drastically reduce leakage inductance. This condition also exists on the secondary, when the secondary is a full-wave, center-tapped circuit. A bifilar winding is a pair of insulated wires, wound simultaneously and contiguously, (i.e., close enough to touch each other); Warning: do not use bifilar wire or the capacitance will go out of sight. Each wire constitutes a winding; their proximity reduces leakage inductance by several orders of magnitude, more than ordinary interleaving. This arrangement can be applied to the primary, or to the secondary. It can be applied to the primary and secondary together as well. This arrangement will provide the minimum leakage inductance.

Winding Capacitance

Operating at high frequency presents unique problems in the design of transformers to minimize the effect of winding capacitance. Transformer winding capacitance is detrimental in three ways: (1) winding capacitance can drive the transformer into premature resonance; (2) winding capacitance can produce large primary current spikes when operating from a square wave source, (3) winding capacitance can produce electrostatic coupling to other circuits.

When a transformer is operating, different voltage gradients arise almost everywhere. These voltage gradients are caused by a large variety of capacitance throughout the transformer, due to the turns and how they are placed throughout the transformer. When designing high frequency converters, there are several factors that have a control over the turns: (1) the operating flux density or core loss; (2) the operating voltage levels in the primary and secondary; (3) the primary inductance.

Keeping turns to a minimum will keep the capacitance to a minimum. This capacitance can be separated into four categories: (1) capacitance between turns; (2) capacitance between layers; (3) capacitance between windings; and (4) stray capacitance. The net effect of the capacitance is normally seen by the lumped capacitance, C_p, on the primary, as shown in Figure 17-1. The lumped capacitance is very difficult to calculate by itself. It is much easier to measure the primary inductance and the resonant frequency of the transformer or inductor, as shown in Figure 17-11. Then, calculate the capacitance using Equation [17-7]. The test circuit, in Figure 17-11 functions as follows: The input voltage, V1, is held constant while monitoring the voltage, V2, is swept through the frequency with the power oscillator. When the voltage, V2, rises to a peak, and starts to decay at this peak voltage, the transformer or inductor is in resonance. At this point the phase angle is also 0 degrees at resonance when looking at both the curves of, V1 and V2.

$$C_p = \left(\frac{1}{(\omega_r)^2 L} \right) = \frac{1}{4\pi^2 f_r^2 L}, \quad \text{[farads]} \qquad [17\text{-}7]$$

© 2011 by Taylor and Francis Group, LLC

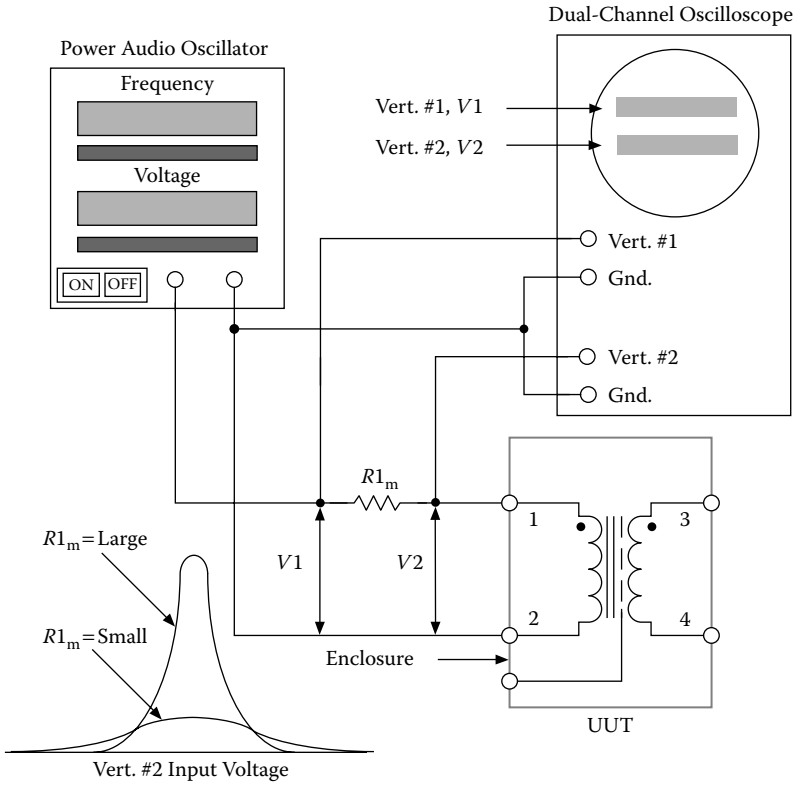

Figure 17-11. Circuit for Measuring either a Transformer or Inductor Self Resonates.

For transformers designed to operate with a square wave, such as a dc-to-dc converter, leakage inductance, L_p, and the lumped capacitance, C_p, should be kept to a minimum. This is because they cause overshoot and oscillate, or ring, as shown in Figure 17-12. The overshoot oscillation, seen in Figure 17-12A, has a resonant frequency, f, that is controlled by, L_p and C_p. This resonant frequency could change and change drastically after potting, depending on the material and its dielectric constant, as shown Figure 17-12B.

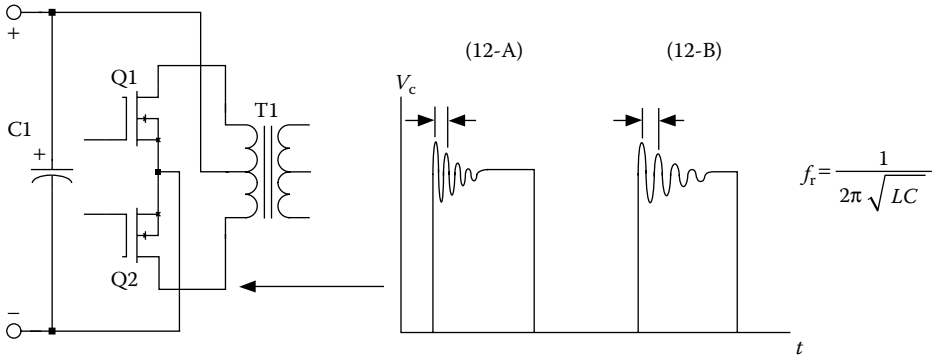

Figure 17-12. Primary Voltage with Leading Edge Ringing.

© 2011 by Taylor and Francis Group, LLC

Winding Capacitance Turn-to-Turn

The turn-to-turn capacitance, C_t, shown in Figure 17-13, should not be a problem if you are operating at high frequency, low voltage power converters, due to the low number of turns. If the turn-to-turn capacitance is important, then change the magnet wire insulation to one with a lower dielectric constant. See Chapter 4.

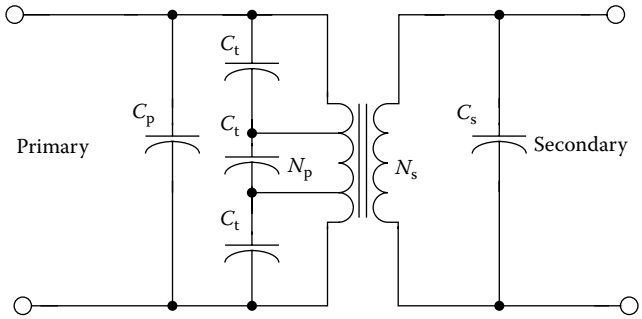

Figure 17-13. Capacitance Turn-to-Turn.

Winding Capacitance Layer-to-Layer

The capacitance between layers on the primary or secondary is the best contributor to the overall, lumped capacitance, C_p. There are three ways to minimize the layer capacitance: (1) Divide the primary and secondary windings into sections, and then sandwich the other winding between them, as shown in Figure 17-7; (2) The foldback winding technique, shown in Figure 17-14, is preferred to the normal U type winding, even though it takes an extra step before starting the next layer. The foldback winding technique will also reduce the voltage gradient between the end of the windings; (3) Increasing the amount of insulation between windings will decrease the amount of capacitance. But remember, this will increase the leakage inductance. If the capacitance is reduced, then the leakage inductance will go up. There is one exception to this rule, and that is, if the windings are sandwiched or interleaved, it will reduce the winding capacitance, but, it will increase the winding-to-winding capacitance.

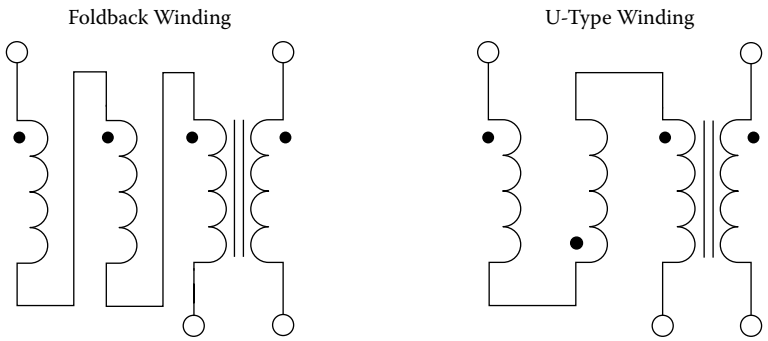

Figure 17-14. Comparing the Foldback to the U Type Winding.

© 2011 by Taylor and Francis Group, LLC

Transformers and inductors wound on toroidal cores can have capacitance problems, just as much if care is not taken in the design at the beginning. It is difficult to control the winding capacitance on a toroidal core because of its odd configuration, but there are ways to control the windings and capacitance. The use of tape barriers to mark a zone for windings, as shown in Figure 17-15, offers a good way to control this capacitance.

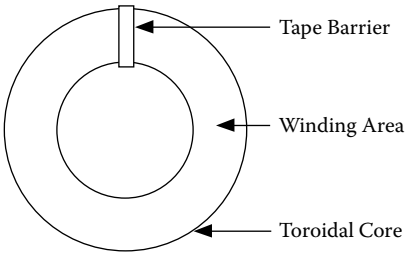

Figure 17-15. Tape Barrier for Winding Toroidal Core.

Another way to help reduce the capacitance effect on toroids is to use the progressive winding technique. The progressive winding technique example is shown in Figure 17-16 and 17-17: Wind five turns forward and wind four turns back, then wind ten turns forward and keep repeating this procedure until the winding is complete.

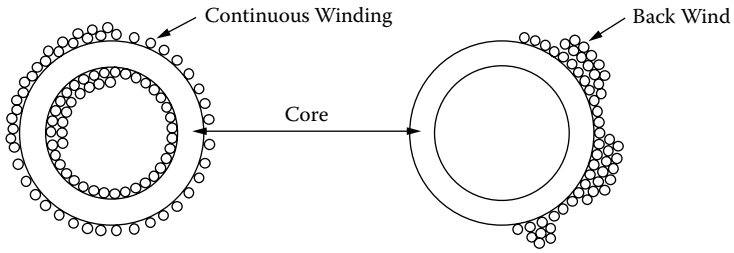

Figure 17-16. Progress Winding Top View.

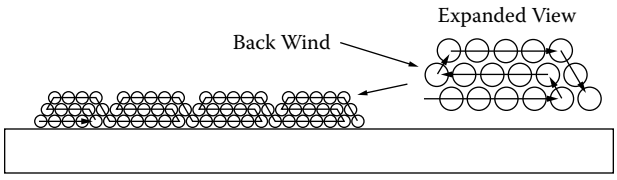

Figure 17-17. Progress Winding Side View.

Capacitance Winding-to-Winding

Balanced windings are very important in keeping down noise and common mode signals that could lead to in-circuit noise and instability problems later on. The capacitance, from winding-to-winding, shown in Figure 17-18, can be reduced, by increasing the amount of insulation between windings. This will decrease the amount of capacitance, but again, this will increase the leakage inductance. The capacitance effect between

© 2011 by Taylor and Francis Group, LLC

windings can be reduced, without increasing the leakage inductance noticeably. This can be done, by adding a Faraday Shield or screen, as shown in Figure 17-19, between primary and secondary windings.

A Faraday Shield is an electrostatic shield, usually made of copper foil. The Faraday Shield is normally added along with the insulation between primary and secondary. In some designs, the Faraday Shield can consist of three independent insulated shields or just one. It all depends on the required noise rejection.

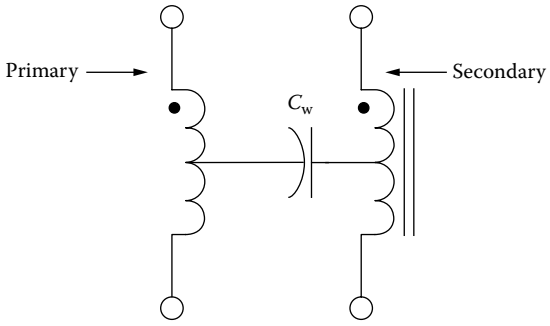

Figure 17-18. Capacitance, C_w, Winding-to-Winding.

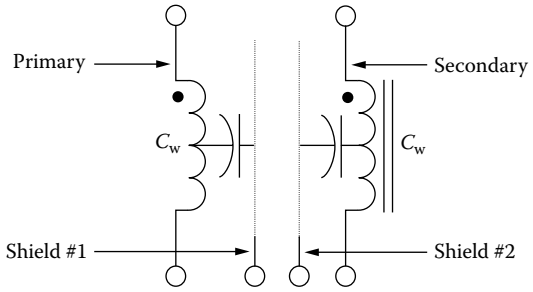

Figure 17-19. Transformer with a Primary and Secondary Shield.

Stray Capacitance

Stray capacitance is very important to minimize because it too, can generate asymmetry currents and could lead to high common mode noise. Stray capacitance is similar to winding-to-winding capacitance except that the capacitance is between the winding next to the core, C_c, and the outer winding next to the surrounding circuitry, C_s, as shown in Figure 17-20. Stray capacitance can be minimized by using a balanced winding, or using a copper shield over the entire winding. A means for measuring leakage current is shown in Figure 17-21. The winding-to-winding capacitance can be calculated, using Equations [17-8] and [17-9].

$$X_c = R1\sqrt{\left(\frac{V_{in}}{V_o}\right) - 1}, \quad \text{[ohms]} \qquad \text{[17-8]}$$

© 2011 by Taylor and Francis Group, LLC

$$C_x = \frac{1}{2\pi f X_c}, \quad \text{[farads]} \qquad \text{[17-9]}$$

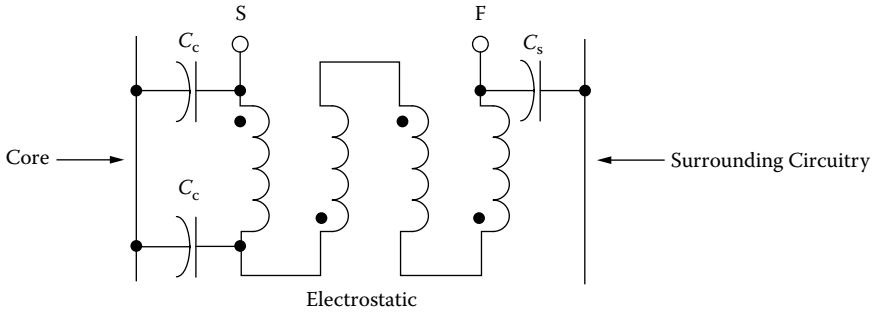

Figure 17-20. Transformer Winding with Stray Capacitance.

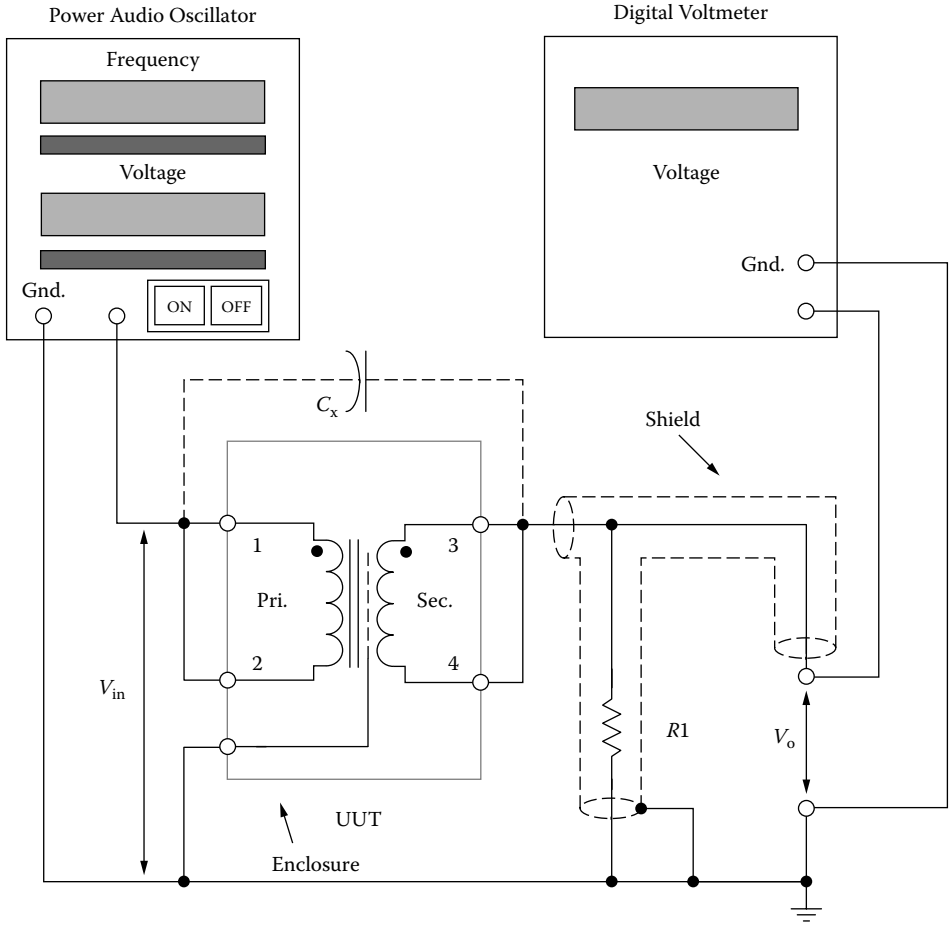

Figure 17-21. Test Circuit for Measuring Primary and Secondary, ac Leakage Current.

© 2011 by Taylor and Francis Group, LLC

References

1. Grossner, N., *Transformer for Electronic Circuits*, McGraw-Hill, New York, 1967.

2. Landee, R., Davis, D., and Albecht, A., *Electronic Designer's Handbook*, McGraw-Hill, New York, 1957, pp. 17–12.

3. Lee, R., *Electronic Transformer and Circuits*, 2nd ed., John Wiley & Sons, New York, 1958.

4. *Reference Data for Radio Engineers*, 4th ed., International Telephone and Telegraph Co., New York.

5. Richardson, I., The Technique of Transformer Design, Electro-Technology, January, 1961, pp. 58–67.

6. Flanagan, W., *Handbook of Transformer Application*, McGraw-Hill, New York, 1986.

© 2011 by Taylor and Francis Group, LLC

Chapter 18

Quiet Converter Design

© 2011 by Taylor and Francis Group, LLC

Table of Contents

1. Introduction 18-3
2. The Voltage-fed Converter 18-3
3. Regulating and Filtering 18-4
4. The Current-fed Converter 18-4
5. The Quiet Converter 18-5
6. Regulating and Filtering 18-6
7. Quiet Converter Waveforms 18-6
8. Technology on the Move 18-10
9. Window Utilization Factor, K_u 18-10
10. Temperature Stability 18-11
11. Calculating the Apparent Power, P_t 18-11
12. Quiet Converter Design Equations 18-12
13. Transformer Design, Using the Core Geometry, K_g, Approach 18-16
14. Design Review 18-21
15. Recognition 18-26
16. References 18-26

© 2011 by Taylor and Francis Group, LLC

Introduction

A few designers have known about the Resonant Converter described here for many years. This type of Resonant Converter has been built mainly in the range of 200 watts to 2 kilowatts, and has been used as a static inverter. However, it has remained relatively obscure in the general literature. The Quiet Converter was developed at Jet Propulsion Laboratory (JPL), Division 38, to power very sensitive instruments. The Quiet Converter produces a sinusoidal voltage across a parallel resonant tank. The dc output voltage is obtained after rectification and filtering of the sinusoidal secondary voltage. The regulation is achieved by controlling the duty-cycle of the switching transistors. A comparison of the standard type of PWM control with the Quiet Converter and its amplitude modulation (AM), is shown in Figure 18-1. The inherent low noise from this converter is how the nickname, Quiet Converter, came about. The low noise can easily be reduced, even further, by the addition of a Faraday Shield and common-mode inductors. Programs at the Jet Propulsion Laboratory (JPL) that have successfully used the low noise environment of the Quiet Converter are WF/PC-II, Articulated Fold, Mirror Actuators, (Hubbell Space Telescope), MISR (Earth Orbiting System), Raman, and the Mars 05 ONC, CCD Camera.

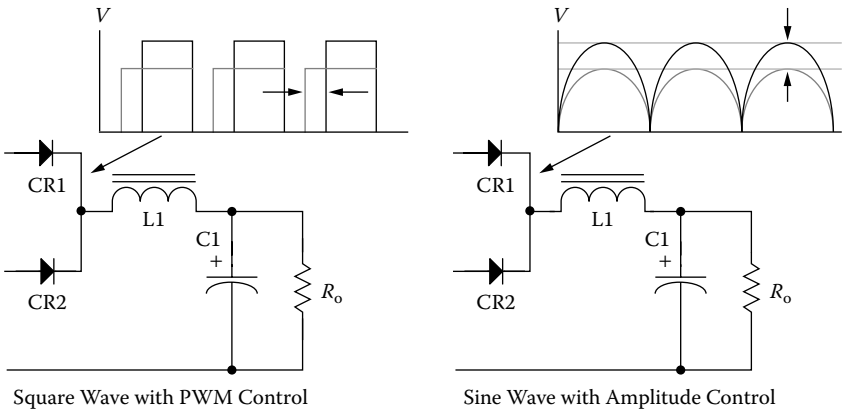

Figure 18-1. Comparing PWM and Amplitude Control.

The Voltage-fed Converter

The voltage-fed converter circuit is the most widely-used, converter topology. In a voltage-fed converter, the powder source, V_{in}, is connected directly to the transformer through a transistor, Q1, as shown in Figure 18-2. When the transistor, Q1, is switched on, the full source voltage is applied to the transformer, T1, primary, (1-2). The transistor saturation is ignored. Conversely, when Q2 is switched on, the full source voltage is applied to the other half of the transformer, T1, primary, (2-3).

In Figure 18-2, the switching drive circuit alternately saturates and cuts off the semiconductors' switches, Q1 and Q2, causing an alternating voltage to be generated across the primary winding of transformer, T1, and then delivered to the secondary to be rectified and filtered before going to the load. The primary source voltage, V_{in}, is

© 2011 by Taylor and Francis Group, LLC

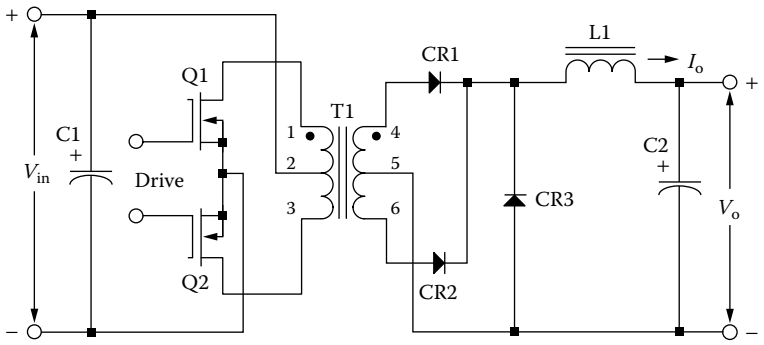

Figure 18-2. Typical, Voltage-fed Power Converter.

directly impressed onto the primary of the transformer, T1, and therefore, the voltage across the transformer, T1, is always a square wave.

Regulating and Filtering

The most effective method of regulation for a voltage-fed converter is Pulse Width Modulation (PWM). A constant output voltage can be obtained for a changing input voltage, by reducing the on time, T_{on}, of Q1 and Q2, as shown in Figure 18-3. The pulse width voltage is applied to the output filter, L1 and C2, averaging circuit to provide the proper output voltage, V_o.

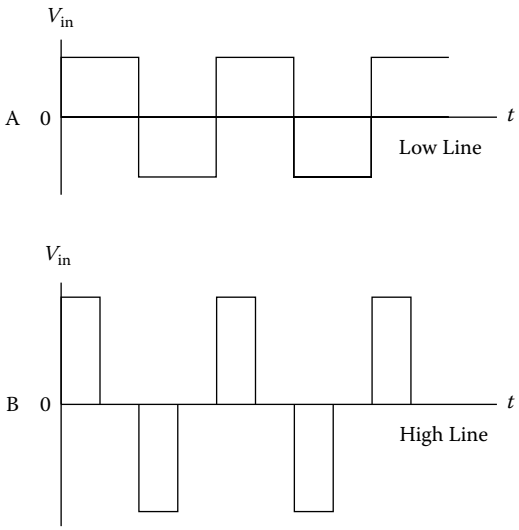

Figure 18-3. Primary Voltage of a PWM Controlled Converter.

The Current-fed Converter

The main difference between a voltage-fed converter and a current-fed converter is the series inductor, L1, shown in Figure 18-4. The inductor, L1, is commonly called a feed-choke or series inductor. It has an inductance large enough in value to maintain a continuous current through the circuit under all conditions of line and load.

© 2011 by Taylor and Francis Group, LLC

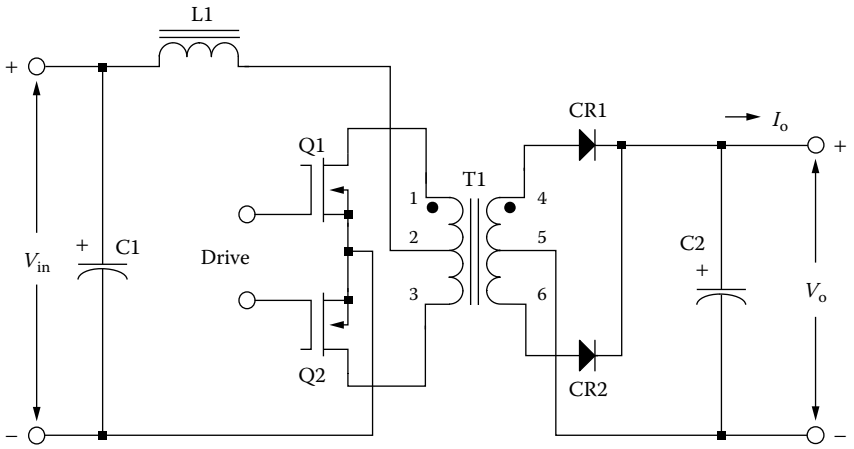

Figure 18-4. Typical Current-fed Power Converter Circuit.

The Quiet Converter

Simple additions to the circuit, in Figure 18-4, change the performance dramatically, and it becomes a whole new converter. The new converter is shown in Figure 18-5. The changes are: 1. The transformer, T1, core material has been changed to Molypermalloy Powder Core, (MPP). The reason for using a powder core is because it has a built-in gap required for the tank circuit and these cores are available with temperature stabilized permeability. The use of a gap ferrite would perform just as well, but the design must be stable over temperature. 2. A commutating winding has been added to the series inductor, L1. 3. A capacitor, C3, was added for the required parallel tuned tank. The tuning capacitor, C3, should be of high quality with a low ESR and stable. The capacitors that were used in the flight power supplies, were plastic film, Type CRH, to MIL-C-83421.

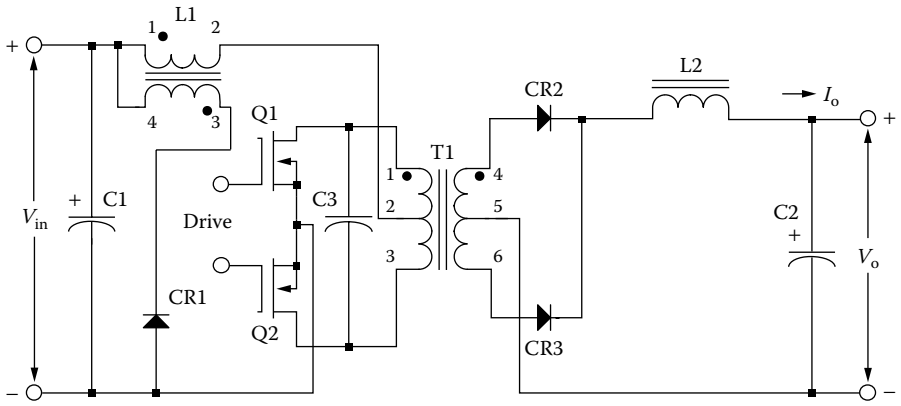

Figure 18-5. Current-fed Parallel Resonant Converter.

With properly designed components, the output voltage of transformer, T1, will always be a sine wave. The sine wave is accomplished by using a tuned parallel resonant tank circuit, (T1C3), to the natural running frequency of the converter. The series inductor, L1, isolates the input dc source from the sine wave voltage across the primary of the transformer, T1.

© 2011 by Taylor and Francis Group, LLC

Regulating and Filtering

The current-fed resonant converter, shown in Figure 18-5, requires a minimum of dead time, (dwell), for the circuit to function properly. The series inductor, L1, when connected, as shown in Figure 18-4, requires continuous conduction of both, Q1 and Q2, along with a small amount of overlap. In this way, there would always be continuous current flowing in, L1. If there is any disruption of current in the series inductor, L1, no matter how small, it would destroy the switching transistors, Q1, and/or Q2.

In order to incorporate Pulse Width Modulation (PWM), or a drive circuit that has inherent dead time that neither transistor is conducting, there must be a means to commutate the current in the series inductor, L1. Adding a winding to the series inductor, L1, is a simple way to commutate the current. When the current flowing in winding, (1-2), is interrupted, the current will now be commutated to the added winding, (3-4). This is done when connected with proper phasing, through a diode CR1, then, back to the dc source to complete the path, as shown in Figure 18-5. Now, when either transistors, Q1 or Q2, are interrupted, the added winding of the series inductor, L1, commutates the current back into the dc source, thus preventing the destruction of the switching transistors, Q1 and Q2.

Quiet Converter Waveforms

The current-fed, sine wave converter waveforms will be referenced from Figure 18-6. In Figure 18-7 through Figure 18-15, refer back to (A)–(J) points in Figure 18-6. The waveforms presented here are copies drawn from an actual photo taken with an oscilloscope camera.

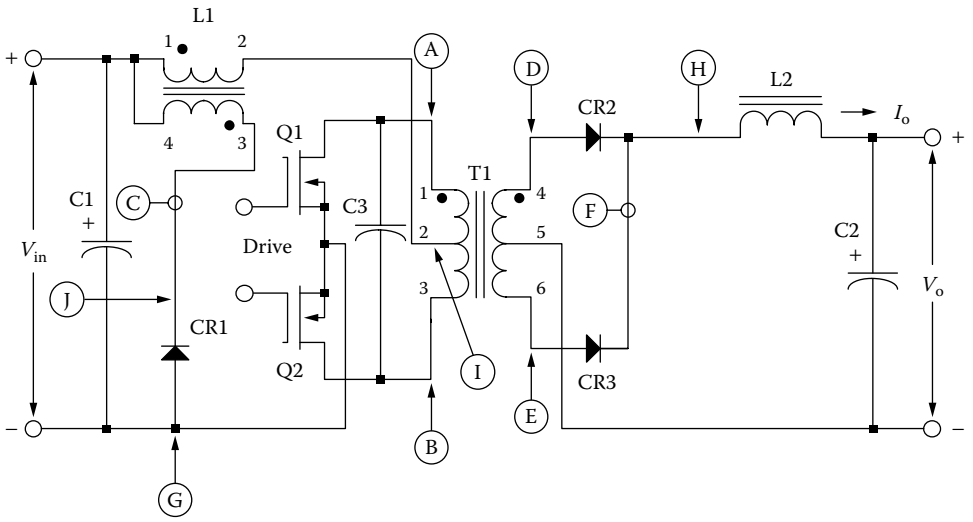

Figure 18-6. Quiet Converter Schematic with Reference Points.

© 2011 by Taylor and Francis Group, LLC

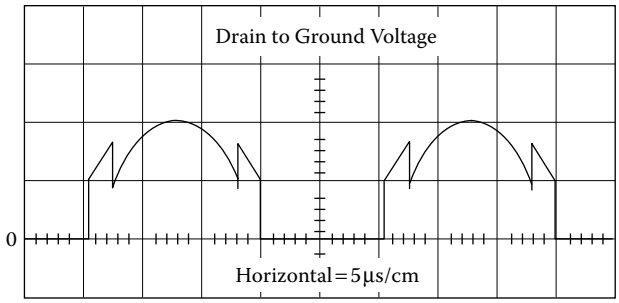

Figure 18-7. Drain to Ground, Voltage Waveform of, Q1 and Q2.

The drain voltage waveform of, Q1, is shown in Figure 18-7. Waveform is taken between points A and G. The converter is properly tuned to the natural frequency.

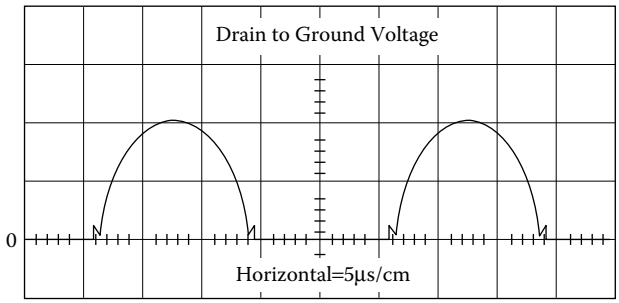

Figure 18-8. Drain to Ground, Voltage Waveform of, Q1 and Q2.

The drain voltage waveform of, Q1, is shown in Figure 18-8, with minimum dead time. Waveform is taken between points A and G. The converter is properly tuned to the natural frequency.

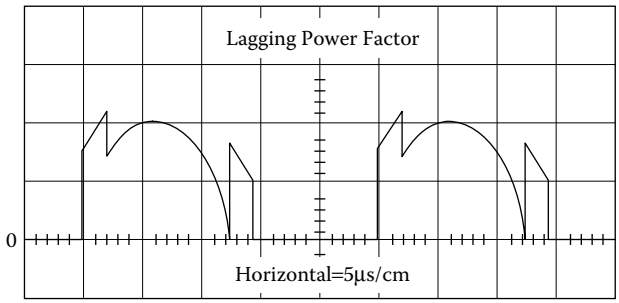

Figure 18-9. Drain to Ground, Voltage Waveform of, Q1 and Q2.

The drain voltage waveform of, Q1, is shown in Figure 18-9. Waveform is taken between points A and G. The converter is improperly tuned to the natural frequency. The resonant tank capacitor is too small in value.

© 2011 by Taylor and Francis Group, LLC

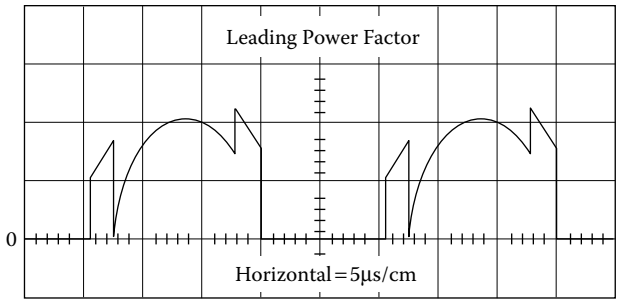

Figure 18-10. Drain to Ground, Voltage Waveform of, Q1 and Q2.

The drain voltage waveform of, Q1, is shown in Figure 18-10. Waveform is taken between points A and G. The converter is improperly tuned to the natural frequency. The resonant tank capacitor is too large in value.

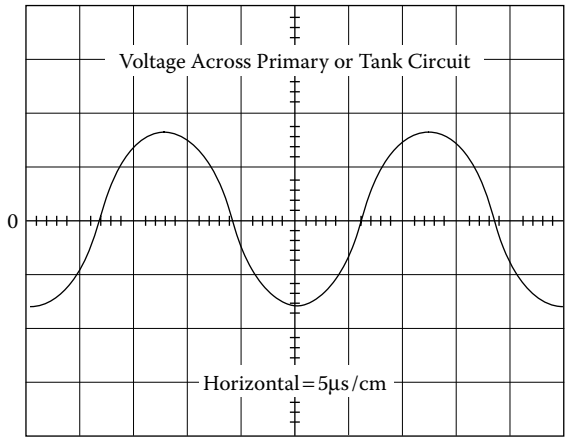

Figure 18-11. Voltage Waveform Across Transformer Primary.

The primary voltage waveform is shown in Figure 18-11, across transformer, T1. Waveform is taken between points A and B. The converter is properly tuned to the natural frequency.

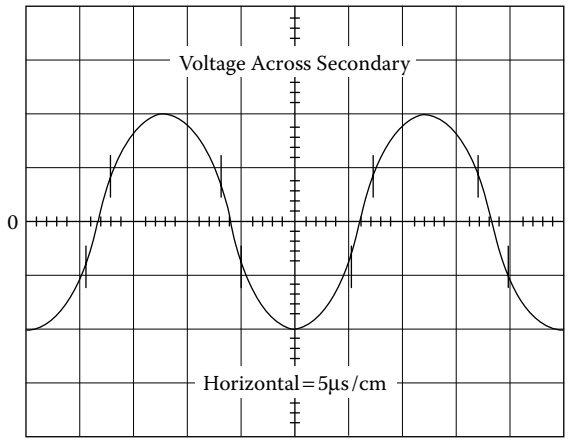

Figure 18-12. Voltage Waveform Across Transformer Secondary.

© 2011 by Taylor and Francis Group, LLC

The secondary voltage waveform of transformer, T1, is shown in Figure 18-12. Waveform is taken between points D and E. The converter is properly tuned to the natural frequency.

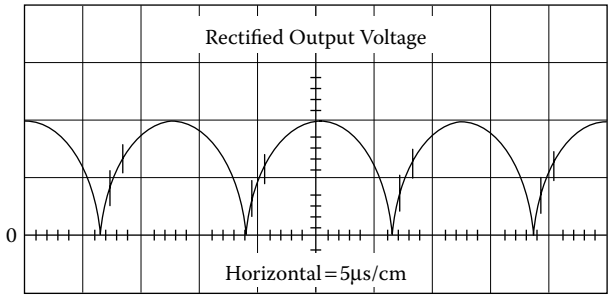

Figure 18-13. Secondary Rectified Voltage Waveform at, CR2 and CR3.

The secondary, rectified voltage waveform, at the cathodes of, CR2 and CR3, is shown in Figure 18-13. Waveform is taken at point H. The converter is properly tuned to the natural frequency.

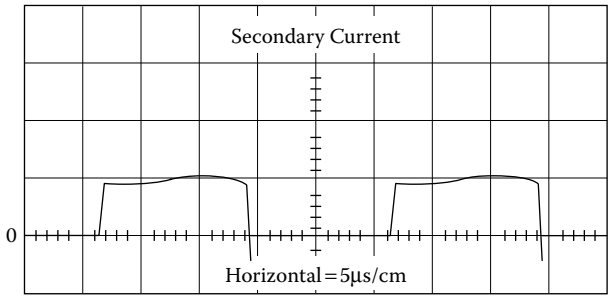

Figure 18-14. Secondary Current Waveform.

The secondary current waveform is shown in Figure 18-14. The current waveform is taken at point F.

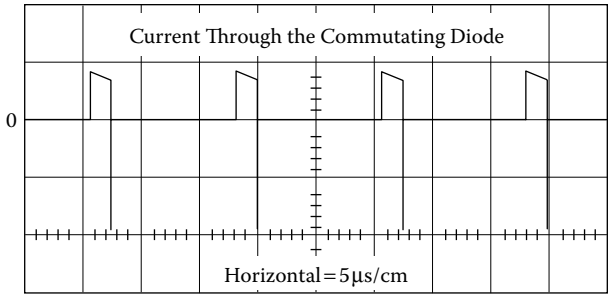

Figure 18-15. Current Through the Commutating Diode, CR1.

Commutating diode current waveform is shown in Figure 18-15. The current is through the series inductor, L1, winding (3-4). Waveform is taken at point C. The converter is properly tuned to the natural frequency.

© 2011 by Taylor and Francis Group, LLC

Technology on the Move

As technology moves ahead, instruments become more sophisticated, smaller in size, and require less power. Less power normally relates to lower current. Lower current requires smaller wire to carry the current. There is a practical point where the wire size can no longer be reduced, even though the current is very small. Reliability is affected when the wire size becomes very small. It becomes a handling and termination problem. If a larger wire size can be tolerated, and it does not impact the size a great deal, then, the larger wire should be used. The smallest wire size that seems to be tolerable, depending on the application, ranges from #35 to #39 AWG and this would be from a specialty house.

Window Utilization Factor, K_u

When designing a transformer or inductor, the window utilization factor, K_u, is the amount of copper that appears in the window area. See Chapter 4. The window utilization factor, K_u, is influenced by five main factors:

1. Wire insulation, S_1.
2. Wire lay fill factor, S_2.
3. Effective window area, S_3.
4. Winding insulation, S_4.
5. Workmanship.

These factors multiplied together will give a normalized window utilization factor of, $K_u = 0.4$.

$$K_u = (S_1)(S_2)(S_3)(S_4) = 0.4 \quad [18\text{-}1]$$

The design of the current-fed sine wave converter is much more detailed and complex, compared to the simple voltage-fed, square wave converter. The sole reason to use the Quiet Converter is because of its inherent low noise, (EMI). The noise of the Quiet Converter can be reduced even further by adding a primary and a secondary Faraday Shield. When a Faraday Shield is added between the primary and secondary, the transformer must be designed to accommodate the shield. Transformer size is mainly determined by the loads. The window utilization, K_u, has to be adjusted during the design to accommodate the Faraday Shield. When the core size is selected for the transformer, it will be a little larger core, do to the added space required by the Faraday Shield.

After the preliminary design, the engineer selects the proper core size for the power transformer. The core geometry, K_g, selects the molypermalloy powder core size. After the molypermalloy powder core size has been selected, the engineer now selects a core with a permeability best-suited for the application. The molypermalloy powder cores come with a range of permeability from 14 to 550, all with the same core geometry, K_g.

© 2011 by Taylor and Francis Group, LLC

Temperature Stability

For the Quiet Converter to function properly over a wide temperature range, the components must be stable over that temperature range. The components that control the oscillator frequency must be stable. The LC tank circuit must be stable and not drift with temperature. Molypermalloy powder cores are offered with stabilized permeability, with code letters M, W, and D from Magnetics, Inc. The W material temperature stability is shown in Figure 18-16.

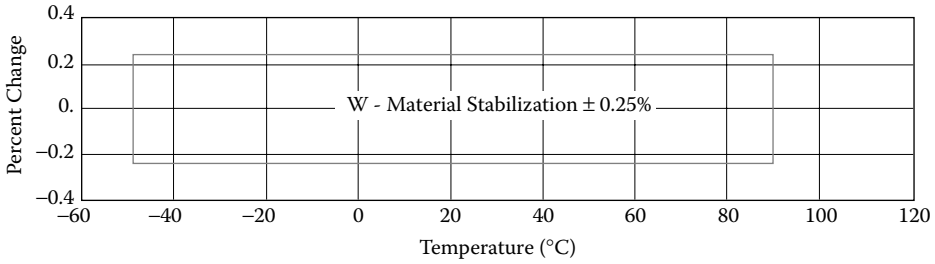

Figure 18-16. Typical, Stabilized Molypermalloy Material.

Calculating the Apparent Power, P_t

The apparent power, P_t, is the power associated with the geometry of the transformer. The designer must be able to make allowances for the rms power in each winding. The primary winding handles, P_{in}, the secondaries handle, P_o, to the load. Since the power transformer has to be designed to accommodate the primary power, P_{in}, and the secondary, P_o, then by definition,

$$P_t = P_{in} + P_\Sigma, \quad \text{[watts]}$$

$$P_\Sigma = P_{o1} + P_{o2} + ...P_{on}$$

$$P_{in} = \frac{P_\Sigma}{\eta}, \quad \text{[watts]} \qquad \text{[18-2]}$$

$$P_t = \frac{P_\Sigma}{\eta} + P_\Sigma, \quad \text{[watts]}$$

$$\eta = \text{efficiency}$$

The designer must be concerned with the apparent power-handling capability, P_t, of the transformer core and winding. The apparent power, P_t, may vary by a factor ranging from 2 to 2.828 times the input power, P_{in}, depending upon the type of circuit in which the transformer is used. If the current in the transformer becomes interrupted, such as a center-tapped secondary or push-pull primary, its effective rms value changes.

© 2011 by Taylor and Francis Group, LLC

Transformer size is thus determined not only by the load demand, but also by application, because of the different copper losses incurred owing to current waveforms.

Because of the different winding configurations, the apparent power, P_t, of the transformer will have to be summed to reflect these differences. When the winding has a center tap and produces a discontinuous current, then the power in that winding, whether it is primary or secondary, has to be multiplied by the factor, U, to correct for the rms current in that winding. If the winding has a center tap, then, U = 1.41; if not, then, U = 1. Summing the output power of a multiple-output transformer would be:

$$P_{\Sigma} = P_{o1}(U) + P_{o2}(U) + ...P_{on}(U) \quad [18\text{-}3]$$

Quiet Converter Design Equations

The transformer secondary voltage, V_s, is shown in Equation [18-4].

V_o = Output voltage

V_d = Diode Drop

$$V_s = (V_o + V_d), \quad [\text{volts}] \quad [18\text{-}4]$$

The maximum secondary true power, $P_{s(max)}$, is shown in Equation [18-5].

$$P_{s(\max)} = V_s\left(I_{o(\max)}\right), \quad [\text{watts}] \quad [18\text{-}5]$$

The minimum secondary true power, $P_{s(min)}$, is shown in Equation [18-6].

$$P_{s(\min)} = V_s\left(I_{o(\min)}\right), \quad [\text{watts}] \quad [18\text{-}6]$$

The secondary apparent power, P_{sa}, is shown in Equation [18-7].

U = 1.41, center tapped winding

U = 1.0, single winding

$$P_{sa} = V_s\left(I_{o(\max)}\right)(U), \quad [\text{watts}] \quad [18\text{-}7]$$

If, there is more than one output, then, sum the total secondary maximum apparent load power, $P_{sa\Sigma}$.

$$P_{sa\Sigma} = P_{sa01} + P_{sa02} + ..., \quad [\text{watts}] \quad [18\text{-}8]$$

If, there is more than one output, then, sum the total secondary maximum load power, $P_{ot(max)}$.

$$P_{ot(\max)} = P_{o01(\max)} + P_{o02(\max)} + ..., \quad [\text{watts}] \quad [18\text{-}9]$$

© 2011 by Taylor and Francis Group, LLC

If, there is more than one output, then, sum the total secondary minimum load power, $P_{ot(min)}$.

$$P_{ot(\min)} = P_{o01(\min)} + P_{o02(\min)} + ..., \quad [\text{watts}] \qquad [18\text{-}10]$$

The maximum reflected secondary load resistance, $R_{(max)}$, is shown in Equation [18-11].

$R_{(max)}$ = Resistance Value

η = Efficiency

$$R_{(\max)} = \frac{(V_{in})^2(\eta)}{P_{ot(\min)}}, \quad [\text{ohms}] \qquad [18\text{-}11]$$

The required series inductor inductance, L1, is shown in Equation [18-12].

$\omega = 2\pi f$

f = fundamental frequency

$$L1 = \frac{(R_{(\max)})}{3\omega}, \quad [\text{henrys}] \qquad [18\text{-}12]$$

The total period, T, is shown in Equation [18-13].

$$T = \frac{1}{f}, \quad [\text{seconds}] \qquad [18\text{-}13]$$

The maximum transistor on time, $t_{on(max)}$, is shown in Equation [18-14].

Transistor drive circuits, such as a Pulse Width Modulator (PWM), will have a minimum of dead time, t_d. Dead time or dwell is shown in Figure 18-17.

$$t_{on(\max)} = \left(\frac{T}{2}\right) - t_d, \quad [\mu\text{sec}] \qquad [18\text{-}14]$$

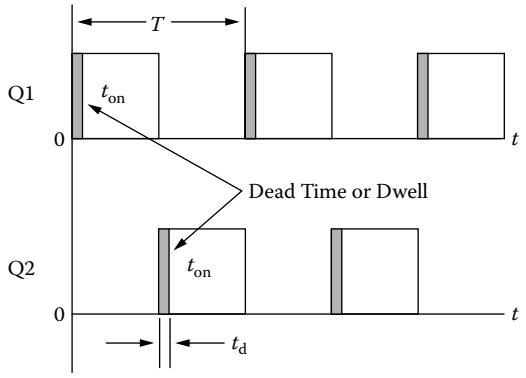

Figure 18-17. Transistor Drive Waveforms, Showing Dead Time or Dwell.

© 2011 by Taylor and Francis Group, LLC

The conversion ratio, K_a, is shown in Equation [18-15].

$$K_a = \frac{\left(4t_{on(\max)} - T\right)}{T\,Sin\left(\frac{t_{on(\max)}180}{T}\right)} \quad [18\text{-}15]$$

The peak voltage, $V_{c(pk)}$, on the resonant capacitor, C3, as shown in Figure 18-5, is:

$K_b = 2$, center tapped winding.

$K_b = 1$, single winding.

$$V_{c(pk)} = \frac{\pi\left(K_a V_{in} K_b\right)}{2}, \quad \text{[volts]} \quad [18\text{-}16]$$

The primary rms voltage, $V_{p(rms)}$, is shown in Equation [18-17].

$K_b = 2$, center tapped winding.

$K_b = 1$, single winding.

$$V_{p(rms)} = \frac{0.707\left(V_{c(pk)}\right)}{K_b}, \quad \text{[volts]} \quad [18\text{-}17]$$

The primary maximum reflected secondary current, I_{ps}, is shown in Equation [18-18].

$$I_{ps} = \frac{P_{ot(\max)}}{V_{p(rms)}\eta}, \quad \text{[amps]} \quad [18\text{-}18]$$

The secondary reflected loads to the primary, R_{SR}, is shown in Equation [18-19].

$K_b = 2$, center tapped winding.

$K_b = 1$, single winding.

$$R_{SR} = \frac{K_a V_{p(rms)} \left(K_b\right)^2}{I_{sp}}, \quad \text{[ohms]} \quad [18\text{-}19]$$

Note: The capacitance reactance affects the total percentage of harmonic distortion when:

$$\omega R_{SR} C = 1, \approx [12\%], \quad \omega R_{SR} C = 2, \approx [6\%], \quad \omega R_{SR} C = 3, \approx [4\%]$$

As a general rule:

$$C_x = \frac{2}{2\pi f\left(R_{SR}\right)}, \quad \text{[farads]} \quad [18\text{-}20]$$

The resonant capacitance, C_x, is shown in Equation [18-21].

© 2011 by Taylor and Francis Group, LLC

Q_T, is a variable that provides the engineer a little latitude with the capacitance value. ($1 < Q_T < 3$)

$$C_x = \frac{Q_T}{2\pi f\left(R_{SR}\right)}, \quad \text{[farads]} \tag{18-21}$$

The reactance, X_{cx}, of capacitor, C_x, is shown in Equation [18-22].

Use a standard capacitor.

$$X_{cx} = \frac{1}{2\pi f C_x}, \quad \text{[ohms]} \tag{18-22}$$

The capacitor rms current, $I_{cx(rms)}$, is shown in Equation [18-23].

$$I_{cx(rms)} = \frac{(0.707)\left(V_{c(pk)}\right)}{X_{cx}}, \quad \text{[amps]} \tag{18-23}$$

The total primary current, $I_{tp(rms)}$, is shown in Equation [18-24].

$$I_{pt(rms)} = \sqrt{\left(\left(I_{p(rms)}\right)^2 + \left(I_{cx(rms)}\right)^2\right)}, \quad \text{[amps]} \tag{18-24}$$

The primary tank inductance, L_x, is shown in Equation [18-25].

$$L_x = \frac{1}{\left(2\pi f\right)^2 C_x}, \quad \text{[henrys]} \tag{18-25}$$

The total transformer apparent power, P_t, is shown in Equation [18-26].

$$\begin{aligned} P_t &= \left(\text{Primary VA}\right) + \left(\text{Secondary VA}\right) + \left(\text{Capacitor VA}\right), \quad \text{[watts]} \\ P_t &= \left(\frac{P_{ot(\max)}(U)}{\eta}\right) + \left(P_{sa\Sigma}\right) + \left(K_b V_{p(rms)} I_{cx}\right), \quad \text{[watts]} \end{aligned} \tag{18-26}$$

The core geometry, K_g, is shown in Equation [18-27].

K_f is the waveform factor = 4.44

B_{ac} is the operating flux density and its value is an engineering judgment based on the frequency and core material.

$$K_g = \left(\frac{P_t}{0.000029\left(K_f\right)^2 (f)^2 \left(B_{ac}\right)^2 \alpha}\right), \quad \left[\text{cm}^5\right] \tag{18-27}$$

© 2011 by Taylor and Francis Group, LLC

Transformer Design, Using the Core Geometry, K_g, Approach

The following information is the Design specification for a 2.2 watt push-pull transformer, operating at 32kHz, using the K_g, core geometry approach. For a typical design example, assume a push-pull, full wave bridge circuit, with the following specification:

1. Input voltage, $V_{(min)} = 22$ volts
2. Output voltage #1, $V_{s01} = 5.0$ volts
3. Output current #1, $I_{s01(max)} = 0.2$ amps
4. Output current #1, $I_{s01(min)} = 0.1$ amps
5. Output voltage #2, $V_{s02} = 12.0$ volts
6. Output current #2, $I_{s02(max)} = 0.1$ amps
7. Output current #2, $I_{s02(min)} = 0.05$ amps
8. Frequency, f = 32kHz
9. Switching dead time, $t_d = 0.625$ μsec
10. Efficiency, $\eta = 95\%$
11. Regulation, $\alpha = 1.0\%$
12. Diode voltage drop, $V_d = 0.5$ volt
13. Operating flux density, $B_{ac} = 0.05$ tesla
14. Core Material = MPP
15. Window utilization, $K_u = 0.4$
16. Temperature rise goal, $T_r = 15°C$
17. Waveform coefficient, $K_f = 4.44$
18. Notes:

    Using a center tapped winding, U = 1.41

    Using a single winding, U = 1.0

Step 1: Calculate the total secondary voltage, $V_{s,}$ for each output.

$$V_s = (V_o) + (2V_d), \quad \text{[volts]}$$

$$V_{s01} = (5.0) + (1.0) = 6.0, \quad \text{[volts]}$$

$$V_{s02} = (12) + (1.0) = 13.0, \quad \text{[volts]}$$

Step 2: Calculate the maximum secondary true power, $P_{s(max)}$.

$$P_{s(\max)} = V_s \left(I_{o(\max)}\right), \quad \text{[watts]}$$

$$P_{s01(\max)} = 6.0(0.2) = 1.2, \quad \text{[watts]}$$

$$P_{s02(\max)} = 13.0(0.1) = 1.3, \quad \text{[watts]}$$

© 2011 by Taylor and Francis Group, LLC

Step 3: Calculate the minimum secondary true power, $P_{s(min)}$.

$$P_{s(\min)} = V_s\left(I_{o(\min)}\right), \quad \text{[watts]}$$

$$P_{s01(\min)} = 6.0(0.1) = 0.6, \quad \text{[watts]}$$

$$P_{s02(\min)} = 13.0(0.05) = 0.65, \quad \text{[watts]}$$

Step 4: Calculate the secondary apparent power, P_{sa}.

$$P_{sa} = V_s\left(I_{o(\max)}\right)(U), \quad \text{[watts]}$$

$$P_{sa01} = 6.0(0.2)(1.0) = 1.2, \quad \text{[watts]}$$

$$P_{sa02} = 13.0(0.1)(1.0) = 1.3, \quad \text{[watts]}$$

Step 5: Calculate the secondary total maximum apparent load power, $P_{sa\Sigma}$.

$$P_{sa\Sigma} = P_{sa01} + P_{sa02}, \quad \text{[watts]}$$

$$P_{sa\Sigma} = (1.2) + (1.3), \quad \text{[watts]}$$

$$P_{sa\Sigma} = 2.5, \quad \text{[watts]}$$

Step 6: Calculate the secondary total maximum load power, $P_{ot(max)}$.

$$P_{ot(\max)} = P_{o01(\max)} + P_{o02(\max)}, \quad \text{[watts]}$$

$$P_{ot(\max)} = (1.2) + (1.3), \quad \text{[watts]}$$

$$P_{ot(\max)} = 2.5, \quad \text{[watts]}$$

Step 7: Calculate the secondary total minimum load power, $P_{ot(min)}$.

$$P_{ot(\min)} = P_{o01(\min)} + P_{o02(\min)}, \quad \text{[watts]}$$

$$P_{ot(\min)} = (0.6) + (0.65), \quad \text{[watts]}$$

$$P_{ot(\min)} = 1.25, \quad \text{[watts]}$$

Step 8: Calculate the secondary maximum reflected load resistance, $R_{(max)}$.

$R_{(max)}$ = Resistance Value

η = Efficiency

$$R_{(\max)} = \frac{(V_{in})^2(\eta)}{P_{ot(\min)}}, \quad \text{[ohms]}$$

$$R_{(\max)} = \frac{(22)^2(0.95)}{1.25}, \quad \text{[ohms]}$$

$$R_{(\max)} = 368, \quad \text{[ohms]}$$

© 2011 by Taylor and Francis Group, LLC

Step 9: Calculate the inductance of the series inductor, L1.

$$L1 = \frac{R_{(\max)}}{3\omega}, \quad \text{[henrys]}$$

$$L1 = \frac{(368)}{3\left(2(3.14)(32{,}000)\right)}, \quad \text{[henrys]}$$

$$L1 = 0.000610, \quad \text{[henrys]}$$

Step 10: Calculate the total period, T.

$$T = \frac{1}{f}, \quad \text{[seconds]}$$

$$T = \frac{1}{32{,}000}, \quad \text{[seconds]}$$

$$T = 31.25, \quad \text{[micro-seconds]}$$

Step 11: Calculate the maximum transistor on time, $T_{on(max)}$. Dead time is shown in Figure 18-17.

$$t_{on(\max)} = \left(\frac{T}{2}\right) - t_d, \quad \text{[usec]}$$

$$t_{on(\max)} = \left(\frac{31.25}{2}\right) - 0.625, \quad \text{[usec]}$$

$$t_{on(\max)} = 15, \quad \text{[usec]}$$

Step 12: Calculate the conversion ratio, K_a.

$$K_a = \frac{\left(4t_{on(\max)} - T\right)}{T\,Sin\left(\frac{t_{on(\max)}180}{T}\right)}$$

$$K_a = \frac{\left(4(15) - (32.25)\right)}{(32.25)Sin\left(\frac{(15)180}{32.25}\right)}$$

$$K_a = 0.866$$

Step 13: Calculate the peak voltage, $V_{c(pk)}$, on the resonant capacitor, C3, as shown in Figure 18-5.

$K_b = 2$, center tapped winding.

$K_b = 1$, single winding.

© 2011 by Taylor and Francis Group, LLC

$$V_{c(pk)} = \frac{\pi\left(K_a V_{in} K_b\right)}{2}, \quad \text{[volts]}$$

$$V_{c(pk)} = \frac{(3.1415)(0.866)(22)(2)}{2}, \quad \text{[volts]}$$

$$V_{c(pk)} = 59.85, \quad \text{[volts]}$$

Step 14: Calculate the primary rms voltage, $V_{p(rms)}$.

$K_b = 2$, center tapped winding.

$K_b = 1$, single winding.

$$V_{p(rms)} = \frac{0.707\left(V_{c(pk)}\right)}{K_b}, \quad \text{[volts]}$$

$$V_{p(rms)} = \frac{0.707(59.85)}{2}, \quad \text{[volts]}$$

$$V_{p(rms)} = 21.2, \quad \text{[volts]}$$

Step 15: Calculate the primary maximum reflected secondary current, I_{ps}.

$$I_{ps} = \frac{P_{ot(\max)}}{V_{p(rms)}\eta}, \quad \text{[amps]}$$

$$I_{ps} = \frac{2.5}{(21.2)(0.95)}, \quad \text{[amps]}$$

$$I_{ps} = 0.124, \quad \text{[amps]}$$

Step 16: Calculate the secondary reflected loads to the primary, R_{SR}.

$K_b = 2$, center tapped winding.

$K_b = 1$, single winding.

$$R_{SR} = \frac{K_a V_{p(rms)} (K_b)^2}{I_{sp}}, \quad \text{[ohms]}$$

$$R_{SR} = \frac{(0.866)(21.2)(2)^2}{0.124}, \quad \text{[ohms]}$$

$$R_{SR} = 592, \quad \text{[ohms]}$$

Note: The capacitance reactance effects the total percentage of harmonic distortion when:

$$\omega R_{SR} C = 1, \approx [12\%], \quad \omega R_{SR} C = 2, \approx [6\%], \quad \omega R_{SR} C = 3, \approx [4\%]$$

© 2011 by Taylor and Francis Group, LLC

As a general rule:

$$C_x = \frac{2}{2\pi f(R_{SR})}, \quad \text{[farads]}$$

Step 17: Calculate the resonant capacitance, C_x.

$$C_x = \frac{2}{2\pi f(R_{SR})}, \quad \text{[farads]}$$

$$C_x = \frac{2}{(6.28)(32{,}000)(592)}, \quad \text{[farads]}$$

$$C_x = 1.68\left(10^{-8}\right), \quad \text{[farads]}$$

$$C_x = 0.0168 \text{ use a } 0.015, \quad \text{[micro-farads]}$$

Step 18: Calculate the reactance, X_{cx}, of capacitor, C_x. Use a standard capacitor. Let, C_x, equal 0.015 µf.

$$X_{cx} = \frac{1}{2\pi f C_x}, \quad \text{[ohms]}$$

$$X_{cx} = \frac{1}{(6.28)(32{,}000)\left(0.015\left(10^{-6}\right)\right)}, \quad \text{[ohms]}$$

$$X_{cx} = 332, \quad \text{[ohms]}$$

Step 19: Calculate the capacitor current, $I_{cx(rms)}$.

$$I_{cx(rms)} = \frac{(0.707)\left(V_{c(pk)}\right)}{X_{cx}}, \quad \text{[amps]}$$

$$I_{cx(rms)} = \frac{(0.707)(59.85)}{332}, \quad \text{[amps]}$$

$$I_{cx(rms)} = 0.127, \quad \text{[amps]}$$

Step 20: Calculate the total primary current, $I_{tp(rms)}$.

$$I_{pt(rms)} = \sqrt{\left(\left(I_{p(rms)}\right)^2 + \left(I_{cx(rms)}\right)^2\right)}, \quad \text{[amps]}$$

$$I_{pt(rms)} = \sqrt{\left((0.124)^2 + (0.127)^2\right)}, \quad \text{[amps]}$$

$$I_{pt(rms)} = 0.177, \quad \text{[amps]}$$

© 2011 by Taylor and Francis Group, LLC

Step 21: Calculate primary tank inductance, L_x.

$$L_x = \frac{1}{(2\pi)^2 \left(f\right)^2 C_x}, \quad \text{[henrys]}$$

$$L_x = \frac{1}{(6.28)^2 (32{,}000)^2 \left(0.015\left(10^{-6}\right)\right)}, \quad \text{[henrys]}$$

$$L_x = 0.00165, \quad \text{[henrys]}$$

Step 22: Calculate the total transformer apparent power, P_t.

$$P_t = \left(\text{Primary VA}\right) + \left(\text{Secondary VA}\right) + \left(\text{Capacitor VA}\right), \quad \text{[watts]}$$

$$P_t = \left(\frac{P_{ot(\max)}(U)}{\eta}\right) + \left(P_{sa\Sigma}\right) + \left(K_b V_{p(rms)} I_{cx}\right), \quad \text{[watts]}$$

$$P_t = \left(\frac{(2.5)(1.41)}{0.95}\right) + (2.5) + \left((2)(21.2)(0.127)\right), \quad \text{[watts]}$$

$$P_t = 11.6, \quad \text{[watts]}$$

Step 23: Calculate the core geometry, K_g. B_{ac} is the operating flux density and its value is an engineering judgment based on the frequency and core material.

$$K_g = \left(\frac{P_t}{0.000029\left(K_f\right)^2 \left(f\right)^2 \left(B_{ac}\right)^2 \alpha}\right), \quad [\text{cm}^5]$$

$$K_g = \left(\frac{11.6}{0.000029(4.44)^2 (32{,}000)^2 (0.05)^2 (1)}\right), \quad [\text{cm}^5]$$

$$K_g = 0.00793, \quad [\text{cm}^5]$$

Design Review

Conversion factor, $K_a = 0.866$

Tank Capacitance, $C_x = 0.015$ μf

Tank Capacitance Peak Voltage, $V_{cx} = 59.85$ volts

Tank Capacitance rms Current, $I_{cx(rms)} = 0.127$ amps

Primary Inductance, $L_x = 0.00165$ henrys

Series Inductor, L1 = 0.000610 henrys

Primary Reflected Current, $I_{ps(rms)} = 0.124$ amps

Primary rms Voltage, $V_{p(rms)} = 21.2$ volts

Primary Total rms Current, $I_{tp(rms)} = 0.177$ amps

Secondary Total Load Power, $P_{ot(max)} = 2.5$ watts

© 2011 by Taylor and Francis Group, LLC

Transformer Total Apparent Power, $P_t = 11.6$ watts

Transformer Core Geometry, $K_g = 0.0107$ cm^2

Step 24: From Chapter 3, select a MPP powder core, comparable in core geometry, K_g.

Core part number = 55848-W4

Manufacturer = Magnetics

Magnetic path length, MPL = 5.09 cm

Core weight, $W_{tfe} = 9.4$ gm

Copper weight, $W_{tcu} = 11.1$ gm

Mean length turn, MLT = 2.8 cm

Iron area, $A_c = 0.226$ cm^2

Window area, $W_a = 1.11$ cm^2

Area product, $A_p = 0.250$ cm^4

Core geometry, $K_g = 0.008$ cm^5

Surface area, $A_t = 22.7$ cm^2

Permeability, $\mu = 60$

Millihenrys per 1000 turns, AL = 32

Step 25: Calculate the total number of primary turns, N_{tp}.

$$N_{tp} = 1000\sqrt{\frac{L_{(new)}}{L_{(1000)}}}, \quad \text{[turns]}$$

$$N_{tp} = 1000\sqrt{\frac{1.65}{32}}, \quad \text{[turns]}$$

$$N_{tp} = 226, \quad \text{round-down [turns]}$$

$$N_p = 113, \quad \text{[each side center tap]}$$

Step 26: Calculate the operating flux density, B_{ac}.

$$B_{ac} = \frac{V_{p(rms)}\left(10^4\right)}{K_f N_p f A_c}, \quad \text{[teslas]}$$

$$B_{ac} = \frac{(21.2)\left(10^4\right)}{(4.44)(113)(32{,}000)(0.226)}, \quad \text{[teslas]}$$

$$B_{ac} = 0.0587, \quad \text{[teslas]}$$

Step 27: Calculate the watts per kilogram, WK, using the MPP 60 perm loss Equation in Chapter 2.

$$WK = 0.788\left(10^{-3}\right)(f)^{(1.41)}(B_{ac})^{(2.24)}, \quad \text{[watts/kilogram]}$$

$$WK = 0.788\left(10^{-3}\right)(32{,}000)^{(1.41)}(0.0587)^{(2.24)}, \quad \text{[watts/kilogram]}$$

$$WK = 3.09, \quad \text{[watts/kilogram] or 3.09, [milliwatts/gram]}$$

© 2011 by Taylor and Francis Group, LLC

Step 28: Calculate the core loss, P_{fe}.

$$P_{fe} = \left(\frac{\text{milliwatts}}{\text{grams}}\right) W_{tfe}\left(10^{-3}\right), \quad \text{[watts]}$$

$$P_{fe} = (3.09)(9.4)\left(10^{-3}\right), \quad \text{[watts]}$$

$$P_{fe} = 0.0290, \quad \text{[watts]}$$

Step 29: Calculate the volts per turn, $K_{N/V}$.

$$K_{N/V} = \frac{N_p}{V_p}, \quad \text{[turns/volt]}$$

$$K_{N/V} = \frac{(113)}{(21.2)}, \quad \text{[turns/volt]}$$

$$K_{N/V} = 5.33, \quad \text{[turns/volt]}$$

Step 30: Calculate the secondary number of turns N_s. α is regulation in percent. See Chapter 6.

$$K = \left(1 + \frac{\alpha}{100}\right) = 1.01$$

$$N_{s01} = K_{N/V} V_{s01} K = (5.33)(6.0)(1.01) = 32, \quad \text{[turns]}$$

$$N_{s02} = K_{N/V} V_{s02} K = (5.33)(13.0)(1.01) = 70, \quad \text{[turns]}$$

Step 31: Calculate the current density, J, using a window utilization, $K_u = 0.4$.

$$J = \frac{P_t 10^4}{A_p B_m f K_f K_u}, \quad \text{[amps per cm}^2\text{]}$$

$$J = \frac{(11.6)10^4}{(0.25)(0.0587)(32{,}000)(4.44)(0.4)}, \quad \text{[amps per cm}^2\text{]}$$

$$J = 139, \quad \text{[amps per cm}^2\text{]}$$

Step 32: Calculate the secondary required wire area, A_{ws}.

$$A_{ws01} = \frac{I_{s(01)(rms)}}{J} = \frac{0.2}{139} = 1.44 \times 10^{-3}, \quad \text{[cm}^2\text{]}$$

$$A_{ws02} = \frac{I_{s(02)(rms)}}{J} = \frac{0.1}{139} = 0.719 \times 10^{-3}, \quad \text{[cm}^2\text{]}$$

© 2011 by Taylor and Francis Group, LLC

Step 33: Then, select the wire from the Wire Table, in Chapter 4. Record μΩ/cm.

$$A_{ws01} = 1.44 \times 10^{-3}, \text{ use } \#26 = 1.28 \times 10^{-3}, \quad [\text{cm}^2]$$

$$\#26, \frac{\mu\Omega}{cm} = 1345$$

$$A_{ws02} = 0.719 \times 10^{-3}, \text{ use } \#29 = 0.647 \times 10^{-3}, \quad [\text{cm}^2]$$

$$\#29, \frac{\mu\Omega}{cm} = 2664$$

Step 34: Calculate the primary required wire area, A_{wp}.

$$A_{wp} = \frac{I_{tp(rms)}}{J}, \quad [\text{cm}^2]$$

$$A_{wp} = \frac{(0.177)}{139}, \quad [\text{cm}^2]$$

$$A_{wp} = 1.27 \times 10^{-3}, \quad [\text{cm}^2]$$

Step 35: Then, select the wire from the Wire Table, in Chapter 4. Record μΩ/cm.

$$A_{wp} = 1.27 \times 10^{-3}, \text{ use } \#26 = 1.28 \times 10^{-3}, \quad [\text{cm}^2]$$

$$\#26, \frac{\mu\Omega}{cm} = 1345$$

Step 36: Calculate the total secondary window utilization, K_{uts}.

$$K_{us01} = \frac{\left(N_{01} A_{w01}\right)}{W_a} = \frac{(32)(0.00128)}{1.11} = 0.0369$$

$$K_{us02} = \frac{\left(N_{02} A_{w02}\right)}{W_a} = \frac{(70)(0.000647)}{1.11} = 0.0408$$

$$K_{uts} = K_{us01} + K_{us02} = 0.0777$$

Step 37: Calculate the primary window utilization, K_{up}.

$$K_{up} = \frac{\left(N_{tp} A_w\right)}{W_a}$$

$$K_{up} = \frac{(226)(0.00128)}{1.11}$$

$$K_{up} = 0.261$$

Step 38: Calculate the total window utilization, K_u.

$$K_u = K_{up} + K_{uts}$$

$$K_u = 0.261 + 0.0777$$

$$K_u = 0.339$$

© 2011 by Taylor and Francis Group, LLC

Step 39: Calculate the primary, winding resistance, R_p.

$$R_p = \text{MLT}(N_p)\left(\frac{\mu\Omega}{\text{cm}}\right)\left(10^{-6}\right), \quad \text{[ohms]}$$

$$R_p = 2.80(113)(1345)\left(10^{-6}\right), \quad \text{[ohms]}$$

$$R_p = 0.426, \quad \text{[ohms]}$$

Step 40: Calculate the primary, copper loss, P_p.

$$P_p = \left(I_{p(rms)}\right)^2 R_p, \quad \text{[watts]}$$

$$P_p = (0.177)^2 (0.426), \quad \text{[watts]}$$

$$P_p = 0.0133, \quad \text{[watts]}$$

Step 41: Calculate the secondary, winding resistance, R_s.

$$R_s = \text{MLT}(N_s)\left(\frac{\mu\Omega}{\text{cm}}\right)\left(10^{-6}\right), \quad \text{[ohms]}$$

$$R_{s01} = 2.80(32)(1345)\left(10^{-6}\right) = 0.121, \quad \text{[ohms]}$$

$$R_{s02} = 2.80(70)(2664)\left(10^{-6}\right) = 0.186, \quad \text{[ohms]}$$

Step 42: Calculate the secondary, copper loss, P_s.

$$P_s = \left(I_{s(rms)}\right)^2 R_s, \quad \text{[watts]}$$

$$P_{s01} = (0.2)^2 (0.121) = 0.00484, \quad \text{[watts]}$$

$$P_{s02} = (0.1)^2 (0.186) = 0.00186, \quad \text{[watts]}$$

Step 43: Calculate the total secondary, copper loss, P_{ts}.

$$P_{ts} = P_{s01} + P_{s02}, \quad \text{[watts]}$$

$$P_{ts} = 0.00484 + 0.00186, \quad \text{[watts]}$$

$$P_{ts} = 0.0067, \quad \text{[watts]}$$

Step 44: Calculate the total loss, core and copper, P_Σ.

$$P_\Sigma = P_p + P_{ts} + P_{fe}, \quad \text{[watts]}$$

$$P_\Sigma = (0.0133) + (0.0067) + (0.0290), \quad \text{[watts]}$$

$$P_\Sigma = 0.049, \quad \text{[watts]}$$

© 2011 by Taylor and Francis Group, LLC

Step 45: Calculate the watts per unit area, ψ.

$$\psi = \frac{P_{\Sigma}}{A_t}, \quad [\text{watts per cm}^2]$$

$$\psi = \frac{(0.049)}{(22.7)}, \quad [\text{watts per cm}^2]$$

$$\psi = 0.00216, \quad [\text{watts per cm}^2]$$

Step 46: Calculate the temperature rise, T_r.

$$T_r = 450(\psi)^{(0.826)}, \quad [°\text{C}]$$

$$T_r = 450(0.00216)^{(0.826)}, \quad [°\text{C}]$$

$$T_r = 2.83, \quad [°\text{C}]$$

Step 47: Calculate the, Q_t, of the tank.

$$Q_t = 2\pi f C_x R_{SR}$$

$$Q_t = (6.28)(32,000)\left(0.015\left(10^{-6}\right)\right)(592)$$

$$Q_t = 1.79$$

For more information, see Equation [18-20].

Recognition

The author would like to thank **Dr. V. Vorperian**, Senior Engineer, Power and Sensor Electronics Group, Jet Propulsion Laboratory (JPL), for his help with the Quiet Converter design equations.

References

1. V. Vorperian, and C. McLyman, “Analysis of a PWM-Resonant DC-to-DC Converter.” IEEE transaction.

2. S. Lendena, “Current-Fed Inverter.” 20th Annual Proceedings Power Sources Conference, May 24, 1966.

3. S. Lendena, “Single Phase Inverter for a Three Phase Power Generation and Distribution System.” Electro-Optical-System, Contract #954272, from Jet Propulsion Laboratory, January, 1976.

© 2011 by Taylor and Francis Group, LLC

Chapter 19

Rotary Transformer Design

© 2011 by Taylor and Francis Group, LLC

Table of Contents

1. Introduction 19-3
2. Basic Rotary Transformer 19-3
3. Square Wave Technology 19-4
4. Rotary Transformer Leakage Inductance 19-5
5. Current-fed Sine Wave Converter Approach 19-6
6. Rotary Transformer Design Constraints 19-8
7. References 19-10

© 2011 by Taylor and Francis Group, LLC

Introduction

There are many requirements to transfer signals and power across rotary interfaces. Most things that use slip rings or brushes can be replaced with a rotary transformer. Science instruments, antennas and solar arrays are elements needing rotary power transfer for certain spacecraft (S/C) configurations, such as a spin, stabilized (S/C). Delivery of signals and power has mainly been done by slip rings. There are problems in using slip rings for long life and high reliability: contact wear, noise, and contamination. Contact wear will lead to a conductive path to ground. This conductive path will generate noise and upset the original designed common-mode noise rejection. A simple slip ring assembly and a rotary transformer are shown in Figure 19-1. High data rates and poor slip ring life forced the Galileo (S/C) to replace the signal interface with rotary transformers. The use of a rotary transformer to transfer power on the Galileo (S/C) was contemplated, but it was thought the impact on the (S/C) delivery was too great. The rotary transformers on the Galileo (S/C) lasted the life of the spacecraft, from 1989 to 2003 without a glitch.

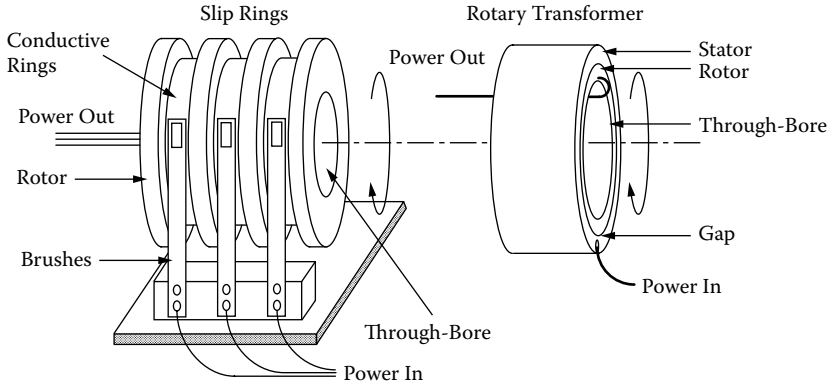

Figure 19-1. Comparing a Slip Ring Assembly and a Rotary Transformer.

Existing approaches to rotary power transfer use square wave converter technology. However, there are problems caused by the inherent gap in a rotary transformer, coupled with the fast rate of change in the square wave voltage. Undue stress is placed on the power electronics and the interface becomes a source of Electromagnetic Interference (EMI) that impacts the overall system's operating integrity.

Basic Rotary Transformer

The rotary transformer is essentially the same as a conventional transformer, except that the geometry is arranged so that the primary and secondary can be rotated, with respect to each other with negligible changes in the electrical characteristics. The most common of the rotary transformers are the axial rotary transformer, shown in Figure 19-2, and the flat plane, (pot core type), rotary transformer, shown in Figure 19-3. The power transfer is accomplished, electro-magnetically, across an air gap. There are no wearing contacts, noise, or contamination problems due to lubrication or wear debris.

© 2011 by Taylor and Francis Group, LLC

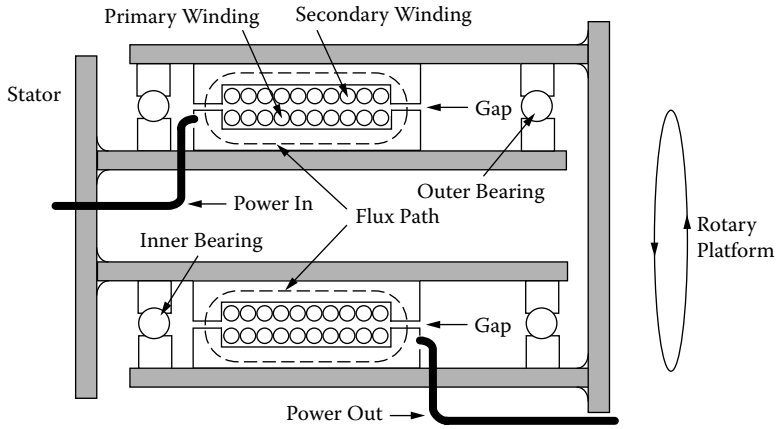

Figure 19-2. Pictorial of an Axial, Type Rotary Transformer.

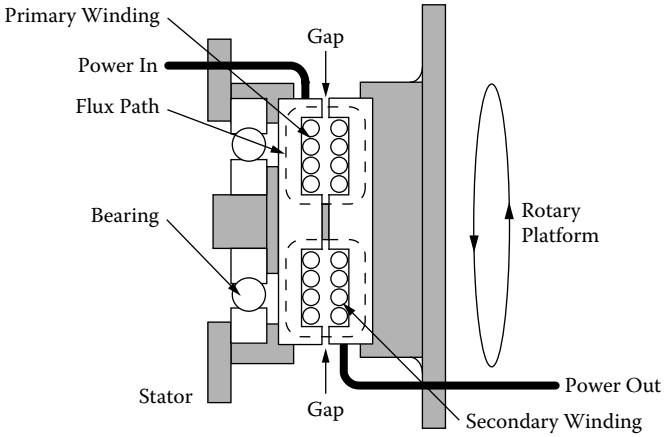

Figure 19-3. Pictorial of a Flat Plane, Type Rotary Transformer.

Square Wave Technology

The ideal converter transformer would have a typical square B-H loop, as shown in Figure 19-4. A converter transformer is normally designed to have a minimum of leakage inductance. The voltage spikes that are normally seen on the primary of a square wave converter transformer are caused by the leakage inductance. To design a converter transformer to have a minimum of leakage inductance, the primary and secondary must have a minimum of distance between them. Minimizing the leakage inductance will reduce the need for power-wasting, snubber circuits. Although there are rotary power transformers designed with the use of square wave converter technology, they are not without problems.

There are two basic problems not found in the normal transformer: (1) the inherent gap in a rotary transformer is one problem, and (2) the required spacing between primary and secondary that leads to large leakage inductance is the other. These problems, along with a square wave drive, are what leads to a high loss, snubber circuit, and become a source of Electromagnetic Interference (EMI) that impacts the adjoining systems

© 2011 by Taylor and Francis Group, LLC

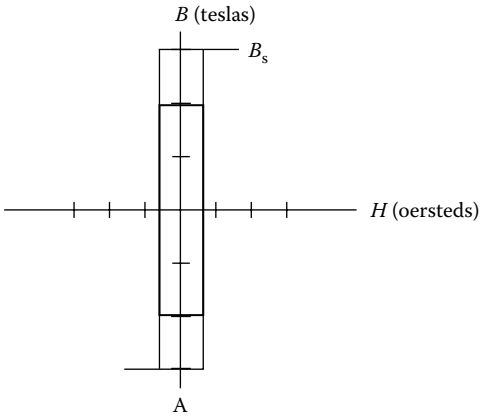

Figure 19-4. Typical, Transformer BH Loop.

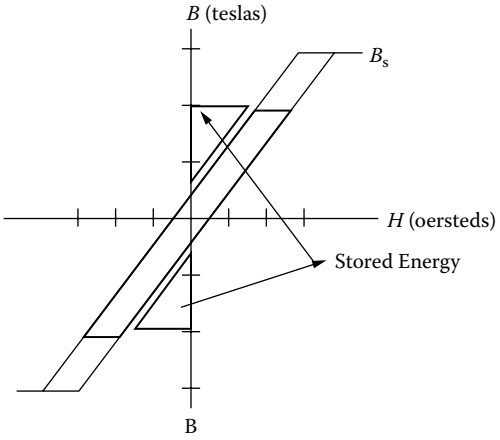

Figure 19-5. Typical, Rotary Transformer BH Loop.

operating integrity. The rotary transformer, because of its inherent gap, has a B-H loop similar to an inductor, as shown in Figure 19-5. Basically, the transformer transforms power, and the inductor stores energy in the gap. The rotary transformer does not have any of the traits of an ideal transformer. It is, more accurately, a trans-inductor having a gap and a secondary, spaced away from the primary.

Rotary Transformer Leakage Inductance

The rotary transformer has an inherent gap and spacing of the primary and secondary. The gap and spacing in the rotary transformer result in a low primary magnetizing inductance. This low primary inductance leads to a high magnetizing current. The leakage inductance, L_p, can be calculated for both axial and flat plane using Equation 19-1. The axial rotary transformer winding dimensions are shown in Figure 19-6. The flat plane rotary transformer winding dimensions are shown in Figure 19-7.

$$L_p = \frac{4\pi(MLT)N_p^2}{a}\left(c + \frac{b_1 + b_2}{3}\right)\left(10^{-9}\right), \quad \text{[henrys]} \qquad [19\text{-}1]$$

© 2011 by Taylor and Francis Group, LLC

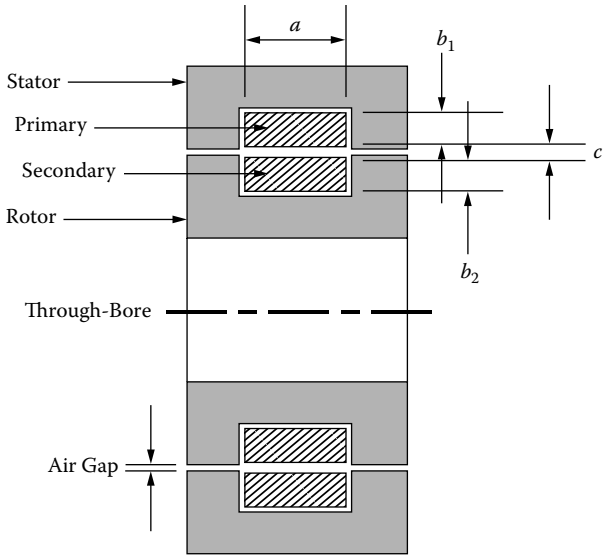

Figure 19-6. Axial Rotary Transformer, Showing Winding Dimensions.

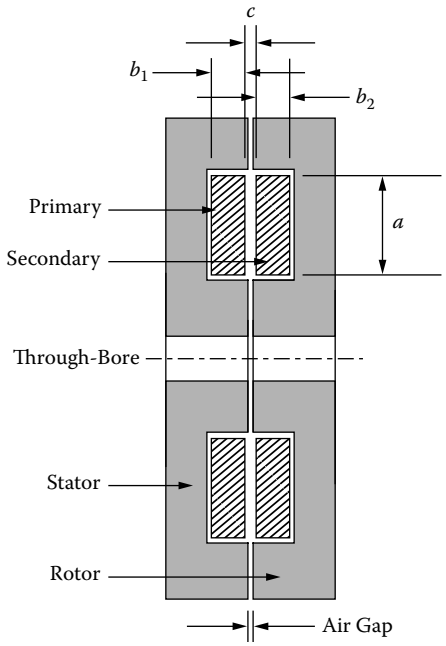

Figure 19-7. Flat Plane Rotary Transformer, Showing Winding Dimensions.

Current-fed Sine Wave Converter Approach

The current-fed, sine wave converter topology is a good candidate to power the rotary transformer. The design would be a current-fed, push-pull, tuned tank converter requiring a gapped transformer. A comparison between a standard, square wave converter, shown in Figure 19-8, and a current-fed, sine wave converter, is

© 2011 by Taylor and Francis Group, LLC

shown in Figure 19-9. Using the rotary transformer in this topology, the energy that is stored in the rotary gap that causes so much trouble in the standard square wave driving a rotary transformer, is recovered and is used in the tank circuit. There would not be any need of power-wasting snubbers using the rotary transformer approach. See Chapter 18.

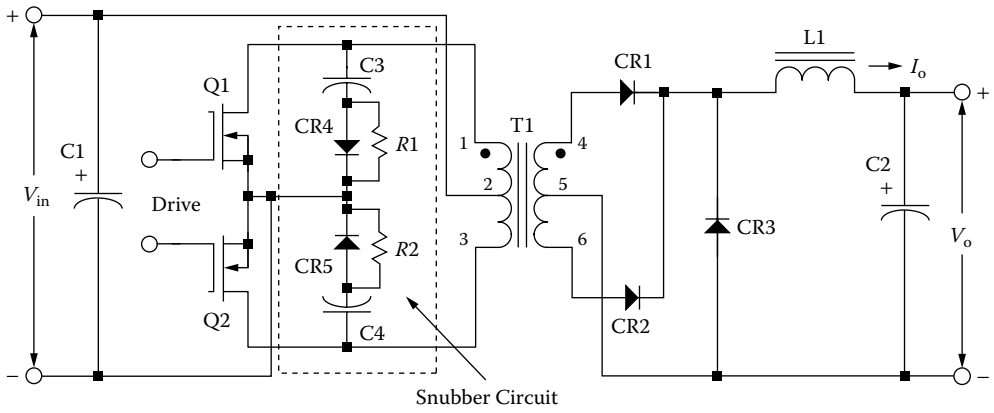

Figure 19-8. Typical, Voltage-fed, Square Wave Converter Circuit with Snubbers.

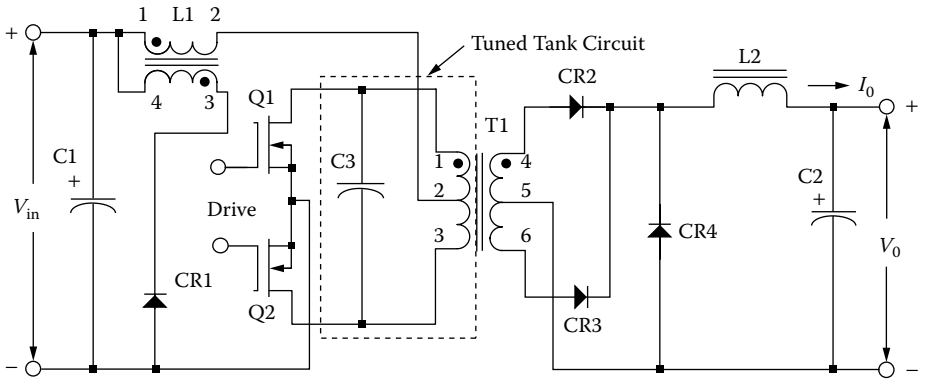

Figure 19-9. Typical, Current-fed, Resonant Converter Circuit.

The current-fed sine wave converter requires a resonant, LC, tank circuit to operate properly. The primary of the rotary transformer would be the ideal inductor, because of the inherent gap of the rotary transformer. There are several advantages to incorporating the resonant tank circuit into the rotary transformer. First, it minimizes the number of components in the power stage. Secondly, the output of the inverter is a natural sine wave, as shown in Figure 19-10, and usually requires no additional filtering. Thirdly, energy stored in the gap of the transformer is released when either power switch is turned off. This energy is commutated in the resonant tank circuit. This provides the capability for direct exchange of power between the tank circuit and the load. There is not a noticeable drive torque in a rotary transformer. The tuning or tank capacitor must be of high quality, stable, and with low ESR.

© 2011 by Taylor and Francis Group, LLC

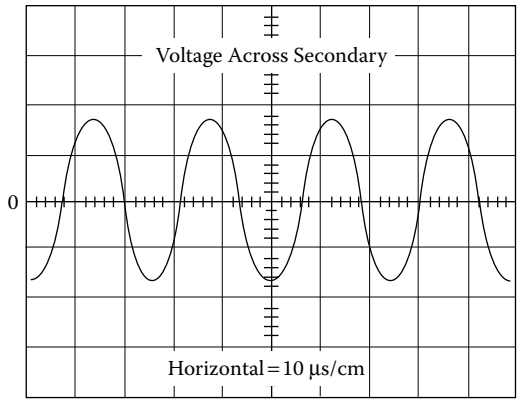

Figure 19-10. Current-fed Converter, Secondary Sine Wave Secondary Voltage.

Rotary Transformer Design Constraints

The rotary transformer requirements pose some unusual design constraints compared to the usual transformer design. The first is the relatively large gap in the magnetic circuit. This gap size depends on the eccentric dimension and the tolerance of the rotating shaft. The gap results in a low primary magnetizing inductance. Secondly, the large space separating primary and secondary windings results in an unusually high primary-to-secondary leakage inductance. Thirdly, the large through-bore requirement results in an inefficient utilization of the core material and copper, due to the fixed mean-length turn. This large diameter results in requiring more copper area for the same regulation. Finally, the core has to be more robust than the normal transformer because of the structural requirement. See Figure 19-11.

Rotary transformer dimensions are usually governed by the mechanical interface, in particular the relatively large gap and the large through-bore, resulting in a long Mean Length Turn (MLT). The rotary transformer is not an ideal magnetic assembly. A toroidal core is an ideal magnetic assembly. Manufacturers use test data, taken from toroidal cores, to present magnetic material characteristics. The magnetic flux in a toroidal core

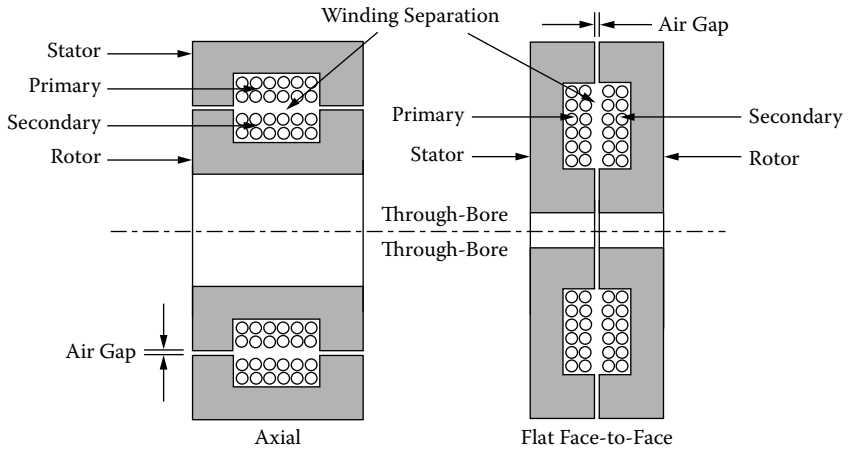

Figure 19-11. Geometries of the Basic Type Rotary Transformers.

© 2011 by Taylor and Francis Group, LLC

travels through a constant core cross-section, A_c, throughout the whole Magnetic Path Length, MPL, as shown in Figure 19-12, and provides ideal magnetic characteristics. It can be seen that the core cross-section throughout the rotary transformers, shown in Figure 19-13 and Figure 19-14, does not provide constant flux density or an ideal magnetic assembly. The rotary transformers for the Galileo spacecraft were about 10 cm in diameter, and manufactured by CMI (Ref. 4.)

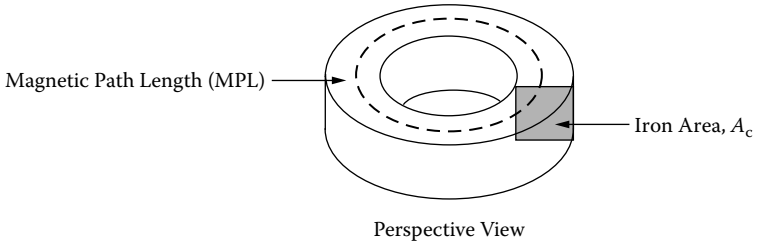

Figure 19-12. Typical Perspective View of a Toroidal Core.

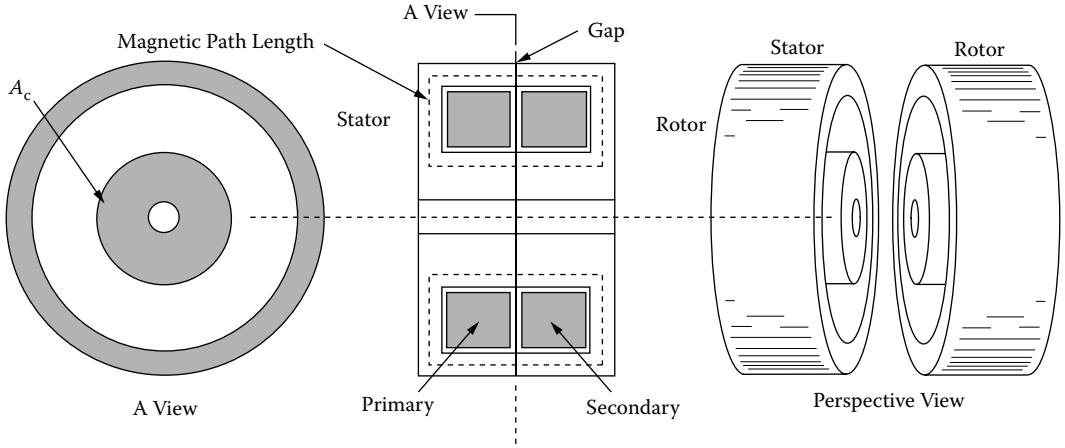

Figure 19-13. Open View of a Flat Plane, Type Rotary Transformers.

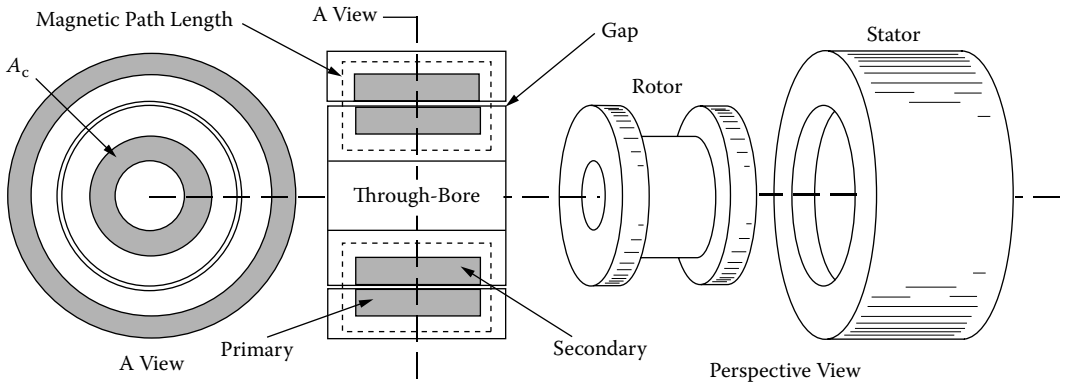

Figure 19-14. Open View of an Axial Type Rotary Transformers.

© 2011 by Taylor and Francis Group, LLC

References

1. E. Landsman, “Rotary Transformer Design.” Massachusetts Institute Technology, PCSC-70 Record, pp. 139–152.

2. L. Brown, “Rotary Transformer Utilization in a Spin Stabilized Spacecraft Power System.” General Electric, pp. 373–376.

3. S. Marx, “A Kilowatt Rotary Power Transformer.” Philco-Ford Corp., *IEEE Transactions on Aerospace and Electronic Systems* Vol. AES-7, No. 6 November, 1971.

4. Ceramic Magnetics, Inc. 16 Law Drive Fairfield, NJ 07006.

© 2011 by Taylor and Francis Group, LLC

Chapter 20

Planar Transformers and Inductors

© 2011 by Taylor and Francis Group, LLC

Table of Contents

1. Introduction....20-3
2. Planar Transformer Basic Construction....20-3
3. Planar Integrated PC Board Magnetics....20-5
4. Core Geometries....20-6
5. Planar Transformer and Inductor Design Equations....20-7
6. Window Utilization, K_u....20-8
7. Current Density, J....20-9
8. Printed Circuit Windings....20-11
9. Calculating the Mean Length Turn, MLT....20-12
10. Winding Resistance and Dissipation....20-13
11. PC Winding Capacitance....20-14
12. Planar Inductor Design....20-16
13. Winding Termination....20-16
14. PC Board Base Materials....20-17
15. Core Mounting and Assembly....20-18
16. References....20-19

© 2011 by Taylor and Francis Group, LLC

Introduction

The planar transformer, or inductor, is a low profile device that covers a large area, whereas, the conventional transformer would be more cubical in volume. Planar Magnetics is the new "buzz" word in the field of power magnetics. It took a few engineers with the foresight to come up with a way to increase the power density, while at the same time increasing the overall performance, and also, making it cost effective. One of the first papers published on planar magnetics was by Alex Estrov, back in 1986. After reviewing this paper, you really get a feeling of what he accomplished. A whole new learning curve can be seen on low profile ferrite cores and printed circuit boards if one is going to do any planar transformer designs. It is an all-new technology for the transformer engineer. The two basic items that made this technology feasible were the power, MOSFETs that increased the switching frequency and enabled the designer to reduce the turns, and the ferrite core, which can be molded and machined into almost any shape. After this paper was written the interest in planar magnetics seems to increase each year.

Planar Transformer Basic Construction

Here, shown in Figure 20-1 through Figure 20-4 are four views of a typical EE core, planar construction method. The assembled planar transformers have very unique characteristics in their finished construction. In the assembled planar transformer, every primary turn is at a precise location, governed by the PC board. The primary is always the same distance from the secondary. This provides a tight control over the primary to secondary leakage inductance. Using the same insulating material will always provide the same capacitance between primary and secondary; in this way, all parasitics will be the same from unit-to-unit. With this type of planar construction, the engineer will have a tight control over leakage inductance, the resonant frequency, and the common-mode rejection. A tight control is necessary on all materials used.

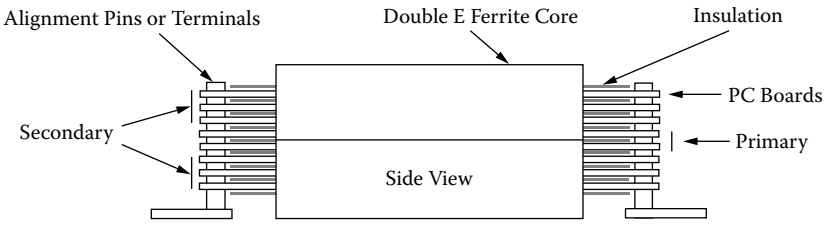

Figure 20-1. Side View of a Typical EE Planar Transformer.

© 2011 by Taylor and Francis Group, LLC

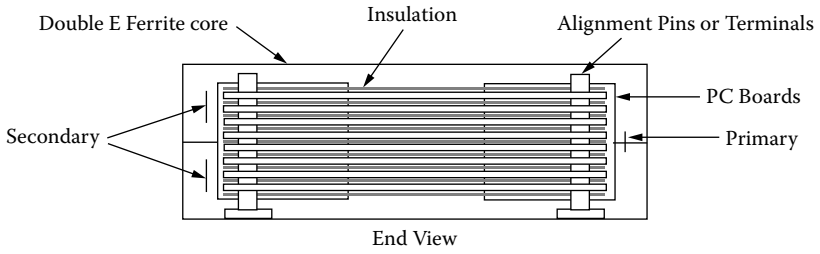

Figure 20-2. End View of a Typical EE Planar Transformer.

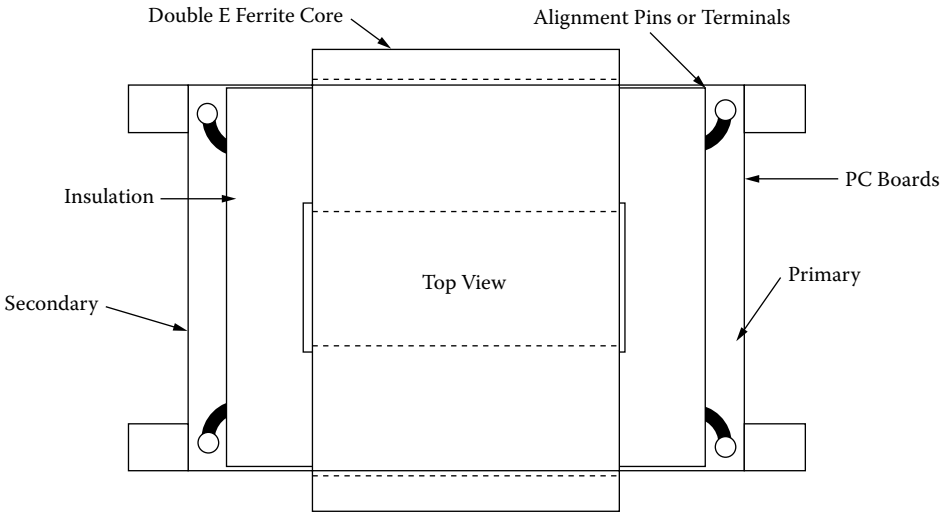

Figure 20-3. Top View of a Typical EE Planar Transformer.

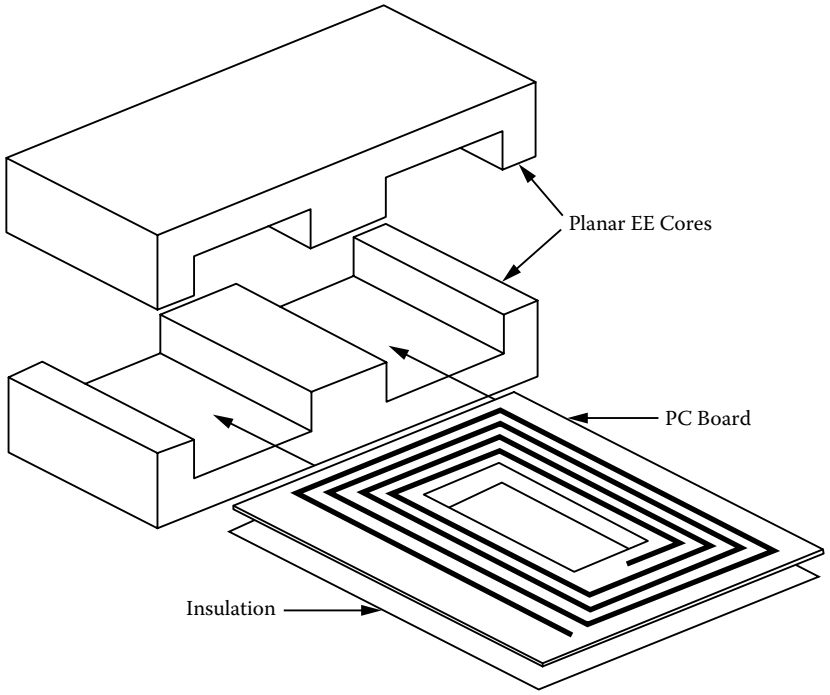

Figure 20-4. A Perspective View of a Typical EE Planar Transformer.

© 2011 by Taylor and Francis Group, LLC

Planar Integrated PC Board Magnetics

Planar transformers and inductors are now being integrated right on the main PC board. Design engineers are pushing the operating frequency higher and higher to where it is commonplace to operate at frequency range between 250-500kHz. As the frequency increases the power supplies are getting smaller and smaller. In order to reduce the size of the power supply even further, engineers are going to planar magnetics that are integrated into the main PC board. An exploded view to show the multi-layers PC board of a planar transformer that has been integrated into the main PC board is shown in Figure 20-5. The final assembly of the same planar transformer is shown in Figure 20-6.

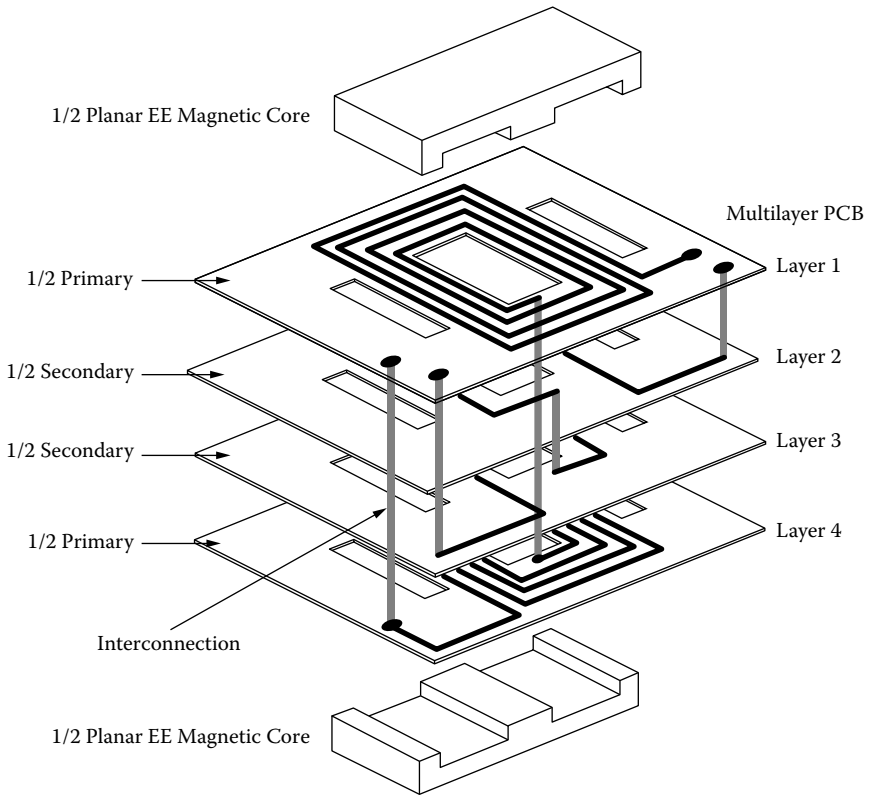

Figure 20-5. A Planar Transformer Integrated into the Main PC Board.

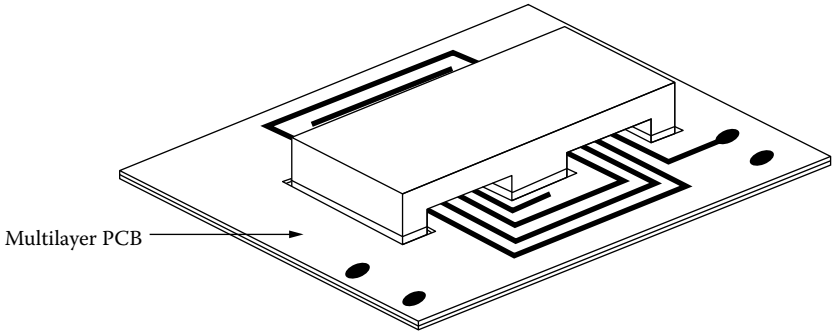

Figure 20-6. PC Board Planar Transformer in Final Assembly.

© 2011 by Taylor and Francis Group, LLC

Core Geometries

The EE and EI are not the only planar geometries now available. There are a few firms in the ferrite industry that offer low profile versions of their standard cores, giving the engineer a few more choices in his design. There are EE and EI cores available from Magnetics Inc. as shown in Figure 20-7; there are ER cores available from Ferroxcube, as shown in Figure 20-8; there are ETD-lp cores available from Ferrite International, as shown in Figure 20-9; there are PQ-lp cores available from Ferrite International, as shown in Figure 20-10; and there are RM-lp cores available from Ferroxcube, as shown in Figure 20-11. There are several advantages, with cores with a round center post, such as PQ-lp, RM-lp, ETD-lp and ER. A round center post results in a more efficient use of copper and a more efficient use of board space. There is a company, Ceramic Magnetics, Inc. (CMI), that can modify any of these cores to your specification or machine a special core for your application. The IEC has a new standard 62313 for planar cores that supercedes standard 61860.

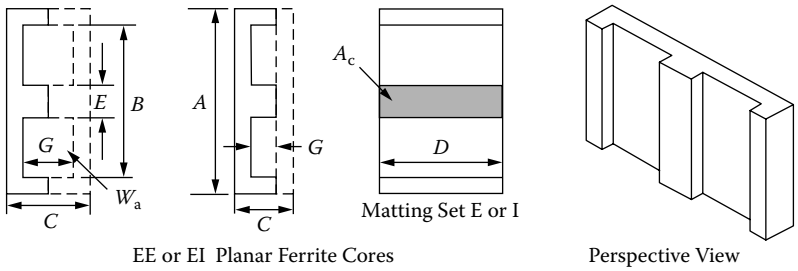

Figure 20-7. Magnetic Inc. EE and EI Low Profile Planar Cores.

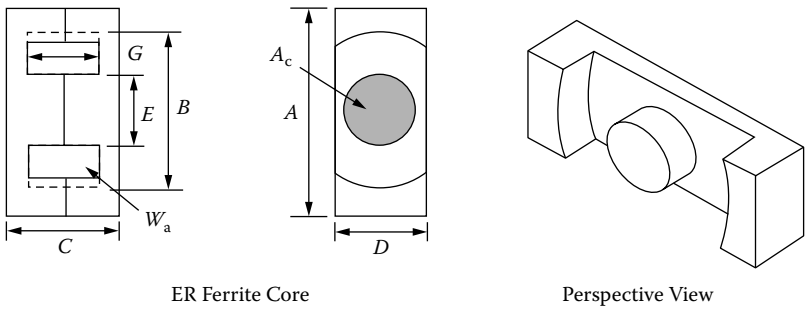

Figure 20-8. Ferroxcube ER Low Profile Planar Cores.

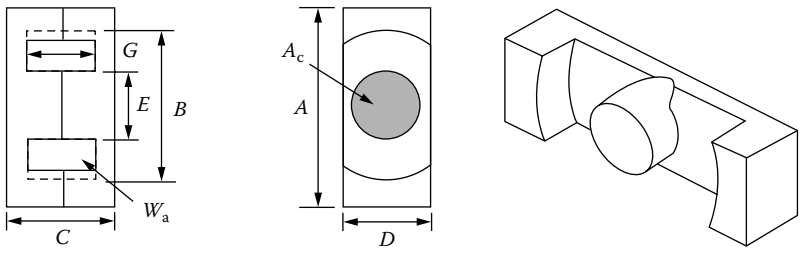

Figure 20-9. Ferrite International ETD Low Profile Planar Cores.

© 2011 by Taylor and Francis Group, LLC

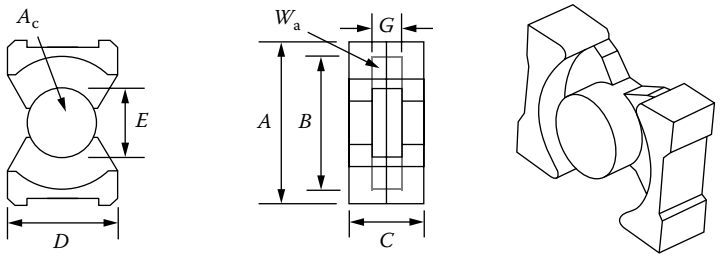

Figure 20-10. Ferrite International PQ Low Profile Planar Cores.

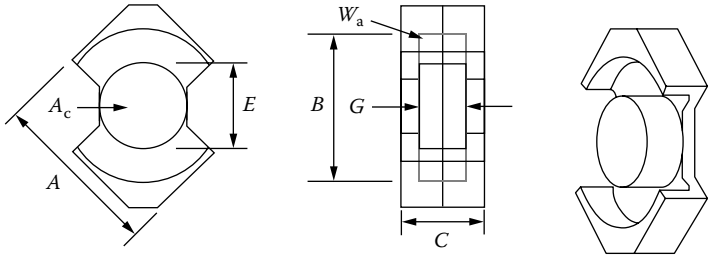

Figure 20-11. Ferroxcube RM Low Profile Planar Cores.

Planar Transformer and Inductor Design Equations

The same design Equations are used, as well as the criteria used to select the proper core, to design a planar transformer as a conventional transformer. Faraday's Law is still used to calculate the required turns, as shown in Equation [20-1].

$$N = \frac{V_p(10^4)}{K_f f A_c B_{ac}}, \quad \text{[turns]} \tag{20-1}$$

The area product, A_p, is the power handling capability of the core for transformers, as shown in Equation [20-2].

$$A_p = \frac{P_t(10^4)}{K_f K_u f A_c B_{ac} J}, \quad [\text{cm}^4] \tag{20-2}$$

In the gapped inductor Equation, L, is shown in Equation [20-3].

$$L = \frac{0.4\pi N^2 A_c (10^{-8})}{l_g + \left(\frac{MPL}{\mu_m}\right)}, \quad \text{[henrys]} \tag{20-3}$$

The area product, A_p, is the energy handling capability of the core for inductors, as shown in Equation [20-4].

$$A_p = \frac{2(\text{Energy})}{K_u B_{ac} J}, \quad [\text{cm}^4] \tag{20-4}$$

© 2011 by Taylor and Francis Group, LLC

Window Utilization, K_u

The window utilization factor in the conventional transformer is about 0.40. This means that 40% of the window is filled with copper. The other 60% of the area is devoted to the bobbin or tube, to the insulation both layer and wire, and to the winding technique. The window utilization is explained, in detail, in Chapter 4. Designing a planar transformer and using the PC winding technique, reduces the window utilization factor even further. The window utilization, K_u, comparison of the two different winding techniques is shown in Figure 20-12.

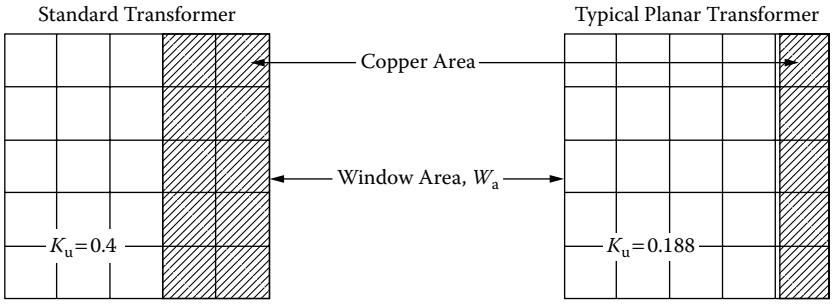

Figure 20-12. Comparing the Window Utilization of a Standard Transformer and a Planar Transformer.

A PC board window utilization, K_u, calculation example will be as follows:

The windings will be placed on a double-sided 2oz PC board 10 mils thick, giving a total thickness of 15.4 mils (0.0391 cm). The Mylar insulation material is between the PC boards, and between the PC boards, and the core will add another 4 mils (0.0102 cm) to the thickness. This will give 19.4 mils (0.0493 cm) per layer. There will be a 20 mil space (margin) between the edge of the board and the copper clad. The copper width will be the window width of 0.551cm, minus 2x the margin of 0.102. This will give a total copper width of 0.449. The window utilization, K_u, will be summed in Table 20-1, using Figure 20-13 as a guide.

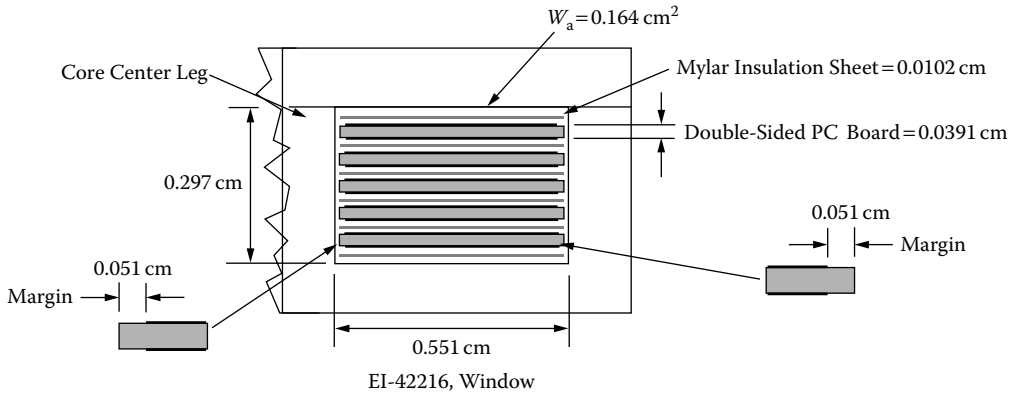

Figure 20-13. Window Utilization of a Typical EI Planar Transformer.

© 2011 by Taylor and Francis Group, LLC

Table 20-1. EI-42216 Window Utilization

EI-42216 Window Utilization	
Window Height, cm	0.2970
Window Width, cm	0.5510
Window Area, cm^2	0.1640
PC Board Thickness with Copper, cm	0.0391
Sheet Insulator, cm	0.0102
Total Insul. 5+1 Layers Thick, cm	0.0612
Total Thickness 5 Layers, cm	0.2570
Copper Thickness 5 Layers, cm	0.0686
Copper Width, cm	0.4494
Total Copper Area, cm^2	0.0308
Window Utilization, K_u	0.1878

Current Density, J

One of the unknown factors in designing planar transformers is the current density, J. The current density controls the copper loss (regulation) and the inherit temperature rise caused by the copper loss. The temperature rise is normally controlled by the surface dissipation of the transformer. The size of a transformer goes up by the cubic law, and the surface area goes up by the square law. Large transformers, such as 60 Hz, are designed with a low current density, while 400 Hz are designed with higher current density for the same temperature rise. There used to be an old rule of thumb, for a large transformer, that you use 1000 circular mils per amp, and for a small transformer, you use 500 circular mils (CM) per amp:

$$500\text{CM/Amp} \approx 400\,\text{Amps/cm}^2, \quad \text{[400 Hertz Aircraft]}$$
$$1000\text{CM/Amp} \approx 200\,\text{Amps/cm}^2, \quad \text{[60 Hertz]}$$

Planar transformer designers handle the current density in a different way. When designing planar transformer PC windings, designers use the same technology used by the printed, circuit board designers, and that is the current rating for a given voltage drop and temperature rise. It is another way of saying the same thing. The printed circuit boards are covered with a copper clad. The thickness of this copper is called out in ounces, such as 1oz, 2oz, and 3oz. The weight in ounces comes from an area of one square foot of material. So 1oz of copper clad would be 1 square foot, and have a thickness of 0.00135 of an inch; 2oz would be 0.0027 of an inch; and 3oz would be 0.00405 of an inch. Tables have been made to show the current capacity for a constant temperature rise with different line width. The design data for 1oz copper is shown in Table 20-2. The 2oz copper is shown in Table 20-3, and 3oz copper is shown in Table 20-4. Planar transformer engineers are using the industrial guidelines for their selection of copper trace thickness and line width, based on temperature rise. For the first effort for a planar transformer, the PC winding should be around:

$$100\text{CM/Amp} \approx 2000\,\text{Amps/cm}^2, \quad \text{[500 kHertz Planar Transformers]}$$

© 2011 by Taylor and Francis Group, LLC

If the current density is based on Table 20-1, with a line width of 0.06 inches, then use:

$$35\text{CM/Amp} \approx 5700\,\text{Amps/cm}^2, \quad \text{[500 kHertz Planar Transformers]}$$

Table 20-2. Design Data for 0.00135 Inch Thick Copper Clad

Printed Circuit Trace Data for 1oz Copper (Based on 10 Inches Long)							
Line Width	Line Width	Resistance micro-ohm	Copper Weight 1oz Thickness 0.00135		Temp. °C Increase above Amb. vs. Current in Amperes		
Inches	mm	per-mm	cm^2	AWG[a]	5°	20°	40°
0.0200	0.51	989.7	0.000174	35	1.00	3.00	4.00
0.0400	1.02	494.9	0.000348	32	2.25	5.00	6.50
0.0600	1.52	329.9	0.000523	30	3.00	6.50	8.00
0.0800	2.03	247.4	0.000697	29	4.00	7.00	9.50
0.1000	2.54	197.9	0.000871	28	4.50	8.00	11.00
0.1200	3.05	165.0	0.001045	27	5.25	9.25	12.00
0.1400	3.56	141.4	0.001219	26	6.00	10.00	13.00
0.1600	4.06	123.7	0.001394	26	6.50	11.00	14.25
0.1800	4.57	110.0	0.001568	25	7.00	11.75	15.00
0.2000	5.08	99.0	0.001742	25	7.25	12.50	16.60

Source: Data From: Handbook of Electronic Packaging.

[a] This is a close approximation to an equivalent AWG wire size.

Table 20-3. Design Data for 0.0027 Inch Thick Copper Clad

Printed Circuit Trace Data for 2oz Copper (Based on 10 Inches Long)							
Line Width	Line Width	Resistance micro-ohm	Copper Weight 2oz Thickness 0.0027		Temp. °C Increase above Amb. vs. Current in Amperes		
Inches	mm	per-mm	cm^2	AWG[a]	5°	20°	40°
0.0200	0.51	494.9	0.000348	32	2.00	4.00	6.25
0.0400	1.02	247.4	0.000697	29	3.25	7.00	9.00
0.0600	1.52	165.0	0.001045	27	4.25	9.00	11.25
0.0800	2.03	123.7	0.001394	26	5.00	10.25	13.25
0.1000	2.54	99.0	0.001742	25	5.25	11.00	15.25
0.1200	3.05	82.5	0.002090	24	5.75	12.25	17.00
0.1400	3.56	70.7	0.002439	23	6.25	13.25	18.50
0.1600	4.06	61.9	0.002787	23	6.50	14.25	20.50
0.1800	4.57	55.0	0.003135	22	7.00	15.25	22.00
0.2000	5.08	49.5	0.003484	22	7.25	16.25	24.00

Source: Data From: Handbook of Electronic Packaging.

[a] This is a close approximation to an equivalent AWG wire size.

© 2011 by Taylor and Francis Group, LLC

Table 20-4. Design Data for 0.00405 Inch Thick Copper Clad

Printed Circuit Trace Data for 3oz Copper (Based on 10 Inches Long)							
Line Width	Line Width	Resistance micro-ohm	Copper Weight 3oz Thickness 0.00405		Temp. °C Increase above Amb. vs. Current in Amperes		
Inches	mm	per-mm	cm^2	AWG[a]	5°	20°	40°
0.0200	0.51	329.9	0.000523	30	2.50	6.00	7.00
0.0400	1.02	165.0	0.001045	27	4.00	8.75	11.00
0.0600	1.52	110.0	0.001568	25	4.75	10.25	13.50
0.0800	2.03	82.5	0.002090	24	5.50	12.00	15.75
0.1000	2.54	66.0	0.002613	23	6.00	13.25	17.50
0.1200	3.05	55.0	0.003135	22	6.75	15.00	19.50
0.1400	3.56	47.1	0.003658	22	7.00	16.00	21.25
0.1600	4.06	41.2	0.004181	21	7.25	17.00	23.00
0.1800	4.57	36.7	0.004703	20	7.75	18.25	25.00
0.2000	5.08	33.0	0.005226	20	8.00	19.75	27.00

Source: Data From: Handbook of Electronic Packaging.
[a] This is a close approximation to an equivalent AWG wire size.

Printed Circuit Windings

There will be a few paths of mystery along the way when engineers first get started in the design of a planar transformer. Therefore, it is easier to start on a simple design and use magnet wire, then convert that into a truly all-planar approach, using a PC winding board design. In this way the engineer will slide up the learning curve slowly. There are several benefits to a printed circuit winding. Once the printed winding board is finished and the layout is fixed, the winding will not vary and all of the parasitics, including the leakage inductance, will be frozen. This is not necessarily true in conventional transformers. There are two basic core configurations available to the engineer for planar design. The first configuration is the EE or EI with the rectangular center post. A typical high current and low current winding PC board for E cores is shown in Figure 20-14.

The second configuration is shown in Figure 20-15. These are four cores with round center legs. Winding PC boards with round center legs are used on PQ-lp, RM-lp, ETD-lp and ER cores. There is an advantage to cores with round center legs. Cores with round center leg will produce a round ID, OD resulting in a more efficient use of copper.

© 2011 by Taylor and Francis Group, LLC

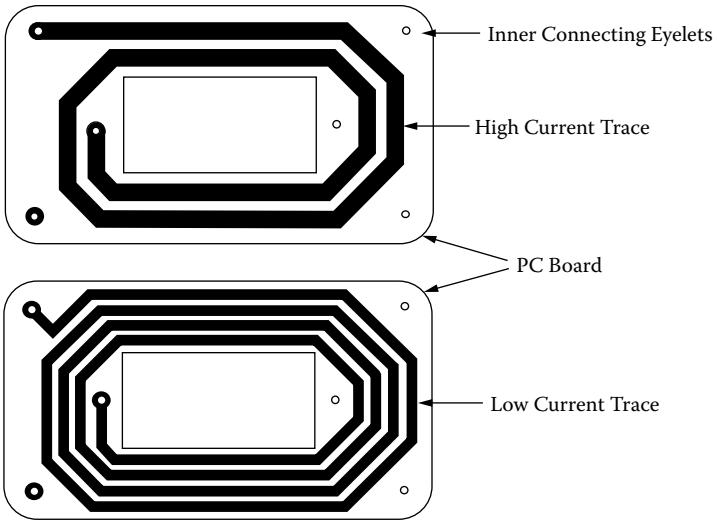

Figure 20-14. Typical Planar E Core Winding PC Board.

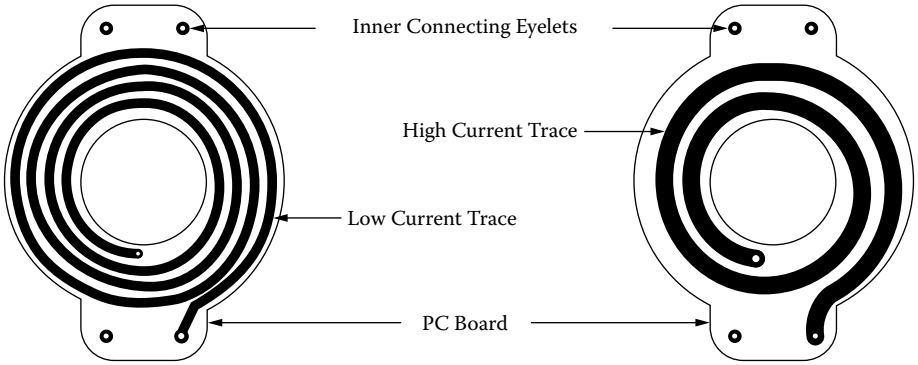

Figure 20-15. Typical Circular Winding PC Board for Cores with Round Center Leg.

Calculating the Mean Length Turn, MLT

The Mean Length Turn (MLT), is required to calculate the dc winding resistance. With the winding resistance known, the winding voltage drop can be calculated at rated load. The winding dimensions, relating to the Mean Length Turn (MLT) for a rectangular winding, is shown in Figure 20-16, along with the MLT equation, and a circular winding is shown in Figure 20-17, along with the MLT equation.

$$\text{MLT} = 2B + 2C + 2.82A, \quad \text{[mm]} \qquad \text{[20-5]}$$

$$\text{MLT} = \frac{\pi(OD + ID)}{2}, \quad \text{[mm]} \qquad \text{[20-6]}$$

© 2011 by Taylor and Francis Group, LLC

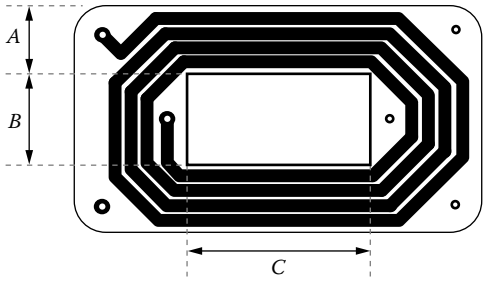

Figure 20-16. Dimensions, Relating to a Rectangular Winding, Mean Length Turn (MLT).

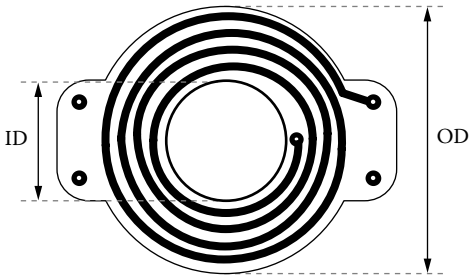

Figure 20-17. Dimensions, Relating to a Circular Winding, Mean Length Turn (MLT).

Winding Resistance and Dissipation

The winding dc resistance and voltage drop will be calculated as follows:

Calculate the Mean Length Turn (MLT) using the winding board configuration and Equation in Figure 20-17. Use the printed winding data in Table 20-5.

Table 20-5. PC Board Winding Data

PC Winding Data		
Item		Units
PC Board Turns Each Side	4	
Winding Trace Thickness	0.0027	inches
Winding Trace Width	2.54	mm
Trace Resistance	99	μΩ/mm
Winding Board, OD	31.5	mm
Winding Board, ID	14.65	mm
Winding Current, I	3	amps
PC Board Thickness	0.5	mm
PC Board Dielectric Constant, K	4.7	

© 2011 by Taylor and Francis Group, LLC

Step 1: Calculate the Mean Length Turn, MLT:

$$\text{MLT} = \frac{\pi(OD + ID)}{2}, \quad [\text{mm}]$$
$$\text{MLT} = \frac{3.14(31.5 + 14.65)}{2}, \quad [\text{mm}]$$
$$\text{MLT} = 72.5, \quad [\text{mm}]$$

Step 2: Calculate the winding resistance, R:

$$R = MLT(N)\left(\frac{\mu\Omega}{\text{mm}}\right)(10^{-6}), \quad [\text{ohms}]$$
$$R = (72.5)(8)(99.0)(10^{-6}), \quad [\text{ohms}]$$
$$R = 0.057, \quad [\text{ohms}]$$

Step 3: Calculate the winding voltage drop, V_w:

$$V_w = IR, \quad [\text{volts}]$$
$$V_w = (3.0)(0.057), \quad [\text{volts}]$$
$$V_w = 0.171, \quad [\text{volts}]$$

Step 4: Calculate the winding dissipation, P_w:

$$P_w = I^2R, \quad [\text{watts}]$$
$$P_w = (3)^2(0.057), \quad [\text{watts}]$$
$$P_w = 0.513, \quad [\text{watts}]$$

PC Winding Capacitance

The PC winding board trace will have capacitance, to the other side of the board, as shown in Figure 20-18. This capacitance could be to another winding, or to a Faraday shield to ground.

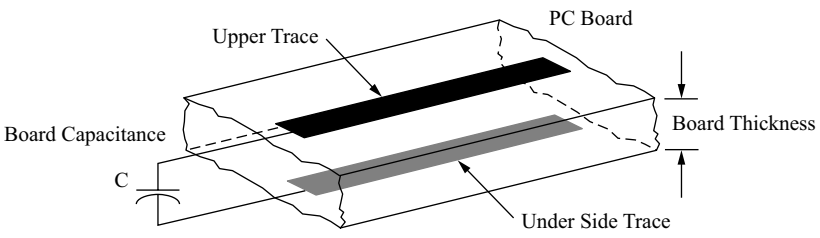

Figure 20-18. PC Board Trace Capacitance.

The formula for calculating the winding trace capacitance, to either another winding trace or ground plane, is given in Equation 20.7.

© 2011 by Taylor and Francis Group, LLC

$$C_p = \frac{0.0085KA}{d}, \quad [\text{pf}] \qquad [20.7]$$

Where:

C_p = capacitance, [pf]
K = dielectric constant
A = area of the trace, [mm^2]
d = thickness of the PC board, [mm]

A typical square wave power converter, operating at 250kHz, will have extremely fast rise and fall times in the order of 0.05 micro-seconds. This fast excursion will generate a fairly high current pulse depending on the capacitance and source impedance.

The calculation of the winding capacitance is as follows:

Use the PC board winding data in Table 20-5, the outline drawing in Figure 20-19, and Equation 20-7:

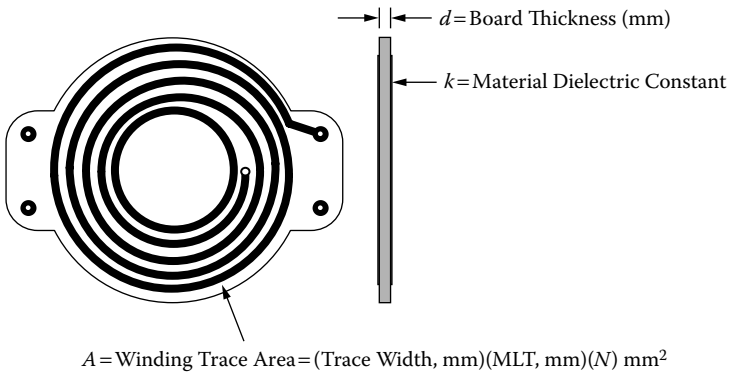

Figure 20-19. PC Board Winding Capacitance.

Step 1: Calculate the winding trace area, A.

$$A = (\text{trace width, mm})(\text{MLT, mm})(\text{turns, N}), \quad [\text{mm}^2]$$
$$A = (2.54)(72.5)(8), \quad [\text{mm}^2]$$
$$A = 1473, \quad [\text{mm}^2]$$

Step 2: Calculate the winding capacitance, C_p.

$$C_p = \frac{0.0085KA}{d}, \quad [\text{pf}]$$
$$C_p = \frac{0.0085(4.7)(1473)}{(0.50)}, \quad [\text{pf}]$$
$$C_p = 118, \quad [\text{pf}]$$

© 2011 by Taylor and Francis Group, LLC

Planar Inductor Design

Planar inductors are designed the same way as the conventional inductors. See Chapter 8. Planar inductors use the same planar cores and PC winding board techniques as the transformers. The main difference is the inductor will have a gap to prevent the dc current from prematurely saturating the core. It is normal to operate planar magnetics at a little higher temperature than conventional designs. It is important to check the maximum operating flux level at maximum operating temperature.

Fringing flux can be severe in any gapped ferrite inductor, but, even more so, on planar construction, because of the printed winding board, as shown in Figure 20-20. When the flux intersects the copper winding, eddy currents are generated, which produces hot spots and reduces the overall efficiency. The use of a PC winding board, (flat traces), can give the eddy currents an added degree of freedom. The resulting loss could be a disaster.

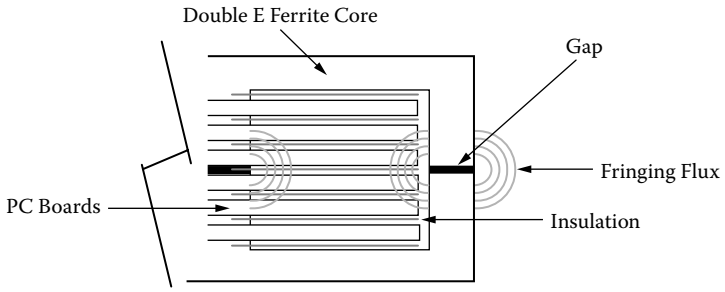

Figure 20-20. Fringing Flux Cutting Across PC Winding Boards.

Winding Termination

Making connections from a planar transformer to the outside world could be very clumsy, if not enough thought is put in for termination. It has to be remembered that this is a high frequency transformer, and skin effect, (ac resistance), has to be addressed. Because of the skin effect it is important the external leads of the planar transformer must be kept as short as possible. Terminations are very important for currents of one amp and above. A poor connection will only get worse. It is recommended to use plated-through holes and eyelets, where possible, but cost will control that. If the transformer has many interconnections, or only a few, there must be provisions made for those connections. When the PC winding boards are stacked, and because of the high density, all connections and interconnections have to be done with extended area pads, as shown in Figure 20-21. The PC winding boards require good artwork registry to make sure the interconnections can be made between boards. Interconnections are usually done, by passing a bus wire through a hole, and at the same time making the connection on the other board. If the solder terminations are to be made on the board, then it is important to leave as much room as possible especially if the connection is to be made with copper foil, as shown in Figure 20-22. When the PC windings have to be paralleled, because of the increased current, the interconnecting jumpers will also have to be increased.

© 2011 by Taylor and Francis Group, LLC

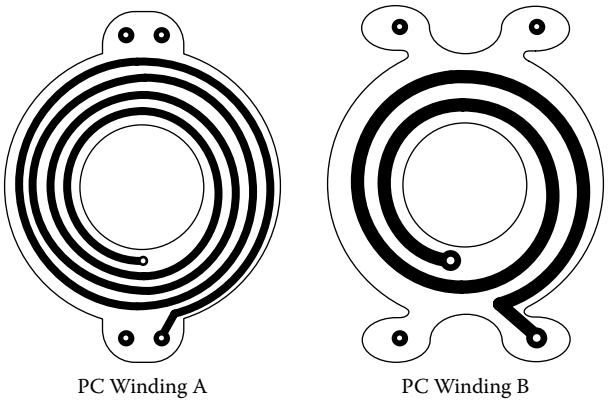

Figure 20-21. PC Winding Boards Showing Butterfly Pads.

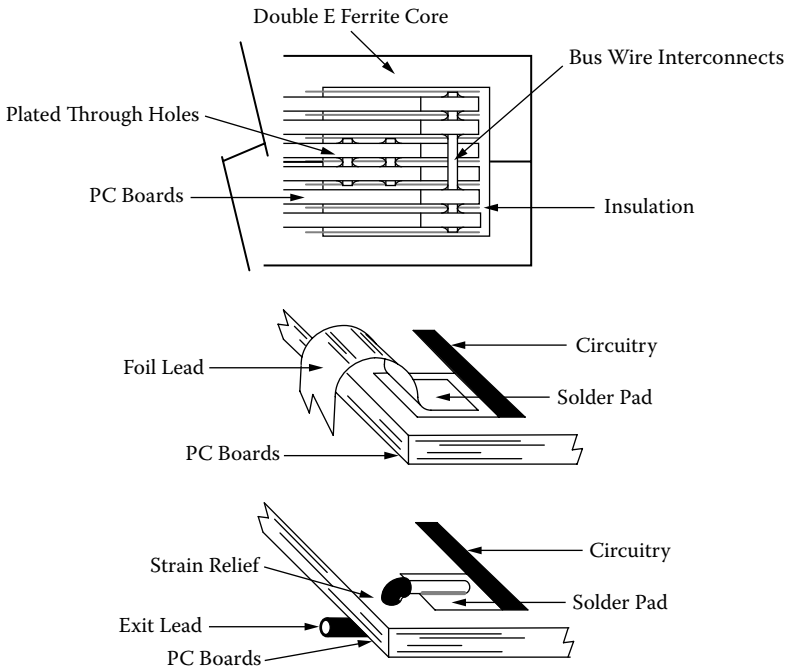

Figure 20-22. PC Winding Boards, Showing Interconnections and Exit Leads.

PC Board Base Materials

PC Board materials are available in various grades, as defined by the National Electrical Manufacturers Association (NEMA). The important properties for PC Board materials are tabulated in Table 20-6. It is very important to choose the correct PC board material for your application. Planar transformers are normally stressed to the last watt for a given temperature rise. This could give rise to hot spots at winding terminations and cause PC Board discoloration. Due to their inherit design Planar transformers will have a wide temperature delta, Δt. It would be wise to stay away from paper/phenolic materials and materials that absorb moisture.

© 2011 by Taylor and Francis Group, LLC

Table 20-6. Properties of Typical Printer Circuit Board Materials

Properties of Typical Printed Circuit Board Materials							
Material/Comments	NEMA Grade						
	FR-1 Paper Phenolic	FR-2 Paper Phenolic	FR-3 Paper Epoxy	FR-4 Glass/ Cloth Epoxy	FR-5 Glass/ Cloth Epoxy	G10 Glass/ Cloth Epoxy	G11 Glass/ Cloth Epoxy
Mechanical Strength	good	good	good	excellent	excellent	excellent	excellent
Moisture Resistant	poor	good	good	excellent	excellent	excellent	excellent
Insulation	fair	good	good	excellent	excellent	excellent	excellent
Arc Resistance	poor	poor	fair	good	good	good	good
Tool Abrasion	good	good	good	poor	poor	poor	poor
Max. Cont. Temp. °C	105	105	105	130	170	130	170
Dielectric Constant, K	4.2	4.2	4.4	4.7	4.3	4.6	4.5

Core Mounting and Assembly

Core assembly and mounting should be strong and stable with temperature. One of the most viable methods for securing core halves together is epoxy adhesive. There is one epoxy adhesive that has been around a long time and that's 3M EC-2216A/B. This bonding technique is shown in Figure 20-23, and it seems to work quite well. When the core halves are properly bonded with epoxy adhesive, there will be little or no effect on the electrical performance. This means the epoxy adhesive added little or no gap to the mating surface. Large temperature excursions are normal in planar magnetics. Care should be taken into account for the coefficients of thermal expansion between the core and mounting surfaces. It has to be remembered ferrite is a ceramic and is very brittle. Planar cores have a low silhouette with thin sections that cannot absorb as much strain as other geometries. After the planar transformer has been assembled, there should be a small amount of play in the PC winding assembly to guarantee there will be a minimum of stress over temperature.

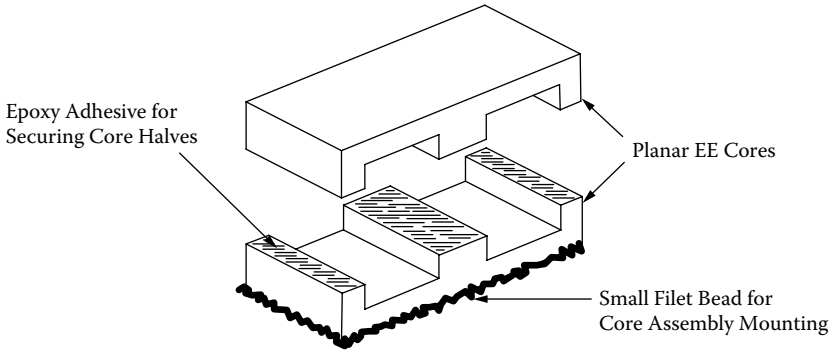

Figure 20-23. Epoxy Adhesive for Securing Transformer Assembly.

© 2011 by Taylor and Francis Group, LLC

References

1. Designing with Planar Ferrite Cores, Technical Bulletin FC-S8, Magnetics, Division of Spang and Company, 2001.

2. Brown, E., "Planar Magnetics Simplifies Switchmode Power Supply Design and Production," *PCIM*, June, 1992, p. 46.2.

3. Van der Linde, Boon, and Klassens, "Design of High-Frequency Planar Power Transformer in Multilayer Technology," *IEEE Transaction on Industrial Electronics*, Vol. 38, No. 2, April, 1991, pp. 135–141.

4. Bloom, E., "Planar Power Magnetics: New Low Profile Approaches for Low-Cost Magnetics Design," *Magnetic Business & Technology*, June, 2002, pp. 26, 27.

5. Charles A. Harper, *Handbook of Electronic Packaging*, McGraw-Hill Book Company, 1998, pp. 1.51–1.53.

6. *Reference Data for Radio Engineers*, Fourth Edition, International Telephone and Telegraph Corp. March, 1957, pp. 107–111.

7. PC Boards, Casco Circuits, Inc., 10039 D Canoga Ave., Chatsworth, CA 91311.

© 2011 by Taylor and Francis Group, LLC

Chapter 21

Derivations for the Design Equations

© 2011 by Taylor and Francis Group, LLC

Table of Contents

1. Output Power, P_o, Versus Apparent Power, P_t, Capability 21-3
2. Transformer Derivation for the Core Geometry, K_g 21-4
3. Transformer Derivation for the Area Product, A_p 21-7
4. Inductor Derivation for the Core Geometry, K_g 21-9
5. Inductor Derivation for the Area Product, A_p 21-12
6. Transformer Regulation 21-15
7. Recognition 21-17

© 2011 by Taylor and Francis Group, LLC

Output Power, P_o Versus Apparent Power, P_t Capability

Introduction

Output power, P_o, is of the greatest interest to the user. To the transformer designer, the apparent power, P_t, which is associated with the geometry of the transformer, is of greater importance. Assume, for the sake of simplicity, that the core of an isolation transformer has only two windings in the window area, a primary and a secondary. Also, assume that the window area, W_a, is divided up in proportion to the power-handling capability of the windings, using equal current density. The primary winding handles, P_{in}, and the secondary handles, P_o, to the load. Since the power transformer has to be designed to accommodate the primary, P_{in}, and, P_o, then,

By definition:

$$P_t = P_{in} + P_o, \quad \text{[watts]}$$
$$P_{in} = \frac{P_o}{\eta}, \quad \text{[watts]} \qquad \text{[21-A1]}$$

The primary turns can be expressed using Faraday's Law:

$$N_p = \frac{V_p\left(10^4\right)}{A_c B_{ac} f K_f}, \quad \text{[turns]} \qquad \text{[21-A2]}$$

The winding area of a transformer is fully utilized when:

$$K_u W_a = N_p A_{wp} + N_s A_{ws} \qquad \text{[21-A3]}$$

By definition the wire area is:

$$A_w = \frac{I}{J}, \quad [\text{cm}^2] \qquad \text{[21-A4]}$$

Rearranging the Equation shows:

$$K_u W_a = N_p\left(\frac{I_p}{J}\right) + N_s\left(\frac{I_s}{J}\right) \qquad \text{[21-A5]}$$

Now, substitute in Faraday's Equation:

$$K_u W_a = \frac{V_p\left(10^4\right)}{A_c B_{ac} f K_f}\left(\frac{I_p}{J}\right) + \frac{V_s\left(10^4\right)}{A_c B_{ac} f K_f}\left(\frac{I_s}{J}\right) \qquad \text{[21-A6]}$$

© 2011 by Taylor and Francis Group, LLC

Rearranging shows:

$$W_a A_c = \frac{\left[\left(V_p I_p\right)+\left(V_s I_s\right)\right]\left(10^4\right)}{B_{ac} f J K_f K_u}, \quad [\text{cm}^4] \qquad [21\text{-A7}]$$

The output power, P_o, is:

$$P_o = V_s I_s, \quad [\text{watts}] \qquad [21\text{-A8}]$$

The input power, P_{in}, is:

$$P_{in} = V_p I_p, \quad [\text{watts}] \qquad [21\text{-A9}]$$

Then:

$$P_t = P_{in} + P_o, \quad [\text{watts}] \qquad [21\text{-A10}]$$

Transformer Derivation for the Core Geometry, K_g

Introduction

Although most transformers are designed for a given temperature rise, they can also be designed for a given regulation. The regulation and power-handling ability of a core are related to two constants, K_g and K_e by the equation:

$$P_t = 2K_g K_e \alpha, \quad [\text{watts}] \qquad [21\text{-B1}]$$

Where:

$$\alpha = \text{Regulation}, \quad [\%]$$

The constant, K_g, is a function of the core geometry:

$$K_g = f\left(A_c, W_a, \text{MLT}\right) \qquad [21\text{-B2}]$$

The constant, K_e, is a function of the magnetic and electrical operating conditions:

$$K_e = g\left(f, B_m\right) \qquad [21\text{-B3}]$$

The derivation of the specific functions for, K_g and K_e, is as follows: First, assume there is a two-winding transformer with equal primary and secondary regulation, as schematically shown in Figure 21-B1. The primary winding has a resistance of, R_p, ohms, and the secondary winding has a resistance of, R_s ohms:

© 2011 by Taylor and Francis Group, LLC

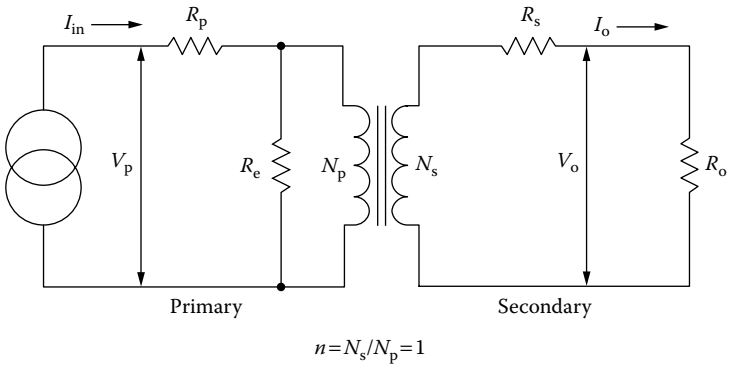

Figure 21-B1. Isolation Transformer.

$$\alpha = \frac{\Delta V_p}{V_p}(100) + \frac{\Delta V_s}{V_s}(100) \quad [21\text{-B4}]$$

The assumption, for simplicity, is that R_e is infinity (no core loss).

And:

$$I_{in} = I_o \quad [21\text{-B5}]$$

Then:

$$\Delta V_p = I_p R_p = \Delta V_s = I_s R_s, \quad \text{[volts]} \quad [21\text{-B6}]$$

$$\alpha = 2\frac{I_p R_p}{V_p}(100) \quad [21\text{-B7}]$$

Multiply the numerator and denominator by V_p:

$$\alpha = 200\frac{I_p R_p}{V_p}\left(\frac{V_p}{V_p}\right) \quad [21\text{-B8}]$$

$$\alpha = 200\frac{R_p VA}{V_p^2} \quad [21\text{-B9}]$$

From the resistivity formula, it is easily shown that:

$$R_p = \frac{(\text{MLT})N_p^2}{W_a K_p}\rho \quad [21\text{-B10}]$$

Where:

$\rho = 1.724\ (10^{-6})$ ohm cm

K_p is the window utilization factor (primary)

K_s is the window utilization factor (secondary)

© 2011 by Taylor and Francis Group, LLC

$$K_p = \frac{K_u}{2} = K_s \qquad [21\text{-B11}]$$

Faraday's Law expressed in metric units is:

$$V_p = K_f f N_p A_c B_m \left(10^{-4}\right) \qquad [21\text{-B12}]$$

Where:

$K_f = 4.0$ for a square wave.

$K_f = 4.44$ for a sine wave.

Substituting Equation 21-B10 and 21-B12, for R_p and V_p, in Equation [21-B13]:

$$VA = \frac{E_p^2}{200 R_p}\alpha \qquad [21\text{-B13}]$$

The primary VA is:

$$VA = \frac{\left(K_f f N_p A_c B_m \left(10^{-4}\right)\right)\left(K_f f N_p A_c B_m \left(10^{-4}\right)\right)}{200\left(\frac{(\mathrm{MLT}) N_p^2}{W_a K_p}\rho\right)}\alpha \qquad [21\text{-B14}]$$

Simplify:

$$VA = \frac{K_f^2 f^2 A_c^2 B_m^2 W_a K_p \left(10^{-10}\right)}{2(\mathrm{MLT})\rho}\alpha \qquad [21\text{-B15}]$$

Inserting $1.724(10^{-6})$ for ρ:

$$VA = \frac{0.29 K_f^2 f^2 A_c^2 B_m^2 W_a K_p \left(10^{-4}\right)}{\mathrm{MLT}}\alpha \qquad [21\text{-B16}]$$

Let the primary electrical equal:

$$K_e = 0.29 K_f^2 f^2 B_m^2 \left(10^{-4}\right) \qquad [21\text{-B17}]$$

Let the primary core geometry equal:

$$K_g = \frac{W_a A_c^2 K_p}{\mathrm{MLT}}, \quad [\mathrm{cm}^5] \qquad [21\text{-B18}]$$

The total transformer window utilization factor is:

$$K_p + K_s = K_u$$

$$K_p = \frac{K_u}{2} = K_s \qquad [21\text{-B19}]$$

© 2011 by Taylor and Francis Group, LLC

When this value for, K_p, is put into Equation [21-B16], then:

$$VA = K_e K_g \alpha \qquad [21\text{-B20}]$$

Where:

$$K_e = 0.145 K_f^2 f^2 B_m^2 \left(10^{-4}\right) \qquad [21\text{-B21}]$$

The above VA is the primary power, and the window utilization factor, K_u, includes both the primary and secondary coils.

$$K_g = \frac{W_a A_c^2 K_u}{\text{MLT}}, \quad [\text{cm}^5] \qquad [21\text{-B22}]$$

Regulation of a transformer is related to the copper loss, as shown in Equation [21-B23]:

$$\alpha = \frac{P_{cu}}{P_o}(100), \quad [\%] \qquad [21\text{-B23}]$$

The total VA of the transformer is primary plus secondary:

$$\begin{aligned} &\text{Primary, } VA = K_e K_g \alpha \\ &\text{plus} \\ &\text{Secondary, } VA = K_e K_g \alpha \end{aligned} \qquad [21\text{-B24}]$$

The apparent power, P_t, then is:

$$\begin{aligned} P_t &= (\text{Primary}) K_e K_g \alpha + (\text{Secondary}) K_e K_g \alpha \\ P_t &= 2 K_e K_g \alpha \end{aligned} \qquad [21\text{-B25}]$$

Transformer Derivation for the Area Product, A_p

Introduction

The relationship between the power-handling capability of a transformer and the area product, A_p, can be derived as follows:

Faraday's Law expressed in metric units is:

$$V = K_f f N_p A_c B_m \left(10^{-4}\right) \qquad [21\text{-C1}]$$

Where:

$K_f = 4.0$ for a square wave.

$K_f = 4.44$ for a sine wave.

© 2011 by Taylor and Francis Group, LLC

The winding area of a transformer is fully utilized when:

$$K_u W_a = N_p A_{wp} + N_s A_{ws} \quad [21\text{-C2}]$$

By definition the wire area is:

$$A_w = \frac{I}{J}, \quad [\text{cm}^2] \quad [21\text{-C3}]$$

Rearranging the equation shows:

$$K_u W_a = N_p \left(\frac{I_p}{J} \right) + N_s \left(\frac{I_s}{J} \right) \quad [21\text{-C4}]$$

Now, substitute in Faraday's Equation:

$$K_u W_a = \frac{V_p \left(10^4\right)}{A_c B_{ac} f K_f} \left(\frac{I_p}{J} \right) + \frac{V_s \left(10^4\right)}{A_c B_{ac} f K_f} \left(\frac{I_s}{J} \right) \quad [21\text{-C5}]$$

Rearranging shows:

$$W_a A_c = \frac{\left[\left(V_p I_p\right) + \left(V_s I_s\right) \right] \left(10^4\right)}{B_{ac} f J K_f K_u}, \quad [\text{cm}^4] \quad [21\text{-C6}]$$

The output power, P_o, is:

$$P_o = V_s I_s, \quad [\text{watts}] \quad [21\text{-C7}]$$

The input power, P_{in}, is:

$$P_{in} = V_p I_p, \quad [\text{watts}] \quad [21\text{-C8}]$$

Then:

$$P_t = P_{in} + P_o, \quad [\text{watts}] \quad [21\text{-C9}]$$

Therefore:

$$W_a A_c = \frac{P_t \left(10^4\right)}{B_{ac} f J K_f K_u}, \quad [\text{cm}^4] \quad [21\text{-C10}]$$

By definition:

$$A_p = W_a A_c \quad [21\text{-C11}]$$

© 2011 by Taylor and Francis Group, LLC

Then:

$$A_p = \frac{P_t\left(10^4\right)}{B_{ac} f J K_f K_u}, \quad [\text{cm}^4] \qquad [21\text{-C12}]$$

Inductor Derivation for the Core Geometry, K_g

Introduction

Inductors, like transformers, are designed for a given temperature rise. They can also be designed for a given regulation. The regulation and energy-handling ability of a core are related to two constants, K_g and K_e, by the equation:

$$\left(\text{Energy}\right)^2 = K_g K_e \alpha, \qquad [21\text{-D1}]$$

Where:

$$\alpha = \text{Regulation}, \quad [\%]$$

The constant, K_g, is a function of the core geometry:

$$K_g = f\left(A_c, W_a, \text{MLT}\right) \qquad [21\text{-D2}]$$

The constant, K_e, is a function of the magnetic and electrical operating conditions:

$$K_e = g\left(P_o, B_m\right) \qquad [21\text{-D3}]$$

The derivation of the specific functions for, K_g and K_e, is as follows: First, assume a dc inductor could be an input or output, as schematically shown in Figure 21-D1. The inductor resistance is R_L.

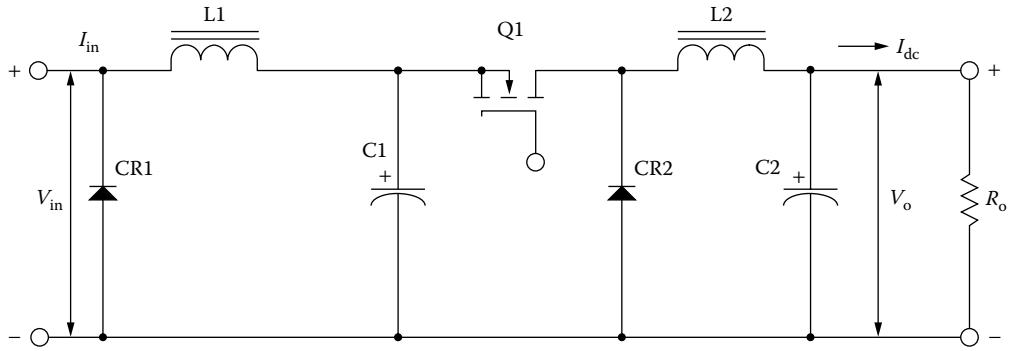

Figure 21-D1. Typical Buck Type Switching Converter.

© 2011 by Taylor and Francis Group, LLC

The output power is:

$$P_o = I_{dc} V_o, \quad \text{[watts]} \tag{21-D4}$$

$$\alpha = \frac{I_{dc} R_L}{V_o}(100), \quad [\%] \tag{21-D5}$$

The inductance equation is:

$$L = \frac{0.4\pi N^2 A_c \left(10^{-8}\right)}{l_g}, \quad \text{[henrys]} \tag{21-D6}$$

The inductor flux density is:

$$B_{dc} = \frac{0.4\pi N I_{dc} \left(10^{-4}\right)}{l_g}, \quad \text{[teslas]} \tag{21-D7}$$

Combine Equations [21-D6] and [21-D7]:

$$\frac{L}{B_{dc}} = \frac{N A_c \left(10^{-4}\right)}{I_{dc}} \tag{21-D8}$$

Solve for N:

$$N = \frac{L I_{dc} \left(10^{4}\right)}{B_{dc} A_c}, \quad \text{[turns]} \tag{21-D9}$$

From the resistivity formula, it is easily shown that:

$$R_L = \frac{(\text{MLT}) N_p^2}{W_a K_u} \rho, \quad \text{[ohms]} \tag{21-D10}$$

Where:

$\rho = 1.724\ (10^{-6})$ ohm cm

Combining Equations [21-D5] and [21-D10]:

$$\alpha = \left(\frac{I_{dc}}{V_o}\right)\left(\frac{(\text{MLT}) N_p^2}{W_a K_u} \rho\right)(100), \quad [\%] \tag{21-D11}$$

Take Equation [21-D9] and square it:

$$N^2 = \left(\frac{L I_{dc}}{B_{dc} A_c}\right)^2 \left(10^8\right) \tag{21-D12}$$

© 2011 by Taylor and Francis Group, LLC

Combine Equations [21-D11] and [21-D12]:

$$\alpha = \left(\frac{I_{dc}\,(\mathrm{MLT})}{V_o W_a K_u} \rho \right) \left(\frac{L I_{dc}}{B_{dc} A_c} \right)^2 \left(10^{10} \right) \qquad \text{[21-D13]}$$

Combine and simplify:

$$\alpha = \left(\frac{I_{dc}\,(\mathrm{MLT}) \left(L I_{dc} \right)^2}{V_o W_a K_u B_{dc}^2 A_c^2} \rho \right) \left(10^{10} \right) \qquad \text{[21-D14]}$$

Multiply the Equation by I_{dc} / I_{dc} and combine:

$$\alpha = \left(\frac{(\mathrm{MLT}) \left(L I_{dc}^2 \right)^2}{V_o I_{dc} W_a K_u B_{dc}^2 A_c^2} \rho \right) \left(10^{10} \right) \qquad \text{[21-D15]}$$

The energy equation is:

$$\mathrm{Energy} = \frac{L I_{dc}^2}{2}, \quad \text{[watt-seconds]} \qquad \text{[21-D16]}$$

$$2\mathrm{Energy} = L I_{dc}^2$$

Combine and simplify:

$$\alpha = \left(\frac{\left(2\mathrm{Energy} \right)^2}{P_o B_{dc}^2} \right) \left(\frac{\rho (\mathrm{MLT})}{W_a K_u A_c^2} \right) \left(10^{10} \right) \qquad \text{[21-D17]}$$

The resistivity is:

$$\rho = 1.724\,(10^{-6})\,[\mathrm{ohm\,cm}] \qquad \text{[21-D18]}$$

Combine the resistivity:

$$\alpha = \left(\frac{6.89 \left(\mathrm{Energy} \right)^2}{P_o B_{dc}^2} \right) \left(\frac{(\mathrm{MLT})}{W_a K_u A_c^2} \right) \left(10^4 \right) \qquad \text{[21-D19]}$$

Solving for energy:

$$\left(\mathrm{Energy} \right)^2 = 0.145 P_o B_{dc}^2 \left(\frac{W_a A_c^2 K_u}{\mathrm{MLT}} \right) \left(10^{-4} \right) \alpha \qquad \text{[21-D20]}$$

The core geometry equals:

$$K_g = \frac{W_a A_c^2 K_u}{\mathrm{MLT}}, \quad [\mathrm{cm}^5] \qquad \text{[21-D21]}$$

© 2011 by Taylor and Francis Group, LLC

The electrical conditions:

$$K_e = 0.145 P_o B_{dc}^2 \left(10^{-4}\right) \quad \text{[21-D22]}$$

The regulation and energy-handling ability is:

$$\left(\text{Energy}\right)^2 = K_g K_e \alpha \quad \text{[21-D23]}$$

The copper loss is:

$$\alpha = \frac{P_{cu}}{P_o}(100), \quad [\%] \quad \text{[21-D24]}$$

Inductor Derivation for the Area Product, A_p

Introduction

The area product, A_p, can determine the energy-handling capability of an inductor. The area product, A_p, relationship is obtained by the following: (Note that symbols marked with a prime, such as H′, are mks (meter-kilogram-second) units.)

$$E = L\frac{dI}{dt} = N\frac{d\phi}{dt} \quad \text{[21-E1]}$$

Combine and simplify:

$$L = N\frac{d\phi}{dI} \quad \text{[21-E2]}$$

Flux density is:

$$\phi = B_m A_c' \quad \text{[21-E3]}$$

$$B_m = \frac{\mu_o NI}{l_g' + \left(\frac{\text{MPL}'}{\mu_\text{m}}\right)} \quad \text{[21-E4]}$$

$$\phi = \frac{\mu_o NI\, A_c'}{l_g' + \left(\frac{\text{MPL}'}{\mu_\text{m}}\right)} \quad \text{[21-E5]}$$

© 2011 by Taylor and Francis Group, LLC

$$\frac{d\phi}{dI} = \frac{\mu_o N A_c'}{l_g' + \left(\frac{\text{MPL}'}{\mu_m}\right)} \quad [21\text{-E6}]$$

Combine Equations [21-E2] and [21-E6]:

$$L = N\frac{d\phi}{dI} = \frac{\mu_o N^2 A_c'}{l_g' + \left(\frac{\text{MPL}'}{\mu_m}\right)} \quad [21\text{-E7}]$$

The Energy Equation is:

$$\text{Energy} = \frac{LI^2}{2}, \quad \text{[watt-seconds]} \quad [21\text{-E8}]$$

Combine Equations [21-E7] and [21-E8]:

$$\text{Energy} = \frac{LI^2}{2} = \frac{\mu_o N^2 A_c' I^2}{2\left(l_g' + \left(\frac{\text{MPL}'}{\mu_m}\right)\right)} \quad [21\text{-E9}]$$

If B_m is specified:

$$I = \frac{B_m\left(l_g' + \left(\frac{\text{MPL}'}{\mu_m}\right)\right)}{\mu_o N} \quad [21\text{-E10}]$$

Combine Equations [21-E7] and [21-E10]:

$$\text{Energy} = \frac{\mu_o N^2 A_c'}{2\left(l_g' + \left(\frac{\text{MPL}'}{\mu_m}\right)\right)}\left(\frac{B_m\left(l_g' + \left(\frac{\text{MPL}'}{\mu_m}\right)\right)}{\mu_o N}\right)^2 \quad [21\text{-E11}]$$

Combine and simplify:

$$Energy = \frac{B_m^2\left(l_g' + \left(\frac{\text{MPL}'}{\mu_m}\right)\right)A_c'}{2\mu_o} \quad [21\text{-E12}]$$

The winding area of a inductor is fully utilized when:

$$K_u W_a' = N A_w' \quad [21\text{-E13}]$$

© 2011 by Taylor and Francis Group, LLC

By definition the wire area is:

$$A'_w = \frac{I}{J'} \qquad \text{[21-E14]}$$

Combining Equations [21-E13] and [21-E14]:

$$K_u W'_a = N\left(\frac{I}{J'}\right) \qquad \text{[21-E15]}$$

Solving for I:

$$I = \frac{K_u W_a J}{N} = \frac{B_m\left(l'_g + \left(\frac{\text{MPL}'}{\mu_\text{m}}\right)\right)}{\mu_\text{o} N} \qquad \text{[21-E16]}$$

Rearrange Equation [21-E16]:

$$l'_g + \left(\frac{\text{MPL}'}{\mu_\text{m}}\right) = \frac{K_u W'_a J' \mu_o}{B_m} \qquad \text{[21-E17]}$$

Now, substitute in Energy Equation [21-E11]:

$$\text{Energy} = \frac{B_m^2\left(\frac{K_u W'_a J'\mu_o}{B_m}\right)A'_c}{2\mu_o} \qquad \text{[21-E18]}$$

Rearrange Equation [21-E18]:

$$\text{Energy} = \left(\frac{B_m^2 A'_c}{2\mu_o}\right)\left(\frac{K_u W'_a J' \mu_o}{B_m}\right) \qquad \text{[21-E19]}$$

Combine and simplify:

$$\text{Energy} = \left(\frac{B_m K_u W'_a J' A'_c}{2}\right) \qquad \text{[21-E20]}$$

Now, multiply mks units to return cgs.

$$W'_a = W_a\left(10^{-4}\right)$$

$$A'_c = A_c\left(10^{-4}\right)$$

$$J' = J\left(10^{4}\right)$$

$$\text{MPL}' = \text{MPL}\left(10^{-2}\right)$$

$$l'_g = l_g\left(10^{-2}\right)$$

© 2011 by Taylor and Francis Group, LLC

We can substitute into the energy equation to obtain:

$$\text{Energy} = \frac{B_m K_u W_a J A_c}{2}\left(10^{-4}\right) \qquad [21\text{-E21}]$$

Solve for the area product:

$$A_p = W_a A_c$$
$$A_p = \frac{2(\text{Energy})}{B_m J K_u}, \quad [\text{cm}^4] \qquad [21\text{-E22}]$$

Transformer Regulation

The minimum size of a transformer is usually determined either by a temperature rise limit, or by allowable voltage regulation, assuming that size and weight are to be minimized. Figure 21-F1 shows a circuit diagram of a transformer with one secondary.

Note that α = regulation (%).

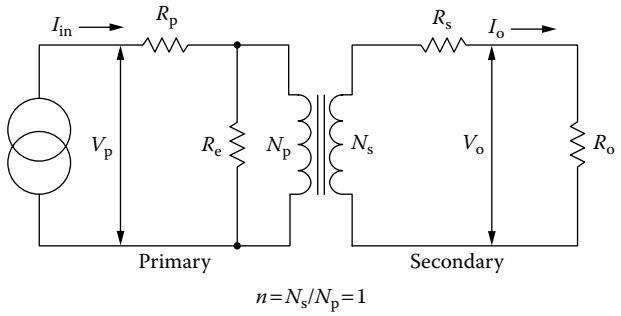

Figure 21-F1. Transformer Circuit Diagram.

The assumption is that distributed capacitance in the secondary can be neglected because the frequency and secondary voltage are not excessively high. Also, the winding geometry is designed to limit the leakage inductance to a level low enough to be neglected under most operating conditions. The transformer window allocation is shown in Figure 21-F2.

$$\frac{W_a}{2} = \text{Primary} = \text{Secondary} \qquad [21\text{-F1}]$$

© 2011 by Taylor and Francis Group, LLC

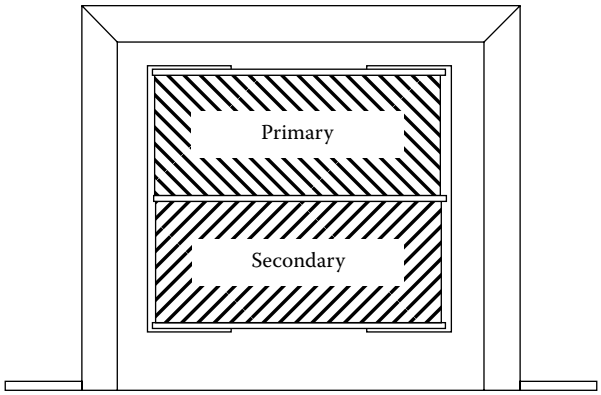

Figure 21-F2. Transformer Window Allocation.

Transformer voltage regulation can now be expressed as:

$$\alpha = \frac{V_o\,(\text{N.L.}) - V_o(\text{F.L.})}{V_o\,(\text{F.L.})}(100), \quad [\%] \qquad [21\text{-F2}]$$

In which, V_o(N.L.) is the no load voltage, and V_o(F.L.) is the full load voltage. For the sake of simplicity, assume the transformer in Figure 21-F1 is an isolation transformer, with a 1:1 turns ratio, and the core impedance, R_e, is infinite.

If the transformer has a 1:1 turns ratio and the core impedance is infinite, then:

$$I_{in} = I_o, \quad [\text{amps}]$$

$$R_p = R_s, \quad [\text{ohms}] \qquad [21\text{-F3}]$$

With equal window areas allocated for the primary and secondary windings, and using the same current density, J:

$$\Delta V_p = I_{in} R_p = \Delta V_s = I_o R_s, \quad [\text{volts}] \qquad [21\text{-F4}]$$

Regulation is then:

$$\alpha = \frac{\Delta V_p}{V_p}(100) + \frac{\Delta V_s}{V_s}(100), \quad [\%] \qquad [21\text{-F5}]$$

Multiply the Equation by currents, I_{in}/I_{in}:

$$\alpha = \frac{\Delta V_p I_{in}}{V_p I_{in}}(100) + \frac{\Delta V_s I_o}{V_s I_o}(100), \quad [\%] \qquad [21\text{-F6}]$$

© 2011 by Taylor and Francis Group, LLC

Primary copper loss is:

$$P_p = \Delta V_p I_{in}, \quad \text{[watts]} \qquad \text{[21-F7]}$$

Secondary copper loss is:

$$P_s = \Delta V_s I_o, \quad \text{[watts]} \qquad \text{[21-F8]}$$

Total copper loss is:

$$P_{cu} = P_p + P_s, \quad \text{[watts]} \qquad \text{[21-F9]}$$

Then, the Regulation Equation can be rewritten to:

$$\alpha = \frac{P_{cu}}{P_o}(100), \quad [\%] \qquad \text{[21-F10]}$$

Recognition

The author would like to thank **Richard Ozenbaugh** of Linear Magnetics for his help with the derivations.

© 2011 by Taylor and Francis Group, LLC

Chapter 22

Autotransformer Design

© 2011 by Taylor and Francis Group, LLC

Table of Contents

1. Introduction....22-3
2. The Voltage and Current Relationship of an Autotransformer....22-3
3. Autotransformer Step-up or Boost....22-5
4. Autotransformer Step-down or Buck....22-6
5. 250 Watt Step-up Autotransformer Design, (Using the Core Geometry, K_g, Approach)....22-8
6. Confirming the Window Utilization....22-13
7. 250 Watt Step-up Autotransformer Design Test Data (Using the Core Geometry, K_g, Approach)....22-14
8. Comparing the Step-up Autotransformer Design With Isolation Transformer....22-14
9. 250-Watt Step-down Autotransformer Design (Using the Core Geometry, K_g, Approach)....22-15
10. Confirming the Window Utilization....22-21
11. 250 Watt Step-down Autotransformer Design Test Data (Using the Core Geometry, K_g, Approach)....22-21
12. Comparing the Autotransformer Design With a Standard Isolation Transformer....22-22
13. Engineering Note....22-23
14. Recognition....22-23
15. References....22-23

© 2011 by Taylor and Francis Group, LLC

Introduction

The autotransformer is a unique and special transformer. The autotransformer can provide a step-up voltage or a step-down voltage with respect to the input with good regulation. The biggest advantage of an autotransformer is the reduction in size, weight, and cost compared with an equivalent isolation transformer shown in Figure 22-1, as long as the designed secondary voltage is within limits of the primary voltage. What makes the autotransformer undesirable is that it does not provide isolation between the primary and secondary, as shown in Figure 22-2. A big application for the autotransformer is to boost the line voltage at the end of a long power line, when there is no auxiliary power available.

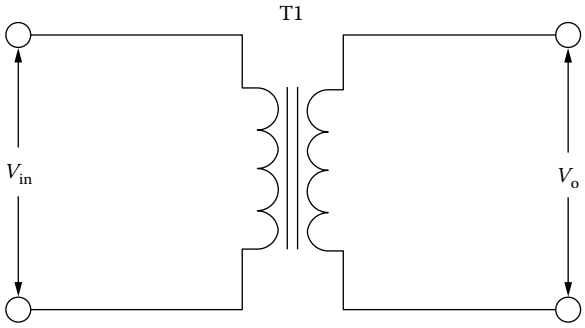

Figure 22-1. Standard Isolation Transformer Schematic.

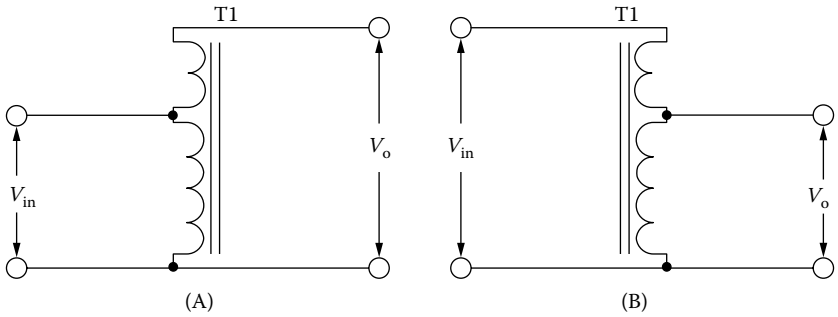

Figure 22-2. (A) is a Step-up and (B) is a Step-down Autotransformer Schematic.

The Voltage and Current Relationship of an Autotransformer

The easiest way to explain the voltage, current and VA rating of an autotransformer is to compare it with a simple two winding isolation transformer shown in Figure 22-3. For this design review the losses will be neglected.

© 2011 by Taylor and Francis Group, LLC

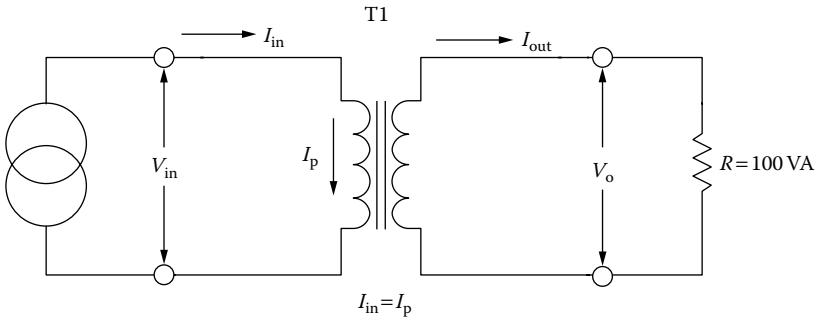

Figure 22-3. Standard Isolation Transformer Schematic.

The output power P_o is of greatest interest to the user. To the transformer designer, the apparent power, P_t, which is associated with the geometry of the transformer, is of greater importance. Assume the core of an isolation transformer has only two windings in the window area, a primary and a secondary, as shown in Figure 22-3. Also assume that the window area, W_a, is divided up in proportion of the power-handling capability of the windings using equal current density. The primary winding handles, P_{in}, and the secondary winding handles, P_o, to the load.

The output power, P_o, is:

$$P_o = V_o I_o, \quad \text{[watts]} \tag{22-1}$$

The input power, P_{in}, is:

$$P_{in} = V_{in} I_{in}, \quad \text{[watts]} \tag{22-2}$$

The apparent power, P_t, is:

$$P_t = P_{in} + P_o, \quad \text{[watts]} \tag{22-3}$$

The apparent power, P_t, for an output, P_o, of 100 watts is:

$$\begin{aligned} P_t &= P_{in} + P_o, \quad \text{[watts]} \\ P_t &= 100 + 100, \quad \text{[watts]} \\ P_t &= 200, \quad \text{[watts]} \end{aligned} \tag{22-4}$$

The apparent power, P_t, is required for calculating both, area product, A_p, in Equation [22-5] and core geometry K_g, in Equation [22-6] when the proper core size is selected, for a design.

The area product, A_p, is:

$$A_p = \frac{P_t(10^4)}{K_u K_f B_m f J}, \quad [\text{cm}^4] \tag{22-5}$$

$$A_p = W_a A_c, \quad [\text{cm}^4]$$

© 2011 by Taylor and Francis Group, LLC

The core geometry, K_g, is:

$$K_g = \frac{P_t}{2K_e\alpha}, \quad [\text{cm}^5]$$
$$K_e = 0.145K_f^2 f^2 B_m^2 (10^{-4})$$
$$K_g = \frac{W_a A_c^2 K_u}{\text{MLT}}, \quad [\text{cm}^5] \qquad [22\text{-}6]$$

The regulation or copper loss, α for an isolation transformer is shown in Equation [22-7].

$$\alpha = \frac{P_{cu}}{P_o}(100), \quad [\%] \qquad [22\text{-}7]$$

Autotransformer Step-up or Boost

The voltage, current and VA rating of a step-up autotransformer is the same as an isolation transformer. The main difference is, the apparent power P_t, calculation and the fact that there is no electrical isolation between primary and secondary. The turns-ratio for primary and secondary is the same as the isolation transformer. The step-up autotransformer schematic is shown in Figure 22-4 and the Design Equations follow.

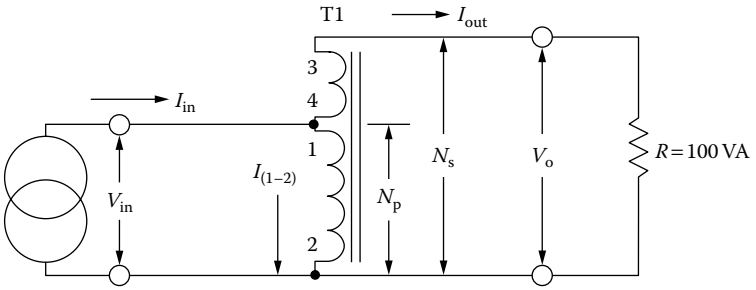

Figure 22-4. A 100 watt Step-up or Boost Autotransformer.

It is assumed for this explanation, that there is not a core loss or copper loss for the autotransformer.

The autotransformer turns ratio is:

$$\frac{N_p}{N_s} = \frac{V_{in}}{V_o}, \quad [\text{volts}] \qquad [22\text{-}8]$$

The output voltage, V_o, is:

$$V_o = \frac{N_s}{N_p} V_{in}, \quad [\text{volts}] \qquad [22\text{-}9]$$

The input output power relationship, P_{in}, is:

$$V_{in} I_{in} = V_o I_o, \quad [\text{VA}] \qquad [22\text{-}10]$$

© 2011 by Taylor and Francis Group, LLC

The autotransformer current, $I_{(1\text{-}2)}$, is:

$$I_{(1-2)} = I_{in} - I_o, \quad \text{[amps]} \tag{22-11}$$

The volt-amp rating for a boost autotransformer, VA, is:

$$V_{in} I_{(1-2)} = \left(V_o - V_{in}\right) I_o, \quad \text{[VA]} \tag{22-12}$$

The autotransformer input power volt-amps, P_{tin}, is:

$$P_{tin} = V_{in} I_{(1-2)} = V_{in}\left(I_{in} - I_o\right), \quad \text{[VA]} \tag{22-13}$$

The autotransformer boost output power volt-amps, P_{AT}, is:

$$P_{AT} = \left(V_o - V_{in}\right) I_o, \quad \text{[VA]} \tag{22-14}$$

The autotransformer apparent power, P_t, is:

$$P_t = V_{in}\left(I_{in} - I_o\right) + \left(V_o - V_{in}\right) I_o, \quad \text{[VA]} \tag{22-15}$$

$$P_t = P_{AT} + P_{tin}, \quad \text{[VA]} \tag{22-16}$$

It can be seen quite easily from Equation [22-14], when the difference between the output voltage V_o, and the input voltage V_{in}, becomes very small the apparent power P_t, also becomes very small.

The core geometry, K_g, is:

$$\begin{aligned} K_g &= \frac{P_t}{2K_e \alpha}, \quad [\text{cm}^5] \\ K_e &= 0.145 K_f^2 f^2 B_m^2 \left(10^{-4}\right) \\ K_g &= \frac{W_a A_c^2 K_u}{\text{MLT}}, \quad [\text{cm}^5] \end{aligned} \tag{22-17}$$

The copper loss ratio, α in percent for an autotransformer is shown in Equation [22-18].

$$\alpha = \frac{P_{cu}}{P_{AT}}(100), \quad [\%] \tag{22-18}$$

Autotransformer Step-down or Buck

The voltage, current and VA rating of a buck autotransformer is the same as an isolation transformer. The main difference is the apparent power, P_t, calculation and there is no electrical isolation between primary and secondary.

© 2011 by Taylor and Francis Group, LLC

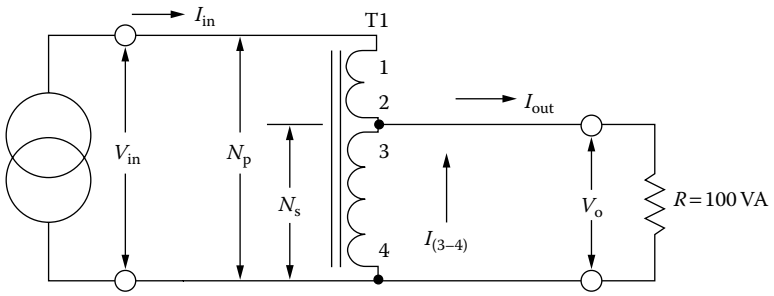

Figure 22-5. A 100 watt Step-down or Buck Autotransformer.

The turns-ratio for primary and secondary is the same as the isolation transformer. The step-down or buck autotransformer schematic is shown in Figure 22-5.

It is assumed for this explanation, that there is not a core loss or copper loss for the autotransformer.

The autotransformer turns ratio is:

$$\frac{N_p}{N_s} = \frac{V_{in}}{V_o}, \quad \text{[volts]} \qquad \text{[22-19]}$$

The output voltage, V_o, is:

$$V_o = \frac{N_s}{N_p} V_{in}, \quad \text{[volts]} \qquad \text{[22-20]}$$

The input output power relationship, P_o, is:

$$V_{in} I_{in} = V_o I_o, \quad \text{[VA]} \qquad \text{[22-21]}$$

The autotransformer winding (3-4) current, $I_{(3-4)}$, is:

$$I_{(3-4)} = I_o - I_{in}, \quad \text{[amps]} \qquad \text{[22-22]}$$

The volt-amp rating for a buck autotransformer, VA, is:

$$V_o I_{(3-4)} = I_{in} \left(V_{in} - V_o \right), \quad \text{[VA]} \qquad \text{[22-23]}$$

The autotransformer buck winding (1-2) volt-amp, P_{AT}, is:

$$P_{AT} = I_{in} \left(V_{in} - V_o \right), \quad \text{[VA]} \qquad \text{[22-24]}$$

© 2011 by Taylor and Francis Group, LLC

The autotransformer winding (3-4) volt-amps, P_{tin}, is:

$$P_{tin} = V_o I_{(3-4)}, \quad [\text{VA}] \tag{22-25}$$

The autotransformer apparent power P_t, is:

$$P_t = (V_{in} - V_o) I_{in} + V_o (I_o - I_{in}), \quad [\text{VA}] \tag{22-26}$$

$$P_t = P_{AT} + P_{tin}, \quad [\text{VA}] \tag{22-27}$$

It can be seen quite easily from Equation [22-24], that when the difference between the output voltage, V_o, and the input voltage, V_{in}, become very small, the apparent power, P_t, also becomes very small.

The core geometry, K_g, is:

$$\begin{aligned} K_g &= \frac{P_t}{2K_e \alpha}, \quad [\text{cm}^5] \\ K_e &= 0.145 K_f^2 f^2 B_m^2 (10^{-4}) \\ K_g &= \frac{W_a A_c^2 K_u}{\text{MLT}}, \quad [\text{cm}^5] \end{aligned} \tag{22-28}$$

The copper loss ratio, α for an autotransformer is shown in Equation [22-29].

$$\alpha = \frac{P_{cu}}{P_{AT}}(100), \quad [\%] \tag{22-29}$$

250 Watt Step-up Autotransformer Design, (Using the Core Geometry, K_g, Approach)

The following information is the Design specification for a 250 watt autotransformer, as shown in Figure 22-6, operating at 60 Hz, using the, K_g, core geometry approach. For a typical design example, assume the design with the following specifications:

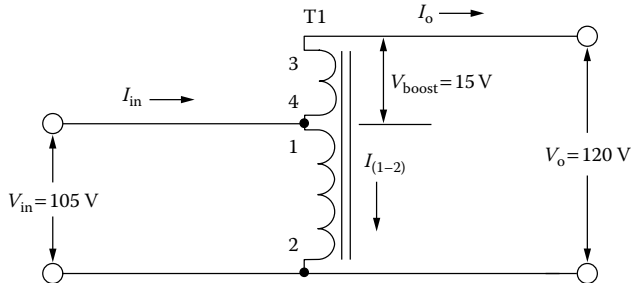

Figure 22-6. Step-up Autotransformer.

© 2011 by Taylor and Francis Group, LLC

Electrical Design Specification

1. Input voltage, V_{in} = 105 volts
2. Output voltage, V_o = 120 volts
3. Boost voltage, V_{bost} = 15 volts
4. Output current, I_o = 2.08 amps
5. Output power, P_o = 250 watts
6. Frequency, f = 60Hz
7. Efficiency, η = 95%
8. Copper loss ratio, α = 5%
9. Operating flux density, B_{ac} = 1.4 teslas
10. Core Material = Silicon M6X
11. Window utilization, K_u = 0.4
12. Temperature rise goal, $T_r < 20°C$

Step No. 1: Calculate the input current, I_{in}.

$$I_{in} = \frac{P_o}{V_{in}\,\eta}, \quad \text{[amps]}$$
$$I_{in} = \frac{250}{(105)(0.95)}, \quad \text{[amps]}$$
$$I_{in} = 2.51, \quad \text{[amps]}$$

Step No. 2: Calculate the autotransformer current in winding (1–2), $I_{(1\text{-}2)}$.

$$I_{(1-2)} = I_{in} - I_o, \quad \text{[amps]}$$
$$I_{(1-2)} = 2.51 - 2.08, \quad \text{[amps]}$$
$$I_{(1-2)} = 0.43, \quad \text{[amps]}$$

Step No. 3: Calculate the autotransformer volt-amps in winding (1–2), P_{tin}.

$$P_{tin} = V_{in}\,I_{(1-2)}, \quad \text{[watts]}$$
$$P_{tin} = (105)(0.43), \quad \text{[watts]}$$
$$P_{tin} = 45.1, \quad \text{[watts]}$$

Step No. 4: Calculate the autotransformer boost winding volt-amps in winding (3–4), P_{AT}.

$$P_{AT} = (V_o - V_{in})I_o, \quad \text{[watts]}$$
$$P_{AT} = (120 - 105)(2.08), \quad \text{[watts]}$$
$$P_{AT} = 31.2, \quad \text{[watts]}$$

© 2011 by Taylor and Francis Group, LLC

Step No. 5: Calculate the autotransformer apparent power, P_t.

$$P_t = P_{tin} + P_{AT}, \quad \text{[watts]}$$
$$P_t = 45.1 + 31.2, \quad \text{[watts]}$$
$$P_t = 76.3, \quad \text{[watts]}$$

Step No. 6: Calculate the electrical conditions, K_e.

$$K_e = 0.145 K_f^2 f^2 B_m^2 (10^{-4})$$
$$K_e = 0.145(4.44)^2(60)^2(1.4)^2(10^{-4})$$
$$K_e = 2.02$$

Step No. 7: Calculate the core geometry, K_g.

$$K_g = \frac{P_t}{2K_e \alpha}, \quad [\text{cm}^5]$$
$$K_g = \frac{76.3}{2(2.02)(5)}, \quad [\text{cm}^5]$$
$$K_g = 3.78, \quad [\text{cm}^5]$$

Step No. 8: Select a lamination from Chapter 3, comparable to core geometry, K_g.

1. Lamination = EI-100
2. Manufacturer = Temple
3. D Dimension = 2.54 cm
4. E Dimension = 2.54 cm
5. F Dimension = 1.27 cm
6. Core Geometry, $K_g = 4.93\ \text{cm}^5$
7. Area Product, $A_p = 29.7\ \text{cm}^4$
8. Core Weight, $W_t = 676$ grams
9. Surface Area, $A_t = 213\ \text{cm}^2$
10. Iron Area, $A_c = 6.13\ \text{cm}^2$
11. Window Area, $W_a = 4.84\ \text{cm}^2$
12. Magnetic Material, 14 mil = Si-Fe
13. Efficiency = 95%
14. Mean Length Turn, MLT = 14.8 cm

Step No. 9: Calculate the number of turns required for winding (1–2), $N_{(1\text{-}2)}$.

$$N_{(1-2)} = \frac{V_{in}(10^4)}{K_f B_{ac} f A_c}, \quad \text{[turns]}$$
$$N_{(1-2)} = \frac{105(10^4)}{(4.44)(1.4)(60)(6.13)}, \quad \text{[turns]}$$
$$N_{(1-2)} = 459, \quad \text{[turns]}$$

© 2011 by Taylor and Francis Group, LLC

Step No. 10: Calculate the current density, J.

$$J = \frac{P_t(10^4)}{K_u K_f B_{ac} f A_p}, \quad [\text{amps/cm}^2]$$

$$J = \frac{76.3(10^4)}{(0.4)(4.44)(1.4)(60)(29.7)}, \quad [\text{amps/cm}^2]$$

$$J = 172, \quad [\text{amps/cm}^2] \quad \text{use, } J = 200$$

Reviewing, K_u, in Step 27, a current density, J, of 200 amps/cm^2 would be more feasible.

Step No. 11: Calculate the autotransformer bare wire area, $A_{w(1\text{-}2)(B)}$.

$$A_{w(1-2)(B)} = \frac{I_{(1-2)}}{J}, \quad [\text{cm}^2]$$

$$A_{w(1-2)(B)} = \frac{(0.43)}{200}, \quad [\text{cm}^2]$$

$$A_{w(1-2)(B)} = 0.00215, \quad [\text{cm}^2]$$

Step No. 12: Select the wire from the Wire Table in Chapter 4.

$$AWG = \#24$$

$$A_{w(1-2)(B)} = 0.00205, \quad [\text{cm}^2]$$

$$A_{w(1-2)} = 0.00251, \quad [\text{cm}^2]$$

$$\left(\frac{\mu\Omega}{\text{cm}}\right) = 842, \quad [\text{micro-ohm/cm}]$$

Step No. 13: Calculate the autotransformer winding (1-2) resistance, $R_{(1\text{-}2)}$.

$$R_{(1-2)} = \text{MLT}\left(N_{(1-2)}\right)\left(\frac{\mu\Omega}{\text{cm}}\right)(10^{-6}), \quad [\text{ohms}]$$

$$R_{(1-2)} = (14.8)(459)(842)(10^{-6}), \quad [\text{ohms}]$$

$$R_{(1-2)} = 5.72, \quad [\text{ohms}]$$

Step No. 14: Calculate the autotransformer winding (1–2) copper loss, $P_{(1\text{-}2)}$.

$$P_{(1-2)} = I_{(1-2)}^2 R_{(1-2)}, \quad [\text{watts}]$$

$$P_{(1-2)} = (0.43)^2(5.72), \quad [\text{watts}]$$

$$P_{(1-2)} = 1.058, \quad [\text{watts}]$$

Step No. 15: Calculate the secondary boost winding (3-4) turns, $N_{(3\text{-}4)}$.

$$N_{(3-4)} = \frac{N_{(1-2)}V_{bost}}{V_{in}}\left(1 + \frac{\alpha}{100}\right), \quad [\text{turns}]$$

$$N_{(3-4)} = \frac{(459)(15)}{(105)}\left(1 + \frac{5}{100}\right), \quad [\text{turns}]$$

$$N_{(3-4)} = 68.8 \text{ use } 69, \quad [\text{turns}]$$

© 2011 by Taylor and Francis Group, LLC

Step No. 16: Calculate the autotransformer boost winding (3-4) bare wire area, $A_{w(3\text{-}4)(B)}$.

$$A_{w(3-4)(B)} = \frac{I_o}{J}, \quad [\text{cm}^2]$$
$$A_{w(3-4)(B)} = \frac{(2.08)}{200}, \quad [\text{cm}^2]$$
$$A_{w(3-4)(B)} = 0.0104, \quad [\text{cm}^2]$$

Step No. 17: Select the wire from the Wire Table in Chapter 4.

$$AWG = \#17$$
$$A_{w(3-4)(B)} = 0.0104, \quad [\text{cm}^2]$$
$$A_{w(3-4)} = 0.0117, \quad [\text{cm}^2]$$
$$\left(\frac{\mu\Omega}{\text{cm}}\right) = 166, \quad [\text{micro-ohm/cm}]$$

Step No. 18: Calculate the boost winding (3-4) resistance, $R_{(3\text{-}4)}$.

$$R_{(3-4)} = \text{MLT}\left(N_{(3-4)}\right)\left(\frac{\mu\Omega}{\text{cm}}\right)(10^{-6}), \quad [\text{ohms}]$$
$$R_{(3-4)} = (14.8)(69)(166)(10^{-6}), \quad [\text{ohms}]$$
$$R_{(3-4)} = 0.170, \quad [\text{ohms}]$$

Step No. 19: Calculate the boost winding (3-4) copper loss, $P_{(3\text{-}4)}$.

$$P_{(3-4)} = I_o^2 R_{(3-4)}, \quad [\text{watts}]$$
$$P_{(3-4)} = (2.08)^2(0.170), \quad [\text{watts}]$$
$$P_{(3-4)} = 0.735, \quad [\text{watts}]$$

Step No. 20: Calculate the total copper loss, P_{cu}.

$$P_{cu} = P_{(1-2)} + P_{(3-4)}, \quad [\text{watts}]$$
$$P_{cu} = 1.058 + 0.735, \quad [\text{watts}]$$
$$P_{cu} = 1.793, \quad [\text{watts}]$$

Step No. 21: Calculate the autotransformer regulation, α.

Use, P_{AT} = 31.2 calculated in Step 4.

$$\alpha = \frac{P_{cu}}{P_{AT}}(100), \quad [\%]$$
$$\alpha = \frac{(1.793)}{(31.2)}(100), \quad [\%]$$
$$\alpha = 5.7, \quad [\%]$$

© 2011 by Taylor and Francis Group, LLC

Step No. 22: Calculate the watts per kilogram, W/K. Use the Equation for this material presented in Chapter 2.

$$W/K = 0.000557(f)^{1.68}(B_{ac})^{1.86}$$
$$W/K = 0.000557(60)^{1.68}(1.4)^{1.86}$$
$$W/K = 1.011$$

Step No. 23: Calculate the core loss, P_{fe}.

$$P_{fe} = (W/K)(W_{tfe})(10^{-3}), \quad \text{[watts]}$$
$$P_{fe} = (1.011)(0.676), \quad \text{[watts]}$$
$$P_{fe} = 0.683, \quad \text{[watts]}$$

Step No. 24: Calculate the total loss, P_{Σ}.

$$P_{\Sigma} = P_{cu} + P_{fe}, \quad \text{[watts]}$$
$$P_{\Sigma} = (1.793) + (0.683), \quad \text{[watts]}$$
$$P_{\Sigma} = 2.476, \quad \text{[watts]}$$

Step No. 25: Calculate the watts per unit area, ψ.

$$\psi = \frac{P_{\Sigma}}{A_t}, \quad \text{[watts/cm}^2\text{]}$$
$$\psi = \frac{(2.476)}{(213)}, \quad \text{[watts/cm}^2\text{]}$$
$$\psi = 0.0116, \quad \text{[watts/cm}^2\text{]}$$

Step No. 26: Calculate the temperature rise, T_r.

$$T_r = 450(\psi)^{(0.826)}, \quad [°C]$$
$$T_r = 450(0.0116)^{(0.826)}, \quad [°C]$$
$$T_r = 11.3, \quad [°C]$$

Confirming the Window Utilization

Step No. 27: Calculate the total window utilization, K_u.

$$K_u = K_{u(1-2)} + K_{u(3-4)}$$
$$K_{u(3-4)} = \frac{N_{(3-4)} A_{w(3-4)(B)}}{W_a}$$
$$K_{u(3-4)} = \frac{(69)(0.0104)}{(4.84)} = 0.148$$
$$K_{u(1-2)} = \frac{N_{(1-2)} A_{w(1-2)(B)}}{W_a}$$
$$K_{u(1-2)} = \frac{(459)(0.00205)}{(4.84)} = 0.194$$
$$K_u = (0.194) + (0.148)$$
$$K_u = 0.342$$

© 2011 by Taylor and Francis Group, LLC

250 Watt Step-up Autotransformer Design Test Data (Using the Core Geometry, K_g, Approach)

The following information is the test data for the above 250 watt Step-up Autotransformer, as shown in Figure 22-7, operating at 60 Hz, using the, K_g, core geometry approach.

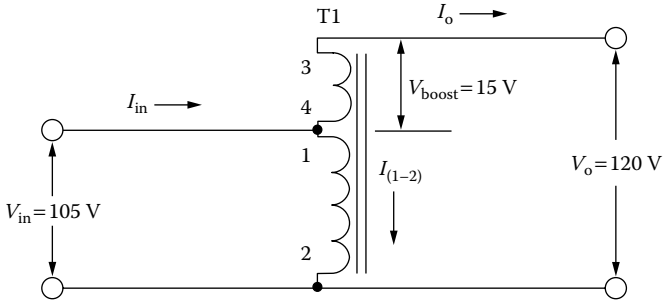

Figure 22-7. Step-up Autotransformer.

Test Data

1. Input voltage, V_{in} = 105 volts
2. Output voltage, V_o, No Load = 121 volts
3. Output voltage, V_o, Full Load = 120.3 volts
4. Output current, I_o = 2.08 amps
5. Output power, P_o = 250 watts
6. Current, $I_{(1-2)}$ = 0.351 amps
7. Current, I_{in} = 2.43 amps
8. Resistance, $R_{(1-2)}$ = 4.916 ohms
9. Resistance, $R_{(3-4)}$ = 0.170 ohms
10. Temperature rise, T_r = 14.2°C

Comparing the Step-up Autotransformer Design With a Standard Isolation Transformer

When comparing the Step-up Autotransformer Design with a Standard Isolation Transformer, use the same electrical requirements.

The output power P_o, is:

$$P_o = V_o I_o, \quad \text{[watts]}$$

© 2011 by Taylor and Francis Group, LLC

The input power P_{in} is:

$$P_{in} = \frac{V_o I_o}{\eta}, \quad [\text{watts}]$$

Step No. 1: Calculate the apparent power P_t for an output P_o, of 250 watts:

$$P_t = P_o\left(\frac{1}{\eta} + 1\right), \quad [\text{watts}]$$
$$P_t = (250)\left(\frac{1}{0.95} + 1\right), \quad [\text{watts}]$$
$$P_t = 513, \quad [\text{watts}]$$

Step No. 2: Calculate the electrical conditions, K_e.

$$K_e = 0.145 K_f^2 f^2 B_m^2 (10^{-4})$$
$$K_e = 0.145(4.44)^2(60)^2 (1.4)^2 (10^{-4})$$
$$K_e = 2.02$$

Step No. 3: Calculate the core geometry, K_g.

$$K_g = \frac{P_t}{2K_e \alpha}, \quad [\text{cm}^5]$$
$$K_g = \frac{513}{2(2.02)(5)}, \quad [\text{cm}^5]$$
$$K_g = 25.4, \quad [\text{cm}^5]$$

Step No. 4: Select a lamination from Chapter 3, comparable to core geometry, K_g.

1. Lamination = EI-138
2. Core Geometry, $K_g = 24.5$ cm^5
3. Core Weight, $W_t = 1786$ grams
4. Copper Weight, $W_{tcu} = 653$ cm^2
5. Iron Area, $A_c = 11.59$ cm^2
6. Window Area, $W_a = 9.148$ cm^2

250-Watt Step-down Autotransformer Design (Using the Core Geometry, K_g, Approach)

The following information is the Design specification for a 250-Watt Step-down Autotransformer, as shown in Figure 22-8, operating at 60 Hz, using the, K_g, core geometry approach. For a typical design example, assume the design with the following specifications:

© 2011 by Taylor and Francis Group, LLC

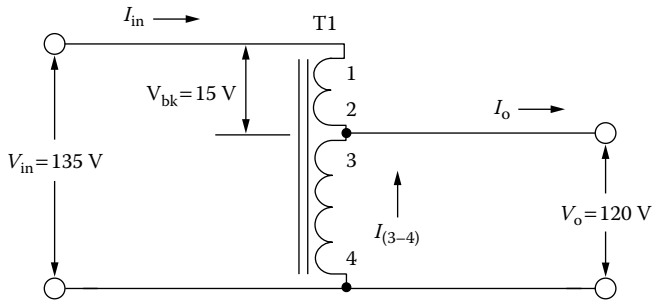

Figure 22-8. Step-down Autotransformer.

Electrical Design Specification

1. Input voltage, V_{in} = 135 volts
2. Output voltage, V_o = 120 volts
3. Buck voltage, V_{bk} = 15 volts
4. Output current, I_o = 2.08 amps
5. Output power, P_o = 250 watts
6. Frequency, f = 60 Hz
7. Efficiency, η = 95%
8. Copper loss, α = 5 %
9. Operating flux density, B_{ac} = 1.4 teslas
10. Core Material = Silicon M6X
11. Window utilization, K_u = 0.4
12. Temperature rise goal, $T_r < 20°C$

Step No. 1: Calculate the input current, I_{in}.

$$I_{in} = \frac{P_o}{V_{in}\,\eta}, \quad \text{[amps]}$$

$$I_{in} = \frac{250}{(135)(0.95)}, \quad \text{[amps]}$$

$$I_{in} = 1.95, \quad \text{[amps]}$$

Step No. 2: Calculate the autotransformer winding (3-4) current, $I_{(3-4)}$.

$$I_{(3-4)} = I_o - I_{in}, \quad \text{[amps]}$$

$$I_{(3-4)} = 2.08 - 1.95, \quad \text{[amps]}$$

$$I_{(3-4)} = 0.13, \quad \text{[amps]}$$

Step No. 3: Calculate the autotransformer winding (3-4) volt-amp rating VA, P_{to}.

$$P_{to} = V_o\, I_{(3-4)}, \quad \text{[watts]}$$

$$P_{to} = (120)(0.13), \quad \text{[watts]}$$

$$P_{to} = 15.6, \quad \text{[watts]}$$

© 2011 by Taylor and Francis Group, LLC

Step No. 4: Calculate the autotransformer buck winding (1-2) volt-amps rating, P_{AT}.

$$P_{AT} = I_{in}\left(V_{in} - V_o\right), \quad \text{[watts]}$$
$$P_{AT} = (1.95)(135 - 120), \quad \text{[watts]}$$
$$P_{AT} = 29.25, \quad \text{[watts]}$$

Step No. 5: Calculate winding (1-2) and winding (3-4) apparent power, P_t.

$$P_t = P_{AT} + P_{to}, \quad \text{[watts]}$$
$$P_t = 29.25 + 15.6, \quad \text{[watts]}$$
$$P_t = 44.85, \quad \text{[watts]}$$

Step No. 6: Calculate the electrical conditions, K_e.

$$K_e = 0.145 K_f^2 f^2 B_m^2 \left(10^{-4}\right)$$
$$K_e = 0.145(4.44)^2(60)^2 (1.4)^2 \left(10^{-4}\right)$$
$$K_e = 2.02$$

Step No. 7: Calculate the core geometry, K_g.

$$K_g = \frac{P_t}{2K_e\alpha}, \quad [\text{cm}^5]$$
$$K_g = \frac{44.85}{2(2.02)(5)}, \quad [\text{cm}^5]$$
$$K_g = 2.22, \quad [\text{cm}^5]$$

Step No. 8: Select a lamination from Chapter 3, comparable to core geometry, K_g.

1. Lamination = EI-875
2. Manufacturer = Temple
3. D Dimension = 2.22 cm
4. E Dimension = 2.22 cm
5. F Dimension = 1.11 cm
6. Core Geometry, K_g = 2.513 cm^5
7. Area Product, A_p = 17.4 cm^4
8. Core Weight, W_t = 457 grams
9. Surface Area, A_t = 163 cm^2
10. Iron Area, A_c = 4.69 cm^2
11. Window Area, W_a = 3.705 cm^2
12. Magnetic Material, 14 mil = Si-Fe
13. Efficiency = 95%
14. Mean Length Turn, MLT = 13.0 cm

© 2011 by Taylor and Francis Group, LLC

Step No. 9: Calculate the number of turns for winding (3-4), $N_{(3\text{-}4)}$.

$$N_{(3-4)} = \frac{V_o(10^4)}{K_f B_{ac} f A_c}, \quad [\text{turns}]$$

$$N_{(3-4)} = \frac{120(10^4)}{(4.44)(1.4)(60)(4.69)}, \quad [\text{turns}]$$

$$N_{(3-4)} = 686, \quad [\text{turns}]$$

Step No. 10: Calculate the current density, J.

$$J = \frac{P_t(10^4)}{K_u K_f B_{ac} f A_p}, \quad [\text{amps/cm}^2]$$

$$J = \frac{44.85(10^4)}{(0.4)(4.44)(1.4)(60)(17.4)}, \quad [\text{amps/cm}^2]$$

$$J = 173, \quad [\text{amps/cm}^2] \quad \text{use, } J = 200$$

Reviewing, K_u, in Step 27, a current density, J, of 200 amps/cm^2 would be more feasible.

Step No. 11: Calculate the bare wire area for winding (3-4), $A_{w(3\text{-}4)(B)}$.

$$A_{w(3-4)(B)} = \frac{I_{(3-4)}}{J}, \quad [\text{cm}^2]$$

$$A_{w(3-4)(B)} = \frac{(0.13)}{200}, \quad [\text{cm}^2]$$

$$A_{w(3-4)(B)} = 0.00065, \quad [\text{cm}^2]$$

Step No. 12: Select the wire from the Wire Table, in Chapter 4.

$$AWG = \#29$$

$$A_{w(3-4)(B)} = 0.000647, \quad [\text{cm}^2]$$

$$A_{w(3-4)} = 0.000855, \quad [\text{cm}^2]$$

$$\left(\frac{\mu\Omega}{\text{cm}}\right) = 2664, \quad [\text{micro-ohm/cm}]$$

Step No. 13: Calculate winding (3-4) resistance, $R_{(3\text{-}4)}$.

$$R_{(3-4)} = \text{MLT}(N_p)\left(\frac{\mu\Omega}{\text{cm}}\right)(10^{-6}), \quad [\text{ohms}]$$

$$R_{(3-4)} = (13)(686)(2664)(10^{-6}), \quad [\text{ohms}]$$

$$R_{(3-4)} = 23.8, \quad [\text{ohms}]$$

Step No. 14: Calculate winding (3-4) copper loss, $P_{(3\text{-}4)}$.

$$P_{(3-4)} = I^2_{(3-4)} R_{(3-4)}, \quad [\text{watts}]$$

$$P_{(3-4)} = (0.13)^2(23.8), \quad [\text{watts}]$$

$$P_{(3-4)} = 0.402, \quad [\text{watts}]$$

© 2011 by Taylor and Francis Group, LLC

Step No. 15: Calculate the buck winding (1-2) turns, $N_{(1-2)}$.

$$N_{(1\text{-}2)} = \frac{N_{(3-4)}V_{bk}}{V_o}, \quad [\text{turns}]$$
$$N_{(1\text{-}2)} = \frac{(686)(15)}{(120)}, \quad [\text{turns}]$$
$$N_{(1\text{-}2)} = 85.7 \text{ use } 86, \quad [\text{turns}]$$

Step No. 16: Calculate the buck winding (1-2) bare wire area, $A_{w(1\text{-}2)(B)}$.

$$A_{w(1-2)(B)} = \frac{I_{in}}{J}, \quad [\text{cm}^2]$$
$$A_{w(1-2)(B)} = \frac{(1.95)}{200}, \quad [\text{cm}^2]$$
$$A_{w(1-2)(B)} = 0.00975, \quad [\text{cm}^2]$$

Step No. 17: Select the wire from the Wire Table, in Chapter 4.

$$AWG = \#18$$
$$A_{w(1-2)(B)} = 0.00823, \quad [\text{cm}^2]$$
$$A_{w(1-2)} = 0.00933, \quad [\text{cm}^2]$$
$$\left(\frac{\mu\Omega}{\text{cm}}\right) = 210, \quad [\text{micro-ohm/cm}]$$

Step No. 18: Calculate the buck winding (1-2) resistance, $R_{(1\text{-}2)}$.

$$R_{(1-2)} = \text{MLT}\left(N_{(1-2)}\right)\left(\frac{\mu\Omega}{\text{cm}}\right)(10^{-6}), \quad [\text{ohms}]$$
$$R_{(1-2)} = (13)(86)(210)(10^{-6}), \quad [\text{ohms}]$$
$$R_{(1-2)} = 0.235, \quad [\text{ohms}]$$

Step No. 19: Calculate the buck winding (1-2) copper loss, $P_{(1\text{-}2)}$.

$$P_{(1-2)} = I_{in}^2 R_{(1-2)}, \quad [\text{watts}]$$
$$P_{(1-2)} = (1.95)^2(0.235), \quad [\text{watts}]$$
$$P_{(1-2),_s} = 0.894, \quad [\text{watts}]$$

Step No. 20: Calculate winding (1-2) and winding (3-4) total copper loss, P_{cu}.

$$P_{cu} = P_{(1-2)} + P_{(3-4)}, \quad [\text{watts}]$$
$$P_{cu} = 0.894 + 0.402, \quad [\text{watts}]$$
$$P_{cu} = 1.296, \quad [\text{watts}]$$

© 2011 by Taylor and Francis Group, LLC

Step No. 21: Calculate the transformer regulation, α.

Use, P_{AT} = 29.25 calculated in Step 4.

$$\alpha = \frac{P_{cu}}{P_{tin}}(100), \quad [\%]$$
$$\alpha = \frac{(1.296)}{(29.25)}(100), \quad [\%]$$
$$\alpha = 4.43, \quad [\%]$$

Step No. 22: Calculate the watts per kilogram, W/K. Use the Equation for this material found in Chapter 2.

$$W/K = 0.000557(f)^{1.68}(B_{ac})^{1.86}$$
$$W/K = 0.000557(60)^{1.68}(1.4)^{1.86}$$
$$W/K = 1.01$$

Step No. 23: Calculate the core loss, P_{fe}.

$$P_{fe} = (W/K)(W_{tfe})(10^{-3}), \quad [\text{watts}]$$
$$P_{fe} = (1.01)(0.457), \quad [\text{watts}]$$
$$P_{fe} = 0.462, \quad [\text{watts}]$$

Step No. 24: Calculate the total loss, P_{Σ}.

$$P_{\Sigma} = P_{cu} + P_{fe}, \quad [\text{watts}]$$
$$P_{\Sigma} = (1.296) + (0.462), \quad [\text{watts}]$$
$$P_{\Sigma} = 1.758, \quad [\text{watts}]$$

Step No. 25: Calculate the watts per unit area, ψ.

$$\psi = \frac{P_{\Sigma}}{A_t}, \quad [\text{watts/cm}^2]$$
$$\psi = \frac{(1.758)}{(163)}, \quad [\text{watts/cm}^2]$$
$$\psi = 0.0108, \quad [\text{watts/cm}^2]$$

Step No. 26: Calculate the temperature rise, T_r.

$$T_r = 450(\psi)^{(0.826)}, \quad [°\text{C}]$$
$$T_r = 450(0.0108)^{(0.826)}, \quad [°\text{C}]$$
$$T_r = 10.7, \quad [°\text{C}]$$

© 2011 by Taylor and Francis Group, LLC

Confirming the Window Utilization

Step No. 27: Calculate the total window utilization, K_u.

$$K_u = K_{u(1-2)} + K_{u(3-4)}$$

$$K_{u(1-2)} = \frac{N_{(1-2)} A_{w(1-2)(B)}}{W_a}$$

$$K_{u(1-2)} = \frac{(86)(0.00823)}{(3.705)} = 0.191$$

$$K_{u(3-4)} = \frac{N_{(3-4)} A_{w(3-4)(B)}}{W_a}$$

$$K_{up} = \frac{(686)(0.000647)}{(3.705)} = 0.120$$

$$K_u = (0.191) + (0.120)$$

$$K_u = 0.311$$

250 Watt Step-down Autotransformer Design Test Data (Using the Core Geometry, K_g, Approach)

The following information is the test data for the above 250 watt buck autotransformer, as shown in Figure 22-9, operating at 60 Hz, using the, K_g, core geometry approach.

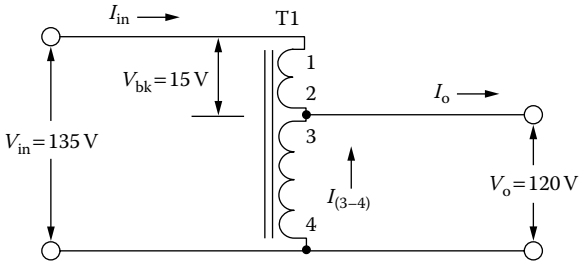

Figure 22-9. Step-down Autotransformer.

Test Data

1. Input voltage, V_{in} = 135 volts
2. Output voltage, V_o, No Load = 120.3 volts
3. Output voltage, V_o, Full Load = 119.6 volts
4. Output current, I_o = 2.08 amps
5. Output power, P_o = 250 watts
6. Current, $I_{(3-4)}$ = 0.24 amps
7. Current, I_{in} = 1.86 amps
8. Resistance, $R_{(1-2)}$ = 0.237 ohms
9. Resistance, $R_{(3-4)}$ = 19.72 ohms
10. Temperature rise, T_r = 19.1°C

© 2011 by Taylor and Francis Group, LLC

Comparing the Autotransformer Design With a Standard Isolation Transformer

When comparing the Step-up Autotransformer Design with a standard isolation transformer use the same electrical requirements.

The output power P_o, is:

$$P_o = V_o I_o, \quad \text{[watts]}$$

The input power P_{in} is:

$$P_{in} = \frac{V_o I_o}{\eta}, \quad \text{[watts]}$$

Step No. 1: Calculate the apparent power P_t for an output P_o, of 250 watts:

$$P_t = P_o\left(\frac{1}{\eta} + 1\right), \quad \text{[watts]}$$
$$P_t = (250)\left(\frac{1}{0.95} + 1\right), \quad \text{[watts]}$$
$$P_t = 513, \quad \text{[watts]}$$

Step No. 2: Calculate the electrical conditions, K_e.

$$K_e = 0.145 K_f^2 f^2 B_m^2 (10^{-4})$$
$$K_e = 0.145(4.44)^2(60)^2 (1.4)^2 (10^{-4})$$
$$K_e = 2.02$$

Step No. 3: Calculate the core geometry, K_g.

$$K_g = \frac{P_t}{2K_e \alpha}, \quad [\text{cm}^5]$$
$$K_g = \frac{513}{2(2.02)(5)}, \quad [\text{cm}^5]$$
$$K_g = 25.4, \quad [\text{cm}^5]$$

Step No. 4: Select a lamination from Chapter 3, comparable to core geometry, K_g.

1. Lamination = EI-138
2. Core Geometry, K_g = 24.5 cm^5
3. Core Weight, W_t = 1786 grams
4. Copper Weight, W_{tcu} = 653 cm^2
5. Iron Area, A_c = 11.59 cm^2
6. Window Area, W_a = 9.148 cm^2

© 2011 by Taylor and Francis Group, LLC

Engineering Note

The copper loss regulation, α, for a standard transformer, as shown in Figure 22-1, has to do with the total copper loss, P_{cu}, and the output power, P_o, as shown in Equation [22-30].

$$\alpha = \frac{P_{cu}}{P_o}(100) \quad [\%] \qquad [22\text{-}30]$$

$$P_{cu} = P_p + P_s, \quad [\text{watts}] \qquad [22\text{-}31]$$

$$P_o = V_o I_o, \quad [\text{watts}] \qquad [22\text{-}32]$$

The copper loss, α, for an Autotransformer, as shown in Figure 22-2, has to do with the total copper loss, P_{cu}, and the volt-amps, and the VA of the boost or buck winding, as shown in Equation [22-33].

$$\alpha = \frac{P_{cu}}{P_{AT}}(100) \quad [\%] \qquad [22\text{-}33]$$

$$P_{cu} = P_{(1-2)} + P_{(3-4)}, \quad [\text{watts}] \qquad [22\text{-}34]$$

Autotransformer Boost

$$P_{AT} = (V_o - V_{in})I_o, \quad [\text{watts}] \qquad [22\text{-}35]$$

Autotransformer Buck

$$P_{AT} = (V_{in} - V_o)I_{in}, \quad [\text{watts}] \qquad [22\text{-}36]$$

Recognition

I would like to give thanks to Charles Barnett, an engineer at Leightner Electronics Inc., for building and testing the 250 watt step-up and step-down autotransformer design examples.

Leightner Electronics Inc.
1501 S. Tennessee St.
McKinney, TX. 75069

References

1. Flanagan, W.M., *Handbook of Transformer Applications*, McGraw-Hill Book Co., Inc., New York, 1986, pp. 3.10–3.12.

2. Lee, R., *Electronic Transformers and Circuits*, John Wiley & Sons, New York, N.Y., 1958, pp. 250–252.

3. Nordenberg, H.M., *Electronic Transformers*, Reinhold Publishing Corporation, New York, 1964, pp. 147–149.

4. Grossner, N.R., *Transformers for Electronic Circuits*, McGraw-Hill Book Co., Inc., New York, 1983, pp. 31–32.

© 2011 by Taylor and Francis Group, LLC

Chapter 23

Common-Mode Inductor Design

© 2011 by Taylor and Francis Group, LLC

Table of Contents

1. Introduction....23-3
2. Differential Mode Noise....23-3
3. Common Mode Noise....23-5
4. Semiconductors Common Mode Noise Source....23-6
5. Transformers and Inductors Common Mode Noise Source....23-8
6. Faraday Shield....23-10
7. The Common Mode Filter....23-11
8. The Common Mode Filter Inductor....23-12
9. Choosing the Magnetic Material....23-12
10. Ferrite Temperature Characteristics....23-13
11. Ferrite Stress Characteristics....23-14
12. Core Saturation....23-15
13. Common Mode Filter Inductor Design Specification....23-16
14. References....23-19

© 2011 by Taylor and Francis Group, LLC

Introduction

Switch Mode Power Supplies (SMPS) are normally one of the biggest generators of noise. The SMPS generates two types of noise: common mode and differential mode. Common mode noise occurs simultaneously on both lines of a conductor pair with respect to a common ground chassis, whereas differential noise occurs between the input conductor paths. The common mode filters are generally relied upon to suppress line conducted common mode noise, whereas the input LC filter is used to minimize the differential noise (ripple current) back to the source.

Differential Mode Noise

The differential mode noise diagram is shown in Figure 23-1. The differential mode noise follows the same path as the input power. A typical SMPS generating differential mode noise is shown in Figure 24-2.

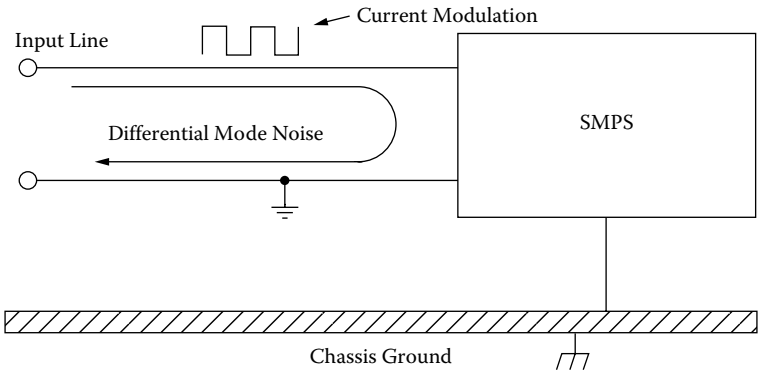

Figure 23-1. The Differential Mode Noise Path Diagram from a SMPS.

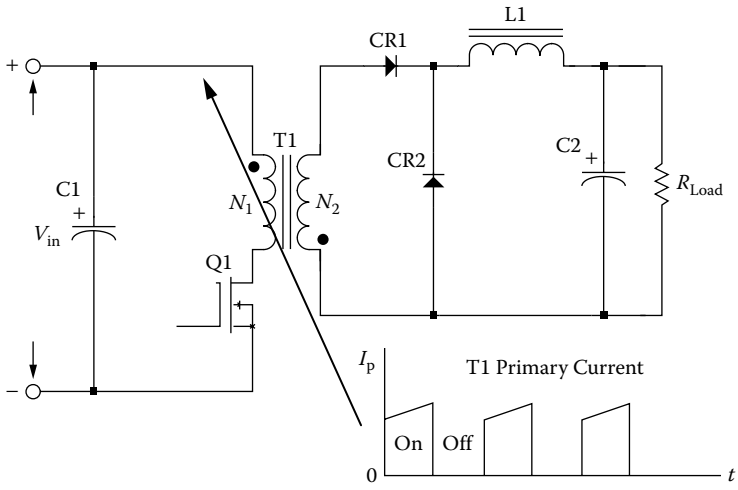

Figure 23-2. Input Current Modulation from a Flyback Converter.

© 2011 by Taylor and Francis Group, LLC

A simple LC filter can normally reduce the noise to a reasonable limit, as shown in Figure 23-3.

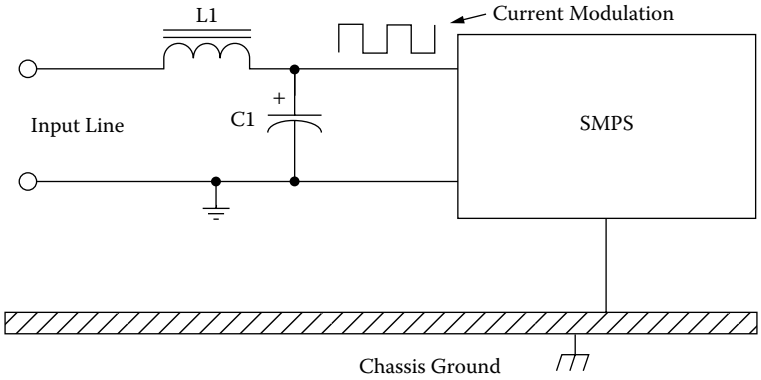

Figure 23-3. Typical Differential Mode Noise Input Filter.

The input LC filter is designed to reduce the input current modulation at the power source. The input current modulation generates a noise voltage within power source, as shown in Figure 23-4. It is shown in Figure 23-4 that any noise $V_{(noise)}$ generated by the Switch Mode Power Supply (SMPS) can be seen by the other users of the power source. The magnitude of the noise $V_{(noise)}$ is shown in Equation [23-1]. The ripple current $I_{L(pk\text{-}pk)}$ is calculated, using Equation [23-2]. R_X is an external non-inductive resistor that is used to measure the ripple voltage $V_{I(ripple)}$ to calculate the ripple current $I_{L(pk\text{-}pk)}$.

$$V_{(noise)} = I_{L(pk-pk)} R_Z, \quad \text{[volts]} \tag{23-1}$$

$$I_{L(pk-pk)} = \frac{V_{I(ripple)}}{R_X}, \quad \text{[amps]} \tag{23-2}$$

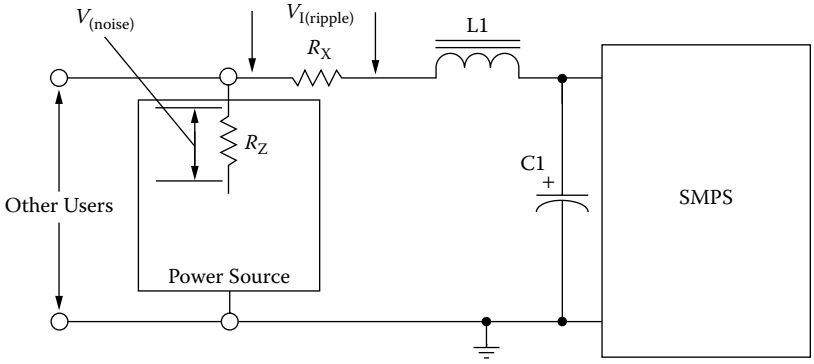

Figure 23-4. Noise Disturbances Generated in the Power Source.

© 2011 by Taylor and Francis Group, LLC

The differential mode (DM) noise, $V_{(noise)}$ will generally be designed to have a magnitude of less than 100 millivolts, peak to peak. The common mode (CM) noise can have an amplitude of several volts and give erroneous measurements. The test setup should be clean without ground loops and the test equipment should have good common mode (CM) rejection.

Common Mode Noise

A simple common mode noise diagram is shown in Figure 23-5. The common mode noise occurs simultaneously on both lines of the input conductor pair with respect to a common ground (chassis). The primary source of this noise is the charging and discharging of stray capacitance, C_s from the high switching rate within the power supply, as shown in Figure 23-6.

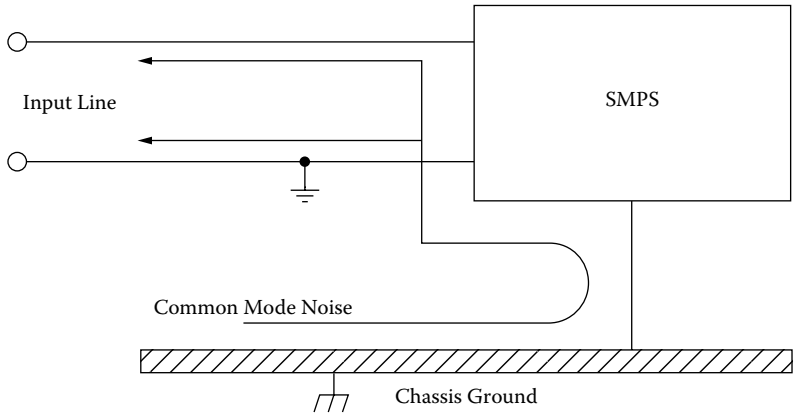

Figure 23-5. Common Mode Noise and Its Trail.

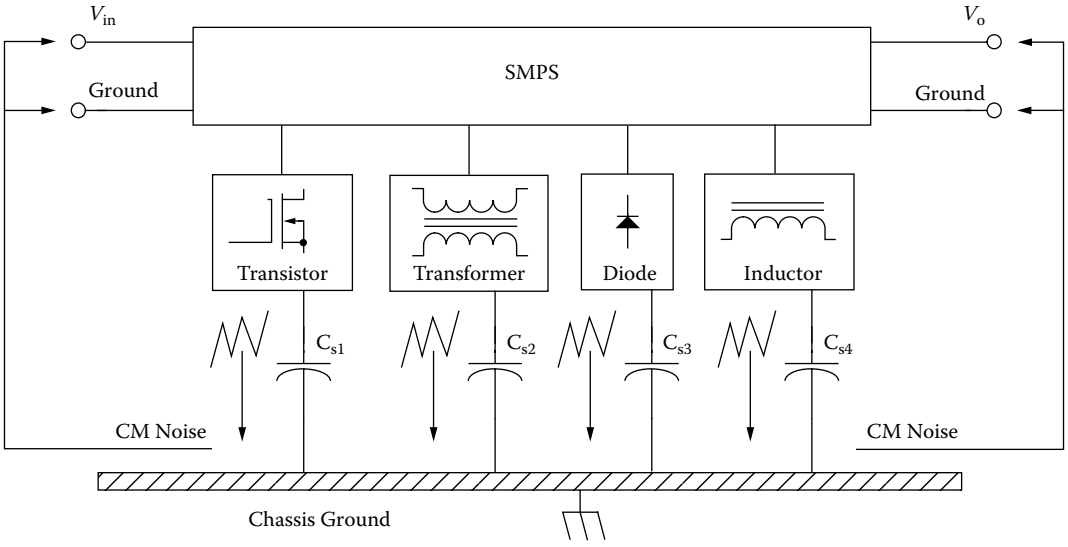

Figure 23-6. The Common Mode Noise Can Travel Down Both Input and Output Lines.

© 2011 by Taylor and Francis Group, LLC

The main source of common mode noise in the SMPS is the stray capacitance to chassis ground that can be found in switching power transformer, inductors, transistors and diodes connected to the heat sink and any wiring carrying high ac currents. The primary source of this noise is the di/dt and dv/dt of the fast switching power MOSFET transistors. See Figure 23-7. This sub-microsecond rise and fall time causes fast charging and discharging of the stray parasitic capacitance, C_s, which creates high pulse currents to flow. The delta current, ΔI can be calculated using Equation [23-3].

$$\Delta I = \frac{C_s V_{(pk)}}{\Delta t}, \quad \text{[amps]} \qquad \text{[23-3]}$$

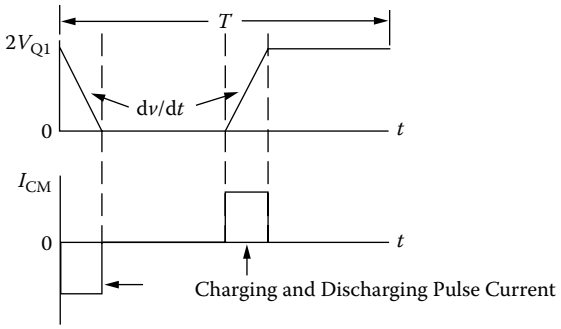

Figure 23-7. Charging and Discharging Stray Capacitance in Switch Mode Power Supply.

Semiconductors Common Mode Noise Source

The primary noise generators that couple noise into the chassis are transistors and diodes. This is because they are bolted to a heat sink and the heat sink is connected to the chassis. If the transistors and diodes are not mounted on a heat sink, then this stray capacitance, C_s problem is minimized. To a lesser extent power transformers and switching inductors that are bolted to the chassis provide their share of common mode noise. There are some simple ways to reduce the common mode noise at the noise source. The power switching transistor connected to the heat sink generating common mode noise through the stray capacitance, C_s is shown in Figure 23-8. The noise generated is from the current charging and discharging the stray capacitance, C_s created by the insulating hardware used to mount the power transistor to the heat sink. This noise current that is generated with the stray capacitance, C_s must return to the point of origin. The only way for the current, I_s to return is through the input lines, unless there is an alternate path provided.

© 2011 by Taylor and Francis Group, LLC

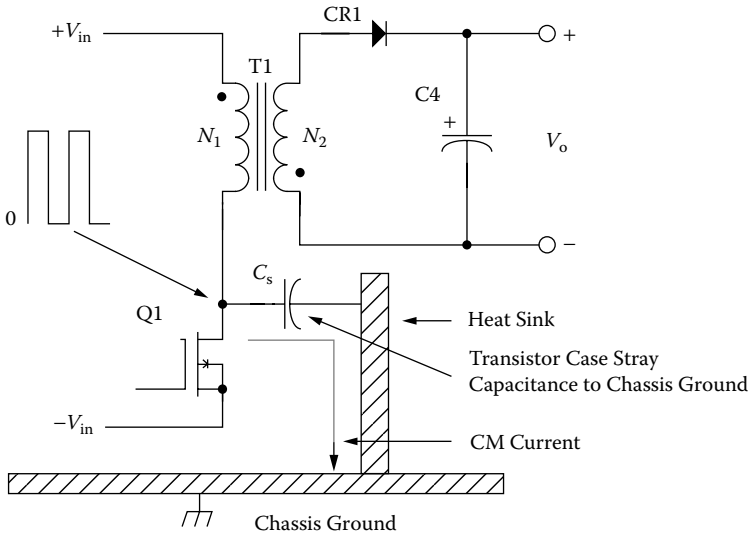

Figure 23-8. Charging and Discharging Stray Capacitance in Switch Mode Power Supply.

The noise current, I_s, that flows through the stray capacitance, C_s, can be diverted to the input ground. Doing this bypass will keep the noise current within the power supply, as shown in Figure 23-9. Using insulated copper foil between the transistor and the heat sink and then grounding the foil can do this. The output power rectifiers have the same stray capacitance, C_s, mounting problem as the transistors, as shown in Figure 23-10. The noise current, I_s, that flows through the stray capacitance, C_s, can be diverted to ground also, but this time it is the output ground, as shown in Figure 23-11. Using insulated copper foil between the rectifiers and the heat sink, followed by grounding the foil to the output ground can accomplish this goal.

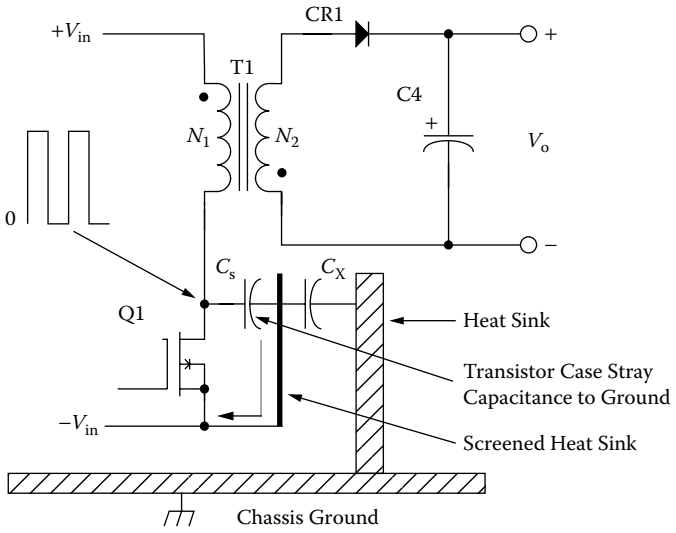

Figure 23-9. Transistor Mounting to Bypass the Stray Capacitance to the Input Ground.

© 2011 by Taylor and Francis Group, LLC

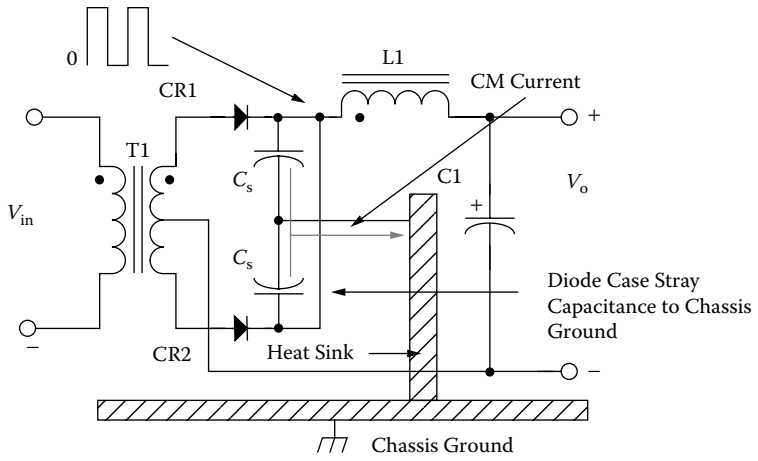

Figure 23-10. Rectifier Mounting Stray Capacitance, C_s, to the Heat sink.

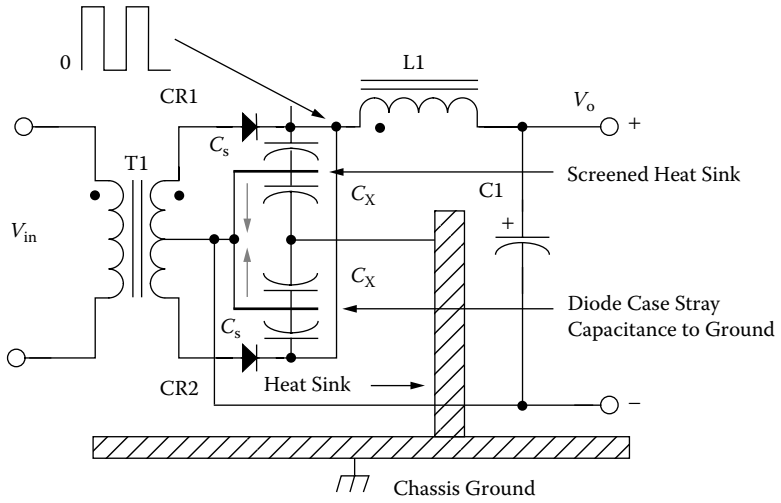

Figure 23-11. Mounting the Rectifier to Bypass the Stray Capacitance, C_s, to the Output Ground.

Transformers and Inductors Common Mode Noise Source

Transformers and multi-winding inductors have two paths for their common mode noise with their stray capacitance, C_s. The two paths are winding-to-winding and winding to the core. The stray capacitance, C_s, between the winding and the core is much easier to handle than the stray capacitance, C_s, between the primary and secondary. A buck type flyback inductor, L1, is shown with the stray capacitance, C_s, from the coil to the core in Figure 23-12. A flyback transformer, T1, with its stray capacitance, C_s, between the coil and the core is shown in Figure 23-13. If the transformer is not mounted directly on the chassis, but on a printed circuit board, it might be a good idea to ground it, just in case. A way to minimize the stray capacitance, C_s to the core is to add an insulated copper shield, as shown in Figure 23-14. This copper shield would be placed around the center

© 2011 by Taylor and Francis Group, LLC

leg and the outer surface of the coil, being very careful not to create a shorted turn, as shown in Figure 23-14. The copper shield should be terminated at the center to eliminate voltage gradient effects, as shown.

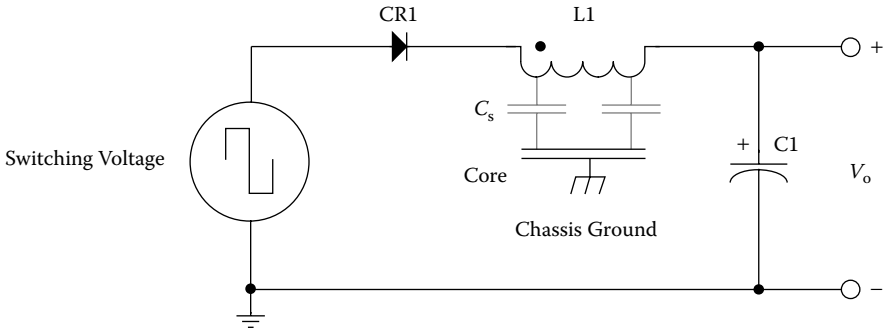

Figure 23-12. Stray Capacitance, C_s from the Inductor Winding to the Core.

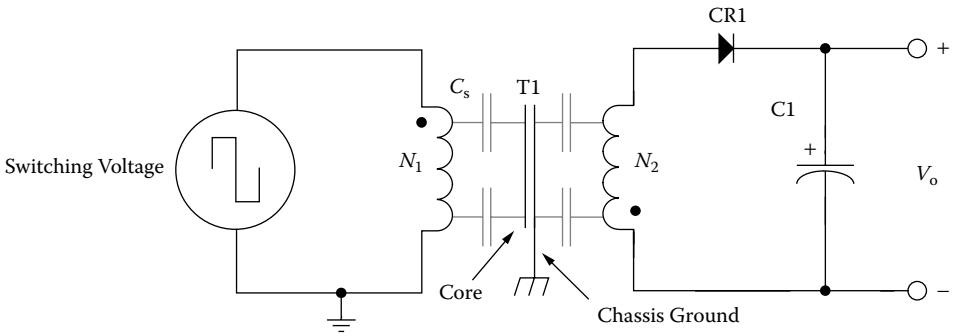

Figure 23-13. Stray Capacitance, C_s from a Flyback Transformer Windings to the Core.

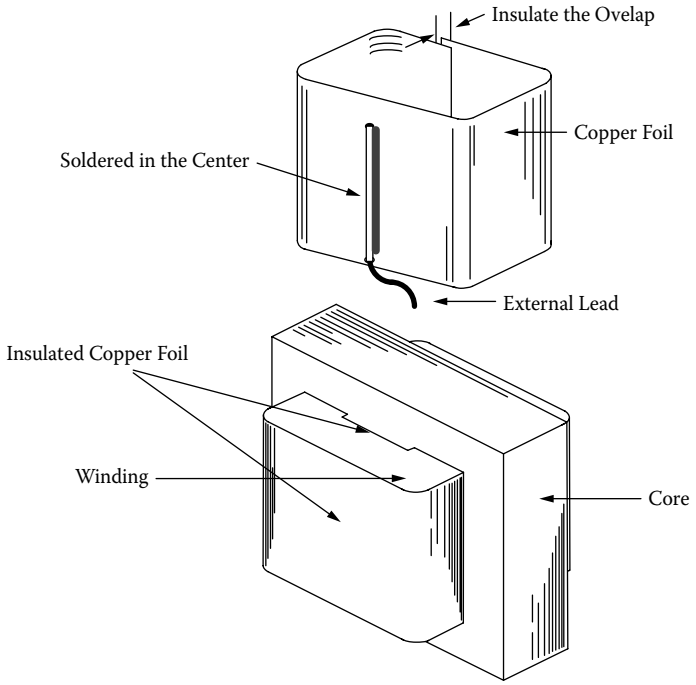

Figure 23-14. Shielding Stray Capacitance, C_s from the Power Transformer Windings to the Core.

© 2011 by Taylor and Francis Group, LLC

Faraday Shield

The stray capacitance, C_s, between primary and secondary, is shown in Figure 23-15, on Side A. This stray capacitance, C_s, between winding and winding is much harder to handle, because, as the stray capacitance, C_s is decreased, the leakage inductance, L_s, will increase. The performance of a high frequency converter power transformer and/or inductor is normally designed to have a very tight coupling between the primary and secondary to minimize the leakage inductance. Designing a transformer to minimize the stray capacitance, C_s, between primary and secondary will greatly increase the leakage inductance, L_s, which has an undesirable side effect.

The common mode noise produced by the stray capacitance, C_s can be reduced with the addition of a Faraday copper shield, as shown in Figure 23-15, Side B. This copper shield would be placed between the primary and the secondaries, as shown in Figure 23-15B. The copper shield would be installed the same way as in Figure 23-14, and should be terminated at the center to eliminate voltage gradient effects, as shown. To reduce the common mode noise even more, multiple Faraday shields can be added, as shown in Figure 23-16.

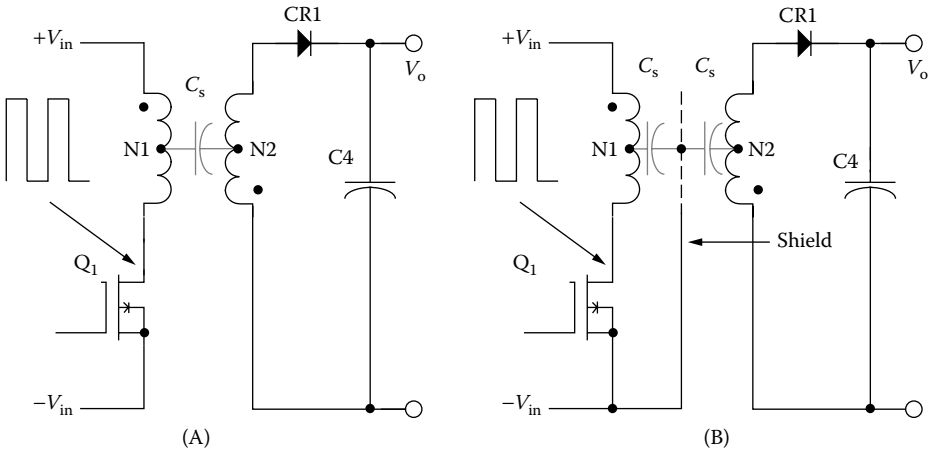

Figure 23-15. A Faraday Shield is Added to Bypass the Common Mode Noise to Ground.

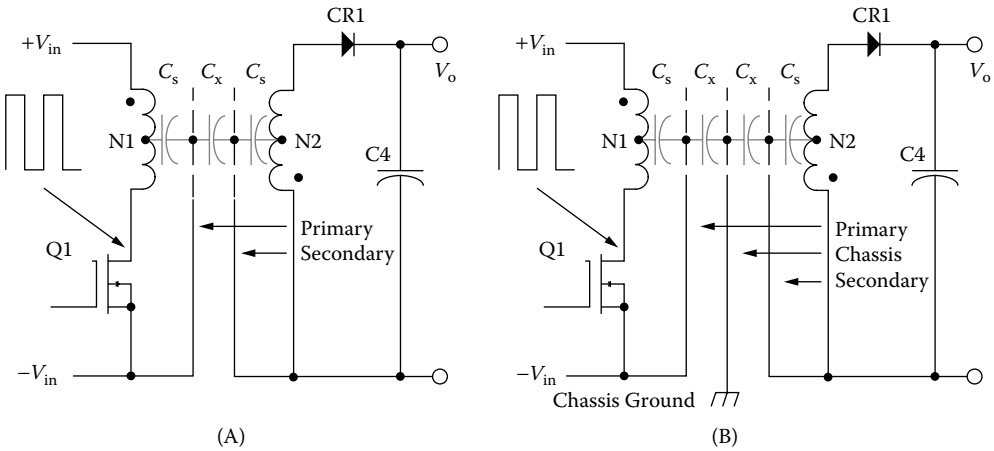

Figure 23-16. Multiple Faraday Shields to Get Better Common Mode Rejection.

© 2011 by Taylor and Francis Group, LLC

The Common Mode Filter

The typical input common mode filter components; L1, C2 and C3 are shown in Figure 23-17. The common mode inductor, L1, has two identical windings, N1 and N2. The input current from the power source goes into lead #1 of L1 and comes out of lead 3 of L1. Since both leads are starts, the net flux change is zero. This is because the amp-turn of N1 is equal to the amp-turn of N2, and they cancel each other. The capacitors, C2 and C3 are of high quality with low ESR, and are used to bypass the noise current created from the stray capacitance, C_s, within the power supply. The capacitors, C2 and C3, keep the common mode noise current created by the stray capacitance, C_s within the power supply. The output common mode filter is shown in Figure 23-18. The output common mode filter components are, L4, C4 and C5. The output common mode filter performs the same way as the input common mode filter.

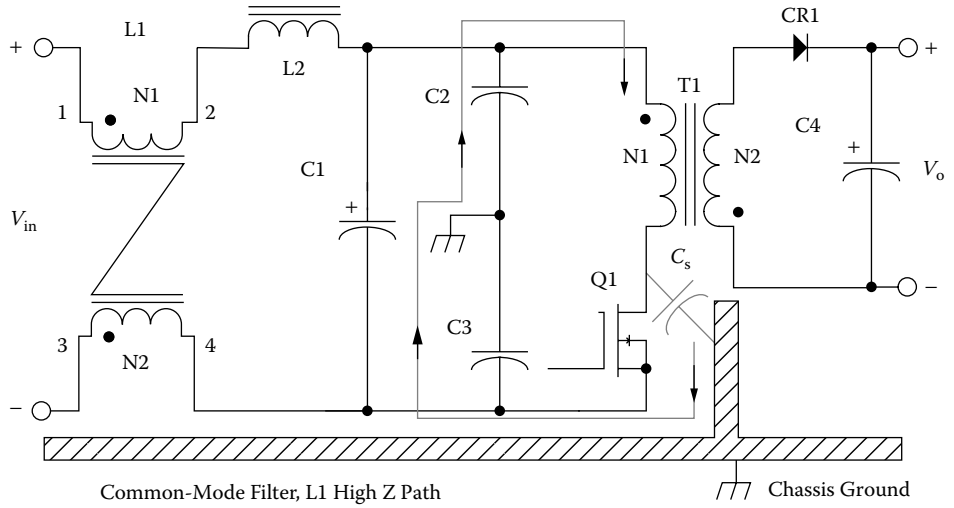

Figure 23-17. Input Common Mode Filter with an Alternate Path for the Stray Capacitance Current.

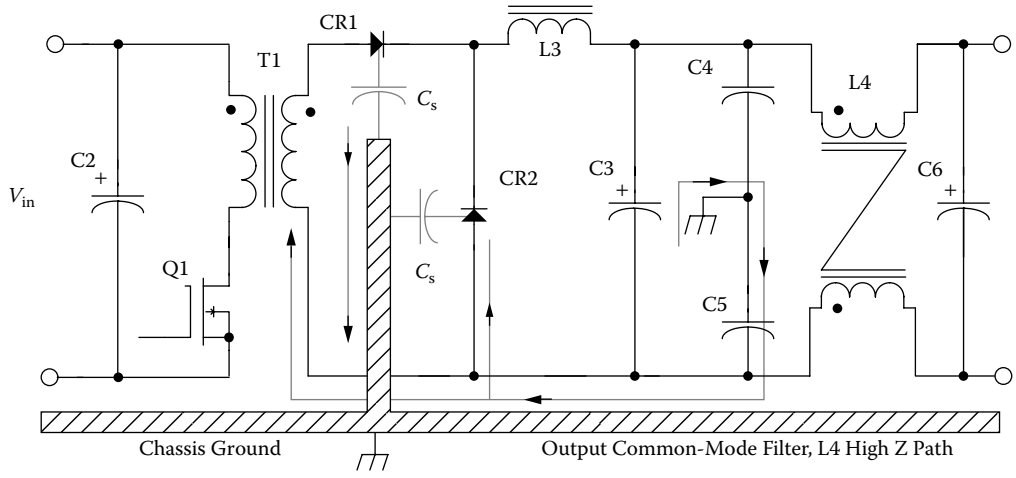

Figure 23-18. Output Common Mode Filter with an Alternate Path for the Stray Capacitance Current.

© 2011 by Taylor and Francis Group, LLC

The Common Mode Filter Inductor

The toroidal core is the most popular for the common mode filter inductor, because of its high permeability and usually requires very few turns, as shown in Figure 23-19. The windings are placed on the toroidal core with the alignment spacer. The alignment spacer helps provide a tight control of the windings space and provides a good control of the parasitics. As mentioned earlier, the differential current or amp-turns through the common mode filter inductor cancel and produce zero net flux because of the phasing of N1 to N2, as shown in Figure 23-20. Because of the phasing on the common mode inductor the differential current produces zero net flux. This means the common mode inductor can be designed more effectively with a core of high permeability.

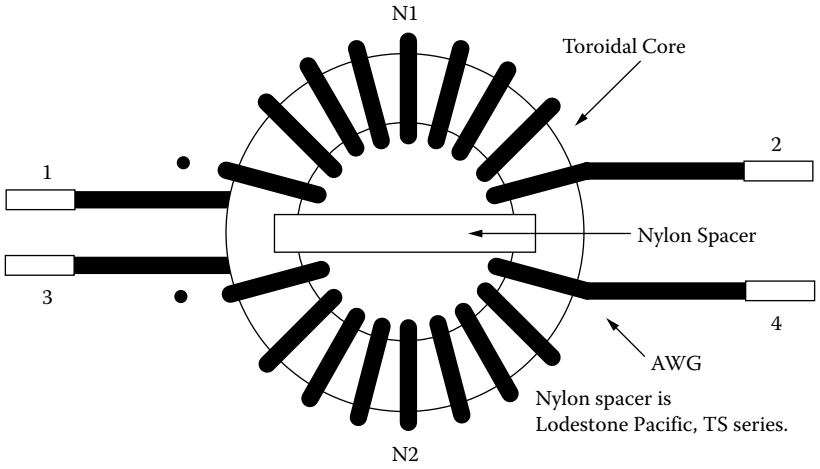

Figure 23-19. Outline of a Toroidal Common Mode Filter Inductor.

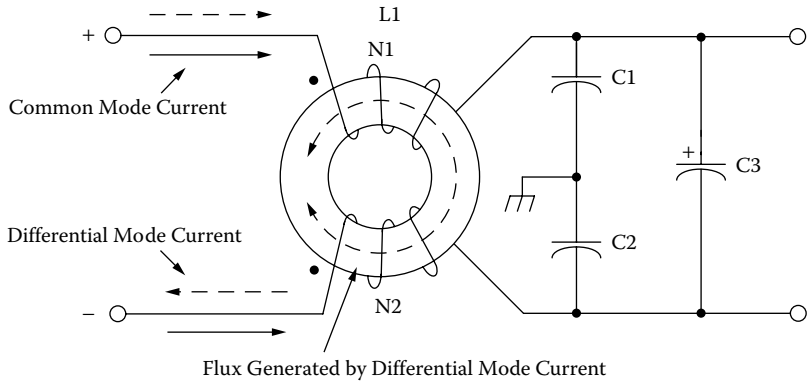

Figure 23-20. A Common Mode Filter Showing the Applied Currents.

Choosing the Magnetic Material

The engineer will usually know how much space is available for the common mode inductor. In the norm, the design of common mode filters is done after the design is finished. The space left will go to the filter. The engineer also knows how much insertion loss can be tolerated. This insertion loss can be in the form of power

© 2011 by Taylor and Francis Group, LLC

or voltage drop. The engineer can control the watts loss, the temperature rise, and/or the voltage drop by selecting the proper cores and wire size.

The noise spectrum generated by switching power supplies usually runs anywhere from 10kHz to 50MHz. To provide proper attenuation, the impedance of the inductor must be sufficiently high over this frequency range. The magnetic material must have a high initial permeability and a low cost. High permeability ferrites, such as Magnetics J with 5,000u and W with 10,000u, are the materials of choice for most common mode inductors. There is an amorphous material by Vacuumschmelze, (VAC) which is successful on the common mode inductor market with a nanocrystalline material called Vitroperm 500F. VAC's Vitroperm 500F can be compared with ferrites in Table 23-1.

Table 23-1. Magnetic Material Properties

Magnetic Material Properties					
Manufacturer Name	Material Name	Trade Name Composition	Initial Permeability μ_i	Flux Density Teslas B_s	Typical Operating Frequency
Magnetics	Ferrite J	MnZn	5,000	0.43	10k-2M
Magnetics	Ferrite W	MnZn	10,000	0.43	10k-2M
CMI	CMD5005	NiZn	1600	0.3	0.2M-100M
VAC	Vitroperm 500F	Nanocrystalline	30,000	1.2	10k-2M

Ferrite Temperature Characteristics

Ferrite materials with a medium to high permeability, μ_m do have a "down" side. Ferrites are very temperature-sensitive regarding permeability, μ_m, as shown in Figure 23-21. As can be seen in Figure 23-21, the permeability, μ_m changes quite readily with temperature. The inductance is directly proportional permeability, μ_m, as shown by Equation [23-4]. When an inductor is designed with a gap, then the permeability, μ_m, changes to the relative permeability, μ_r. The relative permeability, μ_r, is about 600 or less depending on the gap, l_g, dimension, as shown in Equation [23-5]. The gap, l_g, will stabilize the inductance changes with temperature. Temperature also effects the saturation, or B_{max}, of a ferrite core. The flux density, B_{max}, will decrease, as shown in Figure 23-22. As the temperature goes up the saturation flux goes down. This definitely has a negative effect when designing for high temperature.

$$L = \frac{0.4\pi N^2 A_c \mu_m (10^{-8})}{\text{MPL}}, \quad \text{[henrys]} \qquad [23\text{-}4]$$

$$\mu_r = \frac{\mu_m}{1 + \left(\frac{l_g}{\text{MPL}}\right)\mu_m}, \quad \text{[relative perm]} \qquad [23\text{-}5]$$

© 2011 by Taylor and Francis Group, LLC

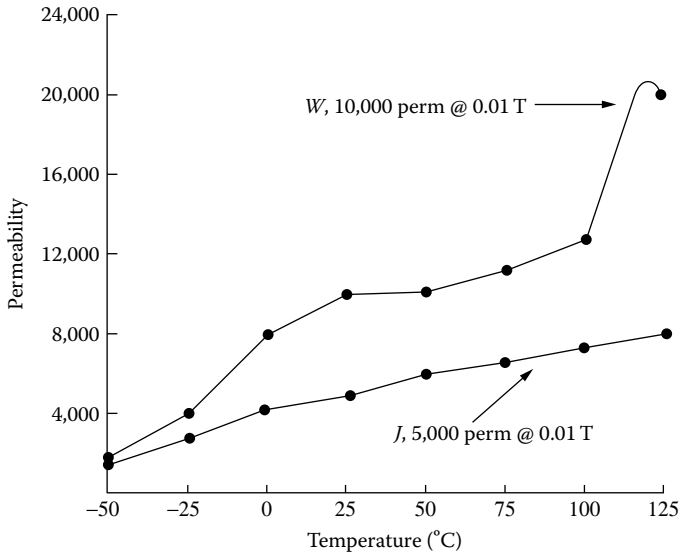

Figure 23-21. Changes in Permeability with Temperature.

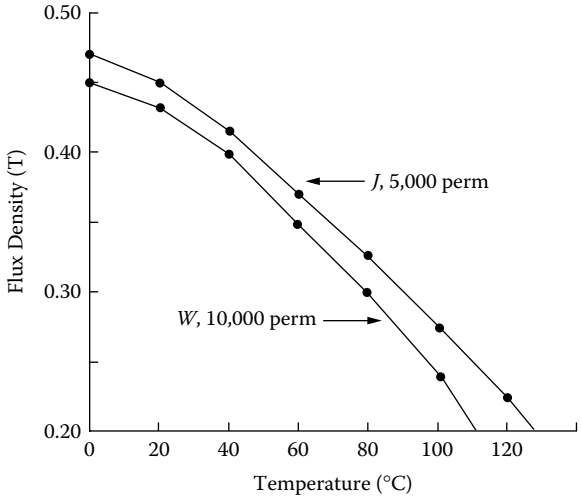

Figure 23-22. Changes in Flux Density with Temperature.

Ferrite Stress Characteristics

Ferrite Materials are susceptible to mechanical stress, both in compression and tension. High permeability materials are particularly affected with negative changes in permeability under moderate stresses. If it is important that the inductance be fairly stable in operation, then, after the units are built, temperature cycling will help relieve the pressure and stabilize the core. Also, if the turns are kept to a minimum and the epoxy encapsulant is brushed on with a very thin coating, it will help. The ferrite core should be checked before using for cracks and fissures. Below are two conditions to remember when using ferrites:

1. An encapsulant will cause stresses.
2. Winding directly on the core will cause stresses.

© 2011 by Taylor and Francis Group, LLC

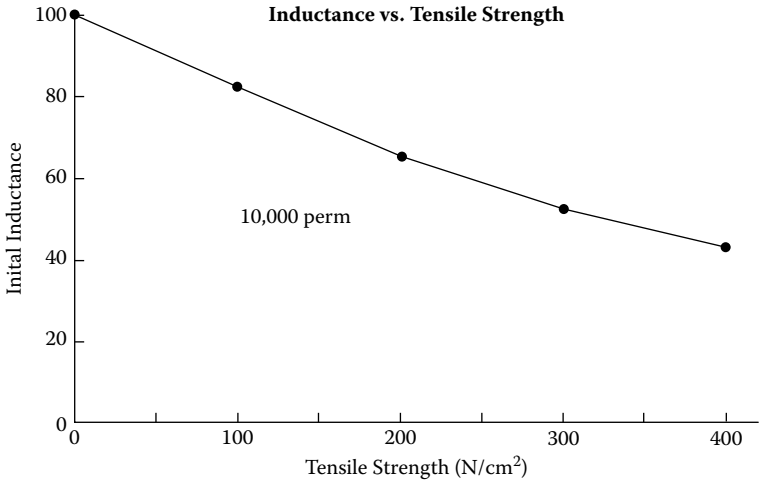

Figure 23-23. Toroidal Common Mode Filter Inductor

Core Saturation

It has been shown that some amount of differential flux exits the core from each winding. This leakage flux is proportional to both the line current and leakage inductance of the winding. Because the leakage flux leaves the core and is not canceled, it is then possible to saturate the core under high currents. Care must be taken to reduce the leakage inductance. The windings on the core should be wound identical so they look like a mirror image of each other. When selecting a core and you have a choice, always pick a core that has the highest permeability. A core selected with the highest permeability requires fewer turns for the required inductance. A design with fewer turns means less leakage flux.

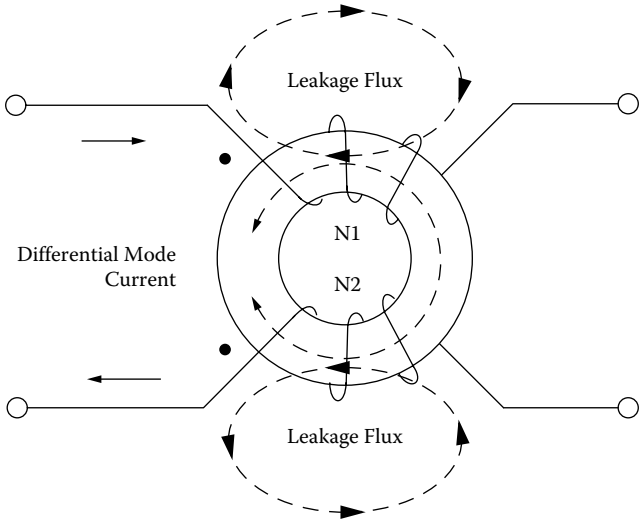

Figure 23-24. Toroidal Common Mode Filter Inductor with Leakage Flux.

© 2011 by Taylor and Francis Group, LLC

Common Mode Filter Inductor Design Specification

1. Core Configuration = Toroid
2. Core Material = Ferrite
3. Material Permeability, W (+/–30) = 10,000 u
4. Line Current, I_{in} = 0.5 amps
5. Coil Reactance at 10 kHz, X_L = 100 ohms
6. Current Density = 400 per cm^2
7. It will use a Nylon Spacer = LP, TS series*
8. Mounting = LP, Vertical*
9. Core Selected P/N = TC-41605
10. Outside Diameter, O.D = 1.664 cm
11. Inside Diameter, I.D = 0.812 cm
12. Core Height, Ht = 0.521 cm

* See Reference #9

Step No. 1: Calculate the bare wire area, $A_{w(B)}$.

$$A_{w(B)} = \frac{I_{in}}{J}, \ [cm^2]$$

$$A_{w(B)} = \frac{0.5}{400}, \ [cm^2]$$

$$A_{w(B)} = 0.00125, \ [cm^2]$$

Step No. 2: Go to the wire Table in Chapter 4, Table 4-9, column 2 and select a wire area with the closest calculated bare wire area, $A_{w(B)}$ from Step Number 1. Then, record the wire size AWG from Column 1, the bare wire area from Column 2, and the resistance in micro-ohms from Column 4 and the wire diameter with insulation from Column 7.

Column 1, #26 [AWG]
Column 2, 0.00128 cm^2 [Wire Area]
Column 4, 1345 [μohms per cm]
Column 7, 0.0452 cm [Diameter with Insulation]

Step No. 3: The design will have a nylon spacer to separate the coils, as shown.

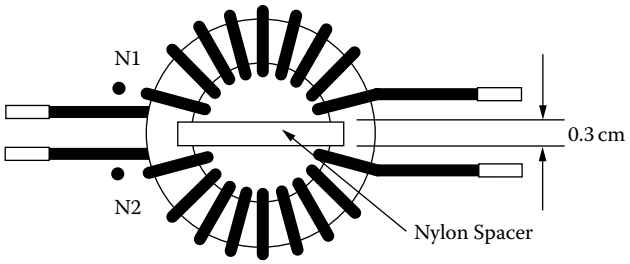

© 2011 by Taylor and Francis Group, LLC

Step No. 4: Calculate the minimum inductance, L.

$$L_{(\min)} = \frac{X_L}{2\pi f}, \quad \text{[henrys]}$$

$$L_{(\min)} = \frac{100}{2(3.14)(10000)}, \quad \text{[henrys]}$$

$$L_{(\min)} = 0.00159, \quad \text{[henrys]}$$

Step No. 5: Choose a core size from Chapter 3, Table 3-52. Then record ID and the AL value for the 1 Kperm core. Choosing the correct core on the first or second go-around takes a little skill and luck.

$$\text{Core} = \text{TC-41605}$$

$$ID = 0.812, \quad \text{[cm]}$$

$$\text{A}_\text{L}\text{, for a 1000 perm, } \frac{\text{mh}}{1000\text{T}} = 548, \quad \text{[factor]}$$

Step No. 6: Calculate the millihenrys per 1000 turns for W material in kiloperm.

$$A_L = \left(\frac{mh}{1000\text{T}}\right)\left(W_{kiloperm}\right), \quad \text{[mh per 1000 turns]}$$

$$A_L = (548)(10), \quad \text{[mh per 1000 turns]}$$

$$A_L = 5480, \quad \text{[mh per 1000 turns]}$$

Step No. 7: Calculate the total winding mean length.

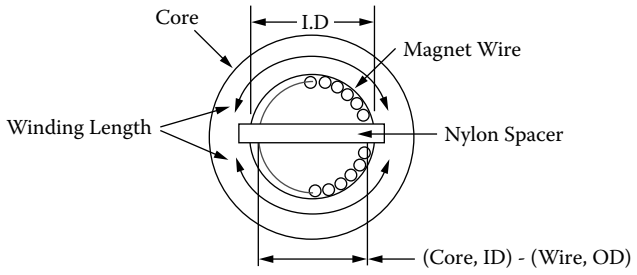

$$\text{Winding Length} = \pi(\text{Core, ID} - \text{Wire, OD}) - 2(\text{Spacer, Width})$$

$$\text{Winding Length} = 3.14(0.812 - 0.0452) - 2(0.3)$$

$$\text{Winding Length} = 1.81, \quad \text{[cm]}$$

Step No. 8: Calculate the winding length per coil.

$$\text{Winding Length per coil} = \frac{\text{Total Winding Length}}{2}, \quad \text{[cm]}$$

$$\text{Winding Length per coil} = \frac{1.81}{2}, \quad \text{[cm]}$$

$$\text{Winding Length per coil} = 0.905, \quad \text{[cm]}$$

© 2011 by Taylor and Francis Group, LLC

Step No. 9: Calculate the number of turns possible using #26 for each coil.

$$\text{Turns} = \frac{\text{Winding Length (cm)}}{\text{Wire Diameter (cm)}}, \quad \text{[turns]}$$
$$\text{Turns} = \frac{0.905}{0.0452}, \quad \text{[turns]}$$
$$\text{Turns} = 20, \quad \text{[turns]}$$

Step No. 10: Calculate the inductance, L using the low end of the permeability (–30%).

$$L = \left(\frac{mh}{1000T}\right) N^2 (10^{-6}), \quad \text{[millihenrys]}$$
$$L = (3836)(20)^2 (10^{-6}), \quad \text{[millihenrys]}$$
$$L = 1.53, \quad \text{[millihenrys]}$$

Step No. 11: Calculate the mean length turn.

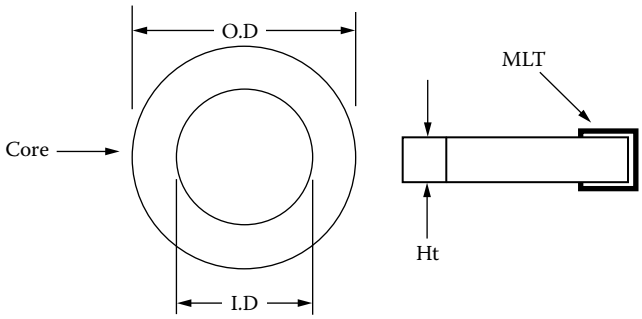

$$\text{MLT} = (OD - ID) + 2(Ht), \quad \text{[cm]}$$
$$\text{MLT} = (1.664 - 0.812) + 2(0.521), \quad \text{[cm]}$$
$$\text{MLT} = 1.894, \quad \text{[cm]}$$

Step No. 12: Calculate the winding resistance of a coil, R.

$$R = \text{MLT}(N1)\left(\frac{\mu\Omega}{\text{cm}}\right) x10^{-6}, \quad \text{[ohms]}$$
$$R = 1.89(20)(1345)\, x10^{-6}, \quad \text{[ohms]}$$
$$R = 0.0508, \quad \text{[ohms]}$$

Step No. 13: Calculate the total copper loss for both coils, P_{cu}.

$$P_{cu} = I_{in}^2\, 2(R), \quad \text{[watts]}$$
$$P_{cu} = (0.5)^2\, 2(0.0508), \quad \text{[watts]}$$
$$P_{cu} = 0.0254, \quad \text{[watts]}$$

© 2011 by Taylor and Francis Group, LLC

Step No. 14: The common mode inductor is assembled in the vertical mount and ready for test.

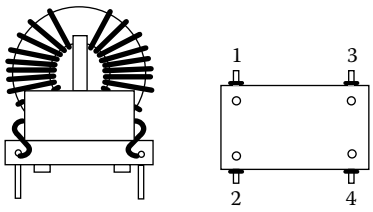

Vertical Toriodal Mount

References

1. Magnetics Technical Bulletin, FC-S5, 1997.

2. Magnetics Technical Bulletin, FC-S2, 1995.

3. Magnetics Ferrite Catalog, FC-601, 2006.

4. Sebranig, Steve and Leonard Crane, *Guide for Common Mode Filter Design Coilcraft*, 1985.

5. Kociecki, John, Predicting the Performance of Common-Mode Inductors, Data General Corporation, n.d.

6. Nave, Mark, A Novel Differential Mode Rejection Network for Conducted Emissions Diagnostics, IEEE, 1089.

7. Leonard Crane, Sebranig, Steve, *Common Mode Filter Inductor Analysis*, Coilcraft Publication, 1985.

8. Ozenbaugh, Richard, *EMI Filter Design*, CRC Press, New York, 2001.

9. Lodestone Pacific, VTM Series, Vertical Toroid Mount, 2002.

© 2011 by Taylor and Francis Group, LLC

Chapter 24

Series Saturable Reactor Design

© 2011 by Taylor and Francis Group, LLC

Table of Contents

1. Introduction 24-3
2. The Series Saturable Reactor 24-3
3. Basic Operation 24-4
4. How the Series Saturable Reactor Operates 24-6
5. Control Winding 24-8
6. Saturated Inductance and Winding Resistance 24-9
7. Saturable Reactor Power Gain 24-10
8. Response Time for Saturable Reactors 24-11
9. Saturable Reactor Apparent Power, P_t 24-12
10. Mean Length Turn for E Cores 24-13
11. Calculating, MLT for Toroidal Cores 24-14
12. Toroidal Saturable Reactor Surface Area 24-15
13. E Core Saturable Reactor Surface Area 24-16
14. Designing with Toroidal Tape Cores 24-17
15. Comparing the Toroidal Tape Cores with the Laminations 24-17
16. Series Saturable Reactor Design Example 24-18
17. Specification and Design 24-19
18. Series Saturable Reactor Design Test Data (Core Geometry, K_g, Approach) 24-24
19. Ultra Low Power 0-15 Amp Current Transducer (Saturable Reactor) 24-26
20. Summary 24-30
21. Recognition 24-30
22. References 24-31

© 2011 by Taylor and Francis Group, LLC

Introduction

The saturable reactor is a magnetic device that had great popularity in 1950 and 1960, but when the transistor and silicon controlled rectifier came along, the saturable reactor nearly fell out of sight. The saturable reactor is still being used in motor control, power supplies and current transducers. It is also rugged and provides good electrical isolation between input and output.

The Series Saturable Reactor

The saturable reactor circuit diagram is shown in Figure 24-1. The saturable reactor being used as a current transducer is shown in Figure 24-2. The saturable reactor has two gate windings connected in series opposing and a single control winding. The saturable reactor can be constructed using two toroidal cores, DU or EI lamination. The saturable reactor works best when using a square loop and high permeability magnetic material. The saturable reactor is an amp-turn device. Amp-turns in the control winding will produce amp-turns in the gate winding. The amp-turn Equation is [24-1]:

$$N_{c(5-6)}I_c = N_{g(1-2)}I_g \qquad [24\text{-}1]$$

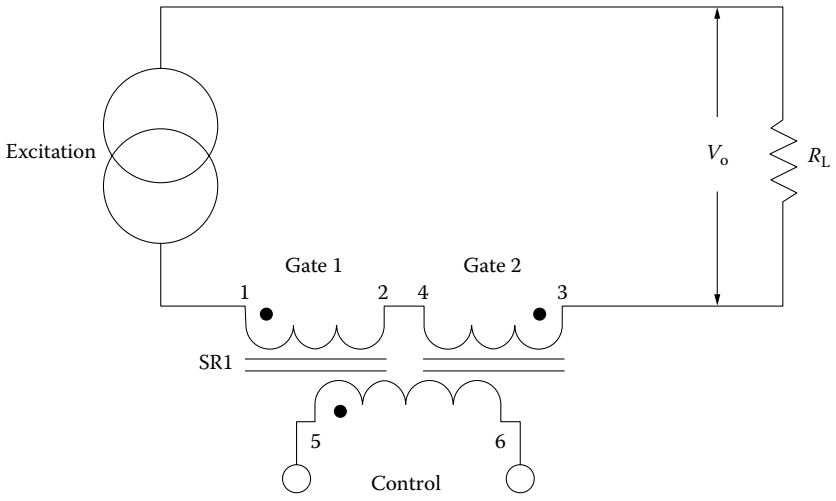

Figure 24-1. The Basic Two Core Series Saturable Reactor.

© 2011 by Taylor and Francis Group, LLC

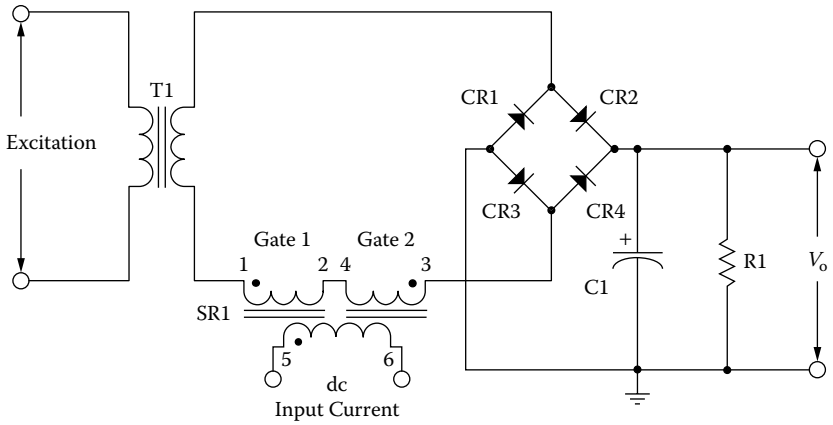

Figure 24-2. Series Saturable Reactor used as a Current Transducer.

Basic Operation

To understand the saturable reactor operation, we will go through the functional steps of the operation using an EI core, as shown in Figure 24-3. The core material is a square-loop, grain-oriented type 50-50 Nickel-Iron (Orthonol) with a high relative permeability. The gate windings, N_{g1}, and N_{g2}, on the outer legs of the EI core both have the same number of turns. The control winding, N_c, is wound on the center leg of the EI core. As shown in Figure 24-3, a dc current is applied to the control winding, N_c, via the battery, E_c. Under these conditions a magnetic flux is generated in the core. As can be seen by the arrows, the flux travels up in the center leg and down in the outer legs. If the dc control current is reversed, the direction of the flux is reversed, but nothing else changes.

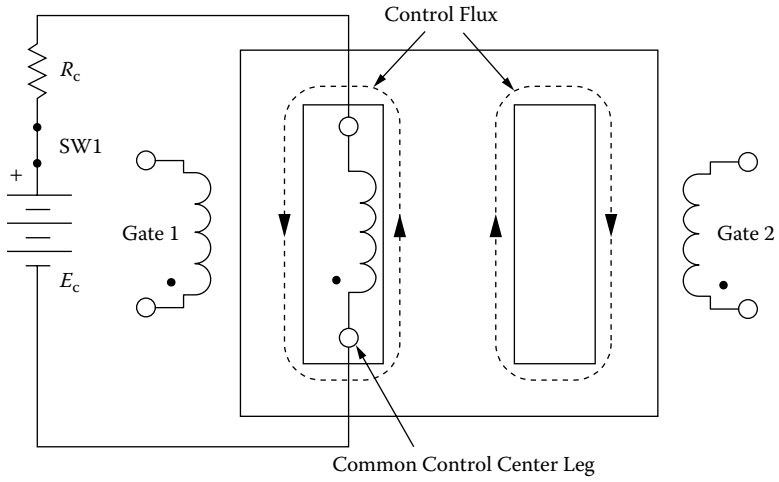

Figure 24-3. Magnetic Flux Produced by the Control Winding Alone.

The ac excitation will now be applied to the gate windings connected in series, which are opposing along with the load resistor, R_L. The dc current will be removed from the control winding, as shown in Figure 24-4. Each gate is designed to support ½ of the applied ac excitation voltage. The direction of the magnetic flux generated by the gate windings is shown in Figure 24-4. The flux is in the downward direction in the right leg, and in

© 2011 by Taylor and Francis Group, LLC

an upward direction in the left leg of the EI core, as indicated by the arrows. The flux generated by the gate windings is opposite and equal, and is relatively independent of each other. The flux in each gate is in a static mode when there is no dc control current, as shown in Figure 24-5.

When the gates are supporting all of the applied voltage and the control winding dc current is zero, then the output voltage, V_o, measured across the load resistor, R_L, will be caused by the magnetizing current, I_m, as shown in Figure 24-6. The magnetizing current, I_m, can be calculated using Equation [24-2]. If the magnetizing current, I_m, is to be reduced the engineer have two alternatives: reduce the operating flux density, B_m, or change the magnetic material to a material that requires less drive.

$$I_m = \frac{V_o}{R_L}, \quad \text{[amps]} \qquad \text{[24-2]}$$

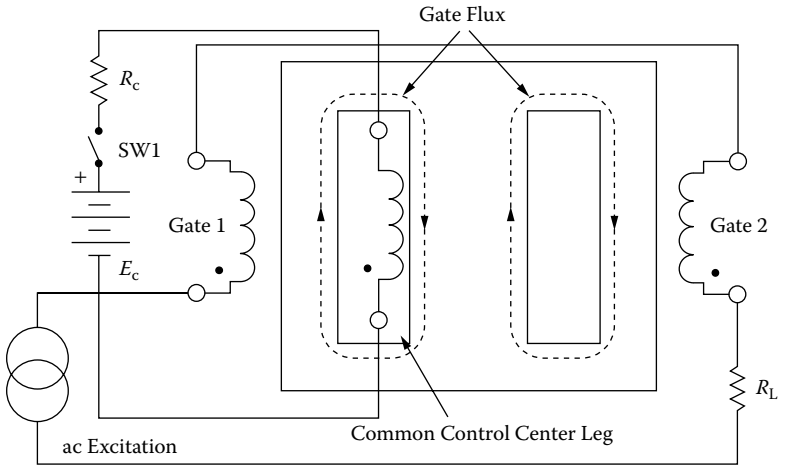

Figure 24-4. Magnetic Flux Produced by Both Gate Windings.

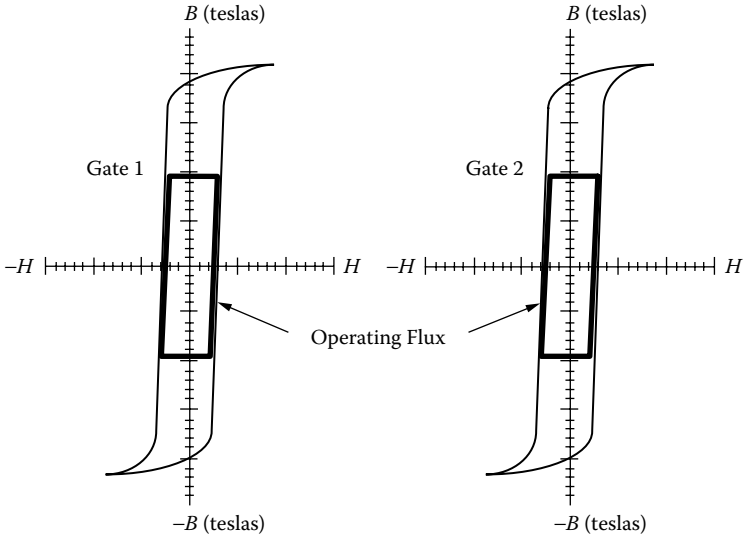

Figure 24-5. Gate Operating Flux with No dc Control Current.

© 2011 by Taylor and Francis Group, LLC

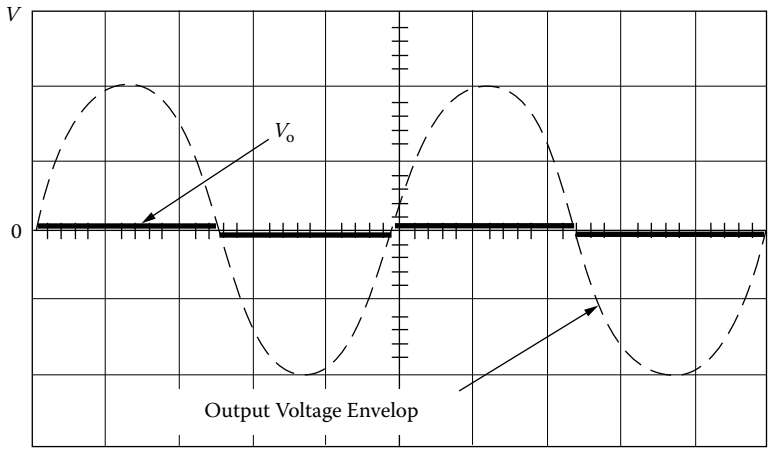

Figure 24-6. Output Voltage Caused by the Magnetizing Current I_m.

How the Series Saturable Reactor Operates

Now both conditions can be combined. Enough current needs to be applied in the control winding to produce a 50% duty cycle and ac excitation then is applied to the gates, as shown in Figure 24-7. The control winding produces flux in the center leg and in both outer legs in the same direction. The flux, produced by Gate 1 in the left leg, is in the opposite direction to the flux produced by the control winding in the center leg. The flux, produced by Gate 2 in the right leg, is in the same direction as the flux produced by the control winding in the center leg. The net result is the amp-turns (N_cI_c) in the control winding will bias the core into saturation to satisfy the Equation [24-3]. This saturation of the core leg will create an output voltage across the load resistor, R_L as shown in Figure 24-8.

$$I_{g2} = \frac{N_c I_c}{N_{g2}}, \qquad [24\text{-}3]$$

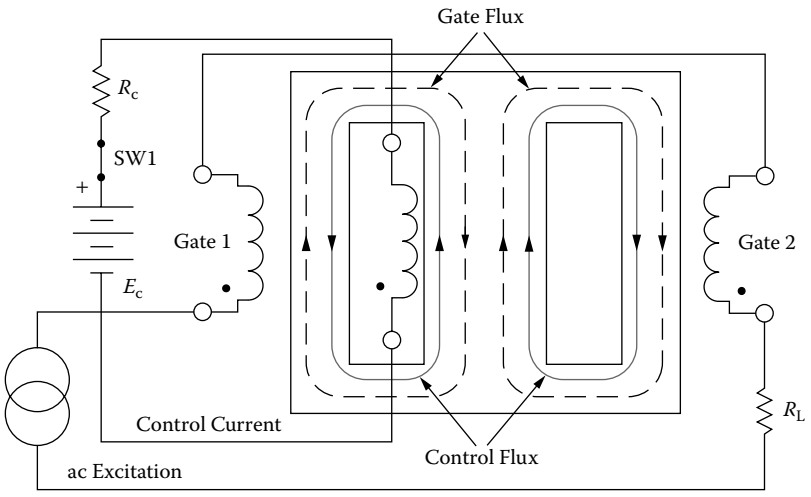

Figure 24-7. The Magnetic Flux for Is Shown for Both Gate Windings and the Control Winding.

© 2011 by Taylor and Francis Group, LLC

The saturable reactor gates are connected in series. Whatever current is flowing in Gate 2 is also flowing in Gate 1, but the amp-turns flowing in the control winding is in the opposite direction to Gate 1 and the net result is they cancel each other, as shown in Equation [24-4].

$$0 = N_{g1}I_{g1} - N_cI_c \qquad [24\text{-}4]$$

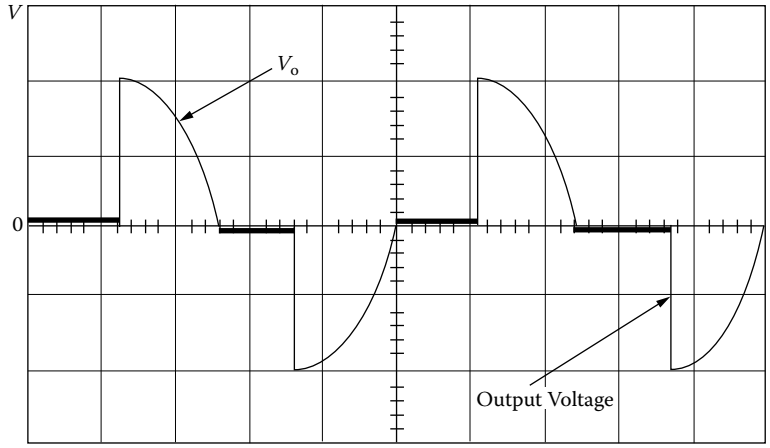

Figure 24-8. Output Voltage Across the Load Operating at a 50% Duty Cycle.

This condition reverses every half cycle and Gate 1 will go into saturation, while Gate 2 will come out of saturation. The B-H loops in Figure 24-5 will now change, when the current is flowing in the control winding. The flux in Gate 1 is still symmetrical around the origin, while Gate 2 goes into saturation, as shown in Figure 24-9. When the input ac excitation reverses on the next half cycle, the gate flux also reverses and Gate 1 goes into saturation and Gate 2 goes out of saturation, as shown in Figure 24-10.

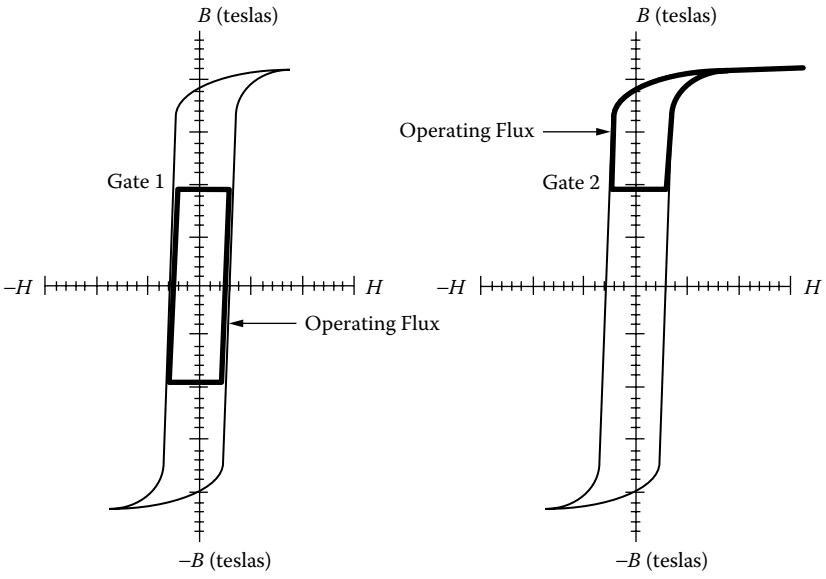

Figure 24-9. The Control Current Is Forcing Gate 2 into Saturation.

© 2011 by Taylor and Francis Group, LLC

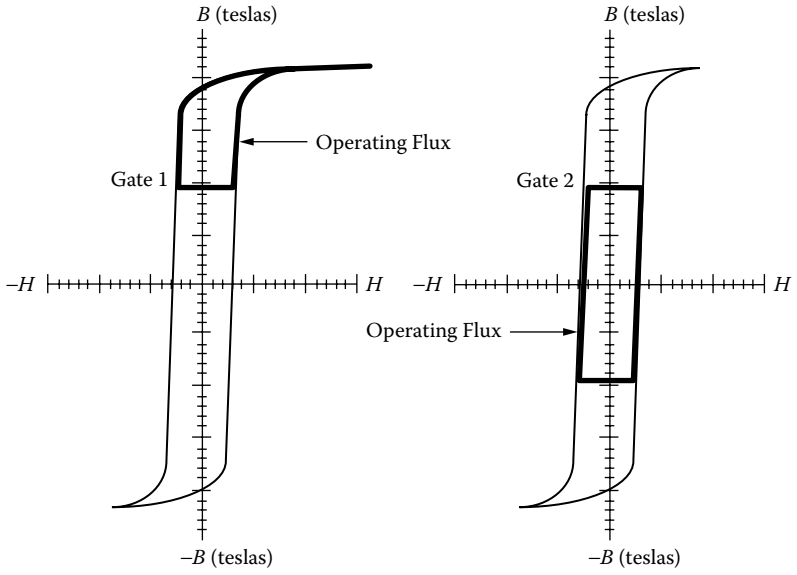

Figure 24-10. The Control Current Is Forcing Gate1 into Saturation.

Control Winding

With the ac excitation applied to the gates and without any dc control current applied, the net change in flux through the control winding is zero, making the induced voltage in the control winding zero. This condition is true because the flux generated by the opposing gates in the center leg of the EI core cancels. It can only be true if there are equal turns on each gate and the permeability of the outer legs of the EI core is equal. To minimize the unbalance that can occur because of the gate windings and core material, there is usually a test specification written to control the gate turns and the permeability of the material.

The induced voltage in the control winding is from the above example operating at a 50% duty cycle, as shown in Figure 24-11. If the ac excitation to the gates were a square wave then the induced voltage would be a square

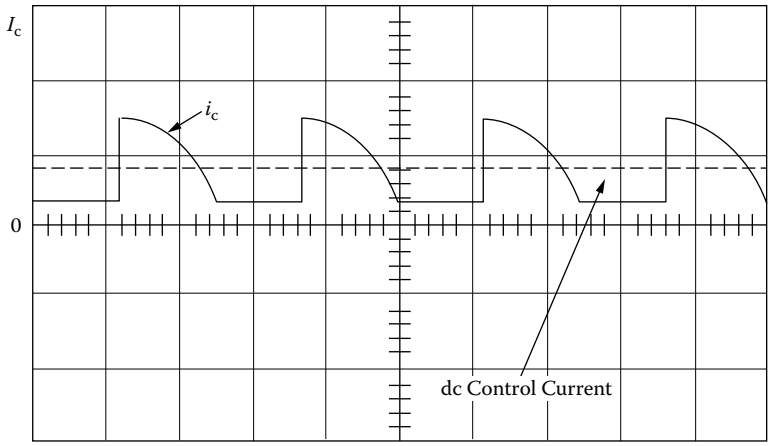

Figure 24-11. The Induced Voltage in the Control Winding Is from a Sine Wave Excitation.

© 2011 by Taylor and Francis Group, LLC

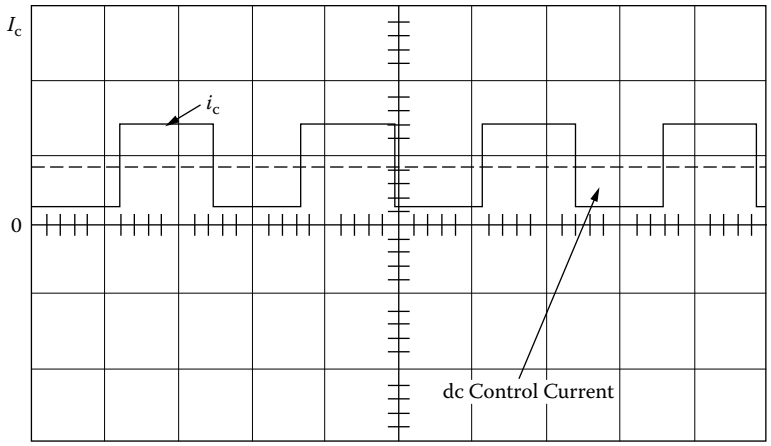

Figure 24-12. The Induced Voltage in the Control Winding Is from a Square Wave Excitation.

wave, as shown in Figure 24-12. The induced voltage in the control winding is always the second harmonic of the operating frequency. The second harmonic is caused by the changing flux in the core not at saturation.

Saturated Inductance and Winding Resistance

After the saturable reactor has been built it would be wise to measure all of the parameters before designing the rest of the circuit. This is because the output voltage at the load could be lower than the design voltage, as shown in Figure 24-13. This discrepancy is because of the winding resistance and the saturated inductance of the saturable reactor. The saturated inductance is a built-in ac resistor that will support voltage after the magnetic core has been saturated with the control amp-turns. If the magnetic material is ideal and the core is saturated, the permeability will drop to zero. All you will have then is an air core inductor. The saturated

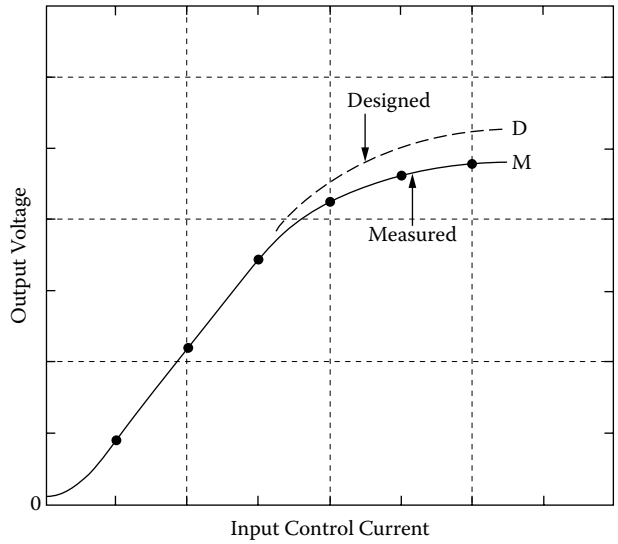

Figure 24-13. Comparing the Design and Measured Output Voltage at the Load.

© 2011 by Taylor and Francis Group, LLC

inductance is very dependent on the magnetic material and its configuration. Depending on the design the engineer has the choice of laminations, C cores or toroids. Toroidal cores, by their construction, have the minimum of air gap. Both laminations and C cores have air gaps and this results in shearing over the hysteresis loop. See Chapter 2. To minimize the saturated inductance pick a material and construction that will provide a minimum of air gap, high permeability and a high flux density, if possible.

The magnetic materials provide two types of B-H loops, a high permeability square loop and a round loop to do the design, as shown in Figure 24-14. The square B-H loop found in Figure 24-14 is typical of what is found in toroidal cores. The X marks the B_{sat} of the magnetic material. If the excitation is increased, the horizontal line above the X will just become longer and B_{sat} remains constant. The round B-H loop found Figure 24-14 is typical of what is found with laminations because of the small air-gaps. The Y marks the, B_{sat}, for the high permeability magnetic material within the core. If the excitation is increased the diagonal line above the Y will also increase upward. The diagonal line above Y shows, B_{sat}, has not been completely reached because of the small air gaps and will take more H to accomplish, B_{sat}.

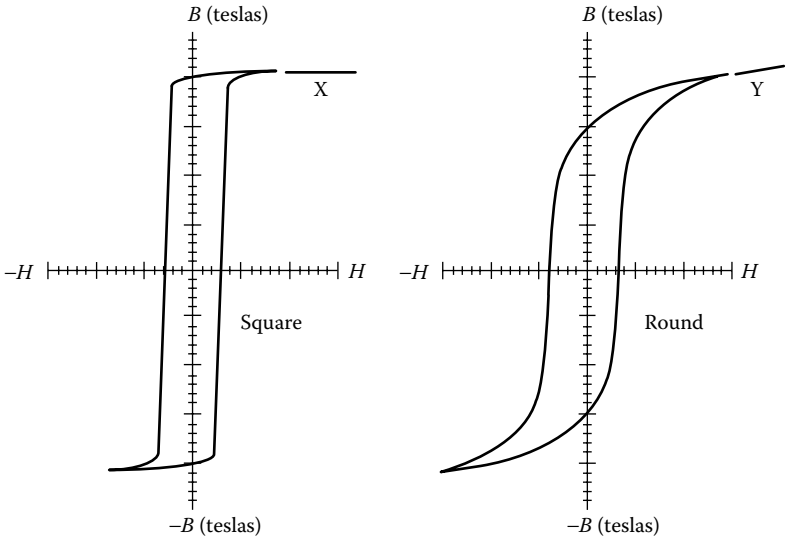

Figure 24-14. Comparing Square and Round B-H Loops.

Saturable Reactor Power Gain

One of the qualities of a saturable reactor is based on its power gain. The power gain is dependent to a great deal upon the design, type, and physical size of the saturable reactor. Power gain of a saturable reactor is the ratio of the input control power, P_c, to the output or load power, P_o. The input control power is the power

© 2011 by Taylor and Francis Group, LLC

dissipated in the control winding. The control power, P_c, is the power dissipated in the control winding, as shown in Equation [24-5]. The control current is, I_c, and the winding resistance is, R_c. The output power, P_o, is the power delivered to the load, as shown in Equation [24-6]. The current flowing in the gate winding is, I_g, and the load resistance is, R_L. The power gain then is the output power, P_o, divided by the control power, P_c, as shown in Equation [24-7].

$$P_c = I_c^2 R_c, \quad \text{[watts] [control]} \tag{24-5}$$

$$P_o = I_o^2 R_L, \quad \text{[watts] [load]} \tag{24-6}$$

$$P_{(gain)} = \frac{\left(I_o^2 R_L\right)}{\left(I_c^2 R_c\right)}, \quad \text{[power gain]} \tag{24-7}$$

The currents in the saturable reactor are inversely proportional to the turn's ratio, so Equation [24-7] can be rewritten to Equation [24-8]. The control turns are, N_c, and the gate turns (single gate) are, N_g.

$$P_{(gain)} = \frac{\left(N_{c(5-6)}^2 R_L\right)}{\left(N_{g(1-2)}^2 R_c\right)}, \quad \text{[power gain]} \tag{24-8}$$

The above two Equations [24-7] and [24-8] are without feedback.

Response Time for Saturable Reactors

The response time, t_r, for a saturable reactor is very slow for a step change in the control signal. This is because the control winding is very inductive. Any step change in current in the control winding will take time to reach its final value. The response time, t_r, is given as a time constant of the control circuit. The response time is the time it takes for the load current to reach 63 percent of its final value for a step input change as shown in Figure 24-15. It can be seen in Figure 24-15, when there is an input step change, t_1, in the control circuit, the output current, I_1, will rise from its initial value at, t_1, to its final value of, I_3, at time, t_3. The value of, I_2, is the current at 63 percent of the final current, I_3, which is a one time constant. The time constant is shown in Equation [24-9].

$$t_r = \frac{L_c}{R_c}, \quad \text{[seconds]} \tag{24-9}$$

t_r = [seconds], [time constant]

L_c = [henries], [contral winding inductance]

R_c = [ohms], [contral winding resistance]

This concept was derived from linear systems. It yields sufficiently accurate results for most purposes.

© 2011 by Taylor and Francis Group, LLC

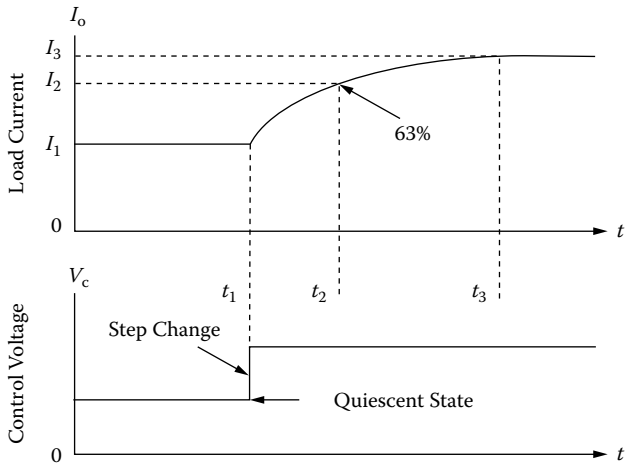

Figure 24-15. Output Response Time for an Input Signal Step Change.

Saturable Reactor Apparent Power, P_t

Each gate of the saturable reactor, SR1, will support half of the output voltage to the load. The volt-amps, VA, of the saturable reactor, SR1, are equal to the volt-amps, VA, of the load. The amp-turns in the control winding will produce amp-turns in the gate winding, as shown in Equation [24-10]. If the volt-amps of the gates are equal to the volt-amps of the control, then the window area is divided equally between the gate and the control, as shown in Figure 24-16.

$$N_{c(5-6)}I_c = N_{g(1-2)}I_g \qquad [24\text{-}10]$$

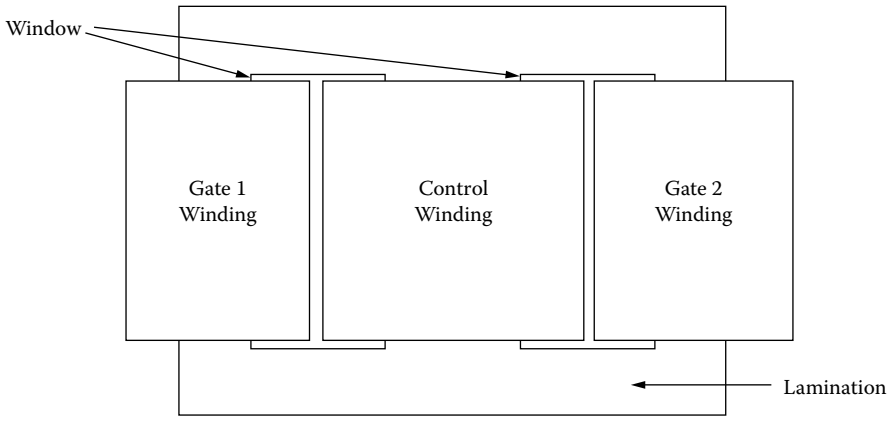

Figure 24-16. Series Saturable Reactor Showing Gate and Control Window Allocation.

To have full control of the output voltage from, T1, as shown in Figure 24-2, the volt-amps of the saturable reactor, SR1, must equal the volt-amps of the load, P_o. The saturable reactor, SR1, has a gate winding and a common control winding. Both are equal to one-half the load power, P_o, as shown in Equation [24-11].

© 2011 by Taylor and Francis Group, LLC

$$P_t = 0.5P_o\left(\frac{1_{(gate)}}{\eta} + 1_{(control)}\right), \quad \text{[watts]} \tag{24-11}$$

The apparent power, P_t, calculated in Equation 24-11 is for each core of a saturable reactor using two cores, such as a toroid, as shown in Figure 24-18. The total apparent power, P_t, is shown in Equation [24-12]. The Equation [24-12] would be used for designs using laminations. It must be remembered that the gates are wound on the outer legs of the lamination where the cross-section, A_c, is normally only half the center leg.

$$P_t = P_o\left(\frac{1_{(gate)}}{\eta} + 1_{(control)}\right), \quad \text{[watts]} \tag{24-12}$$

The electrical conditions, K_e, for the core geometry, K_g, are shown in Equation [24-13].

$$K_e = 0.145K_f^2 f^2 B_m^2 (10^{-4}) \tag{24-13}$$

The calculation for the core geometry, K_g, is shown in Equation [24-14].

$$K_g = \frac{P_t}{2K_e\alpha}, \quad [\text{cm}^5] \tag{24-14}$$

Note: Alpha, α, is the combined copper loss of the saturable reactor control and gate windings. The core calculation for the core geometry, K_g, is shown in Equation [24-15].

$$K_g = \frac{W_a A_c^2 K_u}{\text{MLT}}, \quad [\text{cm}^5] \tag{24-15}$$

Mean Length Turn for E Cores

The Mean Length Turn, (MLT), is required to calculate both winding resistance and weight for given winding. Using the EI lamination in a saturable reactor design requires the calculation of the resistance of both control and gate windings. The winding dimensions, relating to the Mean Length Turn, (MLT) for a tube or bobbin coil, are shown in Figure 24-17. The Mean Length Turn, (MLT) for the control winding is shown in Equation 24-16 and the Mean Length Turn, (MLT) for the gate windings, is shown in Equation [24-17].

$$\text{MLT}_{(control)} = 2(D + 2B) + 2(E + 2B) + 2\pi\left(\frac{F}{4}\right), \quad \text{[cm]} \tag{24-16}$$

$$\text{MLT}_{(gate)} = 2(D + 2B) + 2\left(\frac{E}{2} + 2B\right) + 2\pi\left(\frac{F}{4}\right), \quad \text{[cm]} \tag{24-17}$$

© 2011 by Taylor and Francis Group, LLC

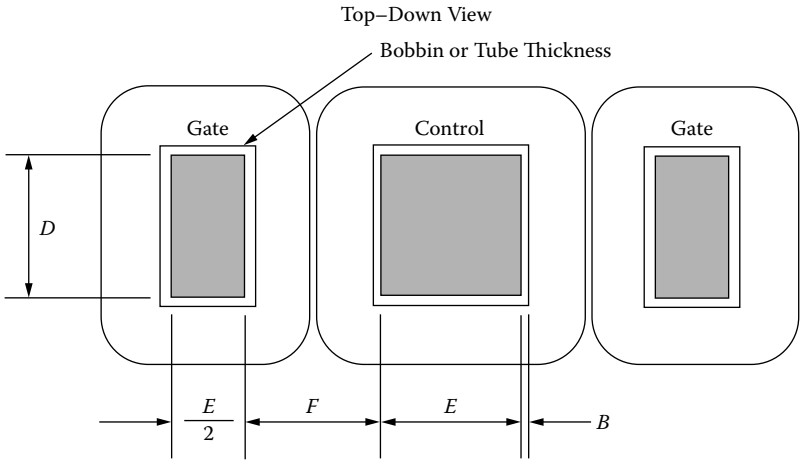

Figure 24-17. Dimensions, Relating to the Mean Length Turn, (MLT).

Calculating, MLT for Toroidal Cores

In order to wind the toroidal core, there has to be room to allow free passage of the wire shuttle. The wire shuttle could be a machine shuttle or a hand wind shuttle. Winding a saturable reactor is not any different than winding any other toroidal core. Half of the inside diameter will be set aside for the shuttle clearance. This will leave 75% of the window, W_a, for the windings. It is very difficult to calculate the Mean Length Turn (MLT) for a toroidal core used in saturable reactor design that would satisfy all conditions. The saturable reactor has two cores and each core has its own gate winding. The gate winding is wound first. After the gate winding is wound, the cores are tested and matched, then they are assembled for the common control winding to be wound. The assembly of the toroidal cores can be seen in Figure 24-18. The fabrication of a toroidal design is weighted heavily on the skill of the winder. The toroidal core saturable reactor requires special attention, when wound by hand or wound by machine, because of the angle it imposes when two cores are stacked. The Mean Length Turn, (MLT) for a toroidal saturable reactor is very difficult to obtain, because its shape is very non-linear. A good approximation for a toroidal core, Mean Length Turn (MLT) for the gate winding is Equation [24-18] and Equation [24-19] for the control winding, shown in Figure 24-18. There is a correction factor of 0.85 for the gate winding and a correction factor of 0.70 for the control winding.

Nomenclature clarification:

1. A = Core strip width including the case. Core Height
2. B = Core build including the case. (OD – ID) / 2
3. C = Is the build of both gate and control winding = W/4
4. D = Is the build of the gate, = W/8
5. W = Is the inside diameter of the core including the case.

© 2011 by Taylor and Francis Group, LLC

$$\text{MLT} = (2A) + (2B) + \pi 0.125W)(0.85), \quad \text{approximation [Gate]} \tag{24-18}$$

$$\text{MLT} = (4A + 0.25W) + (2B) + 2\pi(0.375W)(0.70), \quad \text{approximation [Control]} \tag{24-19}$$

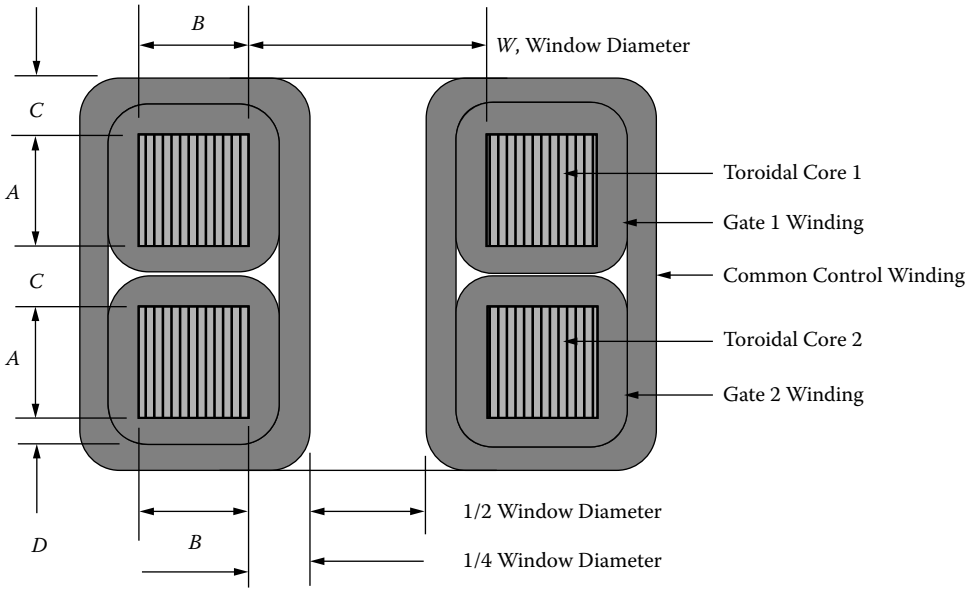

Figure 24-18. Toroidal Core Saturable Reactor Mean Length Turn, (MLT) is a Good Approximation.

Toroidal Saturable Reactor Surface Area

The data such as height and outside diameter required for the surface area calculation, was taken from Figure 24-18. The height, Ht, of the saturable reactor is shown in Equation [24-20] and the outside diameter, OD, is shown in Equation [24-21]. The saturable reactor outline is shown in Figure 24-19.

$$Ht = (3C + 2A)$$
$$OD = (2C + 2B + W)$$

$$A = (\text{Core Height, Ht}),\ B = (\text{Core Build, (OD-ID)}/2),\ C = (\text{Winding Build, } W/4 = ID/4)$$

$$SR_{Ht} = \left(3\left(\frac{ID}{4}\right) + 2Ht\right) \tag{24-20}$$

$$SR_{OD} = \left(\left(\frac{ID}{2}\right) + (OD - ID) + ID\right) \tag{24-21}$$

© 2011 by Taylor and Francis Group, LLC

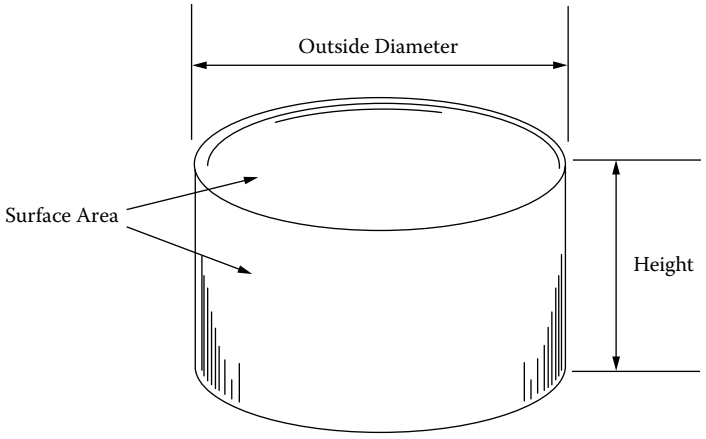

Figure 24-19. The Outline of a Toroidal Wound Saturable Reactor.

The surface area of the saturable reactor can be calculated using Equation, [24-24].

$$\text{Top and Bottom Surface} = 2\left(\frac{\pi\left(SR_{OD}\right)^2}{4}\right), \quad [\text{cm}^2] \qquad [24\text{-}22]$$

$$\text{Periphery Surface} = \left(\pi\left(SR_{OD}\right)\right)\left(\text{SR}_{\text{Ht}}\right), \quad [\text{cm}^2] \qquad [24\text{-}23]$$

$$A_t = \frac{\pi\left(SR_{OD}\right)^2}{2} + \left(\pi\left(SR_{OD}\right)\right)\left(\text{SR}_{\text{Ht}}\right), \quad [\text{cm}^2] \qquad [24\text{-}24]$$

E Core Saturable Reactor Surface Area

The data for height, width and length required for the surface area calculation was taken from Chapter 3. The height, Ht, is (E+G), the width, is (D+F), and length is (2E+3F). The saturable reactor outline is shown in Figure 24-20. The surface area for an E core saturable reactor can be calculated using Equation, [24-28].

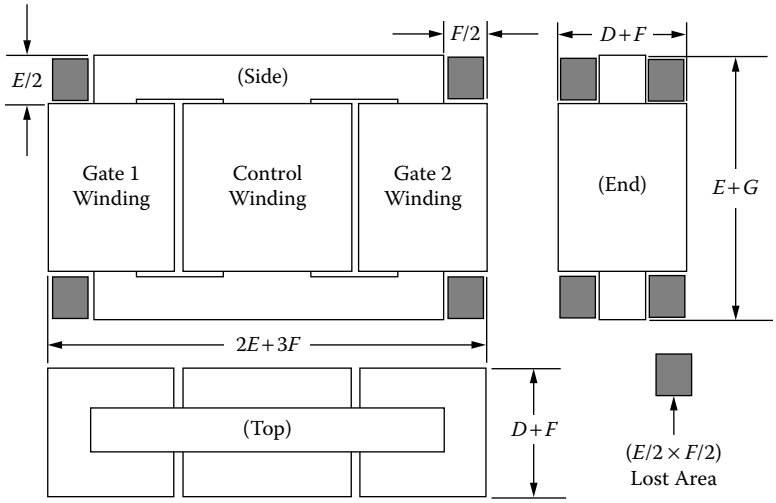

Figure 24-20. The Outline of an E Core Wound Saturable Reactor.

© 2011 by Taylor and Francis Group, LLC

$$\text{Side Area} = (2E + 3F)(E + G) - (EF), \quad [\text{cm}^2] \qquad [24\text{-}25]$$

$$\text{End Area} = (E + G)(D + F) - (EF), \quad [\text{cm}^2] \qquad [24\text{-}26]$$

$$\text{Top Area} = (2E + 3F)(D + F), \quad [\text{cm}^2] \qquad [24\text{-}27]$$

$$A_t = 2(\text{Side Area}) + 2(\text{End Area}) + 2(\text{Top Area}), \quad [\text{cm}^2] \qquad [24\text{-}28]$$

Designing with Toroidal Tape Cores

The performance of a saturable reactor using tape toroidal cores, as shown in Figure 24-21, is far more superior to using laminations. The tape toroidal core comes in a lot of sizes and shapes. The tape toroidal cores with a large window are known for their high power gain. The tape toroidal cores have a much higher permeability and can be matched to a much tighter tolerance. The tape toroidal cores, because of their construction, do not have an air gap. A core without an air gap will provide a minimum of magnetizing current. The net result is a minimum of offset voltage on the output when the control current is zero. Also, having cores with high permeability and operating at a high frequency does have a drawback. When magnetic components with high permeability cores are operating at high frequency, special care must be taken so the magnetic components do not go into self-resonates.

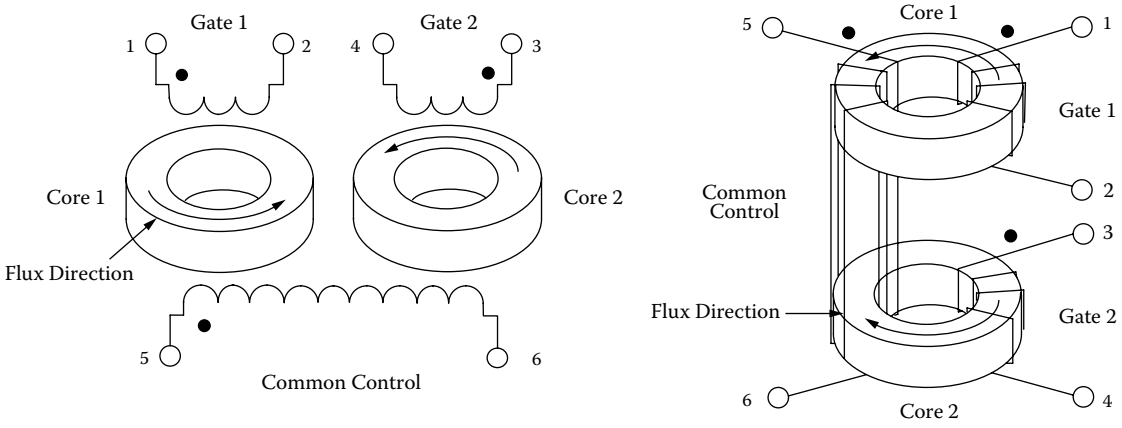

Figure 24-21. Saturable Reactor Designed Using Toroidal Cores.

Comparing the Toroidal Tape Cores with the Laminations

The schematics of a saturable reactor, using toroidal tape cores and a saturable reactor using laminations are shown in Figure 24-22. There is truly not much difference between the saturable reactor designed with laminations or toroidal tape cores, but it does bring out why the toroidal cores have to be matched.

© 2011 by Taylor and Francis Group, LLC

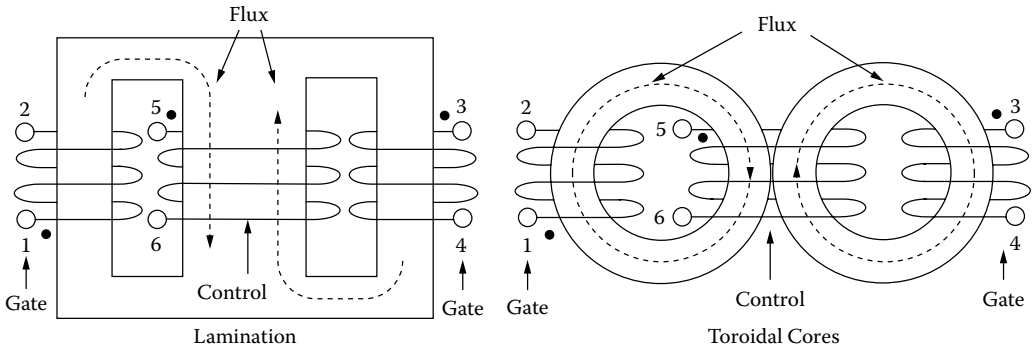

Figure 24-22. Comparing Saturable Reactors with Toroidal Cores and Laminations.

Series Saturable Reactor Design Example

The saturable reactor will control the voltage of 12.6 volts at 1.0 amps to the power an incandescent lamp. The load resistor, R1, as shown in Figure 24-23, will be 12 ohms. The load resistor, R1, is used in place of the incandescent lamp for testing. The reason for using a resistor in place of the lamp is because the lamp is a non-linear load and the transfer function looks much cleaner and more representative of the saturable reactive, SR1, output.

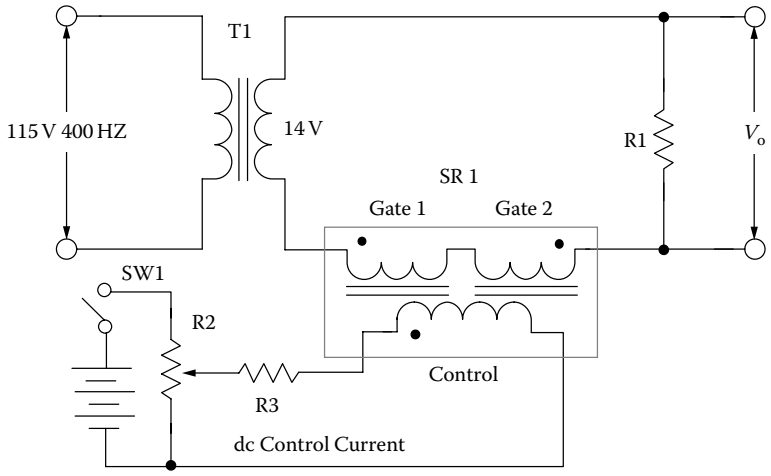

Figure 24-23. AC Power Supply being controlled by a Saturable Reactor, SR1.

© 2011 by Taylor and Francis Group, LLC

Specification and Design

1. Transformer, T1 Output Voltage = 14 volts ac
2. Operating Frequency = 400 Hz
3. Load voltage, V_o = 12.6 volts ac
4. Load Current, I_o = 1.0 amps
5. Magnetic Core Type = Toroid
6. Magnetic Material, 4 mil = 50-50 NiFe
7. Efficiency, η = 95%
8. Regulation (copper loss), α = 5%
9. Operating Flux Density, B_{ac} = 1.0 T
10. Control Current, I_c = 0.10 amps

Step No. 1: Calculate the load power, P_o.

$$P_o = V_o I_o, \quad \text{[watts]}$$
$$P_o = (12.6)(1.0), \quad \text{[watts]}$$
$$P_o = 12.6, \quad \text{[watts]}$$

Step No. 2: Calculate the saturable reactor apparent power, P_t, for a single core.

$$P_t = (0.5)P_o\left(\frac{1_{(gate)}}{\eta} + 1_{(control)}\right), \quad \text{[watts]}$$
$$P_t = (0.5)(12.6)\left(\frac{1}{0.95} + 1\right), \quad \text{[watts]}$$
$$P_t = 12.9, \quad \text{[watts]}$$

Step No. 3: Calculate the electrical conditions, K_e.

$$K_e = 0.145K_f^2 f^2 B_m^2 (10^{-4})$$
$$K_f = 4.44$$
$$K_e = 0.145(4.44)^2(400)^2(1.0)^2(10^{-4})$$
$$K_e = 45.7$$

Step No. 4: Calculate the core geometry, K_g.

$$K_g = \frac{P_t}{2K_e\alpha}, \quad [\text{cm}^5]$$
$$K_g = \frac{12.9}{2(45.7)(5)}, \quad [\text{cm}^5]$$
$$K_g = 0.0282, \quad [\text{cm}^5]$$

© 2011 by Taylor and Francis Group, LLC

Step No. 5: This core was selected from "Magnetics Tape Wound Cores Catalog," TWC 500, comparable to core geometry, K_g.

1. Toroid = 52029-4A
2. Manufacturer = Magnetics
3. OD Dimension = 3.78 cm
4. ID Dimension = 2.25 cm
5. Ht Dimension = 0.978 cm
6. Core Geometry, $K_g = 0.0256\ cm^5$
7. Area Product, $A_p = 1.08\ cm^4$
8. Core Weight, $W_t = 19.66$ grams
9. Iron Area, $A_c = 0.272\ cm^2$
10. Window Area, $W_a = 3.97\ cm^2$
11. Magnetic Path Length, MPL = 9.47 cm
12. Magnetic Material, 4 mil = Orthonol
13. Efficiency = 95%
14. Copper Loss, $\alpha = 5\%$

Step No. 6: Calculate the window area for the gate winding, A_{cg}.

$$W_{ag} = \frac{W_a}{2}, \quad [\text{cm}^2]$$

$$W_{ag} = \frac{3.97}{2}, \quad [\text{cm}^2]$$

$$W_{ag} = 1.98, \quad [\text{cm}^2]$$

Step No. 7: Calculate the number of turns for the gate winding, N_g.

$$N_g = \frac{0.5V_o(10^4)}{K_f B_{ac} f A_c}, \quad [\text{turns}]$$

$$N_g = \frac{0.5(14)(10^4)}{(4.44)(1.0)(400)(0.272)}, \quad [\text{turns}]$$

$$N_g = 145, \quad [\text{turns}]$$

Step No. 8: Calculate the current density, J.

$$J = \frac{P_t(10^4)}{K_u K_f B_{ac} f A_p}, \quad [\text{amps/cm}^2]$$

$$J = \frac{(12.9)(10^4)}{(0.4)(4.44)(1.0)(400)(1.08)}, \quad [\text{amps/cm}^2]$$

$$J = 168, \quad [\text{amps/cm}^2]$$

© 2011 by Taylor and Francis Group, LLC

Step No. 10: Calculate the gate bare wire area, $A_{wg(B)}$.

$$A_{wg(B)} = \frac{I_o}{J}, \quad [\text{cm}^2]$$
$$A_{wg(B)} = \frac{1.0}{168}, \quad [\text{cm}^2]$$
$$A_{wg(B)} = 0.00595, \quad [\text{cm}^2]$$

Step No. 11: Select the wire from the Wire Table in Chapter 4.

$$AWG = 20$$
$$A_{w(B)} = 0.005188, \quad [\text{cm}^2]$$
$$A_{wg} = 0.006065, \quad [\text{cm}^2]$$
$$\left(\frac{\mu\Omega}{cm}\right) = 332, \quad [\text{micro-ohm/cm}]$$

Step No. 12: Calculate the Mean Length Turn, (MLT) for the gate. Use Figure 24-18 for a reference.

A = Core with case Ht Dimension = 0.978

B = Core with case Build = (OD-ID)/2 = 0.765

W = Core with case Inside Diameter = 2.25

$$\text{MLT} = ((2A) + (2B) + (\pi 0.125W))(0.85), \quad [\text{cm}]$$
$$\text{MLT} = ((2(0.978)) + (2(0.765)) + (\pi 0.125(2.25)))(0.85), \quad [\text{cm}]$$
$$\text{MLT} = 3.71, \quad [\text{cm}]$$

Step No. 13: Calculate the gate winding resistance, R_g.

$$R_g = \text{MLT}(N_g)\left(\frac{\mu\Omega}{\text{cm}}\right)(10^{-6}), \quad [\text{ohms}]$$
$$R_g = 3.71(145)(332)(10^{-6}), \quad [\text{ohms}]$$
$$R_g = 0.179, \quad [\text{ohms}]$$

Step No. 14: Calculate the gate winding copper loss, P_g.

$$P_g = I_g^2 R_g, \quad [\text{watts}]$$
$$P_g = (1.0)^2 (0.179), \quad [\text{watts}]$$
$$P_g = 0.179, \quad [\text{watts}]$$

Step No. 15: Calculate the required control turns, N_c.

$$N_c = \left(\frac{N_g I_g}{I_c}\right), \quad [\text{turns}]$$
$$N_c = \left(\frac{(145)(1.0)}{0.1}\right), \quad [\text{turns}]$$
$$N_c = 1450, \quad [\text{turns}]$$

© 2011 by Taylor and Francis Group, LLC

Step No. 16: Calculate the control bare wire area, $A_{w(B)}$.

$$A_{wc(B)} = \frac{I_c}{J}, \quad [\text{cm}^2]$$
$$A_{wc(B)} = \frac{0.10}{168}, \quad [\text{cm}^2]$$
$$A_{wc(B)} = 0.000595, \quad [\text{cm}^2]$$

Step No. 17: Select the wire from the Wire Table, in Chapter 4.

$$AWG = 30$$
$$A_{wc(B)} = 0.000507, \quad [\text{cm}^2]$$
$$A_{wc} = 0.000678, \quad [\text{cm}^2]$$
$$\left(\frac{\mu\Omega}{cm}\right) = 3402, \quad [\text{micro-ohm/cm}]$$

Step No. 18: Calculate the Mean Length Turn, (MLT) for the control winding. Use Figure 24-18 for reference.

A = Core with case Ht Dimension = 0.978

B = Core with case Build = (OD-ID)/2 = 0.765

W = Core with case Inside Diameter = 2.25

$$\text{MLT} = ((4A + 0.25W) + (2B) + 2\pi(0.375W))(0.70), \quad [\text{cm}]$$
$$\text{MLT} = (4(0.978) + 0.25(2.25) + 2(0.765) + 2\pi(0.375(2.25)))(0.70), \quad [\text{cm}]$$
$$\text{MLT} = 7.91, \quad [\text{cm}]$$

Step No. 19: Calculate the control winding resistance, R_c.

$$R_c = \text{MLT}(N_c)\left(\frac{\mu\Omega}{\text{cm}}\right)(10^{-6}), \quad [\text{ohms}]$$
$$R_c = 7.91(1450)(3402)(10^{-6}), \quad [\text{ohms}]$$
$$R_c = 39.0, \quad [\text{ohms}]$$

Step No. 20: Calculate the control winding copper loss, P_c.

$$P_c = I_c^2 R_c, \quad [\text{watts}]$$
$$P_c = (0.1)^2(39.0), \quad [\text{watts}]$$
$$P_c = 0.39, \quad [\text{watts}]$$

Step No. 21: Calculate the total copper loss for the gates and control, P_{cu}.

$$P_{cu} = P_{g1} + P_{g2} + P_c, \quad [\text{watts}]$$
$$P_{cu} = (0.179) + (0.179) + (0.39), \quad [\text{watts}]$$
$$P_{cu} = 0.748, \quad [\text{watts}]$$

© 2011 by Taylor and Francis Group, LLC

Step No. 22: Calculate the percent of total copper loss, α.

$$\alpha = \frac{P_{cu}}{P_o}(100), \quad [\%]$$
$$\alpha = \frac{(0.748)}{(12.6)}(100), \quad [\%]$$
$$\alpha = 5.94, \quad [\%]$$

Step No. 23: Calculate the watts per kilogram, W/K. Use the Equation for this material in Chapter 2.

$$W/K = 0.000618(f)^{1.48}(B_{ac})^{1.44}$$
$$W/K = 0.000618(400)^{1.48}(1.0)^{1.44}$$
$$W/K = 4.38$$

Step No. 24: Calculate the core loss, P_{fe}.

$$P_{fe} = (W/K)2(W_{tfe})(10^{-3}), \quad [\text{watts}]$$
$$P_{fe} = (4.38)2(19.7)(10^{-3}), \quad [\text{watts}]$$
$$P_{fe} = 0.173, \quad [\text{watts}]$$

Step No. 25: Calculate the total loss, P_{Σ}.

$$P_{\Sigma} = P_{cu} + P_{fe}, \quad [\text{watts}]$$
$$P_{\Sigma} = (0.748) + (0.173), \quad [\text{watts}]$$
$$P_{\Sigma} = 0.921, \quad [\text{watts}]$$

Step No. 26: Calculate the saturable reactor height, Ht using Figure 24-19 for reference. See Chapter 5.

$$SR_{Ht} = \left(3\left(\frac{ID}{4}\right) + 2Ht\right), \quad [\text{cm}]$$
$$SR_{Ht} = \left(3\left(\frac{2.25}{4}\right) + 2(0.978)\right), \quad [\text{cm}]$$
$$SR_{Ht} = 3.64, \quad [\text{cm}]$$

Step No. 27: Calculate the saturable reactor outside diameter, OD using Figure 24-19 for reference. See Chapter 5.

$$SR_{OD} = \left(\left(\frac{ID}{2}\right) + (OD - ID) + ID\right), \quad [\text{cm}]$$
$$SR_{OD} = \left(\left(\frac{2.25}{2}\right) + (3.78 - 2.25) + 2.25\right), \quad [\text{cm}]$$
$$SR_{OD} = 4.91, \quad [\text{cm}]$$

Step No. 28: Calculate the saturable reactor surface area using Figure 24-19 for reference. See Chapter 5.

$$A_t = \frac{\pi(SR_{OD})^2}{2} + \left(\pi(SR_{OD})(\mathrm{SR_{Ht}})\right), \quad [\text{cm}^2]$$
$$A_t = \frac{\pi(4.91)^2}{2} + (\pi(4.91)(3.64)), \quad [\text{cm}^2]$$
$$A_t = 85.8, \quad [\text{cm}^2]$$

© 2011 by Taylor and Francis Group, LLC

Step No. 29: Calculate the watts per unit area, ψ.

$$\psi = \frac{P_{\Sigma}}{A_t}, \quad [\text{watts/cm}^2]$$
$$\psi = \frac{0.921}{85.8}, \quad [\text{watts/cm}^2]$$
$$\psi = 0.0107, \quad [\text{watts/cm}^2]$$

Step No. 30: Calculate the temperature rise, T_r.

$$T_r = 450(\psi)^{0.826}, \quad [°\text{C}]$$
$$T_r = 450(0.0107)^{0.826}, \quad [°\text{C}]$$
$$T_r = 10.6, \quad [°\text{C}]$$

Step No. 31: Calculate the window utilization, K_u, for both control and gate.

$$K_{uc} = \left(\frac{N_c A_{wc(B)}}{\frac{W_a}{2}} \right), \quad K_{uc} = \frac{(1450)(0.000507)}{(1.98)} = 0.371$$

$$K_{ug} = \left(\frac{N_g A_{wg(B)}}{\frac{W_a}{2}} \right), \quad K_{ug} = \frac{(145)(0.005188)}{(1.98)} = 0.380$$

Series Saturable Reactor Design Test Data (Core Geometry, K_g, Approach)

Summary

The above series saturable reactor was built, and tested. The following information is the test data for the above series saturable reactor design. The input control current versus the output voltage test data is shown in Table 24-1. The input current versus output voltage transfer function is shown in Figure 24-24. The author hopes that this design, with its step-by-step approach, helps the readers understand the design of a series saturable reactor.

Test Data

1. Frequency, f = 400 Hz
2. Output voltage, V_o = 12.7 volts
3. Output current, I_o = 1.0 amps
4. Control current, I_c = 0.10 amps
5. Gate resistance, R_g = 0.176 ohms
6. Control resistance, R_c = 38.4 ohms
7. Temperature Rise, T_r = 10.4°C

© 2011 by Taylor and Francis Group, LLC

Table 24-1. Series Saturable Reactor Showing Input Current versus Output Voltage

Saturable Reactor		
Steps	Control Current Amps	Output Voltage Volts
1	0.00	0.200
2	0.01	1.600
3	0.02	2.900
4	0.03	4.400
5	0.04	5.700
6	0.05	7.100
7	0.06	8.400
8	0.07	9.900
9	0.08	11.400
10	0.09	12.500
11	0.10	12.700
12	0.11	12.700

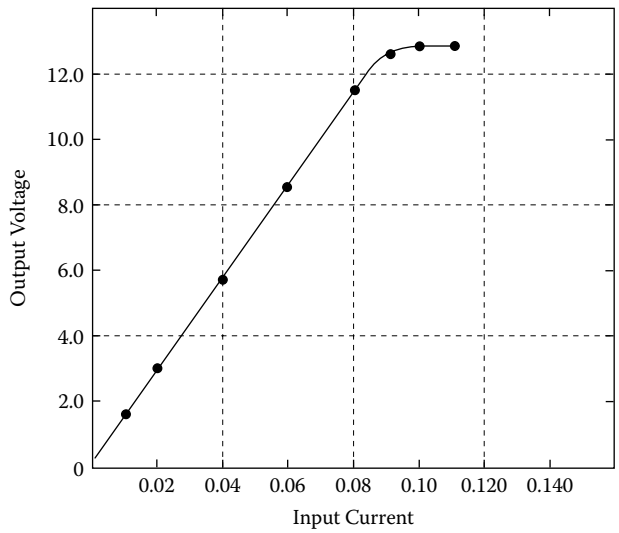

Figure 24-24. Transfer Function Using the Data in Table 24-1.

© 2011 by Taylor and Francis Group, LLC

Ultra Low Power 0-15 Amp Current Transducer (Saturable Reactor)

Introduction

A unique, ultra low power current transducer was developed to measure the charge and discharge current on the Mariner Mark II battery. It provides current detection and isolation, via a series connected saturable reactor. The current transducer, shown in Figure 24-25, provides a 0-3 volt output for a 0-15 amps input. The power source is +5 volts and consumes 22 milliwatts of power. The current transducer performance can best be seen by looking at the transfer function of input current versus output voltage, as shown in Figure 24-26. The data for Figure 24-26 is taken from Table 24-2.

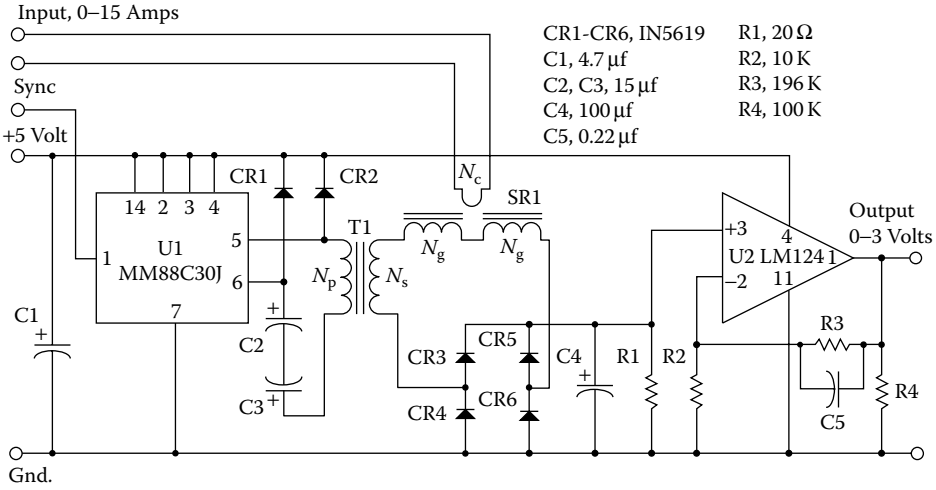

Figure 24-25. Schematic for the Ultra Low, Power Current Transducer.

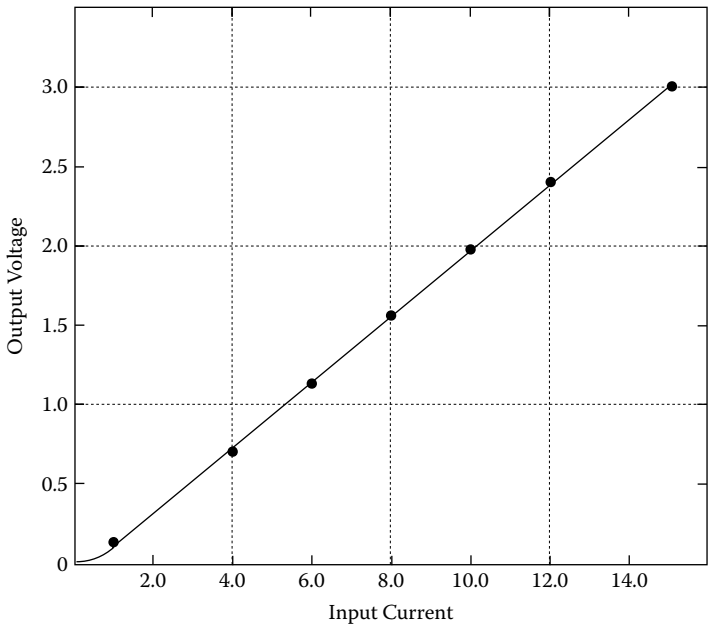

Figure 24-26. Input Current versus Output Voltage.

© 2011 by Taylor and Francis Group, LLC

Table 24-2.

Milliwatt Current Transducer		
Steps	Input Current Amps	Output Voltage Volts
1	0.00	0.020
2	0.50	0.051
3	1.00	0.136
4	2.00	0.298
5	3.00	0.475
6	4.00	0.669
7	5.00	0.875
8	6.00	1.089
9	7.00	1.306
10	8.00	1.525
11	9.00	1.744
12	10.00	1.962
13	11.00	2.178
14	12.00	2.392
15	13.00	2.603
16	14.00	2.814
17	15.00	3.022

The saturable reactor can be used for both power and signal. The typical output power transfer function is shown in Figure 24-27A. The output power transfer function becomes nonlinear at the higher output voltages, as shown in Figure 24-27A. This non-linearity is fine for controlling lamps, heaters and motor control, but will not cut it as a transducer. The input-output transfer function for a telemetry transducer must be very linear. To get a good linear transfer function from a saturable reactor it is wise to use only 40 percent of its output capability, as shown in Figure 24-27B. The selection of a magnetic material with a square BH loop will also help.

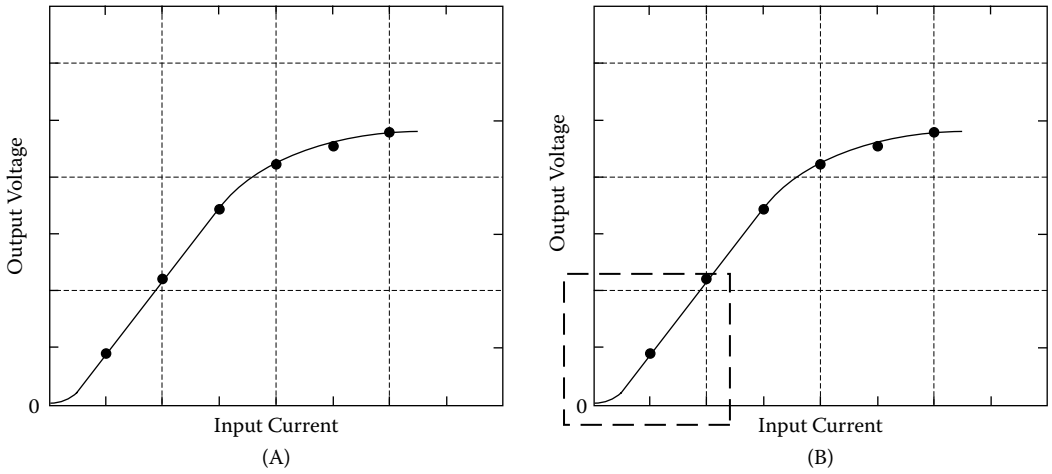

Figure 24-27. Typical Saturable Reactor Input-Output Transfer Function.

© 2011 by Taylor and Francis Group, LLC

Circuit Description

The current detection and isolation is accomplished with a saturable reactor, (SR1). The line driver, (U1) provides the excitation power for the transducer. The inverter transformer, (T1), supplies power to the current-sensing, series saturable reactor, SR1. The output of the saturable reactor is then rectified with diodes (CR3-CR6) and provides the signal to the operational amplifier, (U2). The operational amplifier has a gain of 20 and produces a corresponding output of 0-3 volt for a 0-15 amp input. The transducer is powered from a 5-volt dc power source.

Specification

1. Input Current, I_{in} = 0-15 amps dc
2. Output voltage, V_o = 0-3 volts dc
3. Supply Voltage, V_{in} = 5 volts dc
4. Maximum Supply Power @ 10 amps Input Current = 50 milliwatts
5. Operating Frequency, f = 2.3kHz
6. External Drive Signal = 0-5 volts
7. Power Source Line Driver = MM78C30

Design Discipline

Power Transformer, (T1)

The power transformer, (T1), was designed for high efficiency and minimum capacitance for optimum performance. To minimize core loss, the transformer was designed, using an 80/20 nickel-iron core. The core is a Magnetics type, 52056-2D. The primary and secondary windings were interleaved and progressively wound 350° to minimize the capacitance. The winding procedure is shown in Figure 24-28. The primary has 408 turns of number #34 AWG and the secondary has 660 turns of number #34 AWG.

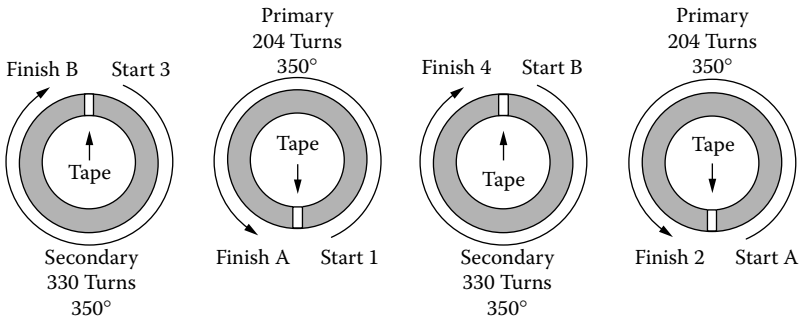

Figure 24-28. Transformer, T1, Winding Configuration.

Saturable Reactor, (SR1)

The saturable reactor was designed to have a one-turn, current sense winding. The design was to have an output current set at approximately 10 ma at 15 amps input. This process was done in order to keep the power

© 2011 by Taylor and Francis Group, LLC

consumption to a minimum. In the design of a saturable reactor, the amp-turns in the control winding must equal the amp-turns in the gate windings, as shown in Equation [24-29].

$$\begin{aligned} I_g N_g &= I_c N_c \\ N_g &= \frac{I_c N_c}{I_g}, \quad \text{[turns]} \\ N_g &= \frac{(15)(1)}{(0.01)}, \quad \text{[turns]} \\ N_g &= 1500, \quad \text{[turns]} \end{aligned} \qquad \text{[24-29]}$$

The saturable reactor has two opposing gates with a common control, as shown in Figure 24-28. With 1500 turns on the gates and a high permeability core, an effort must be made to minimize the capacitance in the gate winding in order to remove any chance of resonance. In this design the gate windings were wound progressively with 750 turns, 350° then insulated, and another 750 turns, 350° were wound progressively. The windings are rotated 180° to each other on the core. The cores are Magnetics 52057-2D, 80/20 nickel-iron, with a standard 5 percent, sine current match.

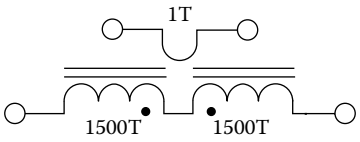

Figure 24-29. Simple Schematic of a Series Saturable Reactor.

Line Driver, (U1)

The line driver, IC, is a National Semiconductor MM78C30 dual differential line driver, which provides sufficient power to drive transformer, T1. The input signal to the line driver is a 2.3 kHz square wave, 0-5 volts.

Operational Amplifier (U2)

The operational amplifier is a National Semiconductor, LM124. The LM124 was chosen because of its input common-mode characteristics and its output voltage can swing to ground while operating from a single power supply.

Commutating Diodes (CR1, CR2)

The commutating diodes are 1N5619, and they are used to commutate the reactive current in the primary of T1, back to the source. The reactive current on the primary is caused by the reactive component of the saturable reactors (SR1) gates connected on the secondary. These two diodes commutate the reactive current back to the source on each half cycle. Without these diodes there would be large voltage spikes on the primary that waste power and could destroy the line driver. The input current to the transducer operating in a quiescent state is about 1.2 ma. With a signal current of 10amps the input current rose to 4.4 ma and 7.2 ma at 15 amps. The input power with a 10amp signal is 22 milliwatts, which is well within the specification of 50-mw requirement.

© 2011 by Taylor and Francis Group, LLC

Rectifier Diodes (CR3-CR6)

These rectifier diodes are 1N5619 and are used to rectify the output of the saturable reactor.

Capacitor (C1)

The filter capacitor C1 is 4.7uf. It is required to store the energy from CR1 and CR2.

Capacitors (C2 and C3)

The line driver, U1, requires a 2.3kHz, 0-5 volt signal at pin 1 to function. If this signal is removed the line driver will go into an unknown state, and will not provide an ac source to the transformer, T1. The capacitors, C2 and C3, are used for blocking dc into the transformer. If the line driver can be assured of always getting a drive signal, then capacitors, C2 and C3, can be eliminated.

Summary

As you can see, the performance of this current transducer is adequate for most applications. The circuit is simple and does not require a lot of calibration. The circuit can be easily modified to handle other input currents. The line driver circuit can be designed and/or modified to become a self-contained oscillator or an oscillator can be simply added. The reason for operating at such a low frequency is because of the saturable reactors. The gate inductance of the saturable reactors is extremely high. This high inductance requires the operation frequency to keep well below the self-resonate frequency of the saturable reactors.

Recognition

I would like to give thanks to Charles Barnett, an engineer at Leightner Electronics Inc. for building and testing the 12watt, saturable reactor design example.

Leightner Electronics Inc.
1501 S. Tennessee St.
McKinney, TX. 75069

I would like to give thanks to Zack Cataldi, a Senior Applications Engineer at Magnetics for supplying the cores for the saturable reactor design example.

Magnetics
110 Delta Drive
Pittsburgh, PA 15238

© 2011 by Taylor and Francis Group, LLC

References

1. Flanagan, W.M., *Handbook of Transformer Applications*, McGraw-Hill Book Co., Inc., New York, 1986, pp. 14.9–14.20.

2. Lee, R., *Electronic Transformers and Circuits*, John Wiley & Sons, New York, 1958, pp. 259–291.

3. Platt, S., *Magnetic Amplifiers Theory and Application*, Prentice-Hall, Inc., Englewood Cliffs, N.J., 1958, Chapter 4.

4. National Aeronautics and Space Administration, New Technology, NPO-16888, Low Power 0-15 Amp Current Transducer.

© 2011 by Taylor and Francis Group, LLC

Chapter 25

Self-Saturating, Magnetic Amplifiers

© 2011 by Taylor and Francis Group, LLC

Table of Contents

1. Introduction....25-3
2. Self-Saturating, Magnetic Amplifier Overview....25-3
3. Basic Operation of the Self-Saturating, Mag-Amp....25-4
4. Square and Round B-H Loop Performance....25-6
5. Adding the Bias Winding....25-7
6. Control Winding and Rectifiers....25-8
7. Self-Saturating Magnetic Amplifier Apparent Power, P_t....25-9
8. Magnetic Amplifier Power Gain....25-11
9. Self-Saturating Magnetic Amplifier Response Time....25-11
10. Mean Length Turn for DU Lamination....25-12
11. Calculating, MLT for Toroidal Cores....25-13
12. Toroidal Magnetic Amplifier Surface Area....25-14
13. DU Lamination Magnetic Amplifier Surface Area....25-15
14. Control Winding Calculation....25-16
15. Bias Winding Calculation....25-17
16. Control Winding Precautions....25-18
17. Self-Saturating Magnetic Amplifier Design Example....25-18
18. Self-Saturating, Magnetic Amplifier Design Test Data....25-26
19. Recognition....25-27
20. References....25-28

© 2011 by Taylor and Francis Group, LLC

Introduction

The self-saturating magnetic amplifier had great popularity in 1950 and 1960 like the saturable reactors, but when the transistor and silicon controlled rectifier came along, the magnetic amplifier nearly became obsolete. One of the early successes for the magnetic amplifier was power supplies for military aircraft operating at 400 Hz. The magnetic amplifier is still being used in motor control, power supplies. It also provides good electrical isolation between input and output. Magnetic amplifiers are inherently rugged, with a long life, and good reliability. Magnetic amplifiers are still being used in very remote locations. Only the operational and design highlights of the basic self-saturating, two-core magnetic amplifier will be discussed in this chapter. It would take a book to cover all of the attributes of a magnetic amplifier. A review of Chapter 2, "Magnetic Materials and Their Characteristics", will help one to understand how the magnetic core operates.

Self-Saturating, Magnetic Amplifier Overview

The basic self-saturating two-core magnetic amplifier with a controllable dc output is shown in Figure 25-1, and the two-core, self-saturating magnetic amplifier with a controllable ac output is shown in Figure 25-2. An overview description of the self-saturating magnetic amplifier is done with a resistive load, R_L.

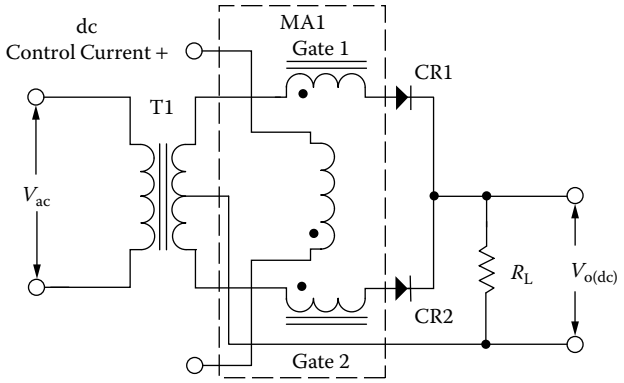

Figure 25-1. Magnetic Amplifier Circuit with a Controllable dc Voltage Output.

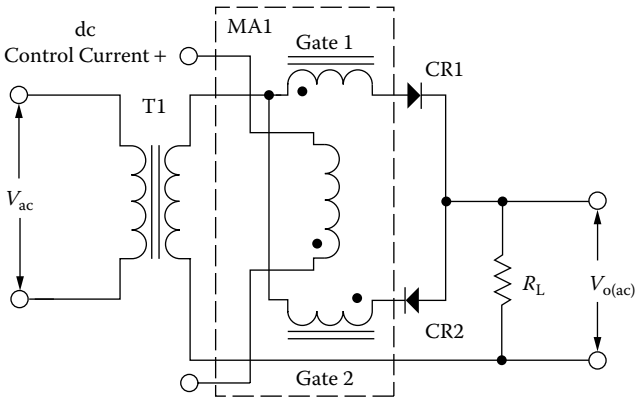

Figure 25-2. Magnetic Amplifier Circuit with a Controllable ac Voltage Output.

© 2011 by Taylor and Francis Group, LLC

The performance and design complexity of a self-saturating magnetic amplifier design is based on the magnetic material used in the magnetic amplifier. The engineer can choose a magnetic material that has a square or round B-H loop, as shown in Figure 25-3 for the design. A good percentage of the magnetic amplifiers designed, will be designed on a toroidal core and have a magnetic material with a square loop and a high permeability at the operating conditions.

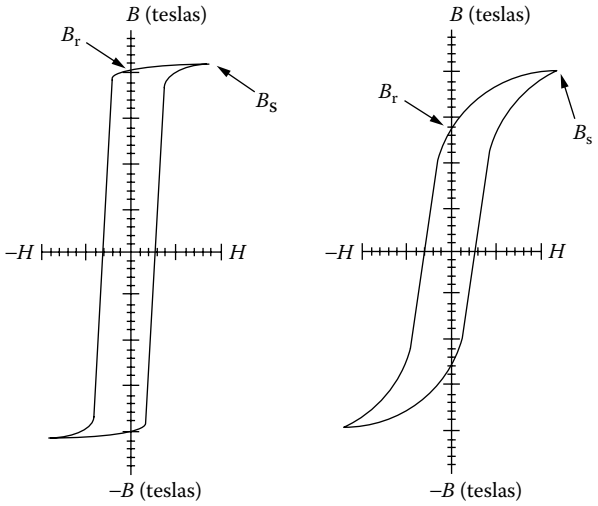

Figure 25-3. Comparing the (A) Square and (B) Round B-H Loop.

Basic Operation of the Self-Saturating, Mag-Amp

The core material and configuration used in the design of a self-saturating magnetic amplifier controls the overall performance of the magnetic amplifier. The gate from a magnetic amplifier is shown in Figure 25-4A, with the ac excitation from the transformer, T1 into a resistance load, R_L.

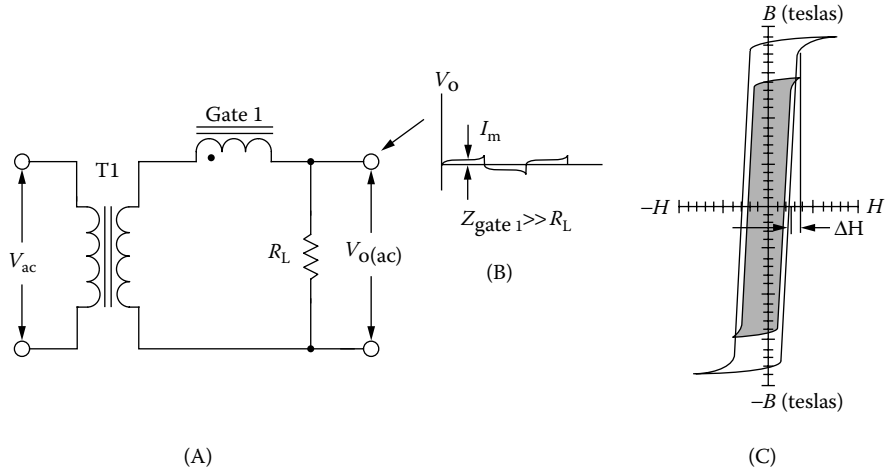

Figure 25-4. Magnetic Amplifier Gate Being Excited, Having a Square B-H Loop.

© 2011 by Taylor and Francis Group, LLC

The core configuration for Gate-1, shown in Figure 25-4A, is a toroid. The magnetic material is a square loop with high permeability. The impedance of the gate, $Z_{(gate)}$, is much greater than the load resistance, R_L ($Z_{(gate)} >> R_L$). The magnetizing current, shown in Figure 25-4B, is that of a magnetic material with a square B-H loop. In Figure 25-C, note how the magnetizing current follows the outline of the B-H loop.

The ΔH, shown in Figure 25-4C, is the magnetizing force required to drive the core into saturation, or out of saturation. The magnetizing force, H, can be in amp-turns, as shown in Equation [25-1], or oersteds, as shown in Equation [25-2]. The magnetizing force, H, is different for all magnetic materials, and it will change with frequency and material thickness. To change amp-turns/meter to oersteds, multiply (amp-turns × 0.01256) and to change oersteds to amp-turns/meter, divide (oersteds/0.01256).

$$H = \frac{NI}{(\text{MPL})}, \quad \text{[amp-turns/meter]} \qquad [25\text{-}1]$$

$$H = \frac{0.4\pi NI}{(\text{MPL})}, \quad \text{[oersteds]} \qquad [25\text{-}2]$$

The basic two-core self-saturating magnetic amplifier is shown in Figure 25-5. The self-saturating magnetic amplifier gets its name because the rectifier diodes, CR1 and CR2. The diodes are in series with the gates and put a unidirectional current into Gates 1 and 2 of the magnetic amplifier, which drive the cores to saturation. The output of the magnetic amplifier, MA1, can be seen in Figure 25-5B. With the Gates 1 and 2 saturated, the output is that of a center-tap, full wave rectifier. The dc current flowing into the Gates 1 and 2 drives the cores into saturation, as shown in Figure 25-5C.

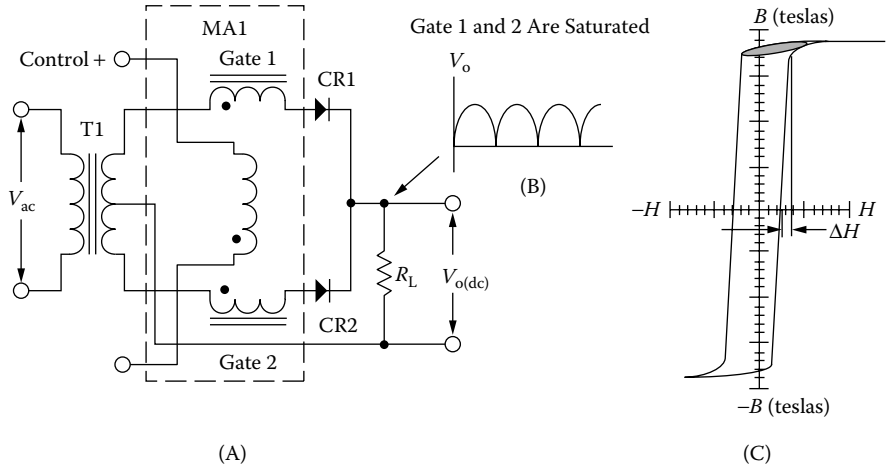

Figure 25-5. Two-Core, Self-Saturating Magnetic Amplifier with dc Output.

To make the gates operate as a variable switch, a current must be applied to the control winding in reverse to the amp-turns in the gate winding. The current in the gate winding is flowing into the dot, as shown in Figure 25-5A. The current in the control winding must have the current flowing out of the dot. It can be seen in Figure 25-6 as the control magnetizing current is increased from core saturation in Figure 25-6A to a 50 percent duty cycle in

© 2011 by Taylor and Francis Group, LLC

Figure 25-6B, and then increases even further to where the gate is absorbing the total applied voltage in Figure 25-6C. This can only be done if the gates are designed to support the full voltage from the secondary of T1. There are some magnetic amplifier design circuits where the gate does not support the total secondary voltage.

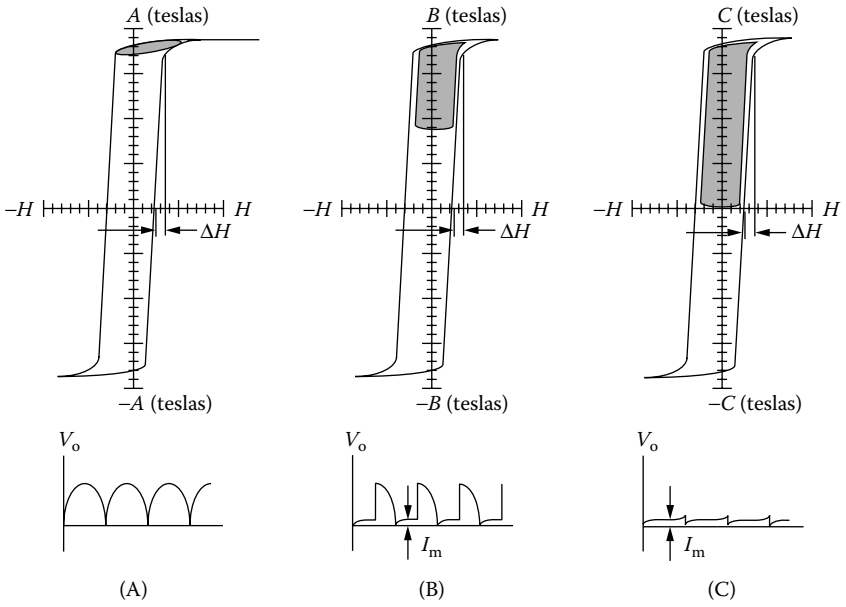

Figure 25-6. Two-Core, Self-Saturating Magnetic Amplifier with dc Output.

Square and Round B-H Loop Performance

The functional difference between the square B-H loop and the round B-H loop can best be shown by looking at the output voltage waveform across the load resistor, R_L with the control winding open (no dc current). This condition is best illustrated when the self-saturating magnetic amplifier is driven by a square wave, as shown in Figure 25-7.

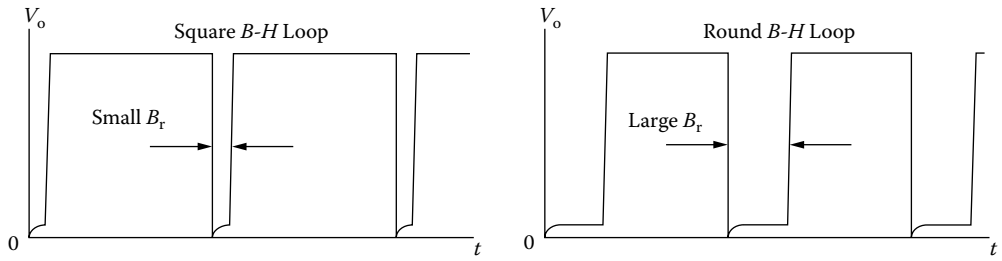

Figure 25-7. Comparing the Performance of Round and Square B-H Loop Magnetic Materials.

It can be seen in Figure 25-7 that the round magnetic material has a large gap between half cycles. What happens is that every time the transformer, T1 switches, (See Figure 25-1), diode CR1 turns off and diode, CR2 turns on. This cycle causes the flux in Gate 1 to fall back to residual flux, B_r, and then, on the next half cycle, the flux starting point will be at the residual flux, B_r, as shown in Figure 25-3. Round or square B-H loop magnetic materials will always fall back to the residual flux, B_r, when the excitation is removed. It is easy to see that

© 2011 by Taylor and Francis Group, LLC

the round loop material is not being used to its full flux capacity. There are times when round loop magnetic material is a requirement because of the cost or the other assets of the material.

Adding the Bias Winding

If the round loop magnetic material is the choice then the B-H loop will have to be shifted over to get the full core capability. A typical transfer function of a self-saturating magnetic amplifier is shown in Figure 25-8, showing magnetic materials with both square and round B-H loops.

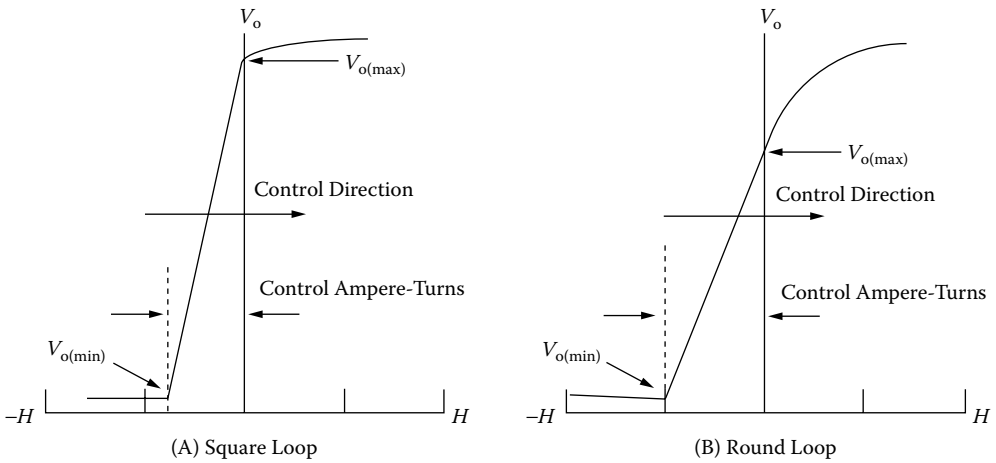

Figure 25-8. Comparing Transfer Function for Both Round and Square Magnetic Material.

As seen in Figure 25-8 the control amp-turns can bias the core, as shown by the arrow in the control direction, to get the output voltage down to minimum, $V_{o(min)}$. A bias winding can be added to the magnetic amplifier, shown in Figure 25-1, to bias the core with amp-turns in the opposite direction to the control amp-turns, as shown in Figure 25-9.

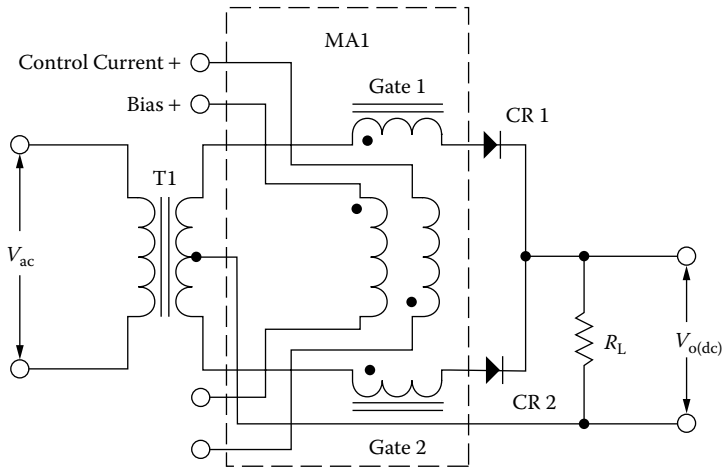

Figure 25-9. A Magnetic Amplifier Showing a Control and Bias Winding.

© 2011 by Taylor and Francis Group, LLC

The new bias winding amp-turns will bias the gates in the same direction as the rectifiers, CR1 and CR2. The output load current travels into the start (dot) of the gate windings. The bias winding will also have the current travel into the start (dot). The current in the bias winding will shift both cores and hold the flux even though the switching load current has been removed from CR1 and CR2 by transformer action. The control current now controls the full range of the output voltage from minimum, $V_{o(min)}$ to maximum, $V_{o(max)}$ and uses the full capacity of the core, as shown in Figure 25-10. Comparing the square B-H loop in Figure 25-8A with the biased round B-H loop in Figure 25-10B, both have the same output voltage range, but the round B-H loop material requires more control current, I_c. This is because the control current, I_c, now has overcome the bias amp-turns to get the same output voltage, V_o, range.

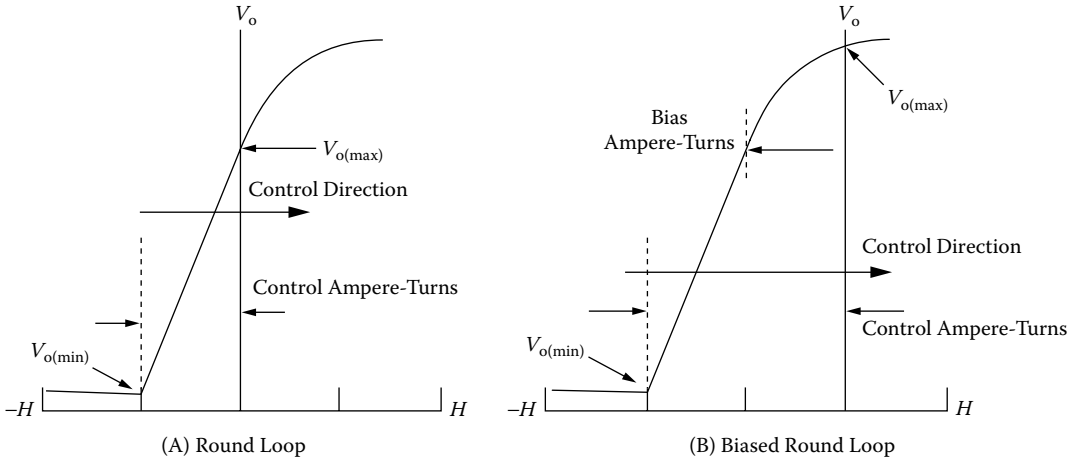

Figure 25-10. Showing How the B-H Loop can be shifted with the Bias Winding.

Control Winding and Rectifiers

The window area of the magnetic amplifier, MA1, has to accommodate both power and control windings. The rectifiers have a big impact on the control winding. Back in the 50's and 60's the mag-amp engineer had a lot of problems just with the diode rectifiers, CR1 and CR2, as shown in Figure 25-9. The rectifiers that were available at this time were selenium, germanium, and the new silicon. At that time the forward voltage drop and the reverse leakage were not tightly controlled. The semiconductor manufacturers were just beginning to get their process down. The problem caused by the reverse leakage current in the rectifiers is shown in Figure 25-11. The reverse leakage current would reset the core with amp-turns every half cycle. To be able to get full use of the core, a bias winding would have to be added to overcome this reverse rectifier leakage current. The rectifiers have to be well-balanced in both forward and reverse directions to keep the ac, unbalanced noise generated in the control winding to a minimum. Early self-saturating magnetic amplifiers required a lot of room in the window for the control and bias windings, because of the loss of gain caused by the reverse leakage current.

As time went on the manufacturers of semiconductors got their processes down and produced rectifiers with very tight specification for both forward and reverse conditions. A well-balanced magnetic amplifier has a minimum

© 2011 by Taylor and Francis Group, LLC

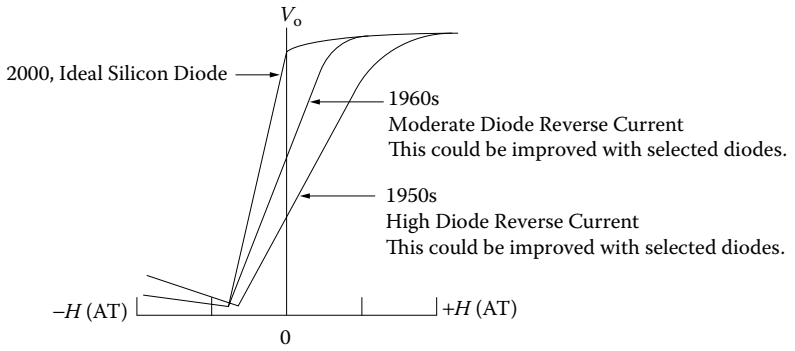

Figure 25-11. How the Transfer Function can be shifted with Reverse Diode Leakage.

of disturbance in the control winding. The engineers would use a transistor to drive the magnetic amplifier and would not depend on the gain of the mag-amp itself. This reduced the number of turns required for the control. The window area required for the control winding is up to the engineer on how to incorporate the control.

Self-Saturating Magnetic Amplifier Apparent Power, P_t

The designer must be concerned with the apparent power, P_t, and power handling capability of the mag-amp core and windings, when selecting the correct core. The mag-amp has two gate windings and a control winding and could include a bias winding, as shown in Figure 25-12. For more information on apparent, power, P_t, and power-handling capability, see Chapters 7 and 21. Each gate of the self-saturating magnetic amplifier, MA1, is designed to support the full output voltage, V_o. The current, I_g, in each gate is interrupted every half cycle. This affects the RMS value and changes the volt-amps, VA, of the gate winding, as shown in Equation [25-3] and Equation [25-4]. The apparent power, P_t, for the two gate windings is the same as the apparent power, P_t for the transformer, T1 secondary.

$$I_{g(rms)} = 0.707(I_o), \quad [25\text{-}3]$$

$$VA_{(gates)} = P_o\sqrt{2}, \quad [25\text{-}4]$$

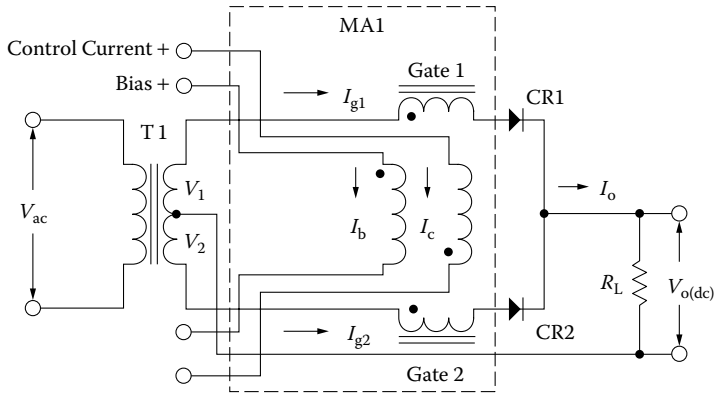

Figure 25-12. Self-Saturating Magnetic Amplifier Showing Gate and Control Current.

© 2011 by Taylor and Francis Group, LLC

There must be area in the window assigned to the control and bias windings when a core is selected. The Equation for the apparent power, P_t, for a transformer is shown in Equation [25-5]. The Equation [25-5] for the transformer apparent power, P_t can be simplified to Equation [25-6].

$$P_t = \text{Primary Power} + \text{ Secondary Power}, \quad \text{[watts]} \tag{25-5}$$

$$P_t = P_{in} + P_o \quad \text{[watts]} \tag{25-6}$$

The apparent power, P_t, Equation [25-6] can be modified for the magnetic amplifier by substituting the input power, P_{in}, with the gate volt-amps, $VA_{(gates)}$. The control and bias windings coefficient, K_{cw}, can be substituted for the output power, P_o. The new apparent power, P_t, for a magnetic amplifier is shown in Equation [25-7].

$$P_t = P_o\left(\left(\sqrt{2}\right)_{(gate)} + K_{cw}\right), \quad \text{[watts]} \tag{25-7}$$

The engineer can adjust the apparent power, P_t, to accommodate the control and bias windings by using the winding coefficient, K_{cw}. The window is divided up to where the gates get 60% and the control and bias windings will get 40% of the available winding area when the winding coefficient, $K_{cw} = 1$, as shown in Figure 25-13. This is a good starting point and not a hard fast rule. There will be many designs in which that ratio will change.

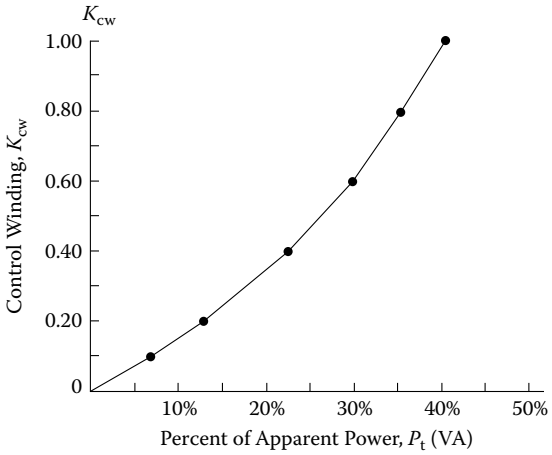

Figure 25-13. How the Control Winding Coefficient, K_{cw}, affects the apparent power, P_t, in percent.

The apparent power, P_t, calculated in Equation [25-8] is for each core of a magnetic amplifier using two cores, such as a toroid or a double stack DU lamination.

$$P_t = 0.5P_o\left(\sqrt{2}_{(gate)} + K_{cw}\right), \quad \text{[watts]} \tag{25-8}$$

The electrical conditions, K_e, are shown in Equation [25-9].

$$K_e = 0.145K_f^2 f^2 B_m^2\left(10^{-4}\right) \tag{25-9}$$

© 2011 by Taylor and Francis Group, LLC

The calculation for the core geometry, K_g, is shown in Equation [25-10].

$$K_g = \frac{P_t}{2K_e\alpha}, \quad [\text{cm}^5] \qquad [25\text{-}10]$$

Note: Alpha, α, is the combined copper loss for the control and gate windings of the magnetic amplifier. The core calculation for the core geometry, K_g, is shown in Equation [25-11].

$$K_g = \frac{W_a A_c^2 K_u}{\text{MLT}}, \quad [\text{cm}^5] \qquad [25\text{-}11]$$

Magnetic Amplifier Power Gain

One of the qualities of a magnetic amplifier is based on its power gain. The power gain is dependent to a great deal upon the design, type, and physical size of the magnetic amplifier. The power gain of a self-saturating magnetic amplifier is normally very high compared to a saturable reactor. Power gain of a magnetic amplifier is the ratio of the input control power, P_c to the output or load power, P_o. The input control power is the power dissipated in the control winding. The control power, P_c is the power dissipated in the control winding, as shown in Equation [25-12]. The control current is, I_c and the winding resistance is, R_c. The output power, P_o is the power delivered to the load, as shown in Equation [25-13]. The current flowing in the gate winding is, I_g and the load resistance is, R_L. The power gain then is the output power, P_o divided by the control power, P_c as shown in Equation [25-14].

$$P_c = I_c^2 R_c, \quad [\text{watts}]\ [\text{control}] \qquad [25\text{-}12]$$

$$P_o = I_o^2 R_L, \quad [\text{watts}]\ [\text{load}] \qquad [25\text{-}13]$$

$$P_{(gain)} = \frac{\left(I_o^2 R_L\right)}{\left(I_c^2 R_c\right)}, \quad [\text{power gain}] \qquad [25\text{-}14]$$

Self-Saturating Magnetic Amplifier Response Time

The response time, t_r for a magnetic amplifier is very slow for a step change in the control signal. This is because the control winding is very inductive. Any step change in current in the control winding will take time to reach its final value. The response time, t_r is given as a time constant of the control circuit. The response time is the time it takes for the load current to reach 63 percent of its final value for a step input change, as shown in Figure 25-14. It can be seen in Figure 25-14, when there is an input step change, t_1, in the control circuit. The output current, I_1, will rise from its initial value at, t_1, to its final value of, I_3, at the time, t_3. The value of I_2 is the current at 63 percent of the final current, I_3, which is one time constant. The time constant is shown in Equation [25-15].

© 2011 by Taylor and Francis Group, LLC

$$t_r = \frac{L_c}{R_c}, \quad \text{[seconds]}$$

$t_r =$ [seconds], [time constant] [25-15]

$L_c =$ [henries], [control winding inductance]

$R_c =$ [ohms], [control winding resistance]

This concept was derived from linear systems. It yields sufficiently accurate results for most purposes.

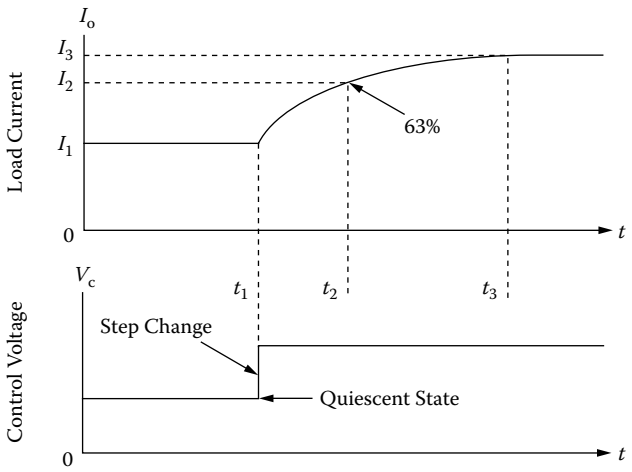

Figure 25-14. Output Response Time for a Input Signal Step Change.

Mean Length Turn for DU Laminations

The Mean Length Turn, (MLT), is required to calculate both winding resistance and weight for a given winding. Using the DU lamination in a magnetic amplifier design requires the calculation of the resistance of both control and gate windings. The winding dimensions, relating to the Mean Length Turn, (MLT) for a tube or bobbin coil, are shown in Figure 25-15. The Mean Length Turn, (MLT) for the control winding is shown in Equation [25-16] and the Mean Length Turn, (MLT) for the gate windings, is shown in Equation [25-17].

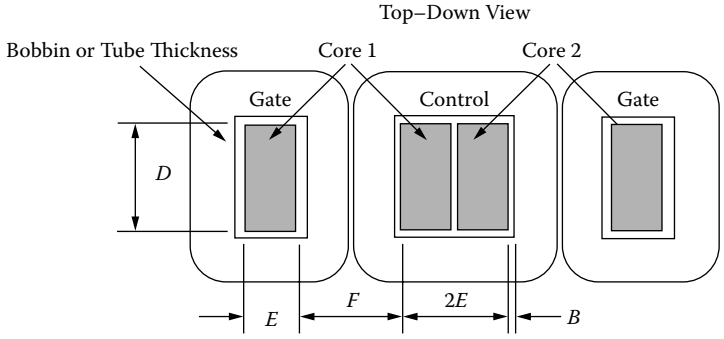

Figure 25-15. Dimensions, Relating to the Mean Length Turn, (MLT) for a DU Lamination.

© 2011 by Taylor and Francis Group, LLC

$$\mathrm{MLT}_{(control)} = 2(D+2B)+4(E+B)+\pi\left(\frac{F}{2}\right), \quad [\mathrm{cm}] \qquad [25\text{-}16]$$

$$\mathrm{MLT}_{(gate)} = 2(D+2B)+2(E+2B)+\pi\left(\frac{F}{2}\right), \quad [\mathrm{cm}] \qquad [25\text{-}17]$$

Calculating, MLT for Toroidal Cores

In order to wind the toroidal core, there has to be room to allow free passage of the wire shuttle. The wire shuttle could be a machine shuttle or a hand-wind shuttle. Winding a magnetic amplifier is not any different than winding any other toroidal core. Half of the inside diameter will be set aside for the shuttle clearance. This will leave 75% of the window, W_a, for the windings. It is very difficult to calculate the Mean Length Turn, (MLT) for a toroidal core used in magnetic amplifier design that would satisfy all conditions. The magnetic amplifier has two cores and each core has its own gate winding. The gate windings are wound first. After the gate windings are wound the cores are tested and matched. Then they are assembled for the common control winding to be wound over both. The assembly of the toroidal cores can be seen in Figure 25-16. The fabrication of a toroidal design is weighted heavily on the skill of the winder. The toroidal core magnetic amplifier requires special attention, when wound by hand or wound by machine, because of the angle it imposes when two cores are stacked. The Mean Length Turn, (MLT) for a toroidal magnetic amplifier is very difficult to obtain, because its shape is very nonlinear. A good approximation for a toroidal core, Mean Length Turn (MLT) for the gate winding is Equation [25-18] and Equation [25-19] for the control winding that is shown in Figure 25-16. There is a correction factor of 0.85 for the gate winding and a correction factor of 0.70 for the control winding.

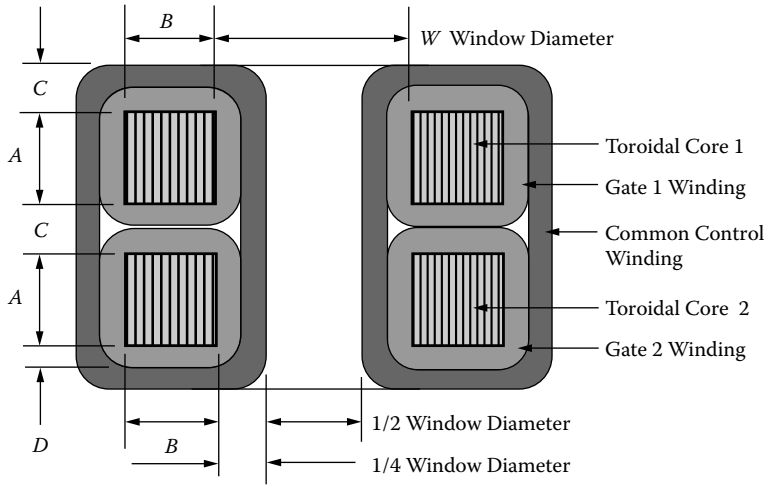

Figure 25-16. Toroidal Core Mag-Amp Mean Length Turn, (MLT) is a Good Approximation.

$$\mathrm{MLT} = \big((2A)+(2B)+(\pi 0.125W)\big)(0.85), \quad \text{Approximation [Gate]} \qquad [25\text{-}18]$$

$$\mathrm{MLT} = \big(4A+0.25W+2B+2\pi(0.375W)\big)(0.70), \quad \text{Approximation [Control]} \qquad [25\text{-}19]$$

© 2011 by Taylor and Francis Group, LLC

Nomenclature clarification:

1. A = Core strip width including the case.
2. B = Core build including the case.
3. C = Is the build of both gate and control winding = W/4
4. D = Is the build of the gate, = W/8
5. W = Is the inside diameter of the core including the case.

Toroidal Magnetic Amplifier Surface Area

The data such as height and outside diameter, required for the surface area calculation was taken from Figure 25-16. The Height, Ht, of the magnetic amplifier is shown in Equation [25-20] and the Outside Diameter, OD, is shown in Equation [25-21]. The magnetic amplifier outline is shown in Figure 25-17.

$$Ht = (3C + 2A)$$

$$OD = (2C + 2B + W)$$

$$A = (\text{Core Height, Ht}),\ B = (\text{Core Build},\ (\text{OD} - \text{ID})/2),\ C = (\text{Winding Build},\ W/4 = ID/4)$$

$$MA_{Ht} = \left(3\left(\frac{ID}{4}\right) + 2Ht\right), \qquad [25\text{-}20]$$

$$MA_{OD} = \left(\left(\frac{ID}{2}\right) + (OD - ID) + ID\right), \qquad [25\text{-}21]$$

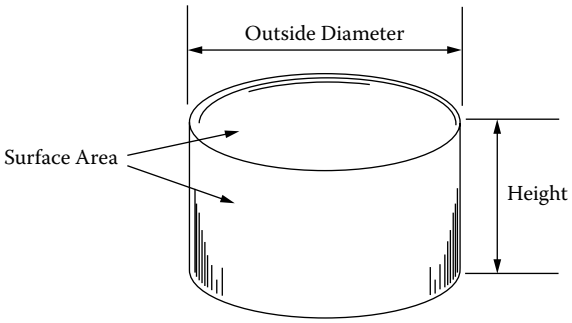

Figure 25-17. The Outline of a Toroidal Wound Magnetic Amplifier.

The surface area of a Toroidal Magnetic Amplifier can be calculated using Equation, [25-24].

$$\text{Top and Bottom Surface} = 2\left(\frac{\pi(MA_{OD})^2}{4}\right), \quad [\text{cm}^2], \qquad [25\text{-}22]$$

© 2011 by Taylor and Francis Group, LLC

$$\text{Periphery Surface} = \left(\pi\left(MA_{OD}\right)\right)\left(MA_{\text{Ht}}\right), \quad [\text{cm}^2], \tag{25-23}$$

$$A_t = \frac{\pi\left(MA_{OD}\right)^2}{2} + \left(\pi\left(MA_{OD}\right)\right)\left(MA_{\text{Ht}}\right), \quad [\text{cm}^2] \tag{25-24}$$

DU Lamination Magnetic Amplifier Surface Area

The data for height, width and length required for the surface area calculation was taken from Chapter 3. The height, Ht, is (H + G), the width, is (D + F), and length is (4E + 3F). The magnetic amplifier outline is shown in Figure 25-18. The surface area for a DU lamination magnetic amplifier can be calculated using Equation, [24-28].

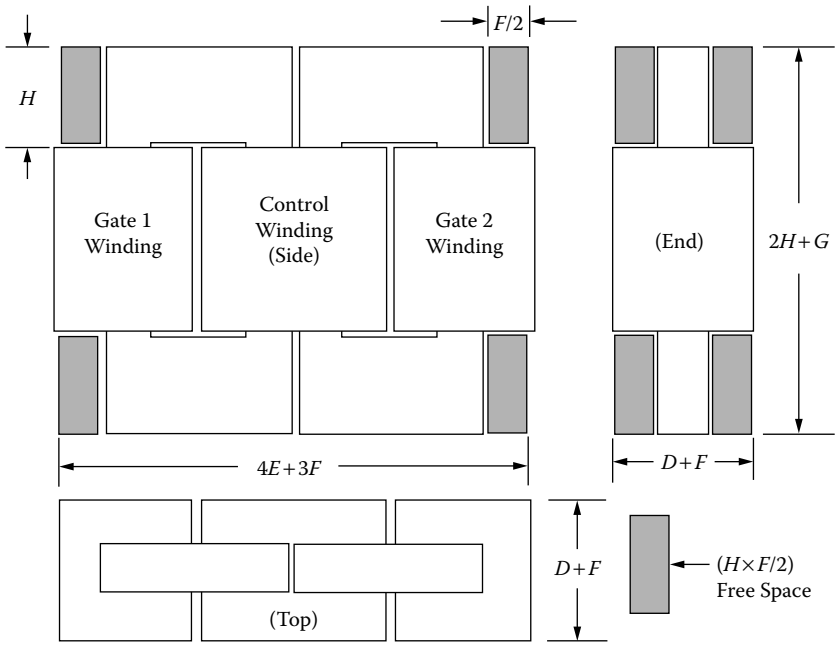

Figure 25-18. The Outline of a DU Lamination Core Wound Magnetic Amplifier.

$$\text{Side Area} = \left(4E + 3F\right)\left(H + G\right) - 2\left(HF\right), \quad [\text{cm}^2] \tag{25-25}$$

$$\text{End Area} = \left(2H + G\right)\left(D + F\right) - 2\left(HF\right), \quad [\text{cm}^2] \tag{25-26}$$

$$\text{Top Area} = \left(4E + 3F\right)\left(D + F\right), \quad [\text{cm}^2] \tag{25-27}$$

$$A_t = 2\left(\text{Side Area}\right) + 2\left(\text{End Area}\right) + 2\left(\text{Top Area}\right), \quad [\text{cm}^2] \tag{25-28}$$

© 2011 by Taylor and Francis Group, LLC

Control Winding Calculation

The control winding must have enough amp-turns to pull the gates out of saturation to where the gates are supporting the total applied voltage, as shown in Figure 25-6. Each magnetic material type has its own electrical characteristic. The magnetic materials that are used in laminations and tape cores are supplied in different thicknesses, so the engineer can design and get best performance at the operating frequency. See Chapter 3. The area within, the hysteresis loop are losses. As the frequency is increased the eddy current loss in the magnetic material increases, and the hysteresis loop gets wider as the losses go up, as shown in Figure 25-19.

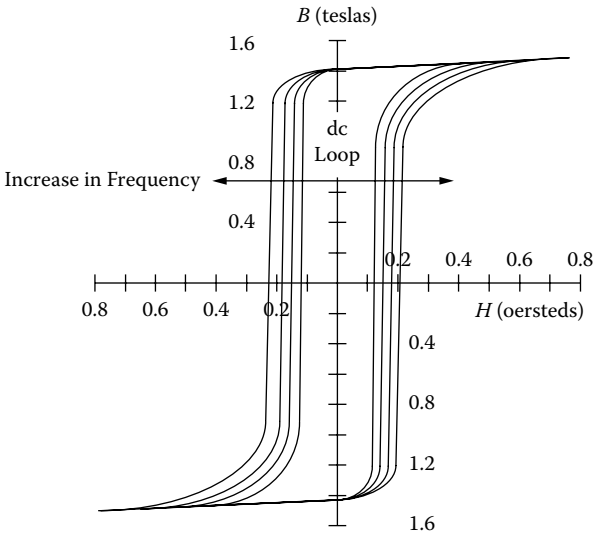

Figure 25-19. Showing How the B-H Loop Changes with Frequency.

The widening of the hysteresis loop has to be taken into consideration when calculating the control turns. When calculating the number of turns required for a control current of 5 ma and a Magnetic Path Length, (MPL), of 9.5 cm, use Figure 25-20 as a guide. The value for A in Figure 25-20 is 0.26 oersteds. The tolerance set by the manufacturers for the magnetizing force (oersteds) is +/–25%. The turns can be calculated using Equation [25-29] for oersteds and Equation [25-30] for amp-turns per meter.

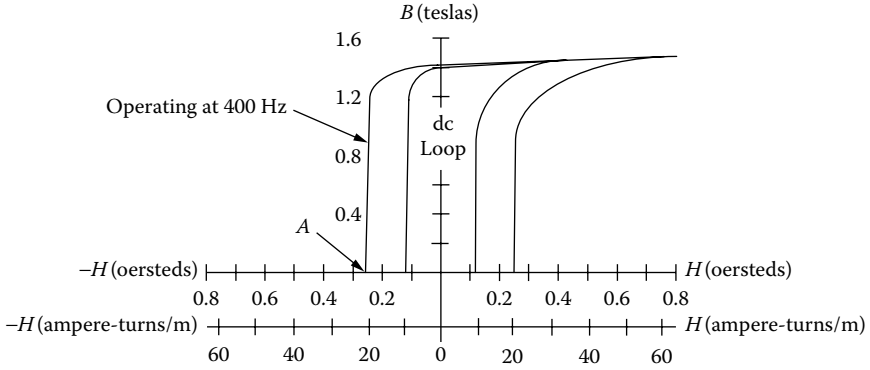

Figure 25-20. The Required Magnetizing Force, A, Operating at 400 Hertz.

© 2011 by Taylor and Francis Group, LLC

$$N = \frac{H(\text{MPL})}{0.4\pi I_c}, \quad [\text{turns}]$$

$$N = \frac{(0.26)(9.5)}{(0.4)(3.415)(0.005)}, \quad [\text{turns}] \qquad [25\text{-}29]$$

$$N = 393, \quad [\text{turns}]$$

$$N = \frac{H(\text{MPL})\left(10^{-2}\right)}{I_c}, \quad [\text{turns}]$$

$$N = \frac{(20.7)(9.5)\left(10^{-2}\right)}{0.005} \qquad [25\text{-}30]$$

$$N = 393, \quad [\text{turns}]$$

Bias Winding Calculation

The bias winding must have enough amp-turns to shift the B-H loop over to get the full core capability, as shown in Figure 25-21. The magnetic material, shown in Figure 25-22, is Square Permalloy 80 in a toroidal configuration. Square Permalloy 80 is considered a square loop material even though it is a little rounded at the top. Although a bias winding could improve its performance, it is not considered mandatory.

Normally the round B-H loop is caused by laminations that introduce a small amount of air-gap. Even a small amount of air-gap will shear the B-H loop over, and this produces the round B-H loop. The amount rounding or shearing of the B-H loop is hard to determine. If the manufacturer does not have the curves or data, it might be wise to wind a sample unit to get the actual data. Then, take a look at the output voltages as shown in Figure 25-7. This will show what is really required and what will be gained with the bias winding. There is another way and that is to look at the B-H loop. Looking at the B-H loop can be done by using one of the cores

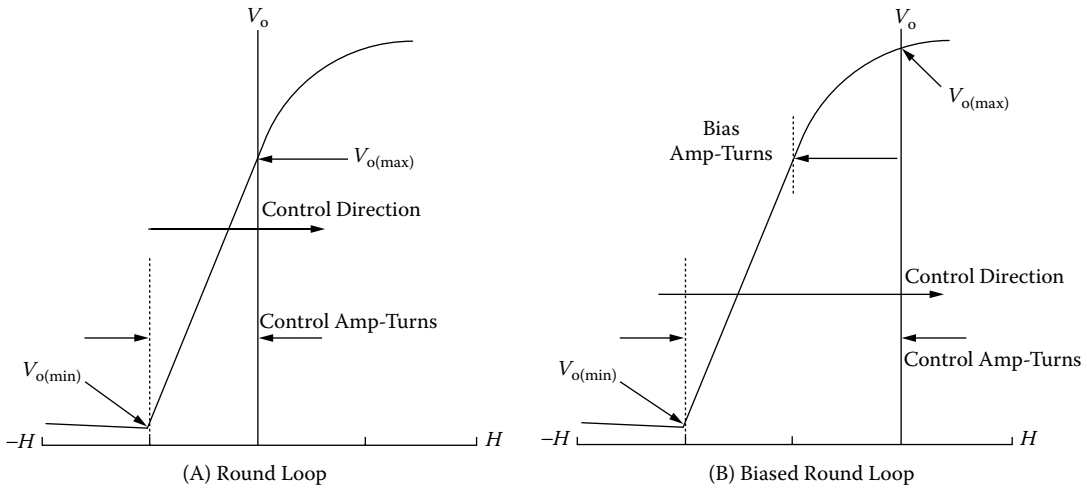

Figure 25-21. Showing How the Bias Amp-Turns Shifts the B-H Loop.

© 2011 by Taylor and Francis Group, LLC

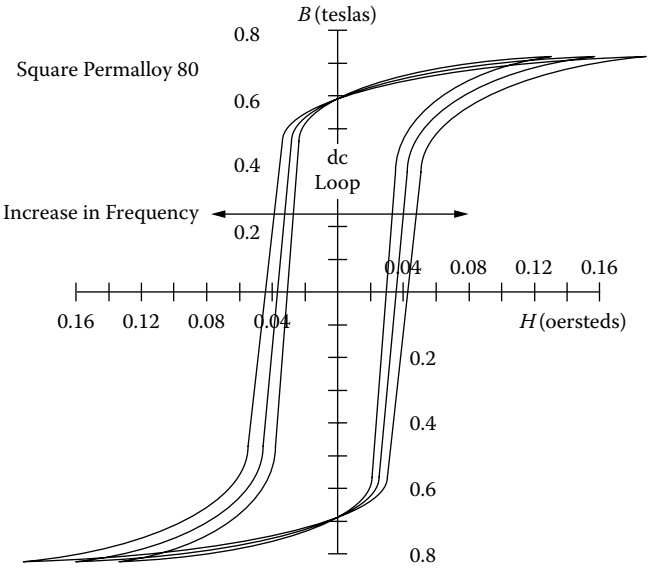

Figure 25-22. Square Permalloy 80 B-H Loop with Increasing Frequency.

and putting on a few turns to see the rounding or shearing over. See Chapter 2. If the self-saturating magnetic amplifier is connected, as shown in Figure 25-12, then the bias current goes into the dot. The amp-turn bias required to shift the B-H loop is shown in Equation [25-31].

$$H = \frac{NI}{\text{MPL}}, \quad \text{[amp-turns/meter]} \qquad [25\text{-}31]$$

Control Winding Precautions

If good design procedures are used, where the cores are matched and high quality diodes are used, the fundamental a-c voltage induced in the control winding by the gates will cancel each other. There could easily be a high voltage induced in the control winding that could require very special attention. This high voltage condition could easily happen if the voltage on the gate was high and there was a large turns ratio between the gate and control winding, as shown in Equation [25-32]. It would be wise to take this precaution taking steps to insulate the control winding to minimize the chances of voltage breakdown. There are conditions that can happen that could be unforeseen at the time, such as wiring error, phase reversing and or a bad component.

$$V_c = \frac{N_c V_g}{N_g}, \quad \text{[volts]} \qquad [25\text{-}32]$$

Self-Saturating Magnetic Amplifier Design Example

The design example will just be the magnetic amplifier used to control and regulate a 12.0 volt at 1.0 amp power supply. The magnetic amplifier test schematic is shown in Figure 25-23. The design will operate from a 14 volt, 400 Hz power source. The core configuration will be toroidal in shape. The cores are matched

© 2011 by Taylor and Francis Group, LLC

using the Constant Current Flux Reset test method. A description of this method can be found in Magnetics manual, "Tape Wound Cores Design Manual TWC-500". The magnetic material will be 50-50 Ni-Fe with a material thickness of 4 mils. The B-H loop for this magnetic material is shown in Figure 25-24. The B-H loop is very square and will not require a bias winding. The magnetic amplifier control current, I_c, is 3 ma with the current going out of the dot. The winding coefficient is $K_{cw} = 1$. In this way the window will be divided up to where the gates get 60% and the control winding will get 40% of the available winding area, as shown in Figure 25-13.

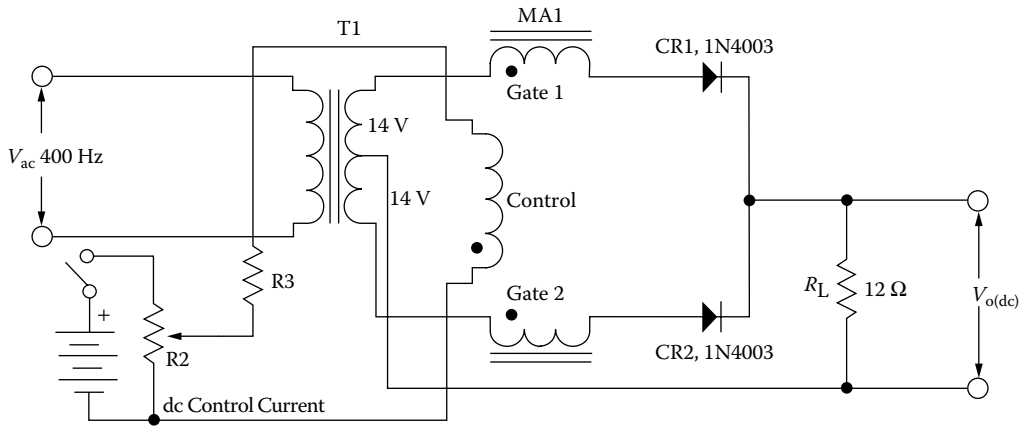

Figure 25-23. Schematic of a Self-Saturating Magnetic Amplifier Test Circuit.

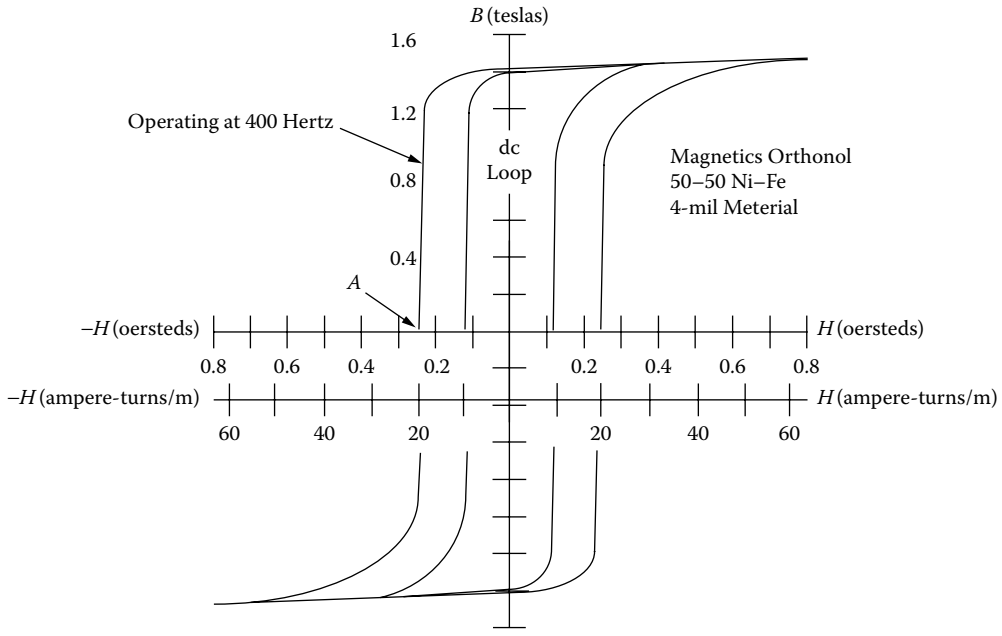

Figure 25-24. Showing the B-H Loop for 50-50 Ni-Fe 4 mil Magnetic Material.

© 2011 by Taylor and Francis Group, LLC

Specification and Design

1. Transformer, T1 Output Voltage, V_t = 14 volts ac
2. Operating Frequency = 400 Hz
3. Load voltage, V_o = 12.0 volts dc
4. Load Current, I_o = 1.0 amps
5. Magnetic Core Type = Toroid
6. Magnetic Material, 4 mil = 50-50 NiFe
7. Efficiency, η = 95%
8. Regulation (copper loss), α = 5%
9. Operating Flux Density, B_{ac} = 1.1T
10. Control Current, I_c = 0.003 amps
11. Magnetizing Force, H = 0.26 oersteds
12. Control Winding Coefficient, K_{cw} = 1.0

Step No. 1: Calculate the load power, P_o.

$$P_o = V_o I_o, \quad \text{[watts]}$$

$$P_o = (12.0)(1.0), \quad \text{[watts]}$$

$$P_o = 12, \quad \text{[watts]}$$

Step No. 2: Calculate the magnetic amplifier, MA1 apparent power, P_t, for a single core. Let, K_{cw} = 1.

$$P_t = (0.5) P_o \left(\sqrt{2_{(gate)}} + K_{cw} \right), \quad \text{[watts]}$$

$$P_t = (0.5)(12)(1.41 + 1), \quad \text{[watts]}$$

$$P_t = 14.5, \quad \text{[watts]}$$

Step No. 3: Calculate the electrical conditions, K_e.

$$K_e = 0.145 K_f^2 f^2 B_m^2 \left(10^{-4}\right)$$

$$K_f = 4.44$$

$$K_e = 0.145(4.44)^2 (400)^2 (1.1)^2 \left(10^{-4}\right)$$

$$K_e = 55.3$$

Step No. 4: Calculate the core geometry, K_g.

$$K_g = \frac{P_t}{2 K_e \alpha}, \quad [\text{cm}^5]$$

$$K_g = \frac{14.5}{2(55.3)(5)}, \quad [\text{cm}^5]$$

$$K_g = 0.0262, \quad [\text{cm}^5]$$

© 2011 by Taylor and Francis Group, LLC

Step No. 5: This core was selected from Magnetics Tape Wound Cores catalog, TWC 500, comparable to core geometry, K_g.

1. Toroid = 52029-4A
2. Manufacturer = Magnetics
3. OD Dimension = 3.78 cm
4. ID Dimension = 2.25 cm
5. Ht Dimension = 0.978 cm
6. Core Geometry, $K_g = 0.0256\ cm^5$
7. Area Product, $A_p = 1.08\ cm^4$
8. Core Weight, $W_t = 19.66$ grams
9. Iron Area, $A_c = 0.272\ cm^2$
10. Window Area, $W_a = 3.97\ cm^2$
11. Magnetic Path Length, MPL = 9.47 cm
12. Magnetic Material, 4 mil = Orthonol

Step No. 6: Calculate the window area for both gate and control winding.

$$W_{ag} = W_a(0.60) = (3.97)(0.60) = 2.38, \quad [cm^2] \ \text{[Gate]}$$

$$W_{ac} = W_a(0.40) = (3.97)(0.40) = 1.59, \quad [cm^2] \ \text{[Control]}$$

Step No. 7: Calculate the number of turns for the gate winding, N_g.

$$N_g = \frac{(V_t - V_d)(10^4)}{K_f B_{ac} f A_c}, \quad \text{[turns]}$$

$$N_g = \frac{(14-1)(10^4)}{(4.44)(1.1)(400)(0.272)}, \quad \text{[turns]}$$

$$N_g = 245, \quad \text{[turns]}$$

Step No. 8: Calculate the gate rms current, $I_{g(rms)}$.

$$I_{g(rms)} = (0.707)I_o, \quad \text{[amps]}$$

$$I_{g(rms)} = (0.707)(1.0), \quad \text{[amps]}$$

$$I_{g(rms)} = (0.707), \quad \text{[amps]}$$

Step No. 9: Calculate the gate wire area, A_{wg}.

$$A_{wg} = \frac{K_u W_{ag}}{N_g}$$

$$A_{wg} = \frac{(0.4)(2.38)}{245}$$

$$A_{wg} = 0.00389$$

© 2011 by Taylor and Francis Group, LLC

Step No. 10: Select the wire from the Wire Table in Chapter 4.

$$AWG = 22$$

$$A_{w(B)} = 0.00324, \quad [\text{cm}^2]$$

$$A_{wg} = 0.00386, \quad [\text{cm}^2]$$

$$\left(\frac{\mu\Omega}{cm}\right) = 531, \quad [\text{micro-ohm/cm}]$$

Step No. 11: Calculate the Mean Length Turn, (MLT) for the gate. Use Figure 25-16 for a reference.

A = Core with case Ht Dimension = 0.978, [cm]

B = Core with case Build = (OD − ID)/2 = 0.765, [cm]

W = Core with case Inside Diameter = 2.25, [cm]

$$\text{MLT} = (2A + 2B + \pi 0.125W)(0.85), \quad [\text{cm}]$$

$$\text{MLT} = \big(2(0.978) + 2(0.765) + \pi 0.125(2.25)\big)(0.85), \quad [\text{cm}]$$

$$\text{MLT} = 3.71, \quad [\text{cm}]$$

Step No. 12: Calculate the gate winding resistance, R_g.

$$R_g = \text{MLT}(N_g)\left(\frac{\mu\Omega}{\text{cm}}\right)\left(10^{-6}\right), \quad [\text{ohms}]$$

$$R_g = 3.71(245)(531)\left(10^{-6}\right), \quad [\text{ohms}]$$

$$R_g = 0.483, \quad [\text{ohms}]$$

Step No. 13: Calculate the gate winding copper loss, P_g.

$$P_g = I_g^2 R_g, \quad [\text{watts}]$$

$$P_g = (0.707)^2 (0.483), \quad [\text{watts}]$$

$$P_g = 0.241, \quad [\text{watts}]$$

Step No. 14: Calculate the required control turns, N_c.

$$N_c = \left(\frac{H(\text{MPL})}{0.4\pi I_c}\right), \quad [\text{turns}]$$

$$N_c = \left(\frac{(0.260)(9.47)}{(1.256)(0.003)}\right), \quad [\text{turns}]$$

$$N_c = 653 \text{ use } 660, \quad [\text{turns}]$$

© 2011 by Taylor and Francis Group, LLC

Step No. 15: Calculate the control wire area, A_{wc}.

$$A_{wc} = \frac{K_u W_{ac}}{N_c}$$

$$A_{wc} = \frac{(0.4)(1.59)}{660}$$

$$A_{wc} = 0.000964$$

Step No. 16: Select the wire from the Wire Table in Chapter 4.

$$AWG = 28$$

$$A_{wc(B)} = 0.000805, \quad [\text{cm}^2]$$

$$A_{wc} = 0.00105, \quad [\text{cm}^2]$$

$$\left(\frac{\mu\Omega}{cm}\right) = 2142, \quad [\text{micro-ohm/cm}]$$

Step No. 17: Calculate the Mean Length Turn, (MLT) for the control winding. Use Figure 25-16 for reference.

A = Core with case Ht Dimension = 0.978

B = Core with case Build = (OD − ID)/2 = 0.765

W = Core with case Inside Diameter = 2.25

$$\text{MLT} = \big((4A + 0.25W) + (2B) + 2\pi(0.375W)\big)(0.70), \quad [\text{cm}]$$

$$\text{MLT} = \big(4(0.978) + 0.25(2.25)) + (2(0.765)\big) + 2\pi\big(0.375(2.25)\big)(0.70), \quad [\text{cm}]$$

$$\text{MLT} = 7.91, \quad [\text{cm}]$$

Step No. 18: Calculate the control winding resistance, R_c.

$$R_c = \text{MLT}(N_c)\left(\frac{\mu\Omega}{\text{cm}}\right)\left(10^{-6}\right), \quad [\text{ohms}]$$

$$R_c = 7.91(660)(2142)\left(10^{-6}\right), \quad [\text{ohms}]$$

$$R_c = 11.2, \quad [\text{ohms}]$$

Step No. 19: Calculate the control winding copper loss, P_c.

$$P_c = I_c^2 R_c, \quad [\text{watts}]$$

$$P_c = (0.003)^2 (11.2), \quad [\text{watts}]$$

$$P_c = 0.0001, \quad [\text{watts}]$$

© 2011 by Taylor and Francis Group, LLC

Step No. 20: Calculate the total copper loss for the gates and control, P_{cu}.

$$P_{cu} = P_{g1} + P_{g2} + P_c, \quad \text{[watts]}$$
$$P_{cu} = (0.241) + (0.241) + (0.0001), \quad \text{[watts]}$$
$$P_{cu} = 0.482, \quad \text{[watts]}$$

Step No. 21: Calculate the percent of total copper loss, α.

$$\alpha = \frac{P_{cu}}{P_o}(100), \quad [\%]$$
$$\alpha = \frac{(0.482)}{(12.0)}(100), \quad [\%]$$
$$\alpha = 4.02, \quad [\%]$$

Step No. 22: Calculate the watts per kilogram, W/K. Use the equation for this material in Chapter 2.

$$W/K = 0.000618(f)^{1.48}(B_{ac})^{1.44}$$
$$W/K = 0.000618(400)^{1.48}(1.1)^{1.44}$$
$$W/K = 5.03$$

Step No. 23: Calculate the core loss, P_{fe}.

$$P_{fe} = (W/K)2(W_{tfe})(10^{-3}), \quad \text{[watts]}$$
$$P_{fe} = (5.03)2(19.7)(10^{-3}), \quad \text{[watts]}$$
$$P_{fe} = 0.198, \quad \text{[watts]}$$

Step No. 24: Calculate the total loss, P_Σ.

$$P_\Sigma = P_{cu} + P_{fe}, \quad \text{[watts]}$$
$$P_\Sigma = (0.482) + (0.198), \quad \text{[watts]}$$
$$P_\Sigma = 0.68, \quad \text{[watts]}$$

Step No. 25: Calculate the magnetic amplifier height, Ht, using Figure 25-17 for reference, See Chapter 5.

$$MA_{Ht} = \left(3\left(\frac{ID}{4}\right) + 2Ht\right), \quad \text{[cm]}$$
$$MA_{Ht} = \left(3\left(\frac{2.25}{4}\right) + 2(0.978)\right), \quad \text{[cm]}$$
$$MA_{Ht} = 3.64, \quad \text{[cm]}$$

© 2011 by Taylor and Francis Group, LLC

Step No. 26: Calculate the magnetic amplifier outside diameter, OD using Figure 25-17 for reference. See Chapter 5.

$$MA_{OD} = \left(\left(\frac{ID}{2}\right) + (OD - ID) + ID\right), \quad [\text{cm}]$$

$$MA_{OD} = \left(\left(\frac{2.25}{2}\right) + (3.78 - 2.25) + 2.25\right), \quad [\text{cm}]$$

$$MA_{OD} = 4.91, \quad [\text{cm}]$$

Step No. 27: Calculate the magnetic amplifier surface area using Figure 25-17 for reference, See Chapter 5.

$$A_t = \frac{\pi(MA_{OD})^2}{2} + (\pi(MA_{OD})(MA_{\text{Ht}}), \quad [\text{cm}^2]$$

$$A_t = \frac{\pi(4.91)^2}{2} + (\pi(4.91)(3.64), \quad [\text{cm}^2]$$

$$A_t = 85.8, \quad [\text{cm}^2]$$

Step No. 28: Calculate the watts per unit area, ψ.

$$\psi = \frac{P_\Sigma}{A_t}, \quad [\text{watts/cm}^2]$$

$$\psi = \frac{0.68}{85.8}, \quad [\text{watts/cm}^2]$$

$$\psi = 0.00793, \quad [\text{watts/cm}^2]$$

Step No. 29: Calculate the temperature rise, T_r.

$$T_r = 450(\psi)^{0.826}, \quad [°\text{C}]$$

$$T_r = 450(0.00793)^{0.826}, \quad [°\text{C}]$$

$$T_r = 8.28, \quad [°\text{C}]$$

Step No. 30: Calculate the window utilization, K_u, for both control and gate.

$$K_{uc} = \left(\frac{N_c A_{wc(B)}}{\frac{W_a}{2}}\right), \quad K_{uc} = \frac{(660)(0.000805)}{(1.59)} = 0.334$$

$$K_{ug} = \left(\frac{N_g A_{wg(B)}}{\frac{W_a}{2}}\right), \quad K_{ug} = \frac{(245)(0.00324)}{(2.38)} = 0.334$$

© 2011 by Taylor and Francis Group, LLC

Self-Saturating, Magnetic Amplifier Design Test Data

Summary

The above self-saturating, magnetic amplifier was built, and tested. The following information is the test data for the above magnetic amplifier design. The input control current versus the output voltage test data is shown in Table 25-1. The input current versus output voltage transfer function is shown in Figure 25-25. The author hopes that this design, with its step-by-step approach, helps the readers understand the design of a self-saturating, magnetic amplifier.

Test Data

1. Frequency, f = 400 Hz
2. Output voltage, V_o = 12.05 volts
3. Output current, I_o = 1.0 amps
4. Control current, I_c = 0.003 amps
5. Gate resistance, R_g = 0.475 ohms
6. Control resistance, R_c = 10.56 ohms
7. Temperature Rise, T_r = 8.1°C

Table 25-1. Self-Saturating, Magnetic Amplifier, Showing Input Current versus Output Voltage

Self-Saturating Magnetic Amplifier		
Steps	Control Current ma	Output Voltage Volts
1	0.000	12.050
2	0.250	12.020
3	0.500	12.000
4	0.750	11.880
5	1.000	11.550
6	1.250	10.350
7	1.500	8.770
8	1.750	7.130
9	2.000	5.220
10	2.250	3.570
11	2.500	2.360
12	2.750	1.270
13	3.000	0.480
14		

© 2011 by Taylor and Francis Group, LLC

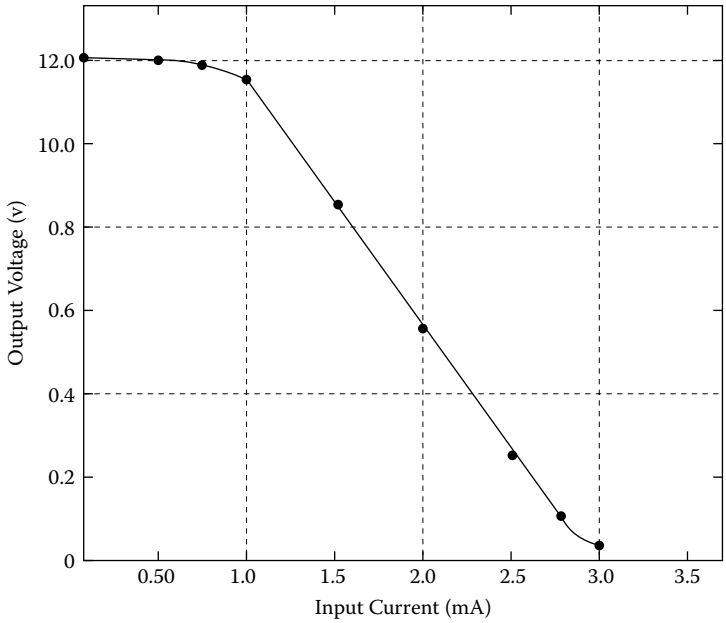

Figure 25-25. Transfer Function Using the Data in Table 25-1.

Recognition

I would like to thank Charles Barnett, an engineer at Leightner Electronics Inc., for building and testing the magnetic amplifier design example.

Leightner Electronics Inc.
1501 S. Tennessee St.
McKinney, TX. 75069

I would like to thank Zack Cataldi, a Senior Applications Engineer at Magnetics, for supplying the cores for the magnetic amplifier design example.

Magnetics
110 Delta Drive
Pittsburgh, PA 15238

© 2011 by Taylor and Francis Group, LLC

References

1. Flanagan, W.M., *Handbook of Transformer Applications*, McGraw-Hill Book Co., Inc., New York, 1986, pp. 14.9–14.20.

2. Lee, R., *Electronic Transformers and Circuits*, John Wiley & Sons, New York, 1958, pp. 259–291.

3. Platt, S., *Magnetic Amplifiers Theory and Application*, Prentice-Hall, Inc., Englewood Cliffs, N.J., 1958, Chapter 9.

4. ITT, Corp, *Reference Data for Radio Engineers,* fourth edition, Stratford Press, Inc., New York, 1956, Chapter 13, pp. 323–343.

© 2011 by Taylor and Francis Group, LLC

Chapter 26

Designing Inductors for a Given Resistance

© 2011 by Taylor and Francis Group, LLC

Table of Contents

1. Introduction....26-3
2. Design Overview....26-3
3. Powder Core Inductor Design Example (Core Geometry, K_g, Approach)....26-4
4. Powder Core Inductor Design Test Data (Core Geometry, K_g, Approach)....26-9
5. Gapped Ferrite Inductor Design Example (Core Geometry, K_g, Approach)....26-10
6. Gapped, Ferrite Inductor Design Test Data (Core Geometry, K_g, Approach)....26-15
7. Powder Core, Input Inductor Design Example (Core Geometry, K_g, Approach)....26-16
8. Powder Core, Input Inductor Design Test Data (Core Geometry, K_g, Approach)....26-20
9. Recognition....26-21

© 2011 by Taylor and Francis Group, LLC

Introduction

There are times when the engineer is required to design around a black box. This means the engineer does not get an overview of the complete picture. The parameters given to the engineer are inductance, dc current, ac current, dc resistance, temperature rise, and volume. If the engineer is lucky, a sample unit will show up. With a design example in hand the engineer can get more of a feel for what core was used in the design. I have been asked many times, by engineers, to write a step-by-step approach using my equations to design an inductor for a given dc resistance. An inductor with its internal equivalent resistance is shown in Figure 26-1.

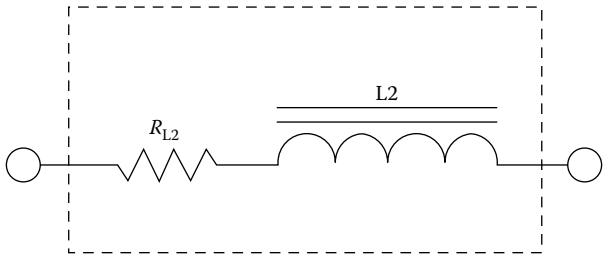

Figure 26-1. Output Inductor, L2, Showing the Internal Equivalent Resistance.

Design Overview

This chapter will present a straight forward approach for selecting the core and the proper wire size to meet the specification for the winding resistance that can be used for both an input inductor, L1, and an output inductor, L2, as shown in Figure 26-2.

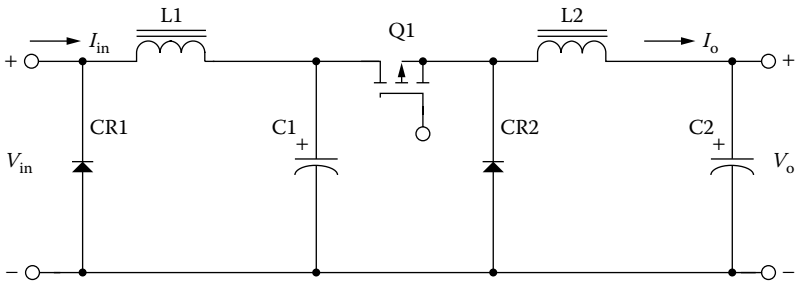

Figure 26-2. Schematic of a Simple Buck Regulator.

Designing to meet a given resistance is very difficult and requires more than several iterations using the area product, A_p, method. The core geometry, K_g, approach is very precise and will lead you to the correct core, with a minimum of time.

The losses in the magnetic material will increase significantly when the converter is operating at a higher frequency. However, the core loss in the output inductor of a switching regulator is much lower compared to

© 2011 by Taylor and Francis Group, LLC

the core loss in the main converter transformer. The core loss in the output inductor is caused by the change in current or ΔI, which induces a change in flux, B_{ac}, as shown in Figure 26-3.

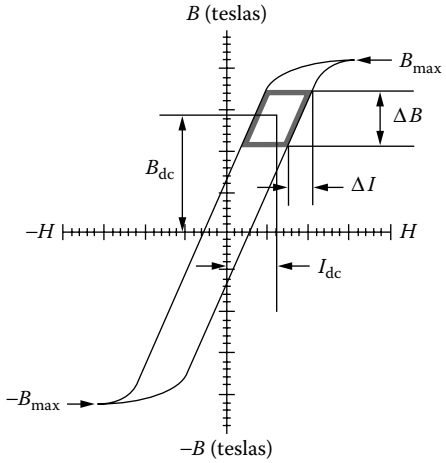

Figure 26-3. Typical, Output Inductor, B-H Loop.

Powder Core Inductor Design Example (Core Geometry, K_g, Approach)

The magnetic cores and wire data have been taken from Chapters 3 and 4. A powder core inductor design example, assume an output filter, L2, as shown in Figure 26-2, with the following specifications:

1. Frequency, f = 100kHz
2. Inductance, L = 50 µh
3. Output current, I_o = 5.0 amps
4. Delta current, ΔI = 1.0 amps
5. DC Resistance, R = 0.01 ohms
6. Temperature Rise, T_r = <20°C
7. Window utilization, K_u = 0.4
8. Operating Flux, B_m = 0.3 T

This design procedure will work equally well with all of the various powder cores. Care must be taken regarding maximum flux density with different materials and core loss.

Step No. 1: Calculate the peak current, I_{pk}.

$$I_{pk} = I_{o(\max)} + \left(\frac{\Delta I}{2}\right) \quad \text{[amps]}$$

$$I_{pk} = (5.0) + \left(\frac{1.0}{2}\right) \quad \text{[amps]}$$

$$I_{pk} = 5.5 \quad \text{[amps]}$$

© 2011 by Taylor and Francis Group, LLC

Step No. 2: Calculate the energy-handling capability in watt-seconds, w-s.

$$\text{Energy} = \frac{LI_{pk}^2}{2} \quad \text{[w-s]}$$

$$\text{Energy} = \frac{\left(50 \times 10^{-6}\right)(5.5)^2}{2} \quad \text{[w-s]}$$

$$\text{Energy} = 0.000756 \quad \text{[w-s]}$$

Step No. 3: Calculate the electrical conditions, K_e.

$$K_e = \frac{345L}{B_m^2 R_{(L)}}$$

$$K_e = \frac{345\left(50 \times 10^{-6}\right)}{(0.3)^2(0.01)}$$

$$K_e = 19.2$$

Step No. 4: Calculate the core geometry, K_g.

$$K_g = K_e\left(\text{Energy}\right) \quad [\text{cm}^5]$$

$$K_g = (19.2)(0.000756) \quad [\text{cm}^5]$$

$$K_g = 0.0145 \quad [\text{cm}^5]$$

Step No. 5: Select a MPP powder core, from Chapter 3, comparable in core geometry, K_g.

Core number = 55059-A2
Manufacturer = Magnetics
Magnetic path length, MPL = 5.7 cm
Core weight, W_{tfe} = 15.0 grams
Copper weight, W_{tcu} = 15.2 grams
Mean length turn, MLT = 3.2 cm
Iron area, A_c = 0.331 cm^2
Window Area, W_a = 1.356 cm^2
Area Product, A_p = 0.449 cm^4
Core geometry, K_g = 0.0186 cm^5
Surface area, A_t = 28.6 cm^2
Permeability, μ = 60
Millihenrys per 1000 turns, AL = 43

© 2011 by Taylor and Francis Group, LLC

Step No. 6: Calculate the number of turns, N.

$$N = 1000\sqrt{\frac{L_{(new)}}{L_{(1000)}}} \quad [\text{turns}]$$

$$N = 1000\sqrt{\frac{.05}{43}} \quad [\text{turns}]$$

$$N = 34 \quad [\text{turns}]$$

Step No. 7: Calculate the rms current, I_{rms}.

$$I_{rms} = \sqrt{I_{o(\max)}^2 + \Delta I^2} \quad [\text{amps}]$$

$$I_{rms} = \sqrt{(5)^2 + (1)^2} \quad [\text{amps}]$$

$$I_{rms} = 5.1 \quad [\text{amps}]$$

Step No. 8: Calculate the current density, J, using a window utilization, $K_u = 0.4$.

$$J = \frac{NI}{W_a K_u} \quad [\text{amps/cm}^2]$$

$$J = \frac{(34)(5.1)}{(1.356)(.4)} \quad [\text{amps/cm}^2]$$

$$J = 320 \quad [\text{amps/cm}^2]$$

Step No. 9: Calculate the required permeability, $\Delta\mu$.

$$\Delta\mu = \frac{(B_m)(MPL)\times 10^4}{0.4\pi(W_a)(J)(K_u)}$$

$$\Delta\mu = \frac{(0.3)(5.7)\times 10^4}{(1.256)(1.356)(320)(0.4)}$$

$$\Delta\mu = 78.4 \text{ use } 60 \text{ perm}$$

Step No. 10: Calculate the peak flux density, B_m.

$$B_m = \frac{0.4\pi(N)(I_{pk})(\mu_r)\times 10^{-4}}{MPL} \quad [\text{teslas}]$$

$$B_m = \frac{1.256(34)(5.5)(60)\times 10^{-4}}{(5.7)} \quad [\text{teslas}]$$

$$B_m = 0.247 \quad [\text{teslas}]$$

© 2011 by Taylor and Francis Group, LLC

Step No. 11: Calculate the required bare wire area, $A_{w(B)}$.

$$A_{w(B)} = \frac{I_{rms}}{J} \quad [\text{cm}^2]$$

$$A_{w(B)} = \frac{5.1}{320} \quad [\text{cm}^2]$$

$$A_{w(B)} = 0.0159 \quad [\text{cm}^2]$$

Step No. 12: Select a wire size with the required area from the Wire Table in Chapter 4. If the area is not within a few percent of required area, then go to the next smallest size.

$$\text{AWG} = \#15$$

$$A_{w(B)} = 0.0165$$

$$\mu\Omega / cm = 104$$

Step No. 13: Calculate the winding resistance, R.

$$R = \text{MLT}(N)\left(\frac{\mu\Omega}{\text{cm}}\right)\left(10^{-6}\right), \quad [\text{ohms}]$$

$$R = (3.2)(34)(104)\left(10^{-6}\right), \quad [\text{ohms}]$$

$$R = 0.0113, \quad [\text{ohms}]$$

Step No. 14: Calculate the winding copper loss, P_{cu}.

$$P_{cu} = I^2 R, \quad [\text{watts}]$$

$$P_{cu} = (5.1)^2(0.0113), \quad [\text{watts}]$$

$$P_{cu} = 0.294, \quad [\text{watts}]$$

Step No. 15: Calculate the magnetizing force in oersteds, H.

$$H = \frac{(0.4\pi)NI_{pk}}{MPL} \quad [\text{oersteds}]$$

$$H = \frac{(1.256)(34)(5.5)}{5.7} \quad [\text{oersteds}]$$

$$H = 41.2 \quad [\text{oersteds}]$$

© 2011 by Taylor and Francis Group, LLC

Step No. 16: Calculate the ac flux density in teslas, B_{ac}.

$$B_{ac} = \frac{(0.4\pi)(N)\left(\frac{\Delta I}{2}\right)(\mu_r)\times 10^{-4}}{MPL} \quad \text{[teslas]}$$

$$B_{ac} = \frac{(1.256)(34)(0.5)(60)\times 10^{-4}}{5.7} \quad \text{[teslas]}$$

$$B_{ac} = 0.0225 \quad \text{[teslas]}$$

Step No. 17: Calculate the watts per kilogram, WK, using MPP 60 perm powder cores, as shown in Chapter 7.

$$WK = 0.788\times 10^{-3}\,(f)^{(1.41)}\,(B_{ac})^{(2.24)} \quad \text{[watts/kilogram]}$$

$$WK = 0.788\times 10^{-3}\,(100000)^{(1.41)}\,(0.0225)^{(2.24)} \quad \text{[watts/kilogram]}$$

$$WK = 1.80 \quad \text{[watts/kilogram] or [milliwatts/gram]}$$

Step No. 18: Calculate the core loss, P_{fe}.

$$P_{fe} = \left(\frac{\text{milliwatts}}{\text{gram}}\right) W_{tfe}\times 10^{-3} \quad \text{[watts]}$$

$$P_{fe} = (1.8)(15)\times 10^{-3} \quad \text{[watts]}$$

$$P_{fe} = 0.027 \quad \text{[watts]}$$

Step No. 19: Calculate the total loss P_{Σ}, core P_{fe} and copper P_{cu}, in watts.

$$P_{\Sigma} = P_{fe} + P_{cu} \quad \text{[watts]}$$

$$P_{\Sigma} = (0.027) + (0.294) \quad \text{[watts]}$$

$$P_{\Sigma} = 0.321 \quad \text{[watts]}$$

Step No. 20: Calculate the watt density, ψ.

$$\psi = \frac{P_{\Sigma}}{A_t} \quad \text{[watts/cm}^2\text{]}$$

$$\psi = \frac{0.321}{28.6} \quad \text{[watts/cm}^2\text{]}$$

$$\psi = 0.0112 \quad \text{[watts/cm}^2\text{]}$$

© 2011 by Taylor and Francis Group, LLC

Step No. 21: Calculate the temperature rise in degrees C.

$$T_r = 450(\psi)^{(0.826)} \quad \text{[degrees C]}$$
$$T_r = 450(0.0112)^{(0.826)} \quad \text{[degrees C]}$$
$$T_r = 11.0 \quad \text{[degrees C]}$$

Step No. 22: Calculate the window utilization, K_u.

$$K_u = \frac{NA_{w(B)}}{W_a}$$
$$K_u = \frac{(34)(0.0165)}{(1.356)}$$
$$K_u = 0.414$$

Powder Core Inductor Design Test Data (Core Geometry, K_g, Approach)

Summary

The following information is the test data for the above powder core inductor. It is difficult to design and achieve the required resistance with just one wire and also have a compact design. If the engineer is required to get closer to the required resistance called out in the design specification, the inductor could be wound bifilar using a large wire and a smaller wire. It would be like having two resistors in parallel to get the correct resistance. The author hopes that this chapter, with its step-by-step approach, helps the readers understand the design of a filter inductor with the required resistance. The above example of this inductor was built, and tested. It meets the intent of the specification and shows the reader a typical design.

Test Data

1. Frequency, f = 100kHz
2. Inductance, L = 54 µh
3. Inductance, L, (at 5.0 amps) = 50 µh
4. Output current, I_o = 5.0 amps
5. DC Resistance, R_L = 0.0119 ohms
6. Temperature Rise, T_r = 12.5°C
7. Window utilization, K_u (See Chapter 4) = 0.404
8. Max. Operating Flux, B_m = 0.247 T

© 2011 by Taylor and Francis Group, LLC

Gapped Ferrite Inductor Design Example (Core Geometry, K_g, Approach)

The magnetic cores and wire data have been taken from Chapters 3 and 4. For a gapped inductor design example, assume an output filter, L2, as shown in Figure 26-2, with the following specifications:

Step No. 1: Design Specifications.

1. Frequency, f = 100kHz
2. Inductance, L = 50 µh
3. Output current, I_o = 4.0 amps
4. Delta current, ΔI = 0.4 amps
5. DC Resistance, R = 0.01 ohms
6. Temperature Rise, T_r = <20°C
7. Window utilization, K_u (See Chapter 4) = 0.313
8. Operating Flux, B_m = 0.25 T

Step No. 2: Calculate the peak current, I_{pk}.

$$I_{pk} = I_{o(\max)} + \left(\frac{\Delta I}{2}\right) \quad \text{[amps]}$$

$$I_{pk} = (4.0) + \left(\frac{0.4}{2}\right) \quad \text{[amps]}$$

$$I_{pk} = 4.2 \quad \text{[amps]}$$

Step No. 3: Calculate the energy-handling capability in watt-seconds, w-s.

$$\text{Energy} = \frac{LI_{pk}^2}{2} \quad \text{[w-s]}$$

$$\text{Energy} = \frac{\left(50 \times 10^{-6}\right)(4.2)^2}{2} \quad \text{[w-s]}$$

$$\text{Energy} = 0.000441 \quad \text{[w-s]}$$

Step No. 4: Calculate the electrical conditions, K_e.

$$K_e = \frac{345L}{B_m^2 R_{(L)}}$$

$$K_e = \frac{345\left(50 \times 10^{-6}\right)}{(0.25)^2(0.01)}$$

$$K_e = 27.6$$

© 2011 by Taylor and Francis Group, LLC

Step No. 5: Calculate the core geometry, K_g. Since this design is using a ferrite core the core geometry, K_g, has to be increased approximately 20%. See Chapter 4 on window utilization, K_u, for bobbin ferrites.

$$K_g = K_e\,(\text{Energy})(1.20) \quad [\text{cm}^5]$$

$$K_g = (27.6)(0.000441)(1.20) \quad [\text{cm}^5]$$

$$K_g = 0.0146 \quad [\text{cm}^5]$$

Step No. 6: Select a Pot core from Chapter 7, comparable in core geometry, K_g.

Core number = PC-42213
Manufacturer = Magnetics
Magnetic path length, MPL = 3.12 cm
Core weight, W_{tfe} = 13 grams
Copper weight, W_{tcu} = 6.2 grams
Mean length turn, MLT = 4.4 cm
Iron area, A_c = 0.634 cm^2
Window Area, W_a = 0.414 cm^2
Area Product, A_p = 0.262 cm^4
Core geometry, K_g = 0.0151 cm^5
Winding Length, G = 0.940 cm
Surface area, A_t = 16.4 cm^2
Permeability, μ = 2500 (P)
Millihenrys per 1000 turns, AL = 4393

Step No. 7: Calculate the current density, J, using the area product Equation, A_p.

$$J = \frac{2(\text{Energy})(10^4)}{B_m A_p K_u}, \quad [\text{amps-per-cm}^2]$$

$$J = \frac{2(0.000441)(10^4)}{(0.25)(0.262)(0.4)}, \quad [\text{amps-per-cm}^2]$$

$$J = 337, \quad [\text{amps-per-cm}^2]$$

Step No. 8: Calculate the rms current, I_{rms}.

$$I_{rms} = \sqrt{I_o^2 + \Delta I^2}, \quad [\text{amps}]$$

$$I_{rms} = \sqrt{(4.0)^2 + (0.4)^2}, \quad [\text{amps}]$$

$$I_{rms} = 4.02, \quad [\text{amps}]$$

© 2011 by Taylor and Francis Group, LLC

Step No. 9: Calculate the required bare wire area, $A_{w(B)}$.

$$A_{W(B)} = \frac{I_{rms}}{J}, \quad [\text{cm}^2]$$

$$A_{W(B)} = \frac{(4.02)}{(337)}, \quad [\text{cm}^2]$$

$$A_{W(B)} = 0.0119, \quad [\text{cm}^2]$$

Step No. 10: Select a wire from the Wire Table in Chapter 4. If the area is not within a few percent, take the next smallest size. Also, record the micro-ohms per centimeter.

$$\text{AWG} = \#17$$

$$\text{Bare, } A_{W(B)} = 0.01039, \quad [\text{cm}^2]$$

$$\text{Insulated, } A_W = 0.0117, \quad [\text{cm}^2]$$

$$\left(\frac{\mu\Omega}{\text{cm}}\right) = 166, \quad [\text{micro-ohm/cm}]$$

Step No. 11: Calculate the effective window area, $W_{a(eff)}$. Use the window area found in Step 6. A typical value for, S_3, is 0.6, as shown in Chapter 4.

$$W_{a(eff)} = W_a S_3, \quad [\text{cm}^2]$$

$$W_{a(eff)} = (0.414)(0.60), \quad [\text{cm}^2]$$

$$W_{a(eff)} = 0.248, \quad [\text{cm}^2]$$

Step No. 12: Calculate the number turns possible, N, using the insulated wire area, A_w, found in Step 10. A typical value for, S_2, is 0.61, as shown in Chapter 4.

$$N = \frac{W_{a(eff)} S_2}{A_W}, \quad [\text{turns}]$$

$$N = \frac{(0.248)(0.61)}{(0.0117)}, \quad [\text{turns}]$$

$$N = 12.9 \text{ use } 13, \quad [\text{turns}]$$

Step No. 13: Calculate the required gap, l_g.

$$l_g = \frac{0.4\pi N^2 A_c (10^{-8})}{L} - \left(\frac{\text{MPL}}{\mu_m}\right), \quad [\text{cm}]$$

$$l_g = \frac{(1.26)(13)^2(0.634)(10^{-8})}{(0.00005)} - \left(\frac{3.12}{2500}\right), \quad [\text{cm}]$$

$$l_g = 0.0257, \quad [\text{cm}]$$

© 2011 by Taylor and Francis Group, LLC

Step No. 14: Calculate the equivalent gap in mils.

$$\text{mils} = \text{cm}(393.7)$$

$$\text{mils} = (0.0257)(393.7)$$

$$\text{mils} = 10, \text{ then cm} = 0.0254$$

Step No. 15: Calculate the fringing flux factor, F.

$$F = 1 + \frac{l_g}{\sqrt{A_c}} \ln\left(\frac{2G}{l_g}\right)$$

$$F = 1 + \frac{(0.0254)}{\sqrt{0.634}} \ln\left(\frac{2(0.940)}{0.0254}\right)$$

$$F = 1.14$$

Step No. 16: Calculate the new number of turns, N_n, by inserting the fringing flux, F.

$$N_n = \sqrt{\frac{l_g L}{0.4\pi A_c F\left(10^{-8}\right)}}, \quad \text{[turns]}$$

$$N_n = \sqrt{\frac{(0.0254)(0.00005)}{(1.26)(0.634)(1.14)\left(10^{-8}\right)}}, \quad \text{[turns]}$$

$$N_n = 12, \quad \text{[turns]}$$

Step No. 17: Calculate the winding resistance, R_L. Use the MLT from Step 6 and the micro-ohm per centimeter from Step 10.

$$R_L = (\text{MLT})(N_n)\left(\frac{\mu\Omega}{\text{cm}}\right)\left(10^{-6}\right), \quad \text{[ohms]}$$

$$R_L = (4.4)(12)(166)\left(10^{-6}\right), \quad \text{[ohms]}$$

$$R_L = 0.0088, \quad \text{[ohms]}$$

Step No. 18: Calculate the copper loss, P_{cu}.

$$P_{cu} = I_{rms}^2 R_L, \quad \text{[watts]}$$

$$P_{cu} = (4.02)^2(0.0088), \quad \text{[watts]}$$

$$P_{cu} = 0.142, \quad \text{[watts]}$$

© 2011 by Taylor and Francis Group, LLC

Step No. 19: Calculate the ac flux density, B_{ac}.

$$B_{ac} = \frac{0.4\pi N_n F\left(\frac{\Delta I}{2}\right)\left(10^{-4}\right)}{l_g + \left(\frac{\text{MPL}}{\mu_m}\right)}, \quad \text{[teslas]}$$

$$B_{ac} = \frac{(1.26)(12)(1.14)\left(\frac{0.4}{2}\right)\left(10^{-4}\right)}{(0.0254) + \left(\frac{3.12}{2500}\right)}, \quad \text{[teslas]}$$

$$B_{ac} = 0.0129, \quad \text{[teslas]}$$

Step No. 20: Calculate the watts per kilogram for ferrite, P, material in Chapter 2. Watts per kilogram can be written in milliwatts per gram.

$$\text{mW/g} = k f^{(m)} B_{ac}^{(n)}$$

$$\text{mW/g} = (0.00004855)(100000)^{(1.63)}(0.0129)^{(2.62)}$$

$$\text{mW/g} = 0.0769$$

Step No. 21: Calculate the core loss, P_{fe}.

$$P_{fe} = (\text{mW/g})\left(W_{tfe}\right)\left(10^{-3}\right), \quad \text{[watts]}$$

$$P_{fe} = (0.0769)(13)\left(10^{-3}\right), \quad \text{[watts]}$$

$$P_{fe} = 0.001, \quad \text{[watts]}$$

Step No. 22: Calculate the total loss, copper plus iron, P_{Σ}.

$$P_{\Sigma} = P_{fe} + P_{cu}, \quad \text{[watts]}$$

$$P_{\Sigma} = (0.001) + (0.265), \quad \text{[watts]}$$

$$P_{\Sigma} = 0.266, \quad \text{[watts]}$$

Step No. 23: Calculate the watt density, ψ. The surface area, A_t, can be found in Step 6.

$$\psi = \frac{P_{\Sigma}}{A_t}, \quad \text{[watts/cm}^2\text{]}$$

$$\psi = \frac{(0.266)}{(16.4)}, \quad \text{[watts/cm}^2\text{]}$$

$$\psi = 0.0162, \quad \text{[watts/cm}^2\text{]}$$

Step No. 24: Calculate the temperature rise, T_r.

$$T_r = 450(\psi)^{(0.826)}, \quad [^{\circ}\text{C}]$$

$$T_r = 450(0.0162)^{(0.826)}, \quad [^{\circ}\text{C}]$$

$$T_r = 14.9, \quad [^{\circ}\text{C}]$$

© 2011 by Taylor and Francis Group, LLC

Step No. 25: Calculate the peak flux density, B_{pk}.

$$B_{pk} = \frac{0.4\pi N_n F\left(I_{dc} + \frac{\Delta I}{2}\right)\left(10^{-4}\right)}{l_g + \left(\frac{\text{MPL}}{\mu_m}\right)}, \quad \text{[teslas]}$$

$$B_{pk} = \frac{(1.26)(12)(1.14)(4.2)\left(10^{-4}\right)}{(0.0254) + \left(\frac{3.12}{2500}\right)}, \quad \text{[teslas]}$$

$$B_{pk} = 0.271, \quad \text{[teslas]}$$

Step No. 26: Calculate the total window utilization, K_u.

$$K_u = \frac{NA_{w(B)}}{W_a}$$

$$K_u = \frac{(12)(0.01039)}{(0.414)}$$

$$K_u = 0.301$$

Gapped, Ferrite Inductor Design Test Data (Core Geometry, K_g, Approach)

Summary

The following information is the test data for the above gapped ferrite inductor. It is difficult to design and achieve the required resistance with just one wire and also have a compact design. If the engineer is required to get closer to the required resistance called out in the design specification, the inductor could be wound bifilar using a large wire and a smaller wire. It would be like having two resistors in parallel to get the correct resistance. The author hopes that this chapter, with its step-by-step approach, helps the readers understand the design of a filter inductor with the required resistance. The above example of this inductor was built, and tested. It meets the intent of the specification and shows the reader a typical design.

Test Data

1. Frequency, f = 100kHz
2. Inductance, L = 52 µh
3. Inductance, L, (at 4.0 amps) = 49 µh
4. Output current, I_o = 4.0 amps
5. DC Resistance, R_L = 0.0088ohms
6. Temperature Rise, T_r = 12.1°C
7. Window utilization, K_u (See Chapter 4) = 0.301
8. Max. Operating Flux, B_m = 0.271 T

© 2011 by Taylor and Francis Group, LLC

Powder Core, Input Inductor Design Example (Core Geometry, K_g, Approach)

For a typical design example, assume an input filter circuit, as shown in Figure 26-2, with the following specifications:

1. Frequency, f = 100kHz
2. Inductance, L = 125 uh
3. Input current, I_{in} = 2.5 amps
4. Delta current, ΔI = 0.010 amps
5. DC Resistance, R = 0.05 ohms
6. Temperature Rise, T_r = <20°C
7. Window utilization, K_u = 0.4
8. Operating Flux, B_m = 0.3

This design procedure will work equally well with all of the various powder cores. Care must be taken regarding maximum flux density with different materials and core loss.

Step No. 1: Calculate the peak current, I_{pk}.

$$I_{pk} = I_{in(\max)} + \left(\frac{\Delta I}{2}\right) \quad \text{[amps]}$$

$$I_{pk} = (2.5) + \left(\frac{0.01}{2}\right) \quad \text{[amps]}$$

$$I_{pk} = 2.505 \quad \text{[amps]}$$

Step No. 2: Calculate the energy-handling capability in watt-seconds, w-s.

$$\text{Energy} = \frac{LI_{pk}^2}{2} \quad \text{[w-s]}$$

$$\text{Energy} = \frac{\left(125\times10^{-6}\right)(2.505)^2}{2} \quad \text{[w-s]}$$

$$\text{Energy} = 0.000392 \quad \text{[w-s]}$$

Step No. 3: Calculate the electrical conditions, K_e.

$$K_e = \frac{345L}{B_m^2 R_{(L)}}$$

$$K_e = \frac{345\left(125\times10^{-6}\right)}{(0.3)^2(0.05)}$$

$$K_e = 9.58$$

© 2011 by Taylor and Francis Group, LLC

Step No. 4: Calculate the core geometry, K_g.

$$K_g = K_e\left(\text{Energy}\right) \quad [\text{cm}^5]$$

$$K_g = (9.58)(0.000392) \quad [\text{cm}^5]$$

$$K_g = 0.00376 \quad [\text{cm}^5]$$

Step No. 5: Select a Sendust powder core from Chapter 3 comparable in core geometry, K_g.

Core number = 77121-A7
Manufacturer = Magnetics
Magnetic path length, MPL = 4.11 cm
Core weight, W_{tfe} = 5.524 grams
Copper weight, W_{tcu} = 6.10 grams
Mean length turn, MLT = 2.5 cm
Iron area, A_c = 0.192 cm^2
Window Area, W_a = 0.684 cm^2
Area Product, A_p = 0.131 cm^4
Core geometry, K_g = 0.00403 cm^5
Surface area, A_t = 16.0 cm^2
Permeability, μ = 60
Millihenrys per 1000 turns, AL = 35

Step No. 6: Calculate the number of turns, N.

$$N = 1000\sqrt{\frac{L_{(new)}}{L_{(1000)}}} \quad [\text{turns}]$$

$$N = 1000\sqrt{\frac{.125}{35}} \quad [\text{turns}]$$

$$N = 59.7 \text{ use } 60 \quad [\text{turns}]$$

Step No. 7: Calculate the rms current, I_{rms}.

$$I_{rms} = \sqrt{I_{o(\max)}^2 + \Delta I^2} \quad [\text{amps}]$$

$$I_{rms} = \sqrt{(2.5)^2 + (0.01)^2} \quad [\text{amps}]$$

$$I_{rms} = 2.50 \quad [\text{amps}]$$

© 2011 by Taylor and Francis Group, LLC

Step No. 8: Calculate the current density, J, using a window utilization, $K_u = 0.4$.

$$J = \frac{NI}{W_a K_u} \quad [\text{amps/cm}^2]$$

$$J = \frac{(60)(2.5)}{(0.684)(.4)} \quad [\text{amps/cm}^2]$$

$$J = 458 \quad [\text{amps/cm}^2]$$

Step No. 9: Calculate the required permeability, $\Delta\mu$.

$$\Delta\mu = \frac{(B_m)(MPL)\times 10^4}{0.4\pi(W_a)(J)(K_u)}$$

$$\Delta\mu = \frac{(0.3)(4.11)\times 10^4}{(1.256)(0.684)(458)(0.4)}$$

$\Delta\mu = 78.3$ use 60 perm

Step No. 10: Calculate the peak flux density, B_m.

$$B_m = \frac{0.4\pi(N)(I_{pk})(\mu_r)\times 10^{-4}}{MPL} \quad [\text{teslas}]$$

$$B_m = \frac{1.256(60)(2.5)(60)\times 10^{-4}}{(4.11)} \quad [\text{teslas}]$$

$B_m = 0.275$ [teslas]

Step No. 11: Calculate the required bare wire area, $A_{w(B)}$.

$$A_{w(B)} = \frac{I_{rms}}{J} \quad [\text{cm}^2]$$

$$A_{w(B)} = \frac{2.5}{458} \quad [\text{cm}^2]$$

$$A_{w(B)} = 0.00546 \quad [\text{cm}^2]$$

Step No. 12: Select a wire size with the required area from the Wire Table in Chapter 4. If the area is not within 10% of required area, then go to the next smallest size.

$$\text{AWG} = \#20$$
$$A_{w(B)} = 0.00519$$
$$\mu\Omega / cm = 332$$

Step No. 13: Calculate the winding resistance, R.

$$R = \text{MLT}(N)\left(\frac{\mu\Omega}{\text{cm}}\right)(10^{-6}), \quad [\text{ohms}]$$

$$R = (2.5)(60)(332)(10^{-6}), \quad [\text{ohms}]$$

$$R = 0.0498, \quad [\text{ohms}]$$

© 2011 by Taylor and Francis Group, LLC

Step No. 14: Calculate the winding copper loss, P_{cu}.

$$P_{cu} = I^2 R, \quad \text{[watts]}$$

$$P_{cu} = (2.5)^2 (0.0498), \quad \text{[watts]}$$

$$P_{cu} = 0.311, \quad \text{[watts]}$$

Step No. 15: Calculate the magnetizing force in oersteds, H.

$$H = \frac{(0.4\pi) N I_{pk}}{MPL} \quad \text{[oersteds]}$$

$$H = \frac{(1.256)(60)(2.5)}{4.11} \quad \text{[oersteds]}$$

$$H = 45.8 \quad \text{[oersteds]}$$

Step No. 16: Calculate the ac flux density in teslas, B_{ac}.

$$B_{ac} = \frac{(0.4\pi)(N)\left(\frac{\Delta I}{2}\right)(\mu_r) \times 10^{-4}}{MPL} \quad \text{[teslas]}$$

$$B_{ac} = \frac{(1.256)(60)(0.005)(60) \times 10^{-4}}{4.11} \quad \text{[teslas]}$$

$$B_{ac} = 0.00055 \quad \text{[teslas]}$$

Note: Normally the ac flux is very low for the input filter inductor.

Step No. 17: Calculate the watts per kilogram, WK, using Sendust 60 perm powder cores, as shown in Chapter 2.

$$WK = 0.634 \times 10^{-3} (f)^{(1.46)} (B_{ac})^{(2.0)} \quad \text{[watts/kilogram]}$$

$$WK = 0.634 \times 10^{-3} (100000)^{(1.46)} (0.00055)^{(2.0)} \quad \text{[watts/kilogram]}$$

$$WK = 0.00383 \quad \text{[watts/kilogram] or [milliwatts/gram]}$$

Step No. 18: Calculate the core loss, P_{fe}.

$$P_{fe} = \left(\frac{\text{milliwatts}}{\text{gram}}\right) W_{tfe} \times 10^{-3} \quad \text{[watts]}$$

$$P_{fe} = (0.00383)(5.524) \times 10^{-3} \quad \text{[watts]}$$

$$P_{fe} = 4.5\left(10^{-7}\right) \quad \text{[watts]}$$

© 2011 by Taylor and Francis Group, LLC

Step No. 19: Calculate the total loss, P_Σ core P_{fe} and copper P_{cu}, in watts.

$$P_\Sigma = P_{fe} + P_{cu} \quad \text{[watts]}$$

$$P_\Sigma = (0.000) + (0.311) \quad \text{[watts]}$$

$$P_\Sigma = 0.311 \quad \text{[watts]}$$

Step No. 20: Calculate the watt density, ψ.

$$\psi = \frac{P_\Sigma}{A_t} \quad [\text{watts/cm}^2]$$

$$\psi = \frac{0.311}{16} \quad [\text{watts/cm}^2]$$

$$\psi = 0.0194 \quad [\text{watts/cm}^2]$$

Step No. 21: Calculate the temperature rise in degrees C.

$$T_r = 450(\psi)^{(0.826)} \quad \text{[degrees C]}$$

$$T_r = 450(0.0194)^{(0.826)} \quad \text{[degrees C]}$$

$$T_r = 17.3 \quad \text{[degrees C]}$$

Step No. 22: Calculate the window utilization, K_u.

$$K_u = \frac{NA_{w(B)}}{W_a}$$

$$K_u = \frac{(60)(0.00519)}{(0.684)}$$

$$K_u = 0.455$$

Powder Core, Input Inductor Design Test Data (Core Geometry, K_g, Approach)

Summary

The following information is the test data for the above powder core inductor. It is difficult to design and achieve the required resistance with just one wire and also have a compact design. If the engineer is required to get closer to the required resistance called out in the design specification, the inductor could be wound bifilar using a large wire and a smaller wire. It would be like having two resistors in parallel to get the correct resistance. The author hopes that this chapter, with its step-by-step approach, helps the readers understand the design of a filter inductor with the required resistance. The above example of this inductor was built, and tested. It meets the intent of the specification and shows the reader a typical design.

© 2011 by Taylor and Francis Group, LLC

Test Data

1. Frequency, f = 100kHz
2. Inductance, L = 125 µh
3. Inductance, L, (at 2.5 amps) = 103 µh
4. Output current, I_o = 2.5 amps
5. DC Resistance, R_L = 0.0503 ohms
6. Temperature Rise, T_r = 16.6°C
7. Window utilization, K_u (See Chapter 4) = 0.455
8. Max. Operating Flux, B_m = 0.275 T

Recognition

I would like to give thanks to Charles Barnett, an engineer at Leightner Electronics Inc., for building and testing the inductor design examples.

Leightner Electronics Inc.
1501 S. Tennessee St.
McKinney, TX. 75069

The Author would like to thank Paul A. Levin for his work he did to develop these Equations from my original Core Geometry (Kg) Equations.

© 2011 by Taylor and Francis Group, LLC

Index

A

AC inductor design, 10–3
  AC inductor design example, 10-9–13
  AC inductor loss, 10-7
  AC inductor VA, 10-3
  fundamental considerations, 10-4–5
AC inductor volt-amp (VA) capability
  relationship of A_p to, 10-3–4
  relationship of K_g to, 10-4
AC leakage current measurement, 17-12, 17-13
Adjacent conductors, 1-5
Air-core coil, 1-6
Air-core coil emitting magnetic flux, 1-8
Air gap
  controlling the dc flux with, 1-20–21
  types of, 1-21–22
Air gap effect, 2-42
Alternating flux, 3-6–7
Amorphous materials
  core loss coefficients for, 2-27
  magnetic properties for, 2-10
Amplitude modulation, 18-3
Amp turn equation, 24-3
Annealing, 3-8–9
Apparent power, 7-5–8, 12-11, 18-11–12, 24-12–13
Apparent power total, 7-7
Area product (A_p), 5-4, 5-6, 7-4, 7-13, 8-13, 10-3
  inductor derivation for, 21-12–15
  transformer core geometry, K_g and, 5-18–20
  transformer current density and, 5-15–18
  transformer derivation for, 21-7–9
  transformer surface area and, 5-11–14
  transformer volume and, 5-6–9
  transformer weight and, 5-9–11
Autotransformer design
  apparent power, 22-5, 22-8
  step-down, 22-6–8, 22-15–20
  step-up, 22-5–6, 22-14–15
  voltage and current relationship of, 22-3–5
  250 watt step-down, 22-15–20
    design example, 22-15
  250 watt step-up, 22-8–13, 22-14, 22-21
    design example, 22-8
  window utilization, 22-13, 22-21
Autotransformer turns ratio, 22-5, 22-7
AWG ac/dc resistance ratio, 4-27
Axial rotary transformer, 19-6

B

Bare wire area, 14-8, 14-19
Base film insulation, 4-20–21
Base materials
  PC board, 20-17
Basic rotary transformer, 19-3–4
B-H loops, 11-8, 13-4
  dynamic, 2-37
  ferrite, 2-14, 2-15
  ideal square, 2-30
  magnesil (K), 2-37, 2-39, 2-45
  orthonol, 2-37, 2-39, 2-45
  silicon, 2-7
  square permalloy, 2-8, 2-38, 2-40, 2-45
  supermalloy, 2-9, 2-38, 2-40, 2-46
  supermendur, 2-7
Bias winding calculation, 25-17
Bifilar windings, 17-8
Bondable magnet wire, 4-20
Bondable overcoats, 4-21
Bonding methods, 4-20
Boost converter, 13-8
  design example, 13-29–37
  PFC converter, 13-37
    design example, 13-37–47
Bowing
  in transformer windings, 4-9
Buck converter, 13-5
Buck regulator converter, 8-5
Buck type converters, 8-5–7
Bulk gaps, 1-21

C

Calculate capacitance, 17-8
Calculation
  MLT, 4-40–41
  skin effect, 4-24–27
Capacitance layer-to-layer, 17-10–11
Capacitance turn-to-turn, 17-10
Capacitance winding-to-winding, 17-11–12
Capacitor, 15-4, 24-30
  current, 11-9
  step-up winding, 11-6
Capacitor input bridge rectifier filter, 13-38
C core, 7-14
Center-tapped full-wave circuit, 7-7, 7-8

© 2011 by Taylor and Francis Group, LLC

Circuit operation, 14-3
Circular mil, 4-14
Circular mils per amp, 20-9
Clamp diodes, 15-9
Coercive force, 1-11
Coercivity, 2-4
Coil proximity, 1-26–27
Common mode filter, 23-12
  inductor design specification, 23-16–19
Common-mode inductor design, 23-3
  choosing the magnetic material, 23-12
  CM core saturation, 23-15
  CM filter inductor, 23-12
  CM inductor design example, 23-16
  CM noise source, 23-6
  common-mode noise, 23-5
  differential-mode noise, 23-3
  DM noise source, 23-3
  ferrite stress characteristics, 23-14
  ferrite temperature characteristics, 23-13
  semiconductor noise, 23-6–8
  transformer noise, 23-9
Common mode noise
  semiconductors, 23-6–8
  transformers and inductors, 23-8–9
Commutating diodes, 24-29
Commutating winding, 18-5
Comparing B-H loops, 14-4
Comparing transformer, 12-4–5
Composite core configuration, 2-50–53
Constant Voltage Transformer (CVT)
  B-H loop of, 11-8
  design equations, 11-5–8
  design example, 11-8–15
  electrical parameters of, 11-4–5
  primary voltage, 11-8
  regulating characteristics, 11-3
  series AC inductor, 11-15–19
Continuous boundary, 13-5
Continuous current
  boost converter design equations, 13-8–10
  buck converter design equations, 13-6–7
  inverting buck-boost design equations, 13-12–13
  isolated buck-boost design equations, 13-15–16
  mode, 13-4
Control winding, 24-8–9
  calculation, 25-16
  coefficient, 25-10
  precautions, 25-18
  and rectifiers, 25-8
Convection
  transformer dissipation by, 6-5–6
Conventional current flow, 1-3
Conversion process, 5-3
Converter regulation, 18-3
Converter waveforms
  double-ended forward, 14-6
  single-ended forward, 14-5
Copper
  loss, 6-3
  resistance, 4-41
  weight, 4-41
Core assembly, 20-18
Core configuration
  comparing, 10-8
Core geometry, 5-5, 7-4, 7-12, 8-14, 8-15–20, 9-6, 9-10, 10-4, 18-15–21, 24-13
  and area product, 5-18–20
  inductor derivation for, 21-9–12
  and regulation, 7-12
  transformer derivation for, 21-4–7
Core loss, 2-24–25, 6-3, 14-14
  equations, 2-25–28
Core materials
  fundamental considerations, 8-9–11
  in PWM converters, 8-8–9
  types of, 3-5–6
Core mounting, 20-18
Core saturation, 23-15
Core saturation margin, 10-7
Core type construction, 3-5
Core type transformer, 12-5
Critical inductance point, 8-4
Current carrying conductor, 1-3
Current density, 5-6, 20-9–11
  and area product, 5-15–18
Current-fed resonant converter, 18-6
Current-fed sine wave converter, 19-6–8
Current spikes, 17-4
Current transformer
  circuit applications, 16-7–8
  current transformer design, 16-2
  design example, 16-9–13
  design performance, 16-13
  diode drop, 16-9
  electrical data, 16-13
  equivalent circuit for, 16-4
  error compensation, 16-7
  exciting current, 16-4
  input current *versus* output voltage, 16-13
  secondary AC current monitor, 16-3
  uniqueness of, 16-5–7

© 2011 by Taylor and Francis Group, LLC

Current waveforms
voltage, 15-4
Cut and uncut cores, 2-47, 2-50, 2-51
CVT, *see* Constant Voltage Transformer

D

DC inductor design
buck type converters, 8-5–7
fundamental considerations, 9-7–9
inductance, 8-3–7
sine wave rectification, 8-3–5
DC inductor skin effect, 4-24
DC magnetizing force, 2-43, 9-7, 9-14, 9-19
Delta circuit, 12-6
Delta connection, 12-3
Delta phase current, 12-6
Demag
winding delta current, 14-13
winding inductance, 14-12
winding rms current, 14-13
wire area, 14-14
Demagnetizing
current, 14-5
force, 2-48
winding, 14-3
Design constraints, 19-8–9
Design equations, 14-6
derivation for
inductor area product, 21-12–15
inductor core geometry, 21-9–12
transformer area product, 21-7–9
transformer core geometry, 21-4–7
transformer regulation, 21-15–17
Designing Ind. for a given resistance, 26-3
calculating the core geometry, 26-5
calculating the electrical conditions, 26-5
gapped inductor design example, 26-10–15
overview, 26-3
powder core design example, 26-4–9
Design performance, 16-13
Dielectric constants, 4-40
Different core configurations, 1-22
Discontinuous boundary, 13-5
Discontinuous current
boost converter
design equations, 13-8–9
design example, 13-29–37
buck converter design equations, 13-5–6
inverting buck-boost design equations, 13-11–12
isolated buck-boost
design equations, 13-14–15
design example, 13-17–29
mode, 13-4
Distributed gaps, 1-21
Domain theory, 2-41
Double-ended forward converter, 14-5
Dowell curves, 4-31–33
Drain voltage waveform, 18-7, 18-8
Dwell time, 18-13
Dynamic B-H loops, 2-38, 14-4

E

Eddy currents, 4-22, 4-23, 4-28
and insulation, 3-6–7
loss, 2-4–5
Electrical coefficient, 14-8
Electrical conditions, 5-5
Electrical design specification, 22-16–20
Electrical insulating materials, 4-41
Electrostatic shield, 17-12
Energy-handling capability
relationship of A_p to inductor's, 9-5
relationship of K_g to inductor's, 9-6
Energy storage inductor, 13-3
Energy transfer, 13-3
Epoxy adhesive, 20-18
Equivalent circuit, 16-4
Equivalent Series Resistance (ESR), 15-3
Error compensation, 16-7
Exciting current, 3-11–12, 16-4

F

Faraday's equation, 7-5
Faraday shield, 17-12, 18-10, 23-10
Faraday's law, 7-5, 10-5, 20-7, 21-3, 21-6, 21-7
Ferrite B-H loop, 2-14, 2-15
Ferrite cross reference, 2-16
Ferrite materials, 2-13, 2-16, 8-8
magnetic properties for, 2-14
Ferrite stress, 23-14–15
Ferrite temperature characteristics, 23-13–14
Ferroresonant regulator
CVT capacitor, 11-3
CVT design equations, 11-5–6
CVT design example, 11-2
input inductor, 11-6
LC relationship, 11-5
primary voltage waveform, 11-3
Ferroresonant voltage stabilizer, 11-3
Flat plane rotary transformer, 19-6

© 2011 by Taylor and Francis Group, LLC

Flux crowding, 3-10
Flux density, 2-4, 2-25, 2-43, 16-12
Flyback converters, 13-3
  boost converter, 13-8
    design equations, 13-8–10
  buck converter, 13-5
    design equations, 13-5–7
  continuous mode, 13-3
  design example, 13-17, 13-29
  discontinuous mode, 13-3
  inverting buck-boost converter, 13-10
    design equations, 13-11–13
  isolated buck-boost converter, 13-13
    design example, 13-17–29
  standard boost, 13-39
Foil
  capacitance equation, 4-39
  with sharp burrs, 4-38
  use of, 4-37–40
Forward converter, 14-3
  design equations, 14-6
  design example, 14-2
  double-ended forward converter, 14-5
    double-ended waveforms, 14-6
  output filter inductor, 14-17
  output inductor design, 14-15–17
  single-ended forward
    single-ended waveforms, 14-5
Forward converter waveforms, 14-4–6
Frequency change, 11-4
Fringing flux, 1-22, 8-11–12, 10-5–8, 11-17, 20-16
  air gaps, 1-23–24
  coil proximity and, 1-26–27
  crowding, 1-27–28
  dc inductor design, 1-25–26
  at the gap, 8-11
  material permeability, 1-23
  powder cores and, 1-29
Full-wave bridge, 8-3
  secondary circuit, 7-7
Full-wave center tap, 8-3
Full-wave center-tapped secondary circuit, 7-7

G

Gap inductor design example, 8-2
Gap loss, 10-7
Gapped cores, 2-43, 2-52, 15-6, 15-7
Gapped ferrite inductor
  design example, 26-10–15
  design test data, 26-15
Gapped inductor design
  using the area product, A_p, 8-21–26
  using the core geometry, K_g, 8-15–20
Gapping effect, 2-42–49
Gapping materials, 1-21
Gap placement, 1-22

H

Hardware
  and brackets, 3-12
Heat bonding, 4-20
Heat dissipation, 6-6, 6-7
Heavy film magnetic wire, 4-6
HF, *see* High Flux Powder Cores
High Flux Powder Cores (HF), 2-20, 3-46, 9-3
  permeability *versus* dc bias for, 2-22
High frequency transformers, 4-29, 4-36
Hipernik, 2-5
Hysteresis loop, 1-11, 2-3, 2-4
Hysteresis loss, 2-4–5

I

Ideal square B-H loop, 2-30
IEC/VDE safety, 4-33–34
Incremental permeability, 1-14
Individual ripple, 15-4
Inductance
  buck type converters, 8-5–7
  critical point, 8-4
  versus dc bias, 8-8
  sine wave rectification, 8-3–5
Inductance *versus* DC bias, 9-9
Inductor, 9-5, 15-5
  design, 20-16
    critical inductance sine wave, 8-3
    critical inductance square wave, 8-5
    inductor design-gap, 8-3
    inductor design-powder, 9-3
  flux density, 8-10
  flux density *versus,* $I_{dc} + \Delta I$ current, 9-8
  input bridge rectifier filter, 13-38
  output power, 8-14
  output power, defining, 9-6
Inductors
  energy-handling capability, 8-13–14
  relationship of, A_p, 8-13
  relationship of, K_g, 8-14
Initial permeability, 1-13
Input capacitor voltage, 15-10
Input current component analysis, 16-4–5
Input current *versus* output voltage, 16-13

© 2011 by Taylor and Francis Group, LLC

Input filter
with additional damping, 15-6
design procedure, 15-9–10
inrush current measurement, 15-6
Input filter design
applying power, 15-6
capacitor, 15-3–4
design specification, 15-11–16
inductor, 15-5
oscillation, 15-5
Input inductor design, 15-6
Input-output transfer function, 24-27
Inrush current, 15-7
Insulated powder, 9-3
Intensified magnetic field, 3-4
Interlaminar eddy current, 3-7
Intralaminar eddy current, 3-7
Inverting buck-boost converter, 13-10
Iron-core inductor, 10-5
Iron powder cores, 2-17–23, 3-44, 9-4
core loss coefficients for, 2-28
Isolated buck-boost converter, 13-13
design example, 13-17–29

J

Jet Propulsion Laboratory (JPL), 18-3

L

Lamination burr, 3-9
Laminations, 3-7–8
Large through bore, 19-9
Layer winding, 4-37
LC filter, 8-3, 8-3–5
ripple reduction, 8-5
LC tank, 19-7
Leakage flux, 17-4–7, 23-15
Leakage inductance, 17-3–5, 19-5–6
Level detector, 16-8
Linear reactor
design of, 9-7
Line driver, 24-29
LL laminations, 3-19
Lumped capacitance, 17-3, 17-8, 17-9

M

Magnesil (K) B-H loop, 2-37, 2-39, 2-45
Magnetic conditions, 5-5
Magnetic cores, 1-8–9
with an air gap, 1-18
DS ferrite cores, 3-39
DU laminations, 3-20
EC ferrite cores, 3-27
EE ferrite cores, 3-25
EE iron powder cores, 3-47
EE planar ferrite cores, 3-26
EE sendust cores, 3-48
EFD ferrite cores, 3-31
EI laminations, 3-17
EI planar ferrite cores, 3-26
EPC ferrite cores, 3-32
EP ferrite cores, 3-34
ER ferrite cores, 3-30
ETD ferrite cores, 3-28
ETD/lp low profile ferrite cores, 3-29
fundamental characteristics of, 1-9–10
HF cores, 3-46
introduction to, 3-16
iron powder cores, 3-44
LL laminations, 3-19
MPP powder cores, 3-43
PC ferrite pot cores, 3-33
PQ ferrite cores, 3-35
PQ/lp ferrite cores, 3-36
RM ferrite cores, 3-37
RM/lp ferrite cores, 3-38
sendust powder cores, 3-45
tape wound C cores, 3-22
tape wound EE cores, 3-23
tape wound toroidal cores, 3-24
three-phase laminations, 3-21
toroidal ferrite cores, 3-42
UI laminations, 3-18
UUR ferrite cores, 3-40
UUS ferrite cores, 3-41
Magnetic fields
adjacent conductors, 1-5
changes polarity, 1-4
intensifying, 1-4–7
spaced conductors, 1-5
Magnetic insulators, 2-12
Magnetic material
air gap effect, 2-42
characteristics, 2-30–32
coercivity, 2-4
composite core configuration, 2-50–53
core loss, 2-24–25
equations, 2-25–28
eddy current loss, 2-4–5
ferrite cross reference, 2-16
gapping effect, 2-42–49
hysteresis loss, 2-4–5
iron powder cores, 2-17–23
manganese-zinc ferrites, 2-13

© 2011 by Taylor and Francis Group, LLC

metallic glass, 2-9–12
molypermalloy powder cores, 2-17
nickel-zinc ferrites, 2-13–15
permeability of, 2-4–5
power MOSFET inverter, 2-29
remanence flux, 2-4
resistivity, 2-4–5
saturation
definition, 2-33–35
theory, 2-41–42
silicon steel, 2-5
soft ferrites, 2-12–13
test conditions, 2-36–40
thin tape nickel alloys, 2-5–9
transformers, 2-29
Magnetic materials, 5-3, 7-3, 7-4, 23-12–13
characteristics of, 5-4
properties, 8-9
Magnetic Path Length (MPL), 1-8, 1-18, 3-4, 10-5
Magnetic properties
for amorphous materials, 2-10
of compressed powdered iron, 2-18
for ferrite materials, 2-14
for iron alloys materials, 2-6
Magnetics
hysteresis loop, 1-11
intensifying, 1-4–7
magnetic core, 1-8–9
permeability, 1-11–15
properties in free space, 1-3–4
simple transformer, 1-7
Magnetics kool Mμ, 9-4
Magnetization curve, 1-13
Magnetizing current, 2-43, 14-3
waveform, 14-13
Magnetizing force (H), 1-15–16
Magnetomotive force (mmf), 1-15–16, 4-29, 4-30
Magnet wire, 4-15
aluminum, 4-15
copper, 4-15
data, 4-6
eddy currents generated in, 4-23
film insulation, 4-16
flux distribution in, 4-23
insulation, 4-16, 4-18
litz, 4-27
silver, 4-15
Manganese-zinc ferrites, 2-13
Manufacturers material product list, 3-49
Material characteristics, 2-30–32
Material permeability, 1-15, 1-19, 1-23
Maximum efficiency, 6-3–4
Maximum permeability, 1-14
Mean Length Turn (MLT), 19-8
calculating, 4-40–41, 20-12, 20-13
dimensions, relating to winding, 4-40
lamination, 25-12
self-saturating mag-amp, 25-12
series saturable reactor, 24-13–14
toroid, 25-13
Metallic glass, 2-9–12
Micro-square magnetic wire, 4-21, 4-22
Miniature square magnet wire, 4-21
Minimizing fringing flux, 10-8
MLT, *see* Mean Length Turn
Mode inductor design
common mode noise, 23-5–6
differential mode noise, 23-3–5
Molypermalloy Powder Core (MPP), 2-17, 8-8, 9-3, 18-5, 18-10, 18-11
permeability *versus* dc bias for, 2-22
Monitor line current, 16-8
MPL, *see* Magnetic Path Length
MPP, *see* Molypermalloy Powder Core
Multiple layer high frequency transformers, 4-29–31
Multiple output converter, 7-9
Multistrand litz wire, 4-27
Multistrand wire, 4-22-23

N

Nickel-zinc ferrites, 2-13–15
Ni-Fe alloys, 2-5, 2-6
Noise common-mode, 23-5
Noise differential-mode, 23-3
Normal permeability, 1-14

O

Operational amplifier, 24-29
Orthonol B-H loop, 2-37, 2-39, 2-45
Output filter inductor, 8-7
Output inductor, 26-3
BH loop, 14-15
design
core geometry, K_g, approach, 14-18–24
Output power, 5-3, 7-5–8
versus apparent power, 21-3–4
transfer function, 24-27
Output voltage variation, 11-4

P

Parasitic capacitance, 17-4
Parasitic effects, 17-3–4
Peak current, 14-20
Permalloys, 2-5

© 2011 by Taylor and Francis Group, LLC

Permeability, 1-11–15
versus dc bias, 2-22–23
different kinds of, 1-12
of magnetic materials, 2-6
variation of, 1-13
PFC, *see* Power Factor Correction
Planar transformer, 20-3
calculating MLT, 20-12
core mounting and assembly, 20-18
inductor design, 20-16
and inductor design equations, 20-7
integrated PC board magnetics, 20-5
transformer basic construction, 20-3–4
transformer common-mode, 20-3
transformer core type EE and EI, 20-6
transformer core type ER, 20-6
transformer core type ETD, 20-6
transformer core type PQ, 20-7
transformer core type RM, 20-7
transformer current density, 20-9–11
transformer first effort, 20-9
transformer parasitics, 20-3
transformer PC board, 20-3, 20-8
transformer window utilization, 20-8
Polyfilar magnetic wire, 4-35–36
Powder core inductor
design example, 26-4–9
design test data, 26-9
input inductor
design example, 26-16–20
design test data, 26-20–21
Powder core material properties, 2-19
Powder cores, 1-28, 9-3, 15-6
typical permeability *versus* DC bias curves for, 9-7
Powder inductor designs example, 9-15–19
Powder toroidal core, 3-15
Power Factor Correction (PFC)
designing boost inductors for, 13-37–38
Power factor load, 11-4
Power gain, 25-11
Power handling, 7-4–5, 7-12–13
relationship of A_p to transformer, 5-4–5
relationship of K_g to transformer regulation and, 5-5
Power loss, 6-3
Power transformer, 24-28
Power-wasting snubbers, 19-5, 19-7
Pre-fab foils, 4-38
Primary bare wire area, 14-10
Primary circuit, 12-3
Primary copper loss, 14-11
Primary resistance, 14-11
Primary rms current, 14-10
Primary turns, 14-9
Primary voltage waveform, 11-3
Printed circuit winding, 20-11
PC board base materials, 20-17
PC board connections, 20-16
PC board copper thickness, 20-9
PC board interconnections, 20-16
PC board 1oz copper, 20-10
PC board 2oz copper, 20-10
PC board 3oz copper, 20-11
PC board rectangular center post, 20-11
PC board round center post, 20-11, 20-12
PC board winding capacitance, 20-14–15
PC board winding design, 20-11
PC board winding termination, 20-16
PC winding technique, 20-8
Progressive winding, 17-11
Proper core material, 5-3
Proximity effect, 4-28-29
in transformers, 4-29
using Dowell curves, 4-31–33
Pulse Width Modulation (PWM), 8-8, 18-4, 18-6, 18-13
converters, 8-8
Push-pull buck type converter, 8-5
PWM, *see* Pulse Width Modulation

Q

Quasi-voltage waveform, 11-7
Quiet converter
design
amplitude modulation, 18-3
apparent power, 18-11–12
converter regulation, 18-3
current-fed converter, 18-4–5
current-fed resonant converter, 18-6
dwell time, 18-13
equations, 18-12–15
JPL, 18-3
low EMI noise, 18-10
PWM, 18-4, 18-6
quiet converter waveforms, 18-6–9
regulating and filtering, 18-4, 18-6
resonant converter, 18-3
series inductor, 18-5
sine wave converter, 18-5
sine wave converter waveforms, 18-6
temperature stability, 18-11
voltage-fed converter, 18-3–4
window utilization factor, 18-10
waveforms, 18-6–9

© 2011 by Taylor and Francis Group, LLC

R

Radiation
transformer dissipation by, 6-5–6
Random minor loop, 2-35
Rectifier diodes, 24-30
Reducing skin effect, 4-23-24
Reflected resistance, 11-9
Regenerative drives, 16-8
Regulation equation, 21-17
Remanence, 2-4
flux density, 2-4
Remanent flux, 1-11, 2-4
Residual flux, 2-43
Resistance bonding, 4-21
Resistivity, 2-4–5
Resonant charge, 15-8–9
Resonant converter, 18-3
circuit, 19-7
Resonant frequency, 17-8, 17-9
Ripple voltage, 12-7
Rotary transformer
axial rotary transformer, 19-3, 19-6, 19-8, 19-9
basic rotary transformer, 19-3
flat plane rotary trans, 19-4, 19-6, 19-8, 19-9
transformer core size, 19-8
transformer design constraints, 19-8
transformer inherent gap, 19-3, 19-5
transformer leakage inductance, 19-4, 19-6, 19-8
transformer mechanical interface, 19-9
transformer power transfer, 19-4
transformer square wave, 19-4
Round and square B-H loop, 25-4, 25-6
Rule of thumb, 5-3

S

Saturable reactor, 24-28–29
Saturation
definition, 2-33–35
theory, 2-41–42
Saturation flux density, 11-7
Scrapless laminations, 3-8
Secondary AC current monitor, 16-3
Secondary bare wire area, 14-11
Secondary copper loss, 14-12
Secondary rms current, 14-11
Secondary turns, 14-11
Secondary winding resistance, 14-12
Self-saturating magnetic amplifier
apparent power, 25-9
bias winding, 25-7
bias winding calculation, 25-17
control winding and rectifiers, 25-8
control winding calculation, 25-17
control winding coefficient, 25-10
control winding precautions, 25-18
DU core surface area, 25-15
MLT lamination, 25-12
MLT toroid, 25-13
power gain, 25-11
response time, 25-11
round and square B-H loop, 25-4, 25-6
S-S mag- amp design example, 25-18
toroid surface area, 25-14
two core S-S magnetic amplifier, 25-5
Sendust powder cores, 3-45, 9-4
core loss coefficients for, 2-26
permeability *versus* dc bias for, 2-23
Series AC inductor, 11-15–19
Series inductor turns, 11-17
Series saturable reactor design, 24-3–4
apparent power, 24-12–13
basic operation, 24-4–6
control winding, 24-8–9
core geometry, 24-13
design example, 24-18
E core MLT, 24-13–14
E core surface area, 24-16–17
how SR operates, 24-6–8
power gain, 24-10–11
response time for, 24-11–12
saturated inductance and winding resistance, 24-9–10
specification and design, 24-19–24
test data, 24-24–25
toroidal cores MLT, 24-14–15
toroidal tape cores, 24-17
ultra low power current transducer, 24-26–30
Shearing over the B-H Loop, 2-52
Shell type construction, 3-5
Shell type transformer, 12-5
Shield, common-mode, 23-9
Short circuit current, 11-4
Silicon B-H loop, 2-7
Silicon steel, 2-5
Simple buck regulator, 26-3
Simple transformer, 1-7
Sine wave converter, 18-10
waveforms, 18-6
Sine wave rectification, 8-3–5
Single-ended forward
converter, 14-5
Skin effect, 4-22-23, 13-17, 13-40, 13-41, 14-7
in inductors, calculation, 4-24–27
in transformers, 4-23–24

© 2011 by Taylor and Francis Group, LLC

Slip rings, 19-3
contamination, 19-3
Solderable insulation, 4-19–20
Solder wicking, 4-39
Solvent bonding, 4-21
Spaced conductors, 1-5
Specialty wire, 4-33
Square loop material, 11-8
Square mil, 4-15
Square permalloy B-H loop, 2-38, 2-40, 2-45
Square wave converter circuit, 19-7
Square wave technology, 19-4–5
S-S mag- amp design example, 25-18
Stacking factors, 3-15
Standard dc-to-dc boost flyback converter, 13-39
Standard foils, 4-36–37
Standard isolation transformer, 22-14–15, 22-22
Standard litz wire, 4-27
Standard permeability, 9-4
Standard powder core permeabilities, 2-19
Standard PWM control, 18-3
Standard width foil, 4-37
Stefan-Boltzmann law, 6-5
Step down autotransformer design, 22-6–8, 22-15–20
Step up autotransformer design, 22-5–6, 22-14–15
Stray capacitance, 17-12–13
current, 23-11
Stress-relief, 3-8–9
Supermalloy, 2-9
Supermendur B-H loop, 2-7
Surface area, 6-8
temperature rise *versus,* 6-6
Surface area-area product, 5-12
Switch-Mode Power Supplies (SMPS), 14-15

T

Tape toroidal cores, 3-14–15
Tape wound cores, 3-12–13
Tape wound toroidal cores, 3-24
Temperature class, 4-16
Temperature stability, 18-11
Test data, 22-14, 22-21, 24-24–25
Thermal endurance, 4-19
Thermal expansion, 20-18
Thermal overloads, 4-16
Thin tape nickel alloys, 2-5–9
Three-phase laminations, 3-21
Three phase transformers, 12-3
apparent power, 12-11
area product, 12-10, 12-13
core geometry, 12-10, 12-12
delta circuit, 12-6
delta connection, 12-3
delta phase current, 12-6
design example, 12-2
ripple voltage, 12-7
star connection, 12-3
unbalance line, 12-5
unbalance loads, 12-5
wye circuit, 12-6
wye phase voltage, 12-6
Three single phase, 12-4
Toroidal core, 7-14, 19-9
Toroidal ferrite cores, 3-42
Toroidal powder core design
using area product, A_p , approach, 9-15–19
using core geometry, K_g , approach, 9-9–14
Toroidal powder cores, 9-3
Toroidal tape cores, 24-17–18
Toroid surface area, 25-14
Transformer(s), 2-29, 4-29, 4-30, 4-33, 17-4, 17-5
core geometry (K_g), 5-18–20
current density and area product (A_p), 5-15–18
derivation
for area product, 21-7–9
for core geometry, 21-4–7
design, 7-3, 18-16–21
apparent power, 7-5
area product, 7-4, 7-5
circuit diagram, 7-10
core geometry, 7-4, 14-7–15
current density, 7-3
efficiency, 7-3
with multiple outputs, 7-8–10
output power, 7-3
power handling ability, 7-4
rule of thumb, 7-3
steps in, 5-3
voltage regulation, 7-10–12
dissipation by radiation and convection, 6-5–6
efficiency, 6-3, 6-4
input power, 14-8
output power, 14-8
regulation, 6-3, 14-12, 21-15–17
as function of efficiency, 6-9–11
and power handling capability, 5-5
weight *versus,* 5-20–21
surface area and area product (A_p), 5-11–14
temperature rise, 6-3, 6-6
trade-offs, 5-3

© 2011 by Taylor and Francis Group, LLC

voltage regulation, 21-15
volume and area product (A_p), 5-6–9
weight and area product (A_p), 5-9–11
weight *versus* transformer regulation, 5-20–21
winding capacitance, 17-8–9
Triple insulated litz, 4-34–35
Triple insulated wire, 4-33–34
Two core S-S magnetic amplifier, 25-5

U

Ultra low power current transducer, 24-26–30

V

VA, *see* Volt-amp
Voltage-fed converter, 18-3–4
Voltage regulation, 7-10–12
of transformer, 6-10
Voltage spikes, 17-3
Volt-Amp (VA), 10-3–4
Volume-area product, 5-7

W

250 watt isolation transformer, 7-15–20
38 watt 100kHz transformer design, 7-21–30
Waveforms, 13-6, 13-7, 13-8, 13-9, 13-11, 13-12, 13-14, 13-16
Weight-area product, 5-10
Winding capacitance, 17-8–11
and leakage inductance, 17-3–5
capacitance layer-to-layer, 17-10–11
capacitance turn-to-turn, 17-10
capacitance winding-to-winding, 17-11–12
electrostatic shield, 17-12
Faraday shield, 17-12
leakage flux, 17-4–7
lumped capacitance, 17-3, 17-8, 17-9
minimizing capacitance, 17-10
minimizing leakage inductance, 17-7–8
parasitic capacitance, 17-4
parasitic effects, 17-3–4
progressive winding, 17-11
stray capacitance, 17-12–13
winding configuration, 17-11
Winding data, 2-36
Winding layer parameters, 4-34
Winding resistance and dissipation, 20-13–14
Window utilization, 11-19, 14-9, 22-13, 22-21
effective window, 4-9–11
factor, 18-10
factor, K_u, 4-4–5
fill factor, 4-6–9
hexagonal winding, 4-8
ideal winding, 4-8
insulation factor, 4-12
layer insulation, 4-7, 4-10
square winding, 4-7
transformer winding, 4-10
winding margins, 4-10
wire insulation, 4-5
wire lay, 4-6
wire table, 4-16, 4-17
Window utilization factor, 5-5, 20-8
Window utilization ferrite, 4-13–14
Wire diameter, 14-7, 14-19
Wye circuit, 12-6
Wye phase voltage, 12-6

© 2011 by Taylor and Francis Group, LLC